UNIVERSITY OF CALIFORNIA,
IRVINE

Annulations Initiated by Metal-Hydride Hydrogen Atom Transfer in Terpenoid Total Synthesis

DISSERTATION

submitted in partial satisfaction of the requirements
for the degree of

DOCTOR OF PHILOSOPHY

in Chemistry

by

William Peter Thomas

Dissertation Committee:
Associate Professor Sergey V. Pronin, Chair
Professor Christopher D. Vanderwal
Distinguished Professor Larry E. Overman

2022

TABLE OF CONTENTS

LIST OF FIGURES

LIST OF SCHEMES

LIST OF TABLES

AKNOWLEDGEMENTS

I would like to extend my sincere appreciation to all of those who have supported me throughout my schooling and who have made the accomplishments reported in this dissertation possible.

First, I would like to thank Sergey V. Pronin for his mentorship and dedication to my development as a chemist. I am truly indebted to you for the inordinate amount of time you spent teaching me synthesis, always with an unwavering level of enthusiasm. I am also incredibly grateful for the level of autonomy you gave me to explore my own ideas and for your guidance as I failed, learned, and eventually succeeded throughout my studies. Your mentorship has exceeded all my expectations. It has been a pleasure conducting research with you and I look forward to following your future successes.

I would like to acknowledge my committee members Professor Christopher D. Vanderwal and Distinguished Professor Larry E. Overman, for their support and inspiration throughout my time in graduate school. Thank you both for your insights regarding research and for fostering a truly collaborative environment within the chemistry department at UC Irvine. I have the highest respect for you and your contributions to the sciences.

I would like to thank Professor Brian J. McNelis for his mentorship during my undergraduate studies at Santa Clara University. Your excitement for organic chemistry and patience in training me as an undergraduate researcher were instrumental in my decision to pursue graduate school. I have the deepest appreciation for your support.

I am grateful to all my colleagues in the Pronin group for your camaraderie and the knowledge you have imparted on me. I will also cherish the time we have spent outside of lab and the memories we made. I would like to specifically thank those of you who have been instrumental

in my development as a chemist: Dr. Chris A. Discolo, you were the first person to introduce me to complex organic synthesis and your unparalleled enthusiasm inspired me to pursue a career in chemistry. In graduate school, you were an inspiration as a chemist, mentor, and friend. You have made a monumental impact on my life. Thank you. Dr. David T. George, a remarkable amount of my knowledge regarding chemistry can be traced back to the lessons and skills you taught me. Although we overlapped for less than a year, you have been truly foundational to my success as chemist and for that I thank you. Dr. Devon J. Schatz thank you for your support in developing the MHAT-initiated annulation chemistry. I truly appreciated it. Nick J. Foy, going through graduate school with you has been an absolute pleasure. Your talent as a chemist is inspiring and your friendship has made graduate school all the more enjoyable.

Thank you Dr. David T. George and Dr. Devon J. Schatz for your roles as co-authors. Portions of Chapter 1 and 3 were reproduced with permission from: Thomas, W. P.; Schatz, D. J.; George, D. T.; Pronin, S. V. J. Am. Chem. Soc. 2019, 141, 12246. © 2019 American Chemical Society. Portions of Chapter 5 were reproduced with permission from: Thomas, W. P.; Pronin S. V. J. Am. Chem. Soc. 2022, 144, 118. © 2022 American Chemical Society

I would like to thank my friends not already mentioned for the times we have spent together, which have been welcome reprieves from the challenges of research. I look forward to spending more time with you all now that the commitments of graduate school are behind me.

Finally, I would like to acknowledge my family. To my parents and grandparents, I am indebted for your unwavering support and encouragement throughout all my schooling. To my brothers, Nick and Max, I cannot overstate how impactful you both have been throughout the trials and successes of graduate school and my life. My best memories are with you, and I look forward to the many more to come.

VITA

William P. Thomas

EDUCATION

University of California, Irvine–UCI — Irvine, CA
Ph.D. Organic Chemistry — 2017–2022

Santa Clara University–SCU — Santa Clara, CA
B.S. Biochemistry — 2013–2017

RESEARCH

Pronin Laboratory–UCI — Irvine, CA
Ph.D. Candidate, Advisor: Prof. Sergey V. Pronin — 2018–2022

McNelis Laboratory–SCU — Santa Clara, CA
Undergraduate Researcher, Advisor: Prof. Brian J. McNelis — 2015–2017

PUBLICATIONS

Thomas, W. P.; Pronin, S. V. A concise enantioselective approach to quassinoids. *J. Am. Chem. Soc*. **2022**, 144, 118–122.

Thomas, W. P.; Pronin, S. V. New methods and strategies in the synthesis of terpenoid natural products. *Acc. Chem. Res.* **2021**, 54, 1347–1359.

Thomas, W. P.; Schatz, D. J.; George, D. T.; Pronin, S. V. A radical-polar crossover annulation to access terpenoid motifs. *J. Am. Chem. Soc.* **2019**, 141, 12246–12250.

PRESENTATION

Thomas, W. P.; Schatz, D. J.; George, D. T.; Pronin, S. V. Metal-Hydride Hydrogen Atom Transfer (MHAT) Initiated Annulations in Terpenoid Total Synthesis. Presented at ACS DOC Graduate Research Symposium, Albuquerque, New Mexico, November 18–21, 2021. (poster)

HONORS & AWARDS

Allergan Graduate Fellowship–UCI 2022 • AbbVie Scholar Symposium–UCI 2021 • NSF GRFP Honorable Mention–UCI 2018 • ACS DOC Award–SCU 2017 • American Institute of Chemists Foundation Award–SCU 2017 • Michael Sweeney Endowed Award–SCU 2017 • Phi Lambda Upsilon–SCU 2017 • Phi Beta Kappa–SCU 2017 • ACS Polyed Award–SCU 2015

ABSTRACT OF THE DISSERTATION

Annulations Initiated by Metal-Hydride Hydrogen Atom Transfer in Terpenoid Total Synthesis

by

William Peter Thomas

Doctor of Philosophy in Chemistry

University of California, Irvine, 2022

Associate Professor Sergey V. Pronin, Chair

This dissertation chronicles the development of a metal-hydride hydrogen atom transfer (MHAT) initiated annulation and its implementation in the synthesis of terpenoid natural products. Chapter 1 introduces the concept of MHAT and relevant transformations developed within this reactivity manifold. The second half of Chapter 1 details our development of a novel MHAT-initiated annulation between α,β- and γ,δ-unsaturated carbonyls to access sterically congested terpenoid motifs.

Chapter 2 begins with a brief overview of the biosynthesis and bioactivity of the labdane diterpenoid forskolin. Specific attention is paid to the utility of forskolin as a biological tool to stimulate adenylyl cyclase and its corresponding analogs as therapeutics. The latter half of Chapter 2 focuses on prior total syntheses of this secondary metabolite, highlighting the challenges associated with constructing the carbocyclic core and establishing the stereochemically complex array of oxidation found in the natural product. Chapter 3 details our synthetic efforts towards forskolin, which leveraged the previously described MHAT-initiated annulation culminating in a 14-step synthesis of the target compound.

Chapter 4 begins with a brief overview of the biosynthesis and bioactivity of quassinoid natural products. This section focuses on some of most biologically potent congeners and their antimalarial and anticancer properties. The latter portion of this chapter covers the prior syntheses of the congener quassin, which serves as a logical entry point for groups aiming to establish a general synthetic route to the quassinoids. Specific attention is paid to the challenges associated with introducing the extensive oxidation found in quassin. Chapter 5 details our synthetic efforts towards quassin and the evolution of the MHAT-initiated annulation in a synthetic setting, which led to a 14-step synthesis of the target compound.

Chapter 1: An Introduction to MHAT-Initiated Annulations

1.1 Seminal MHAT Reactions

Metal-hydride hydrogen atom transfer (MHAT) has gained significant attention from the synthetic community in recent years as a mild method to perform hydrofunctionalizations of alkenes. MHAT involves a metal hydride undergoing hydrogen atom transfer (HAT) with an alkene (**1.1**) in a Markovnikov selective fashion to generate an intermediate alkyl radical (**1.2**), which can then be captured by a variety of chemical entities to afford hydrofunctionalized products (**1.3**, Scheme 1.1).[1] The canonical example of MHAT is the Mukaiyama hydration, which involves Markovnikov hydration of alkenes in the presence of cobalt hydrides and molecular oxygen.[2] At the time of this seminal publication the underlying mechanism was not evident and it was not until several decades later that the synthetic community elucidated the elementary steps of these types of chemical transformaitons.[1] This has led to exponential growth in the field of MHAT, spawning an ever growing number of novel alkene hydrofunctionalization methodologies. Several excellent review articles have catalogued these developments and the interested reader is directed here for an in-depth account of MHAT literature.[1] This chapter is intended to highlight the seminal MHAT methodologies involving iron hydrides that result in C–C bond formation, as these examples are the most relevant to our development of an MHAT-initiated annulation (Section 1.3).

Scheme 1.1: MHAT General Mechanism

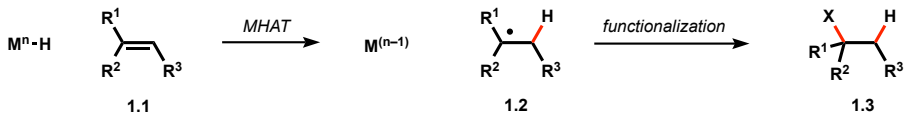

The Boger laboratory, in pursuit of a total synthesis of vinblastine (**1.4**), found that $Fe_2(ox)_3 \cdot 6H_2O$ in the presence of $NaBH_4$ generated a putative iron hydride that was competent at engaging alkenes in an MHAT event (Scheme 1.2).[3] They ultimately leveraged this reactivity to

perform a hydration reaction on a penultimate intermediate in their total synthesis (see inset, Scheme 1.2, bonds highlighted in red of **1.4** constructed via MHAT hydration). Recognizing the value of this type of transformation, the Boger group expanded this methodology to include a variety of alkenes and radicalphiles (Scheme 1.2).[4]

Scheme 1.2: Boger's MHAT Alkene Functionalization

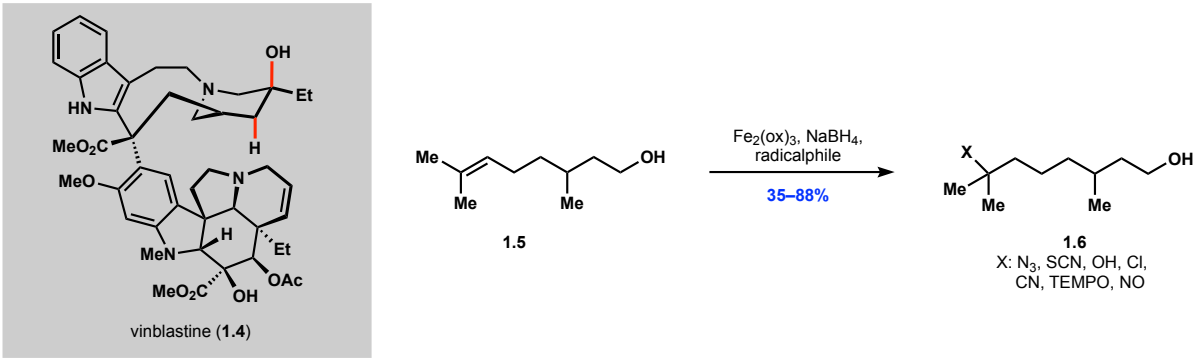

Inspired by these reports from Boger and preceding MHAT literature, in 2014 the Baran group disclosed a practical method to cross-couple alkenes capitalizing on the MHAT reactivity manifold.[5] In their seminal report the Baran group was able to selectively engage electron-rich and electron-neutral alkenes in an MHAT event with a putative iron hydride and then perform Giese additions with the resulting alkyl radicals and electron-deficient alkenes, ultimately affording alkene cross-coupled products (Scheme 1.3). Notably, the conditions Baran developed were far

Scheme 1.3: Baran's MHAT Alkene Cross-Coupling

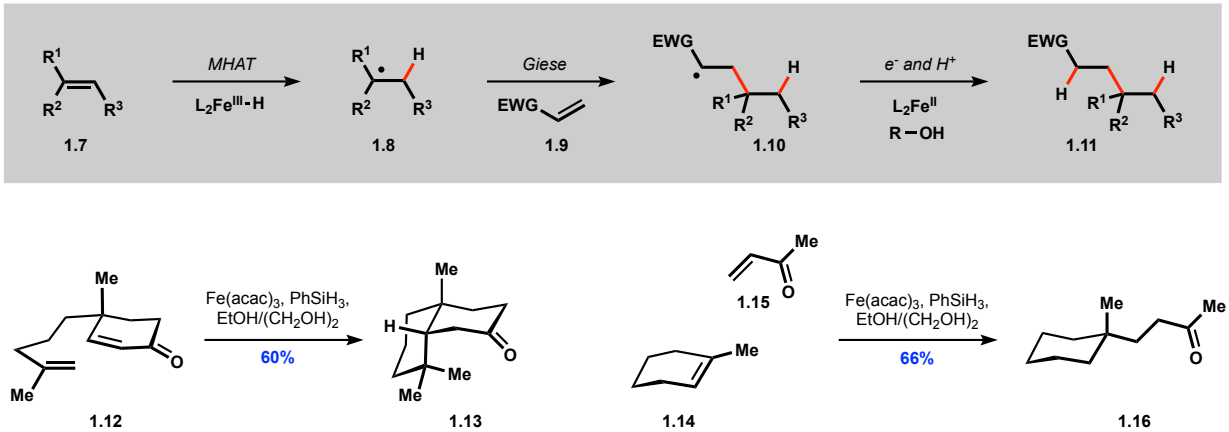

milder than those employed by Boger. Baran was able to generate putative iron hydrides using $Fe(acac)_3$ as the pre-catalyst and $PhSiH_3$ as the hydride source in alcoholic solvents. These mild reaction conditions coupled with the utility of forming C–C bonds through alkene cross-coupling led to rapid and widespread adoption of this methodology by the synthetic community.

In 2019 two mechanistic studies focused on iron-mediated MHAT were published, the first a computational and experimental study of Baran's alkene cross-coupling from the Holland group and the second a computational study from the Chen group focusing on the elementary step of MHAT from iron hydrides to alkenes.[6,7] These reports revealed several key findings: initial formation of the iron hydride is rate-limiting, the resulting iron hydride bond is exceptionally weak with a bond dissociation energy calculated to be 17–20 kcal/mol leading to a highly exergonic MHAT event that is energetically favored over hydrometallation, computations suggest the initial alkyl radical is protected by a persistent radical effect with Fe^{II} species avoiding homo-coupled products, and finally, it is not clear whether the penultimate step from radical **1.10** to the product **1.11** is a stepwise process or a concerted proton-electron transfer (Scheme 1.3). This final point is worth further comment.

The initial hypothesis was that following Giese addition the resulting radical **1.10** was reduced to the enolate by Fe^{II} and then protonated by the alcoholic solvent.[5] This assertion was supported by experimental evidence. First, a three-component coupling was possible where the putative enolate could be captured by an aldehyde (**1.20**, Scheme 1.4). Second, reactions employing deuterated ethanol led to incorporation of deuterium at the α-position of the carbonyl in the product (**1.22**). However, Holland called into question the feasibility of an Fe^{II} mediated reduction of a α-keto radical to the corresponding enolate, with computations suggesting the process involving $Fe(acac)_2$ and an acrylate derived α-keto radical would be endergonic by 35

Scheme 1.4: Mechanistic Studies

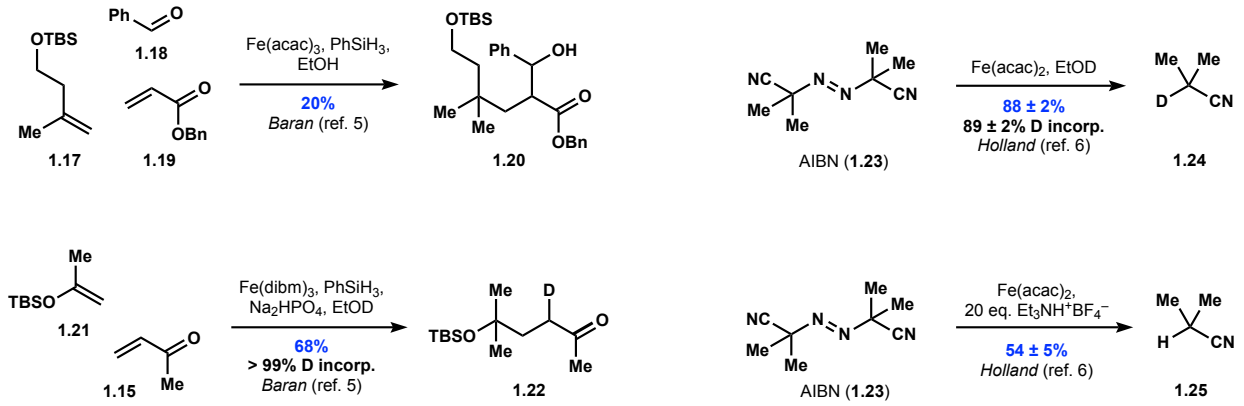

kcal/mol.[6] Further computations by the Holland group suggested a far more feasible pathway would be concerted proton-electron transfer (CPET) from a molecule of ethanol bound to $Fe(acac)_2$, which drastically lowers the bond dissociation energy of the O–H bond from 104 kcal/mol to 74 kcal/mol. However, experimental evidence complicated the mechanistic picture.

In an attempt to experimentally probe this CPET hypothesis Holland heated mixtures of AIBN with $Fe(acac)_2$ and EtOH or EtOD, which led to the expected isobutyronitrile (**1.24**) in 86 ± 3% and 88 ± 2% yield respectively with high levels (89 ± 2%) of deuterium incorporation as expected (Scheme 1.4). Alternatively, when these experiments were run with a non-coordinating acid, $Et_3NH^+BF_4^-$, which should not be able to undergo CPET, they observed 25 ± 2% and 54 ± 5% yield of isobutyronitrile (**1.25**) with 1 and 20 equivalents of acid respectively, implying a possible stepwise proton-electron transfer. Based on these experiments the authors suggested both a stepwise and concerted proton-electron transfer may be operable.

The fate of the radical generated following Giese addition has important implications because several methodologies that were developed following Baran's seminal report aim to intercept this penultimate intermediate with chemical species other than a hydrogen atom (see

below). To date, the complete mechanistic picture surrounding these final elementary steps of iron-mediated MHAT processes remains unclear.[8]

1.2 MHAT-Initiated Polycyclizations

One subset of methodologies that arose following Baran's report on alkene cross-couplings was MHAT-initiated polycyclizations. These polycyclizations leveraged the same reactivity manifold in an intramolecular setting but aimed to capture the putative intermediate enolate with an electrophile.

The first example of an MHAT-initiated polycyclization is from Pronin, who recognized a drastically simplifying disconnection of indole diterpenoid natural products of the paxilline type, which required the development of a novel polycyclization.[9] In their initial foray, targeting emindole SB (**1.31**), Pronin and co-workers envisioned an MHAT-initiated polycyclization of diene **1.26** that would access the tricyclic core of the indole diterpenoid family of natural products (**1.27**, Scheme 1.5). In practice, the group prepared polycyclization precursor **1.26** from 2-methyl-2-cyclopentenone and upon subjecting this material to optimized reaction conditions, generated the desired tricycle **1.27**. This reaction is proposed to proceed by initial MHAT to the 1,1-disubstituted alkene followed by Giese addition, then reduction to the enolate followed by an aldol

Scheme 1.5: Pronin's Synthesis of Emindole SB

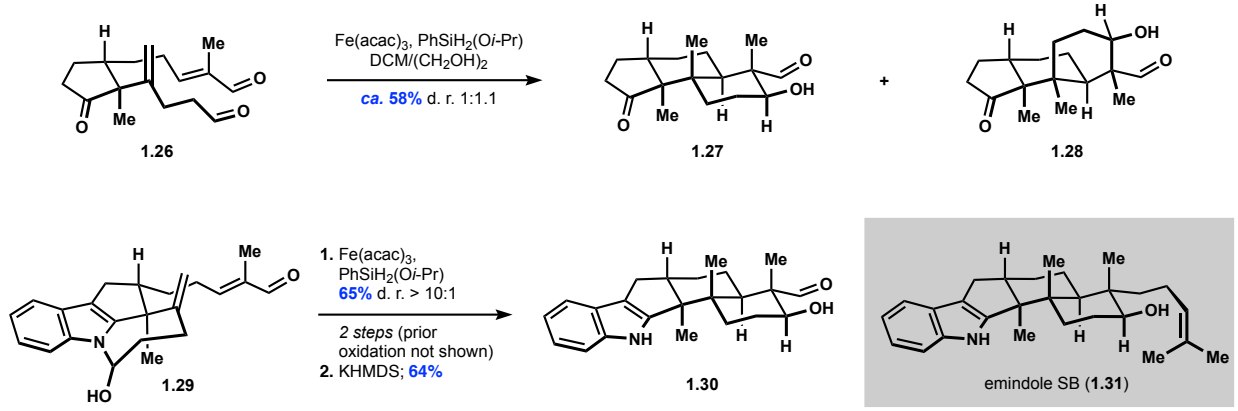

event. Unfortunately, this reaction also afforded an undesired diastereomer **1.28** in nearly equimolar quantities prompting the group to develop a clever solution in the form of tethering the formylpropyl substituent bearing the 1,1-disubstituted alkene to the pendant indole (**1.29**). This then allowed the researchers to accomplish the desired bond-forming events in a stepwise manner, but with high levels of diastereoselectivity. Pronin was able to carry this advanced intermediate **1.30** on to emindole SB, completing a remarkable 11-step synthesis of the target.

In subsequent efforts, Pronin improved upon this polycyclization to achieve a highly diastereoselective process. The key to this success was a fully substituted center at C2. It is postulated that in the first C–C bond forming event the nitrile at C2 incurs pseudodiaxial interactions with the substituents of the adjacent γ,δ-unsaturated aldehyde chain, where orienting the formylethyl fragment in a pseudoaxial configuration is associated with greater steric penalties (Scheme 1.6). This solution led to an efficient synthesis of nodulisporic acid C (**1.33**).[10,11]

Scheme 1.6: Pronin's Synthesis of Nodulisporic Acid C

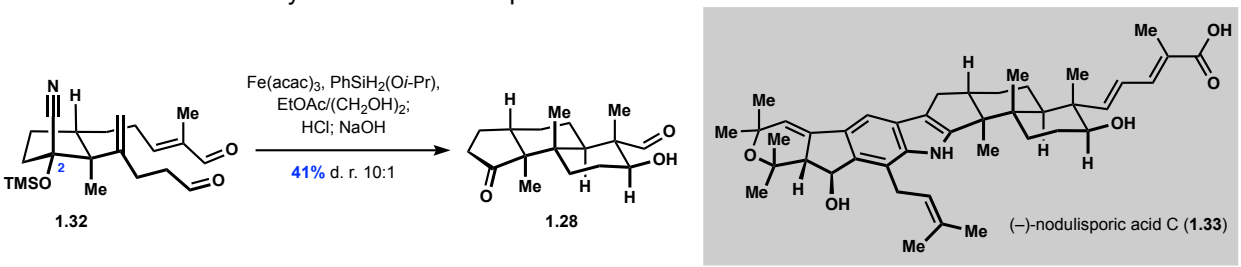

In 2015, the Liu group developed an MHAT-initiated polycyclization in their synthesis of hispidanin A (**1.36**, Scheme 1.7). Liu envisioned a polycyclization that would capitalize on similar reactivity to Baran's MHAT alkene cross-coupling, but that would intercept the putative enolate

Scheme 1.7: Liu's Synthesis of Hispidanin A

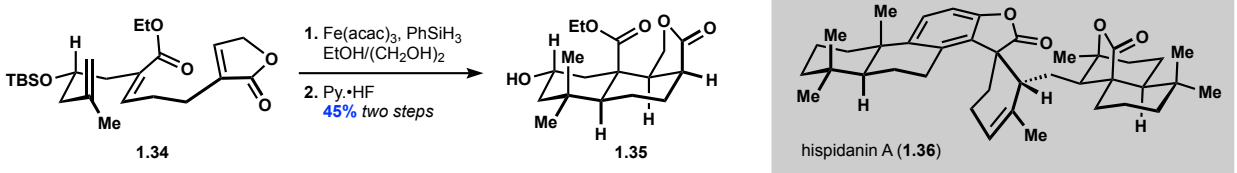

with a butenolide in a 1,4-addition to form the carbocyclic framework of the righthand portion of hispindanin A. Liu prepared polyene **1.34** and upon subjecting this material to standard conditions from Baran's initial report obtained the desired polycyclized product **1.35** following desilylation. The diastereoselectivity observed in this polycyclization can likely be attributed to the OTBS substituent that adopts a pseudoequatorial orientation in the transition state. This element of stereocontrol is ultimately removed in later synthetic manipulations.

1.3 MHAT-Initiated Annulations

It is evident that polycyclizations are powerful transformations to access polycyclic motifs, and MHAT-initiated cascades are no exception. However, there are a host of polycyclic targets that do not necessarily lend themselves to these types of disconnections, but that could be more logically disconnected by annulation transforms. Annulations are valuable because they form multiple bonds in a bimolecular fashion that often proceed in a predictable and stereocontrolled manner. The scope of annulation methodologies is immense ranging from classical reactions like the Robinson and Diels–Alder annulations to a continually growing body of modern methods.[13]

Following the development of MHAT-initiated polycyclizations the Pronin group became interested in a related annulation. This transformation was intended to couple two unsaturated carbonyl components (γ,δ-unsaturated carbonyl **1.37** and α,β-unsaturated carbonyl **1.39**) by engaging the 1,1-disubstituted alkene of **1.37** in an MHAT event, followed by Giese addition of the resulting radical **1.38** to an electron-deficient α,β -unsaturated carbonyl **1.39** and then a formal reduction and aldol event to afford carbocyclic structures such as **1.41** (Scheme 1.8). The impetus

Scheme 1.8: Proposed MHAT Initiated Annulation

for this project was the vast number of natural products that could be logically disconnected by taking advantage of this unrealized annulation (selected examples with disconnections highlighted in red, Figure 1.1). One main class of intended targets was terpenoids with high degrees of steric congestion and high levels of oxidation, structural elements that the proposed MHAT-initiated annulation was expected to accommodate well (see below). Notably, these structural elements are often limiting factors when employing canonical annulations.

Figure 1.1: Annulation Disconnections of Terpenoid Natural Products

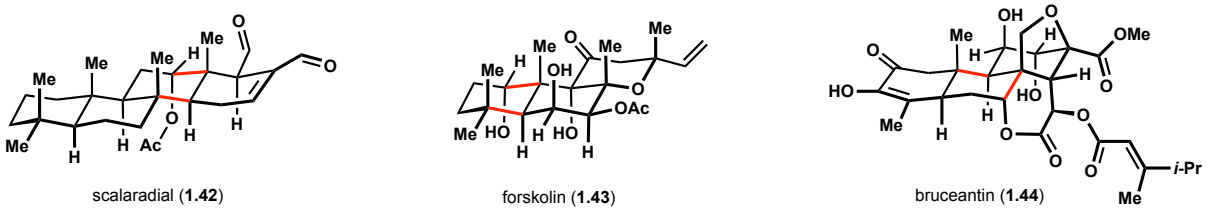

An apt comparison is between the proposed MHAT-initiated annulation and the venerable Diels–Alder annulation (Scheme 1.9). Cyclohexane motifs relevant to terpenoid natural products such as **1.41** can be disconnected along the bonds highlighted in red delivering two sets of hypothetical precurors, either a 1,3-diene **1.45** and dienophile **1.39** in the case of implementing a Diels–Alder transform or a γ,δ-unsaturated carbonyl **1.37** and α,β-unsaturated carbonyl **1.39** in the case of implementing an MHAT-initiated annulation transform. However, in the forward direction the Diels–Alder annulation requires the 1,3-diene component to adopt an s-*cis* conformation in the transition state, which imposes limitation on the degree of substitution at the termini of the 1,3-diene. This makes forming quaternary carbon centers through Diels–Alder annulations particularly

Scheme 1.9: Comparison of MHAT-Initiated Annulation and Diels–Alder Annulation

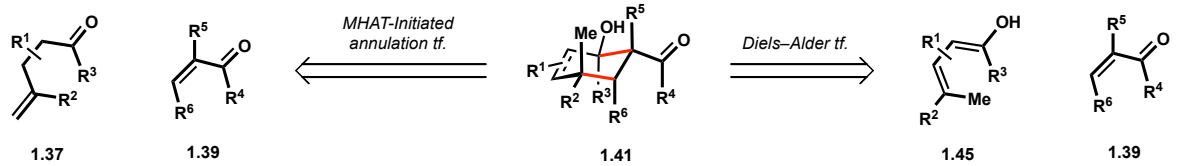

challenging.[14] Alternatively, the envisioned MHAT-initiated annulation would proceed in a stepwise manner and through radical intermediates with presumably early transition states, which should allow for the formation of far more sterically encumbered bonds. As discussed above, the value of being able to form quaternary centers via an annulation is directly relevant in the application of terpenoid total synthesis because a vast number of these natural products contain quaternary carbon motifs like those found in **1.41** as a result of their biosynthetic assembly from isoprenoid precursors. It is also worth highlighting that the proposed MHAT-initiated annulation was expected to tolerate a range of functionality due to the mild nature of precented MHAT reaction conditions, presenting an opportunity to rapidly construct densely functionalized carbon frameworks. In the context of terpenoid synthesis efficient access to highly functionalized carbon scaffolds is essential for concise syntheses. For these reasons the MHAT-initiated annulation seemed well suited for application in terpenoid total synthesis.

With these ideas in mind, my former colleagues Dr. David T. George and Dr. Devon J. Schatz and I set out to develop an MHAT-initiated annulation.[15–17] D.T.G. was the first to investigate this novel reactivity and found that upon subjecting sclareolide derived γ,δ-unsaturated aldehyde **1.46** and methacrolein (**1.47**) to Baran's conditions for alkene cross-coupling, tricycle **1.48** was produced in modest yield along with a reductive aldol product **1.49** (Scheme 1.10). This second component of the reaction mixture presumably arose from an undesired MHAT event, where instead of engaging the 1,1-disubstituted alkene the iron hydride instead engaged the electron-deficient alkene of methacrolein, and the resulting radical or corresponding enolate then participated in unproductive reactivity with starting material.[18] It is worth noting that this type of reductive aldol reactivity in related cobalt-hydride mediated MHAT processes was known at the time.[19] However, in the context of iron-hydride mediated MHAT processes this lack of

Scheme 1.10: Optimization of MHAT-Initiated Annulation

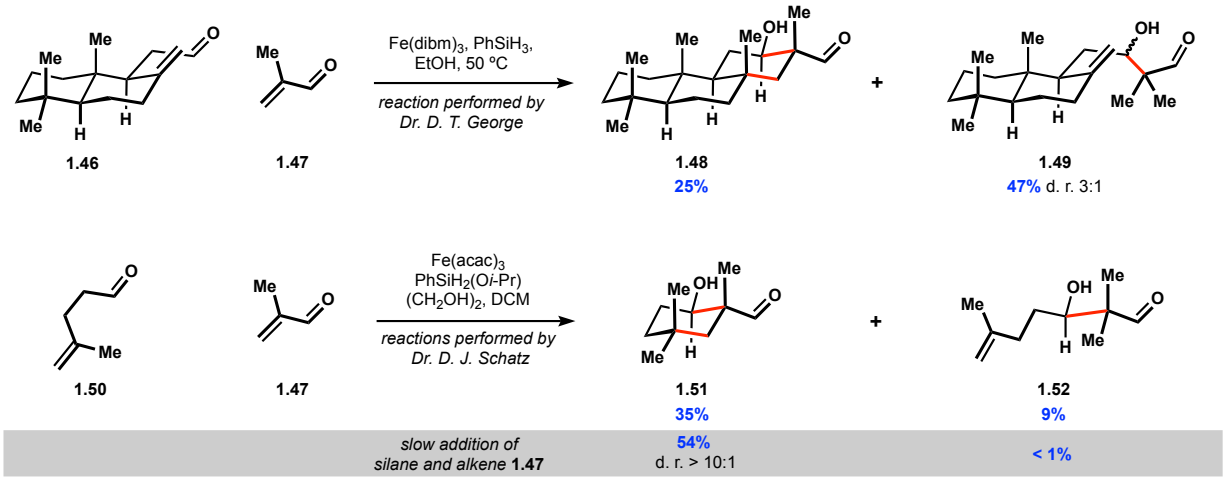

chemoselectivity was somewhat surprising considering the prior instances of apparently high levels of selectivity for electron-neutral and electron-rich alkenes in the presence of electron-deficient alkenes.[5,9–12]

To address this problem, we turned to a simpler γ,δ-unsaturated aldehyde **1.50**, which still produced reductive aldol product **1.52** in considerable yield following initial optimization efforts (Scheme 1.10). It is worth noting that in these initial optimization efforts we exchanged phenylsilane for isopropoxy(phenyl)silane, which was developed in the Shenvi laboratory for MHAT mediated hydrogenations.[20] This more hydridic silane was essential to our development of the MHAT-initiated annulation because it forms the requisite iron hydride far more readily than phenylsilane and allowed us to screen a variety of solvents and temperature regimes in our optimization efforts.[6]

Focusing back on our efforts to mitigate the undesired reductive aldol pathway, our initial attempts revolved around probing Lewis acid additives with the aim that these would coordinate to the α,β-unsaturated carbonyl lowering the electron density of the corresponding alkene and biasing MHAT to the desired 1,1-disubstituted alkene. Unfortunately a variety of Lewis acid

additives were incompatible with the reaction ($FeCl_3$, ZnI_2, $MgBr_2 \cdot OEt_2$, TMSCl, Ti(*i*-PrO)$_4$, $BF_3 \cdot OEt_2$) and although reactivity was not completely shut down with scandium derived Lewis acids ($Sc(OTf)_3$ and $Sc(dpm)_3$) the yields dropped precipitously and no significant change in the ratio of cyclized product to reductive aldol product could be determined.[21] Next we evaluated the possibility of employing a sacrificial aldehyde to capture enolates derived from undesired MHAT events to the α,β-unsaturated carbonyl. Initial attempts with added acetaldehyde did suppress production of the reductive aldol product, but yields were drastically reduced, and this strategy invariably required large excess of the α,β-unsaturated carbonyl and silane leading us to pursue alternative solutions.

Ultimately we reasoned that careful control of the relative concentrations of the α,β-unsaturated carbonyl and γ,δ-unsaturated carbonyl should allow us to statistically bias MHAT to the desired 1,1-disubstituted alkene. Putting this into practice, we developed conditions where the α,β-unsaturated carbonyl and silane were added dropwise as a solution to the reaction mixture over the course of an hour, which led to the effective concentration of the α,β-unsaturated carbonyl being far lower than that of the γ,δ-unsaturated carbonyl. This discrepancy in concentrations led to higher likelihood that the iron hydride would engage the desired γ,δ-unsaturated carbonyl in an MHAT event. The choice to also add the silane slowly was to control the stoichiometry of iron hydride being produced, as overproduction would lead to undesired reaction pathways like hydrogenation of the γ,δ-unsaturated carbonyl. Gratifyingly this strategy proved effective, as exemplified by comparison studies with the γ,δ-unsaturated aldehyde **1.50** and methacrolein **1.47** conducted by D.J.S. (Scheme 1.10).

Table 1.1: Selected Substrate Scope

reactions performed by Dr. D. J. Schatz

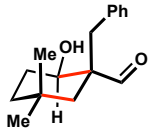

1.53
62% d. r. >10:1

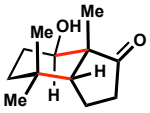

1.54
42% d. r. >10:1

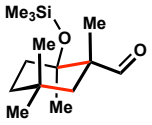

1.55
72% d. r. >10:1
two steps

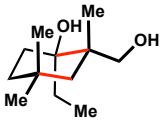

1.56
52% d. r. >10:1
two steps

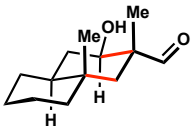

1.57
58% d. r. 5.8:1

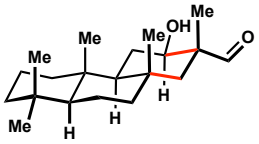

1.48
37% d. r. >10:1

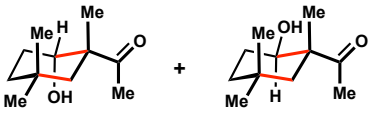

1.58 **1.59**
54% d. r. 1.2:1

D. J. S. went on to further optimize these reaction conditions and evaluate the scope of this transformation, accessing a variety of terpenoid motifs in moderate to good yields with high levels of diastereocontrol (Table 1.1).[17] The method was amenable to engaging α-substituted acroleins (**1.53**), α,β-unsaturated ketones (**1.54**, **1.58**, and **1.59**)[22,23] and remarkably γ,δ-unsaturated ketones, which led to fully substituted aldol motifs (**1.55** and **1.56** were derivatized for purification purposes) that are challenging structures to prepare by other means. Polycyclic scaffolds could also be generated including those related to scalarane sesquiterpenoids (**1.48**).[24]

Having established a set of conditions to affect this novel MHAT-initiated annulation we proceeded to test its applicability in the context of total synthesis. As discussed above, we were particularly interested in pursuing highly oxidized, sterically encumbered terpenoid natural products as we believed the annulation would be uniquely suited to construct these types of motifs. The first target we elected to prepare was the labdane diterpenoid forskolin (**1.43**, Figure 1.1).

1.4 References and Notes

1. For excellent reviews of MHAT, see: (a) Crossley, S. W. M.; Martinez, R. M.; Obradors, C.; Shenvi, R. A. Mn, Fe, and Co-catalyzed radical hydrofunctionalizations of olefins. *Chem. Rev.* **2016**, *116*, 8912. (b) Shevick, S. L.; Wilson, C. V.; Kotesova, S.; Kim, D.; Holland, P. L.; Shenvi, R. A. Catalytic hydrogen atom transfer to alkenes: a roadmap for metal hydrides and radicals. *Chem. Sci.* **2020**, *11*, 12401.
2. (a) Mukaiyama, T.; Yamada, T. Recent advances in aerobic oxygenation. *Bull. Chem. Soc. Jpn.* **1995**, *68*, 17. (b) Isayama, S.; Mukaiyama, T. A New method for preparation of alcohols from olefins with molecular oxygen and phenylsilane by the use of bis(acetylacetonato)cobalt(II). *Chem. Lett.* **1989**, *18*, 1071.
3. Ishikawa, H.; Colby, D. A.; Seto, S.; Va, P.; Tam, A.; Kakei, H.; Rayl, T. J.; Hwang, I.; Boger, D. L. Total synthesis of vinblastine, vincristine, related natural products, and key structural analogues. *J. Am. Chem. Soc.* **2009**, *131*, 4904.
4. Leggans, E. K.; Barker, T. J.; Duncan, K. K.; Boger, D. L. Iron(III)/$NaBH_4$-mediated additions to unactivated alkenes: synthesis of novel 20′-vinblastine analogues. *Org. Lett.* **2012**, *14*, 1428.
5. (a) Lo, J. C.; Yabe, Y.; Baran, P. S. A practical and catalytic reductive olefin coupling. *J. Am. Chem. Soc.* **2014**, *136*, 1304. (b) Lo, J. C.; Gui, J.; Yabe, Y.; Pan, C.-M.; Baran, P. S. Functionalized olefin cross-coupling to construct carbon–carbon bonds. *Nature* **2014**, *516*, 343. (c) Lo, J. C.; Kim, D.; Pan, C.-M.; Edwards, J. T.; Yabe, Y.; Gui, J.; Qin, T.; Gutierrez, S.; Giacoboni, J.; Smith, M. W.; Holland, P. L.; Baran, P. S. Fe-catalyzed C−C bond construction from olefins via radicals. *J. Am. Chem. Soc.* **2017**, *139*, 2484.
6. Kim, D.; Rahaman, S. M. W.; Mercado, B. Q.; Poli, R.; Holland, P. L. Roles of iron complexes in catalytic radical alkene cross-coupling: a computational and mechanistic study. *J. Am. Chem. Soc.* **2019**, *141*, 7473.
7. Jiang, H.; Lai, W.; Chen, H. Generation of carbon radical from iron-hydride/alkene: exchange-enhanced reactivity selects the reactive spin state. *ACS Catal.* **2019**, *9*, 6080.
8. In the proceeding sections and chapters putative enolate intermediates are invoked in the context of iron mediated MHAT reactions, but it should be noted that in most cases a single electron pathway has not been explicitly ruled out.
9. George, T. D.; Kuenstner, E. J.; Pronin, S. V. A Concise Approach to Paxilline Indole Diterpenes. *J. Am. Chem. Soc.* **2015**, *137*, 15410.
10. Godfrey, N. A.; Schatz, D. J.; Pronin, S. V. Twelve-step asymmetric synthesis of (−)-nodulisporic acid C. *J. Am. Chem. Soc.* **2018**, *140*, 12770.
11. For relevant discussion, see: Thomas, W. P.; Pronin, S. V. New methods and strategies in the synthesis of terpenoid natural products. *Acc. Chem. Res.* **2021**, *54*, 1347.
12. Deng, H.; Cao, W.; Liu, R.; Zhang, Y.; Liu, B. Asymmetric total synthesis of hispidanin A. *Angew. Chem. Int. Ed.* **2017**, *56*, 5849.
13. For a selection of reviews, see: (a) Jung, M. E. A review of annulation. *Tetrahedron* **1976**, *32*, 3. (b) Trost, B. M. Fünfgliedrige ringe durch [3+2]-cycloaddition mit trimethylenmethan und syntheseäquivalenten. *Angew. Chem*. **1986**, *98*, 1. (c) Posner, G. H. Multicomponent one-pot annulations forming three to six bonds. *Chem. Rev*. **1986**, *86*, 831. (d) Winkler, J. D. Tandem Diels-Alder cycloadditions in organic synthesis. *Chem. Rev*. **1996**, *96*, 167. (e) Larock, R. C. Palladium-catalyzed annulation. J. *Organomet. Chem.* **1999**, *576*, 111. (f) Molander, G. A. Diverse methods for medium ring synthesis. *Acc.*

Chem. Res. **1998**, *31*, 603. (g) Dötz, K. H.; Tomuschat, P. Annulation reactions of chromium carbene complexes: scope, selectivity and recent developments. *Chem. Soc. Rev.* **1999**, *28*, 187. (h) Rheault, T. R.; Sibi, M. P. Radical-mediated annulation reactions. *Synthesis* **2003**, *6*, 0803. (i) Mal, D.; Pahari, P. Recent advances in the Hauser annulation. *Chem. Rev.* **2007**, *107*, 1892. (j) Zai-Qun, L. An overview on the Robinson annulation. *Current Org. Chem.* **2018**, *22*, 1374. (k) Shen, X.; Thach, D. Q.; Ting, C. P.; Maimone, T. J. Annulative methods in the synthesis of complex meroterpene natural products. *Acc. Chem. Res.* **2021**, *54*, 583.

14. For selected examples of Diels−Alder annulations with highly substituted 1,3-dienes and relevant discussions, see: (a) Roush, W. R.; Limberakis, C.; Kunz, R. K.; Barda, D. A. Diastereoselective synthesis of the endo- and exo-spirotetronate subunits of the quartromicins. The first enantioselective Diels-Alder reaction of an acyclic (Z)-1,3-diene. *Org. Lett.* **2002**, *4*, 1543. (b) Du, X.; Chu, H. V.; Kwon, O. A concise synthesis of the functionalized [5−7−6] tricyclic skeleton of guanacastepene A. *Tetrahedron Lett.* **2004**, *45*, 8843. (c) Usuda, H.; Kuramochi, A.; Kanai, M.; Shibasaki, M. Challenge toward structural complexity using asymmetric catalysis: target-oriented development of catalytic enantioselective Diels-Alder reaction. *Org. Lett.* **2004**, *6*, 4387. (d) Jung, M. E.; Ho, D.; Chu, H. V. Synthesis of highly substituted cyclohexenes via mixed Lewis acid-catalyzed Diels-Alder reactions of highly substituted dienes and dienophiles. *Org. Lett.* **2005**, *7*, 1649. (e) Jung, M. E.; Guzaev, M. Trimethylaluminum-triflimide complexes for the catalysis of highly hindered Diels-Alder reactions. *Org. Lett.* **2012**, *14*, 5169. (f) Huwyler, N.; Carreira, E. M. Total synthesis and stereochemical revision of the chlorinated sesquiterpene (±)-gomerone C. *Angew. Chem., Int. Ed.* **2012**, *51*, 13066. (g) Ishihara, Y.; Mendoza, A.; Baran, P. S. Total synthesis of taxane terpenes: cyclase phase. *Tetrahedron* **2013**, *69*, 5685.
15. Thomas, W. P.; Schatz, D. J.; George, D. T.; Pronin, S. V. A radical-polar crossover annulation to access terpenoid motifs. *J. Am. Chem. Soc*. **2019**, *141*, 12246.
16. The initial optimization of this reaction was a collaborative effort between D.T.G., D.J.S. and myself (W.P.T.). To lay the foundation for discussions in subsequent chapters this section includes research and results obtained by D.T.G and D.J.S., I have made an effort to highlight these contributions in the text and schemes.
17. For a complete account of this reaction development, substrate scope, and experimental details, see: Schatz, S. J. Radical-polar crossover cyclizations in the total synthesis of paxilline indole diterpenes. Ph.D. Dissertation, University of California, Irvine, CA, 2020.
18. Interestingly, the reductive aldol product **1.49** contains a 1,1-disubstituted alkene, which should be competent at engaging in a subsequent MHAT event and Giese addition. Our observation of these 1,1-disubstituted alkenes, rather than further functionalized ones, is likely a result of a discrepancy in concentration of reductive aldol products and the starting γ,δ-unsaturated aldehyde. Where MHAT is statistically biased to the γ,δ-unsaturated aldehyde, which is in far higher concentrations until the end of the reaction.
19. (a) Isayama, S.; Mukaiyama, T. Cobalt(II) catalyzed coupling reaction of α,β-unsaturated compounds with aldehydes by the use of phenylsilane. New method for preparation of β-hydroxy nitriles, amides, and esters. *Chem. Lett.* **1989**, *18*, 2005. (b) Baik, T.-G.; Luis, A. L.; Wang, L.-C.; Krische, M. J. Diastereoselective Cobalt-Catalyzed Aldol and Michael Cycloreductions. *J. Am. Chem. Soc.* **2001**, *123*, 5112.

20. Obradors, C.; Martinez, R. M.; Shenvi, R. A. Ph(i-PrO)SiH_2: an exceptional reductant for metal-catalyzed hydrogen atom transfers. *J. Am. Chem. Soc.* **2016**, *138*, 4962.
21. In retrospect Lewis-acid additives may still be a fruitful area of inquiry considering reports by the Baran group using boron based Lewis acids in MHAT reactions (ref. 5c and 18b), reports from Bradshaw regarding benefits of added $Fe(acac)_2$ to MHAT reactions (ref. 18c), and studies from Overman regarding lanthanide based Lewis-acids effect on photochemical initiated Giese reactions (ref. 18d). Notably, this avenue of investigation would be a logical entry to an asymmetric variant of the MHAT initated annulation if a competent chiral Lewis-acid were to be identified. For references discussed, see: (a) ref. 5c (b) Dao, H. T.; Li, C.; Michaudel, Q.; Maxwell, B. D.; Baran P. S. Hydromethylation of unactivated olefins. *J. Am. Chem. Soc.* **2015**, *137*, 25, 8046. (c) Saladrigas, M.; Puig, J.; Bonjoch, J.; Bradshaw, B. Iron-catalyzed radical intermolecular addition of unbiased alkenes to aldehyde. *Org. Lett.* **2020**, *22*, 8111. (d) Pitre, S. P.; Allred, T. K.; Overman, L. E. Lewis acid activation of fragment-coupling reactions of tertiary carbon radicals promoted by visible-light irradiation of EDA complexes. *Org. Lett.* **2021**, *23*, 1103.
22. Hydroxyketone **1.54** was previously prepared in seven and eight steps from α-cyclocitral, see: Fernández-Mateos, A.; Coca, G. P.; González, R. R.; Hernández, C. T. Synthesis of a CDE fragment of the insect antifeedant 12-hydroxyazadiradione. *J. Org. Chem.* **1996**, *61*, 9097.
23. The poor diastereoselectivity in formation of annulation products **1.58** and **1.59** may reflect the ratio of *E*- and *Z*-enolates produced under the reaction conditions.
24. Kamel, H. N.; Kim, Y. B.; Rimoldi, J. M.; Fronczek, F. R.; Ferreira, D.; Slattery, M. Scalarane sesterterpenoids: semisynthesis and biological activity. *J. Nat. Prod.* **2009**, *72*, 1492.

Chapter 2: A Review of Forskolin

2.1 Forskolin

2.1.1 Forskolin Biosynthesis

Forskolin (**2.6**) is a member of the labdane diterpenoid family of natural products (Scheme 2.1).[1] Biosynthetically, labdane diterpenoids arise from the assembly of four isoprene units, specifically dimethyl allyl diphosphate (**2.1**) and isopentyl diphosphate (**2.2**) which form geranylgeranyl diphosphate (**2.3**). This polyene can then undergo a number of different enzyme catalyzed polycyclizations to generate the labdane diterpene carbon core with varying stereochemical outcomes at C5, C10, C9, C8. In the case of forskolin, the polycyclization produces 8-hydroxy-copalyl diphosphate (**2.4**), which further cyclizes to 13*R*-manoyl oxide (**2.5**). This tricyclic scaffold is then extensively oxidized by a series of cytochrome P450 enzymes to ultimately afford the natural product forskolin (**2.6**, A-, B-, C-rings have been labeled for subsequent discussion).[1b]

Scheme 2.1: Biosynthesis of Forskolin

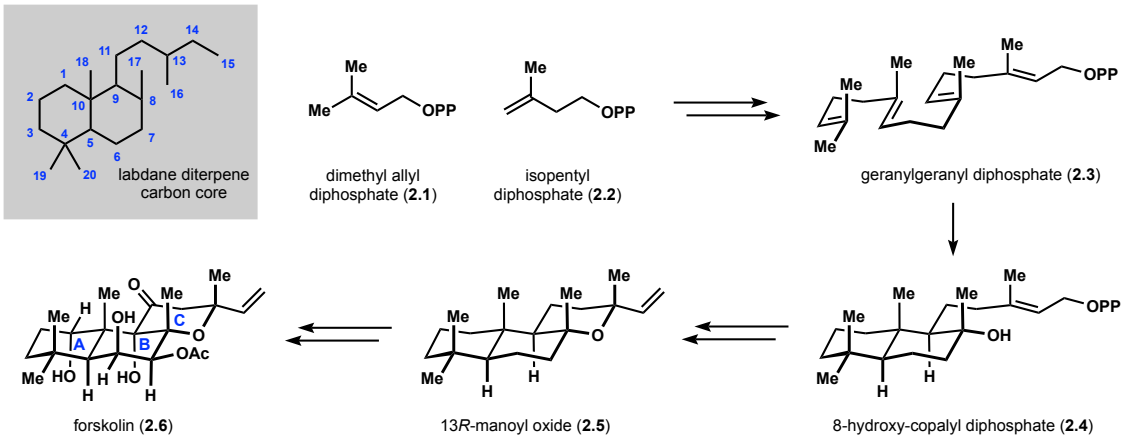

2.1.2 Forskolin Bioactivity

Forskolin was isolated from the root extracts of *Coleus forskohlii* in 1977 by de Souza and co-workers within the context of a broader campaign by Hoechst

Pharmaceuticals to identify drug leads from medicinal plants native to India.[2–4] In this initial report the authors noted that forskolin possesses "interesting blood pressure lowering and cardioactive properties".[2] These observations sparked interest in the potential therapeutic value of forskolin and efforts were undertaken to further understand the mechanism of action. Ultimately, Seamon and Daly identified the primary role of forskolin as an activator of adenylyl cyclase (AC), leading to a rise in the intracellular levels of cyclic adenosine monophosphate (cAMP).[5] Importantly, this modulation of AC activity occurred reversibly *and* in intact cells. Specifically, the researchers found that forskolin (EC_{50}, 25 μM) led to a 35-fold increase in cAMP levels in tissue slices from rat cerebral cortical. This seminal report garnered substantial interest from the scientific community due to the important and ubiquitous role of cAMP as a secondary signaling molecule in numerous biological pathways and its implications in a variety of diseases.[6]

Following these findings and due to its relative abundance (isolated in 0.1% w/w from the dried roots of *C. forskohlii*), forskolin was widely adopted by the biological community as a means to modulate intracellular levels of cAMP.[7] Further studies aimed at probing the mechanism of action of this secondary metabolite culminated in a crystal structure of forskolin bound to a catalytically active AC.[8] Forskolin was found to bind at an allosteric site between the two cytosolic catalytic subunits, C1 and C2, strengthening the bonding interactions between these domains that must associate in the active form of the enzyme. Notably, this represented a novel mode of AC activation.

Currently, forskolin is still an indispensable biological tool for modulating levels of cAMP; however, it lacks selectivity between the nine different membrane-bound isoforms of class III ACs, those relevant to mammals, with the exception of isoform AC9,

which is activated to a lesser extent.[9] These isoforms are united in their function of converting ATP to cAMP, but differ in how they are endogenously activated/inhibited, what tissues they are found in, and the biological pathways they regulate. This lack of isoform selectivity can be beneficial, as it allows for activation of ACs in a variety of cell types. On the other hand, this indiscriminate activation presents a challenge for developing therapeutics and more precise biological tools.[10]

With the intent to develop isoform-selective AC activators and to further understand the biological activity of forskolin, a number of structure-activity relationship (SAR) studies were conducted.[11] These efforts showed that modification of C1, C9, C11, or C13 resulted in a loss of activity (Figure 2.1). However, alterations at C6 and C7 were tolerated, in line with the open pocket observed around these carbons in the crystal structure of forskolin bound to an AC.[8] These SAR studies led to several analogs that were moderately isoform-selective with the most impactful entry being an AC5 selective analog NKH477 (**2.7**), which ultimately became an approved therapeutic in Japan to treat acute heart failure.[12]

Figure 2.1: Forskolin and NKH477

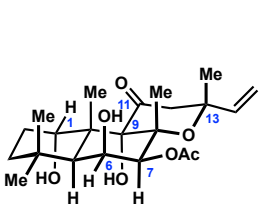

forskolin (**2.6**)

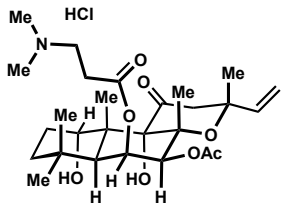

NKH477 (**2.7**)

The wealth of knowledge gained by the biological and medicinal chemistry communities highlighted the utility of forskolin as a biological tool and importantly the value of analogs as therapeutics, which logically led to the desire for fully synthetic routes to this secondary metabolite.

2.2 Prior Syntheses of Forskolin

2.2.1 Ziegler

In 1987 Ziegler and co-workers reported the first total synthesis of racemic forskolin.[13,14] Their strategy relied on initial construction of the A- and B-rings via an intramolecular Diels–Alder cycloaddition and late-stage installation of the C-ring via an oxa-Michael reaction. Starting from citral the group prepared enal **2.8** in four steps (Scheme 2.2). Olefination and acylation with fumarate derivate **2.9** afforded the Diels–Alder precursor **2.10**, which underwent the desired cyclization at elevated temperatures. Following anti-Markovnikov oxidation of the alkene to ketone **2.12**, Ziegler found that epimerization of the lactone was necessary in order to avoid generating the α,β-unsaturated lactone during decarboxylation with $Pb(OAc)_4$. The group then performed a series of redox

Scheme 2.2: Ziegler's Synthesis of Forskolin

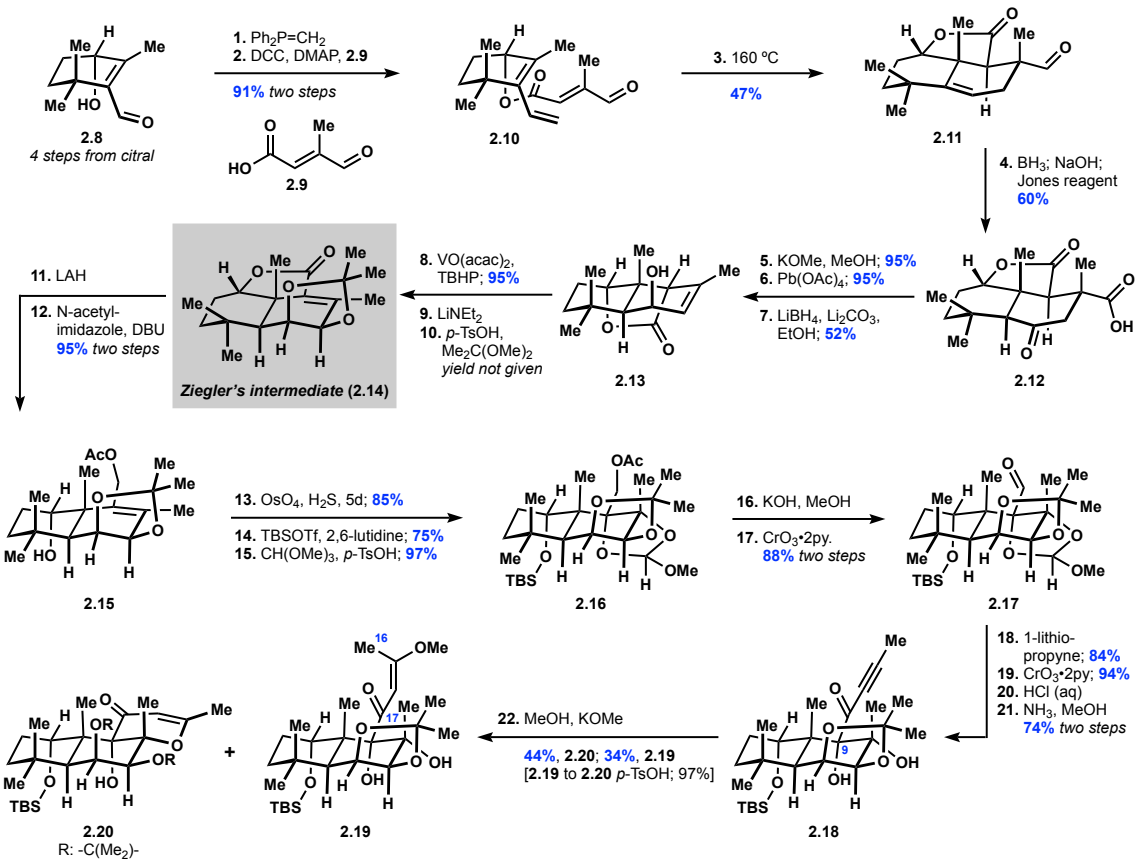

manipulations, ultimately arriving at advanced intermediate **2.18**, which contains the desired oxidation pattern on the A- and B-rings.

The Ziegler group then turned their attention to the C-ring, which they envisioned constructing through an intramolecular oxa-Michael reaction. To investigate this route, they subjected ynone **2.18** to Cs_2CO_3. This exclusively led to the corresponding spiro furanone, resulting from engaging the undesired tertiary alcohol at C9 in the cyclization event. The group postulated that the desired cyclization would be more favorable via a β-alkoxy enone (6-*endo*-trig) rather than with the ynone (6-*endo*-dig). Indeed, subjecting ynone **2.18** to methanolic KOMe afforded the desired dihydro-γ-pyrone **2.20** in 44% yield along with β-methoxy enone **2.19**, which was stable to the reaction conditions, but could be converted to the cyclized dihydro-γ-pyrone **2.20** by treatment with tosic acid. The authors proposed that there is a 1,3-diaxial interaction between the C16 and C17 methyl groups of **2.19** in the transition state of the oxa-Michael addition that prevents this isomer from undergoing cyclization, while the Z-isomer experiences a less demanding 1,3-diaxial interaction between the C17 methyl and methoxy group resulting in the desired dihydro-γ-pyrone **2.20**.

In their initial report Ziegler and co-workers appended the final two carbons, C14 and C15, via an interesting sequence involving a [2+2] cycloaddition with allene (Scheme 2.3).[13b] Notably, straightforward installation of this two-carbon unit by 1,4-addition of a vinyl cuprate into an analogous dihydro-γ-pyrone had been thwarted in efforts by Saksena, which discouraged Ziegler from pursuing this seemingly logical approach.[13c,15]

Scheme 2.3: Ziegler's First Generation C14, C15 Installation

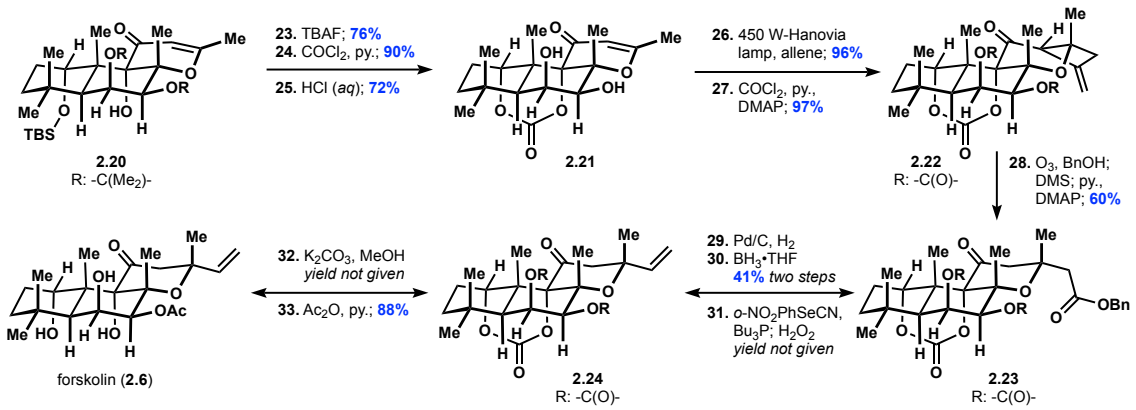

Shortly after this publication however, Lett and co-workers demonstrated that treatment of a dihydro-γ-pyrone analogous to **2.20** (see below) with $(CH_2{=}CH)_2Cu(CN)Li_2$ in the presence of $BF_3{\cdot}OEt_2$ accomplished the desired 1,4-addition.[16] In light of these findings, Ziegler demonstrated that subjecting dihydro-γ-pyrone **2.20** to $BF_3{\cdot}OEt_2$ (20 eq) and $(CH_2{=}CH)_2Cu(CN)Li_2$ (10 eq) afforded the desired tetrahydro-γ-pyrone **2.25** in 54% yield along with the undesired C13 epimer in 6% yield (Scheme 2.4).[13c] Interestingly, following desilylation with TBAF, deprotection of the acetonide under acidic conditions afforded an intractable mixture of products. Empirically, Ziegler found that protecting the 1,3-diol as a carbonate allowed for facile deprotection of the acetonide. Finally, saponification of the carbonate and acylation, reported by de Souza, completed the total synthesis.[2b]

Scheme 2.4: Ziegler's Second Generation C14, C15 Installation

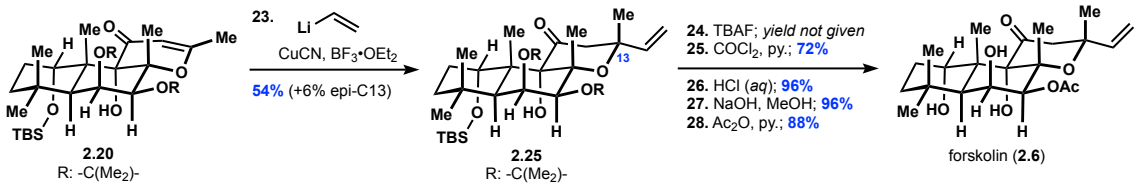

Several aspects of this seminal publication by Ziegler are worth further comment. Notably, lactone **2.14** (commonly referred to as "Ziegler's intermediate") became a key

sub-target in several subsequent syntheses and the focus of numerous formal syntheses of forskolin.[17,18] Furthermore, disconnection of the C-ring via an oxa-Michael transform has proven to be a powerful strategy, implemented successfully by several groups including our own group. Finally, the deprotection of C6/C7 acetonide became a recurring challenge in syntheses of forskolin and Ziegler's serendipitous discovery that a C1/C9 cyclic carbonate allowed for efficient deprotection of this acetonide proved to be a useful solution to the problem.

2.2.2 Ikegami

Shortly after Ziegler's publication the Ikegami and Corey groups reported independent total syntheses of forskolin, published consecutively in the same issue of *JACS*.[19,20] Both notably targeted Ziegler's intermediate **2.14**, but reported novel preparations of this key sub-target and applied unique strategies to forge the C-ring.

The Ikegami group commenced their synthesis with the preparation of butenolide **2.26** from 2,2-dimethylglutarate (Scheme 2.5). This set the stage for construction of the A- and B-ring via a tandem alkene isomerization, intramolecular Diels–Alder cycloaddition favoring the *exo*-product **2.30**. Subsequent dihydroxylation of the resulting alkene from the less hindered face delivered the undesired stereochemistry at C6 and C7. Inversion was accomplished by a Parikh-Doering oxidation, which was accompanied by a [2,3]-sigmatropic rearrangement, followed by reduction of the methoxy group with sodium hydrogen telluride, and borane reduction to the desired diol **2.33**. In order to reach Ziegler's intermediate **2.14**, protection, sulfoxide elimination, and isomerization were executed.

With a route to Ziegler's intermediate **2.14**, the grouped turned their attention to constructing the C-ring. In a similar fashion to Ziegler, the lactone was reduced to the diol

Scheme 2.5: Ikegami's Synthesis of Forskolin

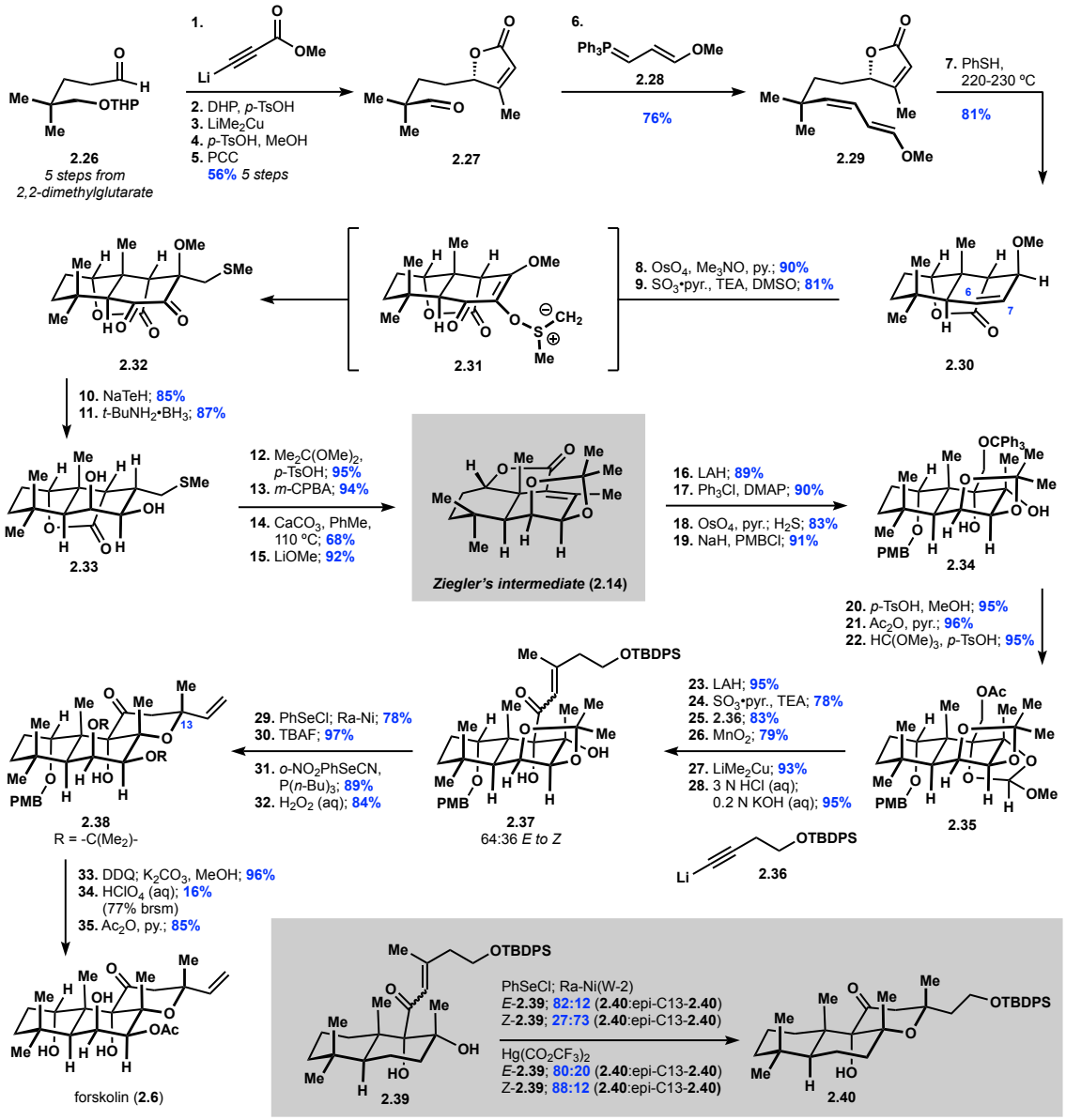

and protected, followed by dihydroxylation of the tetrasubstituted alkene to the corresponding diol **2.34**, which was protected as orthoformate **2.35**. Next, installation of an appropriate five-carbon unit to forge the C-ring was accomplished in six steps providing enone **2.37** as a 64:36 mixture of *E*- and *Z*-alkene isomers. Oxy-selenation of the enones followed by a reductive workup impressively afforded the tetrahydro-γ-pyrone **2.38** with the desired C13 stereochemistry in 78% yield and the undesired C13 epimer in 6% yield.

Subjecting both *E*- and *Z*-alkene isomers separately to the reaction conditions demonstrated insignificant dependence on alkene geometry in forming the desired C13 stereocenter (79%:5% from *E*-**2.37**; 80%:6% from *Z*-**2.37**). The authors attribute the inconsequential nature of the alkene geometry to the intermediacy of a tertiary carbocation long-lived enough to allow for free rotation about the C12–C13 bond. They proposed this carbocation is ultimately trapped via a chair-like transition state placing the less sterically demanding C16 methyl group in a pseudoaxial orientation. Interestingly, the authors note that these findings contrast with model studies they had conducted earlier, where the stereochemical outcome at C13 was highly dependent on alkene geometry of the enone when the cyclization was mediated by PhSeCl, but not when mediated by $Hg(CO_2CF_3)_2$ (Scheme 2.5, see inset).[19b] The authors invoke a similar rationale for the stereochemical outcome of the oxy-mercuration to the one discussed above.

Nevertheless, having successfully constructed the C-ring the Ikegami group oxidatively cleaved the PMB protected alcohol at C1, intercepting a late-stage intermediate in Ziegler's synthesis (Scheme 2.4). At this point the researchers were faced with the challenging deprotection of the C6/C7 acetonide. However, rather than opting for the multistep sequence developed by Ziegler, Ikegami found the acetonide could be hydrolyzed in the presence of aqueous perchloric acid albeit in low conversion. A final acylation delivered forskolin.

2.2.3 Corey

The Corey group's approach to forskolin started from α-ionone and again targeted Ziegler's intermediate **2.14**.[20] The general strategy to this sub-target, reminiscent of Ziegler's approach, relied on an intramolecular Diels–Alder cycloaddition followed by

Scheme 2.6: Corey's Synthesis of Forskolin

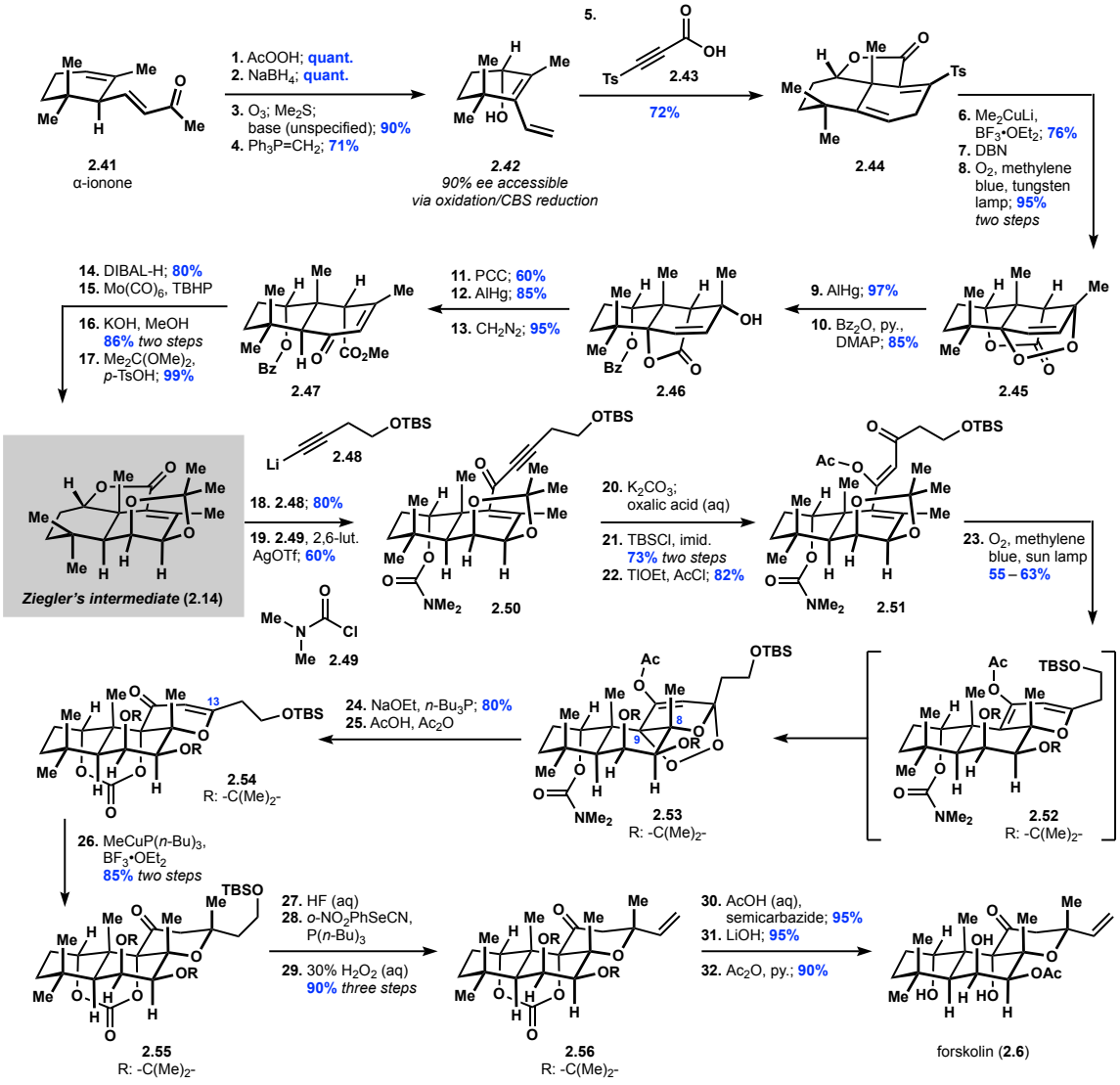

several redox manipulations (Scheme 2.6). Importantly, alcohol **2.42** could be obtained in enantioenriched form via an oxidation/reduction sequence using the Corey–Bakshi–Shibata reduction protocol, rendering this the first asymmetric approach to forskolin. After preparing Ziegler's intermediate **2.14**, the researchers focused on constructing the C-ring. The Corey group accomplished this by accessing β-acetoxy enone **2.51** and then leveraged a clever tandem 6π-photocyclization, [4+2]-cycloaddition to afford endoperoxide **2.53**.

Notably, this sequence set both C8 and C9 stereocenters, and following a reduction and protection provided dihydro-γ-pyrone **2.54**.

At this stage, the researchers aimed to set the C13 stereocenter in a similar manner to prior approaches through 1,4-addition of an organometallic reagent into the dihydro-γ-pyrone. However, Corey opted to install the C16 methyl rather than the C14, C15 vinyl substituent as prior groups had done. This would require the opposite facial selectivity from the reported 1,4-additions reported by Lett and Ziegler.[13,16]

Scheme 2.7: Lett's Studies on 1,4-Additions

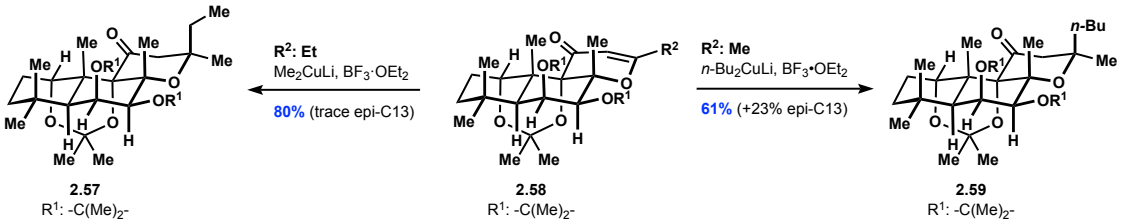

2.57 R1: -C(Me)2-

2.58 R1: -C(Me)2-

2.59 R1: -C(Me)2-

Several aspects surrounding the use of 1,4-additions to set the C13 stereocenter are worth further comment as it is a key disconnection in most syntheses of forskolin. It is important to note that the desired stereochemical outcome envisioned by the Corey group would presumably proceed through a chair-like transition state, but from the more sterically encumbered β-face of the dihydro-γ-pyrone, while Lett and Ziegler's observed 1,4-addition from the less sterically encumbered α-face of the dihydro-γ-pyrone, but likely involved a twist-boat transition state. Complicating the scenario further, Lett observed varying facial selectivity apparently depending on the type of cuprate employed as a nucleophile.[16] Methyl and vinyl cuprates led to addition from the α-face while *n*-butyl cuprate led to β-face selectivity (Scheme 2.7). The origins of this divergence in stereochemical outcome are not clear, leading Lett to conclude that caution should be taken in generalizing these stereochemical results to any related systems.[16]

Quite fortunately for the Corey group, the addition of an organocopper species derived from $MeCuPBu_3$ and $BF_3 \cdot Et_2O$ led to diastereoselective formation of tetrahydro-γ-pyrone **2.55**. The authors do not comment on optimization efforts or origins of this selectivity. Following 1,4-addition and having installed all the necessary carbons, Corey performed a Grieco elimination analogously to Ikegami, intercepting an advanced intermediate in Ziegler's route, **2.56**, which Corey converted to forskolin in a similar manner.

2.2.4 Lett

The Lett group was heavily involved in synthetic research regarding forskolin, reporting their highly impactful studies on cuprate additions in 1987 and ultimately publishing a total synthesis of forskolin in 1996.[16,21] Their general synthetic plan was similar to previous efforts: establish the A-, B-ring system and then append the C-ring. Lett and co-workers commenced their synthesis by elaborating 1,3-dicarbonyl **2.60** to diene **2.42**, the same diene used by Ziegler and Corey, which they could also prepare enantioselectively with a CBS reduction (Scheme 2.8). The researchers then executed a Diels–Alder cycloaddition akin to that performed by Ziegler and Corey. From here a series of redox and functional group manipulations were performed to ultimately arrive at allylic carbamate **2.67**. At this point Lett was able to epoxidize the trisubstituted alkene from the less sterically encumbered face of the decalin core with *m*-CPBA, followed by carbamate assisted opening to diol **2.68**. Acetate (**2.67**, R=Ac) or carbonate (**2.63**, R=C(O)OMe) precursors returned only starting material. This stereochemical relay allowed Lett to establish the appropriate oxidation pattern for the A- and B-rings.

Scheme 2.8: Lett's Synthesis of Forskolin

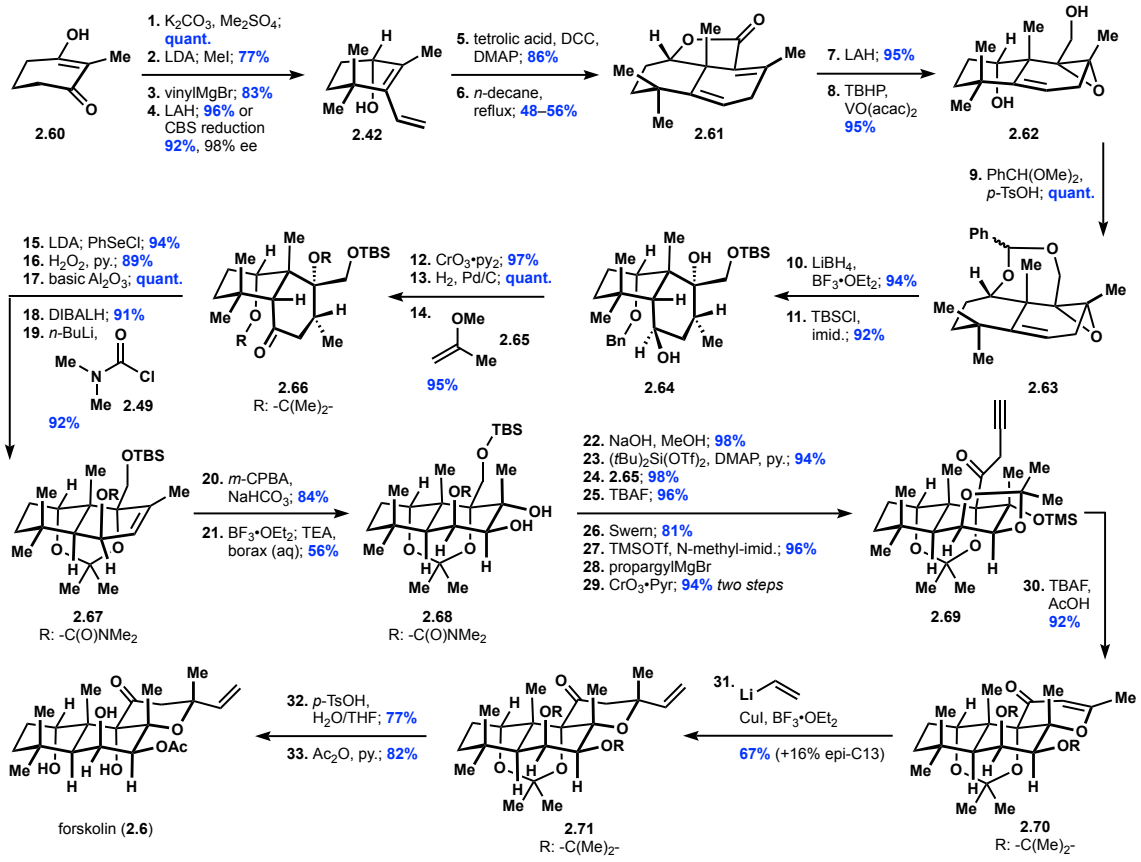

Next the Lett group turned their attention to the C-ring which they envisioned preparing through an oxa-Michael reaction analogously to Ziegler. Their initial attempts to construct an ynone and effect a base mediated *6-endo*-dig cyclization led to a mixture of products, the major being the result of a *5-exo*-dig cyclization. In light of these findings the group prepared propargyl ketone **2.69** to avoid the undesired 5-*exo*-dig pathway. This allowed the group to efficiently access dihydro-γ-pyrone **2.70**. From here, guided by their earlier studies, the Lett group performed a diastereoselective 1,4-addition of a vinyl cuprate to install the final two-carbon unit of forskolin. Like many groups before, Lett was then faced with the challenge of deprotecting the notorious C6/C7 acetonide. Notably, the group found that simply treating the acetonide with tosic acid in aqueous THF led to efficient

formation of deacetyl forskolin although this reaction did require 12 days to reach completion. Finally, an acylation delivered the natural product forskolin.

2.2.5 Švenda

In 2017, Švenda and co-workers reported a 24-step synthesis of racemic forskolin.[22] Their strategy relied on initial construction of the A- and B-rings in the form of an enedione such as **2.72** (Scheme 2.9). The most logical disconnection of this sub-target would be a Diels–Alder transform to the corresponding diene **2.73** and dienophile **2.74**. Unfortunately, Sih had identified this sub-target several decades prior and found that the desired Diels–Alder reaction does not proceed, likely due to the $A^{1,3}$ strain that would be incurred by the 1,3-diene component when adopting the requisite s-*cis* conformation.[23] Several years later, the Kienzle group reported a total synthesis of a related labdane diterpenoid, erigerol, wherein they developed a multistep sequence to arrive at enediones like **2.72**.[24,25] This protocol was leveraged by the Švenda group in their synthesis of forskolin. It also must be highlighted that the utility of Kienzle's findings in pursuit of erigerol went beyond establishing a route to enediones **2.72** and were instrumental in the success of both Švenda's and our own syntheses of forskolin.

Scheme 2.9: Sih's Attempted Diels–Alder Annulation

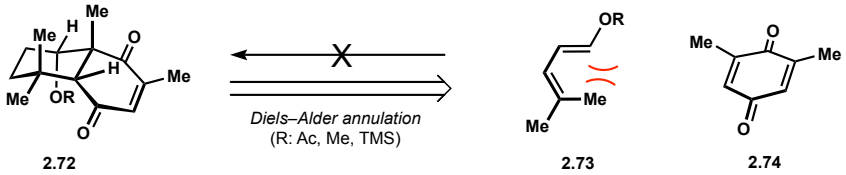

2.72 **2.73** **2.74**

The Švenda lab commenced their synthesis of forskolin following the prior work of Kienzle with preparation of cyclopropyl enedione **2.78** (Scheme 2.10). Then, through a series of redox and functional group manipulations, cyclopropyl enedione **2.78** was

Scheme 2.10: Švenda's Synthesis of Forskolin

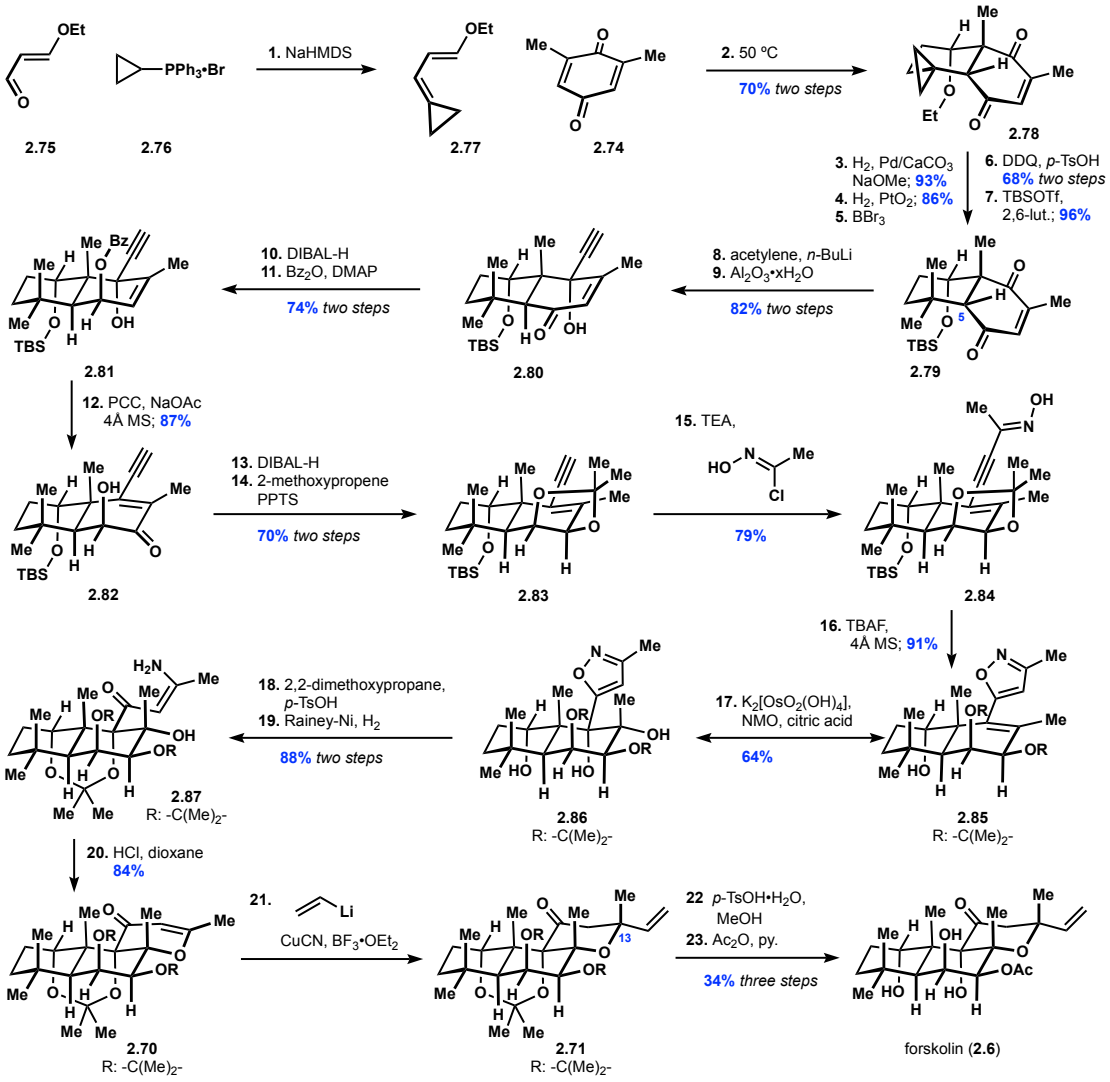

converted to enedione **2.79**. Švenda then adapted a three-step sequence from Kienzle to introduce an acetylene fragment, epimerize C5 and diastereoselectively reduce the enone to an allylic alcohol, which they protected to deliver benzyl ester **2.81**.

At this stage in the synthesis Švenda deviated from Kienzle's previous work and performed a PCC oxidation with allylic transposition to deliver enone **2.82**. A 1,2-reduction and protection as the acetonide secured C6 and C7 in the proper oxidation states. Then, in a stepwise manner, Švenda installed a masked β-amino enone in the form of an isoxazole,

for subsequent installation of the C-ring. Dihydroxylation of the tetrasubstituted alkene proved to be challenging despite precedent in previous syntheses of forskolin, but the group found that three cycles of modified Upjohn conditions provided the desired diol **2.86** in reasonable yield, which was subsequently protected as the acetonide.

Turning their attention to formation of the C-ring, the researchers reductively opened the isoxazole with Rainey-Ni to reveal the β-amino enone, which was then converted to dihydro-γ-pyrone **2.70** in the presence of acid, leveraging similar oxa-Michael reactivity as previous synthetic efforts. Having intercepted the same dihydro-γ-pyrone **2.70** as Lett, Švenda completed the synthesis of forskolin by adapting a three-step protocol reported by the Lett group.

2.3 References and Notes

1. (a) Peters, R. J. Two rings in them all: the labdane-related diterpenoids. *Nat. Prod. Rep.* **2010**, *27*, 1521. (b) Pateraki, I.; et al. Total biosynthesis of the cyclic AMP booster forskolin from Coleus forskohlii. *Elife*. **2017**, *6*, e23001. doi: 10.7554/eLife.23001.001
2. (a) Bhat, S. V.; Bajwa, B. S.; Dornauer, H.; de Souza, N. J.; Fehlhaber, H.-W. Structures and stereochemistry of new labdane diterpenoids from Coleus forskohlii briq. *Tetrahedron Lett.* **1977**, *18*, 1669. (b) Bhat, S. V.; Bajwa, B. S.; Dornauer, H.; de Souza, N. J. Reactions of forskolin, a biologically active diterpenoid from Coleus forskohlii. *J. Chem. Soc., Perkin Trans. 1* **1982**, 767.
3. Tandon and coworkers (ref. 2a), independently from de Souza (ref. 1), isolated an apparent C7 epimer of forskolin from *C. forskohlii*, which they named coleonol. This assignment was later proven incorrect and that in fact coleonol and forskolin were the same compound leading to some confusion in the nomenclature used throughout early literature on forskolin: (a) Tandon, J.; Dhar, M.; Ramakumar, S.; Venkatesan, K. Structure of coleonol, a biologically active diterpene from Coleus forskohlii. *Indian J. Chem.* **1977**, *15*, 880. (b) Saksena, A.K.; Green, M.J.; Shue, H.-J.; Wong, J.K.; Mc Phail, A.T. Identity of coleonol with forskolin: structure revision of a base-catalyzed rearrangement product. *Tetrahedron Lett.* **1985**, *26*, 551.
4. Colombo, M. I.; Zinczuk, J.; Ruveda, E. A. Synthetic routes to forskolin. *Tetrahedron* **1992**, *48*, 963.
5. (a) Seamon, K. B.; Padgett, W.; Daly, J. W. Forskolin: unique diterpene activator of adenylate cyclase in membranes and in intact cells. *Proc. Natl. Acad. Sci. U. S. A.* **1981**, *78*, 3363. (b) Dessauer, C. W.; Scully, T. T.; Gilman, A. G. Interactions of forskolin and ATP with the cytosolic domains of mammalian adenylyl cyclase. *J. Biol. Chem.* **1997**, *272*, 22272.
6. (a) Sapio, L.; Gallo, M.; Illiano, M.; Chiosi, E.; Naviglio, D.; Spina, A.; Naviglio, S. The natural cAMP elevating compound forskolin in cancer therapy: is it time? *J. Cell Physiol.* **2016**, *232*, 922. (b) Sassone-Corsi, P. The Cyclic AMP Pathway *Cold Spring Harb. Perspect. Biol.* **2012**, *4*, a011148. doi: 10.1101/cshperspect.a011148. (c) Pierre, S.; Eshcenhagen, T.; Geisslinger, G.; Scholich, K. Capturing adenylyl cyclases as potential drug targets. *Nature Reviews Drug Discovery* **2009**, *8*, 321.
7. Insel, P. A.; Ostrom, R. S. Forskolin as a tool for examining adenylyl cyclase expression, regulation, and G protein signaling. *Cell. Mol. Neurobiol.* **2003**, *23*, 305.
8. (a) Tesmer, J. J. G.; Sunahara, R. K.; Gilman, A. G.; Sprang, S. R. Crystal Structure of the Catalytic Domains of Adenylyl Cyclase in a Complex with $G_{s\alpha}$•$GTP_{\gamma}S$. *Science* **1997**, *278*, 1907. (b) see ref. 5b
9. Qi, C.; Sorrentino, S.; Medalia, O.; Korkhav, V. M. The structure of a membrane adenylyl cyclase bound to an activated stimulatory G protein. *Sciecne* **2019**, *364*, 389.
10. For relevant considerations in modulating cAMP pathways: Sengupta, S.; Mehta, G. Natural products as modulators of the cyclic-AMP pathway: evaluation and synthesis of lead compounds. *Org. Biomol. Chem.* **2018**, *16*, 6372.

11. (a) Seamon, K.; Daly, J. W.; Metzger, H.; De Souza, N. J.; Reden, J. Structure-activity relationships for activation of adenylate cyclase by the diterpene forskolin and its derivatives. *J. Med. Chem.* **1983**, *26*, 436. (b) Robbins, J. D.; Boring, D. L.; Tang, W.-J.; Shank, R.; Seamon, K. Forskolin Carbamates: Binding and Activation Studies with Type I Adenylyl Cyclase. *J. Med. Chem.* **1996**, *39*, 2745 (c) Onda, T.; Hashimoto, Y.; Nagai, M.; Kuramochi, H.; Saito, S.; Yamazaki, H.; Toya, Y.; Sakai, I.; Homey, C. J.; Nishikawa, K. ; Ishikawa, Y. Type-specific regulation of adenylyl cyclase. *J. Biol.Chem.* **2001**, *276*, 47785. (d) Pinto, C.; Papa, D.; Hübner, M.; Mou, T.-C.; Lushington, G. H.; Seifert, R. Activation and inhibition of adenylyl cyclase isoforms by forskolin analogs. *J. Pharmacol. Exp. Ther*. **2008**, *325*, 27. (e) Egger, M.; Maity, P.; Hübner, M.; Siefert, R.; König, B. Synthesis and pharmacological properties of new tetracyclic forskolin analogues. *Euro. J. Org. Chem.* **2009**, *21*, 3613.
12. (a) Hosono, M.; Takahira, T.; Fujita, A.; Fujihara, R.; Ishijuka, O.; Tatee, T.; Nakamura, K. Cardiovascular and adenylate cyclase stimulant properties of NKH477, a novel water-soluble forskolin derivative. *J. Cardiovasc. Pharmacol.* **1992**, *19*, 625. (b) Hosoda, S.; Motomiya, T.; Katagiri, T.; Takano, T.; Sasayama, S.; Toshima, H.; Ogawa, N. Acute effect of NHK477, a novel forskolin derivative, in patients with acute heart failure. *Jpn. J. Clin. Pharmacol. Ther*. **1997**, *28*, 583.(c) Toya, Y.; Schwencke, C.; Ishikawa, Y. Forskolin Derivatives with Increased Selectivity for Cardiac Adenylyl Cyclase. *J. Mol. Cell. Cardiol.* **1998**, *30*, 97.
13. (a) Ziegler, F. E.; Jaynes, B. H.; Saindane, M. T. A synthetic route to forskolin. *J. Am. Chem. Soc.* **1987**, *109*, 8115. (b) Ziegler, F. E.; Jaynes, B. H. Reconstruction of forskolin from a ring C dihydropyran-4-one degradation product thereof. *Tetrahedron Lett.* **1987**, *28*, 2339. (c) Ziegler, F. E.; Jaynes, B. H. Formation of (±)-forskolin via a cuprate addition to a synthetic dihydropyran-4-one. *Tetrahedron Lett.* **1988**, *29*, 2031.
14. It should be noted that the intermediate diene resulting from olefination of **2.8** was later prepared asymmetrically (ref. 19 and ref. 20), rendering Ziegler's racemic route enantioselective.
15. Saksena, A. K.; Green, M. J.; Shue, H.-J.; Wong, J. K. Forskolin: a convenient degradation to 14,15-dinor-8-13,epoxy-1α,5β,7β,9α-tetrahydroxylabd-12-en-11-one 7-acetate 1,9-carbonate via β-elimination of a aldoxime. *J. Chem. Soc., Chem. Commun.* **1985**, 1748.
16. Delpech, B.; Lett, R. Retrosynthetic studies with forskolin. *Tetrahedron Lett.* **1987**, *28*, 4061.
17. For a representative selection of formal syntheses intercepting Ziegler's intermediate see: (a) Venkataraman, H.; Cha, J. K. A Formal synthesis of forskolin: an electrocyclization approach. *J. Org. Chem.* **1989**, *54*, 2505. (b) Kanematsu, K.; Nagashima, S. An efficient synthesis of a key intermediate of forskolin. *J. Chem. Soc., Chem. Commun.* **1989**, 1028. (c) Begley, M. J.; Cheshire, D. R.; Harrison, T.; Hutchinson, J. H.; Myers, P. L.; Pattenden, G. A new synthetic route to (±)-forskolin. *Tetrahedron* **1989**, *45*, 5215. (d) Colombo, M. I.; Zinczuk, J.; Bacigaluppo, J. A.; Somoza, C.; Rúveda, E. A. Synthesis of the Ziegler key intermediate and related precursors for the synthesis of forskolin and erigerol. *J. Org. Chem.* **1990**, *55*, 5631. (e) Colombo, M. I.; Zinczuk, J.; Bacigaluppo, J. A.;

Somoza, C.; Rúveda, E. A. A practical and efficient synthesis of the Ziegler key intermediate for the synthesis of forskolin. *Tetrahedron Lett.* **1990**, *31*, 39. (f) Nagashima, S.; Kanematsu, K. A synthesis of an optically active forskolin intermediate via allenyl ether intramolecular cycloaddition strategy. *Tetrahedron* **1990**, *1*, 743. (g) Bacigaluppo, J. A.; Colombo, M. I.; Zinczuk, J.; Huber, S. N.; Mischne, M. P.; Rúveda, E. A. Convenient and short route to a key intermediate in the synthesis of forskolin. *Synthetic Comm*. **1991**, *21*, 1361. (h) Anies, C.; Pancrazi, A.; Lallemand, J.-Y. Oxidation and Elimination reactions study in a formal synthesis of (±)-forskolin. *Tetrahedron Lett.* **1995**, *36*, 2074. (i) Leclaire, M.; Pericaud, F.; Lallemand, J. Y. Efficient access to the 'Ziegler intermediate' in the total synthesis of forskolin. *J. Chem. Soc., Chem. Commun*. **1995**, 1333. (j) Leclaire, M.; Levet, R.; Ferreira, F.; Ducrot, P. -H.; Lallemand, J.Y.; Ricard, L. Short cuts toward forskolin synthesis: a pentacyclic approach. *Chem. Commun*. **2000**, 1737.

18. For formal syntheses of forskolin not intercepting Ziegler's intermediate see: (a) Liu, H. J.; Shang, X. Synthetic studies of forskolin. A Diels–Alder approach to Corey's endoperoxide. *Heterocycles*, **1997**, *44*, 143. (b) Hagiwara, H.; Takeuchi, F.; Kudou, M.; Hoshi, T.; Suzuki, T.; Hasimoto, T.; Asakawa, Y. Synthetic transformation of ptychantin into forskolin and 1,9-dideoxyforskolin. *J. Org. Chem.* **2006**, *71*, 4619. (c) Nagasawa, S.; Jones, K. E.; Sarpong, R. Enantiospecific entry to a common decalin intermediate for the syntheses of highly oxygenated terpenoids. *J. Org. Chem*. **2019**, *84*, 12209.
19. (a) Hashimoto, S.; Sakata, S.; Sonegawa, M.; Ikegami, S. A total synthesis of (±)-forskolin. *J. Am. Chem. Soc.* **1988**, *110*, 3670. (b) Hashimoto, S.; Sonegawa, M.; Sakata, S.; Ikegami, S. A Stereocontrolled synthesis of (±)-1,6,7-trideoxyforskolin. *J. Chem. Soc., Chem. Commun.* **1987**, 24.
20. (a) Corey, E. J.; Da Silva Jardine, P.; Mohri, T. Enantioselective route to a key intermediate in the total synthesis of forskolin. *Tetrahedron Lett.* **1988**, *29*, 6409. (b) Corey, E. J.; Da Silva Jardine, P.; Rohloff, J. C. Total synthesis of (±)-forskolin. *J. Am. Chem. Soc.* **1988**, *110*, 3672.
21. (a) Delpech, B.; Calvo, D.; Lett, R. Total synthesis of forskolin - part I. *Tetrahedron Lett.* **1996**, *37*, 1015. (b) Delpech, B.; Calvo, D.; Lett, R. Total synthesis of forskolin - part II. *Tetrahedron Lett.* **1996**, *37*, 1019. (c) Delpech, B.; Port, M.; Calvo, D.; Lett, R. Total synthesis of forskolin - part III studies related to an asymmetric synthesis. *Tetrahedron Lett.* **1996**, *37*, 1023.
22. Hylse, O.; Maier, L.; Kucera, R.; Perečko, T.; Svobodová, A.; Kubala, L.; Paruch, K.; Švenda, J. A concise synthesis of forskolin. *Angew. Chem., Int. Ed.* **2017**, *56*, 12586.
23. Bold, G.; Chao, S.; Bhide, R.; Wu, S.-H.; Patel, D. V.; Sih, C. J. A chiral bicyclic intermediate for the synthesis of forskolin. *Tetrahedron Lett.* **1987**, *28*, 1973.
24. (a) Kienzle, F.; Stadlwieser, J.; Mergelsberg, I. Diels-Alder-Reaktionen mit 3-Cyclopropylidenprop-1-enyl-ethyl-ether als 1,3-Dien. *Helv. Chim. Acta* **1989**, *72*, 348. (b) Kienzle, F.; Stadlwieser, J.; Rank, W.; Schönholzer, P. Die synthese des labdanditerpenes erigerol und analoger verbindungen. *Helv. Chim. Acta* **1990**, *73*, 1108.

25. Our group and the Sarpong group (ref. 18c) have also reported routes to this type of enedione (**2.68**), which will be discussed in more detail in Chapter 3.

Chapter 3: A Total Synthesis of Forskolin

3.1 Synthetic Planning and Considerations

We chose forskolin (**3.1**) as a synthetic target primarily to demonstrate the utility and applicability of the MHAT initiated annulation (Figure 3.1). Forskolin was a logical starting point for this main goal because first, this natural product was biologically relevant both as a tool to modulate intracellular levels of cyclic AMP and its analogs as therapeutics.[1,2] Additionally, the larger family of labdane diterpenoids that forskolin belongs to host an immense wealth of potentially valuable biological activities making a synthetic route to this type of scaffold valuable beyond simply accessing one congener.[3] Second, prior syntheses of labdane diterpenoids had historically relied on classical annulations like the Robinson and Diels–Alder reactions that invariably led to challenges either in producing the sterically congested carbocyclic frameworks or installing the requisite oxidation patterns.[4–9] We believed that an MHAT initiated annulation would be well suited to address these challenges.

In planning our synthetic route to forskolin we first considered the successes and shortcomings of prior routes. All previous efforts followed similar logic in their retrosyntheses: first disconnection of the C-ring and then disconnection of the A- and B-rings. This linear approach seemed logical because it presented the opportunity to set the dense array of stereocenters found in forskolin through stereochemical relay. At the same time, we recognized that a linear approach necessitated the sequential buildup of functionality, often possessing conflicting reactivity, which had presented a challenge in prior work resulting in the bulk of synthetic steps being dedicated to introducing oxidation, protecting/deprotecting, and functional group manipulations. Therefore, in our own synthetic planning we intended minimize sacrificial steps by establishing the requisite

carbon framework with pragmatic functional handles for assembly of the oxidation pattern found in forskolin.

Figure 3.1: Prior Approaches to the C-Ring

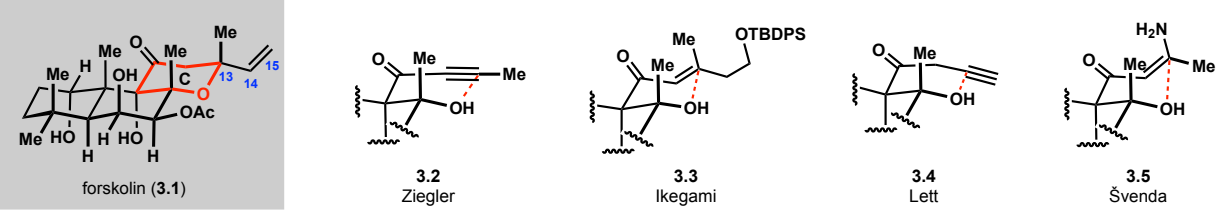

Focusing on specific disconnections from prior works, one of the most strategic seemed to be disconnection of the C14, C15-vinyl substituent via a conjugate addition transform to deliver a dihydro-γ-pyrone synthon. This not only cleared the C13 stereocenter, but the resulting dihydro-γ-pyrone could be logically disconnected along the C13–O bond. In fact, Ziegler, Ikegami, Lett, and Švenda all disconnected the C13–O bond in their respective syntheses of forskolin (**3.2**–**3.5**, Figure 3.1).[5,6,8,9] We intended to take advantage of this precedented strategy; however, in all prior approaches the carbons that ultimately became the C-ring required multiple synthetic steps to install. We envisioned a more concise approach by disconnecting synthon **3.9** along the C9–C11 bond leading to direct introduction of a 1,3-dicarbonyl surrogate in the forward manner (Scheme 3.1).

Scheme 3.1: Retrosynthesis of Forskolin

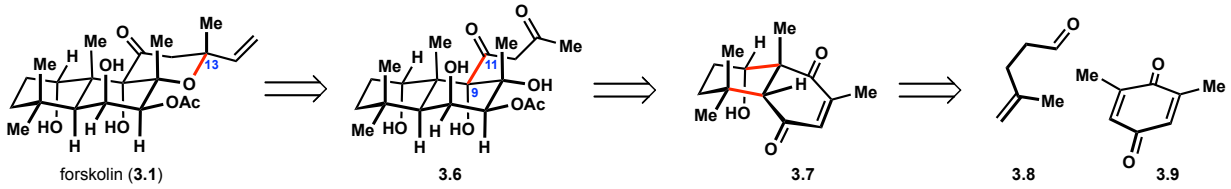

In terms of assembly of the A- and B-rings, all prior efforts relied on Diels–Alder reactions. Ziegler, Corey, Lett, and Ikegami pursued various intramolecular Diels–Alder cyclizations, which established the A- and B-rings early in their respective syntheses, but the resulting cyclization

products were sparsely functionalized and required exhaustive functional group manipulations to reach the complex oxidation pattern found in forskolin (Figure 3.2).[5–8] Alternatively, Švenda took advantage of an intermolecular Diels–Alder annulation, which established the A- and B-rings with pragmatic functional handles.[9] However, this approach was somewhat circuitous because of the inability to form the requisite carbon framework directly via a Diels–Alder annulation (see below).

Figure 3.2: Prior Approaches to the A- and B-Rings

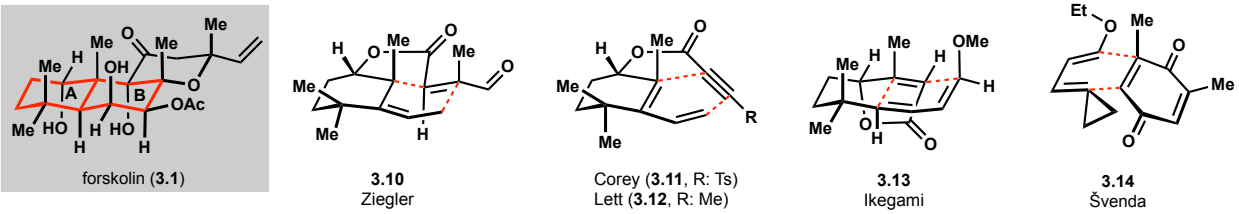

In our assessment of how to disconnect the A- and B-rings we recognized the value of establishing functional handles that would allow for efficient elaboration to the oxidation pattern found in forskolin. Like prior groups we concluded that bicyclic structures **3.15** or **3.7** were logical sub-targets (Scheme 3.1 and 3.2). However, the Sih group had highlighted the challenges associated with preparing enediones like sub-target **3.15**, which were inaccessible by direct annulation between 1,3-dienes like **1.36** and benzoquinone **1.37** because of the $A^{1,3}$ strain imposed on the 1,3-diene component (Scheme 3.2, see Chapter 2 for a detailed discussion).[11] The solution developed by the Kienzle laboratory and implemented by the Švenda group in their synthesis of forskolin was to employ a cyclopropyl 1,3-diene (**3.14**, Figure 3.2) which diminished the severity of the $A^{1,3}$ strain and led to efficient production of the annulated product, but this concession

Scheme 3.2: Sih's Thwarted Diels–Alder Annulation

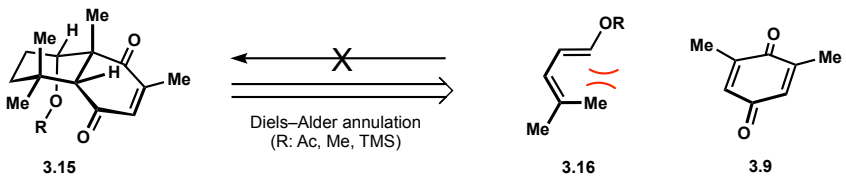

ultimately required multiple synthetic manipulations to convert to the desired carbocyclic framework of the A- and B-rings found in forskolin.[9,10] In our retrosynthetic planning, rather than implementing a Diels–Alder annulation transform to disconnect synthon **3.7**, we reasoned that this sub-target could be more directly prepared by utilizing our recently developed MHAT initiated annulation, which would deliver synthons **3.8** and **3.9** (Scheme 3.1).

It must be emphasized that the prior synthetic work focused on forskolin and related labdane diterpenoids was foundational to the success of our own synthetic efforts and several transformations employed in our synthesis were directly adapted from earlier efforts or inspired by lessons learned in these synthetic campaigns. Guided by the prior art and with a sound retrosynthetic plan we set out to synthesize forskolin.

3.2 A Total Synthesis of Forskolin

3.2.1 Approach to the A- and B-Rings

We commenced our synthesis by preparing the annulation precursors. The γ,δ-unsaturated aldehyde **3.8** was readily accessed through a known reduction of the corresponding ester (Scheme 3.3).[12,13] For the benzoquinone synthon **3.9** we employed enedione **3.17**, which was prepared asymmetrically (96% ee) by an oxazaborolidine catalyzed Diels–Alder annulation developed in the Corey laboratory.[14] The cyclopentadiene adduct was intended to serve both as a handle to render the synthesis asymmetric, but also to protect one of the alkenes of the benzoquinone motif from engaging in undesired reactivity during the annulation.[15] Upon subjecting these coupling

Scheme 3.3: MHAT-Initiated Annulation Towards Forskolin

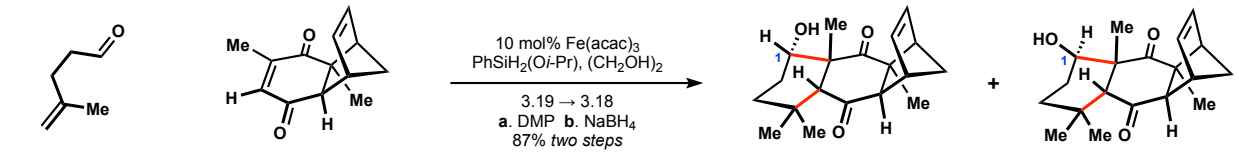

3.8
(3 equivalents)
one step from
commercial material

3.17
one step from
commercial material
(*96% ee*)

3.18
39%

3.19
34%

partners to optimized reaction conditions we obtained the desired annulation product (**3.18**) along with its C1 epimer (**3.19**) in nearly equimolar quantities. Changing to alcoholic solvents (MeOH or *i*-PrOH) did not significantly affect the diastereoselectivity and initial attempts at epimerizing the C1 stereocenter with acid or base were unsuccessful, leading to minimal epimerization or complex mixtures of products. Fortunately, we developed a two-step oxidation-reduction sequence to convert this epimeric material (**3.19**) to the desired compound (**3.18**, Scheme 3.3).

It is worth highlighting the remarkable degree of chemoselectivity among the various alkenes present in this reaction. Although the system benefits from the slow addition protocol (see Chapter 1 for a detailed discussion), where enedione **3.17** is in relatively low concentrations throughout the reaction, the resulting products **3.18** and **3.19** both contain a 1,2-disubstituted alkene, which is does not appear to engage with iron-hydride in an MHAT event to any appreciable degree. Alternatively, if the slow addition protocol was not employed, significant amounts of diones **3.20** and **3.21** were formed presumably through MHAT to the 1,2-disubstituted alkene of **3.17** followed by a 5-*exo* radical cyclization (Scheme 3.4).

Scheme 3.4: Undesired MHAT Pathway

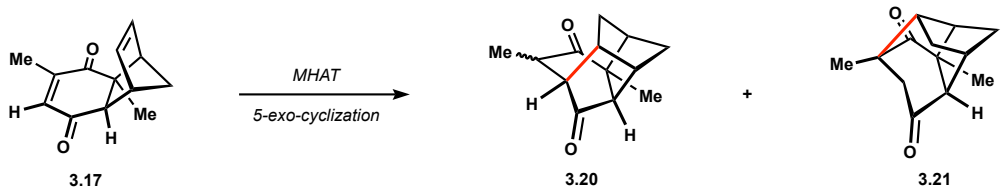

With access to annulation product **3.18** we then investigated removal of the cyclopentene fragment, which had served its purpose to induce asymmetry. Initial attempts to conduct a retro-Diels–Alder reaction at elevated temperatures led to epimerization at C1 presumably through a retro-aldol–aldol sequence. Recognizing that a free alcohol at C1 would likely be a liability in subsequent manipulations and that a protected system would be less prone to epimerization at C1, we opted to protect this functionality prior to performing the retro-Diels–Alder reaction. In the

forward sense, silylation of the C1 alcohol followed by heating the neat silyl ether led to the desired retro-Diels–Alder product **3.23** (Scheme 3.5). Notably, bicyclic ketone **3.23** is an intermediate in Švenda's synthesis of forskolin as well as Kienzle's synthesis of erigerol and may be relevant to other terpenoid natural products. This intermediate was previously prepared as a racemate in eight steps, which we could now access in four steps in an asymmetric fashion.[9,10,16]

Scheme 3.5: Retro-Diels–Alder Reaction to Access A- and B-Rings

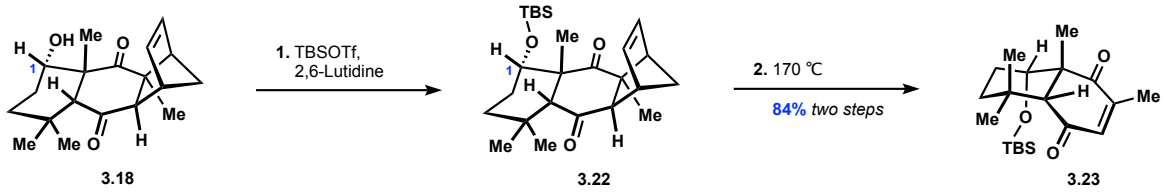

3.2.2 Approach to the C-Ring

Having established the A- and B-rings we turned our attention to introducing a 1,3-dicarbonyl surrogate via a 1,2-addition to the carbonyl at C9, which would ultimately serve as a handle to form the C-ring (Scheme 3.6). Employing enedione **3.23**, or its TMS or free alcohol derivatives (**3.15**), we first attempted addition of lithio-cumulene **3.25**.[17] Unfortunately, this thermally unstable nucleophile led to either recovered starting material or complex mixtures. Next, inspired by Švenda's clever use of an isoxazole as a 1,3-dicarbonyl surrogate, we attempted addition of lithiated 3-methylisothioazole **3.26**, unfortunately to no avail.[18] Several other

Scheme 3.6: 1,2-Addition to C9

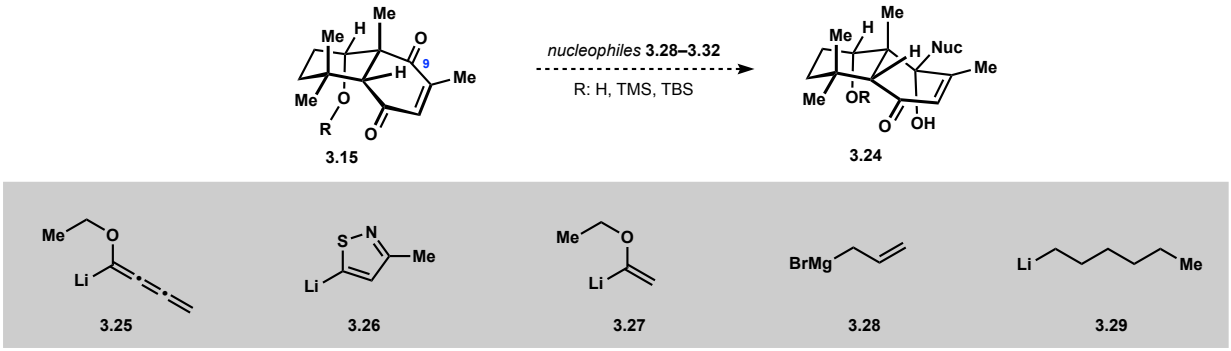

organometallic reagents (**3.27**–**3.29**) used to probe the reactivity of enediones **3.15** were also unsuccessful at delivering the desired 1,2-addion product. Our inability to incorporate sp^3 or sp^2 organometallic species into C9 these enediones was not entirely unexpected. In fact, both Kienzle and Švenda had independently observed challenges with addition of sp^3- or sp^2-hybridized organometallics into enedione **3.23** or its C1 ethyl ether derivative. Alternatively, both groups had successfully performed 1,2-additions of less sterically encumbered sp-hybridized organometallics into the carbonyl at C9.[9,10] We decided to heed the warnings from prior efforts and turned our attention to sp-hybridized nucleophiles.

Our initial efforts focused on forming a protected cyanohydrin at C9. Although this strategy would not introduce all the carbons necessary to install the C-ring, it would provide a useful functional handle and having the resulting alcohol at C9 protected would likely be beneficial for subsequent synthetic manipulations. We were able to form the requisite cyanohydrin (**3.31**) under a variety of conditions, but despite optimization efforts, yields remained prohibitively low. The regioselective functionalization of the carbonyl at C9 in the enedione motif presumably arises as a result of the cyanide nucleophile approaching via the Bürgi–Dunitz angle, where addition into the carbonyl at C6 suffers from steric interactions associated with the two methyl groups vicinal to the carbonyl at C9, whereas approach along the Bürgi–Dunitz angle into the carbonyl at C9 is free from these steric interactions.[10,19]

Table 3.1: C9 Cyanohydrin Formation

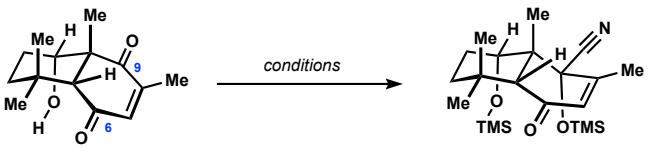

3.30 3.31

entry	conditions	yield[a,b]
1	ZnI_2/TMSCN	N.D.
2	$Sc(OTf)_3$/TMSCN	N.D.
3	I_2/TMSCN	N.D.
4	TEA/TMSCN	10%
5	LiO*t*-Bu/TMSCN	10%
6	LiOMe/TMSCN	28%[c]
7	LiCl/NaCN	N.D.

[a] yield determined by ^{1}H NMR of unpurified reaction mixtures with mesitylene as the internal standard [b] N.D. = not detected by ^{1}H NMR [c] isolated yield

While we were probing the formation of cyanohydrin intermediates, we also pursued the well-precedent addition of acetylide nucleophiles into enedione **3.23**. Early studies from the Liotta group demonstrated that acetylides could be regioselectively incorporated at the C9 carbonyl of related enedione systems.[19] Both Kienzle and Švenda took advantage of this type of reactivity in their syntheses of erigerol and forskolin respectively.[9,10] In our approach we aimed to directly incorporate an acetylide that could serve as a 1,3-dicarbonyl surrogate. With this in mind we prepared dioxolane **3.32**, which we envisioned could be eventually hydrolyzed following 1,2-addition to reveal the desired 1,3-dicarbonyl functionality (Scheme 3.7). Fortunately, treatment of enedione **3.23** with excess of the lithium acetylide of dioxolane **3.32** led to efficient formation of the desired 1,2-addition product **3.34**. The origins of regioselectivity in this case are likely a result of initial deprotonation of the enedione **3.23** to enolate **3.33**, which effectively blocks the C6 carbonyl from nucleophilic attack and then subsequent addition of the acetylide into C9 delivers the desired product. The requirement for at least two equivalents of acetylide to afford appreciable amounts of product **3.34** along with corroborating studies from the Kienzle group support this hypothesis for regiocontrol.[10]

Scheme 3.7: Regioselective Acetylide 1,2-Addition

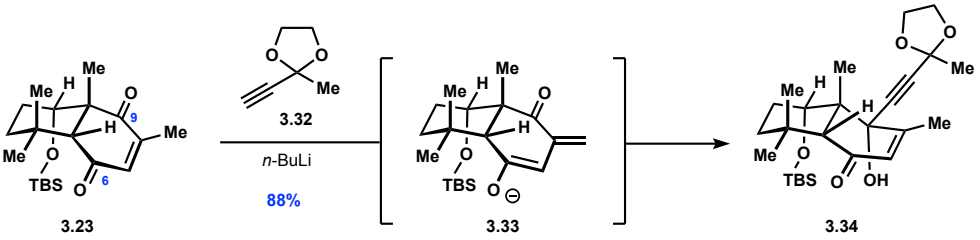

3.2.3 Redox Manipulations of the A- and B-rings

Having installed the requisite carbons to form the C-ring we turned our attention to building up the necessary functionality on the B-ring. This first required epimerization of the C5 stereocenter to form the trans-ring fusion. We capitalized on prior observations from the Kienzle,

Lett, and Švenda groups who had accomplished epimerization of C5 in related systems employing basic aluminum oxide (Brockmann grade IV).[8b,9,10] In accordance with observations from Kienzle and Švenda we found that yields of enone **3.35** were dependent on reaction scale (Scheme 3.8). Where larger scales required multiple additions of aluminum oxide and prolonged reaction times leading a reduction in yield.

At this stage we aimed to install the appropriate oxidation pattern of the B-ring. Initial attempts to epoxidize enone **3.35** with nucleophilic or electrophilic epoxidizing reagents only returned starting material. We suspected that the β-position of the enone was too sterically encumbered to efficiently engage with nucleophilic epoxidizing reagents and that the alkene of the enone was too electron deficient to engage with electrophilic epoxidizing reagents, so we opted to first reduce enone **3.35** to the corresponding allylic alcohol, which we anticipated would increase the electron density of the alkene and allow for more facile epoxidation with electrophilic reagents. Again relying on precedent from prior syntheses we found that treating enone **3.35** with DIBAL–H led to diastereoselective reduction to the desired allylic alcohol **3.36**.[9,10] We were initially concerned that the resulting secondary alcohol would direct epoxidation to the undesired β-face of the alkene, but reaction with *m*-CPBA in DCM resulted in oxidation back to enone **3.35**.[20] Suspecting this product may arise from initial hydrogen-bonding of *m*-CPBA to the secondary alcohol where oxidation back to the enone outcompetes what would be a sterically costly directed epoxidation from the β-face of bicycle **3.36**, we opted to run the reaction with THF as a co-solvent,

Scheme 3.8: B-Ring Functionalization

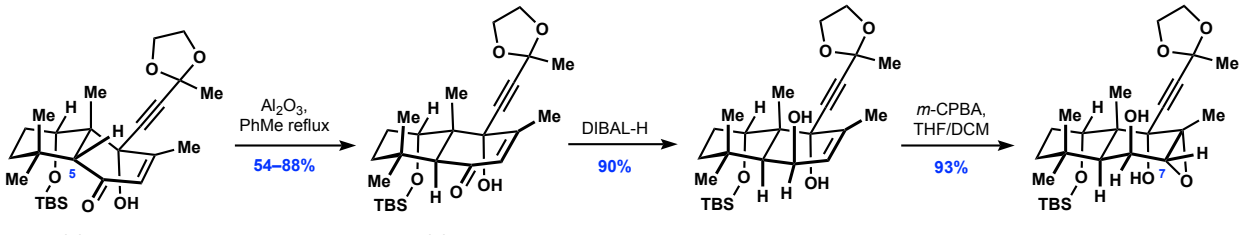

which was expected to act as a hydrogen bond acceptor negating any directing effects. Gratifyingly, this suppressed formation of **3.35** and epoxidized alkene **3.36** from the less sterically encumbered α-face, producing the desired product **3.37** in good yield.

In order to install oxidation at C7 we were inspired by Lett's use of a directed epoxide opening in their synthesis of forskolin.[8] However, we recognized that by capitalizing on work from the Myers group we could potentially accomplish the desired transformation directly from epoxy alcohol **3.37** (Scheme 3.8).[21] In 1988, the Myers group found that treating 2,3-epoxy alcohols with cesium carbonate under an atmosphere of carbon dioxide led to production of the corresponding cyclic carbonates. Interestingly, in our studies we found that the epoxy alcohol **3.37** was inert to the reaction conditions and only underwent the desired transformation following removal of the TBS group at the C1 alcohol. It is not apparent why the presence of a TBS ether at C1 inhibited reactivity. Nevertheless, we developed a protocol to convert allylic alcohol **3.36** to triol **3.38**, which performed exceptionally well under Myers' conditions to afford carbonate **3.40** (Scheme 3.9).

Scheme 3.9: Directed Epoxide Opening

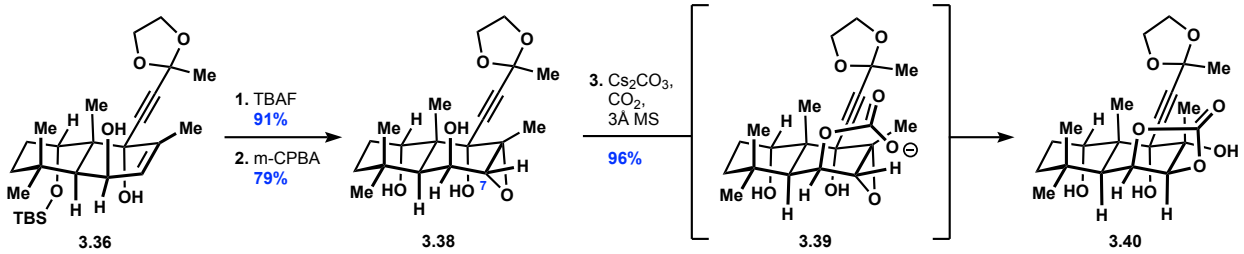

3.2.4 Completion of the C-Ring

With the requisite oxidation installed on both the A- and B-rings we focused our attention on completing the C-ring. In our initial attempts to hydrolyze the propargylic dioxolane motif of carbonate **3.40** to the corresponding 1,3-dicarbonyl or its equivalent with acid we observed production of ketal **3.42**, which was confirmed by X-ray crystallographic studies, rather than the

Scheme 3.10: Ketal Formation

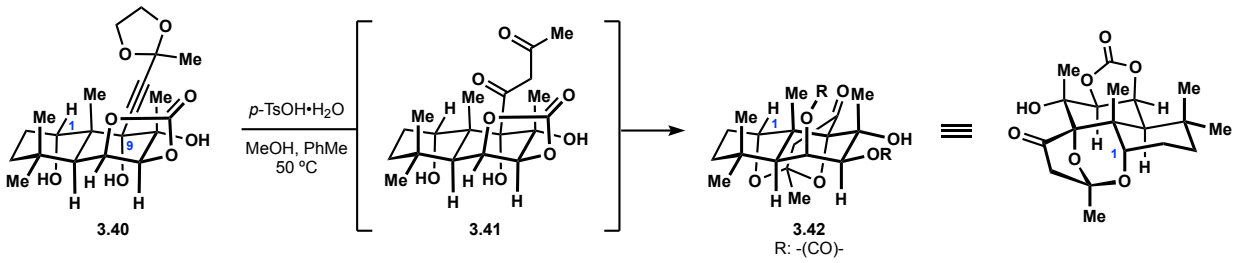

desired dihydro-γ-pyrone. Surprised that this ketal appeared to be the thermodynamic product, we interrogated the effect of protecting groups at the C1 alcohol with the aim that this would shift the equilibrium from, in this case, related hemi-ketal products to the desired dihydro-γ-pyrone. Unfortunately, a variety of protecting groups at the C1 alcohol (Ac, C(O)OMe, PMB, TIPS) were labile under the reaction conditions resulting in solvolysis and formation ketal **3.42**. Similar results were obtained when the C1/C9 diol was protected as the corresponding acetonide or diisopropylsilylene derivative, resulting in formation of ketal **3.42**.

Ultimately, we found that a cyclic carbonate at C1/C9 withstood the reaction conditions necessary to form the desired dihydro-γ-pyrone. Starting back at epoxy alcohol **3.37** we were able subject this material to Myers' conditions for epoxide opening with the addition of cesium fluoride to remove the TBS group at the C1 alcohol (Scheme 3.11). Following opening of the epoxide, carbonyl diimidazole (CDI) was added to the reaction to afford a mixture of biscarbonate products, **3.43** and **3.44**, which equilibrated to a 1:3 ratio under the reaction conditions. In working with

Scheme 3.11: Dihydro-γ-Pyrone Formation

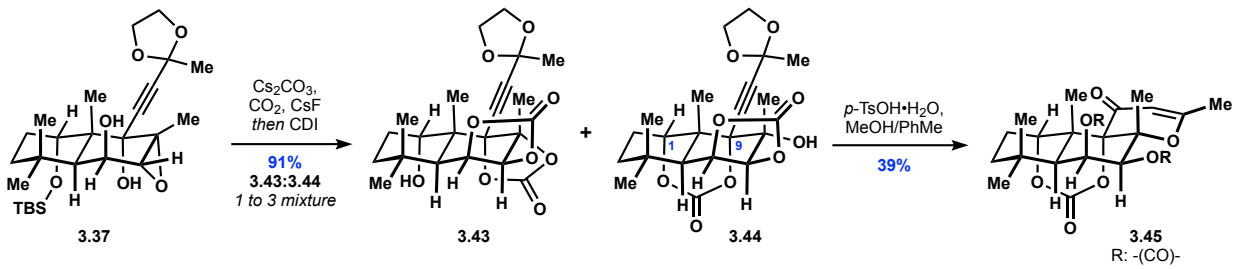

these biscarbonates we found that they not only interconverted under the basic reaction conditions, but also in the presence of acid. Leveraging this reactivity, we found that upon exposure to tosic acid monohydrate in MeOH/PhMe we could convert the equilibrating mixture of biscarbonates to the desired dihydro-γ-pyrone **3.45** in reasonable yield while avoiding formation of ketal **3.42**.

3.2.5 Installation of the C14, C15-Vinyl Substituent

At this stage in the synthesis, dihydro-γ-pyrone **3.45** was only separated from forskolin by a well precedented 1,4-addition of the C14, C15-vinyl substituent, deprotection of the carbonates, and a known acylation. However, this seemingly trivial sequence proved to be far more challenging than initially anticipated. First, dihydro-γ-pyrone **3.45** was poorly soluble in most organic solvents, leading to challenges with conversion and reproducibility in the 1,4-addition of vinyl cuprates. More importantly, upon subjecting dihydro-γ-pyrone **3.45** to a vinyl cuprate in the presence of $BF_3 \cdot OEt_2$, the same conditions developed by Lett and employed by Ziegler and Švenda in their syntheses of forskolin, we only observed formation of the undesired diastereomer **3.48** with respect to the newly formed C13 stereocenter (Scheme 3.12). This was confirmed by saponification of the resulting product with sodium hydroxide in methanol to deliver known C13-epi-deacetyl-forskolin.[9] Although we had not anticipated this result, it was not entirely without precedent considering that Lett had observed α-face selectivity when using *n*-butyl derived cuprates as had Corey when using an organocopper reagent with similar dihydro-γ-pyrones (see Chapter 2).[7,8a] However, when comparing the diastereoselectivity of prior vinyl cuprate additions from Lett (**3.49**), Ziegler (**3.50**), and Švenda (**3.49**) to our system it was apparent that the undesired stereochemical outcome could be attributed to the biscarbonates (Scheme 3.12).[5,8,9]

Recognizing that the biscarbonates were incompatible protecting groups for the C1/C9 and C6/C7 diols we turned our attention to identifying suitable protecting groups that would favor

Scheme 3.12: Vinyl 1,4-Addition to C13

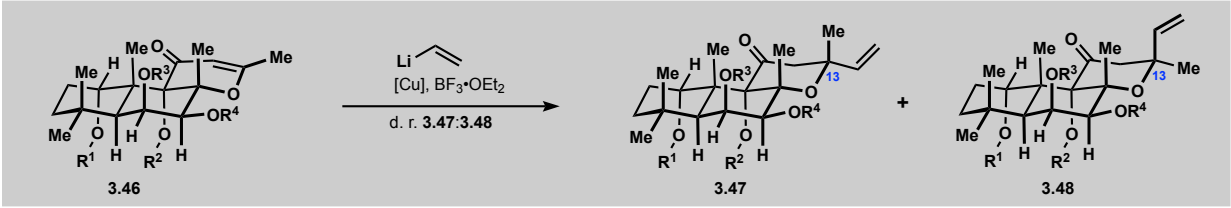

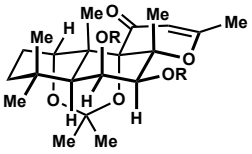

3.49 (*Lett*)
R: -C(Me)$_2$-
d. r. **4.2:1**
83%

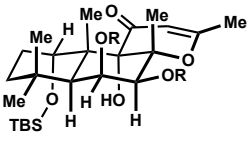

3.50 (*Ziegler*)
R: -C(Me$_2$)-
d. r. **9:1**
60%

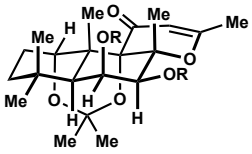

3.49 (*Švenda*)
R: -C(Me)$_2$-
d. r. **5:1**
60%

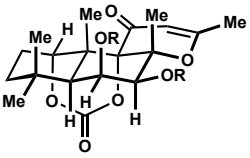

3.45
R: -(CO)-
d. r. **0:1**
yield not determined

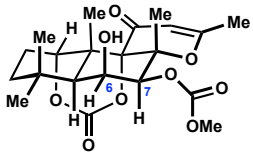

3.51
d. r. **1.4:1**
yield not determined

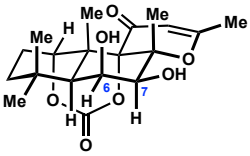

3.52
d. r. **3:1**
yield not determined

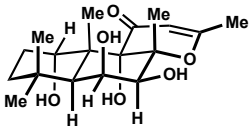

3.53
complex mixture

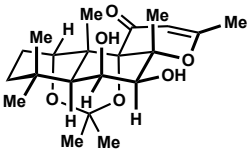

3.54
d. r. **5:1**
44% (61% brsm)

formation of the desired C13 epimer in the vinyl 1,4-addtion. It is worth noting that we did not pursue a bisacetonide system, like Lett and Švenda, because initial attempts to form the desired bisacetonide (**3.49**) from the corresponding tetraol (**3.53**) were unsuccessful. Additionally, the reported deprotection of the bisacetonide functionality following vinyl 1,4-addition required 12 days to reach completion.[8c,9] These two factors encouraged us to identify alternative protecting groups that would allow for a diastereoselective vinyl 1,4-addition, but that could also be readily installed and removed. In pursuit of this goal, we saponified biscarbonate **3.45** with sodium hydroxide in methanol to afford the corresponding tetraol **3.53** with the intention of installing various protecting groups on the C1/C9 and C6/C7 diols. However, we noticed that if the saponification of the biscarbonates was terminated prior to completion a mixture of partially cleaved carbonates could be obtained. Careful separation of these species allowed us to purify carbonates **3.51** and **3.52** (Scheme 3.12). Upon subjecting these carbonates to the same conditions

previously described for vinyl 1,4-addition, we found that carbonates **3.51** and **3.52** both favored production of the desired C13 epimer (**3.48**) delivering a 1.4:1 and 3:1 diastereomeric ratio respectively. Attempts at subjecting the free tetraol **3.53** to conditions for vinyl 1,4-addition led to complex mixtures of products. Although this only represented a few data points, it seemed that having the C6 and C7 alcohols unprotected led to improved stereochemical outcomes. With this in mind, we prepared ketal **3.54**, which afforded a synthetically useful 5:1 ratio of epimers at C13. Satisfied with the results from ketal **3.54** we focused our attention on efficiently preparing this intermediate.

We found that following acid catalyzed formation of the dihydro-γ-pyrone, from biscarbonates **3.43** and **3.44**, we could basicify the reaction mixture to cleave the remaining biscarbonates and deliver tetraol **3.53** (Scheme 3.13). A straightforward ketalization afforded acetonide **3.54**, which upon subjecting to a vinyl cuprate in the presence of $BF_3 \cdot OEt_2$ delivered tetrahydro-γ-pyrone **3.55** in synthetically useful yields, importantly favoring formation of the desired C13 stereocenter. It should be noted that in practice this vinyl 1,4-addition was non-trivial. The dihydro- γ-pyrone **3.54** was slow to react at temperatures below –55 ºC; however, this

Scheme 3.13: Final Approach to Forskolin

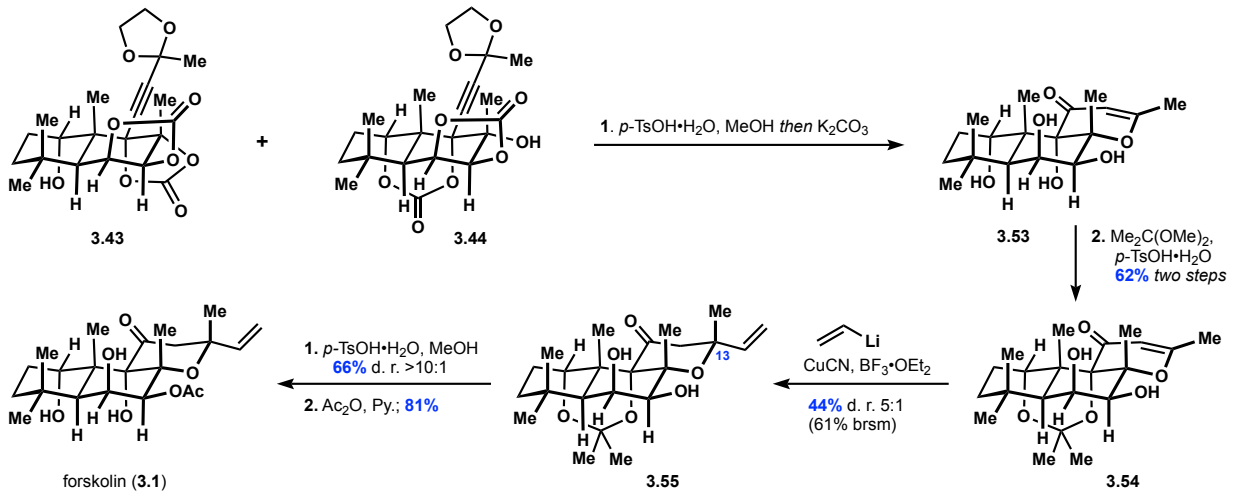

appeared to be the same temperature regime that the generated cuprate decomposed, as indicated by formation of heterogeneous brown residue in the flask and no further conversion to product **3.55**. This competing reactivity ultimately necessitated three sequential additions of freshly prepared cuprate and $BF_3 \cdot OEt_2$ at –78 ºC followed by warming to –55 ºC to achieve reasonable conversion. Nevertheless, with tetrahydro-γ-pyrone **3.55** in hand we executed deprotection of the acetonide, which notably reached completion in just over a day rather than 12 days as was required for the related bisacetonide system.[8c,9] A final, known acylation delivered the natural product forskolin.[22]

3.3 Conclusion

In summation, this work constitutes a 14-step synthesis of forskolin from commercially available material (Scheme 3.14). Our strategy was guided by preceding efforts in the field and aimed to address some of the remaining synthetic challenges. The efficiency of our route can largely be attributed to implementation of an MHAT initiated annulation securing rapid access to the A- and B-rings. Notably, this strategy produced enantioenriched enedione **3.23**, which was previously challenging to prepare as a racemate, and which may have utility in the pursuit of other terpenoids. Additional noteworthy aspects of our synthesis include: the careful relay of stereochemistry to set the dense oxidation pattern found in forskolin, direct addition of a 1,3-carbonyl surrogate enabling efficient formation of the C-ring, and further insights into the diastereoselectivity of vinyl 1,4-additions to dihydro-γ-pyrones relevant to forskolin. We anticipate that our contributions will aid in future synthetic investigations of forskolin and related terpenoids, and that the developed MHAT-initiated annulation will find applicability beyond its implementation in the synthesis of forskolin, specifically in accessing sterically congested carbocyclic motifs that are otherwise challenging to prepare.

Scheme 3.14: Synthesis of Forskolin

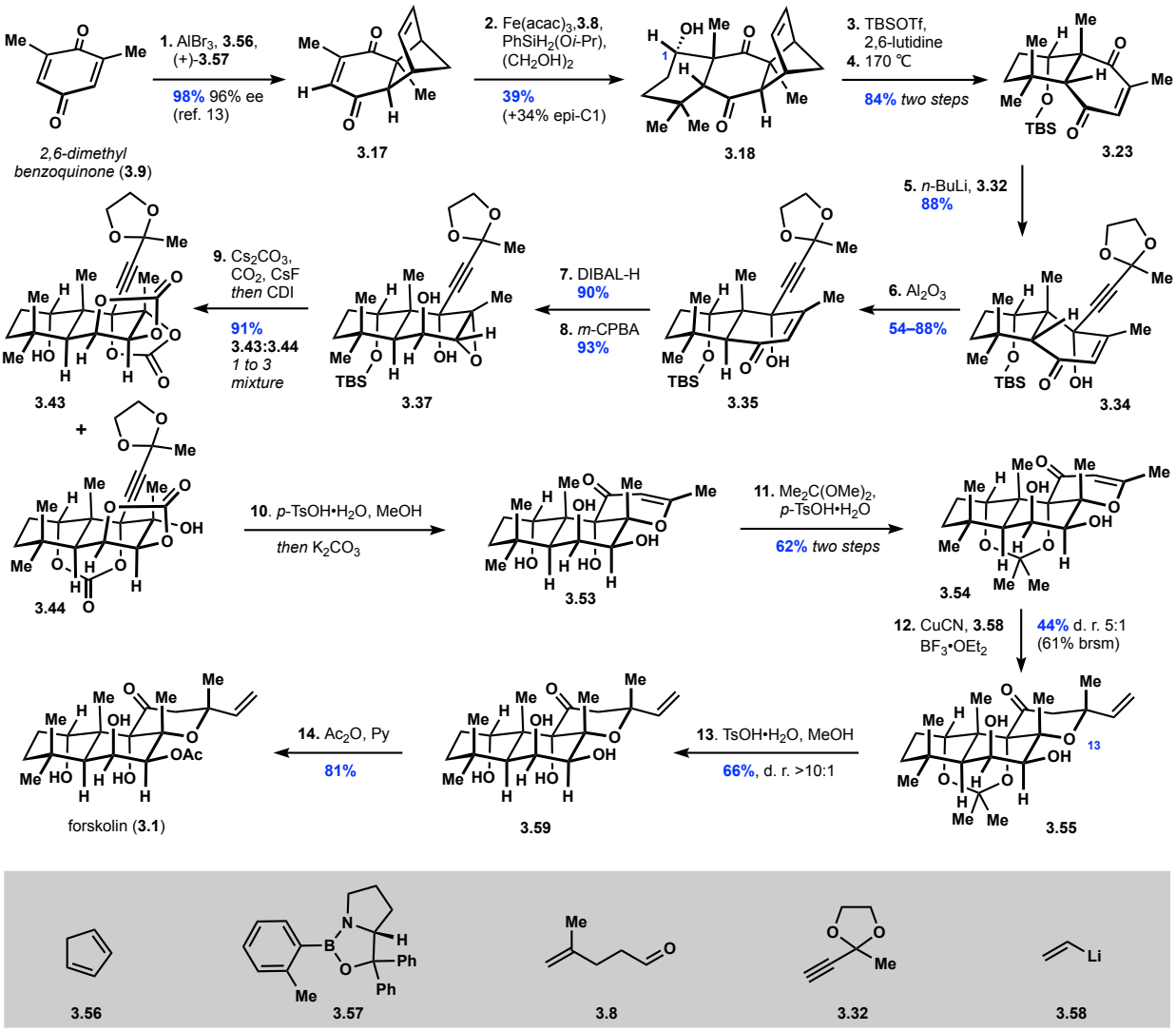

3.4 Experimental Section

3.4.1 Materials and Methods

All reactions were carried out in flame-dried glassware under positive pressure of dry nitrogen unless otherwise noted. Reaction solvents (Fisher, HPLC grade) including tetrahydrofuran (THF), diethyl ether (Et_2O), dichloromethane (DCM), dimethylformamide (DMF), methanol (MeOH) and toluene (PhMe) were dried by percolation through a column packed with neutral alumina and a column packed with a supported copper catalyst for scavenging oxygen (Q5) under positive pressure of argon. Anhydrous 1,2-dichloroethane (DCE, Fisher, ACS Grade), anhydrous pyridine (Fisher) and anhydrous triethylamine (Et_3N, Oakwood Chemical) were distilled from calcium hydride (10% w/v) under positive pressure of nitrogen. Solvents for extraction, thin layer chromatography (TLC), and flash column chromatography were purchased from Fischer (ACS Grade) and VWR (ACS Grade) and used without further purification. Chloroform-d and benzene-d_6 for ^1H and ^{13}C NMR analysis were purchased from Cambridge Isotope Laboratories and used without further purification. Commercially available reagents were used without further purification unless otherwise noted. Reactions were monitored by thin layer chromatography (TLC) using precoated silica gel plates (EMD Chemicals, Silica gel 60 F_{254}). Flash column chromatography was performed over silica gel (Acros Organics, 60 Å, particle size 0.04-0.063 mm). HPLC analysis was performed on an Agilent 1100 series. Optical rotation readings were obtained using JASCO P-1010 polarimeter. ^1H NMR and ^{13}C NMR spectra were recorded on Bruker DRX-500 (BBO probe), Bruker DRX-500 (TCI cryoprobe), Bruker AVANCE600 (TBI probe), and Bruker AVANCE600 (BBFO cryoprobe) spectrometers using residual solvent peaks as internal standards ($CHCl_3$ @ 7.26 ppm ^1H NMR, 77.16 ppm ^{13}C NMR; C_6H_6 @ 7.16 ppm ^1H NMR, 128.00 ppm ^{13}C NMR). High-resolution mass spectra (HRMS) were recorded on Waters LCT Premier TOF spectrometer with ESI and CI sources.

3.4.2 Experimental Procedures

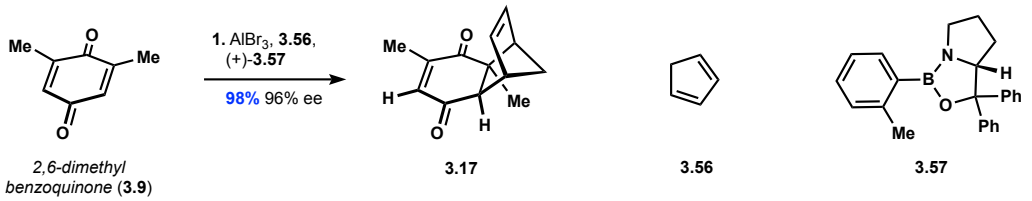

2,6-dimethyl benzoquinone (**3.9**) **3.17** **3.56** **3.57**

(–)-Enedione 3.17.[14] A 100 mL Schlenk flask was charged with (*R*)-(+)-o-Tolyl-CBS-oxazaborolidine **3.57** (0.88 mL of a 0.5 M solution in toluene, 0.44 mmol) and DCM (1.75 mL). The solution was cooled to –40 °C before adding a solution of $AlBr_3$ (0.39 mL of a 1.0 M solution in CH_2Br_2, 0.39 mmol) dropwise. The solution was stirred at –40 °C for 30 min and then cooled to –78 °C and diluted with DCM (40 mL). To the solution was added 2,6-dimethylbenzoquinone (1.50 g, 11.0 mmol) in toluene (10 mL) followed by dropwise addition of freshly prepared cyclopentadiene (4.75 mL, 55.0 mmol). The reaction mixture was stirred for 2 h and quenched with MeOH (1.75 mL) at –78 °C. The solution was then warmed to room temperature and concentrated under reduced pressure. Purification by flash chromatography (elution with 10% v/v ethyl acetate in hexanes) afforded enedione (–)-**3.17** (2.19 g, 98%, 96% ee) as a yellow solid. ^{1}H NMR data matched that provided in the literature.[14] Enantiopurity was assessed by HPLC (Chiralcel AD-H (w/ AD guard); 1 mL/min; 0.3% v/v *i*-PrOH in hexanes): t*R* = 27.757, 29.319 min.

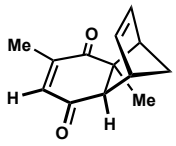

(–)-3.17

$[\alpha]_D^{22}$ –101.8 (c = 2.0, $CHCl_3$); 96% ee

Data File C:\HPCHEM\1\DATA\ALEXB\WPT193.D

Sample Name: wpt-3-193e

Chiralcel ADH w/ guard, 0.3%IPA/Hex, 25uL injection, 1.
0mL/min, 254 nm

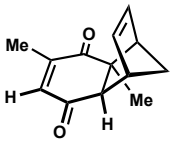

(–)-3.17

Injection Date : 6/25/2019 5:20:58 PM
Sample Name : wpt-3-193e
Location : Vial 24
Acq. Operator : ALEXB
Inj Volume : 25 µl

Acq. Method : C:\HPCHEM\1\METHODS\ALEXB.M
Last changed : 6/25/2019 4:01:43 PM by ALEXB
(modified after loading)
Analysis Method : C:\HPCHEM\1\METHODS\ALEXB.M
Last changed : 6/20/2019 1:38:43 AM by ALEXB

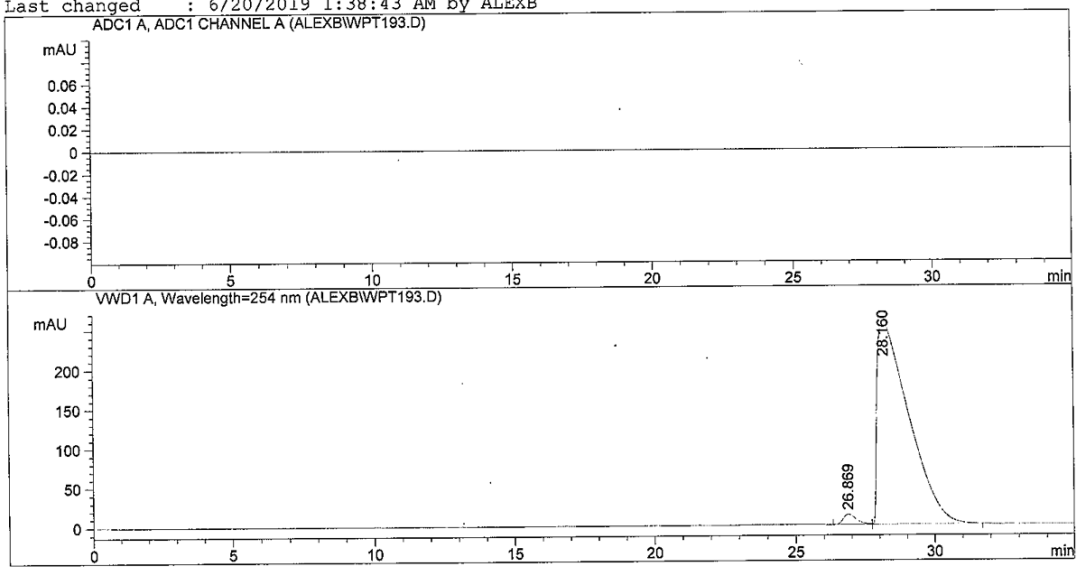

Area Percent Report

Sorted By : Signal
Multiplier : 1.0000
Dilution : 1.0000
Sample Amount : 1.00000 [ng/ul] (not used in calc.)
Use Multiplier & Dilution Factor with ISTDs

Signal 1: ADC1 A, ADC1 CHANNEL A

Signal 2: VWD1 A, Wavelength=254 nm

Peak #	RetTime [min]	Type	Width [min]	Area mAU *s	Height [mAU]	Area %
1	26.869	BV	0.4988	420.16956	12.92051	2.0167
2	28.160	VB	1.0695	2.04148e4	258.19269	97.9833
Totals :				2.08350e4	271.11320	

Results obtained with enhanced integrator!

*** End of Report ***

Data File C:\HPCHEM\1\DATA\ALEXB\WPT3184R.D Sample Name: wpt-3-184-r3

ad-h w/ ad guard, 0.3% IPA/Hex, 25 uL injection, 1.0 mL /min, 254 nm

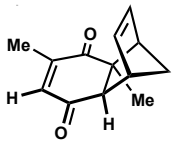

racemic **3.17**

```
Injection Date  : 6/17/2019 11:46:37 AM
Sample Name     : wpt-3-184-r3                  Location : Vial 20
Acq. Operator   : ALEXB                      Inj Volume : 20 µl
Acq. Method     : C:\HPCHEM\1\METHODS\ALEXB.M
Last changed    : 6/17/2019 11:01:18 AM by ALEXB
                  (modified after loading)
Analysis Method : C:\HPCHEM\1\METHODS\ALEXB.M
Last changed    : 2/25/2019 6:27:33 PM by ALEXB
```

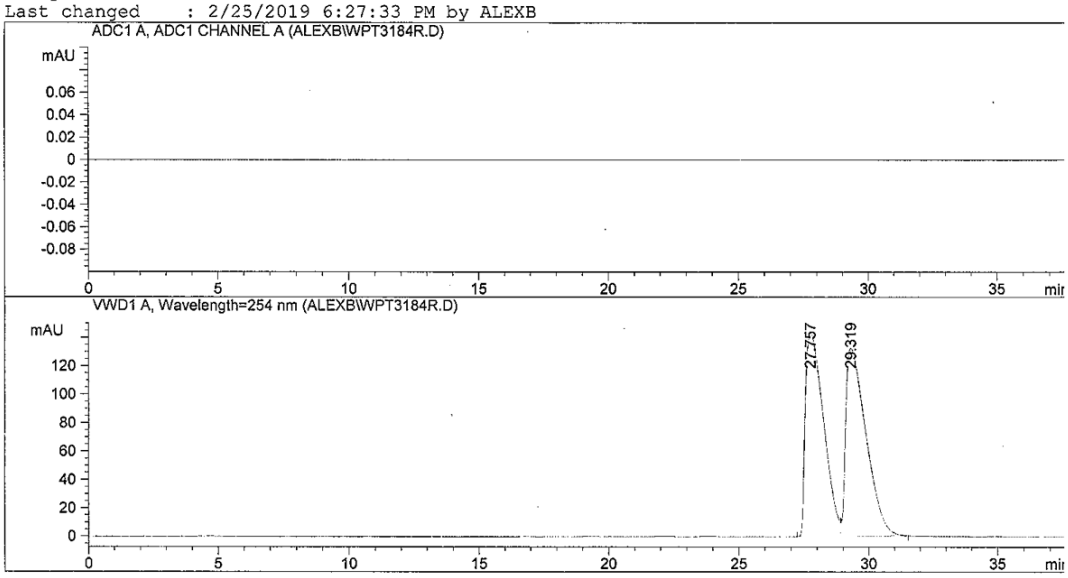


```
                          Area Percent Report

Sorted By             :      Signal
Multiplier            :      1.0000
Dilution              :      1.0000
Sample Amount         :      1.00000  [ng/ul]   (not used in calc.)
Use Multiplier & Dilution Factor with ISTDs

Signal 1: ADC1 A, ADC1 CHANNEL A

Signal 2: VWD1 A, Wavelength=254 nm

Peak RetTime Type  Width     Area      Height     Area
  #   [min]        [min]  mAU   *s   [mAU   ]      %
----|-------|----|-------|----------|----------|--------|
   1  27.757 BV    0.7839 6978.09766  143.59732  49.0839
   2  29.319 VB    0.8477 7238.58105  132.36908  50.9161

Totals :                  1.42167e4   275.96640

 Results obtained with enhanced integrator!

                          *** End of Report ***
```

Racemic **3.17** prepared following protocol previously described in the literature.[23]

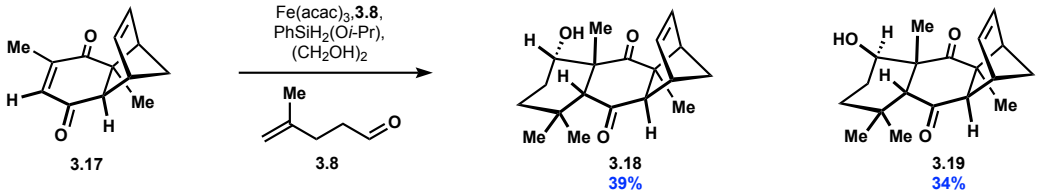

Alcohols (+)-**3.18 and** (+)-**3.19**. A 25 mL Schlenk flask was charged with iron(III) acetylacetonate (87.3 mg, 0.247 mmol), γ,δ-unsaturated aldehyde **3.8**[24] (0.730 g, 7.44 mmol), anhydrous ethylene glycol (0.42 mL, 7.5 mmol) and DCM (10 mL). The solution was degassed by freeze-pump-thaw technique (3 cycles) and charged with nitrogen before cooling the solution to 0 °C. Enedione (–)-**3.17** (0.500 g, 2.47 mmol) and (isopropoxy)phenylsilane[25] (0.62 mL, 3.7 mmol) dissolved in DCM (5 mL sparged under argon for 15 min) were added dropwise to the solution with a syringe pump (2 mL/h). The reaction mixture was then stirred for an additional 3 h at 0 °C, then quenched with 1 N aqueous HCl (12 mL sparged under argon for 15 min) and the flask was warmed to room temperature. The biphasic mixture was diluted with diethyl ether (50 mL) and the layers were separated. The aqueous layer was extracted twice with diethyl ether (100 mL combined). The organic layers were combined and washed with water (15 mL) followed by brine (15 mL). The organic layer was dried over anhydrous magnesium sulfate, filtered and concentrated under reduced pressure. Purification by flash chromatography (gradient elution: 5% to 10% v/v ethyl acetate in hexanes) afforded alcohol (+)-**3.18** (257 mg, 34%) as a white solid and alcohol (+)-**3.19** (289 mg, 39%) as a white solid.

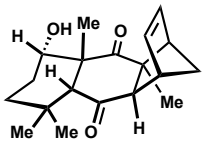

3.18

Alcohol (+)-**3.18**

^{1}H NMR (500 MHz, $CDCl_3$)

δ 6.29 (dd, 1H, *J* = 5.6, 3.0 Hz)	2.77 (d, 1H, *J* = 3.8 Hz)	1.03 (s, 3H)
6.10 (dd, 1H, *J* = 5.6, 3.0 Hz)	2.35 (s, 1H)	1.00 (s, 3H)
4.14–4.12 (m, 1H)	1.63–1.57 (m, 9H)	
3.46 (s, 1H)	1.49 (dt, 1H, *J* = 9.1, 1.7 Hz)	
3.01 (s, 1H)	1.12 (s, 3H)	

^{13}C NMR (126 MHz, $CDCl_3$)

δ 220.2	63.6	47.6	30.1
211.1	61.0	47.4	29.1
138.6	57.1	34.1	26.1
137.7	55.8	32.6	23.6
68.7	53.4	32.5	

HRMS (ES+) calculated for $C_{19}H_{26}O_3Na$ $[M+Na]^+$: 325.1780, found 325.1777

TLC: R_f = 0.19 (20% v/v ethyl acetate in hexanes)

$[\alpha]_D^{22}$ + 15.5 (c = 2.0, $CHCl_3$)

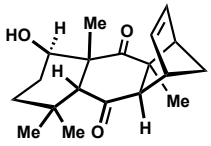

3.19

Alcohol (+)-**3.19**

^{1}H NMR (500 MHz, $CDCl_3$)

δ 6.28 (m, 1H)	2.98 (s, 1H)	1.54–1.45 (m, 2H)
6.07 (m, 1H)	2.80 (d, 1H, *J* = 3.9 Hz)	1.37–1.31 (m, 1H)
4.57 (bs, 1H)	2.13 (s, 1H)	1.17 (s, 3H)
3.47 (s, 1H)	1.84–1.78 (m, 1H)	1.11 (s, 3H)
3.26 (m, 1H)	1.67–1.64 (m, 5H)	0.99 (s, 3H)

^{13}C NMR (126 MHz, $CDCl_3$)

δ 223.8	58.5	32.4
210.4	55.9	30.7
139.2	51.5	29.0
137.7	48.4	28.8
80.4	47.7	27.6
66.7	38.7	
61.2	33.3	

HRMS (ES+) calculated for $C_{19}H_{26}O_3Na$ $[M+Na]^+$: 325.1780, found 325.1770

TLC: R_f = 0.22 (20% v/v ethyl acetate in hexanes)

$[\alpha]_D^{22}$ + 0.6 (c = 2.0, $CHCl_3$)

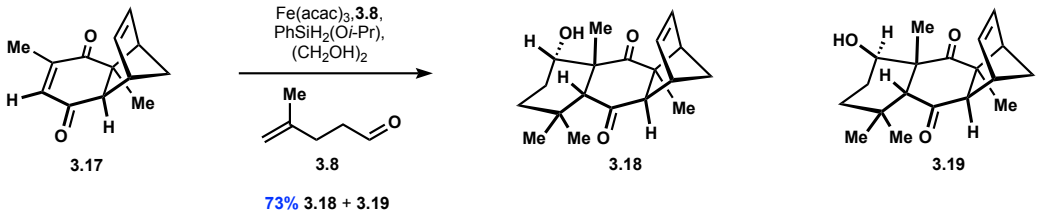

Alcohols 3.18 and 3.19. Subjecting 4.51 g (22.3 mmol) of racemic **3.17** and 4.08 g (41.5 mmol) of γ,δ-unsaturated aldehyde **3.8** to the previously described conditions afforded 2.66 g (39%) of a 6:1 mixture of **3.18** and **3.19**, and 2.28 g (34%) of alcohol **3.19**. ^{1}H NMR data matched that previously reported for alcohols **3.18** and **3.19**.

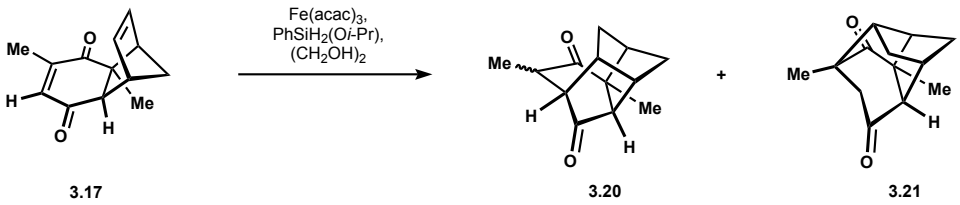

3.17 3.20 3.21

Dione 3.20 and 3.21. A dram vial was charged with enedione **3.17** (40 mg, 0.20 mmol), iron(III) acetylacetonate (7 mg, 0.02 mmol), ethylene glycol (34 μL, 0.60 mmol) and DCM (1.2 mL). The mixture was sparged with argon for 10 min and then (isopropoxy)phenylsilane[25] (67 μL, 0.40 mmol) was added slowly. After 15 h the reaction was concerted under reduced pressure. Purification by preparative thin layer chromatography (elution with 20% v/v ethyl acetate in hexanes) afforded a 1:1 mixture of diones **3.20** and **3.21** (yield not determined).

Note: Further attempts at purification led to isolation of a 2:3 mixture of diones **3.20** and **3.21**, as well as a small quantity of **3.21**. Diones **3.20** and **3.21** were produced in varying quantities from MHAT initiated annulations between **3.17** and γ,δ-unsaturated aldehyde **3.8** depending on rate of addition of **3.17** and (isopropoxy)phenylsilane (see Chapter 3 text for discussion).

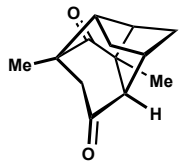

3.21

Dione **3.21**

^{1}H NMR (500 MHz, $CDCl_3$)

δ 2.59 (m, 1H)	2.30 (m, 1H)	1.69 (d, 1H, J = 10.2)
2.58(d, 1H, J = 19.7)	2.23 (d, 1H, J = 19.8)	1.62–1.58 (m, 1H)
2.53 (m, 1H)	1.91 (d, 1H, J = 10.4)	1.11 (s, 3H)
2.36–2.33 (m, 1H)	1.85 (d, 1H, J = 13.2)	1.02 (s, 3H)

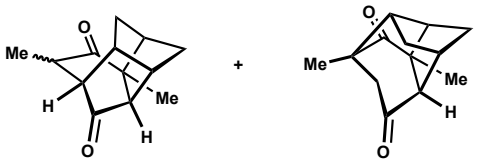

3.20 3.21

Diones **3.20** and **3.21** (1:1 mixture)

^{13}C NMR (126 MHz, $CDCl_3$)

δ 2182	49.4	32.6 (2C)
214.9 (2C)	49.2	31.7
209.3	48.3	21.5
68.2	44.3	19.3
60.8	41.0	16.8
53.1	39.4	16.0
52.3	39.2	

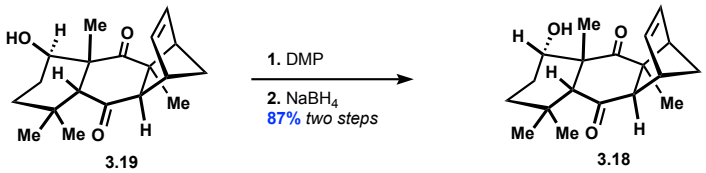

Alcohol 3.18. A 100 mL round bottom flask was charged with Dess–Martin periodinane (5.60 g, 13.2 mmol), DCM (30 mL) and cooled to 0 °C. Racemic alcohol **3.19** (2.63 g, 8.70 mmol) was added over 10 min in DCM (10 mL) followed by solid $NaHCO_3$ (1.60 g, 19.0 mmol). After 1 h saturated aqueous $NaHCO_3$ (10 mL) was added followed by saturated aqueous sodium thiosulfate (25 mL) and water (25 mL). The flask was brought to room temperature and diluted with diethyl ether (50 mL). The layers were separated, and the aqueous layer was extracted twice with diethyl ether (100 mL combined). The organic layers were washed with brine (10 mL), dried over anhydrous magnesium sulfate, filtered, and concentrated under reduced pressure. The crude material was dissolved in a THF (25 mL) and MeOH (25 mL) and cooled to –40 °C. $NaBH_4$ (0.988 g, 26.1 mmol) was added portion-wise over 10 min. After 3 h, 1 N aqueous HCl (25 mL) was added slowly. The biphasic mixture was warmed to room temperature and diluted with ethyl acetate (50 mL). The layers were separated, and the aqueous layer was extracted twice with ethyl acetate (100 mL combined). The organic layers were combined and washed with brine (25 mL). The organic phase was dried over anhydrous magnesium sulfate, filtered and concentrated under reduced pressure. Purification by flash chromatography (elution with 10% v/v ethyl acetate in hexanes) afforded alcohol **3.18** (2.28 g, 87% over two steps). ^1H NMR data matched that previously reported for alcohol **3.18**.

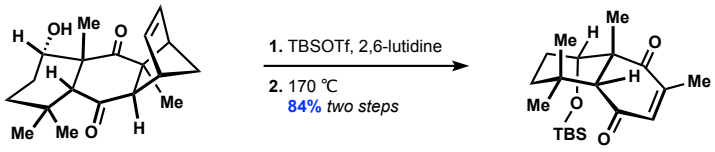

3.18 3.23

Enedione 3.23. A 5 mL round bottom flask was charged with alcohol (+)-**3.18** (51.8 mg, 0.171 mmol), DCM (0.8 mL) and cooled to –78 °C. To the solution was added 2,6-lutidine (30 µL, 0.259 mmol) followed by TBSOTf (48 µL, 0.209 mmol) over 20 min. After 1 h at –78 °C the mixture was added to a stirring solution of 1 M aqueous acetic acid (5 mL) and brine (10 mL). The aqueous layer was extracted three times with DCM (45 mL combined). The organic layers were combined and washed with saturated aqueous $NaHCO_3$ (10 mL) followed by brine (10 mL). The organic layer was dried over magnesium sulfate, filtered and concentrated under reduced pressure. The crude material was then heated neat at 170 °C for 1h. The flask was cooled to room temperature. Purification by flash chromatography (elution with 5% v/v ethyl acetate in hexanes) afforded enedione (–)-**3.23** (50.6 mg, 84%) as a yellow solid.

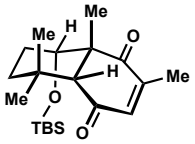

3.23

Enedione (–)-**3.23**

^{1}H NMR (500 MHz, $CDCl_3$)

δ 6.38 (m, 1H)	1.63 (dq, 1H, *J* = 13.4, 3.7 Hz)	0.91 (s, 9H)
3.23 (dd, 1H, *J* = 11.8, 3.8 Hz)	1.49 (dt, 1H, *J* = 13.8, 3.5 Hz)	0.71 (s, 3H)
2.29 (d, 1H, *J* = 1.3 Hz)	1.41 (td, 1H, *J* = 13.7, 3.5 Hz)	0.10 (s, 3H)
2.06–1.98 (m, 1H)	1.32 (s, 3H)	0.03 (s, 3H)
1.96 (d, 3H, *J* = 1.5 Hz)	0.94 (s, 3H)	

^{13}C NMR (126 MHz, $CDCl_3$)

δ 200.5	135.5	51.8	30.8	26.0	16.8
200.0	78.5	41.0	28.2	24.6	– 3.7
151.7	67.7	35.3	27.0	18.2	– 4.7

HRMS (ES+) calculated for $C_{20}H_{34}O_3SiNa$ $[M+Na]^+$: 373.2175, found 373.2174

TLC: R_f = 0.69 (20% v/v ethyl acetate in hexanes)

$[\alpha]_D^{22}$ – 25.1 (c = 2.0, $CHCl_3$)

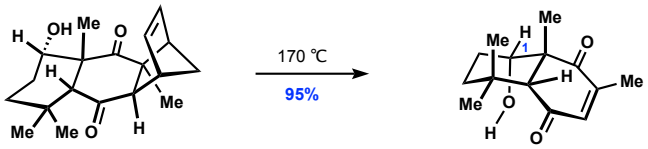

3.18 3.30

Enedione 3.30. Neat alcohol **3.18** (10.0 mg, 0.033 mmol) was heated to 170 ºC for 1h and then cooled to room temperature and placed under vacuum. No further purification was performed affording enedione **3.30** (7.4 mg as a 6:1 mixture of diastereomers at C1, 95%) as a yellow oil.

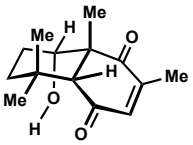

3.30

Enedione **3.30**

^{1}H NMR (500 MHz, $CDCl_3$)

δ 6.49 (m, 1H)	1.99 (d, 1H, J = 1.5 Hz)	1.46 (m, 4H)
3.97 (d, 1H, J = 11.6 Hz)	1.91–1.86 (m, 1H)	0.96 (s, 3H)
3.15 (dt, 1H, J = 11.8, 11.6 Hz)	1.82–1.73 (m, 1H)	0.72 (s, 3H)
2.34 (s, 1H)	1.55–1.52 (m, 3H)*	

* water skews integration

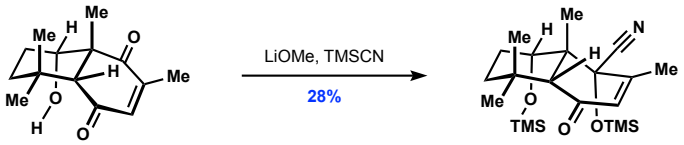

3.30 3.31

TMS Cyanohydrin 3.31. A dram vial was charged with alcohol **3.30** (5.0 mg, 0.021 mmol) and THF (0.3 mL). Then trimethylsilyl cyanide (26 µL, 0.21 mmol) was added and the reaction was stirred for 10 min followed by addition of lithium methoxide (0.8 mg, 0.21 mmol). The reaction was then stirred for 25 h at which point 10% aqueous Na_2CO_3 (2 mL) was added. The aqueous layer was extracted three times with DCM (30 mL combined). The organic layers were combined and washed with brine. The organic layer was dried over magnesium sulfate, filtered and concentrated under reduced pressure. Purification by preparative thin layer chromatography (elution with 10% v/v ethyl acetate in hexanes) afforded TMS cyanohydrin **3.31** (2.3 mg, 28%) as a white solid.

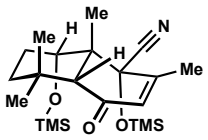

3.31

TMS Cyanohydrin **3.31.**

^{1}H NMR (500 MHz, $CDCl_3$)

δ 5.90 (s, 1H)	2.03 (s, 1H)	1.01 (s, 3H)
3.44 (dd, 1H, J = 12.1, 4.5 Hz)	1.52–1.46 (m, 3H)	0.91 (s, 3H)
2.44–2.35 (m, 1H)	1.41–1.36 (m, 1H)	0.37 (s, 9H)
2.19 (d, 3H, J = 1.2 Hz)	1.29 (s, 3H)	0.21 (s, 9H)

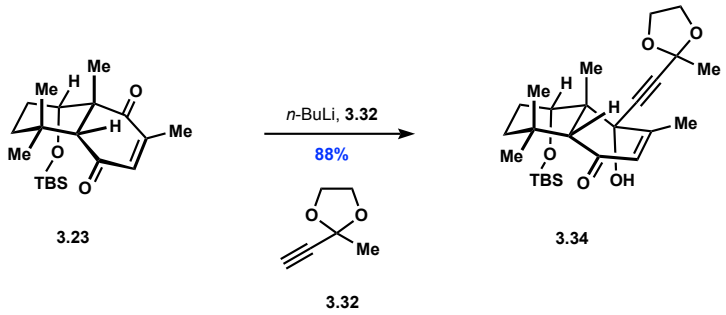

3.23 3.32 3.34

Enedione 3.34. A 250 mL round bottom flask was charged with alkyne **3.32** (3.19 g, 28.4 mmol), THF (50 mL) and cooled to –78 °C. To the solution was added *n*-butyllithium (10.5 mL of a 2.38 M solution in hexanes, 25.0 mmol) dropwise over 30 min and the solution was stirred for 30 min at –78 °C. Then racemic enedione **3.23** (4.12 g, 11.8 mmol) was added in THF (20 mL) over 15 min. The mixture was stirred for 15 min at –78 °C and warmed to 0 °C over 30 min. After 1.5 h at 0 °C the solution was slowly poured into a stirring solution of saturated aqueous NH_4Cl (120 mL) and diluted with diethyl ether (100 mL). The layers were separated and the aqueous layer was extracted twice with diethyl ether (200 mL combined). The organic layers were combined and washed with saturated aqueous $NaHCO_3$ (75 mL). The organic layer was dried over magnesium sulfate, filtered and concentrated under reduced pressure. Purification by flash chromatography (elution with 10% v/v ethyl acetate in hexanes) afforded enedione **3.34** (4.79 g, 88%) as a white solid.

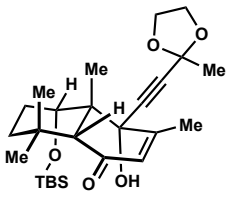

3.34

Enedione **3.34**

^{1}H NMR (500 MHz, $CDCl_3$)

δ 5.84 (d, 1H, *J* = 1.2 Hz)	1.99 (s, 1H)	0.92 (s, 3H)
4.29 (s, 1H)	1.66–1.60 (m, 4H)	0.92 (s, 3H)
3.96 (s, 4H)	1.48 (dt, 1H, *J* =13.6, 3.6 Hz)	0.21 (s, 3H)
3.52 (dd, 1H, *J* = 11.8, 5.4 Hz)	1.34–1.28 (m, 4H)	0.15 (s, 3H)
2.22–2.14 (m, 4H)	0.98 (s, 9H)	

^{13}C NMR (126 MHz, $CDCl_3$)

δ 199.8	64.9	31.1
156.1	64.8	26.2
126.4	64.6	26.1
100.9	43.5	24.3
85.8	40.4	19.3
85.3	33.5	18.1
81.1	32.1	– 4.2
73.4	31.9	– 4.8

HRMS (ES+) calculated for $C_{26}H_{42}O_5SiH$ $[M+H]^+$: 463.2280, found 463.2893

TLC: R_f = 0.47 (20% v/v ethyl acetate in hexanes)

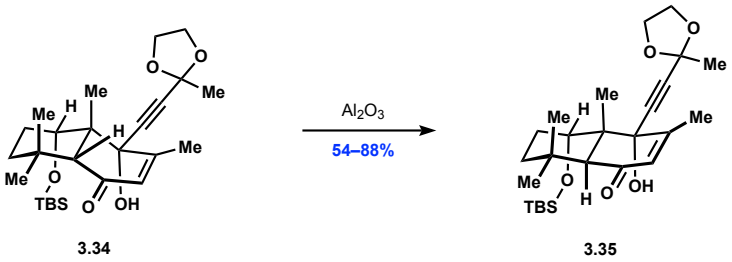

3.34 3.35

***Trans*-octalin 3.35**. A 10 mL round bottom flask was charged with enedione **3.34** (49.4 mg, 0.107 mmol), toluene (1.0 mL) and equipped with a water condenser. The flask was heated to 100 °C and basic aluminum oxide (Brockmann grade IV, 200 mg) was added over 10 sec to the vigorously stirring solution at 100 °C. The solution was heated to a vigorous reflux (oil bath 120 °C) for 30 min and then cooled to 111 °C for 17 h. The reaction mixture was cooled to room temperature and filtered through a pad of celite. The solids were washed with ethyl acetate (50 mL). The filtrate was concentrated under reduced pressure. Purification by flash chromatography (gradient elution: 100% hexanes to 20% v/v ethyl acetate in hexanes) afforded *trans*–octalin **3.35** (43.6 mg, 88%) as a colorless oil that solidified upon storage in the freezer.

Epimerization of 496 mg (1.07 mmol) of enedione **3.34** required initial addition of basic aluminum oxide (Brockmann grade IV, 2.0 g). After 18 h an additional portion of basic aluminum oxide (Brockmann grade IV, 1.0 g) was added. After 7 h the reaction was quenched and purified as described above to afford *trans*–octalin **3.35** (428 mg, 86%) as a colorless oil that solidified upon storage in the freezer.

Epimerization of enedione 4.78 g (10.3 mmol) of **3.34** required initial addition of basic aluminum oxide (Brockmann grade IV, 20 g). After 12 h an additional portion of basic aluminum oxide (Brockmann grade IV, 15 g) was added. After 6 h the reaction was filtered, concentrated, and

resubjected to the reaction conditions with basic aluminum oxide (Brockmann grade IV, 20 g). After 15 h the reaction was quenched and purified as described above to afford *trans*–octalin **3.35** (2.60 g, 54%) as a colorless oil that solidified upon storage in the freezer.

Note: The scale dependent reaction time and quantity of aluminum oxide has been previously noted in the literature for closely related systems.[9,10]

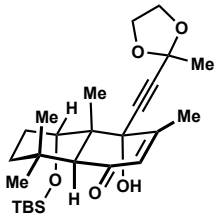

3.35

Trans-octalin **3.35**

^{1}H NMR (500 MHz, $CDCl_3$)

δ 6.55 (s, 1H)	2.07 (d, 3H, J = 1.4 Hz)	1.13–1.10 (m, 4H)
5.73 (d, 1H, *J* = 1.4 Hz)	1.93 (m, 1H)	1.05 (s, 3H)
4.25 (s, 1H)	1.74–1.69 (m, 4H)	0.96 (s, 9H)
4.06–4.00 (m, 4H)	1.56–1.53 (m, 1H)	0.28 (s, 3H)
3.12 (s, 1H)	1.25 (s, 3H)	0.21 (s, 3H)

^{13}C NMR (126 MHz, $CDCl_3$)

δ 199.5	64.9 (2 C)	25.7
154.0	50.9	21.7
127.6	47.0	21.1
100.8	35.3	20.7
86.3	33.7	18.3
82.4	32.2	– 3.8
77.1	26.5	– 4.8
77.0	26.0	

HRMS (ES+) calculated for $C_{26}H_{42}O_5SiNa$ $[M+Na]^+$: 485.2699, found 485.2692

TLC: R_f = 0.47 (20% v/v ethyl acetate in hexanes)

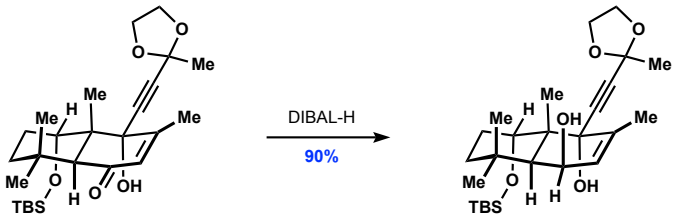

Diol 3.36. A 250 mL round bottom flask was charged with *trans*-octalin **3.35** (2.60 g, 5.62 mmol), THF (50 mL) and cooled to –78 °C. Diisobutylaluminum hydride (3.0 mL, 16.9 mmol) in THF (17 mL) was added dropwise to the solution over 15 min. After 3 h MeOH (5 mL) was added slowly at –78 °C. The solution was poured into 1 N aqueous HCl (100 mL) and extracted three times with ethyl acetate (300 mL combined). The organic layers were combined and washed with 1 N aqueous HCl (50 mL). The organic layer was dried over anhydrous magnesium sulfate, filtered and concentrated under reduced pressure. Purification by flash chromatography (elution with 20% v/v ethyl acetate in hexanes) afforded diol **3.36** (2.36 g, 90%) as a white foam.

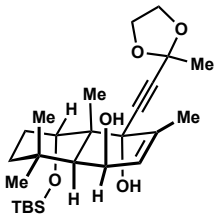

Diol **3.36**

^{1}H NMR (500 MHz, $CDCl_3$)

δ 6.54 (s, 1H)	2.00–1.94 (m, 1H)	1.18 (s, 3H)
5.56–5.57 (m, 1H)	1.92 (d, 3H, *J* = 1.4 Hz)	1.13 (s, 3H)
4.51 (m, 1H)	1.80 (t, 1H, *J* = 13.9 Hz)	1.10–1.05 (m, 1H)
4.20 (m, 1H)	1.71 (s, 3H)	0.93 (s, 9H)
4.06–3.98 (m, 4H)	1.57–1.54 (m, 1H)	0.25 (s, 3H)
2.29 (d, 1H, *J* = 5.1 Hz)	1.32 (s, 3H)	0.18 (s, 3H)

^{13}C NMR (126 MHz, $CDCl_3$)

δ 136.5	64.8	26.5
126.1	64.7	26.0
100.9	42.8	25.9
85.1	40.7	21.1
84.1	37.1	20.8
78.3	34.1	18.3
77.0	32.6	– 3.9
66.1	26.7	– 4.8

HRMS (ES+) calculated for $C_{26}H_{44}O_5SiNa$ $[M+Na]^+$: 487.2856, found 487.2849

TLC: R_f = 0.19 (20% v/v ethyl acetate in hexanes)

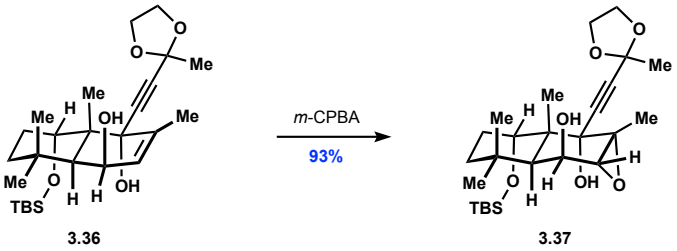

Epoxide 3.37. A 250 mL round bottom flask was charged with diol **3.36** (2.36 g, 5.08 mmol), $NaHCO_3$ (427 mg, 5.08 mmol), THF (25 mL) and cooled to 0 °C. To the solution was added *m*-CPBA (6.30 g, 70-75 wt%) in DCM (25 mL) over 15 min and the reaction mixture was warmed to 30 °C. After 8.5 h the reaction mixture was cooled 0 °C and saturated aqueous $Na_2S_2O_3$ (75 mL) and saturated aqueous $NaHCO_3$ (75 mL) was added slowly to the solution. The aqueous layer was extracted three times with ethyl acetate (300 mL combined) and the combined organic layers were washed with saturated aqueous $NaHCO_3$ (75 mL) followed by saturated aqueous $Na_2S_2O_3$ (50 mL) and saturated aqueous $NaHCO_3$ (50 mL). The organic layer was dried over magnesium sulfate, filtered and concentrated under reduced pressure. Purification by flash chromatography (gradient elution: 20% to 50% v/v ethyl acetate in hexanes) afforded epoxide **3.37** (2.26 g, 93%) as a white solid.

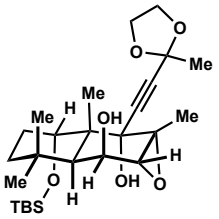

3.37

Epoxide **3.37**

^{1}H NMR (500 MHz, $CDCl_3$)

δ 6.45 (s, 1H)	1.76 (t, 1H, *J* = 13.3 Hz)	1.09 (s, 3H)
4.61 (s, 1H)	1.72 (s, 3H)	1.06–1.03 (m, 1H)
4.16 (s, 1H)	1.61 (bs, 1H)	0.92 (s, 9H)
4.07–3.99 (m, 4H)	1.56 (s, 3H)	0.25 (s, 3H)
3.02 (s, 1H)	1.55–1.50 (m, 1H)	0.17 (s, 3H)
1.98 (d, 1H, *J* = 4.3 Hz)	1.30 (s, 3H)	
1.86 (dt, 1H, *J* = 14.1, 2.1 Hz)	1.22 (s, 3H)	

^{13}C NMR (126 MHz, $CDCl_3$)

δ 100.9	60.0	26.5
85.7	43.5	26.1
83.9	37.3	23.5
78.6	36.9	20.7
75.9	34.0	18.4
67.0	32.5	– 4.3
64.9 (2 C)	27.4	– 4.7
62.7	26.6	

HRMS (ES+) calculated for $C_{26}H_{44}O_6SiNa$ $[M+Na]^+$: 503.2805, found 503.2808

TLC: R_f = 0.57 (70% v/v ethyl acetate in hexanes)

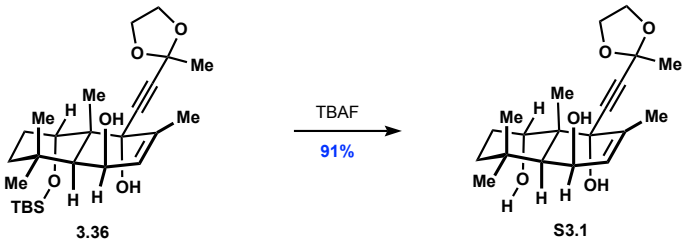

Triol S3.1. A 50 mL round bottom flask was charged with diol **3.36** (338 mg, 0.73 mmol) and THF (5 mL). Then TBAF (0.8 mL, 1M solution in THF, 0.80 mmol) was added at 0 ºC over 5 min and the reaction was warmed to room temperature. After 20 min the reaction was diluted with ethyl acetate (30 mL) and poured into a mixture of 10% aqueous Na_2CO_3 (15 mL) and brine (5mL). The aqueous layer was extracted twice with ethyl acetate (60 mL combined). The organic layers were combined and filtered through a pad of silica to afforded triol **S3.1** (231 mg, 91%) as a white foam.

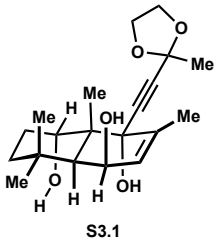

Triol **S3.1**

^{1}H NMR (500 MHz, $CDCl_3$)

δ 5.60 (m, 1H)	2.10 (dt, 1H, J = 14.4, 2.7 Hz)	1.34 (s, 3H)
5.43 (m, 1H)	1.94 (s, 3H)	1.20 (s, 3H)
4.23 (m, 1H)	1.83 (td, 1H, J = 13.9, 2.6 Hz)	1.18–1.15 (m, 4H)
4.10–4.01 (m, 4H)	1.74 (s, 3H)	
2.28 (d, 1H, J = 5.2 Hz)	1.50 (dq, 1H, J = 14.7, 3.2 Hz)	

^{13}C NMR (126 MHz, $CDCl_3$)

δ 135.9	77.4	40.4	26.3
126.6	75.7	37.0	25.6
100.9	66.0	34.1	21.1
84.9	64.7	32.4	20.8
83.4	42.5	27.6	

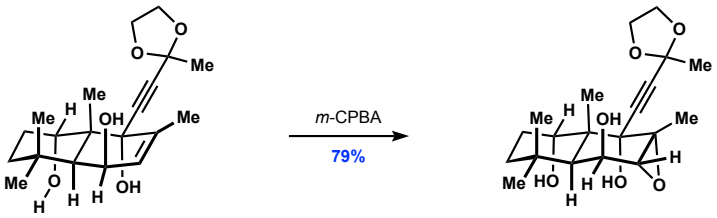

S3.1 3.38

Epoxide 3.38. A round bottom flask was charged with triol **S3.1** (31.8 mg, 0.091 mmol), $NaHCO_3$ (53 mg, 0.63 mmol), and THF (0.8 mL). A suspension of *m*-CPBA (70–75 wt%, 115 mg, 0.45 mmol) in DCM (0.8 mL) was then added to the flask over 15 min and the reaction was warmed to 40 ºC. After 22 h an suspension of *m*-CPBA (115 mg, 0.45 mmol, 70–75 wt%) in DCM (0.8 mL) was added and after 2.5 h the reaction mixture was cooled 0 °C and saturated aqueous $Na_2S_2O_3$ and saturated aqueous $NaHCO_3$ was added slowly to the solution. The aqueous layer was extracted three times with ethyl acetate and the combined organic layers were washed with saturated aqueous $NaHCO_3$. The organic layer was dried over magnesium sulfate, filtered and concentrated under reduced pressure. Purification by flash chromatography (gradient elution: 20% to 50% v/v ethyl acetate in hexanes) afforded epoxide **3.38** (26.9 mg, 79%) as a white solid with a small amount of DCM present (0.8mg, 3% w/w).

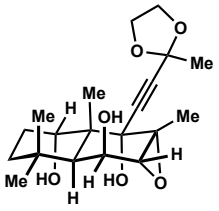

3.38

Epoxide **3.38**

^{1}H NMR (500 MHz, $CDCl_3$)

δ 4.59 (m, 1H)	1.77–1.72 (m, 4H)	1.37 (s, 3H)
4.08–4.02 (m, 5H)	1.61 (d, 1H, J = 4.2)	1.17 (s, 3H)
3.30 (s, 1H)	1.59 (s, 3H)	1.08 (s, 3H)
1.96 (m, 1H)	1.56 (m, 1H)	1.05–1.02 (m, 1H)

^{13}C NMR (126 MHz, $CDCl_3$)

δ 100.7	66.0	36.8	26.1
86.6	65.9	36.7	22.5
80.8	64.9 (2C)	34.2	20.1
76.7	62.2	32.7	
74.7	42.9	27.3	

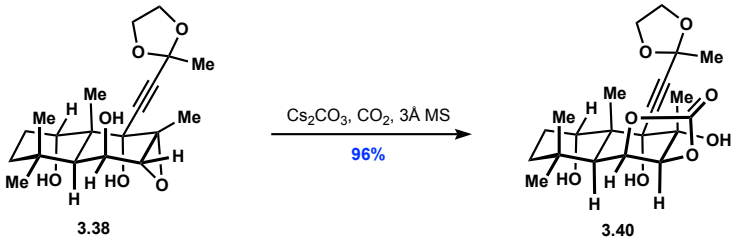

3.38 3.40

Carbonate 3.40. A 50 mL round bottom flask was charged with Cs_2CO_3 (39 mg, 0.12 mmol) and 3 Å molecular sieves (108 mg). The mixture was flamed dried under vacuum and cooled under a balloon of CO_2. To the mixture was added a solution of epoxide **3.38** (217 mg, 0.60 mmol) in DMF (3 mL). The reaction mixture was warmed to 50 °C for 6 h. The flask was then cooled to room temperature and saturated aqueous NH_4Cl (7.5 mL), water (7.5 mL), and ethyl acetate (25 mL) was added. The layers were separated, and the aqueous layer was extracted twice with ethyl acetate (50 mL combined). The organic layers were combined and dried over magnesium sulfate, filtered and concentrated under reduced pressure. No further purification was performed affording carbonate **3.40** (233 mg, 96%) as a white solid.

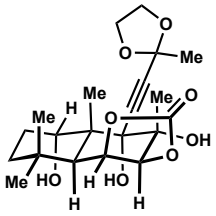

3.40

Carbonate **3.40**

^{1}H NMR (500 MHz, $CDCl_3$)

δ 6.11 (bs, 1H)	2.50 (bs, 1H)	1.55–1.50 (m, 1H)
5.07 (dd, 1H, J = 6.8, 3.6 Hz)	2.39 (d, 1H, J = 3.6)	1.44 (s, 3H)
4.69 (d, 1H, J = 6.9 Hz)	2.21 (m, 1H)	1.28–1.25 (m, 5H)
4.08–4.02 (m, 5H)	1.78 (dt, 1H, J = 13.9, 3.7)	1.19 (s, 3H)
3.52 (s, 1H)	1.73 (s, 3H)	1.13 (s, 3H)

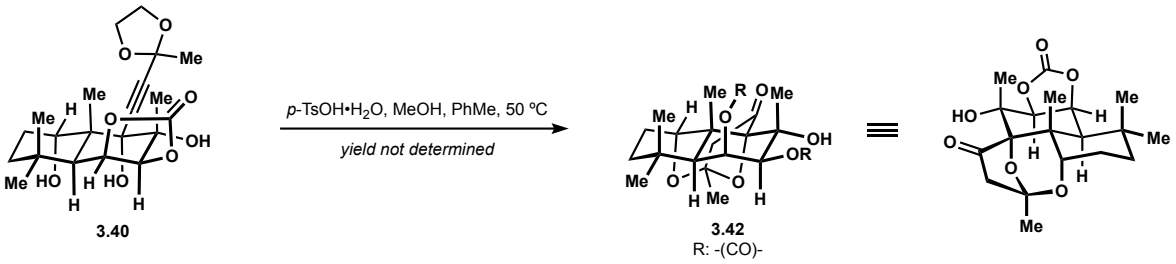

Ketal 3.42. A round bottom flask was charged with carbonate **3.40** (55 mg, 0.13 mmol) and *p*-TsOH·H_2O (29 mg, 0.15 mmol) and toluene (1.5 mL). The reaction was heated to 50 ºC for 2h, then cooled to room temperature diluted with saturated aqueous $NaHCO_3$ and extracted with ethyl acetate. The organic layer was dried over magnesium sulfate, filtered and concentrated under reduced pressure. Purification by flash chromatography afforded ketal **3.42** (yield not determined, characterized by X-ray crystallography).

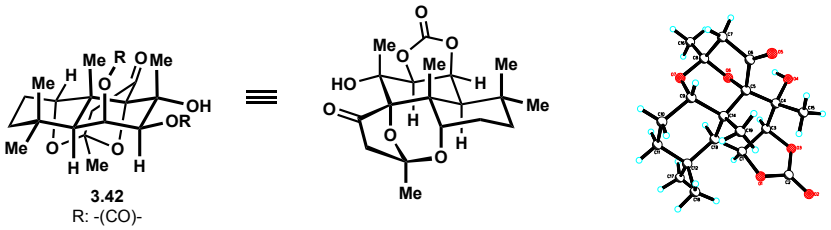

Ketal **3.42**

^{1}H NMR (500 MHz, $CDCl_3$)

δ 5.05 (dd, 1H, J = 6.7, 3.3 Hz)	2.57 (d, 1H, J = 18.3Hz)	1.63 (s, 3H)
4.49 (d, 1H, J = 6.7 Hz)	2.52 (d, 1H, J = 18.3 Hz)	1.56 (m, 3H)*
3.45 (m, 1H)	2.01 (dt, 1H, J = 14.4, 3.6 Hz)	1.27–1.24 (m, 4H)
2.84 (bs, 1H)	1.72 (td, 1H, J = 13.7, 4.2 Hz)	1.16 (s, 3H)
2.66 (d, 1H, J = 3.3 Hz)	1.65 (s, 3H)	1.13 (s, 3H)

* water skews integration

^{13}C NMR (126 MHz, $CDCl_3$)

δ 209.7	78.4	36.4	22.9
155.1	73.7 (2C)	33.9	17.7
103.2	47.8	32.3	16.6
88.3	40.1	24.8	

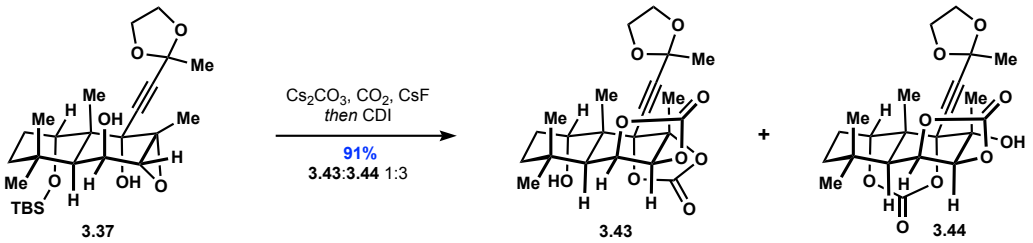

Cyclic carbonates 3.43 and 3.44. A 100 mL round bottom flask was charged with Cs_2CO_3 (301 mg, 0.925 mmol), CsF (768 mg, 5.06 mmol), and 3 Å molecular sieves (1.14 g). The mixture was flamed dried under vacuum and cooled under a balloon of CO_2. To the mixture was added a solution of epoxide **3.37** (2.16 g, 4.49 mmol) in DMF (25 mL). The reaction mixture was warmed to 70 °C for 10 h. The flask was then cooled to 0 °C and carbonyldiimidazole (1.45 g, 8.94 mmol) was added portion wise over 5 min. The flask was warmed to room temperature for 2.5 h and then diluted with ethyl acetate (100 mL), brine (50 mL), and saturated aqueous $CaCO_3$ (25 mL). The layers were separated and the aqueous layer was extracted twice with ethyl acetate (200 mL combined). The organic layers were combined and washed sequentially with brine (25 mL), 1 N aqueous HCl (25 mL), and saturated aqueous $NaHCO_3$ (50 mL). The organic layer was dried over magnesium sulfate, filtered and concentrated under reduced pressure. Purification by flash chromatography (gradient elution: 20% to 50% v/v ethyl acetate in hexanes) afforded a 1:3 mixture of **3.43** and **3.44** (1.78 g, 91%) as a white solid.

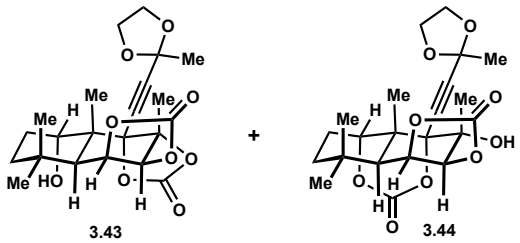

3.43 + 3.44

Cyclic carbonates **3.43** and **3.44**

^{1}H NMR (500 MHz, $CDCl_3$)

δ 5.25 (dd, 1 H, *J* = 8.0, 3.7 Hz)	2.27 (d, 1 H, *J* = 3.6 Hz)	1.46 (s, 9 H)
5.11 (dd, 3 H, *J* = 7.3, 3.1 Hz)	2.12–2.05 (m, 3 H)	1.41–1.37 (m, 3 H)
4.79 (d, 1 H, *J* = 7.9 Hz)	1.99–1.94 (m, 8 H)	1.25–1.21 (m, 17 H)
4.67 (d, 3 H, *J* = 7.4 Hz)	1.75 (s, 3 H)	1.17 (s, 3 H)
4.08–4.01 (m, 16 H)	1.73 (s, 3 H)	1.14 (s, 9 H)
3.99 (m, 1 H)	1.72 (s, 9 H)	
3.05 (bs, 3 H)	1.65 (dt, 3 H, *J* = 14.0, 4.2 Hz)	
2.50 (bs, 1 H)	1.57 (s, 9 H)	

^{13}C NMR (126 MHz, $CDCl_3$)

δ 154.3	82.1	43.4	25.9
153.0	81.7	40.2	25.1
150.8	80.9	38.7	25.0
148.1	76.5	38.0	23.3
100.6	76.2	35.5	22.9
100.6	75.9	35.4	22.9
92.5	75.2	34.6	20.2
91.2	74.4	33.8	19.9
90.8	73.3	32.3	18.9
88.3	65.2	32.2	
87.0	65.1	26.1	

HRMS (ES+) calculated for $C_{22}H_{28}O_9Na$ $[M+Na]^+$: 459.1631, found 459.1631

TLC: R_f of **3.43** = 0.73 (70% v/v ethyl acetate in hexanes)

R_f of **3.44** = 0.62 (70% v/v ethyl acetate in hexanes)

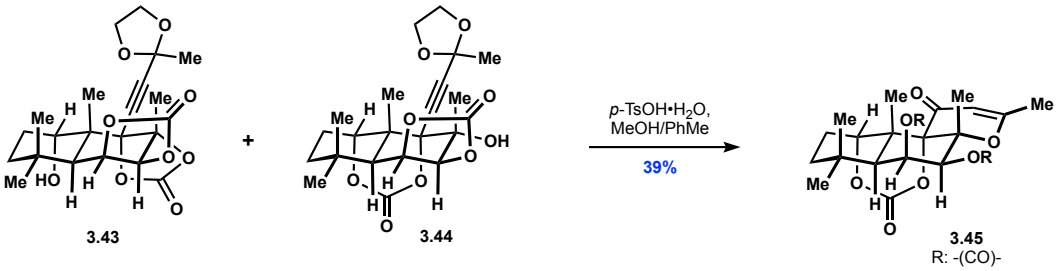

Dihydro-γ-pyrone 3.45. A 10 mL round bottom flask was charged with biscarbonates **3.43** and **3.44** (77.8 mg of a 1:3 mixture, 0.18 mmol), *p*-TsOH·H_2O (34 mg, 0.18), MeOH (36 µL) and toluene (1 mL). The reaction was warmed to 50 ºC for 7h then saturated aqueous $NaHCO_3$ (5 mL) was added followed by DCM (20 mL). The layers were separated and the aqueous layer was extracted twice with DCM (40 mL combined). The organic layers were combined, dried over magnesium sulfate, filtered and concentrated under reduced pressure. Purification by recrystallization from ethyl acetate afforded dihydro-γ-pyrone **3.45** (27.1 mg, 39%) as a white solid.

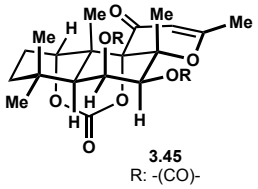

Dihydro-γ-pyrone **3.45**

^{1}H NMR (500 MHz, $CDCl_3$)

δ 5.55 (m, 1H)	2.06 (s, 3H)	1.44 (s, 3H)
5.34 (s, 1H)	1.95–1.90 (m, 1H)	1.38 (m, 1H)
5.16 (dd, 1H, J = 6.7, 3.4 Hz)	1.79 (d, 1H, J = 3.4 Hz)	1.24 (s, 3H)
5.08 (d, 1H, J = 6.8 Hz)	1.67–.160 (m, 4H)	1.15 (s, 3H)
2.18–2.11 (m, 1H)	1.54 (s, 3H)	

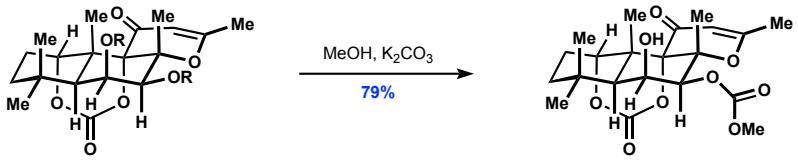

3.45
R: -(CO)-

3.51

Dihydro-γ-pyrone 3.51. A dram vial was charged with dihydro-γ-pyrone **3.45** (4.9 mg, 0.012 mmol), DCM (0.1 mL), and MeOH (0.1 mL). The reaction cooled to 0 ºC and K_2CO_3 (3.9 mg, 0.028 mmol) was added. After 10 min water was added and the aqueous layer was extracted with DCM. The organic layers were combined, dried over magnesium sulfate, filtered and concentrated under reduced pressure. Purification by preparative thin layer chromatography (elution with 33% v/v ethyl acetate in hexanes) afforded dihydro-γ-pyrone **3.51** (4.2 mg, 79%) as a white solid.

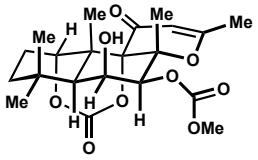

3.51

Dihydro-γ-pyrone **3.51**

^{1}H NMR (500 MHz, $CDCl_3$)

δ 5.68 (m, 1H)	2.30 (d, 1H, 4.0 Hz)	1.64–1.58 (m, 2H)
5.43 (m, 1H)	2.12–2.06 (m, 1H)	1.53 (s, 3H)
5.30 (s, 1H)	2.03 (s, 3H)	1.29–1.24 (m, 2H)
4.40 (t, 1H, J = 4.0 Hz)	1.84 (dq, 1H, J = 15.5, 3.3 Hz)	1.10 (s, 3H)
3.85 (s, 3H)	1.69 (s, 3H)	1.06 (s, 3H)

Key NOESY correlations:

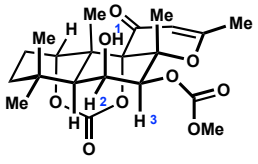

3.51

^{1}H (arbitrary numbering)	Key correlations
H2 (4.40 ppm)	H1 (2.30 ppm) H3 (5.68 ppm)

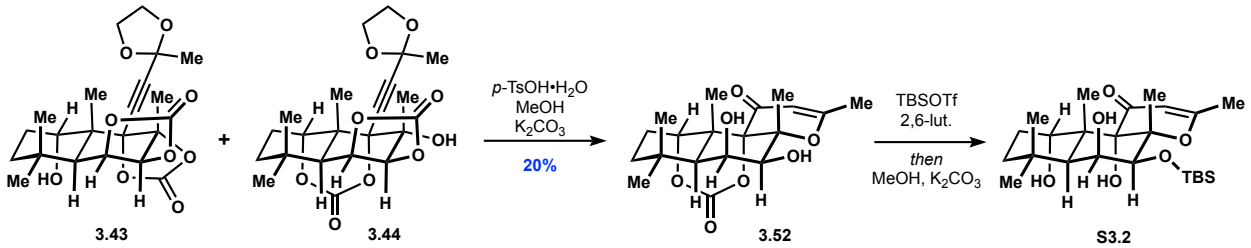

Dihydro-γ-pyrones 3.52 and S3.2. A dram vial was charged with biscarbonates **3.43** and **3.44** (19.7 mg of a 1:3 mixture, 0.045 mmol), *p*-TsOH·H_2O (9.7 mg, 0.51 mmol), MeOH (10 µL, 0.25 mmol) and toluene (0.25 mL) then the reaction was heated to 50 ºC. After 7h K_2CO_3 (38.2 mg, 0.27 mmol), DCM (0.15 mL), and MeOH (0.15 mL) were added and the reaction was stirred for an additional 2 h at which point it was diluted with water and extracted with ethyl acetate (30 mL combined). The organic layers were combined, dried over sodium sulfate, filtered and concentrated under reduced pressure. Purification by preparative thin layer chromatography (elution with 50% v/v ethyl acetate in hexanes) afforded dihydro-γ-pyrone **3.52** (3.3 mg, 20%) as a white solid.

Silyl ether S3.2. For structural characterization silyl ether **S3.2** was prepared according to the following procedures. A dram vial was charged with dihydro-γ-pyrone **3.52** (10.2 mg, 0.028mmol), 2,6-lutidine (15.0 µL, 0.13 mmol), and DCM (0.2 mL). The solution was cooled to 0 ºC and TBSOTf (13.0 µL, 0.056 mmol) was added slowly. After 10 min saturated aqueous $NaHCO_3$ was added and extracted with DCM. Purification by preparative thin layer chromatography (elution with 10% v/v ethyl acetate in hexanes) afforded a tentatively assigned bis-silyl ether that was treated with MeOH and K_2CO_3 at 50 ºC and then isolated by preparative thin layer chromatography (elution with 10% v/v ethyl acetate in hexanes) to afford silyl ether **S3.2** (yield not determined).

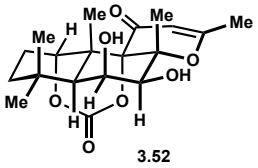

3.52

Dihydro-γ-pyrone **3.52**

^{1}H NMR (500 MHz, $CDCl_3$)

δ 5.40 (m, 1H)	2.27 (s, 1H)	1.62–1.55 (m, 8H)*
5.29 (s, 1H)	2.16–2.08 (m, 1H)	1.44 (d, 1H, J = 2.3 Hz)
4.54 (m, 1H)	2.02 (s, 3H)	1.28–1.23 (m, 4H)
4.22 (d, 1H, J = 3.9 Hz)	1.86 (m, 1H)	1.07 (s, 3H)
2.41 (bs, 1H)	1.73 (s, 3H)	

* water skews integration

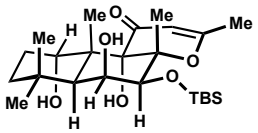

S3.2

Silyl ether **S3.2**

^{1}H NMR (500 MHz, $CDCl_3$)

δ 7.19 (bs, 1 H)	2.13 (d, 1H, J = 1.8 Hz)	1.15 (dt, 1H, J = 13.3, 3.3 Hz)
5.17 (s, 1H)	1.94 (s, 3H)	1.09 (s, 3H)
5.00 (bs, 1H)	1.73 (td, 1H, J = 13.9, 3.3 Hz)	0.95 (s, 9H)
4.40 (d, 1H, J = 4.3 Hz)	1.58 (s, 3H)	0.18 (s, 3H)
4.30 (m, 1H)	1.14–1.38 (m, 1H)	0.15 (s, 3H)
2.54 (s, 1H)	1.36 (s, 3H)	
2.28–2.22 (m, 2H)	1.27 (s, 3H)	

Key NOESY correlations:

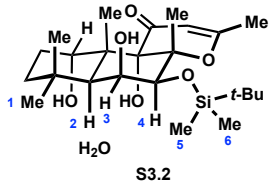

S3.2

^{1}H (arbitrary numbering)	Key correlations
H1 (1.58 ppm)	H2 (2.13 ppm) H3 (4.30 ppm)
H3 (4.30 ppm)	H2 (2.13 ppm) H4 (4.40 ppm)
H4 (4.40 ppm)	H5/H6 (0.18/0.15 ppm)

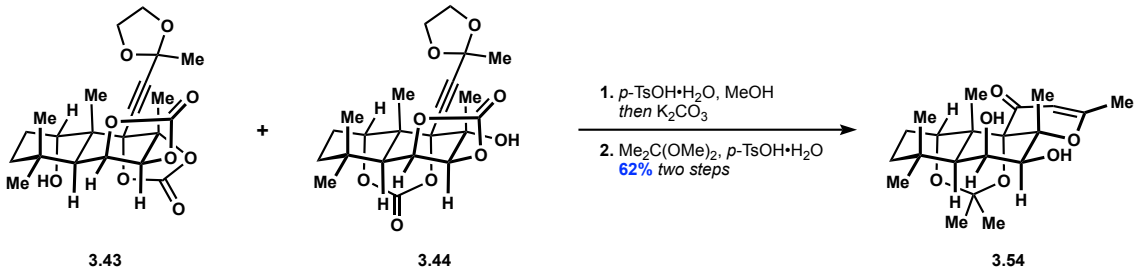

3.43 3.44 3.54

Acetonide 3.54. A 10 mL round bottom flask was charged with cyclic carbonates **3.43** and **3.44** (105.4 mg of a 1:3 mixture of **3.43**:**3.44**, 0.2425 mmol), *p*-TsOH·H_2O (42.0 mg, 0.221 mmol), MeOH (50 µL, 1.2 mmol) and toluene (1.0 mmol). The reaction mixture was heated to 50 °C for 10 h and then cooled to room temperature. To the reaction mixture was added K_2CO_3 (200.0 mg, 1.447 mmol) followed by MeOH (1.0 mL). The solution was heated to 50 °C for 2 h, then cooled to room temperature and diluted with brine (10 mL) and ethyl acetate 15 (mL). The layers were separated and the aqueous layer was extracted twice with ethyl acetate (30 mL combined). The organic layers were combined, dried over magnesium sulfate, filtered and concentrated under reduced pressure. To the crude material was then added *p*-TsOH·H_2O (42.0 mg, 0.221 mmol), acetone (0.5 mL), and 2,2-dimethoxypropane (0.5 mL). The solution was stirred at room temperature for 5 min, quenched with saturated aqueous $NaHCO_3$ (10 mL) and diluted with ethyl acetate (15 mL). The layers were separated and the aqueous layer was extracted twice with ethyl acetate (30 mL combined). The organic layers were combined, dried over magnesium sulfate, filtered and concentrated under reduced pressure. Purification by preparative thin layer chromatography (elution with 20% v/v ethyl acetate in hexanes) afforded acetonide **3.54** (56.9 mg, 62% over two steps) as a white solid. Acetonide **3.54** was crystalized by dissolving in $CDCl_3$ in a dram vial fitted with a septum and allowing for slow evaporation of the solvent.[26]

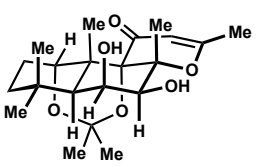

3.54

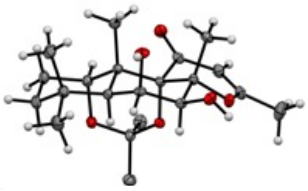

Acetonide **3.54**

^{1}H NMR (500 MHz, $CDCl_3$)

δ 5.17 (s, 1H)	2.20 (d, 1H, *J* = 2.6)	1.48–1.45 (m, 4H)
4.52 (m, 1H)	2.13–2.10 (m, 2H)	1.34 (s, 3H)
4.51 (m, 1H)	1.93 (s, 3H)	1.31 (s, 3H)
4.24 (d, 1H, *J* = 3.8 Hz)	1.78 (dt, 1H, *J* = 13.5, 3.9 Hz)	1.27 (s, 3H)
2.36 (bs, 1H)	1.62 (s, 3H)	1.09–1.05 (m, 4H)

^{13}C NMR (126 MHz, $CDCl_3$)

δ 196.1	71.4	31.9
167.7	70.2	25.0
103.8	43.0	23.8
99.5	38.1	22.3
88.3	36.5	20.9
78.0	34.4	17.8
72.7	33.6	15.6

HRMS (ES+) calculated for $C_{21}H_{32}O_6Na$ $[M+Na]^+$: 403.2097, found 403.2104

TLC: R_f = 0.26 (30% v/v ethyl acetate in hexanes)

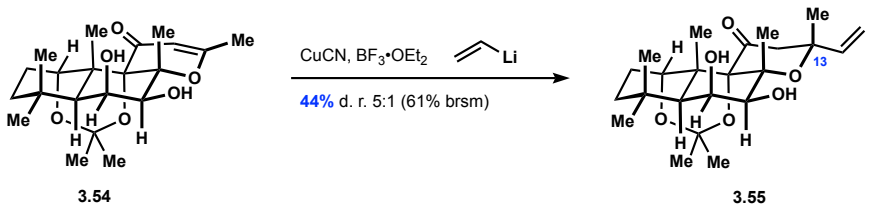

Tetrahydropyranone 3.55. A 5 mL round bottom flask was charged with tetravinyltin (29 µL, 0.16 mmol) followed by dropwise addition of *n*-butyllithium (0.22 mL of a 2.44 M solution in hexane, 0.54 mmol). The solution was stirred at room temperature for 1 h and then diluted with diethyl ether (0.75 mL). The solution of vinyl lithium was added dropwise to a suspension of CuCN (23.5 mg, 0.262 mmol) in diethyl ether (0.25 mL) at –78 °C. The solution was warmed to 0 °C for 5 min and then cooled to –78 °C. To the solution was slowly added $BF_3 \cdot OEt_2$ (32 µL, 0.259) followed by acetonide **3.54** (20.3 mg, 0.0534 mmol). The reaction mixture was then warmed to –55 °C. After 1 h the reaction mixture was cooled to –78 °C and a second portion of divinyl cuprate (0.26 mmol) was added followed by $BF_3 \cdot OEt_2$ (32 µL, 0.259). The reaction mixture was warmed to –55 °C and after 1 h a third portion of divinyl cuprate (0.26 mmol) was added followed by $BF_3 \cdot OEt_2$ (32 µL, 0.259) at –78 °C. The reaction mixture was warmed to –55 °C and after 1 h the reaction was quenched with 1 N aqueous HCl (20 mL sparged under argon for 15 min). The biphasic solution was warmed to room temperature and diluted with ethyl acetate (20 mL). The layers were separated and the aqueous layer was extracted twice with ethyl acetate (40 mL combined). The organic layers were combined and washed sequentially with 1 N aqueous HCl (5 mL) and saturated aqueous $NaHCO_3$ (5 mL). The organic layers were combined and dried over anhydrous sodium sulfate, filtered and concentrated under reduced pressure. Purification by flash chromatography (elution with 5% v/v ethyl acetate in hexanes) afforded tetrahydropyranone **3.55** (9.6 mg as 5:1 mixture of diastereomers at C13, 44%) as a white solid and recovered acetonide **3.54** (6.2 mg, 28%).

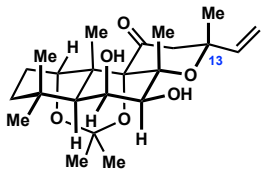

3.55

Tetrahydropryanone **3.55** (5:1 mixture of diastereomers at C13)

^{1}H NMR (500 MHz, $CDCl_3$

δ 6.07 (dd, 5 H, *J* = 17.2, 10.7 Hz)	3.98 (m, 1 H)	1.80–1.74 (m, 6 H)
5.99 (dd, 1 H, *J* = 17.6, 10.9 Hz)	3.02 (d, 1 H, *J* = 17.4 Hz)	1.57 (m, 20 H)*
5.19 (dd, 5 H, *J* = 17.4, 1.2 Hz)	2.97 (d, 5 H, *J* = 19.3 Hz)	1.46 (m, 20 H)
5.09 (d, 1 H, *J* = 17.6 Hz)	2.84 (d, 1 H, *J* = 17.4 Hz)	1.44 (m 4 H)
4.96 (m, 6 H)	2.66 (d, 5 H, *J* = 19.3 Hz)	1.40–1.37 (m, 36 H)
4.48 (m, 6 H)	2.38 (s, 5 H)	1.28 (m, 30 H)
4.29 (m, 5 H)	2.33 (s, 1 H)	1.25 (m, 6 H)
4.22 (m, 1H)	2.14 (s, 5 H)	1.08–1.05 (m, 24 H)
4.00 (d, 5 H, *J* = 2.5 Hz)	2.12–2.06 (m, 17 H)	

* water skews integration

^{13}C NMR (126 MHz, $CDCl_3$)

δ 207.0	74.9	42.9	32.6	21.5
147.8	74.4	42.8	31.8	17.9
147.5	74.3	38.1	31.6	17.8
111.0	70.6	36.3	25.1	
110.4	70.6	36.3	23.8	
99.8	70.3	34.4	23.8	
81.4	50.2	33.7	22.4	
80.8	48.3	33.3	22.3	

HRMS (ES+) calculated for $C_{23}H_{36}O_6Na$ $[M+Na]^+$: 431.2410, found 431.2408

TLC: R_f = 0.55 (30% v/v ethyl acetate in hexanes)

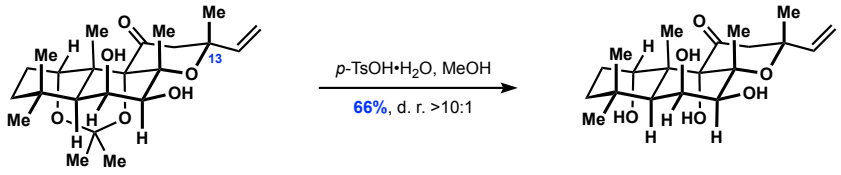

3.55 3.59

7-deacetylforskolin 3.59. 7-deacetylforskolin **3.59** was prepared according to conditions previously described by Lett.[8] A dram vial was charged with acetonide **3.55** (9.5 mg of **3.55** with a 5:1 d.r. at C13, 0.023 mmol), *p*-TsOH·H_2O (5.0 mg, 0.026 mmol), DCM (0.1 mL), and MeOH (0.1 mL), then the vial was sealed. After 27 h the reaction mixture was quenched with saturated aqueous $NaHCO_3$ (5 mL). The aqueous later was extracted three times with ethyl acetate (30 mL combined). The organic layers were combined and dried over anhydrous sodium sulfate, filtered and concentrated under reduced pressure. Purification by flash chromatography (elution with 15% v/v ethyl acetate in hexanes) afforded 7-deacetylforskolin **3.59** (4.7 mg, 66%) as a white solid.

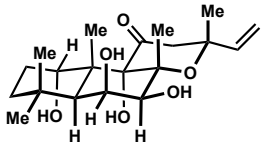

3.59

7-deacetylforskolin **3.59**

^{1}H NMR (500 MHz, $CDCl_3$)

δ 6.41 (s, 1H)	3.18 (d, 1H, *J* = 17.3 Hz)	1.65 (s, 3H)
6.12 (dd, 1H, *J* = 17.4, 10.7 Hz)	2.51 (d, 1H, *J* = 17.3 Hz)	1.41 (m, 7H)
5.20 (d, 1H, *J* = 17.4 Hz)	2.48 (d, 1H, *J* = 2.9 Hz)	1.27 (s, 3H)
4.99 (d, 1H, *J* = 10.7 Hz)	2.38 (d, 1H, *J* = 3.8 Hz)	1.14–1.12 (m, 1H)
4.64 (m, 1H)	2.27–2.20 (m, 2H)	1.07 (s, 3H)
4.49 (m, 1H)	2.11 (s, 1H)	
4.14 (m, 1H)	1.73 (dt, 1H, *J* = 13.9, 3.2 Hz)	

^{13}C NMR (126 MHz, $CDCl_3$)

δ 205.8	82.4	70.6	36.2	27.1
146.7	75.3	48.9	34.5	24.3
110.6	75.0	43.2	33.2	23.6
82.5	74.9	43.0	31.0	20.2

HRMS (ES+) calculated for $C_{20}H_{32}O_6Na$ $[M+Na]^+$: 391.2097, found 391.2101

TLC: R_f = 0.24 (30% v/v ethyl acetate in hexanes)

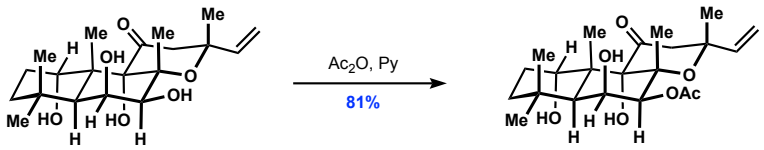

3.59 forskolin (**3.1**)

Forskolin 3.1. Forskolin **3.1** was prepared according to conditions previously described by Bhat.[23] A dram vial was charged with 7-deacetylforskolin **3.59** (4.8 mg, 0.014 mmol) and pyridine (0.25 mL). The solution was cooled to 0 °C and acetic anhydride (0.05 mL) was slowly added. The reaction mixture was stirred at 0 °C for 19 h. Then water (5 mL) was added and mixture was warmed to room temperature. The aqueous layer was extracted three times with $CHCl_3$ (30 mL combined). The organic layers were combined and dried over anhydrous sodium sulfate, filtered and concentrated under reduced pressure. Purification by flash chromatography (gradient elution: 0% to 5% v/v ethyl acetate in DCM) afforded forskolin **3.1** (4.3 mg, 81%) as a white solid.

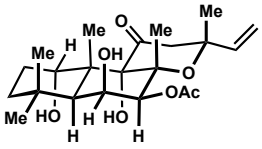

forskolin (**3.1**)

Forskolin **3.1**

^{1}H NMR (500 MHz, $CDCl_3$)

δ 6.00 (s, 1H)	4.46 (s, 1H)	1.71 (s, 3H)
5.94 (dd, 1H, *J* = 17.2, 10.7 Hz)	3.19 (d, 1H, *J* = 17.1 Hz)	1.44–1.41 (m, 4H)
5.48 (d, 1H, *J* = 4.1 Hz)	2.93 (s, 1H)	1.34 (s, 3H)
5.30 (d, 1H, *J* = 17.1 Hz)	2.48 (d, 1H, *J* = 17.1 Hz)	1.26 (s, 3H)
4.98 (d, 1H, *J* = 10.7 Hz)	2.20–2.15 (m, 5H)	1.12–1.09 (m, 1H)
4.58 (s, 1H)	1.79–1.75 (m, 2H)	1.04 (s, 3H)

^{13}C NMR (126 MHz, $CDCl_3$)*

δ 205.5	82.8	74.6	43.0	31.8	21.4
169.8	81.6	70.2	36.3	26.8	20.0
146.4	76.7	48.9	34.6	24.5	
111.0	75.2	43.2	33.2	23.8	

*$CDCl_3$ calibrated to 77.2 ppm for comparison purposes.[9]

HRMS (ES+) calculated for $C_{22}H_{34}O_7Na$ $[M+Na]^+$: 433.2202, found 433.2213

TLC: R_f = 0.39 (15% v/v ethyl acetate in DCM)

Comparison of ^{13}C NMR data for synthetic forskolin (**3.1**) to literature values ($CDCl_3$; δ, ppm)

This work	Švenda et al.[9]	Δ
205.5	205.5	0.0
169.8	169.8	0.0
146.4	146.5	–0.1
111.0	111.0	0.0
82.8	82.9	–0.1
81.6	81.7	–0.1
76.7	76.7	0.0
75.2	75.2	0.0
74.6	74.7	–0.1
70.2	70.2	0.0
48.9	48.9	0.0
43.2	43.2	0.0
43.0	43.0	0.0
36.3	36.3	0.0
34.6	34.7	–0.1
33.2	33.2	0.0
31.8	31.8	0.0
26.8	26.8	0.0
24.5	24.6	–0.1
23.8	23.8	0.0
21.4	21.4	0.0
20.0	20.1	–0.1

3.5 References and Notes

1. Insel, P. A.; Ostrom, R. S. Forskolin as a tool for examining adenylyl cyclase expression, regulation, and G protein signaling. *Cell. Mol. Neurobiol.* **2003**, *23*, 305.
2. (a) Hosono, M.; Takahira, T.; Fujita, A.; Fujihara, R.; Ishijuka, O.; Tatee, T.; Nakamura, K. Cardiovascular and adenylate cyclase stimulant properties of NKH477, a novel water-soluble forskolin derivative. *J. Cardiovasc. Pharmacol.* **1992**, *19*, 625. (b) Hosoda, S.; Motomiya, T.; Katagiri, T.; Takano, T.; Sasayama, S.; Toshima, H.; Ogawa, N. Acute effect of NKH477, a novel forskolin derivative, in patients with acute heart failure. *Jpn. J. Clin. Pharmacol. Ther.* **1997**, *28*, 583.(c) Toya, Y.; Schwencke, C.; Ishikawa, Y. Forskolin Derivatives with Increased Selectivity for Cardiac Adenylyl Cyclase. *J. Mol. Cell. Cardiol.* **1998**, *30*, 97.
3. Peters, R. J. Two rings in them all: the labdane-related diterpenoids. *Nat. Prod. Rep.* **2010**, *27*, 1521.
4. (a) Awen, B. Z. S.; Nozawa, M.; Hagiwara, H. Recent progress in the synthesis of labdane diterpenoids. A review. *The New J. for Org. Synth.* **2008**, *40*, 317. (b) Colombo, M. I.; Zinczuk, J.; Ruveda, E. A. Synthetic routes to forskolin. *Tetrahedron* **1992**, *48*, 963.
5. (a) Ziegler, F. E.; Jaynes, B. H.; Saindane, M. T. A synthetic route to forskolin. *J. Am. Chem. Soc.* **1987**, *109*, 8115. (b) Ziegler, F. E.; Jaynes, B. H. Reconstruction of forskolin from a ring C dihydropyran-4-one degradation product thereof. *Tetrahedron Lett.* **1987**, *28*, 2339. (c) Ziegler, F. E.; Jaynes, B. H. Formation of (±)-forskolin via a cuprate addition to a synthetic dihydropyran-4-one. *Tetrahedron Lett.* **1988**, *29*, 2031.
6. (a) Hashimoto, S.; Sakata, S.; Sonegawa, M.; Ikegami, S. A total synthesis of (±)-forskolin. *J. Am. Chem. Soc.* **1988**, *110*, 3670. (b) Hashimoto, S.; Sonegawa, M.; Sakata, S.; Ikegami, S. A Stereocontrolled synthesis of (±)-1,6,7-trideoxyforskolin. *J. Chem. Soc., Chem. Commun.* **1987**, 24.
7. (a) Corey, E. J.; Da Silva Jardine, P.; Mohri, T. Enantioselective route to a key intermediate in the total synthesis of forskolin. *Tetrahedron Lett.* **1988**, *29*, 6409. (b) Corey, E. J.; Da Silva Jardine, P.; Rohloff, J. C. Total synthesis of (±)-forskolin. *J. Am. Chem. Soc.* **1988**, *110*, 3672.
8. (a) Delpech, B.; Lett, R. Retrosynthetic studies with forskolin. *Tetrahedron Lett.* **1987**, *28*, 4061. (b) Delpech, B.; Calvo, D.; Lett, R. Total synthesis of forskolin - part I. *Tetrahedron Lett.* **1996**, *37*, 1015. (c) Delpech, B.; Calvo, D.; Lett, R. Total synthesis of forskolin - part II. *Tetrahedron Lett.* **1996**, *37*, 1019. (d) Delpech, B.; Port, M.; Calvo, D.; Lett, R. Total synthesis of forskolin - part III studies related to an asymmetric synthesis. *Tetrahedron Lett.* **1996**, *37*, 1023.
9. Hylse, O.; Maier, L.; Kucera, R.; Perečko, T.; Svobodová, A.; Kubala, L.; Paruch, K.; Švenda, J. A concise synthesis of forskolin. *Angew. Chem., Int. Ed.* **2017**, *56*, 12586.
10. Kienzle, F.; Stadlwieser, J.; Rank, W.; Schönholzer, P. Die synthese des labdanditerpenes erigerol und analoger verbindungen. *Helv. Chim. Acta* **1990**, *73*, 1108.
11. Bold, G.; Chao, S.; Bhide, R.; Wu, S.-H.; Patel, D. V.; Sih, C. J. A chiral bicyclic intermediate for the synthesis of forskolin. *Tetrahedron Lett.* **1987**, *28*, 1973.
12. Qian, H.; Han, X.; Widenhoefer, R. A. Platinum-catalyzed intramolecular hydroalkoxylation of γ- and δ-hydroxy olefins to form cyclic ethers. *J. Am. Chem. Soc.* **2004**, *126*, 9536.

13. Thomas, W. P.; Schatz, D. J.; George, D. T.; Pronin, S. V. A radical-polar crossover annulation to access terpenoid motifs. *J. Am. Chem. Soc.* **2019**, *141*, 12246.
14. Liu, D.; Canales, E.; Corey, E. J. Chiral oxazaborolidine– aluminum bromide complexes are unusually powerful and effective catalysts for enantioselective Diels-Alder reactions. *J. Am. Chem. Soc.* **2007**, *129*, 1498.
15. In practice, employing 2,6-dimethyl-1,4-benzoquinone as a coupling partner in the annulation with γ,δ-unsaturated aldehyde **3.8** led to production of small quantities of annulated product (~20%) with the undesired stereochemistry at C1.
16. The Sarpong group also recognized the value of this common intermediate and disclosed their own asymmetric synthesis of bicycle **3.23**, see: Nagasawa, S.; Jones, K. E.; Sarpong, R. Enantiospecific entry to a common decalin intermediate for the syntheses of highly oxygenated terpenoids. *J. Org. Chem.* **2019**, *84*, 12209.
17. Mantione, R.; Alves, A.; Montijn, P. P.; Wildschut, G. A.; Bos, H. J. T.; Brandsma, L. A general method for the preparation of cumulenic ethers and thioethers. *Recueil des Travaux Chimiques des Pays-Bas* **1970**, *89*, 97.
18. The major product in these reactions with TMS derivative **3.15** appeared to be desilylation. It was not clear if this reflected desilylation under the reaction conditions or no reaction and desilylation upon work-up.
19. For a relevant discussion of similar regioselectivity, see: Liotta, D.; Saindane, M.; Sunay, Y.; Jamison, W. C. L.; Grossman, J.; Phillips, P. Acetylide additions to enediones. Regioselectivity based on stereoelectronic control. *J. Org. Chem.* **1985**, *50*, 3241.
20. For an example of relevant reactivity, see: Shih, T.-L.; Lin, Y.-L. Epoxidation of protected (1,4,5)-cyclohex-2-ene-triols and their acid hydrolysis to synthesize quercitols from D-(–)-quinic acid. *Synth. Commun.* **2005**, *35*, 1809.
21. Myers, A. G.; Widdowson, K. L. Direct transformation of 2,3-epoxy alcohols into hydroxyl carbonates under mildly basic conditions. *Tetrahedron Lett.* **1988**, *29*, 6389.
22. Bhat, S. V.; Bajwa, B. S.; Dornauer, H.; de Souza, N. J. Reactions of forskolin, a biologically active diterpenoid from Coleus forskohlii. *J. Chem. Soc., Perkin Trans. 1* **1982**, 767.
23. Northcott, C. J.; Zdenek, V. *Canadian Journal of Chemistry*, **1987**, *65*, 1917.
24. Abdullah, K.; Mustafa, E. *Synthetic Comm.* **2017**, *47*, 2342.
25. Obradors, C.; Martinez, R. M.; Shenvi, R. A. Ph(i-PrO)SiH_2: an exceptional reductant for metal-catalyzed hydrogen atom transfers. *J. Am. Chem. Soc.* **2016**, *138*, 4962.
26. Hydrogens of the acetonide fragment in the provided crystal structure were omitted for clarity.

Chapter 4: A Review of Quassin

4.1 Quassinoid Natural Products

4.1.1 Quassinoid Biosynthesis

Quassinoids are a large collection of natural products isolated from tropical plants belonging to the Simaroubaceae family.[1] The first quassinoid to be isolated was quassin (**4.5**) in 1937 by the Clark group, but the structure was not elucidated until 1961 by Valenta.[2,3] Biosynthetically these secondary metabolites are thought to arise from the degradation of triterpenes (C-30), leading to C-18, C-19, C-20, C-22, C-25, and C-26 quassinoids depending on the extent of degredation.[1] This hypothesis was validated by carbon isotope labeling studies with mevalonate, confirming the triterpene biosynthetic origins. It is postulated that the triterpene precursor may be euphol (**4.1**), which would undergo alkene isomerization and epoxidation, followed by opening of the epoxide and a 1,2-methyl shift (Scheme 4.1). Then exhaustive oxidation and cleavage of ten carbons from this terpenoid would lead to the various quassinoid natural products (quassin is depicted as a representative C-20 quassinoid, A-,B-,C-, and D-rings have been labeled for subsequent discussion). The remainder of Section 4.1 will focus on C-20

Scheme 4.1: Biosynthesis of Quassinoids

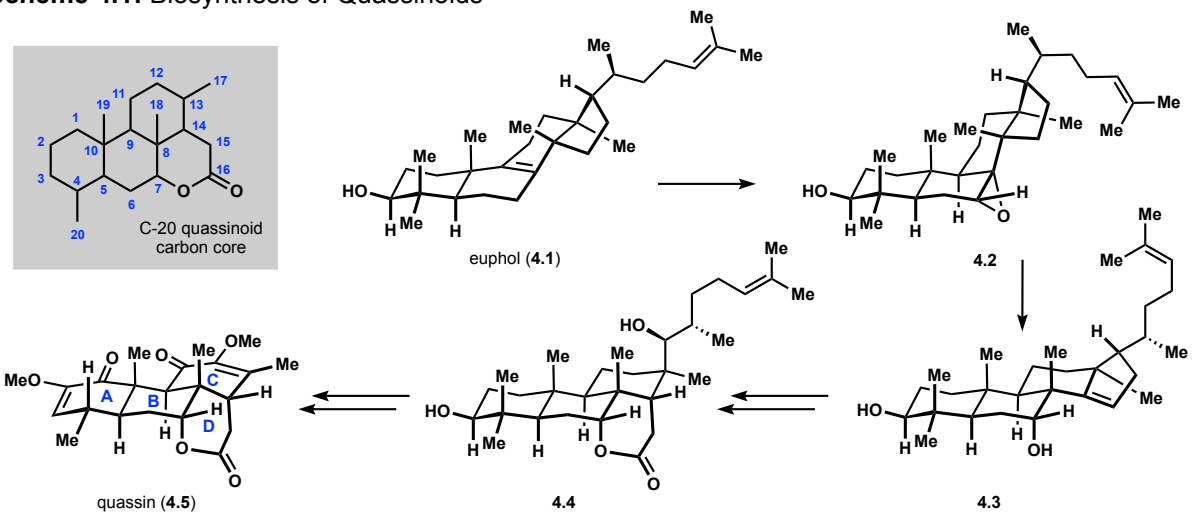

quassinoids as they are the most abundant, bioactive, and well-studied sub-class of quassinoids and the focus of our synthetic work in Chapter 5.

4.1.2 Quassinoid Bioactivity

Quassinoids exhibit a diverse and often potent set of bioactivities. These activities range from antiparasitic, anticancer, anti-HIV, antiviral, antiinflammatory, herbicidal, to insecticidal among others.[1,4] By far the most well-known bioactivities associated with quassinoids are their antimalarial and anticancer properties.

The Simaroubaceae family of plant has been used extensively to treat malaria in parts of the world where these species are endemic. Although several scientific studies corroborated the efficacy of these plant extracts in treating malaria in the early 20th century, it wasn't until the 1980s that there was a concerted effort from the scientific community to study the active components responsible for the pharmacological properites.[4b,5,6] These efforts culminated in the identification of a potent quassinoid, simalikalactone D (**4.6**, Figure 4.1). This congener displayed activity against one of the deadliest strains of malaria, *P. falciparum*, with an IC_{50} of 0.9 ng/mL and completely inhibited parasite growth at 2 ng/mL for in vitro studies.[6] Despite these promising results in vitro, there have been far fewer in vivo studies and the current literature shows potential toxicity issues with many quassinoids that display antimalarial activity.[4b,5] This prompted SAR studies with the aim of improving the pharmacological properties, but the challenges associated

Figure 4.1: Bioactive Quassinoids

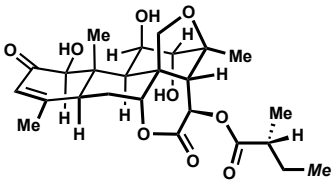

simalikalactone D (**4.6**)

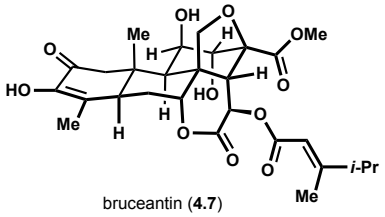

bruceantin (**4.7**)

with synthesizing these highly complex terpenoids has historically made preparing analogs a bottleneck in evaluating potential therapeutics.[4,5]

Aside from antimalarial properties, the other most notable biological activity associated with quassinoids is their antineoplastic properties. The flagship member of this sub-class is bruceantin (**4.7**), which garnered significant attention following its isolation in the 1970s.[7] Ultimately, bruceantin was the subject of two Phase II clinical trials focusing on metastatic breast cancer and malignant melanoma.[8] Unfortunately, these studies in the clinic showed that bruceantin was toxic at higher doses, but more importantly there was minimal or no tumor regression found. These findings effectively terminated any further clinical studies.

Despite these discouraging results, recently there has been a renewed interest in the quassinoids as anticancer agents. This is largely due to further investigations into the mechanism of action of these secondary metabolites and promising results in their application against different cancer types in vitro. The mechanism of action initially attributed to the quassinoids was inhibition of protein synthesis by blocking the P-site of the ribosome, arresting peptidyl transferase activity and peptide chain elongation.[9,10] Bruceantin was one of the more potent congeners with an IC_{50} of 30 nM for inhibition of protein synthesis in HeLa cell lysate.[9a] However, recent investigations have shed light onto a far more complex mechanism of action responsible for the observed pharmacological properties of quassinoids. These include the down-regulation of c-MYC oncoproteins, which plays a key role in cell growth, differentiation and apoptosis; as well as inhibition of transcription factor NF-κB, which is involved in cell differentiation and inflammatory processes.[11,12] These findings spurred a renewed interest in quassinoid natural products and the subsequent research has brought quassinoids back into the spotlight as potentially valuable therapeutic leads, warranting further investigation.[5,13,14,15] Despite this renewed interest, one of the

major hurdles to further investigations is the challenge of preparing analogs, which the synthetic community has been working on for the past several decades.

4.2 Prior Syntheses of Quassin

4.2.1 Grieco

The Grieco laboratory was exceptionally active in the area of quassinoid total synthesis, publishing over a dozen completed total syntheses of these secondary metabolites.[16] Notably, the group also published the first total synthesis of a quassinoid natural product, quassin (**4.5**) in 1980 (Scheme 4.2).[16a] Quassin is the simplest congener of the family and while its biological activity has not received as much attention as other congeners (quassin exhibits antifeedant properties and moderate antimalarial activity)[1] it is a logical entry point to validate synthetic strategies to the quassinoid scaffold and is invariably the initial target for research groups pursuing synthetic routes to these secondary metabolites.

Scheme 4.2: Grieco's Synthesis of Quassin

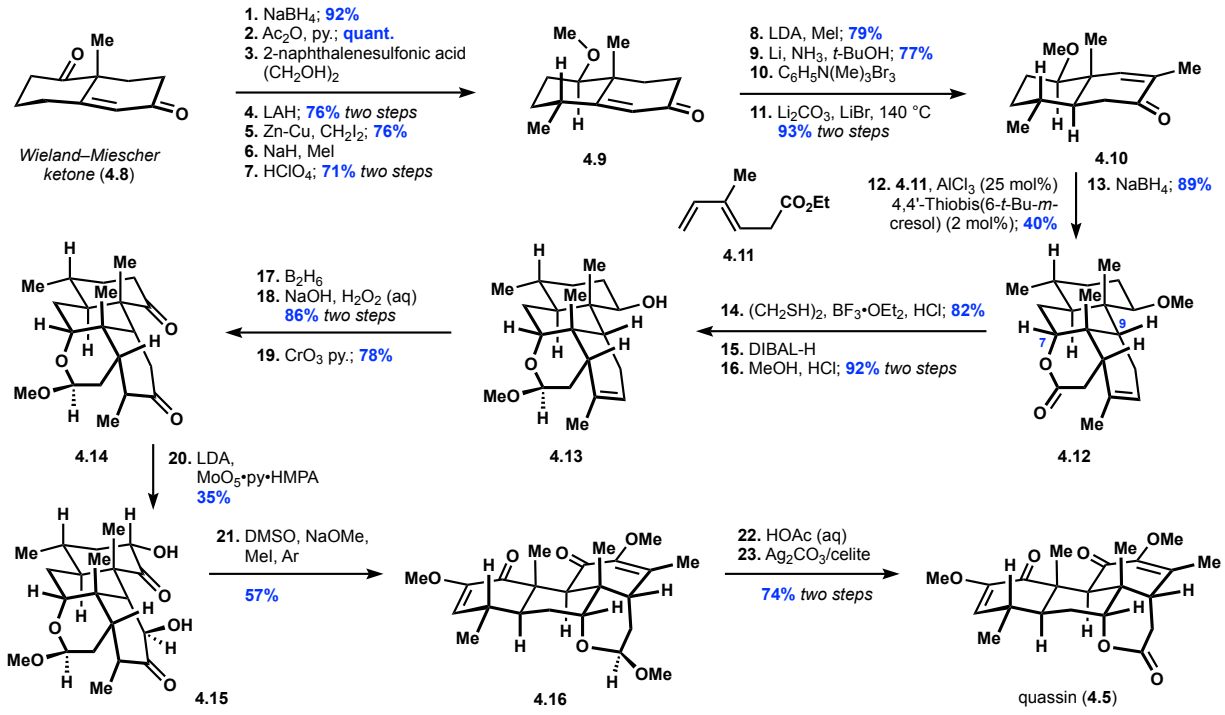

In Grieco's seminal publication, they reported a concise approach to quassin starting from the Wieland–Miescher ketone (**4.8**, Scheme 4.2). Over 11-steps they elaborated this material to enone **4.10**, which served as a dienophile in the subsequent Diels–Alder cycloaddition with diene **4.11**.[16a,16b,17] This sequence rapidly established the tetracyclic core of the quassinoids and although they set the C9 stereocenter incorrectly, precedent suggested this could be epimerized at a later stage.[3] Importantly, the C7 stereocenter was set correctly, which proved to be a challenge in later synthetic efforts. At this stage the Grieco group deprotected the methyl ether at C1 and opted to protect the lactone as lactol **4.13** to avoid undesired reactivity associated with this functionality. The researchers then performed a series of oxidations to arrive at diol **4.15**. In an attempt to epimerize C9 Grieco serendipitously discovered an extraordinary transformation. Treating diol **4.15** with NaOMe in DMSO under an atmosphere of argon, led to oxidation of the α-hydroxy ketones to the bis-1,2-diones, and addition of methyl iodide generated the α-methoxy enone motifs found in quassin. Notably, these conditions also effected epimerization of C9. At this stage lactol **4.16** was deprotected and oxidized completing a succinct synthesis of quassin.

4.2.2 Watt

The next group to synthesize quassin was the Watt laboratory in 1990.[18] Watt's stated goal in targeting quassin was to validate their approach to the quassinoid tetracyclic core with the intention of being able to access more complex, bioactive congeners including pentacyclic members bearing bridging tetrahydrofuran motifs, such as simalikalactone D (**4.6,** Figure 4.1). Watt commenced the synthesis of quassin with the Wieland–Miescher ketone (**4.8**, Scheme 4.3) and elaborated this material to enedione **4.19**, which served as a dienophile in a subsequent Diels–Alder annulation with Danishefsky-type diene **4.20**. This sequence is rather analogous to Grieco's initial steps, but several aspects are worth further comment. Like Grieco, Watt elected to protect

the C1 hydroxyl as a methyl ether citing incompatibilities with downstream chemistry when other protecting groups were employed. Furthermore, the introduction of C18 at the aldehyde oxidation state is seemingly non-strategic as this functionality must be fully reduced later in the synthesis; however, this oxidation theoretically provides a handle to access pentacyclic quassinoids bearing bridging tetrahydrofuran motifs, a goal that was unfortunately never realized.

Scheme 4.3: Watt's Synthesis of Quassin

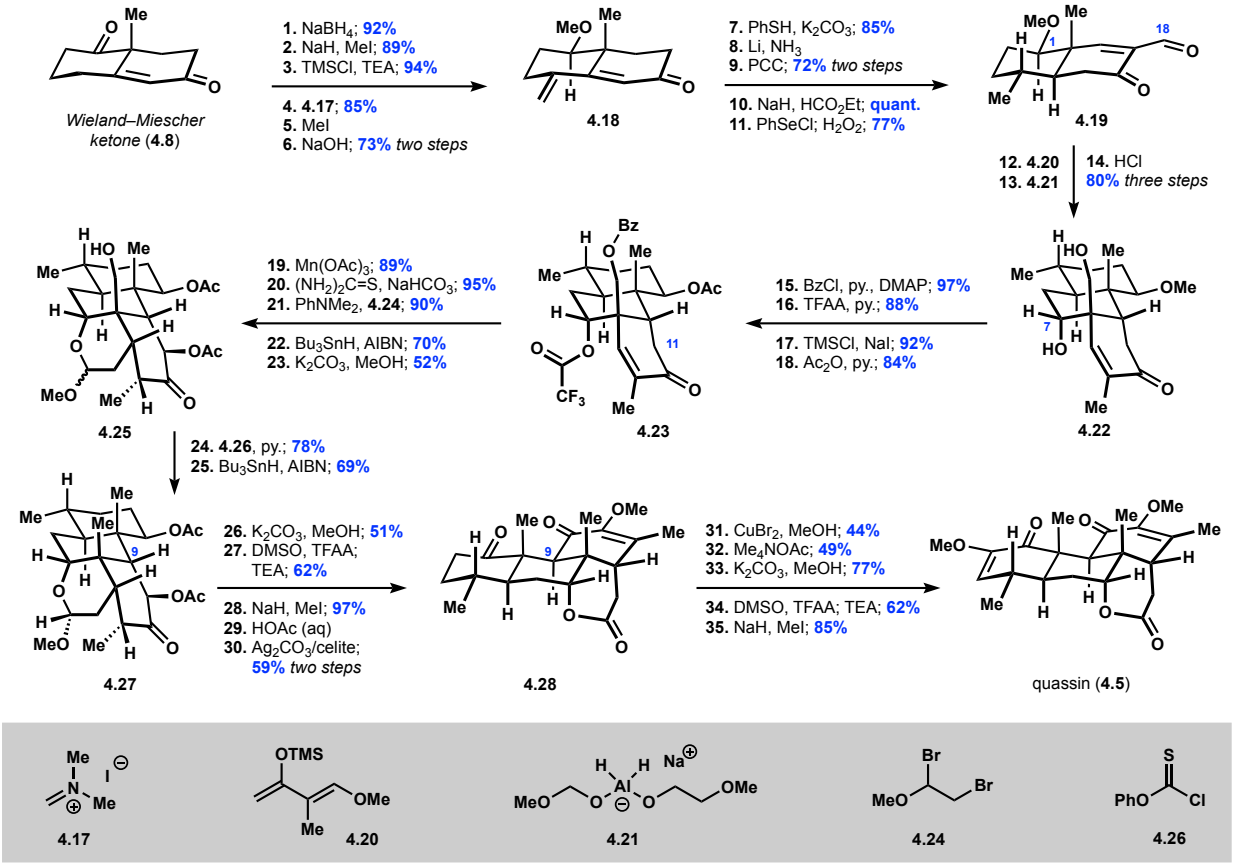

Following the Diels–Alder cycloaddition, Watt reduced the carbonyl at C7 with an aluminum hydride (**4.21**) from the convex face of the tricycle and then performed a series of functional group manipulations to arrive at enone **4.23**. Treatment of this intermediate with $Mn(OAc)_3$ led to oxidation at C11 at which point the trifluoroacetate moiety could be selectively cleaved and the resulting alcohol alkylated with bromide **4.24**. This set the stage for formation of

the D-ring via a radical cyclization, which Watt effected with tributyltin hydride and AIBN, intentionally generating lactol **4.25** to avoid undesired reactivity observed with the corresponding lactone. Having established the tetracyclic core of the quassinoids, Watt converted this material to quassin by deoxygenating C18 and then a series of redox manipulations and epimerization of C9 ultimately afforded the target, quassin.

4.2.3 Valenta

The Valenta group was one of the initial synthetic laboratories to take interest in the quassinoids, dating back to their initial structural elucidation of quassin in the 1960s.[3] After several synthetic studies, Valenta published a total synthesis of quassin in 1991, which was markedly different from the previous two efforts described.[19] The route started with a Diels–Alder cycloaddition between diene **4.30** and benzoquinone **4.31** establishing the B- and C-rings of the quassinoid core (Scheme 4.4). The researchers then epimerized C15 and installed the necessary carbons that would eventually become the A-ring by addition of acetylide **4.34** to ketone **4.33**. Isomerization of this intermediate in the presence of oxalic acid followed by hydrogenation delivered ester **4.36**. Valenta then generated bromide **4.37** providing a functional handle to form the C14–C15 bond of the D-ring. Prior to this bond forming step the group stoichiometrically prepared the osmate ester, followed by treatment with zinc to forge the C14–C15 bond and then cleavage of the osmate ester with hydrogen sulfide delivered diol **4.38**. This carbon scaffold was then rearranged to the desired tetracyclic motif found in the quassinoids over the next several steps. Starting with periodate cleavage of the diol and acetylation the resulting acetal **4.39** could be converted to an intermediate cyanohydrin and upon treatment with lithium pyrrolidide formed the C1–C2 bond of the A-ring (**4.40**). At this stage Valenta performed a series of oxidations followed by a Bi_2O_3 mediated α-ketol rearrangement delivering a carbonyl at C12 and an alcohol at C11,

ultimately forming lactol **4.42**. Treatment with base accomplished epimerization of C4 and elimination of the C9-hydroxyl group establishing the 1,2-dione functionality and affording penultimate intermediate **4.43**. A final methylation delivered quassin.

Scheme 4.4: Valenta's Synthesis of Quassin

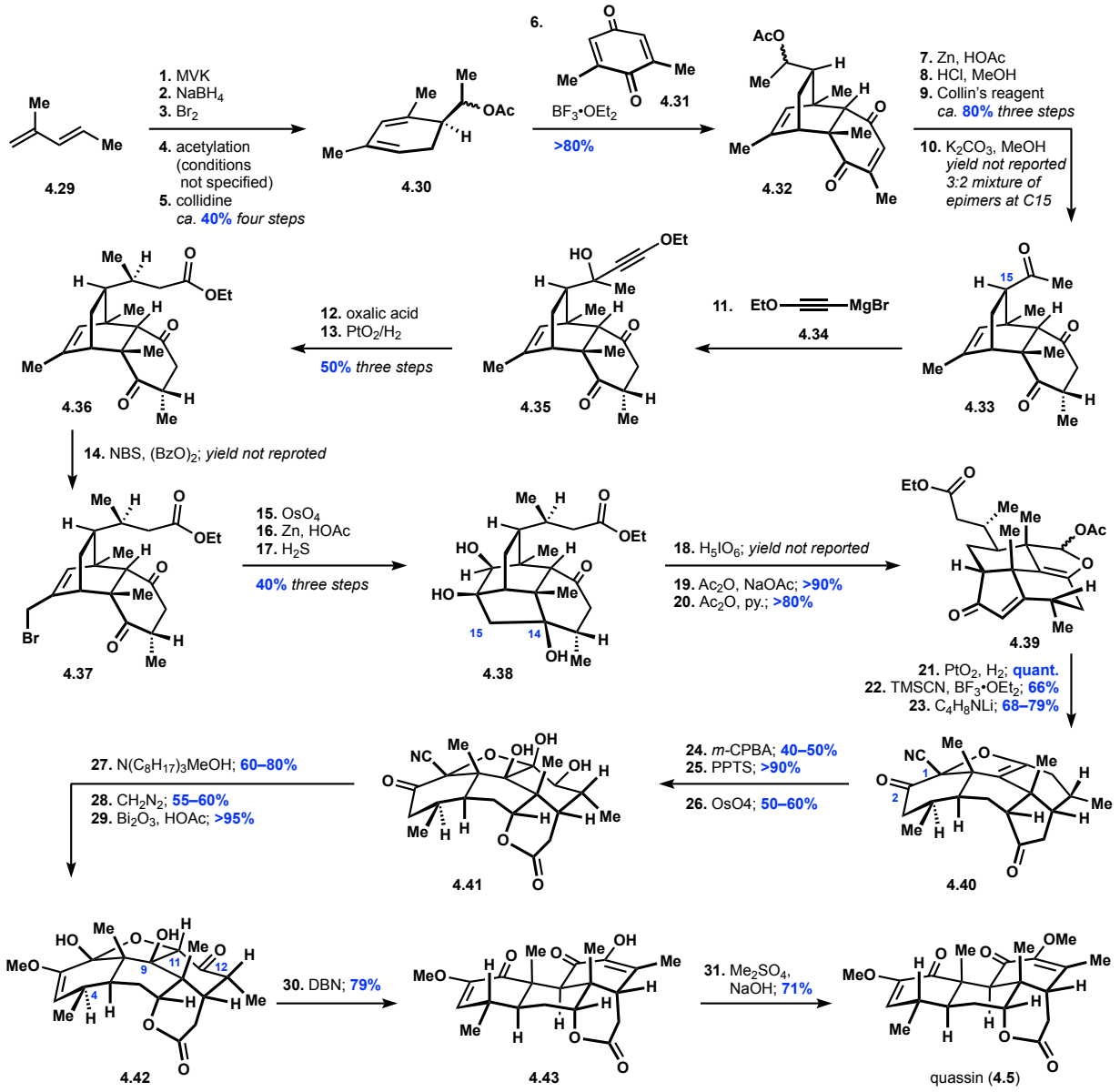

4.2.4 Shing

The Shing group reported their approach to quassin in 1998 starting from S-(+)-carvone and using a clever intramolecular Diels–Alder cycloaddition.[20,21] To prepare the necessary diene and dienophile partners the group performed an aldol reaction between a methylated carvone derived enolate and aldehyde **4.45** (prepared in two steps from 3-methylsulfolene) followed by acylation of the resulting alcohol. From here sulfolene **4.46** underwent a cheletropic reaction at elevated temperatures to reveal a diene that then engaged in a Diels–Alder reaction to afford tricycle **4.47**. This remarkably short sequence established the A-, B-, and C-rings of quassin with the desired *trans-anti-trans* perhydro-phenanthrene motif. Unfortunately, the undesired stereochemistry at C7 needed to be inverted. Shing accomplished this stereoinversion in a four-

Scheme 4.5: Shing's Synthesis of Quassin

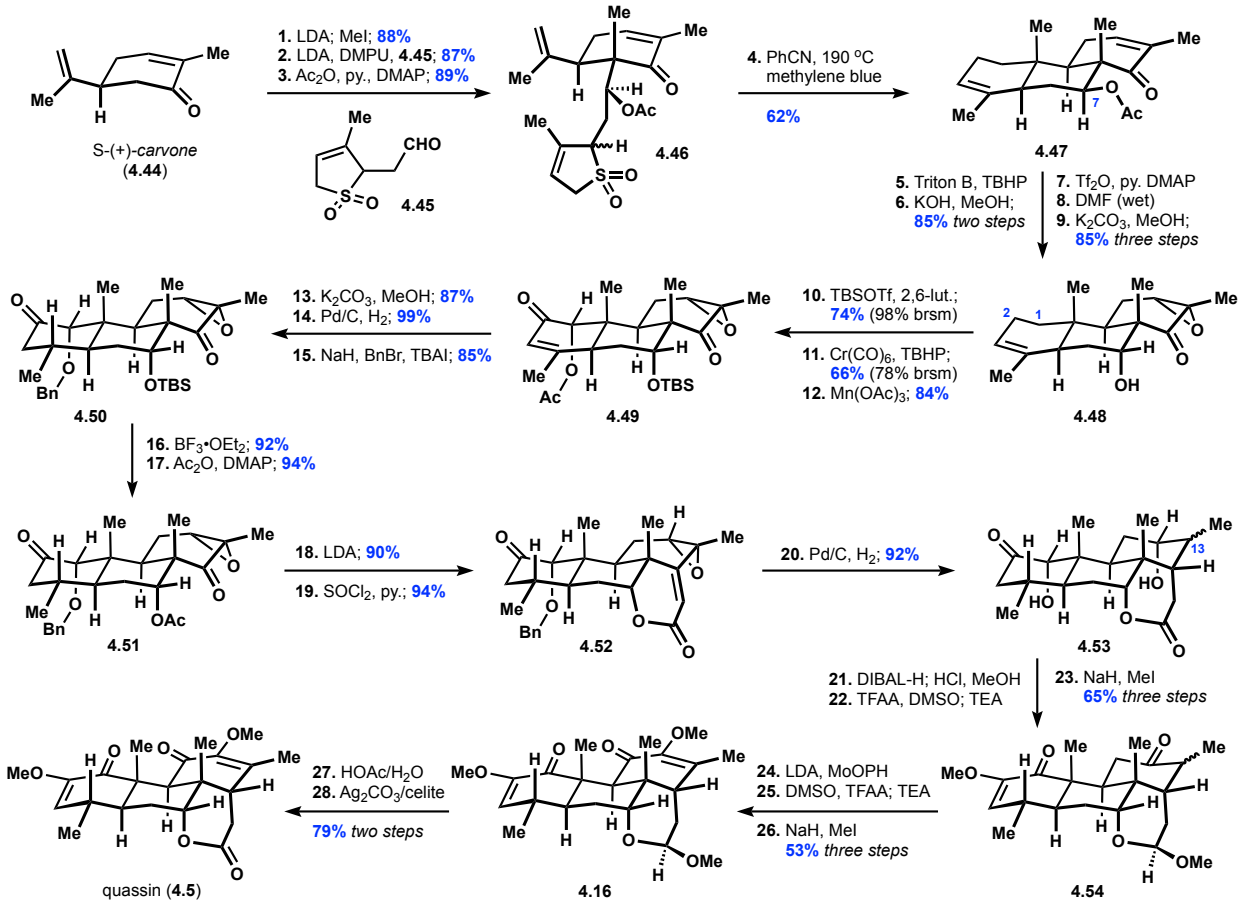

step sequence following epoxidation of the enone functionality. With alcohol **4.48** in hand the Shing laboratory was faced with a series of challenging oxidations at C1 and C2. After extensive experimentation the researchers developed suitable conditions to affect these desired oxidation events and coupled with several protecting group manipulations arrived at acetate **4.51**. The authors then executed a two-step aldol condensation to deliver unsaturated lactone **4.52** containing the tetracyclic core of the quassinoids. With the carbon framework intact, tetracycle **4.52** was separated from quassin by a series of redox manipulations. Shing first performed a hydrogenation, which not only formed the saturated lactone, but also reduced the epoxide to the corresponding alcohol (the stereochemistry at C13 was not unambiguously determined as it was inconsequential). Like many groups before them, they then protected lactone **4.53** as lactol **4.54** and carried out a series of oxidations ultimately arriving at quassin.

4.3 Conclusion

These prior syntheses of quassin culminated in a wealth of valuable knowledge. In our analysis of these past efforts, it appeared that many groups were able to rapidly construct the carbocyclic scaffold of quassin, as highlighted by Shing's exceptionally concise preparation of tricycle **4.47** from S-(+)-carvone. Alternatively, accessing the dense array of oxidation present in the target proved challenging. This led to the majority of synthetic steps in prior syntheses being dedicated to redox manipulations or functional group interconversions. In our view, the major challenge associated with the synthesis of quassin was efficient access to the complex oxidation pattern found in this secondary metabolite.

4.4 References and Notes

1. For reviews on the quassinoids see: (a) Polonsky, J. Quassinoid Bitter Principles. *Fortschritte Der Chemie Organischer Naturstoffe* **1973**, 101. (b) Guo, Z.; Vangapandu, S.; Sindelar, R. W.; Walker, L. A.; Sindelar, R. D. Biologically active quassinoids and their chemistry: potential leads for drug design. *Current Medicinal Chemistry* **2005**, *12*, 173. (c) Curcino Vieira, I. J.; Braz-Filho, A. R. Quassinoids: structual diversity, biological activity and studies synthetic. *Studies in Nat. Prod. Chem.* **2005**, 33, 433. (d) Duan, Z.-K.; Zhang, Z.-J.; Dong, S.-H.; Wang, Y.-X.; Song, S.-J.; Huang, X.-X. Quassinoids: phytochemistry and antitumor prospect. *Phytochemistry* **2021**, *187*, 112769.
2. Clark, E. P. Quassin. I. The preparation and purification of quassin and neoquassin, with information concerning their molecular formulas. *J. Am. Chem. Soc.* **1937**, *59*, 927.
3. (a) Valenta, Z.; Papadopoulos, S.; Podesva, C. Quassin and neoquassin. *Tetrahedron* **1961**, 15, 100. (b) Valenta, Z.; Gray, A. H.; Orr, D. E.; Papadopoulos, S.; Podesva, C. The stereochemistry of quassin. *Tetrahedron* **1962**, *18*, 1433.
4. For reviews on the biological activity of quassinoids see: (a) Fiaschetti, G.; Grotzer, M.A.; Shalaby, T.; Castelletti, A.; Arcaro, A. Quassinoids: from traditional drugs to new cancer therapeutics. *Curr. Med. Chem*. **2011**, *18*, 316. (b) Houël, E.; Stien, D.; Bourdy, G.; Deharo, E. Quassinoids: anticancer and antimalarial activities. *Natural Products* **2013**, 3775. (c) Li, Z.; Ruan. J.-y.; Sun, F.; Yan, J.-j.; Wang, J.-l.; Zhang, Z.-x.; Wang, T. Relationship between structural characteristics and plant sources along with pharmacology research of quassinoids. *Chem. Pharm. Bull.* **2019**, *67*, 654.
5. Muhammad, I.; Samoylenko, V. Antimalarial quassinoids: past, present and future. *Expert Opin. Drug Discov.* **2007**, *2*, 1065.
6. (a) Trager, W.; Polonsky, J. Antimalarial activity of quassinoids against chloroquine-resistant *Plasmodium falciparum* in vitro. *Am. J. Trop. Med. Hyg*. **1981**, *30*, 531. (b) O'Neill, M J; Bray, D H; Boardman, P; Phillipson, J D; Warhurst, D C; Peters, W; Suffness, M Plants as sources of antimalarial drugs: in vitro antimalarial activities of some quassinoids. *Antimicrob. Agents Chemother.* **1986**, *30,* 101. (c)Ang, H. H.; Chan, K. L.; Mak, J. W. In vitro antimalarial activity of quassinoids from Eurycoma longifolia against Malaysian chloroquine-resistant *Plasmodium falciparum* isolates. *Planta Med.* **1995**, *61*, 177. (d) Ekong, R. M.; Kirby, G. C.; Patel, G.; Phillipson, J. D.; Warhurst, D. C. Comparison of the in vitro activities of quassinoids with activity against *Plasmodium falciparum,* anisomycin and some other inhibitors of eukaryotic protein synthesis. *Biochem. Pharmacol.* **1990**, *40*, 297.
7. Kupchan, S. M.; Britton, R. W.; Lacadie, J. A.; Ziegler, M. F.; Sigel, C. W. The isolation and structural elucidation of bruceantin and bruceantinol, new potent antileukemic quassinoids from Brucea antidysenterica. *J. Org. Chem.* **1975**, *40*, 648.
8. (a) Wiseman, C. L.; Yap, H. Y.; Bedikian, A. Y.; Bodey, G. P.; Blumenschein, G. R. Phase II trial of bruceantin in metastatic breast carcinoma. *Am. J. Clin. Oncol.* **1982***, 5,* 389. (b) Arseneau, J.; Wolter, J.; Kuperminc, M.; Ruckdeschel, J. A phase II study of bruceantin (NSC-165, 563) in advanced malignant melanoma. *Invest. New Drugs* **1983**, *1*, 239.
9. (a) Liao, L. L.; Kupchan, S. M.; Horwitz, S. B. Mode of action of the antitumor compound bruceantin, and inhibitor of protein synthesis. *Mol. Pharmacol*. **1976**, *12*, 167. (b) Fresno, M.; Gonzales, A.; Vazquez, D.; Jimenez, A. Bruceantin, a novel inhibitor of peptide bond formation. *Biochim. Biophys. Acta* **1978**, *518*, 104.

10. Kirby, G. C.; O'Neill, M. J.; Phillipson, J. D.; Warhurst, D. C. In vitro studies on the mode of action of quassinoids with activity against chloroquine-resistant *Plasmodium falciparum*. *Biochem. Pharmacol.* **1989**, *38*, 4367.
11. Mata-Greenwood, E.; Cuendet, M.; Sher, D.; Gustin, D.; Stock, W.; Pezzuto, J. M. Brusatol-mediated induction of leukemic cell differentiation and G_1 arrest is associated with down-regulation of c-myc. *Leukemia* **2002**, *16*, 2275.
12. Cuendet, M.; Gills, J. J.; Pezzuto, J. M. Brusatol-induced HL-60 cell differentiation involves NF-, B activation. *Cancer Lett*. **2004**, *206*, 43.
13. Cuendet, M.; Pezzuto, J. M. Antitumor activity of bruceantin: an old drug with new promise. *J. Nat. Prod.* **2004**, *67*, 269.
14. For examples, see: (a) Cuendet, M.; Christov, K.; Lantvit, D. D.; Deng, Y.; Hedayat, S.; Helson, L.; McChesney, J. D.; Pezzuto, J. M. Multiple myeloma regression mediated by bruceantin. *Clin. Cancer Res.* **2004**, *10*, 1170. (b) Fukamiya, K.; Lee, K.-H.; Muhammad, I.; Murakami, C.; Okano, M.; Harvey, I.; Pelletier, J. Structure–activity relationships of quassinoids for eukaryotic protein synthesis. *Cancer Lett.* **2005**, *220*, 37. (c) Kim, J.-A.; Lau, E. K.; Pan, L.; Carcache De Blanco, E. J. NF-cB inhibitors from Brucea javanica exhibiting intracellular effects on reactive oxygen species. *Anticancer Res.* **2010**, *30*, 3295. (d) Castelletti1, D.; Fiaschetti, G.; Di Dato, V.; Ziegler, U.; Kumps, C.; De Preter, K.; Zollo, M.; Speleman, F.; Shalaby, T.; De Martino, D.; Berg, T.; Eggert, A.; Arcaro, A.; Grotzer, M. A. The Quassinoid Derivative NBT-272 Targets Both the AKT and ERK Signaling Pathways in Embryonal Tumors. *Mol. Cancer Ther*. **2010**, *9*, 3145. (e) Issa, M. E.; Berndt, S.; Carpentier, G.; Pezzuto, J. M.; Cuendet, M. Bruceantin inhibits multiple myeloma cancer stem cell proliferation. *Cancer Biol. Ther.* **2016**, *17*, 966.
15. For innovative approaches to the quassinoids in the 21st century, see: (a) Barrero, A. F.; Alvarez-Manzaneda, E. J.; Alvarez-Manzaneda, R.; Chahboun, R.; Meneses, R.; Cuerva, J. M.; Aparicio, M.; Romera, J. L. Approach to the synthesis of antitumor quassinoids from labdane diterpenes: an efficient synthesis of a picrasane-related intermediate. *Org. Lett.* **2001**, *3*, 647. (b) Spino, C.; Hill, B.; Dubé, P.; Gingras, S. A diene-transmissive approach to the quassinoid skeleton. *Can. J. Chem.* **2003**, *81*, 81. (c) Perreault, S.; Spino, C. Meldrum's acid-derived thione dienophile in a convergent and stereoselective synthesis of a tetracyclic quassinoid intermediate. *Org. Lett.* **2006**, *8*, 4385. (d) Marcos, I. S.; García, N.; Sexmero, M. J.; Hernandez, F. A.; Escola, M. A.; Basabe, P.; Díez, D.; Urones, J. G. Synthetic studies towards picrasane quassinoids. *Tetrahedron* **2007**, *63*, 2335. (e) Caron, P.-Y.; Deslongchamps, P. Versatile strategy to access tricycles related to quassinoids and triterpenes. *Org. Lett.* **2010**, *12*, 508. (f) Burns, D. J.; Mommer, S.; O'Brien, P.; Taylor, R. J. K.; Whitwood, A. C.; Hachisu, S. Stereocontrolled synthesis of the AB rings of samaderine C. *Org. Lett.* **2013**, *15*, 394. (g) Ravindar, K.; Caron, P.-Y.; Deslongchamps, P. Anionic polycyclization entry to tricycles related to quassinoids and terpenoids: a stereocontrolled total synthesis of (+)-cassaine. *J. Org. Chem.* **2014**, *79*, 7979. (h) Usui, K.; Suzuki, T.; Nakada, M. A highly stereoselective intramolecular Diels−Alder reaction for construction of the AB ring moiety of bruceantin. *Tetrahedron Lett.* **2015**, *56*, 1247. (i) Oki, Y.; Nakada, M. Research on Au(I)-catalyzed ene-yne cycloisomerization for construction of quassinoid scaffold. *Tetrahedron Lett.* **2018**, *59*, 926. (j) Condakes, M. L.; Rosen, R. Z.; Harwood, S. J.; Maimone, T. J. A copper-catalyzed double coupling enables a 3-step synthesis of the quassinoid core architecture. *Chem. Sci.* **2019**, *10*, 768.

16. For total syntheses of quassinoid natural products from the Grieco laboratory, see: (a) Grieco, P. A.; Ferrino, S.; Vidari, G. Total synthesis of dl-quassin. *J. Am. Chem. Soc.* **1980**, *102*, 7586. (b) Vidari, G.; Ferriño, S.; Grieco, P. A. Quassinoids: total synthesis of dl-quassin. *J. Am. Chem. Soc*. **1984**, *106*, 3539. (c) Grieco, P. A.; Lis, R.; Ferrino, S.; Law, J. Y. Quassinoids: total synthesis of dl-castelanolide. *J. Org. Chem*. **1984**, *49*, 2342. (d) Grieco, P. A.; Nargund, R. P.; Parker, D. T. Total synthesis of the highly oxygenated quassinoid (±)-klaineanone. *J. Am. Chem. Soc.* **1989**, *111*, 6287. (e) Collins, J. L.; Grieco, P. A.; Gross, R. S. Synthetic studies on quassinoids: total synthesis of (±)-shinjulactone C. *J. Org. Chem.* **1990**, *55*, 5816. (f) Gross, R. S.; Grieco, P. A.; Collins, J. L. Synthetic studies on quassinoids: total synthesis of (±)-chaparrinone. *J. Am. Chem. Soc.* **1990**, *112*, 9436. (g) Gross, R. S.; Grieco, P. A.; Collins, J. L. Synthesis of the highly oxygenated quassinoid shinjulactone D. *J. Org. Chem.* **1991**, *56*, 7167. (h) Fleck, T. J.; Grieco, P. A. Synthetic studies on quassinoids: total synthesis of (±)-glaucarubolone and (±)-holacanthone. *Tetrahedron Lett*. **1992**, *33*, 1813. (i) Moher, E. D.; Collins, J. L.; Grieco, P. A. Synthetic studies on quassinoids: total synthesis of simalikalactone D and assignment of the absolute configuration of the u-methylbutyrate ester side chain. *J. Am. Chem. Soc.* **1992**, *114*, 2764. (j) Moher, E. D.; Grieco, P. A.; Collins, J. L. (R)-(+)- and (S)-(−)-5-Ethyl-5-methyl-1,3-dioxolane-2,4-dione reagents for the direct preparation of α-hydroxy-α-methylbutyrate esters: assignment of the absolute configuration of the α-acetoxy-α-methylbutyrate ester side chain of quassimarin via total synthesis. *J. Org. Chem.* **1993**, *58*, 3789. (k) VanderRoest, J. M.; Grieco, P. A. Total synthesis of (±)-bruceantin. *J. Am. Chem. Soc.* **1993**, *115*, 5841. (l) Grieco, P. A.; Collins, J. L.; Moher, E. D.; Fleck, T. J.; Gross, R. S. Synthetic studies on quassinoids: total synthesis of (−)-chaparrinone, (−)-glaucarubolide, and (+)-glaucarubinone. *J. Am. Chem. Soc.* **1993**, *115*, 6078. (m) Grieco, P. A.; Piñeiro-Nuñez, M. M. C19 quassinoids: total synthesis of dl-samaderin B. *J. Am. Chem. Soc.* **1994**, *116*, 7606. (n) Grieco, P. A.; Cowen, S. D.; Mohammadi, F. Synthetic studies on highly oxygenated quassinoids: total synthesis of (±)-141,15,-dihydroxyklaineanone. *Tetrahedron Lett.* **1996**, *37*, 2699. (o) Grieco, P. A.; Collins, J. L.; Huffman, J. C. Synthetic studies on quassinoids: synthesis of (±)-shinjudilactone and (±)-13-epi-shinjudilactone. *J. Org. Chem.* **1998**, *63*, 9576.
17. Grieco, A. P.; Oguri, R.; Gilman, S. Sesquiterpene lactones. Total synthesis of (±)-eriolanin and (±)-eriolangin. *J. Am. Chem. Soc.* **1980**, *102*, 5891.
18. Kim, M.; Kawada, K.; Gross, R. S.; Watt, D. S. An enantioselective synthesis of (+)-picrasin B, (+)-Δ^2-picrasin B, and (+)-quassin from the R-(−) enantiomer of the Wieland-Miescher ketone. *J. Org. Chem.* **1990**, *55*, 504.
19. (a) Stojanac, N.; Sood, A.; Stojanac, Ž.; Valenta, Z. A synthetic approach to quassin. Introduction of functionality and stereochemistry by a Diels-Alder reaction. *Can. J. Chem.* **1975**, *53*, 619. (b) Stojanac, N.; Stojanac, Ž.; White, P. S.; Valenta, Z. A synthetic approach to quassin. Synthesis of a ring A seco derivative. *Can. J. Chem.* **1979**, *57*, 3346. (c) Stojanac, N.; Valenta, Z. Total synthesis of d,l-quassin. *Can. J. Chem.* **1991**, *69*, 853.
20. Shing, T. K. M.; Tang, Y.; Malone, J. F. An expeditious and enantioselective entry to the ABC ring of the quassinoid skeleton. *J. Chem. Soc., Chem. Commun.* **1989**, 1294
21. (a) Shing, T. K. M.; Jiang, Q.; Mak, T. C. W. Total synthesis of (+)-quassin from (+)-carvone. *J. Org. Chem.* **1998**, *63*, 2056. (b) Shing, T. K. M.; Jiang, Q. Total synthesis of (+)-quassin. *J. Org. Chem.* **2000**, *65*, 7059.

Chapter 5: A Total Synthesis of Quassin

5.1 Synthetic Planning and Considerations

Our interest in quassinoids stemmed from both the expansive and often potent bioactivity these secondary metabolites possess and from their intriguing chemical architectures that have challenged the synthetic community for the past several decades (see Chapter 4 for a detailed discussion).[1,2] Like many groups before us, we chose to first target one of the simpler congeners, quassin (**5.1**), with the intention of validating a synthetic strategy that would be applicable to the broader family of quassinoid natural products.

In planning our synthetic route to quassin, we first considered the successes and shortcomings of prior routes.[3–6] All previous syntheses took linear approaches to quassin. As noted in Chapter 3 regarding forskolin, linear approaches to highly oxidized terpenoids can be strategic, to construct complex oxidation patterns through stereochemical relay. However, this strategy requires careful choreography to navigate conflicting reactivity patterns, which invariably accumulate in the progressively more functionalized intermediates of a linear synthetic sequence. In the prior syntheses of quassin this proved challenging, and the bulk of synthetic transformations

Figure 5.1: Prior Approaches to Quassin

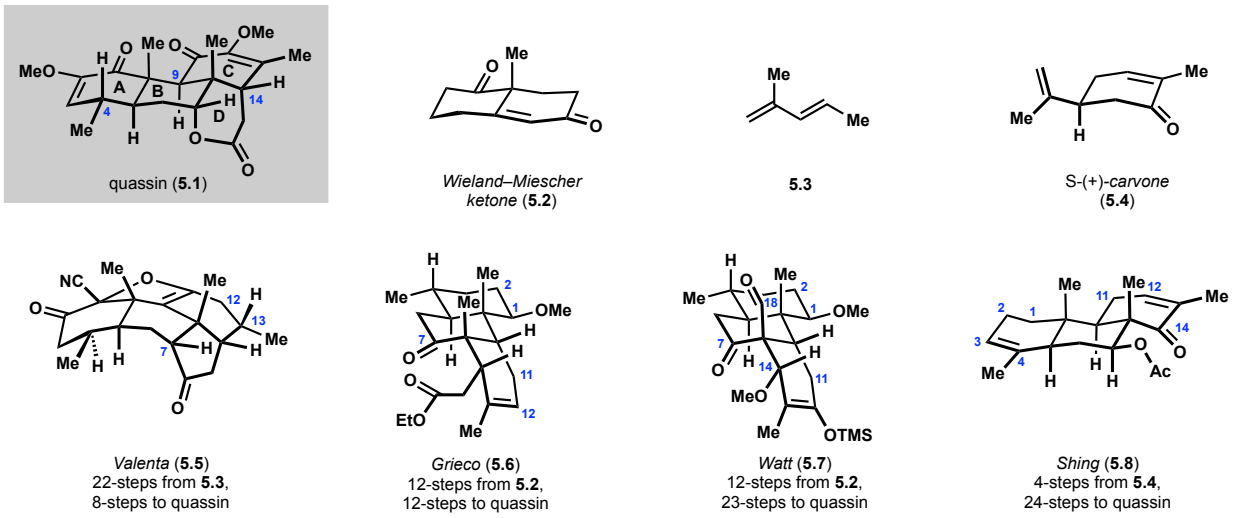

were dedicated to redox manipulations. In our analysis, establishing the dense oxidation patterns found in quassinoids constitutes one of the main synthetic challenges of these secondary metabolites. By comparing past efforts, it is evident that groups who established the tricarbocyclic core (A-, B-, and C-rings) with more carbons in the appropriate oxidation state faced fewer subsequent synthetic steps in their sequences, although preparing these more highly oxidized tricycles almost invariably required more synthetic manipulations due to the linear nature of their construction (numbered carbons are at the undesired oxidation state, Figure 5.1). In our approach to quassin, we aimed to both efficiently prepare the tricarbocylic core of the quassinoids and to make judicious selections regarding the functional handles installed on this carbon framework that would facilitate concise conversion to the target compound.

Having critiqued the prior syntheses, it must be emphasized that any synthesis of quassin or a quassinoid natural product will invariably require redox manipulations and the lessons learned and reactivity manifolds established from prior synthetic efforts are invaluable and were certainly indispensable in our own efforts.[3–7] More broadly, the knowledge gained from the breadth of research focused on quassinoids goes far beyond information pertaining to oxidation events. One important finding comes from the Valenta group in their studies of a related congener to quassin, neoquassin.[8] Valenta found that C4, C9, and C14 in neoquassin underwent deuteration in the presence of sodium methoxide and deuterated methanol.[8] This observation implied that these stereocenters could be corrected late-stage in a synthetic route, if necessary, greatly simplifying the retrosynthetic analysis of quassin. In fact, most syntheses of quassin rely on epimerization of one or more of these stereocenters, including our own.

Armed with an arsenal of knowledge compiled over the decades of research on the quassinoids we commenced our retrosynthetic analysis of quassin. We first envisioned disconnection of the lactone functionality back to an aldol motif **5.9**, which the Shing group had taken advantage of in their synthesis (Scheme 5.1).[6] In our analysis, this was strategic because sub-target **5.9** could be drastically simplified by employing an MHAT-initiated annulation transform, delivering two unsaturated carbonyl synthons (**5.10** and **5.11**). One of the benefits of this convergent approach was the possibility of uniting two functionalized coupling partners in the annulation leading to a more highly oxidized tricarbocyclic core. This would ideally mitigate late-stage redox manipulations, which tend to be challenging due to the presence of more competing reactivity patterns.

Scheme 5.1: Retrosynthesis of Quassin

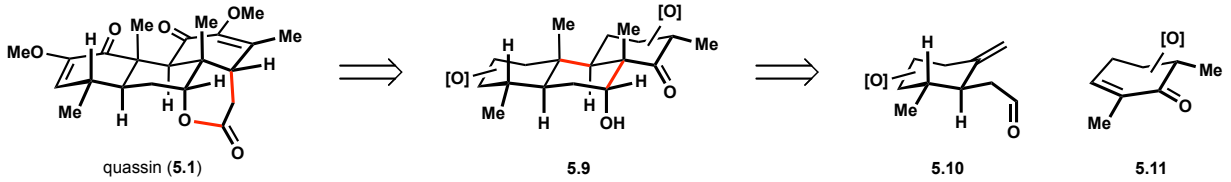

It is worth noting that several decades prior, the Mandell group developed a beautiful retrosynthesis of quassin with key disconnections along the same bonds we identified as strategic (C7–C8 and C9–C10, Scheme 5.2).[9] Mandell envisioned forging these bonds through an intramolecular Diels–Alder cycloaddition between two tethered orthoquinones (**5.12**). Unfortunately, in practice this Diels–Alder reaction never produced the desired product under a

Scheme 5.2: Mandell's Thwarted Diels–Alder Cycloaddition

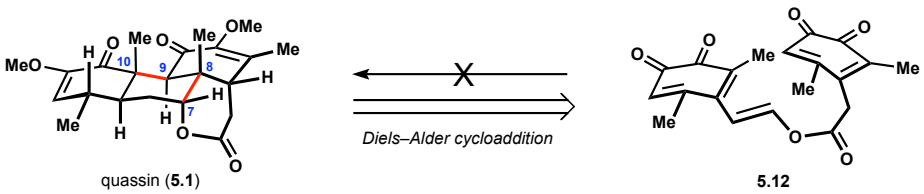

variety of conditions, which was attributed to poor electronic matching between the diene and dienophile as well as the steric constraints of the system.[2d,9] We believed that an MHAT-initiated annulation was well suited to overcome the challenges associated with this retrosynthetic design.

5.2 A Total Synthesis of Quassin

5.2.1 Approach to the A-, B-, and C-Rings

We commenced our studies by evaluating the proposed MHAT-initiated annulation with a panel of γ,δ-unsaturated aldehydes bearing relevant oxidation to that found in the A-ring of quassin (**5.16**–**5.20**, Table 5.1). For the α,β-unsaturated carbonyl component we elected to use cyclopentadiene Diels–Alder adduct **5.13**. This choice was guided by the following factors: Diels–Alder adduct **5.13** was precedented to engage efficiently in MHAT-initiated annulations as demonstrated by its competency in our prior synthesis of forskolin, asymmetric preparation of Diels–Alder adduct **5.13** developed in the Corey group would again provide a handle for stereocontrol in the annulation, and finally, following a retro-Diels–Alder reaction the corresponding enedione motif would provide a pragmatic functional handle to elaborate to the oxidation pattern found in the C-ring of quassin.[10]

Table 5.1: MHAT-Initiated Annulation Towards Quassin

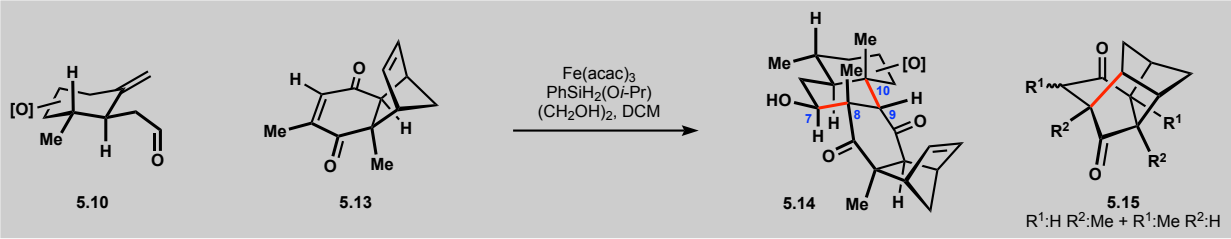

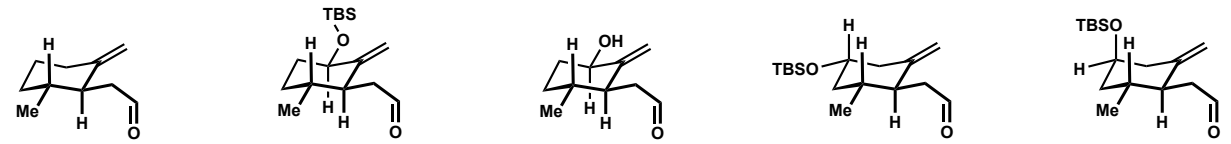

[a] isolated yield [b] yield determined by ^{1}H NMR analysis with mesitylene as internal standard [c] product tentatively assigned

Unfortunately, a preliminary screen resulted in low yields across the panel of substrates evaluated, which was in contrast to the efficient annulation we observed in the context of our synthetic efforts towards forskolin employing a simpler γ,δ-unsaturated aldehyde (4-methylpent-4-enal, see Chapter 3). Despite slow addition of silane and enedione **5.13**, in many cases we observed substantial formation of dione products (**5.15**) arising from MHAT to the 1,2-disubstituted alkene of enedione **5.13**, reactivity that the slow addition protocol had suppressed in our prior studies related to forskolin (see Chapter 3 for a detailed discussion). This suggested that MHAT to the desired 1,1-disubstituted alkenes of the γ,δ-unsaturated aldehydes **3.16**–**3.20** was slower relative to our previous system.

We reasoned that this may be due to the added steric constraints of the γ,δ-unsaturated aldehydes **5.16**–**5.20** and due to the inductive effects of the added oxidation, which would result in a less electron-rich alkene presumably further slowing MHAT. Additionally, these same factors would also decrease the efficiency with which the generated alkyl radical engaged in Giese-type reactivity with enedione **5.13**. Inductive effects would lead to a less electron-rich radical creating a worse electronic match with the electron-deficient alkene of enedione **5.13** slowing the rate of Giese addition and the added steric hinderance would similarly slow the initial bond forming event.

Aside from the desired annulation products **5.14** and diones **5.15**, a large portion of the mass balance seemingly comprised of a complex mixture of products, which may be the manifestation of a slower MHAT event and Giese addition leading to other deleterious reaction pathways predominating. Attempts to optimize reaction conditions by varying reaction times, rate of addition, stoichiometry, solvent, and temperature did not lead to substantially improved yields across the panel of substrates (**5.16**–**5.20**).

It should also be noted that in all cases the annulation favored production of the desired C8 and C10 stereocenters, a mixture of epimers at C7, and the undesired C9 stereocenter. Based on deuteration studies from the Valenta group we were confident that C9 could be readily epimerized, and we intended to address the challenge of C7 epimerization after identifying a competent pair of annulation partners.[5a,8]

5.2.2 C–H Functionalizations of the B-Ring

The poor yields observed from our initial interrogation of MHAT-initiated annulations encouraged us to reevaluate our strategy to quassin. The γ,δ-unsaturated aldehydes **5.17**–**5.20** possessed useful functional handles to elaborate to quassin, a high priority in our synthetic plan, but the efficiency of these annulations was far below synthetically useful yields. Even considering the low conversion, the yields based on recovered starting material were not encouraging with the exception of aldehyde **5.16**. This substrate, initially prepared as a model system, resulted in a tricarbocyclic product that lacked any functional handles on the A-ring seemingly precluding its utility in a succinct synthesis of quassin. However, our initial lack of success with more highly functionalized systems led us to reconsider the value of this material.

We reasoned that following annulation between enedione **5.13** and aldehyde **5.16** oxidation could be installed on the A-ring by capitalizing on recent progress made in the field of aliphatic C–H oxidation chemistry.[11–13] Despite the need for additional oxidation steps, we rationalized the utility of this approach due to the ease with which we could prepare aldehyde **5.16** (see Experimental Section 5.4 for details) and the comparatively high yields with which we could produce the annulated product. Together these factors suggested concise preparation of the quassinoid tricarbocyclic scaffold with pragmatic functional handles was still possible.

In pursuit of this strategy, we investigated two of the more well precedented methodologies for aliphatic C–H oxidations in complex chemical settings: White's C–H oxidation and Alexanian's C–H bromination.[11,12] Although these transformations are mediated by different sets of conditions, both utilize carefully tailored catalysts that differentiate between subtle discrepancies in electronic and steric environments, typically engaging methylenes with the most electron-rich, sterically accessible C–H bonds. These catalysts offer exquisite control in a variety of settings including complex terpenoid motifs.[11–13] A relevant example is the functionalization of the terpenoid sclareolide **5.21** (Scheme 5.3). In our system, we aimed to test these C–H functionalizations on compounds such as tricycle **5.26**, where the cyclopentene motif of **5.14** has been removed as this electron-rich alkene may present a liability under the oxidation conditions. Considering the stereoelectronic environments of the carbons in this system, we believed that C2 would be the most likely site of functionalization followed by C1 and C3, analogous to the selectivity observed by White and Alexanian for sclareolide.

Scheme 5.3: C–H Oxidation Precedent and Strategy

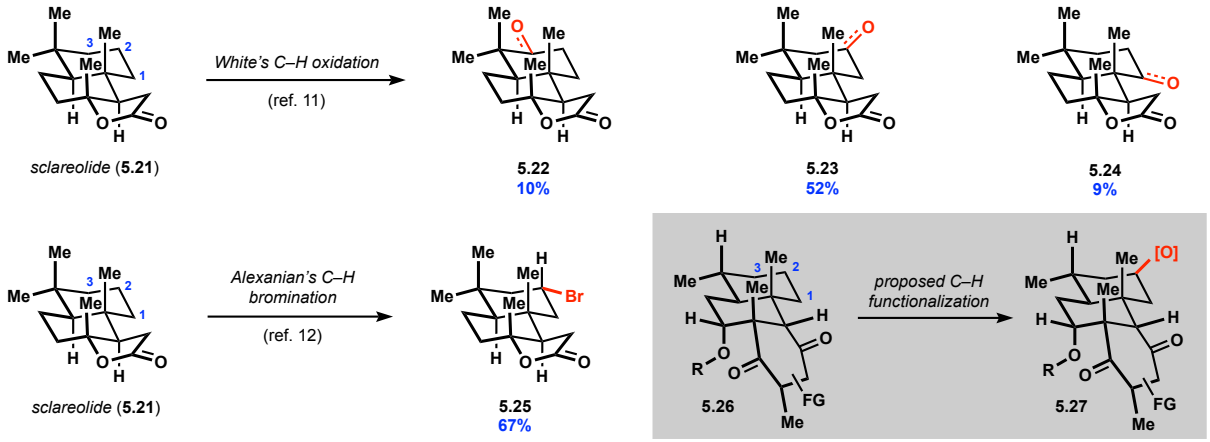

With this new strategy in mind, we set out to prepare suitable tricycles to test C–H functionalizations. Our first goal in elaborating annulation product **5.28** to these C–H

Scheme 5.4: Elaboration to Tricarbocyclic Core

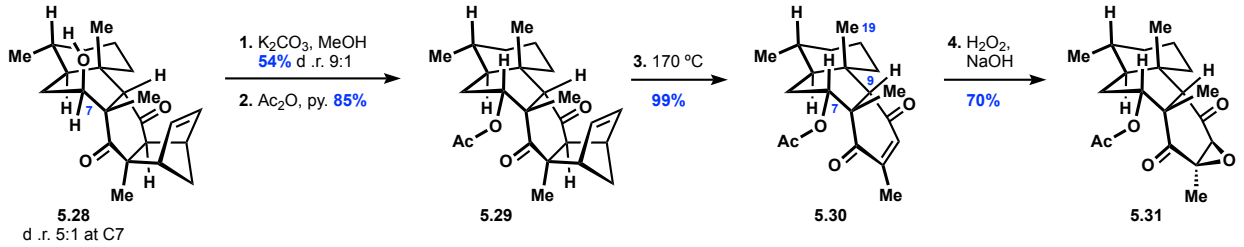

functionalization precursors was to correct the C7 stereocenter, which had been set with poor diastereocontrol in the annulation favoring the undesired configuration (Scheme 5.4). Initially, this appeared to be a nontrivial task because if the *trans-syn-cis* perhydro-phenanthrene motif of **5.28** adopted an all chair-like conformation, then the desired C7 configuration would place the alcohol in an axial orientation (for reference see structure **5.14**, Table 5.1), which would likely not be the thermodynamic epimer. In working with compound **5.28** we also observed apparent epimerization of C7 in the presence of base, ultimately finding that we could achieve production of the desired C7 epimer in basic solutions of methanol, which presumably proceeds through a retro-aldol–aldol sequence. Following acylation and retro-cycloaddition, 2D NMR experiments of enedione **5.30** shed light onto the potential origins of this surprising result. We observed correlations between the C7 proton and the C9 proton and C19 methyl protons, which would not be expected if the B-ring was in a chair-like conformation, suggesting that this cyclohexane may be in a twist-boat configuration. This hypothesis would also explain the thermodynamic preference for the desired C7 configuration, where a twist boat conformation would place the alcohol at C7 in a pseudo-equatorial orientation in the desired configuration. Although this conformational assignment for the B-ring is tentative, our subsequent efforts towards quassin led us to study a related compound by X-ray crystallographic analysis and this system unambiguously displayed the B-ring in a twist-boat conformation, providing plausibility to the above hypothesis (see below).

Having elaborated annulation product **5.28** to suitable precursors for C–H oxidation studies, we commenced these investigations. First, we evaluated White's Fe(CF_3-PDP) pre-catalyst. Gratifyingly we observed production of four major products, two alcohols and two carbonyls (Scheme 5.5). The two alcohols were isolated as an inseparable 1:1 mixture. Treating this mixture with DMP delivered the two carbonyl products, previously isolated, confirming predominant oxidation at two carbons. One set of these products was confirmed to be oxidation at C2, which we established by converting the 1:1 mixture of alcohols to the corresponding TBS ethers, where one of these silyl ethers matched an intermediate prepared from aldehyde **5.19** (Scheme 5.4, see Experimental Section 5.4 for details). At this time, we have not determined which carbonyl product corresponded to C2 oxidation. We have tentatively assigned the carbonyl produced in slightly higher quantities to C2 oxidation. The other site of oxidation remains to be unambiguously confirmed, but we tentatively assigned this set of products to either functionalization of C1 or C3 based on ^{1}H NMR analysis.

Scheme 5.5: C–H Oxidation

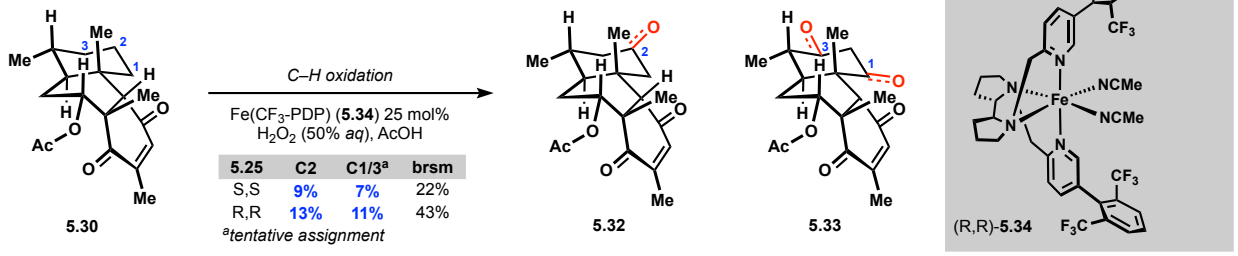

5.25	C2	C1/3[a]	brsm
S,S	9%	7%	22%
R,R	13%	11%	43%

[a]tentative assignment

Unfortunately, preliminary attempts to optimize these reaction conditions were unsuccessful. Both (S,S)- and (R,R)-Fe(CF_3-PDP) resulted in similarly low yields and increased reaction times or catalyst loading did not significantly improve outcomes.[11]

The initial results from attempted C–H oxidations were not ideal in terms of yield, but they were encouraging regarding site-selectivity. While attempting to optimize conditions with White's iron catalyst, we investigated Alexanian's aliphatic C–H bromination with N-bromoamide **3.35** (Figure 5.2). Unfortunately, with several different substrates we were unable to isolate C2 brominated products. In the case of cyclopentene **5.29**, we observed a complex mixture of products potentially a result of reactivity with the alkene functionality. With enedione **5.30** one major product was formed, which we have tentatively assigned to bromination at C17. This site selectivity may reflect the lower BDE at this position due to stabilization of the intermediate radical. Masking the enedione as an epoxide to suppress this reactivity, resulted in only recovered starting material.

Figure 5.2: C–H Bromination

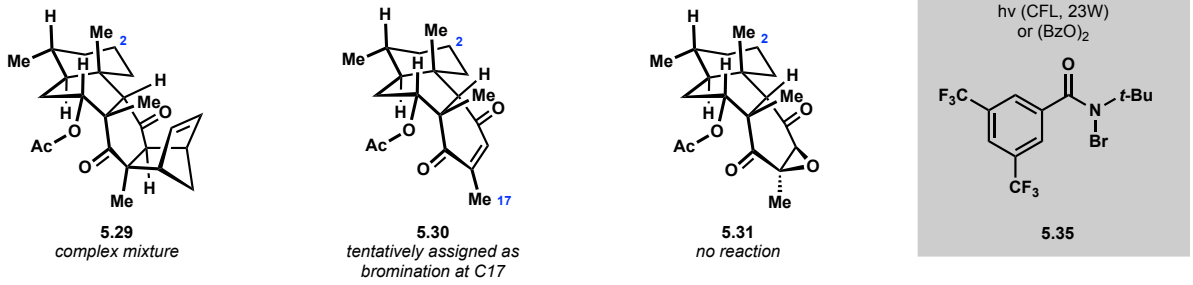

5.29
complex mixture

5.30
tentatively assigned as bromination at C17

5.31
no reaction

5.35

5.2.3 Evolution of Approach to the A-, B-, and C-Rings

The suboptimal results from these C–H functionalization strategies led us to reconsider our synthetic tactics once again. Ideally, we would be able to accomplish an MHAT-initiated annulation with a γ,δ-unsaturated aldehyde bearing relevant oxidation on the A-ring, but based on our past efforts these coupling partners had poor reactivity profiles in annulations with enedione **5.13**. A significant portion of the mass balance could be attributed to formation of diones **5.15**, resulting from MHAT to the 1,2-disubstituted alkene of enedione **5.13** (Table 5.1). It also seemed plausible that intermediates generated following MHAT to enedione **5.13**, either radical in nature

or enolates, may engage unproductively with starting material leading to a portion of the unidentified side products we observed in these reactions. These ideas led us to consider removing the cyclopentene motif of enedione **5.13**, which would eliminate competing MHAT to the 1,2-disubstituted alkene of enedione **5.13** and increase the probability of engaging the 1,1-disubstituted alkene of the γ,δ-unsaturated aldehyde in an MHAT event with the generated iron hydride .

Following this line of thought, we became interested in the epoxyquinone enantiomers **5.36** and **3.59**, which had several potential benefits associated with them (Scheme 5.6). First, these systems lacked functionality that would compete with the 1,1-disubstituted alkene of the γ,δ-unsaturated aldehyde in the MHAT event. Second, the epoxide would install relevant oxidation found in quassin. Finally, the inductive effects of the oxygen may make the enedione a better radical acceptor in the initial Giese reaction. However, from the outset it was not clear if this epoxide would serve as a suitable element for stereocontrol in the annulation.

The stereochemical considerations for this annulation are worth further comment. With either enantiomer of the epoxyquinone we anticipated C10 would be set correctly, where the bulky epoxyquinone would approach the alkyl radical generated from **5.10** away from the formylmethyl substituent. The C8 and C9 stereocenters would likely be set based on facial selectivity of the

Scheme 5.6: Stereochemical Considerations for Epoxyquinones **5.36** and **5.39**

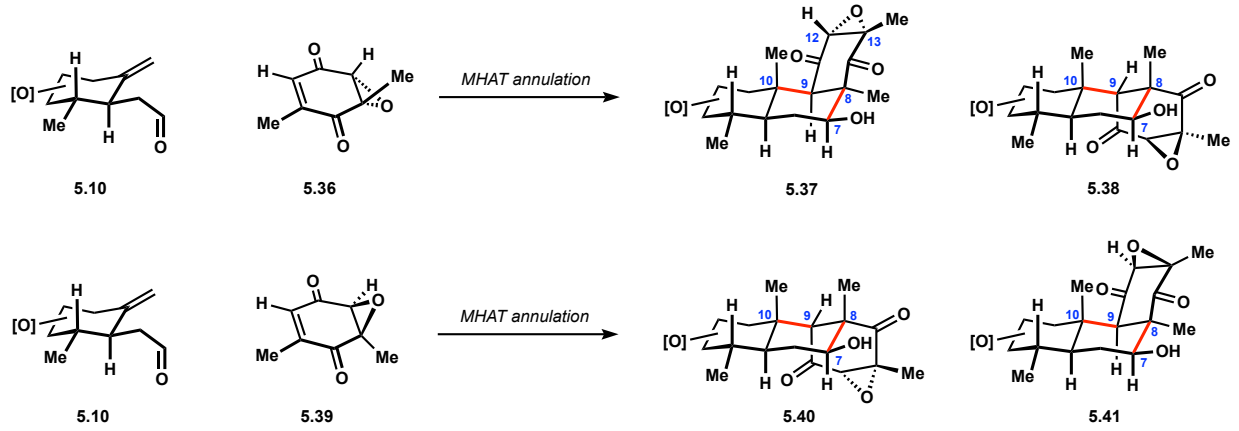

radical addition into the epoxyquinone. Although we were uncertain to what degree the epoxide would control this facial selectivity, we recognized that the C8 stereocenter could potentially be epimerized through a retro-aldol–aldol sequence and that the C9 stereocenter could likely be corrected late-stage based on prior work from Valenta.[5a,8] Importantly, the resulting C12 and C13 stereocenters would ultimately be ablated in the natural product, so regardless of the facial selectivity in the initial Giese addition, or lack thereof, we could potentially utilize both resulting sets of products **3.57** and **3.58** or **5.40** and **5.41**. Finally, we suspected that the C7 stereocenter would be set with the undesired configuration because we anticipated the second bond forming aldol event would proceed through a closed, chair-like transition state resulting in an equatorial alcohol. However, considering Shing's ability to invert the C7 stereocenter we were not dissuaded by this postulation.[6]

In practice, we found that epoxyquinone **5.36** was an exceptional coupling partner in these MHAT-initiated annulations and remarkably produced the annulated products with high levels of diastereocontrol at all four newly established stereocenters (Table 5.2). Annulation with epoxyquinone **5.39** appeared to be inefficient based on analysis of the crude reaction mixture by ^{1}H NMR with internal standard as a guide and isolation of the products was not pursued.

Table 5.2: Annulations with Epoxyquinone **5.36**

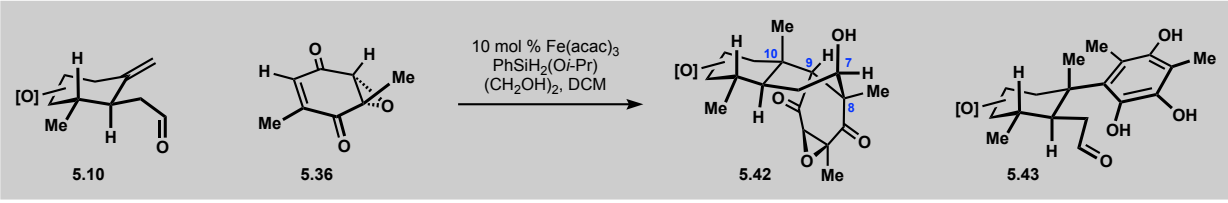

[a] yield determined by ^{1}H NMR analysis with mesitylene as internal standard [b] isolated yield

Interestingly, we later identified a compound in trace quantities produced in the annulation between **5.36** and aldehyde **5.20** that we assigned as a trihydroxyarene (**5.43**). Upon further analysis of the corresponding reaction with epoxyquinone **5.39** we found that this same product was formed in significant quantities (16%). The increased production of trihydroxyarene **5.43** with epoxyquinone **5.39** may reflect a slower second bond forming event leading to an aromatization pathway outcompeting the putative aldol process, where there is effectively a match-mismatch scenario between the enantioenriched aldehyde and enantiomers of the epoxyquinones **5.36** and **5.39**.[14]

Characterization of the annulation product arising from aldehyde **5.20** and epoxyquinone **5.36** by X-ray crystallography and 2D NMR analysis showed that the C8 and C10 stereocenters were set correctly, while the C9 and C7 stereocenters were in the undesired configurations. Surprisingly, it appeared that both in the solid state and in solution the B-ring adopted a twist-boat conformation, placing the C7 alcohol in a pseudoaxial orientation. At this time, it is unclear why the epoxide motif imparts a significant degree of stereocontrol in the initial radical addition, but this observation may be useful beyond its application to quassinoid natural products. It is also not apparent why the B-ring adopts a twist-boat conformation or why the second bond forming event ultimately leads to the secondary alcohol in a pseudoaxial orientation.[15] All questions that warrant further interrogation.

Despite these unpredicted outcomes, we were nevertheless able to improve yields across the panel of γ,δ-unsaturated aldehyde evaluated when compared to annulations with cyclopentadiene Diels–Alder adduct **5.13** (**5.17**, **5.18**, **5.20**, Table 5.2). Encouraged by these results, we investigated γ,δ-unsaturated aldehyde **5.44** with oxidation at both C1 and C2, making it an ideal precursor en route to quassin. A preliminary evaluation revealed that the annulated

product was formed in reasonable yields, but due to the additional synthetic manipulations required to prepare aldehyde **5.44** and challenges associated with differentiating the resulting triol we ultimately pursued an alternative route.

We chose to continue our efforts towards quassin with aldehyde **5.20**, which formed the annulation product in synthetically useful yields and notably contained relevant oxidation at C2. However, subsequent studies revealed that removal of the TBS group on the C2 alcohol was challenging and remained intact in the presence of both acidic and basic fluoride reagents. Because of this we elected to replace it with a more labile TES group.

To prepare this TES protected derivative we could either start from (+)-3-methylcyclohexanone (**5.45**) and perform an IBX-mediated oxidation reported by the Nicolaou laboratory to access enone **5.47** (Scheme5.7).[16] Alternatively, we could execute a dealkenylation of (–)-isopulegol (**5.46**) reported by the Newhouse group and then oxidize the intermediate allylic alcohol to the same enone **5.47**.[17] The latter route proved to be scalable and importantly more cost effective.[18] Enone **5.47** was then converted to epoxynitrile **5.48**, by alkylation of the corresponding enolate with bromoacetonitrile, followed by treatment with basic hydrogen peroxide. This epoxynitrile was then reduced with DIBAL–H to the corresponding homoallylic alcohol and aldehyde. A final silylation afforded the desired γ,δ-unsaturated aldehyde **5.49**.

Scheme 5.7: Synthesis of Aldehyde **5.49**

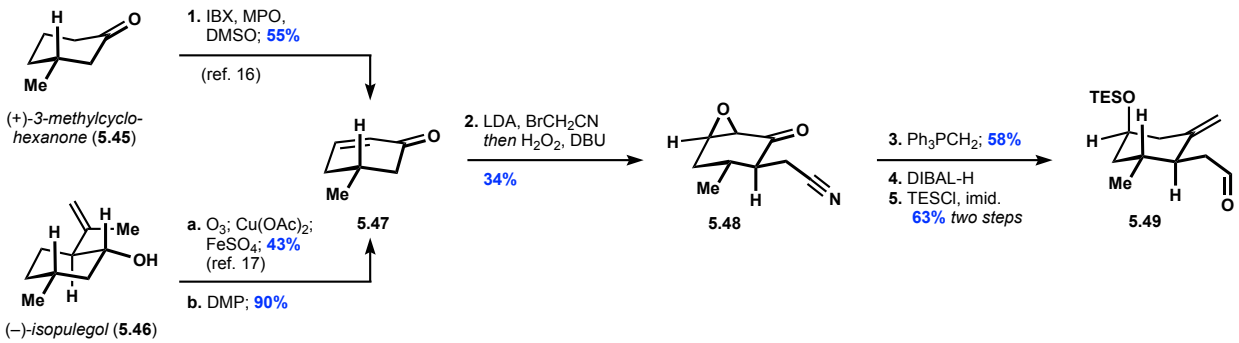

The synthesis of epoxyquinone **5.36** leveraged the same asymmetric Diels–Alder annulation developed by Corey that we had previously employed (Scheme 5.8).[10] Subsequent epoxidation and retro-Diels–Alder reaction afforded the desired epoxyquinone **5.36** in good yield over two steps.

Scheme 5.8: Synthesis of Epoxyquinone **5.36**

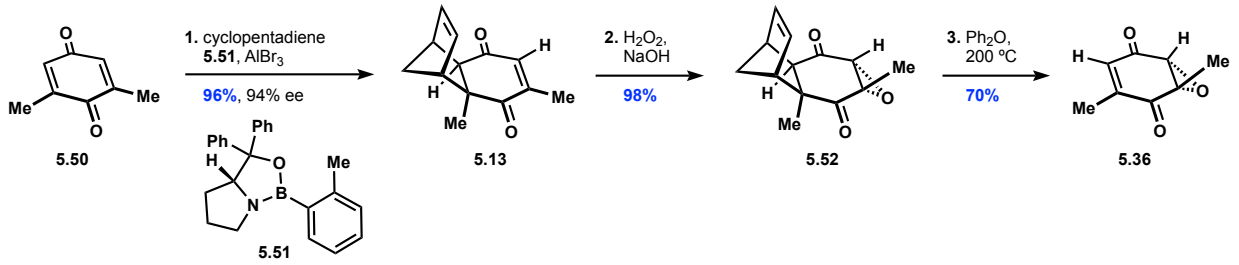

These two coupling partners fared well in the annulation delivering the cyclized product **5.53** (Scheme 5.9). Notably, we could lower the stoichiometry of aldehyde **5.49** from 2 equivalents to 1.5 equivalents while maintaining synthetically useful yields. Further decreases in the amount of aldehyde **5.49** resulted in a precipitous loss of efficiency. Having secured a route to the tricarbocyclic core of the quassinoids, we now turned our attention to epimerizing C7. We were aware that the Shing group had encountered a similar challenge in their synthesis of quassin and had epimerized C7 via a multistep stereoinvertive displacement. However, we recognized that in our system we could leverage the twist-boat conformation of the B-ring to our advantage. Since the annulation produced the alcohol at C7 in a pseudoaxial orientation, we realized this stereocenter should readily epimerize to the more thermodynamically favorable pseudoequatorial

Scheme 5.9: Annulation and Epimerization of C7

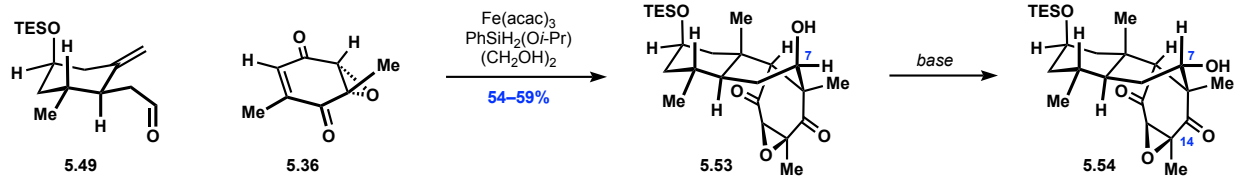

orientation upon exposure to base to induce a retro-aldol–aldol event. It is worth noting that this would not be the case if the B-ring were to adopt a chair-like conformation where the desired alcohol at C7 would then be in an axial orientation. Gratifyingly, we found that under a variety of basic conditions the C7 stereocenter epimerized to the desired configuration.[19]

5.2.4 Approach to the D-Ring

Having established a route to the tricarbocyclic core of the quassinoids we next aimed to introduce the lactone functionality of the D-ring. The first avenue we pursued was based on a Myer–Schuster rearrangement, which would offer a concise entry to the desired lactone.[20] In pursuit of this idea, we subjected TMS derivative **5.55** to lithium phenoxyacetylide delivering the desired 1,2-addition product **5.57** along with hemi-ketal **5.58** (confirmed by X-ray crystallography) following acidic work-up (Scheme 5.10). Production of hemi-ketal **5.58** suggested that the desired Myer–Schuster rearrangement, where the C7 alcohol would cyclize onto C16, was outcompeted by cyclization onto C15. This process seemed to be rather facile as indicated by the significant production of hemi-ketal **5.58** following 1,2-addition of lithium phenoxyacetylide and work-up with aqueous HF or NH_4Cl. Preliminary attempts to catalyze the Myer–Schuster rearrangement with related alkoxyenthynyl derivatives employing silver- or gold-based Lewis acids were also unsuccessful.

Scheme 5.10: Attempted Meyer–Schuster Rearrangement

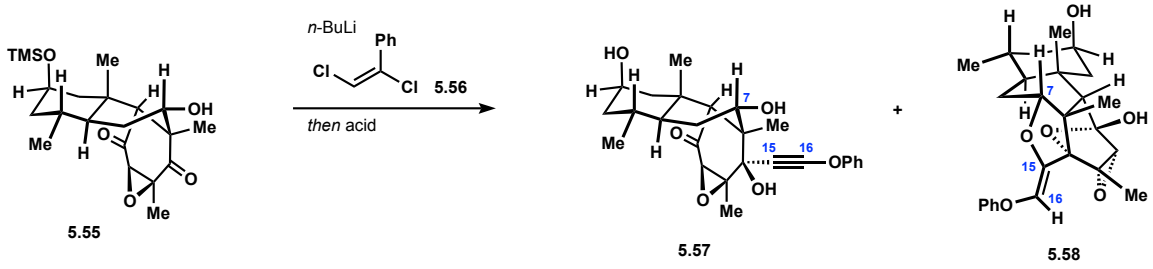

These preliminary results led us to consider alternative methods to form the D-ring lactone. We were aware of Shing's prior work, where the group converted a similar aldol motif found in

Figure 5.3: Attempted D-Ring Formation

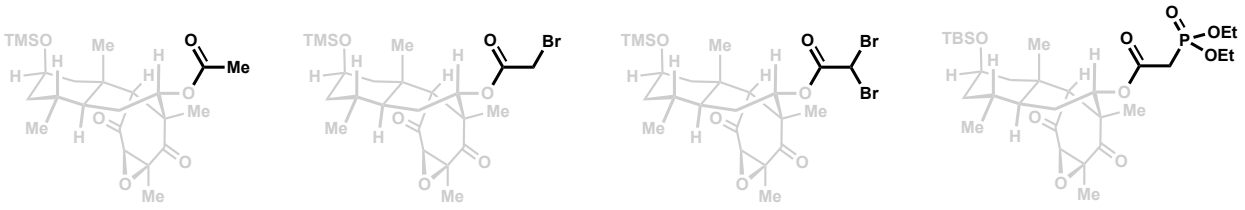

epimerization product **5.54** to the D-ring lactone via acylation of the C7 alcohol followed by intramolecular aldol condensation with the carbonyl at C14 (Scheme 5.9, see Chapter 4 for a detailed discussion). We wondered if we could capitalize on a similar strategy and proceeded to prepare several functionalized aldol products for lactone formation (**5.59**–**5.62**, Figure 5.3). While we were able to form the aldol product from acetate **5.59** in small quantities, unfortunately, all other attempts to forge the desired lactone were unsuccessful leading predominantly to recovered starting material or complex mixtures if forcing conditions were employed. Considering the conformation of these *trans-syn-cis* perhydro-phenanthrenes we rationalized our inability to efficiently form the lactone motif was due to the necessity for the substituent tethered to the C7 alcohol to approach the carbonyl at C14 from the concave face of the *trans-syn-cis* perhydro-phenanthrene likely resulting in severe steric penalties (Figure 5.4). However, we hypothesized that if we were to epimerize C9 to form the *trans-anti-trans* perhydro-phenanthrene, this would unencumber approach into the C14 carbonyl allowing for more facile formation of the desired lactone.

Figure 5.4: Hypothesis Regarding Thwarted D-Ring Formation

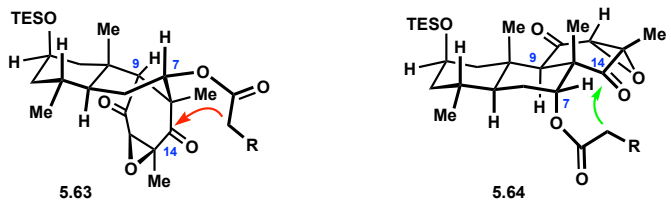

In order to accomplish epimerization of C9, we relied on prior observations made in our synthetic campaign. Earlier, we found that intermediates containing a TBS ether at C2 were resistant to deprotection in the presence of basic fluoride sources. Interestingly, upon heating rather than cleavage of the silyl ether, we observed epimerization of C9. Implementing these tactics with phosphonate **5.65**, we ultimately found that we could induce epimerization at C9 and effect the desired Horner–Wadsworth–Emmons olefination using cesium fluoride (Scheme 5.11). These conditions also partially deprotected the TES ether at C2, and the mixture of products could be oxidized in a subsequent step to the corresponding ketone **5.67**. Preparation of phosphonate **5.66** capitalized on epimerization of C7 with sodium hydride in toluene, followed by coupling with phosphonoacetic acid **5.65**.

Scheme 5.11: Formation of D-Ring

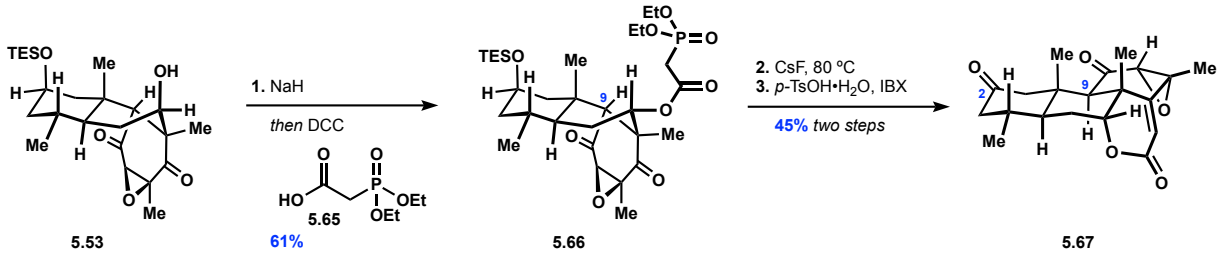

5.2.5 Late-Stage Redox Manipulations

At this stage in the synthesis, we had efficiently established the tetracyclic core of quassin and were separated from the natural product by a series of redox manipulations. We first investigated converting the C- and D-rings to the desired oxidation state. The Shing group had encountered a similar unsaturated epoxylactone (**5.68**) in their synthesis of quassin and found that palladium-catalyzed hydrogenation afforded alcohol **5.69** (Scheme 5.12). In our system utilizing the same hydrogenation conditions with unsaturated epoxylactone **5.67** afforded saturated lactone **5.70** with the epoxide still intact. Further attempts to reductively open the allylic epoxide of **5.67** with Ti^{III} or in an S_N2' fashion at C15 by addition of phenylselenide or a hydrogen atom via MHAT

with Fe, Co, or Mn were unsuccessful.[21] In working with epoxide **5.67**, we observed isomerization to the enol-tautomer of the 1,2-dione **5.71** under a variety of conditions (Scheme 5.13). We believed we could take advantage of this reactivity and found that subjecting epoxide **5.67** to Pd(*t*-$Bu_3P)_2$ resulted in efficient isomerization. Then, a chemoselective hydrogenation afforded the desired saturated lactone, notably maintaining the desired oxidation pattern of the C-ring. The observed chemoselectivity was solvent dependent where methanol proved essential to avoiding over reduction.[22] Notably, the saturated lactone motif had presented a liability in prior syntheses and was invariably protected as the corresponding lactol. By revealing this functionality at the end of our sequence and through the judicious choice of subsequent redox manipulations, we were able to avoid sacrificial steps associated with protecting this functionality.

Having established the desired oxidation state of the C- and D-rings we faced a final oxidation event at C1. This was a non-trivial task because C1 is the more sterically encumbered α-position of the carbonyl at C2 and attempts to form the corresponding enolate under kinetic or thermodynamic conditions resulted in enolization at C3 precluding direct oxidation of enolate intermediates. It is worth noting that Shing encountered a challenging C1 oxidation in their synthesis of quassin as well.[6] In this instance, the group leveraged an enone functionality to

Scheme 5.12: Late-Stage Redox Manipulations

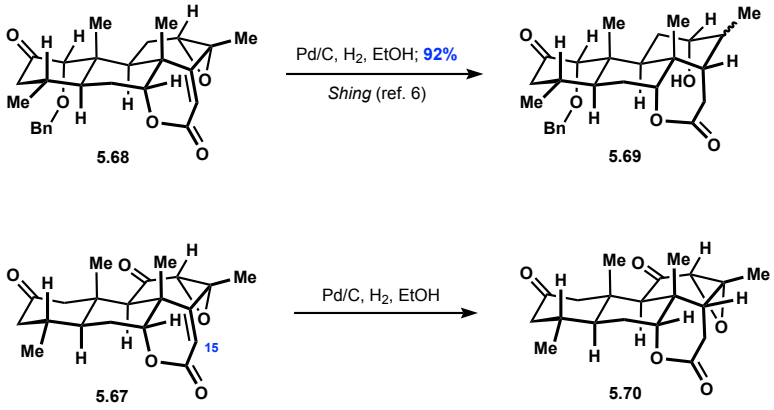

effectively block the C3 position allowing for a $Mn(OAc)_3$ mediated oxidation to deliver the desired C1 acetate product. However, we were not particularly keen on adopting this strategy because in the context of our synthesis this would necessitate a series of unproductive redox manipulations associated with installing and removing the requisite enone. Ultimately, we developed a three-step solution to this problem. First, we prepared TIPS enol ether **5.73**, which allowed us to perform a subsequent SeO_2 mediated allylic oxidation, installing the requisite oxidation at C1 following a subsequent Swern oxidation (**5.74**).[23,24] Finally, enolization of **5.74** with basic fluoride in the presence of methyl iodide delivered quassin.

Scheme 5.13: Final Approach to Quassin

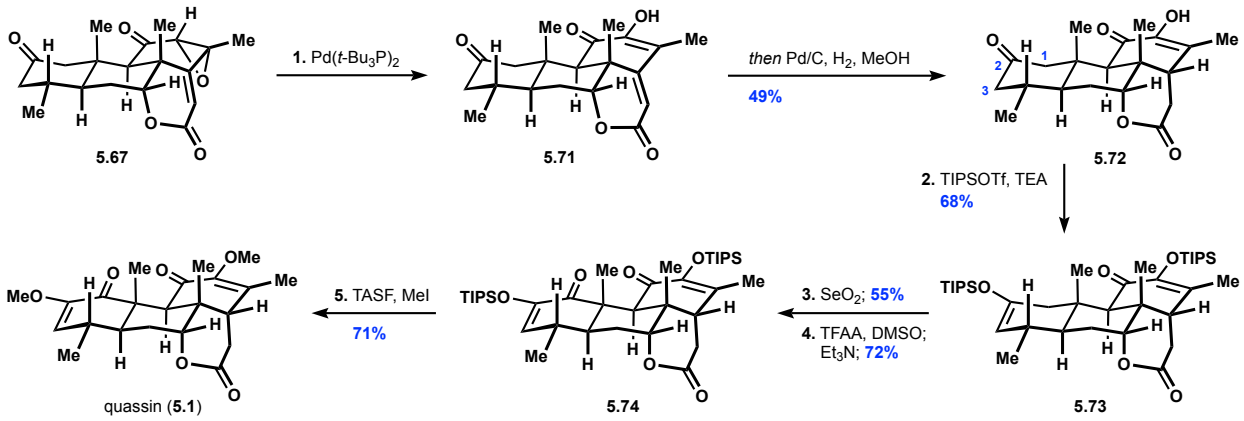

5.3 Conclusion

In summation, this work represents a 14-step synthesis of quassin from commercially available material (Scheme 5.14). Our strategy was guided by preceding efforts in the field and aimed to address some of the remaining synthetic challenges associated with quassinoids. The efficiency of our route can largely be attributed to the rapid construction of the tricarbocyclic core of the quassinoids through an MHAT-initiated annulation and our judicious choice of functional handles, which mitigated subsequent redox manipulations. Regarding the MHAT-initiated annulation, it is worth highlighting the improved efficiency of epoxyquinone **5.36** and the

remarkable degree of stereocontrol imparted by the epoxide motif, which may prove valuable beyond the context of quassinoid synthesis. It is also noteworthy that the resulting *trans-syn-cis* perhydro-phenanthrenes adopted twist-boat conformations, an observation whose origins currently remain ambiguous and warrants further inquiry, but that we nevertheless leveraged to efficiently epimerize the C7 stereocenter.

Regarding our strategy as it pertains to redox manipulations, we identified several useful reactivity pattens including, an isomerization-hydrogenation of epoxylactone **5.67** to access the desired oxidation state of the C- and D-rings, and a SeO_2 mediated allylic oxidation to install oxidation at C1. Despite the overall efficient preparation of quassin and the care taken to avoid unnecessary redox events, these manipulations still account for the bulk of synthetic steps highlighting the challenges of quassinoids and the importance of thoughtful consideration in synthetic planning regarding functional group installation. We anticipate that the lessons learned from our efforts towards quassin will translate to the synthesis other quassinoid congeners and may prove valuable in preparing other highly oxidized terpenoid natural products.

Scheme 5.14: Synthesis of Quassin

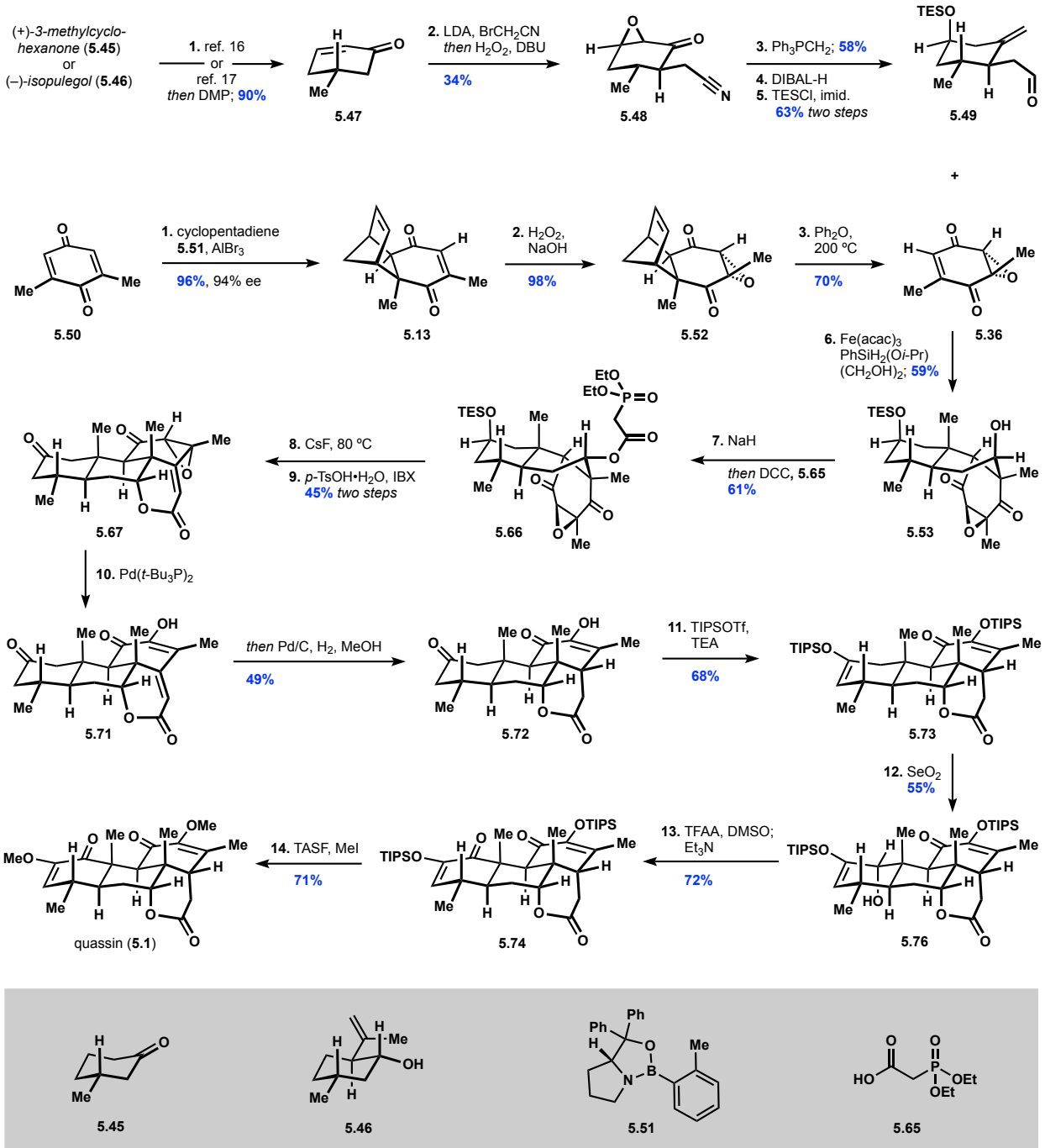

5.4 Experimental

5.4.1 Materials and Methods

All reactions were carried out in flame-dried glassware under positive pressure of dry nitrogen unless otherwise noted. Reaction solvents (Fisher, HPLC grade) including tetrahydrofuran (THF), dichloromethane (DCM), methanol (MeOH) and toluene (PhMe) were dried by percolation through a column packed with neutral alumina and a column packed with a supported copper catalyst for scavenging oxygen (Q5) under positive pressure of argon. Anhydrous dimethyl sulfoxide (DMSO, Sigma Aldrich, reagent grade), anhydrous dimethylacetamide (DMA, Fisher, reagent grade) and anhydrous triethylamine (Et_3N, Oakwood Chemical, reagent grade) were distilled from calcium hydride (10% w/v) under positive pressure of nitrogen. Anhydrous 1,4-dioxane (TCI, reagent grade) was distilled from lithium aluminum hydride under positive pressure of nitrogen. Solvents for extraction, thin layer chromatography (TLC), and flash column chromatography were purchased from Fischer (ACS Grade) and VWR (ACS Grade) and used without further purification. Chloroform-d and benzene-d_6 for ^1H and ^{13}C NMR analysis were purchased from Cambridge Isotope Laboratories and used without further purification. Commercially available reagents were used without further purification unless otherwise noted. Reactions were monitored by thin layer chromatography (TLC) using precoated silica gel plates (EMD Chemicals, Silica gel 60 F_{254}) – also used for preparative TLC. Flash column chromatography was performed over silica gel (Acros Organics, 60 Å, particle size 0.04-0.063 mm). HPLC analysis was performed on an Agilent 1100 series. Optical rotation readings were obtained using JASCO P-1010 polarimeter. ^1H NMR and ^{13}C NMR spectra were recorded on Bruker DRX-500 (BBO probe), Bruker DRX-500 (TCI cryoprobe), Bruker AVANCE600 (TBI probe), and Bruker AVANCE600 (BBFO cryoprobe) spectrometers using residual solvent peaks as internal standards ($CHCl_3$ at 7.26 ppm ^1H NMR, 77.16 ppm ^{13}C NMR; C_6H_6 at 7.16 ppm ^1H NMR, 128.00 ppm ^{13}C NMR). High-resolution mass spectra (HRMS) were recorded on Waters LCT Premier TOF spectrometer with ESI and CI sources.

5.4.2 Experimental Procedures

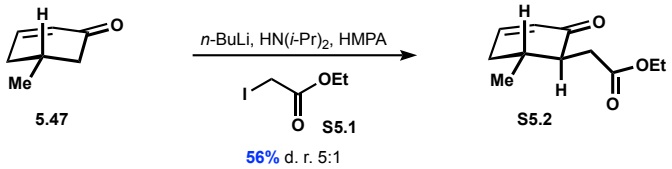

Enone S5.2.[25] LDA was prepared in a 250 mL round bottom flask from diisopropylamine (1.7 mL, 12.0 mmol) and *n*-butyllithium (5.2 mL of a 2.13 M solution in hexanes, 11.0 mmol) in THF (12 mL). The flask was then cooled to –78 ºC and enone **5.47** (1.10 g, 10.0 mmol) was added over 10 min down the walls of the flask as a solution in THF (25 mL). The reaction was stirred for 20 min at which point HMPA (8.7 mL) was added slowly followed by ethyl iodoacetate **S5.1** as a solution inf THF (25 mL) over 15 min down the walls of the flask. After 2.5 h the reaction was warmed to –40 ºC, then after 45 min warmed to 0 ºC for 15 min at which point 1M aqueous HCl (50 mL) was added. The aqueous phase was extracted three times with diethyl ether (150 mL combined). The organic layers were combined and washed sequentially with water (50 mL), saturated aqueous $Na_2S_2O_3$ (25 mL), twice with water (500 mL combined), and brine (25 mL). The organic layer was dried over anhydrous magnesium sulfate, filtered and concentrated under reduced pressure. Purification by flash chromatography (gradient elution: 5% to 50% v/v diethyl ether in pentane) afforded enone **S5.2** (1.10 g as a 5:1 mixture of diastereomers, 56%) as a colorless oil.

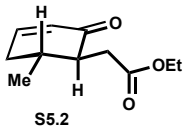

S5.2

Enone **S5.2**

^{1}H NMR (500 MHz, $CDCl_3$)

δ 6.94–6.90 (m, 1H)	2.63–2.51 (m, 2H)	1.27 (t, 3H, J = 7.13 Hz)
6.04–6.02 (m, 1H)	2.46–2.41 (m, 1H)	1.07 (d, 3H, J = 6.4 Hz)
4.16 (q, 2H, J = 7.1 Hz)	2.21–2.11 (m, 1H)	
2.73 (dd, 1H, J = 16.2, 6.1 Hz)	1.57 (s, 3H)	

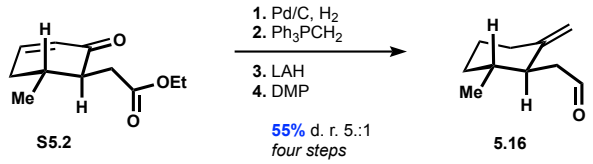

Aldehyde 5.16.[25] A round bottom flask was charged with enone S5.2 (1.10 g, 5.61 mmol) and a suspension of Pd/C (110 mg, 10% w/w) in MeOH (30 mL) was added. The reaction vessel was purged with nitrogen and then a balloon of hydrogen was introduced. The reaction was sparged for 15 min, then stirred for 2.5 h. After which point the reaction mixture was filtered through a plug of celite and then a plug of silica gel.

The semi-purified material was then concentrated under reduced pressure and dissolved in THF (10 mL). This solution was then added to a solution of methylenetriphenylphosphorane, prepared from methyl triphenylphosphonium bromide (2.4 g, 6.7 mmol) and *n*-butyllithium (2.9 mL of a 2.13 M solution in hexanes, 6.2 mmol), in THF (15 mL) at –78 ºC. The reaction was then warmed to room temperature and after 1 h quenched with 1Maqueous HCl. The organic layer was dried over anhydrous magnesium sulfate, filtered through a plug of silica gel and concentrated under reduced pressure.

The semi-purified material was then dissolved in diethyl ether (8 mL) and added to suspension of LAH (203 mg, 5.34 mmol) in diethyl ether (10 mL) at 0 ºC slowly. The reaction was warmed to room temperature for 1 h and then cooled to 0 ºC. At which point water (0.2 mL) followed by 2M aqueous NaOH (0.4 mL) followed by magnesium sulfate was added. The reaction mixture was vigorously stirred then filtered and concentrated under reduced pressure. The semi-purified material was then dissolved in DCM (15 mL) and $NaHCO_3$ (665 mg, 7.9 mmol) was added. The mixture was then cooled to 0 ºC and Dess–Martin periodinane (1.7 g, 4.0 mmol) was added in portions over 5 min. After 1 h another portion of Dess–Martin periodinane (150 mg, 0.35 mmol) was added. After an additional 1 h the reaction was quenched with saturated aqueous

$Na_2S_2O_3$ and $NaHCO_3$. The aqueous layer was extracted three times with diethyl ether. The organic layers were combined and washed sequentially with brine. The organic layer was dried over anhydrous magnesium sulfate, filtered and concentrated under reduced pressure. Purification by flash chromatography (gradient elution: 5% to 50% v/v diethyl ether in pentane) afforded enone **5.16** (472 mg as a 5:1 mixture of diastereomers, 55% four steps) as a colorless oil.

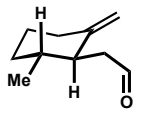

5.16

Enone **5.16**

^{1}H NMR (500 MHz, $CDCl_3$)

δ 9.72 (s, 1H)	2.38–2.32 (m, 1H)	1.50–1.40 (m, 2H)
4.76 (s, 1H)	2.29–2.24 (m, 1H)	1.32–1.26 (m, 1H)
4.54 (s, 1H)	2.09–2.04 (m, 1H)	0.98 (d, 3H, J = 6.9 Hz)
2.59 (m, 2H)	1.75 (m, 2H)	

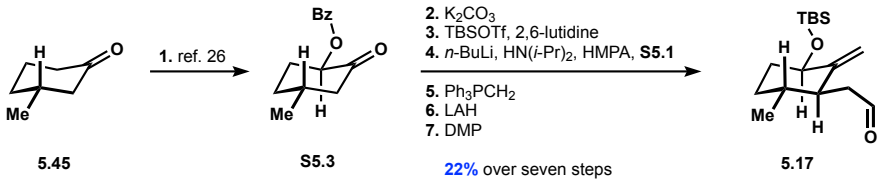

Aldehyde 5.17.[25] Known ketone **S5.3** was prepared from (R)-(+)-3-methylcyclohexanone **5.45** (2.0 mL, 16.3 mmol) following protocol reported from List.[26] This material was then treated with K_2CO_3 (14 g) in MeOH (40 mL), water (40 mL), and THF (30 mL). After 7.5 h the reaction was diluted with water and extracted with DCM. The organic layers were combined and dried over anhydrous magnesium sulfate, filtered, concentrated under reduced pressure and filtered through plug of silica.

This semi-purified material (1.0 g) was then dissolved in DCM (40 mL) and 2,6-lutidine (1.8 mL, 15.6 mmol) was added. The flask was cooled to –78 ºC and TBSOTf (2.0 mL, 8.6 mmol) was added over 10 min. The reaction was warmed to 0 ºC and then quenched with 1M aqueous HCl. The phases were separated, and the organic layer was dried over anhydrous magnesium sulfate, filtered, concentrated under reduced pressure, and filtered through a plug of silica gel.

The semi-purified material (1.55 g) was then alkylated with ethyl iodoacetate **S5.1**, olefinated with methylenetriphenylphosphorane, reduced with LAH, and oxidized with DMP according to the previously described procedure for aldehyde **5.16**. Purification by flash chromatography (eluent: 100% hexanes) afforded aldehyde **5.17** (1.0 g, 22% seven steps) as a colorless oil.

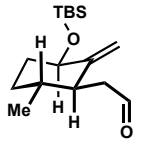

5.17

Aldehyde **5.17**

^{1}H NMR (500 MHz, $CDCl_3$)

δ 9.73 (dd, 1H, J = 2.8, 1.9 Hz)	2.23 (m, 1H)	0.06 (s, 3H)
5.15 (s, 1H)	1.96 (m, 1H)	0.06 (s, 3H)
4.62 (s, 1H)	1.83 (m, 1H)	
4.03 (dd, 1H, J = 10.2, 4.8 Hz)	1.42–1.29 (m, 3H)	
2.69 (ddd, 1H, J = 16.9, 9.1, 2.8 Hz)	0.94 (d, 3H, 6.4 Hz)	
2.60 (ddd, 1H, J = 16.9, 4.8, 1.3 Hz)	0.91 (s, 9H)	

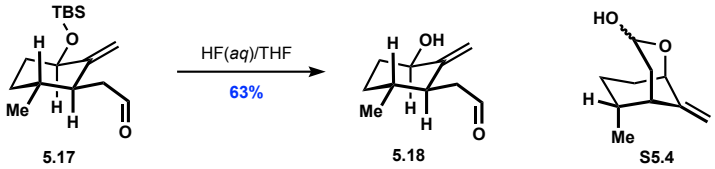

Aldehyde 5.18.[25] A 10 mL round bottom flask was charged with aldehyde **5.17** (108 mg, 0.38 mmol) and THF (2.0 mL) followed by aqueous 49% HF (0.5 mL). After 1h saturated aqueous $CaCO_3$ was added. The aqueous phase was extracted three times with diethyl ether (75 mL combined). The organic layers were combined and washed sequentially with twice with water (20 mL). The organic layer was dried over anhydrous sodium sulfate, filtered and concentrated under reduced pressure. Purification by flash chromatography (eluent: 100% hexanes) afforded aldehyde **5.18** (40.4 mg, 63%) as a white solid along with a small amount of diethyl ether present (5.0 mg, 11% w/w).

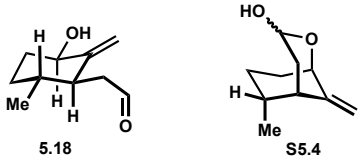

Aldehyde **5.18** was characterized in $CDCl_3$ as a 4:1 mixture with the corresponding lactol **S5.4** (stereochemistry not unambiguously determined). ^{1}H NMR data reported for aldehyde **5.18**

^{1}H NMR (500 MHz, $CDCl_3$)		
δ 9.75 (m, 1H)	2.72–2.62 (m, 2H)	1.39–1.31 (m, 3H)*
5.11 (s, 1H)	2.27–2.22 (m, 1H)	0.96 (d, 4H, J = 5.9 Hz)*
4.66 (s, 1H)	2.13 (m, 1H)	
4.10 (m, 1H)	1.84–1.77(m, 1H)	

*lactol skews integration

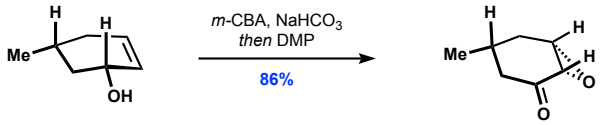

S5.5 S5.6

Epoxyketone S5.6.[25] A 100 mL round bottom flask was charged with alcohol **S5.5**[17] (1.12 g, 10.0 mmol), $NaHCO_3$ (2.94 g, 35.0 mmol), and DCM (20 mL). The flask was cooled to 0 ºC and *m*-CPBA (2.96 g, 70–75 wt%) was added as a suspension in DCM (40 mL) over 30 min. After 2 h $NaHCO_3$ (21 g, 25.0 mmol) was added followed by Dess–Martin periodinane (4.66 g, 11.0 mmol). After 30 min additional Dess–Martin periodinane (4.66 g, 11.0 mmol) was added. After 1.5 h the reaction was quenched with saturated aqueous $Na_2S_2O_3$ (50 mL) slowly at 0 ºC followed by saturated aqueous $NaHCO_3$ (50 mL). The aqueous layer was extracted three times with diethyl ether (200 mL combined). The organic layers were combined and sequentially washed with saturated aqueous $Na_2S_2O_3$ (50 mL), saturated aqueous $NaHCO_3$ (50 mL), water (50 mL), and brine (50 mL). The organic layer was dried over anhydrous sodium sulfate, filtered and concentrated under reduced pressure. Purification by flash chromatography (eluent: 100% hexanes) afforded epoxyketone **S5.6** (1.09 g, 86%) as a colorless oil.

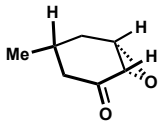

S5.6

Epoxyketone **S5.6**

^{1}H NMR (500 MHz, $CDCl_3$)

δ 3.55 (t, 1H, J = 4.1 Hz)	2.19–2.10 (m, 2H)	1.00 (d, 3H, J = 6.3 Hz)
3.18 (d, 1H, J = 3.8 Hz)	2.07–2.05 (m, 1H)	
2.52 (t, 1H, J = 13.1 Hz)	1.80–1.75 (m, 1H)	

^{13}C NMR (126 MHz, $CDCl_3$)

δ 208.1	54.8	34.0	22.2
58.7	43.8	31.6	

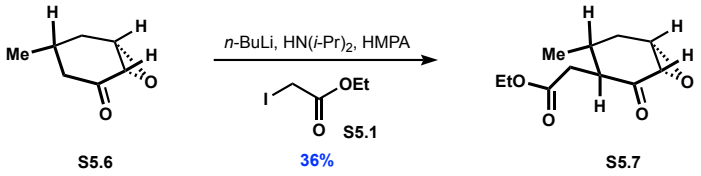

Ester S5.7.[25] LDA was prepared in a 100 mL round bottom flask from diisopropylamine (1.5 mL, 10.6 mmol) and *n*-butyllithium (4.0 mL of a 2.44 M solution in hexanes, 9.76 mmol) in THF (25 mL). The flask was then cooled to –78 ºC and epoxyketone **S5.6** (1.11 g, 8.8 mmol) was added over 10 min down the walls of the flask as a solution in THF (12.5 mL). The reaction was stirred for 20 min and HMPA (7.6 mL) was added slowly. The ethyl iodoacetate **S5.1** (2.1 mL, 17.8 mmol) was added slowly as a solution in THF (5 mL) down the walls of the flask. The reaction was allowed to warm to room temperature and after 15 h quenched with saturated aqueous NH_4Cl. The aqueous layer was extracted three times with diethyl ether (250 mL combined). The organic layers were combined and washed three times with water (300 mL combined) and then bring (50 mL). The organic layer was dried over anhydrous magnesium sulfate, filtered and concentrated under reduced pressure. Purification by flash chromatography (gradient elution: 10% to 20% v/v ethyl acetate in hexanes) afforded ester **S5.7** (664 mg, 36%) as a colorless oil.

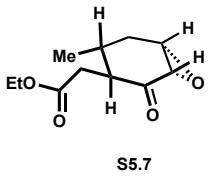

Ester **S5.7**

^{1}H NMR (500 MHz, $CDCl_3$)

δ 4.13 (q, 2H, J = 7.1 Hz)	2.56 (dd, 1H, J = 16.7, 8.2 Hz)	1.25 (t, 3H, J = 7.1 Hz)
3.56 (t, 1H, J = 4.2 Hz)	2.32 (dd, 1H, J = 16.8, 4.9 Hz)	0.98 (d, 3H, J = 6.2 Hz)
3.31 (d, 1H, J = 3.9 Hz)	2.22–2.14 (m, 1H)	
3.12–3.08 (m, 1H)	1.97–1.88 (m, 2H)	

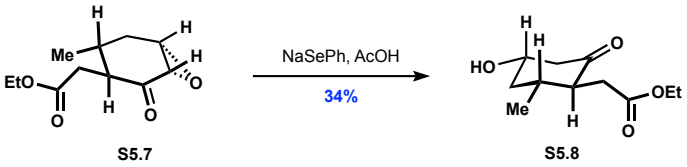

Alcohol S5.8.[25] A 50 mL round bottom flask was charged with diphenyl diselenide (1.33 g, 4.26 mmol) and EtOH (4 mL). The flask was cooled to 0 ºC and $NaBH_4$ (321 mg, 8.48 mmol) in EtOH (14 mL) was added slowly. The reaction was warmed to room temperature for 10 min then cooled to 0 ºC and acetic acid (81 µL, 1.4 mmol) was added. After 5 min, epoxyketone **S5.7** (601 mg, 2.83 mmol) was added slowly as a solution in EtOH (10 mL). After 20 min the reaction was diluted with brine. The aqueous layer was extracted three times with diethyl ether (150 mL combined). The organic layers were combined and washed with brine. The organic layer was dried over anhydrous magnesium sulfate, filtered and concentrated under reduced pressure. Purification by flash chromatography (gradient elution: 20% to 100% v/v ethyl acetate in hexanes) afforded alcohol **S5.8** (205 mg, 34%) as a colorless oil along with a small amount of ethyl acetate (15 mg, 7% w/w).

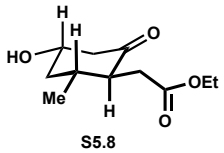

Alcohol **S5.8**

^{1}H NMR (500 MHz, $CDCl_3$)

δ 4.16–4.10 (m, 2H)	2.47–2.42 (m, 1H)	1.10 (d, 3H, J = 6.0 Hz)
3.90 (m, 1H)	2.39 (dd, 1H, J = 16.5, 4.1 Hz)	
2.79 (ddd, 1H, J = 12.7, 4.8, 2.3 Hz)	2.20–2.17 (m, 1H)	
2.62 (dd, 1H, J = 16.5, 8.1 Hz)	1.71 (d, 1H, J = 4.2 Hz)	
2.53–2.47 (m, 1H)	1.26 (t, 3H, J = 7.2 Hz)	

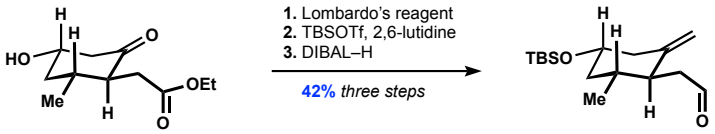

S5.8 5.19

Aldehyde 5.19.[25] A 25 mL round bottom flask was charged with Lombardo's reagent[27] (4.9 mL of a 0.4 mL solution in THF, 1.96 mmol) and the flask was cooled to 0 ºC. Alcohol **S5.8** (210 mg, 0.98 mmol) was added slowly as a solution in DCM (2.5 mL). The reaction was warmed to room temperature for 45 min and then quenched slowly with saturated aqueous $NaHCO_3$. The aqueous layer was extracted three times with diethyl ether. The organic layers were combined and washed with saturated aqueous $NaHCO_3$ followed by brine. The organic layer was dried over anhydrous magnesium sulfate, filtered, concentrated under reduced pressure, and filtered through a plug of silica gel.

The semi-purified material (107 mg) was dissolved in DCM (2.5 mL) and cooled to –78 ºC. Then 2,6-lutidine (0.9 mL, 0.77 mmol) was added followed by TBSOTf (0.13 mL, 0.57 mmol). After 45 min the reaction was warmed to room temperature and after an additional 15 min quenched with aqueous 1M HCl. The aqueous layer was extracted three times with diethyl ether. The organic layers were combined and washed with saturated aqueous $NaHCO_3$ followed by brine. The organic layer was dried over anhydrous magnesium sulfate, filtered, concentrated under reduced pressure, and filtered through a plug of silica gel.

The semi-purified material (164 mg) was dissolved in DCM (2.5 mL) and cooled to –78 ºC. Then DIBAL–H (1.0 mL of a 1M solution in toluene, 1.0 mmol) was added slowly. When the reaction was complete as judged by TLC, aqueous 1M HCl was added. The aqueous layer was extracted three times with diethyl ether. The organic layers were combined and washed with saturated aqueous $NaHCO_3$ followed by brine. The organic layer was dried over anhydrous magnesium sulfate, filtered, and concentrated under reduced pressure. Purification by flash

chromatography (eluent: 5% v/v ethyl acetate in hexanes) afforded aldehyde **5.19** (116 mg, 42% three steps) as light-yellow oil.

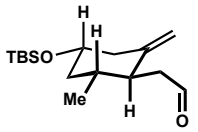

5.19

Aldehyde **5.19**

^{1}H NMR (500 MHz, $CDCl_3$)

δ 9.73 (dd, 1H, J = 3.0, 1.3 Hz)	2.62–2.50 (m, 2H)	1.36–1.28 (m, 1H)
4.81 (s, 1H)	2.17 (m, 1H)	0.99 (d, 3H, J = 6.0 Hz)
4.53 (s, 1H)	2.07 (t, 1H, J = 11.5 Hz)	0.89 (s, 9H)
3.62–3.56 (m, 1H)	1.94–1.91 (m, 1H)	0.06 (s, 6H)

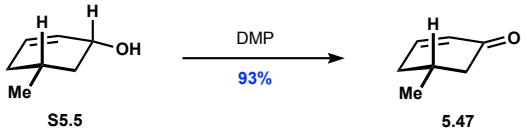

S5.5 5.47

Enone 5.47: Enone **5.47** can be prepared in one step from (R)-(+)-3-methylcyclohexanone using an IBX oxidation reported by the Nicolaou laboratory[16], or it can be prepared from less expensive (–)-isopulegol in two steps. Both methods were employed during these studies. The two-step procedure starts with conversion of (–)-isopulegol to (1R,5R)-5-methylcyclohex-2-en-1-ol can following a reported protocol from the Newhouse laboratory.[17] The second step is as follows: A 500 mL round bottom flask was charged with (1R,5R)-5-methylcyclohex-2-en-1-ol (3.92 g, 34.9 mmol) and dissolved in DCM (125 mL). The solution was cooled to 0 °C and Dess–Martin periodinane (16.5 g, 38.4 mmol) was added over 10 min in DCM (25 mL), then solid $NaHCO_3$ (8.80 g, 104.7 mmol) was added and the reaction was warmed to room temperature. After 1.25 h the reaction was carefully quenched with saturated aqueous $Na_2S_2O_3$ (100 mL) and saturated aqueous $NaHCO_3$ (50 mL). The layers were separated, and the aqueous layer was extracted three times with diethyl ether (300 mL combined). The organic layer was then sequentially washed with saturated aqueous $NaHCO_3$ (50 mL), water (50 mL), and brine (50 mL). The organic layer was dried over anhydrous magnesium sulfate, filtered, and concentrated under reduced pressure. Purification by flash chromatography (gradient elution: 5% to 50% v/v diethyl ether in pentane) afforded enone **5.47** (3.57 g, 93%) as a colorless oil. NMR data matched that provided in the literature.[28]

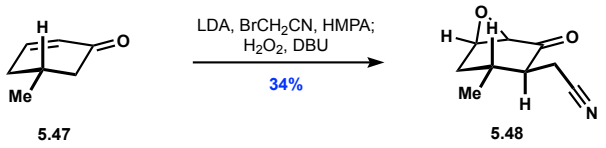

5.47 5.48

Epoxide (+)-**5.48**. A 500 mL round bottom flask was charged with diisopropylamine (5.84mL, 41.3 mmol) and THF (150 mL) and cooled to –78 °C. Then *n*-butyllithium (16.2 mL, 2.44 M solution in hexanes, 39.5 mmol) was added slowly and allowed to warm to room temperature for 1 h. The solution was then cooled to –78 °C and (+)-3-methylcyclohexenone **5.47** (4.141 g, 37.6 mmol) was added over 5 min in THF (12mL) and allowed to stir at –78 °C for 1 h. HMPA (19.6 mL) was then added and the solution was stirred for an additional 5 min at which point bromoacetonitrile (3.1 mL, 44.5 mmol) was added in THF (12 mL) over 15 min down the wall of the round bottom flask to ensure cooling. After the addition the solution was warmed to –40 °C. After 1.5 h an aqueous solution of hydrogen peroxide (38 mL, 30% aqueous solution, 372 mmol) was added slowly followed by DBU (0.56 mL, 3.75 mmol) over 5 min and then the solution was warmed to 0 °C. After stirring for 2 h the reaction was quenched with saturated aqueous $Na_2S_2O_3$ (25 mL) and 10% aqueous Na_2CO_3 (100 mL) using an ice bath to ensure the internal temperature did not exceed 20 °C. The biphasic mixture was diluted with DCM (50 mL) and the layers were separated. The aqueous layer was extracted twice with DCM (100 mL combined). The organic layers were combined and washed with saturated aqueous $NaHCO_3$ (25 mL) and saturated aqueous $Na_2S_2O_3$ (25 mL) followed by saturated aqueous $NaHCO_3$ (50 mL). The organic layer was dried over anhydrous magnesium sulfate, filtered, and concentrated under reduced pressure. Purification by flash chromatography (gradient elution: 20% to 50% v/v ethyl acetate in hexanes) afforded epoxide (+)-**5.48** (2.106 g, 34%) as a light-yellow solid.

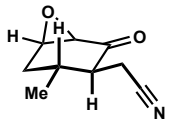

5.48

Epoxide (+)-**5.48**

^{1}H NMR (500 MHz, $CDCl_3$)

δ 3.59 (t, 1H, J = 3.3 Hz)	2.44 (dt, 1H, J = 15.0, 3.6 Hz)	1.10 (d, 3H, J = 6.7 Hz)
3.33 (d, 1H, J = 3.7 Hz)	2.21 (m, 1H)	
2.88 (dd, 1H, J = 17.0, 4.9 Hz)	1.93 (dt, 1H, J = 11.4, 5.1 Hz)	
2.67 (dd, 1H, J = 17.0, 5.3 Hz)	1.77 (dd, 1H, J = 15.1, 11.7 Hz)	

^{13}C NMR (126 MHz, $CDCl_3$)

δ 202.4	53.4	25.6
117.4	50.4	19.3
53.6	31.8	15.8

HRMS (ES+) calculated for $C_9H_{11}NO_2Na$ $[M+Na]^+$: 188.0687, found 188.0693

TLC: R_f = 0.39 (50% v/v ethyl acetate in hexanes)

$[\alpha]_D^{22}$ + 69.5 (c = 1.0, $CHCl_3$)

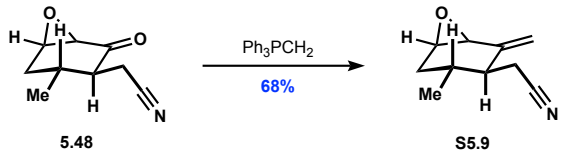

Alkene (–)-**S5.9**. A 500 mL round bottom flask was charged with methyltriphenylphosphonium bromide (16.0 g, 44.8 mmol) and THF (100 mL). The suspension was cooled to –78 °C and *n*-butyllithium (16.0 mL, 2.5 M solution in hexanes, 6.40 mmol) was slowly added. The solution was then warmed to room temperature. After 3 h the solution was cooled to –78 °C and epoxide (+)-**5.48** (5.51g, 33.4 mmol) was slowly added in THF (50 mL) then the solution was warmed to room temperature. After 5.5 h the reaction was diluted with diethyl ether (200 mL) followed by saturated aqueous $NaHCO_3$ (100 mL) and the layers were separated. The aqueous layer was extracted twice with diethyl ether (100 mL combined). The organic layers were combined and washed with brine (50 mL). The organic layer was dried over anhydrous magnesium sulfate, filtered, and concentrated under reduced pressure. Purification by flash chromatography (gradient elution: 10% to 20% v/v ethyl acetate in hexanes) afforded alkene (–)-**S5.9** (3.70 g, 68%) as a light-orange solid.

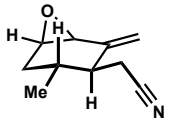

Alkene (–)-**S5.9**

^{1}H NMR (500 MHz, $CDCl_3$)

δ 5.50 (s, 1H)	2.68 (dd, 1H, J = 17.0, 7.1)	1.93 (m, 1H)
5.32 (s, 1H)	2.60 (dd, 1H, J = 17.0, 7.4 Hz)	1.67 (dt, 1H, J = 15.5, 4.4 Hz)
3.49 (d, 1H, J = 3.9 Hz)	2.24 (q, 1H, J = 6.4 Hz)	0.96 (d, 3H, J = 7.0 Hz)
3.36 (t, 1H, J = 3.6 Hz)	2.17 (dd, 1H, J = 15.5, 5.4 Hz)	

^{13}C NMR (126 MHz, $CDCl_3$)

δ 140.8	53.0	22.4
120.6	43.1	21.1
118.8	29.3	
55.5	28.5	

HRMS (ES+) calculated for $C_{10}H_{13}NONa$ $[M+Na]^+$: 186.0895, found 186.0898

TLC: R_f = 0.71 (50% v/v ethyl acetate in hexanes)

$[\alpha]_D^{22}$ – 51.4 (c = 1.0, $CHCl_3$)

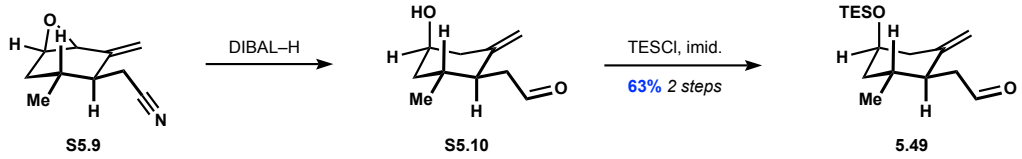

A**ldehyde** (–)-**5.49**. A 500 mL round bottom flask was charged with alkene (–)-**S5.9** (3.69 g, 22.6 mmol) and THF (110 mL) and cooled to –78 °C. DIBAL-H (10 mL, 56.1 mmol) was then added slowly over 5 min. After 15 min the solution was warmed to room temperature and stirred for an additional 6 h. At which point the solution was cooled to 0 °C and a saturated aqueous solution of Rochelle salts (75 mL) was carefully added followed by diethyl ether (200 mL). The biphasic solution was then vigorously stirred for 3h and the layers were separated. The aqueous layer was extracted twice with DCM (100 mL combined). The organic layers were combined dried over anhydrous magnesium sulfate, filtered, and concentrated under reduced pressure. The crude mixture was then passed through a plug of silica gel, flushed with ethyl acetate, and concentrated under reduced pressure. This intermediate alcohol **S5.10** was not stable even upon storage in the freezer overnight, so it was used immediately in the subsequent silylation. The semi purified alcohol **S5.10** (2.99 g) was dissolved in DCM (90 mL) and imidazole (1.33 g, 19.5 mmol) was added followed by TESCl (3.24 mL, 18.7 mmol). The solution was stirred for 15 min at room temperature and then saturated aqueous $NaHCO_3$ (100 mL) was added, and the layers were separated. The aqueous layer was extracted twice with DCM (100 mL combined). The organic layers were combined and washed with brine (50 mL). The organic layer was dried over anhydrous magnesium sulfate, filtered, and concentrated under reduced pressure. Purification by flash chromatography (gradient elution: 1% to 10% v/v ethyl acetate in hexanes) afforded aldehyde (–)-**5.49** (4.01 g, 63% two steps) as a colorless oil.

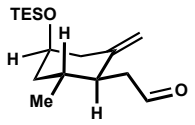

5.49

Aldehyde (–)-**5.49**

^{1}H NMR (500 MHz, $CDCl_3$)

δ 9.71 (t, 1H, J = 2.2 Hz)	2.43 (dt, 1H, J = 10.4, 4.4 Hz)	0.95 (m, 12H)
4.81 (s, 1H)	2.33 (dd, 1H, J = 13.1, 4.2 Hz)	0.58 (q, 6H, J = 7.9 Hz)
4.73 (s, 1H)	2.17 (dd, 1H, J = 13.1, 8.3 Hz)	
3.89 (septet, 1H, J = 4.1 Hz)	1.86 (m, 1H)	
2.64 (ddd, 1H, J = 16.6 8.5, 2.6 Hz)	1.68 (ddd, 1H, J = 13.2, 8.4, 4.4 Hz)	
2.56 (ddd, 1H, J = 16.6, 5.7, 1.9 Hz)	1.54 (m, 1H)	

^{13}C NMR (126 MHz, $CDCl_3$)

δ 202.6	45.8	33.1
145.8	43.6	20.1
111.9	42.7	7.0 (3C)
67.6	39.2	5.0 (3C)

HRMS (ES+) calculated for $C_{16}H_{30}O_2SiNa$ $[M+Na]^+$: 305.1913, found 305.1917

TLC: R_f = 0.69 (10% v/v ethyl acetate in hexanes)

$[\alpha]_D^{22}$ – 3.14 (c = 1.0, $CHCl_3$)

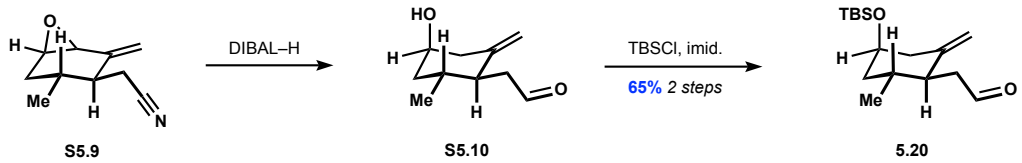

Aldehyde (–)-**5.20**. Aldehyde (–)-**5.20** was prepared in an analogous manner to aldehyde (–)-**5.49**. A 250 mL round bottom flask was charged with alkene (–)-**S5.9** (1.47 g, 9.02 mmol) and DCM (45 mL) and cooled to –78 °C. DIBAL-H (3.4 mL, 19.0 mmol) was then added slowly over 5 min (note: this unoptimized protocol using DCM as a solvent should be avoided since addition of DIBAL-H resulted in the solution becoming a viscous gel). After 5 min the solution was warmed to room temperature and stirred for an additional 30 min. At which point a saturated aqueous solution of Rochelle salts (50 mL) was carefully added followed by diethyl ether (50 mL). The biphasic solution was then vigorously stirred for 12h and the layers were separated. The aqueous layer was extracted twice with DCM (50 mL combined). The organic layers were combined dried over anhydrous magnesium sulfate, filtered, and concentrated under reduced pressure. The crude mixture was then passed through a plug of silica gel, flushed with ethyl acetate, and concentrated under reduced pressure. This intermediate alcohol **S5.10** was not stable even upon storage in the freezer overnight and so it was used immediately in the subsequent silylation. The semi-purified alcohol **S5.10** (1.064 g) was dissolved in DCM (36 mL) and imidazole (516 mg, 7.58 mmol) was added followed by TBSCl (1.05 g, 6.97 mmol). The solution was stirred for 24 h at room temperature then aqueous 1M HCl (25 mL) was added and the layers were separated. The aqueous layer was extracted twice with diethyl ether (40 mL combined). The organic layers were combined and washed with water (20mL) and then brine (20 mL). The organic layer was dried over anhydrous magnesium sulfate, filtered, and concentrated under reduced pressure. Purification by flash chromatography (eluent: 5% v/v ethyl acetate in hexanes) afforded aldehyde (–)-**5.20** (1.66 g, 65% two steps) as a light-yellow oil.

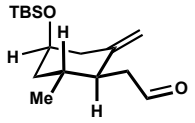

5.20

Aldehyde (–)-**5.20**

^{1}H NMR (500 MHz, $CDCl_3$)

δ 9.72 (s, 1H)	2.41 (m, 1H)	0.96 (d, 3H, J = 7.0 Hz)
4.79 (s, 1H)	2.31 (dd, 1H, J = 13.1, 3.8 Hz)	0.87 (s, 9H)
4.70 (s, 1H)	2.18 (dd, 1H, J = 13.1, 7.6 Hz)	–0.04 (s, 3H)
3.93 (septet, 1H, J = 3.8 Hz)	1.84 (m, 1H)	–0.03 (s, 3H)
2.64 (ddd, 1H, J = 16.6, 8.6, 2.5 Hz)	1.67 (m, 1H)	
2.57 (ddd, 1H, J = 16.9, 5.5, 1.4 Hz)	1.52 (m, 1H)	

^{13}C NMR (126 MHz, $CDCl_3$)

δ 202.7	67.89	42.9	26.0 (3C)	–4.5
145.9	45.5	39.7	20.2	–4.6
111.5	43.8	33.0	18.3	

HRMS (ES+) calculated for $C_{16}H_{30}O_2SiNa$ $[M+Na]^+$: 305.1913, found 305.1922

TLC: R_f = 0.65 (20% v/v ethyl acetate in hexanes)

$[\alpha]_D^{22}$ – 4.62 (c = 1.0, $CHCl_3$)

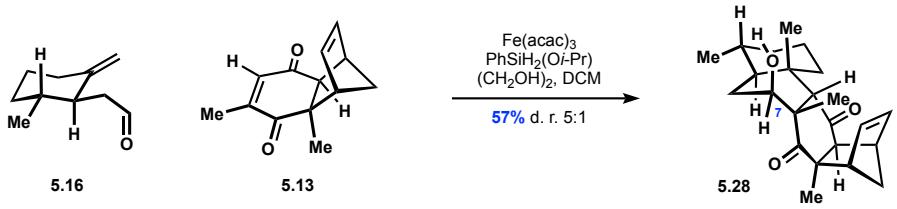

5.16 5.13 5.28

Alcohol 5.28. A 10 mL Schlenk flask was charged with aldehyde **5.16** (450 mg, 3.1 mmol), iron(III) acetylacetonate (164 mg, 0.465 mmol), ethylene glycol (0.26 mL, 4.65 mmol) and DCM (2 mL). The solution was then degassed by freeze-pump-thaw technique and cooled to 0 °C. To this vigorously stirring solution was added enedione **5.13** (344 mg, 1.55 mmol) and isopropoxyphenylsilane[29] (0.52 mL, 3.1 mmol) in DCM (5.5 mL, sparged with argon for 15 min) over the course of 3 h by syringe pump. After an additional 26 h the reaction was concentrated under reduced pressure and directly purified by flash chromatography. Purification by flash chromatography (eluent: 10% v/v ethyl acetate in DCM) afforded alcohol **5.28** (343 mg as a 5:1 mixture of diastereomers at C7, 57%) as white solid.

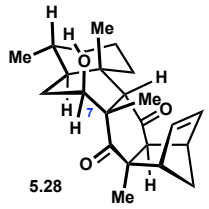

5.28

Alcohol **5.28** (d. r. 5:1 at C7)

^{1}H NMR (500 MHz, $CDCl_3$)

δ 6.42 (dd, 1H, J = 5.4, 3.0 Hz)	2.74 (d, 1H, J = 3.1 Hz)	1.48 (m, 4H)
6.29 (dd, 1H, J = 5.3, 3.1 Hz)	2.68 (s, 1H)	1.31 (s, 3H)
3.59 (dd, 1H, J = 9.4, 4.9 Hz)	2.04 (m, 1H)	1.27–1.19 (m, 4H)*
3.21 (m, 1H)	1.97–1.93 (m, 2H)	1.04–0.97 (m, 6H)*
2.96 (m, 1H)	1.70–1.61 (m, 6H)*	0.82 (d, 3H, J = 6.4 Hz)
2.83 (m, 1H)	1.54–1.48 (m, 5 H)**	

* minor epimer skews integration

** water skews integration

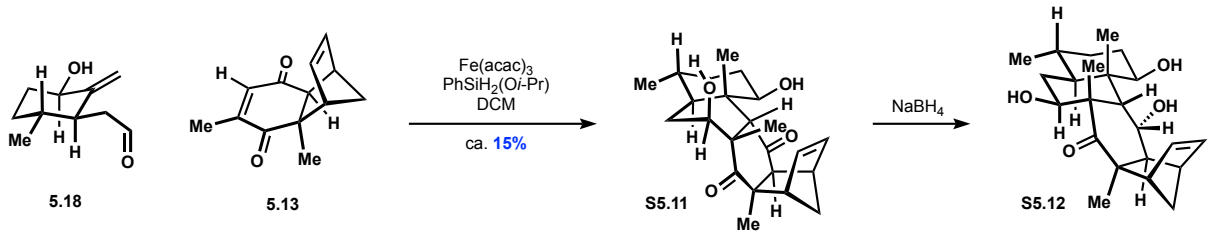

5.18 5.13 S5.11 S5.12

Alcohol S5.11 and Triol S5.12. A 5 mL Schlenk flask was charged with aldehyde **5.18** (8.4 mg, 0.05 mmol), iron(III) acetylacetonate (17.7 mg, 0.05 mmol), ethylene glycol (8.4 µL, 0.15 mmol), enedione **5.13** (20.2 mg, 1.55 mmol) and DCM (0.1 mL). The solution was then degassed by freeze-pump-thaw technique. To this vigorously stirring solution was added and isopropoxyphenylsilane[29] (17 µL, 0.10 mmol) in DCM (0.2 mL, sparged with argon for 15 min) over the course of 3 h by syringe pump. After an additional 4 h the reaction was quenched with 1Maqueous HCl and the aqueous layer was extracted three times with diethyl ether, then the organic layers were combined and washed with brine. The organic layer was dried over anhydrous magnesium sulfate, filtered, and concentrated under reduced pressure. Purification by flash chromatography (eluent: 20% v/v ethyl acetate in hexanes) afforded semi-purified alcohol **S5.11** (*ca.* 15% yield determined by analysis of crude reaction mixture by ^{1}H NMR with mesitylene as internal standard. Resonance at 6.52 ppm integrated for ^{1}H NMR yield). Semi-purified alcohol **S5.11** was then dissolved in MeOH and treated with $NaBH_4$ to provide triol **S5.12**, which was characterized by X-ray crystallography.

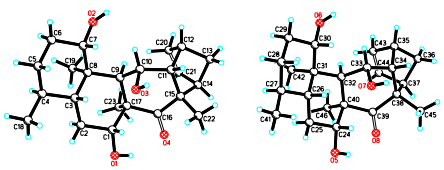

S5.12

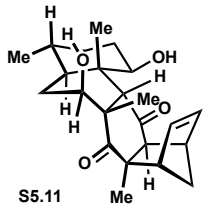

S5.11

Alcohol **S5.11***

^{1}H NMR (500 MHz, $CDCl_3$)

δ 6.52 (m, 1H)	2.95 (d, 1H, J = 2.9 Hz)	1.34 (s, 3 H)
6.32 (m, 1H)	2.52 (m, 1H)	1.30–1.22 (m, 9H)
4.33 (m, 1H)	1.96 (m, 2H)	0.95 (s, 3H)
3.48 (dd, 1H, J = 10.8, 4.7 Hz)	1.86 (m, 2H)	0.81 (d, 3H, J = 6.4 Hz)
3.22 (s, 2H)	1.65 (m, 7H)	
3.06 (m, 1H)	1.44 (s, 3H)	

*impurities skew integrations

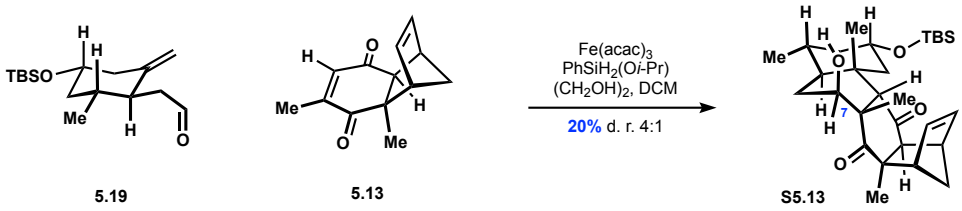

Alcohol S5.13. A 5 mL Schlenk flask was charged with aldehyde **5.19** (27.7 mg, 0.098 mmol), iron(III) acetylacetonate (2.4 mg, 0.007 mmol), ethylene glycol (8.4 µL, 0.15 mmol), and DCM (0.1 mL). The solution was then degassed by freeze-pump-thaw technique. To this vigorously stirring solution was added enedione **5.13** (10.6 mg, 0.52 mmol) and isopropoxyphenylsilane[29] (17 µL, 0.10 mmol) in DCM (0.2 mL, sparged with argon for 15 min) over the course of 1 h by syringe pump. After an additional 4 h the reaction was quenched with 1Maqueous HCl and the aqueous layer was extracted three times with diethyl ether, then the organic layers were combined and washed with brine. The organic layer was dried over anhydrous magnesium sulfate, filtered, and concentrated under reduced pressure. Purification by flash chromatography (eluent: 20% v/v ethyl acetate in hexanes) afforded alcohol **S5.13** (20% yield as a 4:1 mixture of diastereomers at C7, yield determined by analysis of crude reaction mixture by ^{1}H NMR with mesitylene as internal standard. Resonance at 6.45 ppm and 6.02 ppm integrated for ^{1}H NMR yield).

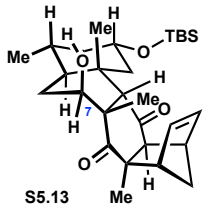

S5.13

Alcohol **S5.13** (d. r. 4:1 at C7)

^{1}H NMR (500 MHz, $CDCl_3$)

δ 6.45 (dd, 1H, J = 5.5, 2.9 Hz)	2.76 (d, 1H, J = 3.2 Hz)	1.49 (s, 3H)
6.27 (dd, 1H, J = 5.2, 3.3 Hz)	2.66 (s, 1H)	1.27 (m, 4H)
3.96–3.90 (m, 1H)	1.99–1.91 (m, 2H)	1.22–1.19 (m, 6H)*
3.63 (dd, 1H, J = 8.9, 5.5 Hz)	1.19–1.84 (m, 3H)	1.02–1.00 (m, 3H)
3.27 (m, 1H)	1.84–1.80 (m, 2H)	0.87 (s, 18H)
2.96 (m, 1H)	1.75 (s, 1H)	0.04 (s, 4H)
2.80 (m, 1H)	1.63 (m, 3H)	0.04 (s, 4H)

*grease skews integration

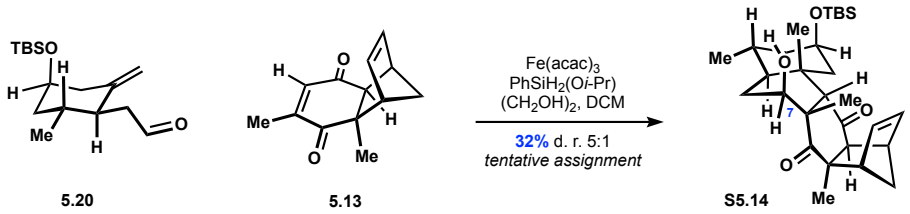

Alcohol S5.14. A 5 mL Schlenk flask was charged with aldehyde **5.20** (20 mg, 0.071 mmol), iron(III) acetylacetonate (1.2 mg, 0.0035 mmol), ethylene glycol (6.0 µL, 0.15 mmol), and DCM (0.1 mL). The solution was then degassed by freeze-pump-thaw technique. To this vigorously stirring solution was added enedione **5.13** (7.2 mg, 0.035 mmol) and isopropoxyphenylsilane[29] (12 µL, 0.105 mmol) in DCM (0.2 mL, sparged with argon for 15 min) over the course of 1 h by syringe pump. After an additional 4 h the reaction was quenched with 1Maqueous HCl and the aqueous layer was extracted three times with diethyl ether, then the organic layers were combined and washed with brine. The organic layer was dried over anhydrous magnesium sulfate, filtered, and concentrated under reduced pressure. Purification by flash chromatography (eluent: 20% v/v ethyl acetate in hexanes) afforded alcohol semi-purified alcohol **S5.14** (32% as a 5:1 mixture of diastereomers at C7, yield determined by analysis of crude reaction mixture by ^{1}H NMR with mesitylene as internal standard. Resonance at 6.32 ppm and 6.21 ppm integrated for ^{1}H NMR yield). Complete ^{1}H NMR data of semi-purified alcohol **S5.14** not tabulated due to lack of purity, structure tentatively assigned based on comparison of diagnostic resonances with **S5.13**.

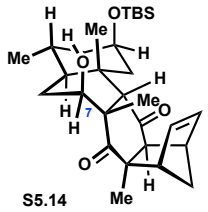

Alcohol **S5.14** (d. r. 5:1 at C7, diagnostic resonances tabulated)

^{1}H NMR (500 MHz, $CDCl_3$)

δ 6.47 (dd, 1H, J = 5.5, 3.0 Hz)	3.20 (m, 1H)	1.45 (s, 3H)
6.30 (dd, 1H, J = 5.4, 3.1 Hz)	2.95 (s, 1H)	1.34 (s, 3H)
4.11 (m, 1H)	2.71 (d, 1H, J = 3.1 Hz)	0.87 (s, 9H)
3.51 (dd, 1H, J = 10.3, 5.1 Hz)	2.69 (s, 1H)	0.01 (s ,6H)

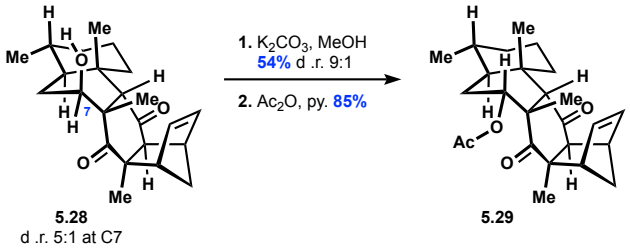

Acetate 5.29. A 50 mL round bottom flask was charged with alcohol **5.28** (343 mg of a 5:1 mixture of diastereomers at C7, 0.96 mmol), K_2CO_3 (133 mg, 0.96 mmol) and MeOH (5 mL). The reaction was stirred for 24 h at which point it was diluted with water and the aqueous layer was extracted three times with diethyl ether. The organic layers were combined and washed with brine. The organic layer was dried over anhydrous magnesium sulfate, filtered, and concentrated under reduced pressure. Purification by flash chromatography (gradient elution: 0% to 5% v/v ethyl acetate in DCM) afforded C7-epi-alcohol **5.28** (186 mg of a 9:1 mixture of diastereomers at C7, 54%).

This material was then dissolved in DCM (2.5 mL) and cooled to 0 ºC. Then DMAP (70 mg, 0.57 mmol) followed by acetic anhydride (75 µL, 0.79 mmol) was added. After 21 h the reaction was quenched with 1Maqueous HCl and the aqueous layer was extracted three times with diethyl ether. The organic layer was dried over anhydrous magnesium sulfate, filtered, and concentrated under reduced pressure. Purification by flash chromatography (eluent: 20% v/v ethyl acetate in hexanes) afforded acetate **5.29** (177 mg, 85%) as white solid.

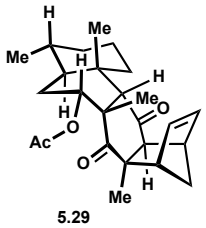

5.29

Acetate **5.29**

^{1}H NMR (500 MHz, $CDCl_3$)

δ 6.34 (dd, 1H, J = 5.5, 3.0 Hz)	2.73 (d, 1H, J = 3.3 Hz)	1.62–1.55 (m, 4H)
6.21 (dd, 1H, J = 5.4, 3.1 Hz)	2.44 (s, 1H)	1.46–1.39 (m, 6H)
4.76 (t, 1H, J = 4.4 Hz)	2.18 (m, 1H)	1.24 (m, 4H)
3.21 (bs, 1H)	1.95 (s, 3H)	1.07–1.01 (m, 2H)
2.91 (bs, 1H)	1.90–1.81 (m, 2H)	0.98 (s, 3H)
		0.72 (d, 3H, J = 6.4 Hz)

^{13}C NMR (126 MHz, $CDCl_3$)

δ 217.1	78.2	36.3	26.6
211.5	62.4	35.7	25.8
169.7	56.9	35.0	22.9
137.7	50.4	31.7	21.4 (2C)
136.9	48.0	28.8	20.0

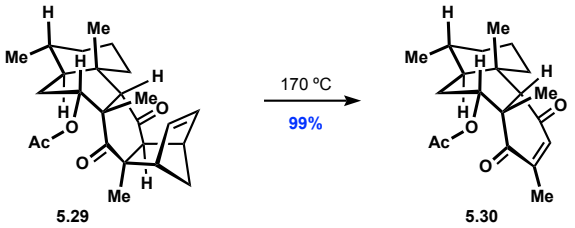

Enedione 5.30. A dram vial was charged with acetate **5.29** (167 mg, 0.42 mmol), heated to 170 ºC for 1.2 h and then cooled to room temperature. Purification by flash chromatography (gradient elution: 2% to 10% v/v ethyl acetate in hexanes) afforded endione **5.30** (138 mg, 99%) as yellow solid.

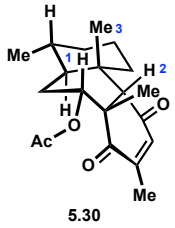

Endione **5.30**

^{1}H NMR (500 MHz, $CDCl_3$)

δ 6.58 (s, 1H)	2.01–1.94 (m, 1H)	1.19 (s, 3H)
4.91 (t, 1H, J = 8.8 Hz)	1.84–1.77 (m, 1H)	1.15 (s, 3H)
2.50 (s, 1H)	1.58–1.55 (m, 3H)	0.92–0.82 (m, 3H)
2.13 (s, 3H)	1.50–1.45 (m, 3H)	0.77 (d, 3H, J = 6.4 Hz)
2.01 (s, 3H)	1.35 (m, 2H)	0.76–0.69 (m, 1H)

^{13}C NMR (126 MHz, $CDCl_3$)

δ 199.6	138.0	45.0	33.8	21.6
199.3	73.6	38.6	29.9	21.2
171.2	69.4	37.1	25.1	19.9
148.7	50.5	35.0	24.8	16.6

Key NOESY correlations:

1H (arbitrary numbering)	Key correlations
H1 (4.91 ppm)	H2 (2.50 ppm) H3 (2.01 ppm)

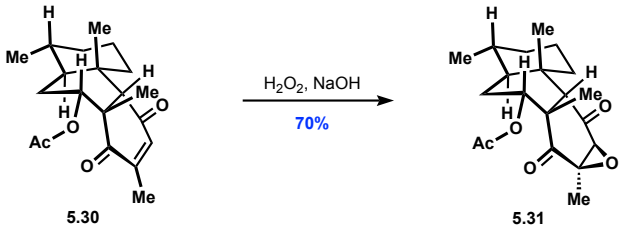

Epoxide 5.31. A dram vial was charged with enedione **5.30** (30 mg, 0.015 mmol) and THF (1.0 mL). An aqueous solution of hydrogen peroxide (0.5 mL, 30% aqueous solution) followed by 2M aqueous NaOH (50 µL) was added. After 2 h the reaction wash quenched with 1Maqueous HCl and extracted three times with ether. The organic layer was dried over anhydrous magnesium sulfate, filtered, and concentrated under reduced pressure. Purification by flash chromatography (elution gradient: 5% to 10% v/v diethyl ether in pentane) afforded epoxide **5.31** (22 mg, 70%) as white solid.

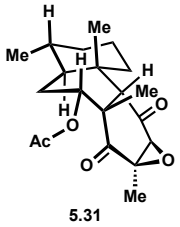

Epoxide **5.31**

^{1}H NMR (500 MHz, $CDCl_3$)

δ 5.10 (s, 1H)	1.82 (s, 3H)	1.14 (dt, 1H, J = 14.5, 6.4 Hz)
3.53 (s, 1H)	1.68–1.59 (m, 3H)	1.04 (s, 3H)
3.20 (s, 1H)	1.51 (s, 3H)	0.99–0.96 (m, 1H)
2.41 (m, 1H)	1.50 (s, 3H)	0.76 (d, 3H, J = 6.4 Hz)
1.99–1.96 (m, 1H)	1.43 (m, 1H)	
1.88 (m, 1H)	1.23 (m, 1H)	

^{13}C NMR (126 MHz, $CDCl_3$)

δ 207.2	68.4	36.1	26.2	20.8
204.7	63.6	35.9	25.5	20.0
169.0	54.8	34.1	21.6	16.0
77.9	39.2	30.9	21.2	

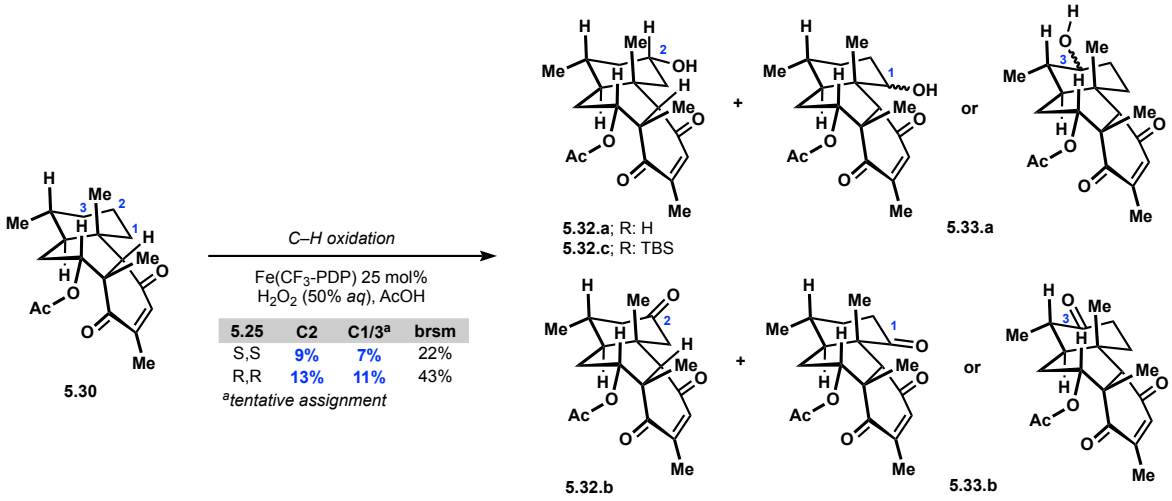

C–H Oxidation. Protocol adapted from White.[11] A dram vial was charged with enedione **5.30** (10.0 mg, 0.030 mmol) and acetic acid (0.85 µL as a solution in 0.3 mL MeCN, 0.015 mmol). Then (S,S)- or (R,R)-Fe(CF_3-PDP) **5.34** (10.2 mg, 0.0075 mmol) in MeCN (0.1 mL) and hydrogen peroxide (8.5 µL, 50% aqueous solution) were added via separate syringes over 1 h. After an additional 30 min. the reaction mixtures were filtered through a plug of silica gel. Purification by preparative thin layer chromatography (elution with 50% v/v ethyl acetate in hexanes) afforded: [reaction with (S,S)-Fe(CF_3-PDP)]: alcohols **5.32.a** and **5.33.a** (9% as a ~1:1 mixture, **5.33.a** C1 or C3 isomer not unambiguously assigned), and ketones **5.32.b** and **5.33.b** (7% as a ~2:1 mixture, **5.33.b** C1 or C3 isomer not unambiguously assigned). [reaction with (R,R)-Fe(CF_3-PDP)]: alcohols **5.32.a** and **5.33.a** (14% as a ~1:1 mixture, **5.33.a** C1 or C3 isomer not unambiguously assigned), and ketones **5.32.b** and **5.33.b** (10% as a ~2:1 mixture, **5.33.b** C1 or C3 isomer not unambiguously assigned). Yields determined by analysis of crude reaction mixture by ^{1}H NMR with mesitylene as internal standard. Resonance at 2.53 ppm and 2.50 ppm (alcohols), 2.64 ppm and 2.58 (ketones) ppm integrated for ^{1}H NMR yield.

Treating alcohols **5.32.a** and **5.33.a** with DMP and $NaHCO_3$ led to production of the same ketones **5.32.b** and **5.33.b**. Treating alcohols **5.32.b** and **5.33.b** with TBSOTf and 2,6-lutidine led

to formation of **5.32.c**, which was independently prepared from silyl ether **S5.13** in an analogous manner to enedione **5.30**.

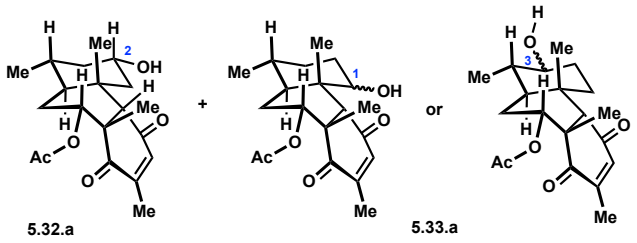

Alcohols **5.32.a** and **5.33.a** (1:1 mixture)

^{1}H NMR (500 MHz, $CDCl_3$)

δ 6.61 (s, 1H)	2.50 (s, 1H)	1.16 (s, 3H)
6.59 (s, 1H)	2.14 (s, 6H)	1.05–0.98 (m, 3H)
4.93 (t, 1H, J = 7.5 Hz)	2.02 (s, 6H)	0.92 (d, 3H, J = 6.3 Hz)
4.89 (t, 1H, J = 7.4 Hz)	2.02–1.96 (m, 4H)	0.85 (d, 3H, J = 6.4 Hz)
3.82 (m, 1H)	1.91–1.75 (m, 6H)	0.84–0.76 (m, 3H)
2.96 (m, 1H)	1.22 (s, 6H)	
2.53 (s, 1H)	1.20 (s, 3H)	

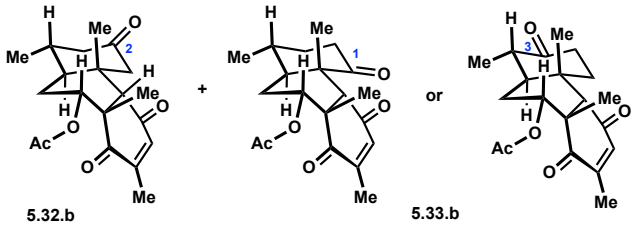

Ketones **5.32** and **5.33** (1:1 mixture)

^{1}H NMR (500 MHz, $CDCl_3$)

δ 6.63 (s, 1H)	2.47 (td, 1H, J = 14.8, 6.0 Hz)	1.87–1.81 (m, 3H)
6.57 (s, 1H)	2.34–2.26 (m, 6H)	1.45 (s, 3H)
4.96 (t, 1H, J = 8.8 Hz)	2.17–2.15 (m, 6 H)	1.32 (s, 3H)
4.91 (t, 1H, J = 7.7 Hz)	2.09 (s, 3H)	1.08 (s, 3H)
2.64 (s, 1H)	2.05 (s, 3H)	0.94 (m, 6H)
2.58 (s, 1H)	2.03–1.98 (m, 7H)	

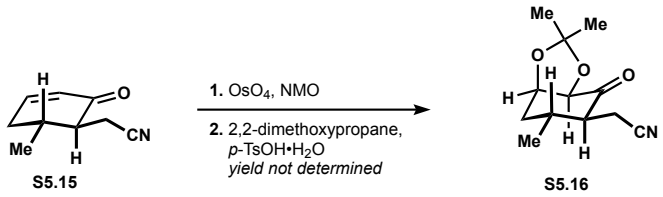

Acetonide S5.16.[25] Enone **S5.15** was prepared following the same procedure to prepare epoxide **5.48** without addition of DBU or hydrogen peroxide. A 250 mL round bottom flask was charged with enone **S5.15** (4.63 g, 31.0 mmol), water (30 mL), acetone (80 mL), and NMO (5.45 g, 36.5 mmol), then OsO_4 (39 mg, 0.15 mmol) was added. After 25 h OsO_4 (250 mg, 0.98 mmol) was added and the reaction was warmed to 40 ºC. After an additional 4 h the reaction was cooled to room temperature and $NaHSO_3$ (11 g) was added slowly (caution: exotherm was observed). The mixture was stirred for 15 min the extracted with ethyl acetate (1L combined) until no longer present by TLC. The organic layers were combined and washed with brine (25 mL), then filtered through a plug of silica gel.

The 500 mg of the semi-purified material was then dissolved in2,2- dimethoxypropane (2.5 mL) and acetone (2.5 mL). Then *p*-TsOH•H_2O (52 mg, 0.27 mmol) and magnesium sulfate (500 mg) were added. After completion as judged by TLC, the reaction was diluted with saturated aqueous $NaHCO_3$ and extracted three times with diethyl ether. The organic layer was dried over anhydrous magnesium sulfate, filtered and concentrated under reduced pressure. Purification by flash chromatography (elution gradient: 10% to 20% v/v diethyl ether in pentane) afforded acetonide **S5.16** (yield not determined).

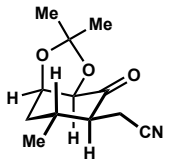

S5.16

Acetonide **S5.16**

^{1}H NMR (500 MHz, $CDCl_3$)	
δ 4.50–4.48 (m, 1H)	2.03 (m, 1H)
4.30 (d, 1H, J = 5.5 Hz)	1.80 (ddd, 1H, J = 15.5, 12.2, 3.4 Hz)
2.55 (d, 2H, J = 5.3 Hz)	1.31 (s, 3H)
2.36 (dt, 1H, J = 12.0, 5.6 Hz)	1.30 (s, 3H)
2.22 (dt, 1H, J = 15.3, 2.9 Hz)	1.07 (d, 3H, J = 6.8 Hz)

Key NOESY correlations:

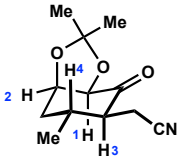

S5.16

^{1}H (arbitrary numbering)	Key correlations	Absent correlations
H1 (4.50–4.48 ppm)	H3 (2.36 ppm)	
H2 (4.30 ppm)		H4 (2.03 ppm)

S5.16 5.44

Aldehyde 5.44.[25] A 500 mL round bottom flask was charged with methyl triphenyl phosphonium bromide (4.6 g, 12.9 mmol) and THF (40 mL). The mixture was cooled to –78 ºC and *n*-butyllithium (4.9 mL of a 2.5 M solution in hexane, 12.2 mmol) was added slowly. Then the mixture was warmed to room temperature for 1 h and acetonide **S5.16** (1.6 g, 7.17 mmol) was added as a solution in THF (20 mL). After 12 h the reaction was quenched with 1Maqueous HCl and extracted with diethyl ether. The organic layers were combined and dried over anhydrous magnesium sulfate, filtered and concentrated under reduced pressure, then filtered through a plug of silica.

The semi-purified material (300 mg) was then dissolved in THF (10 mL) and MeOH (10 mL). 2N aqueous HCl (2 mL) was added, and the reaction was warmed to 40 ºC for 45 min then cooled to room temperature diluted with water and extracted with ethyl acetate. The organic layers were combined and dried over anhydrous magnesium sulfate, filtered and concentrated under reduced pressure, then filtered through a plug of silica.

The semi-purified material (250 mg) was then dissolved in DCM (15 mL) and cooled to 0 ºC. DIBAL–H (3.0 mL of a 1M solution in toluene, 3.0 mmol) was added slowly and the reaction was warmed to room temperature. After 1 h Rochelle salt was added (25 mL of a saturated solution) and the mixture was stirred vigorously for 12 h. The aqueous layer was extracted four times with ethyl acetate and filtered through a plug of silica to afford aldehyde **5.44** (185 mg, 14% three steps) along with remaining DCM (38 mg, 17% w/w) and diethyl ether (3 mg, 6% w/w).

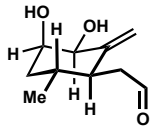

5.44

Aldehyde **5.44**

^{1}H NMR (500 MHz, $CDCl_3$)

δ 9.77 (dd, 1H, J = 2.6, 1.3 Hz)
5.21 (s, 1H)
4.86 (s, 1H)
4.20 (bs, 1H)
4.06 (bs, 1H)
2.75 (ddd, 1H, J = 17.1, 9.0, 2.6 Hz)
2.66 (ddd, 1H, J = 17.1, 4.8, 0.6 Hz)
2.31–2.25 (m, 2H)
1.99 (dt, 1H, J = 14.3, 8.4 Hz)
1.87 (d, 1H, J = 5.7 Hz)
1.50 (ddd, 1H, J = 14.1, 11.1, 2.9 Hz)
0.97 (d, 3H, J = 6.6 Hz)

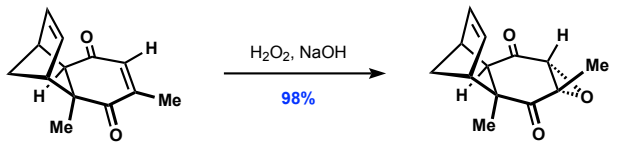

5.13 (94% ee) **5.52**

Epoxide (–)-**5.52**. A 250 mL round bottom flask was charged with enedione **5.13** (4.00 g, 19.8 mmol, 94% ee)[10,30] and MeOH (100mL) then cooled to 0 °C. Then hydrogen peroxide (3.0 mL, 30% aqueous solution, 29.4 mmol) was added over 5 min. Then aqueous 2M NaOH (0.50 mL, 1.00 mmol) was added over 5 min. After 10 min the reaction was quenched by slowly adding a saturated aqueous solution of $Na_2S_2O_3$, maintaining an internal temperature below 10 °C. Then the mixture was diluted with water (50 mL) and DCM (50 mL). The phases were separated, and the aqueous layer was extracted twice with DCM (100 mL combined). The organic layers were combined and washed with brine (25 mL). The organic layer was dried over anhydrous magnesium sulfate, filtered, and concentrated under reduced pressure. Purification by flash chromatography (eluent: 20% v/v ethyl acetate in hexanes) afforded epoxide (–)-**5.52** (4.24 g, 98%) as a white solid.

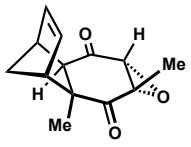

5.52

Epoxide (–)-**5.52**

^{1}H NMR (500 MHz, $CDCl_3$)

δ 6.01 (dd, 1H, J = 5.6, 3.0 Hz)	2.91 (m, 1H)	1.44 (s, 3H)
6.00 (dd, 1H, J = 5.6, 2.8 Hz)	2.85 (d, 1H, J = 3.7 Hz)	1.43–1.41 (m, 1H)
3.35 (s, 1H)	1.59 (s, 3H)	
3.25 (m, 1H)	1.55–1.53 (m, 1H)	

^{13}C NMR (126 MHz, $CDCl_3$)

δ 208.0	65.4	50.7	15.2
205.6	64.2	44.6	
138.3	58.3	44.0	
137.4	54.6	27.6	

HRMS (ES–) calculated for $C_{13}H_{13}O_3$ $[M–H]^-$: 217.0865, found 217.0867

TLC: R_f = 0.64 (20% v/v ethyl acetate in hexanes)

$[\alpha]_D^{22}$ – 83.9 (c = 1.0, $CHCl_3$)

Data File C:\HPCHEM\1\DATA\ALEXB\WT-6-11C.D

Sample Name: wpt-6-11rac2

Chiralcel OD-h w/ guard, 0.3%IPA/Hex, 20uL injection, 1 .0 mL/min, 254nm

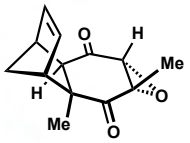

racemic **5.52**

```
Injection Date  : 8/5/2020 3:49:21 PM
Sample Name     : wpt-6-11rac2                    Location : Vial 53
Acq. Operator   : ALEXB
                                                  Inj Volume : 20 µl
Acq. Method     : C:\HPCHEM\1\METHODS\ALEXB.M
Last changed    : 8/5/2020 3:43:46 PM by ALEXB
                  (modified after loading)
Analysis Method : C:\HPCHEM\1\METHODS\ALEXB.M
Last changed    : 2/22/2020 1:07:30 PM by ALEXB
```

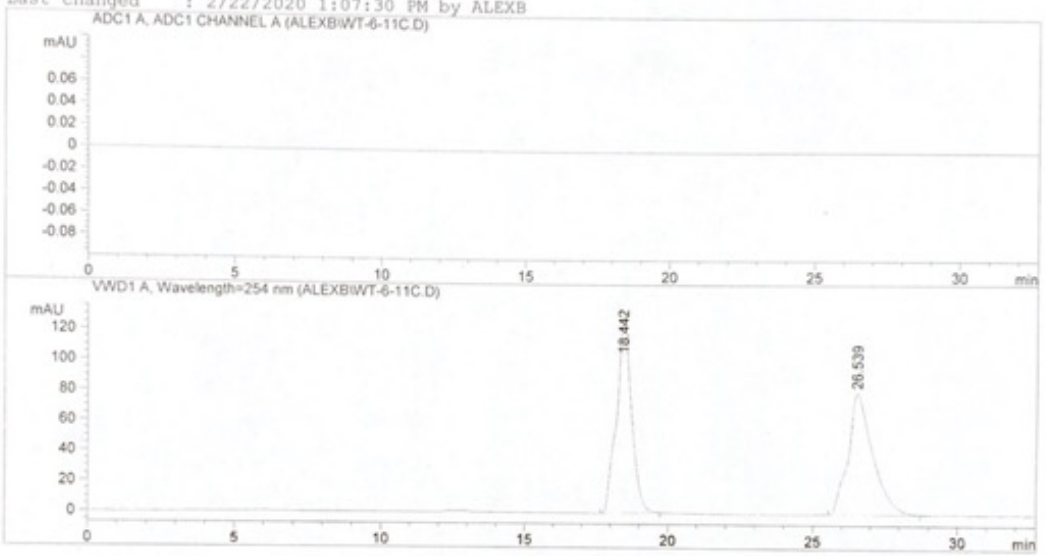


```
                          Area Percent Report

Sorted By             :      Signal
Multiplier            :      1.0000
Dilution              :      1.0000
Sample Amount         :      1.00000  [ng/ul]   (not used in calc.)
Use Multiplier & Dilution Factor with ISTDs


Signal 1: ADC1 A, ADC1 CHANNEL A


Signal 2: VWD1 A, Wavelength=254 nm

Peak RetTime Type  Width     Area      Height     Area
  #   [min]        [min]  mAU   *s   [mAU   ]      %
----|-------|----|-------|----------|----------|--------|
   1  18.442 BB    0.5206 4713.06250  129.09314  49.5728
   2  26.539 BB    0.8340 4794.29248   80.73438  50.4272

Totals :                  9507.35498  209.82752

 Results obtained with enhanced integrator!

                          *** End of Report ***

1100 LC 8/5/2020 4:35:02 PM ALEXB                          Page 1 of 1
```

Data File C:\HPCHEM\1\DATA\ALEXB\WT-6-11D.D Sample Name: wpt-6-11ee2

Chiralcel OD-h w/ guard, 0.3%IPA/Hex, 20uL injection, 1 .0 mL/min, 254nm

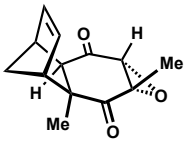

(–)-**5.52** (94% ee)

Injection Date : 8/5/2020 4:28:45 PM
Sample Name : wpt-6-11ee2 Location : Vial 51
Acq. Operator : ALEXB
Inj Volume : 20 µl

Method : C:\HPCHEM\1\METHODS\ALEXB.M
Last changed : 8/5/2020 4:26:27 PM by ALEXB
(modified after loading)

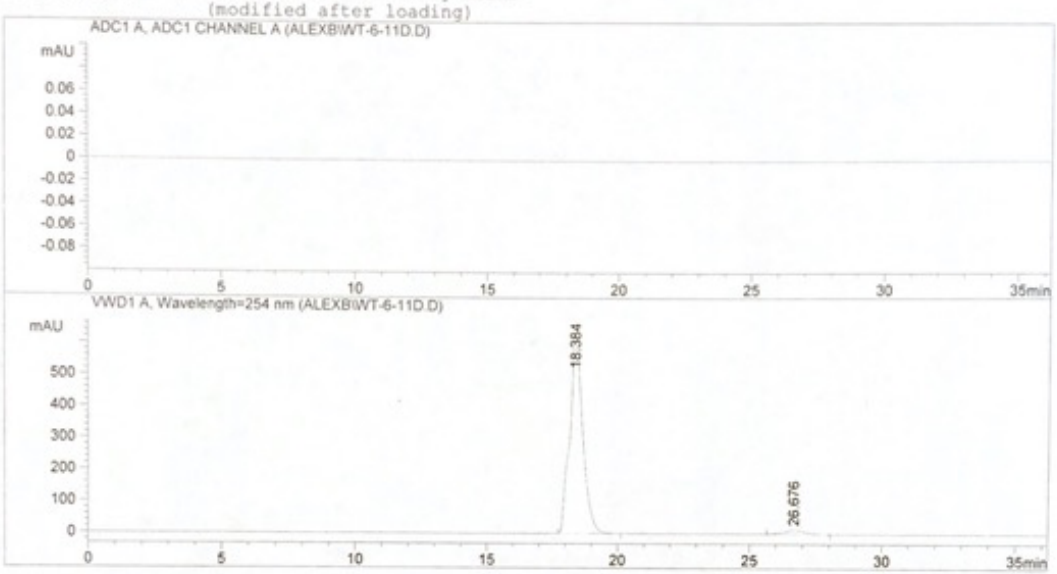

Area Percent Report

Sorted By : Signal
Multiplier : 1.0000
Dilution : 1.0000
Sample Amount : 1.00000 [ng/ul] (not used in calc.)
Use Multiplier & Dilution Factor with ISTDs

Signal 1: ADC1 A, ADC1 CHANNEL A

Signal 2: VWD1 A, Wavelength=254 nm

Peak #	RetTime [min]	Type	Width [min]	Area mAU *s	Height [mAU]	Area %
1	18.384	VB	0.4941	2.19568e4	636.57605	96.8446
2	26.676	BB	0.7465	715.39093	13.85642	3.1554
Totals :				2.26722e4	650.43247	

Results obtained with enhanced integrator!

*** End of Report ***

1100 LC 8/5/2020 5:05:07 PM ALEXB Page 1 of 1

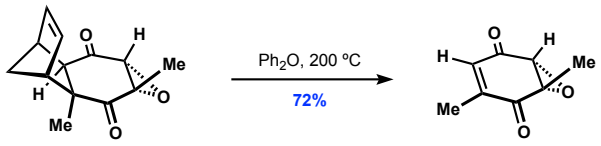

Enedione (+)-**5.36**. A 25 mL round bottom flask was charged with epoxide (–)-**5.52** (1.01 g, 4.60 mmol) and diphenyl ether (2.10 g) and was fitted with a water condenser. The reaction was heated to 200 °C for 1.5 h and then cooled to room temperature, diluted with hexanes, and purified directly by flash chromatography (note: enedione (+)-**5.36** can be seen on the column as a faint yellow band that elutes directly before a dark purple band). Purification by flash chromatography (gradient elution: 0% to 5% v/v ethyl acetate in hexanes) afforded enedione (+)-**5.36** (505 mg, 72%) as a light-yellow solid.

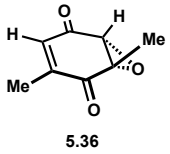

Enedione (+)-**5.36**

^{1}H NMR (500 MHz, $CDCl_3$)

δ 6.39 (s, 1H)	3.63 (s, 1H)	2.02 (s, 3H)	1.62 (s, 3H)

^{13}C NMR (126 MHz, $CDCl_3$)

δ 193.6	147.0	60.2	16.7
192.3	132.9	59.7	14.6

HRMS (ES–) calculated for $C_8H_7O_3$ $[M–H]^-$: 151.0395, found 151.0390

TLC: R_f = 0.32 (10% v/v ethyl acetate in hexanes)

$[\alpha]_D^{22}$ + 87.5 (c = 1.0, $CHCl_3$)

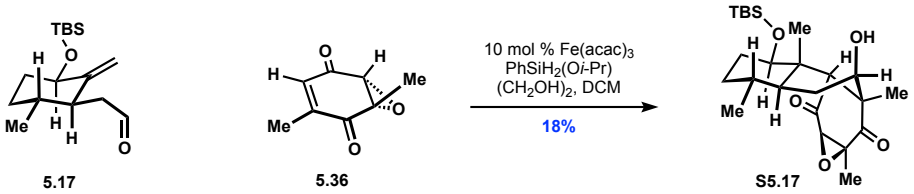

Alcohol S5.17. A 10 mL Schlenk flask was charged with aldehyde **5.17** (28 mg, 0.1 mmol), iron(III) acetylacetonate (1.8 mg, 0.005 mmol), ethylene glycol (8.5 µL, 0.15 mmol) and DCM (0.3 mL). The solution was then degassed by freeze-pump-thaw technique and cooled to 0 °C. To this vigorously stirring solution was added epoxyquinone **5.36** (7.5 mg, 0.05 mmol) and isopropoxyphenylsilane[29] (17 µL, 0.1 mmol) in DCM (0.2 mL, sparged with argon for 15 min) over the course of 1 h by syringe pump. After an additional 3 h the reaction was quenched with 1MHCl and extracted three times with diethyl ether, then washed twice with water and then brine. The organic layer was dried over anhydrous magnesium sulfate, filtered and concentrated under reduced pressure. Purification by preparative thin layer chromatography (eluent: 20% v/v ethyl acetate in hexanes) afforded alcohol **S5.17** (18%, yield determined by analysis of crude reaction mixture by ^{1}H NMR with mesitylene as internal standard. Resonance at 4.42 ppm integrated for ^{1}H NMR yield).

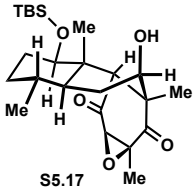

Alcohol **S5.17**

^{1}H NMR (500 MHz, $CDCl_3$)

δ 4.42 (d, 1H, J = 8.7 Hz)	2.17–2.11 (m, 1H)	1.32–1.25 (m, 3H)
4.19 (dd, 1H, J = 10.9, 4.9 Hz)	1.73–1.70 (m, 1H)	1.21 (s, 4H)**
3.49 (d, 1H, J = 0.9 Hz)	1.54 (m, 6H)*	1.05–1.04 (m, 4H)
2.70 (d, 1H, J = 0.9 Hz)	1.51–1.46 (m, 3H)	0.91 (s, 11H)**
2.35 (m, 1H)	1.43 (s, 1H)	0.78 (d, 3H, J = 6.3 Hz)

*water skews integration
**grease skews integration

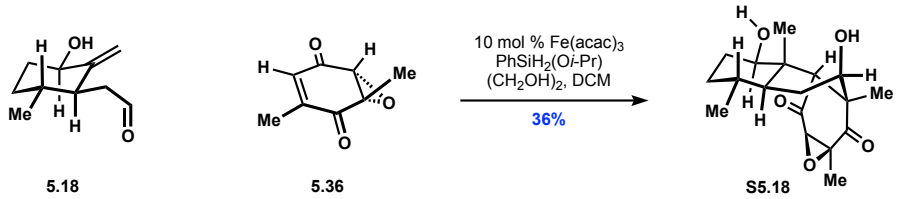

Alcohol S5.18. A 10 mL Schlenk flask was charged with aldehyde **5.18** (90 mg, 0.535 mmol), iron(III) acetylacetonate (9.4 mg, 0.0266 mmol), ethylene glycol (45 μL, 0.804 mmol) and DCM (0.9 mL). The solution was then degassed by freeze-pump-thaw technique and cooled to 0 °C. To this vigorously stirring solution was added epoxyquinone **5.36** (740 mg, 0.267 mmol) and isopropoxyphenylsilane[29] (89 μL, 0.535 mmol) in DCM (0.45 mL, sparged with argon for 15 min) over the course of 1 h by syringe pump. After an additional 3 h the reaction was concentrated under reduced pressure and directly purified by flash chromatography. Purification by flash chromatography (gradient elution: 15% to 50% v/v ethyl acetate in hexanes) followed by flash chromatography (gradient elution: 5% to 15% v/v acetone in hexanes) afforded alcohol **S5.18** (36%, yield determined by analysis of crude reaction mixture by ^{1}H NMR with mesitylene as internal standard. Resonance at 2.77 ppm integrated for ^{1}H NMR yield).

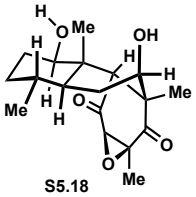

Alcohol **S5.18**

^{1}H NMR (500 MHz, $CDCl_3$)

δ 4.56 (m, 1H)	1.72 (d, 1H, J = 4.8 Hz)	1.24 (s, 3H)
3.61–3.58 (m, 2H)	1.67–1.60 (m, 2H)	1.18 (s, 3H)
2.77 (s, 1H)	1.58 (s, 3H)	1.09–1.02 (m, 1H)
2.68 (m, 1H)	1.54–1.49 (m, 1H)	0.83 (d, 3H, J = 6.2 Hz)
2.24–2.19 (m, 1H)	1.36–1.34 (m, 2H)	

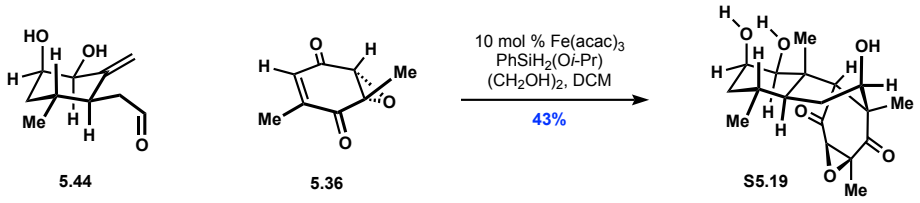

5.44 5.36 S5.19

Alcohol S5.19. A 10 mL Schlenk flask was charged with aldehyde **5.44** (27 mg, 0.147 mmol), iron(III) acetylacetonate (2.6 mg, 0.007 mmol), ethylene glycol (12 μL, 0.215 mmol) and DCM (0.5 mL). The solution was then degassed by freeze-pump-thaw technique and cooled to 0 °C. To this vigorously stirring solution was added epoxyquinone **5.36** (11.5 mg, 0.076 mmol) and isopropoxyphenylsilane[29] (24 μL, 0.144 mmol) in DCM (0.3 mL, sparged with argon for 15 min) over the course of 1 h by syringe pump. After an additional 3 h the reaction was concentrated under reduced pressure and directly purified by flash chromatography. Purification by preparative thin layer chromatography (eluent: 100% ethyl acetate) afforded alcohol **S5.19** (43%, yield determined by analysis of crude reaction mixture by ^{1}H NMR with mesitylene as internal standard. Resonance at 4.54 ppm integrated for ^{1}H NMR yield).

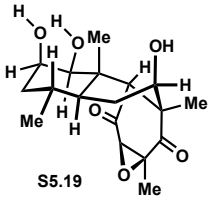

S5.19

Alcohol **S5.19**

^{1}H NMR (500 MHz, $CDCl_3$)

δ 4.54 (m, 1H)	2.34 (bs, 1H)	1.47–1.40 (m, 4H)
3.99 (m, 1H)	2.29 (ddd, 1H, J = 14.1, 8.2, 5.0 Hz)	1.36–1.29 (m, 2H)
3.56 (s, 1H)	2.04 (s, 1H)	1.09–1.02 (m, 1H)
3.50 (t, 1H, J = 4.0 Hz)	1.85 (t, 1H, J = 14.3, 3.2 Hz)	1.18 (s, 3H)
2.82 (d, 1H, J = 4.6 Hz)	1.70 (m, 1H)	0.85 (d, 3H, J = 6.5 Hz)
2.73 (s, 1H)	1.59 (s, 3H)	

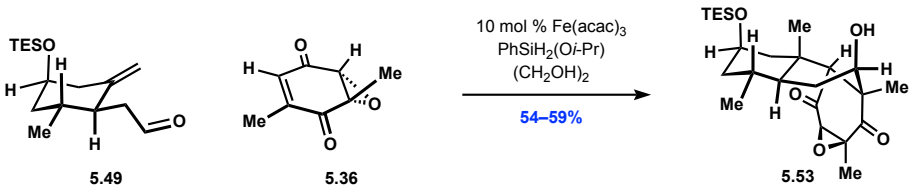

Tricycle (+)-**5.53**. A 25 mL Schlenk flask was charged with aldehyde (–)-**5.49** (930 mg, 3.29 mmol), iron(III) acetylacetonate (58.0 mg, 0.164 mmol), ethylene glycol (0.28 mL, 5.0 mmol) and DCM (5 mL). The solution was then degassed by freeze-pump-thaw technique and cooled to 0 °C. To this vigorously stirring solution was added enedione (+)-**5.36** (252 mg, 1.66 mmol) and isopropoxyphenylsilane[29] (0.41 mL, 2.5 mmol) in DCM (3 mL, sparged with argon for 15 min) over the course of 1 h by syringe pump. After an additional 2 h the reaction was concentrated under reduced pressure and directly purified by flash chromatography. Purification by flash chromatography (gradient elution: 5% to 10% v/v ethyl acetate in hexanes) (note: any impure factions containing tricycle (+)-**5.53** were re-purified by flash chromatography gradient elution: 5% to 15% v/v acetone in hexanes) afforded tricycle (+)-**5.53** (424mg, 59%) as white solid.

Protocol with 1.5 eq of aldehyde (–)-**5.49**: A 25 mL Schlenk flask was charged with aldehyde (–)-**5.49** (810 mg, 2.87 mmol), iron(III) acetylacetonate (67.0 mg, 0.190 mmol), ethylene glycol (0.32 mL, 5.7 mmol) and DCM (6 mL). The solution was then degassed by freeze-pump-thaw technique and cooled to 0 °C. To this vigorously stirring solution was added enedione (+)-**5.36** (280 mg, 1.84 mmol) and isopropoxyphenylsilane[29] (0.48 mL, 2.9 mmol) in DCM (4 mL, sparged with argon for 15 min) over the course of 1 h by syringe pump. After an additional 2 h the reaction was concentrated under reduced pressure and directly purified by flash chromatography. Purification by flash chromatography (gradient elution: 5% to 10% v/v ethyl acetate in hexanes) (note: any impure factions containing tricycle (+)-**5.53** were re-purified by flash chromatography gradient

elution: 5% to 15% v/v acetone in hexanes) afforded tricycle (+)-**5.53** (433mg, 54%) as white solid.

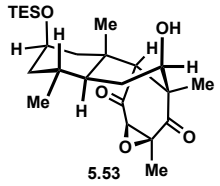

5.53

^{1}H NMR (500 MHz, $CDCl_3$)

δ 4.48 (d, 1H, J = 8.6 Hz)	1.73 (m, 1H)	1.22 (m, 2H)
4.03 (m, 1H)	1.56 (m, 4H)*	1.11 (s, 3H)
3.37 (s, 1H)	1.54 (s, 3H)	0.92 (t, 9H, J = 7.9 Hz)
2.64 (s, 1H)	1.43 (s, 3H)	0.81 (d, 3H, J = 6.6 Hz)
2.37 (ddd, 1H, J = 14.3, 8.8, 5.5 Hz)	1.33 (m, 1H)	0.53 (q, 6H, J = 7.9 Hz)

*water skews integration (expected: 3H)

^{13}C NMR (126 MHz, $CDCl_3$)

δ 206.4	64.2	43.5	32.1	19.7
204.3	63.1	42.8	27.8	16.1
68.4	62.3	42.6	27.1	7.1 (3C)
67.6	52.4	37.2	23.9	4.9 (3C)

HRMS (ES+) calculated for $C_{24}H_{40}O_5SiNa$ $[M+Na]^+$: 459.2543, found 459.2553

TLC: R_f = 0.60 (30% v/v ethyl acetate in hexanes)

$[\alpha]_D^{22}$ + 19.6 (c = 1.0, $CHCl_3$)

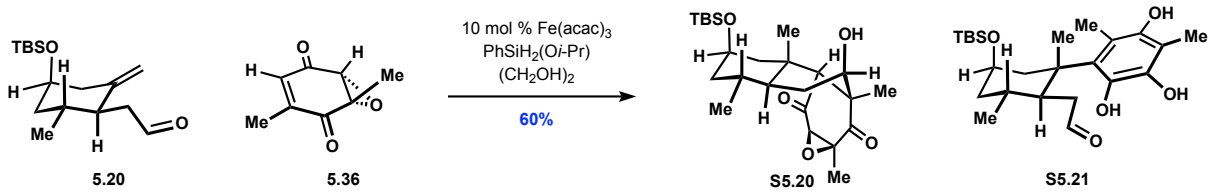

Tricycle (+)-**S5.20**. A 25 mL Schlenk flask was charged with aldehyde (–)-**5.20** (850 mg, 3.01 mmol), iron(III) acetylacetonate (53.0 mg, 0.150 mmol), ethylene glycol (0.25 mL, 4.5 mmol) and DCM (5 mL). The solution was then degassed by freeze-pump-thaw technique and cooled to 0 °C. To this vigorously stirring solution was added enedione (+)-**5.36** (228 mg, 1.50 mmol) and isopropoxyphenylsilane[29] (0.50 mL, 3.0 mmol) in DCM (3 mL, sparged with argon for 15 min) over the course of 1 h by syringe pump. After an additional 2 h the reaction was concentrated under reduced pressure and directly purified by flash chromatography. Purification by flash chromatography (gradient elution: 5% to 10% v/v ethyl acetate in hexanes) (note: any impure factions containing tricycle (+)-**S5.20** were re-purified by flash chromatography gradient elution: 5% to 15% v/v acetone in hexanes) afforded tricycle (+)-**S5.20** (392 mg, 60%) as white solid. Tricycle (+)-**S5.20** was crystalized by dissolving in hexanes/EtOAc (4:1) in a dram vial fitted with a septum and allowing slow evaporation of the solvent.

Note: Trihydroxyarene **S5.21** was produced in trace quantities, see Chapter 5 text for details.

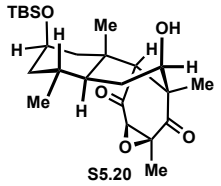

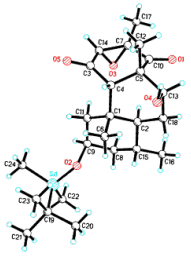

Tricycle (+)-**S5.20**

^{1}H NMR (500 MHz, $CDCl_3$)

δ 4.48 (ddd, 1H, J = 7.4, 4.4, 1.2 Hz)	1.57–1.51 (m, 3H)	0.85 (s, 9H)
4.02 (m, 1H)	1.54 (s, 3H)	0.81 (d, 3H, J = 6.6 Hz)
3.37 (d, 1H, J = 0.74)	1.43 (s, 3H)	0.00 (s, 3H)
2.64 (s, 1H)	1.30 (m, 1H)	–0.01 (s, 3H)
2.37 (ddd, 1H, J = 14.2, 8.8, 5.1 Hz)	1.22 (m, 2H)	
1.71 (m, 1H)	1.11 (s, 3H)	

^{13}C NMR (126 MHz, $CDCl_3$)

δ 206.5	63.1	42.6	25.9 (3C)	–4.9
204.3	62.3	37.2	23.9	–4.9
68.4	52.4	32.1	19.8	
67.8	43.3	27.8	18.1	
64.1	42.8	27.3	16.4	

HRMS (ES+) calculated for $C_{24}H_{40}O_5SiNa$ $[M+Na]^+$: 459.2543, found 459.2450

TLC: R_f = 0.60 (30% v/v ethyl acetate in hexanes)

$[\alpha]_D^{22}$ + 16.1 (c = 1.0, $CHCl_3$)

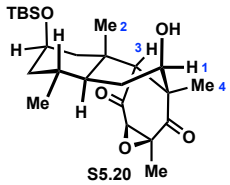

S5.20

Key NOESY correlations:

^{1}H (arbitrary numbering)	Key correlations
H1 (4.48 ppm)	H4 (1.11 ppm)
H3 (2.34 ppm)	H2 (1.43 ppm) H4 (1.11 ppm)

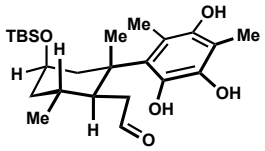

S5.21

Trihydroxyarene **S5.21**.

^{1}H NMR (500 MHz, $CDCl_3$)

δ 9.87 (m, 1H)	2.64–2.58 (m, 1H)	2.89 (s, 3H)
6.58 (s, 1H)	2.22–2.19 (m, 1H)	1.30–1.25 (m, 3H)*
5.82 (s, 1H)	2.15 (s, 6H)	0.92 (d, 3H, J = 6.6 Hz)
4.42 (s, 1H)	1.84–1.82 (m, 1H)	0.85 (s, 10H)*
4.10 (m, 1H)	1.82–1.71 (m, 1H)	0.00 (s, 3H)
2.81 (ddd, 1H, J = 16.4, 7.6, 2.7 Hz)	1.66–1.62 (m, 2H)	–0.02 (s, 3H)

*grease skews integration

^{13}C NMR (126 MHz, $CDCl_3$)

δ 203.8	113.1	43.8	23.2	–4.9 (2C)
148.6	110.5	43.7	20.6	
147.1	84.2	42.9	18.1	
134.2	67.1	28.8	15.8	
121.9	48.7	25.9 (3C)	8.9	

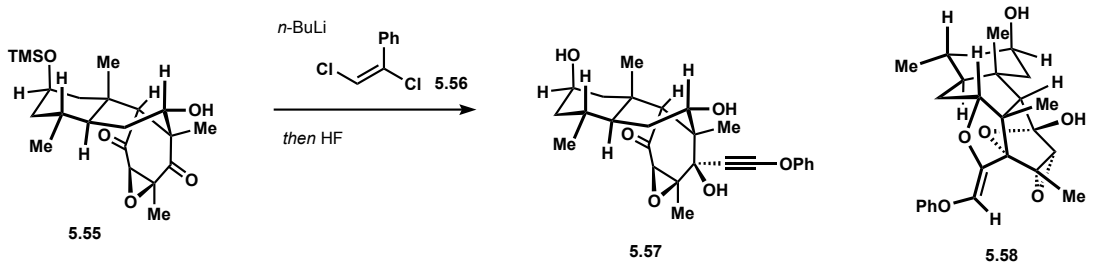

Alkyne 5.57. Alcohol **5.55** was prepared in an analogous manner to phosphonate **5.66**. A dram vial was charged with styrene **5.56** (24 mg, 0.127 mmol) and diethyl ether (0.3 mL) then cooled to –78 ºC. Then *n*-butyllithium (0.1 mL of a 2.5 M solution in hexanes, 0.25 mmol) was added slowly and the reaction was stired for 30 min before warming to –20 ºC for 1 h. The reaction was then cooled to –78 ºC and alcohol 5.55 (17 mg, 0.043 mmol) was added as a solution in THF (0.2 mL). After 15 min the reaction was warmed to room temperature and stirred for 17 h. The reaction was then quenched with saturated aqueous NH_4Cl and extracted with diethyl ether. The organic layer was dried over anhydrous magnesium sulfate, filtered and concentrated under reduced pressure. The crude mixture was then dissolved in THF and aqueous 49% HF was added. After 5 min the reaction was diluted with $NaHCO_3$ and extracted with diethyl ether. The organic layer was dried over anhydrous magnesium sulfate, filtered and concentrated under reduced pressure. Purification by preparative thin layer chromatography (elution with 66% v/v ethyl acetate in hexanes) afforded alkyne **5.57** and alcohol **5.58** (yields not determined). Alcohol **5.58** was crystalized by dissolving in DCM in a dram vial fitted with a septum and allowing slow evaporation of the solvent.

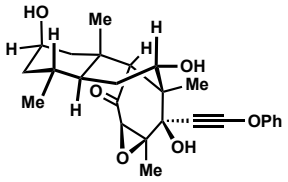

5.57

Alkyne **5.57**

^{1}H NMR (500 MHz, $CDCl_3$)

δ 7.39–7.36 (m, 2H)	2.62 (bs, 1H)	1.69 (s, 3H)
7.18–7.14 (m, 3H)	2.49 (s, 1H)	1.51 (s, 3H)
4.99 (m, 1H)	2.08–2.04 (m, 1H)	1.43 (m, 2H)
4.21 (bs, 1H)	1.88–1.85 (m, 1H)	0.95 (d, 3H, J = 6.4 Hz)
4.14 (m, 1H)	1.81 (m, 1H)	
3.38 (s, 1H)	1.77–1.75 (m, 1H)	

^{13}C NMR (126 MHz, $CDCl_3$)

δ 208.6	90.5	67.6	45.7	30.2	20.3
130.0 (2C)	73.1	64.9	43.4	27.0	17.5
125.0	69.2	47.2	42.4	26.9	
115.2 (2C)	67.9	46.1	38.8	23.5	

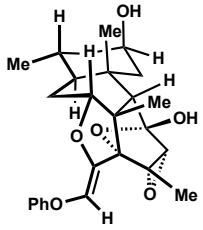

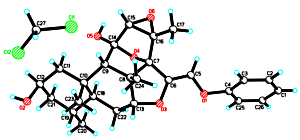

5.58

Alcohol **5.58**

^{1}H NMR (500 MHz, $CDCl_3$)

δ 7.31 (m, 2H)	3.85 (s, 1H)	1.70–1.62 (m, 6H)
7.09 (m, 2H)	3.34 (s, 1H)	1.50 (s, 1H)
7.04 (m, 1H)	2.88 (dd, 1H, J = 14.7, 3.7 Hz)	1.43 (s, 1H)
6.16 (s, 1H)	2.04 (m, 1H)	1.38–1.30 (m, 5H)
4.47 (dd, 1H, J = 10.1, 4.3 Hz)	1.96 (m, 1H)	1.08 (s, 3H)
4.18 (bs, 1H)	1.87 (m, 1H)	0.85 (d, 3H, J = 6.3 Hz)

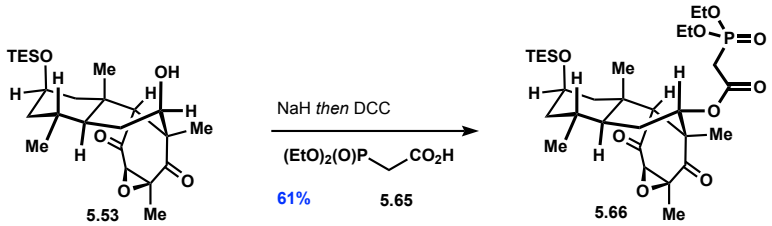

Phosphonate (–)-**5.66**. A 25 mL round bottom flask was charged with sodium hydride (20 mg, 60% dispersion in mineral oil, 0.50 mmol) and washed three times with pentane (1.5 mL combined). Tricycle (+)-**5.53** (411 mg, 0.941 mmol) was then added in toluene (5.0 mL) and the mixture was heated to 60 °C. After 13 h the mixture was cooled to 0 °C and phosphonoacetic acid was added (0.24 mL, 1.5 mmol) followed by DCC (388 mg, 1.88 mmol). The mixture was then warmed to room temperature and stirred for 30 min at which point it was directly purified by flash chromatography (gradient elution: 40% to 70% v/v ethyl acetate in hexanes). The fractions were concentrated, and the crude oil was diluted with pentane (40 mL) resulting in a white precipitate forming, which was filtered and the solution was concentrated to afford phosphonate (–)-**5.66** (354 mg, 61%) as light-yellow viscous oil.

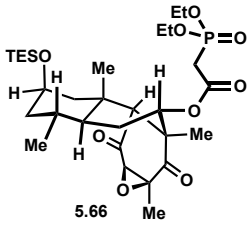

Phosphonate (–)-**5.66**

^{1}H NMR (500 MHz, $CDCl_3$)

δ 4.93 (t, 1H, J = 8.9 Hz)	2.34 (s, 1H)	1.36–1.32 (m, 9H)
4.18 (m, 4H)	1.99 (m, 1H)	1.17 (m, 1H)
4.02 (m, 1H)	1.86 (m, 1H)	1.13 (s, 3H)
3.36 (s, 1H)	1.70 (m, 1H)	0.92 (t, 9H, J = 7.9 Hz)
3.06 (dd, 1H, J = 21.6, 14.2 Hz)	1.57–1.52 (m, 5H)	0.81 (d, 3H, J = 6.5 Hz)
2.99 (dd, 1H, J = 21.6, 14.2 Hz)	1.49 (m, 2H)	0.52 (q, 6H, J = 8.0 Hz)

^{13}C NMR (126 MHz, $CDCl_3$)

δ 204.8	67.3	43.5	29.4	16.4
201.5	62.9	42.8	29.0	16.0
166.0	62.8 (3C)	42.1	28.3	7.0
165.9	62.5	38.2	23.0	4.9
74.2	61.8	35.0	19.4	
69.6	51.5	34.0	16.5	

HRMS (ES+) calculated for $C_{30}H_{52}O_9SiP$ $[M+H]^+$: 615.3118, found 615.3105

TLC: R_f = 0.45 (70% v/v ethyl acetate in hexanes)

$[\alpha]_D^{22}$ – 6.78 (c = 1.0, $CHCl_3$)

Key NOESY correlations:

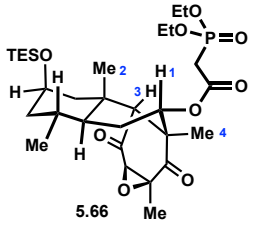

^{1}H (arbitrary numbering)	Key correlations
H1 (4.93 ppm)	H2 (1.33 ppm) H3 (2.34 ppm) H4 (1.13 ppm)
H3 (2.34 ppm)	H1 (4.93 ppm) H2 (1.33 ppm) H4 (1.13 ppm)

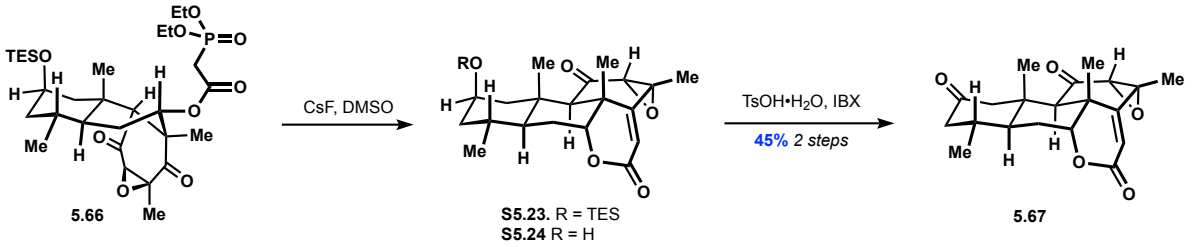

Ketone (–)-**5.67**. A 25 mL round bottom flask was charged phosphonate (–)-**5.66** (344 mg, 0.560 mmol) and CsF (340 mg, 2.24 mmol) and placed under vacuum for 30 min to ensure dryness. The mixture was then dissolved in DMSO (2.5 mL) and heated to 80 °C. After 1 h the reaction was cooled to room temperature and saturated aqueous $NaHCO_3$ (25 mL) and EtOAc (25 mL) were added. The phases were separated, and the aqueous layer was extracted twice with EtOAc (50 mL combined). The organic layers were combined and washed with brine (10 mL). The organic layer was dried over anhydrous sodium sulfate, filtered, and concentrated under reduced pressure. Purification by flash chromatography (gradient elution: 10% to 60% v/v ethyl acetate in hexanes) afforded silyl ether **S5.23** (77 mg, R_f = 0.50, 30% v/v ethyl acetate in hexanes) and semi-purified alcohol **S5.24** (53 mg, R_f = 0.45, 60% v/v ethyl acetate in hexanes). These products were combined and dissolved in DMSO (3.0 mL). To this mixture was added *p*-TsOH•H_2O (115 mg, 0.605 mmol) and IBX (336 mg, 1.20 mmol). The mixture was then heated to 30 °C. After 15 min the mixture was cooled to room temperature and diluted with saturated aqueous $NaHCO_3$ (20 mL) and EtOAc (20 mL). The phases were separated, and the aqueous layer was extracted twice with EtOAc (40 mL combined). The organic layers were combined and washed with brine (10 mL). The organic layer was dried over anhydrous magnesium sulfate, filtered, and concentrated under reduced pressure. Purification by flash chromatography (gradient elution: 20% to 60% v/v ethyl acetate in hexanes) afforded ketone (–)-**5.67** (86.8 mg, 45% over two steps) as a white solid.

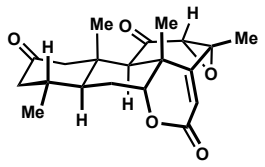

5.67

Ketone (–)-**5.67**

^{1}H NMR (500 MHz, $CDCl_3$)

δ 6.37 (s, 1H)	2.39 (ddd, 1H, J = 14.4, 4.5, 2.7 Hz)	1.73–1.62 (m, 5H)
4.36 (t, 1H, J = 2.8 Hz)	2.23–2.20 (m, 1H)	1.26 (s, 3H)
3.28 (s, 1H)	2.05–2.00 (m, 1H)	1.10 (s, 3H)
2.99 (dd, 1H, J = 13.4, 2.3 Hz)	1.91 (d, 1H, J = 13.4 Hz)	1.04 (d, 3H, J = 3.4 Hz)
2.65 (s, 1H)	1.89–1.81 (m, 1H)	

^{13}C NMR (126 MHz, $CDCl_3$)

δ 209.1	118.3	55.0	41.8	21.3
202.8	78.6	54.0	39.1	20.2
163.8	61.5	49.8	31.9	19.1
160.8	61.1	43.9	25.7	14.3

HRMS (ES+) calculated for $C_{20}H_{25}O_5$ $[M+H]^+$: 345.1702, found 345.1694

TLC: R_f = 0.23 (50% v/v ethyl acetate in hexanes)

$[\alpha]_D^{22}$ – 107.8 (c = 1.0, $CHCl_3$)

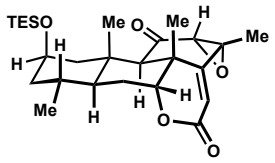

S5.23

Silyl ether **S5.23**

^{1}H NMR (500 MHz, $CDCl_3$)

δ 6.30 (s, 1H)	2.11–2.08 (m, 1H)	1.22–1.16 (m, 1H)
4.30 (t, 1H, J = 2.8 Hz)	1.86 (m, 1H)	1.14–1.09 (m, 1H)
4.00 (m, 1H)	1.68 (m, 2H)	0.96 (t, 9H, J = 8.0 Hz)
3.22 (s, 1H)	1.64 (s, 3H)	0.93–0.90 (m, 1H)
2.45–2.42 (m, 1H)	1.38 (s, 3H)	0.88 (d, 3H, J = 6.6Hz)
2.34 (s, 1H)	1.25 (s, 3H)	0.57 (q, 6H, J = 8.0 Hz)

^{13}C NMR (126 MHz, $CDCl_3$)

δ 203.8	67.3	44.9	24.8	7.1 (3C)
164.3	61.8	44.1	22.2	4.9 (3C)
161.1	61.1	41.6	19.9	
117.5	56.8	36.1	19.2	
79.3	43.4	25.3	15.5	

HRMS (ES+) calculated for $C_{26}H_{40}O_5SiNa$ $[M+Na]^+$: 483.2543, found 483.2552

TLC: R_f = 0.50 (30% v/v ethyl acetate in hexanes)

$[\alpha]_D^{22}$ – 118.0 (c = 1.0, $CHCl_3$)

Key NOESY correlations:

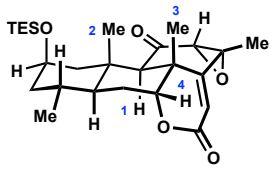

S5.23

^{1}H (arbitrary numbering)	Key correlations	Absent correlations
H1 (2.34 ppm)		H2 (1.25 ppm) H3 (1.38 ppm)
H4 (4.30 ppm)	H3 (1.38 ppm)	
H3 (1.38 ppm)	H2 (1.25 ppm)	

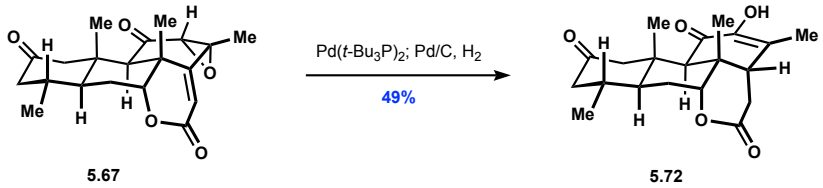

5.67 5.72

Lactone (+)-**5.72**. A dram vial was charged with Pd(*t*-$Bu_3P)_2$ (6.3 mg, 0.012 mmol) and ketone (–)-**5.67** (85.5 mg, 0.248 mmol) and dissolved in 1,4-dioxane (0.5 mL). The mixture was then heated to 100 °C. After 1.5 h the mixture was cooled to room temperature and transferred to a 25 mL round bottom flask with MeOH (2.5 mL) then Pd/C (212 mg, 10% w/w) was added as a suspension in MeOH (2.5 mL) and the mixture was sparged with a balloon of hydrogen for 5 min. Then the mixture was vigorously stirred for 10 h at which point the mixture was filtered over celite, washed with EtOAc (25 mL) and concentrated. Purification by flash chromatography (gradient elution: 20% to 60% v/v ethyl acetate in hexanes) afforded lactone (+)-**5.72** (42.1 mg, 49% over two steps) as a white solid with a small amount of diethyl ether, which was used to transfer material between flasks (2.5 mg, ~5% w/w).

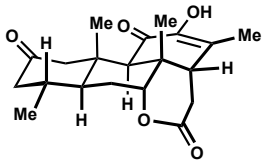

5.72

Lactone (+)-**5.72**

^{1}H NMR (500 MHz, C_6D_6)

δ 6.25 (s, 1H)	2.17 (s, 1H)	0.79 (s, 3H)
3.66 (dd, 1H, J = 13.6, 2.1 Hz)	1.80 (dd, 1H, J = 18.5, 12.3 Hz)	0.58 (d, 3H, J = 5.8 Hz)
3.48 (t, 1H, J = 2.8 Hz)	1.63–1.59 (m, 3H)	0.49 (s, 3H)
2.36 (dd, 1H, J = 18.6, 6.8 Hz)	1.50 (s, 3H)	
2.27–2.23 (m, 1H)	1.36–1.27 (m, 4H)	

^{13}C NMR (126 MHz, C_6D_6)

δ 207.6	124.8	49.7	37.6	22.1
193.0	81.87	46.0	31.5	19.6
167.8	54.9	43.6	31.1	15.4
143.1	51.2	39.1	26.1	14.8

HRMS (ES+) calculated for $C_{20}H_{26}O_5Na$ $[M+Na]^+$: 369.1678, found 369.1672

TLC: R_f = 0.31 (60% v/v ethyl acetate in hexanes)

$[\alpha]_D^{22}$ + 45.4 (c = 1.0, $CHCl_3$)

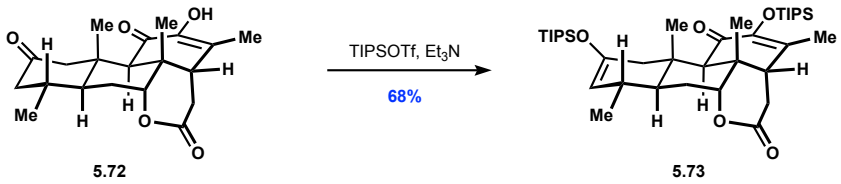

5.72 5.73

Silyl ether (+)-**5.73**. A dram vial was charged with lactone (+)-**5.72** (31.4 mg, 0.0906 mmol) and dissolved in DCM (0.5 mL). The solution was then cooled to 0 °C and triethylamine (76 µL, 0.55 mmol) was added followed by TIPSOTf (0.125 mL, 0.465 mmol) added slowly. The mixture was then warmed to room temperature. After 15 min aqueous 1M HCl (10 mL) and DCM (10 mL) were added, and the biphasic mixture was agitated in a separatory funnel until it turned light pink at which point the phases were separated and the aqueous layer was extracted twice with DCM (20 mL combined). The organic layers were combined and washed with saturated aqueous $NaHCO_3$ (10 mL). The organic layer was dried over anhydrous magnesium sulfate, filtered, and concentrated under reduced pressure. Purification by preparative thin layer chromatography (eluent: 20% v/v ethyl acetate in hexanes) afforded silyl ether (+)-**5.73** (59.7 mg, 68%) as a white solid.

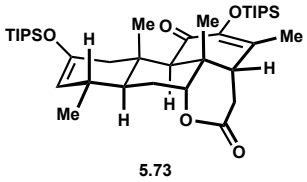

5.73

Silyl ether (+)-**5.73**

^{1}H NMR (500 MHz, $CDCl_3$)

δ 4.69 (s, 1H)	2.06–2.03 (m, 1H)	1.27–1.20 (m, 7H)
4.28 (m, 1H)	1.93 (m, 1H)	1.15–1.11 (m, 6H)
3.01 (d, 1H, J = 17.0 Hz)	1.87 (s, 3H)	1.08–1.01 (m, 36H)
2.95 (dd, 1H, J = 18.5, 6.6 Hz)	1.76–1.73 (m, 1H)	0.96 (d, 3H, J = 6.7 Hz)
2.50–2.32 (m, 3H)	1.62 (m, 1H)	

^{13}C NMR (126 MHz, $CDCl_3$)

δ 192.9	83.5	35.9	18.3 (6C)
170.1	53.4	32.1	18.2 (6C)
148.3	47.0	30.7	16.2
144.5	45.4	26.7	14.3
130.9	41.6	22.9	14.1 (3C)
108.8	37.7	20.3	12.9 (3C)

HRMS (ES+) calculated for $C_{38}H_{67}O_5Si_2$ $[M+H]^+$: 659.4572, found 659.4529

TLC: R_f = 0.35 (20% v/v ethyl acetate in hexanes)

$[\alpha]_D^{22}$ + 28.4 (c = 1.0, $CHCl_3$)

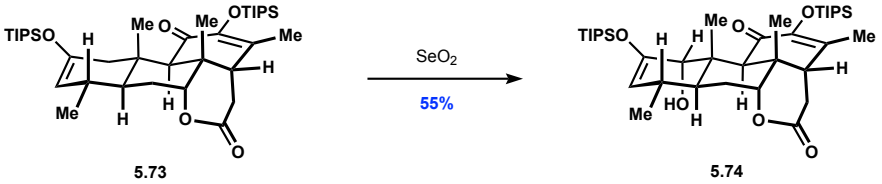

5.73 5.74

Alcohol (+)-**5.74**. A dram vial was charged with silyl ether (+)-**5.73** (18.4 mg, 0.0279 mmol) and SeO_2 (15.4 mg, 0.139 mmol) and dissolved in DMA (0.3 mL). The mixture was heated to 40 °C and stirred vigorously. After 2 h the solution was diluted with saturated aqueous $NaHCO_3$ (10 mL) and EtOAc (10 mL) at which point the phases were separated and the aqueous layer was extracted twice with EtOAc (20 mL combined). The organic layers were combined and washed with brine (5 mL). The organic layer was dried over anhydrous sodium sulfate, filtered, and concentrated under reduced pressure. Purification by preparative thin layer chromatography (eluent: 20% v/v ethyl acetate in hexanes) afforded alcohol (+)-**5.74** (10.4 mg, 55%) as a white solid.

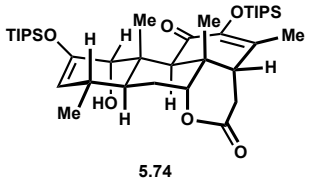

5.74

Alcohol (+)-**5.74**

^{1}H NMR (500 MHz, $CDCl_3$)

δ 4.73 (d, 1H, J = 2.0 Hz)	2.34 (dd, 1H, J = 12.2, 6.5 Hz)	1.27–1.16 (m, 11H)
4.47 (d, 1H, J = 3.7 Hz)	2.08 (dt, 1H, J = 14.5, 3.1 Hz)	1.10–1.08 (m, 21H)
4.25 (t, 1H, J = 2.7 Hz)	1.94–1.86 (m, 4H)	1.05–1.02 (m,18H)
3.39 (s, 1H)	1.70 (d, 1H, J = 4.3 Hz)	0.98 (d, 3H, J = 6.9 Hz)
2.91 (dd, 1H, J = 18.5, 6.5 Hz)	1.68–1.62 (m, 1H)	
2.51 (dd, 1H, J = 18.5, 12.3 Hz)	1.55–1.50 (m, 1H)	

^{13}C NMR (126 MHz, $CDCl_3$)

δ 193.8	110.6	39.6	26.6	18.2 (6C)
170.1	83.3	37.2	23.2	16.3
149.4	73.2	35.3	20.0	14.2 (3C)
144.5	47.5	32.1	18.4 (3C)	13.8
130.8	45.2	31.0	18.3 (3C)	12.8 (3C)

HRMS (ES+) calculated for $C_{38}H_{69}O_6Si_2Na$ $[M+Na]^+$: 697.4296, found 697.4313

TLC: R_f = 0.31 (20% v/v ethyl acetate in hexanes)

$[\alpha]_D^{22}$ + 25.3 (c = 1.0, $CHCl_3$)

Key NOESY correlations:

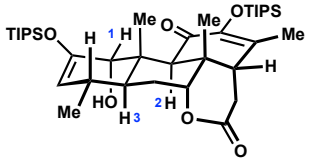

5.74

^{1}H (arbitrary numbering)	Key correlations	Absent correlations
H1 (4.47 ppm)	H2 (3.39 ppm)	H3 (1.55–1.50 ppm)
H2 (3.39 ppm)	H3 (1.55–1.50 ppm) H1 (4.47 ppm)	

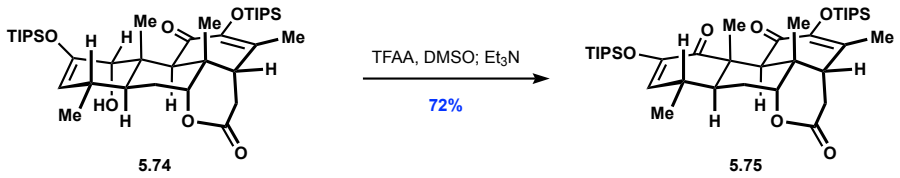

Enone (+)-**5.75**. A dram vial was charged with DMSO (32 µL, 0.45 mmol) and DCM (0.7 mL) and cooled to – 78 °C. Then trifluoroacetic anhydride (53 µL, 0.38 mmol) was added slowly and the mixture was stirred for 15 min. Then alcohol (+)-**5.74** (17.1 mg, 0.0253 mmol) was added in DCM (0.3 mL) slowly and the mixture was stirred at – 78 °C. After 2.5 h triethylamine (140 µL, 1.00 mmol) was added slowly and the mixture was stirred for 10 min. Then the mixture was warmed to room temperature for an additional 15 min at which point water (10 mL) was added followed by EtOAc (10 mL). The phases were separated, and the aqueous layer was extracted twice with EtOAc (20 mL combined). The organic layers were combined and washed with brine (5 mL). The organic layer was dried over anhydrous magnesium sulfate, filtered, and concentrated under reduced pressure. Purification by preparative thin layer chromatography (eluent: 25% v/v ethyl acetate in hexanes) afforded enone (+)-**5.75** (12.2 mg, 72%) as a white solid.

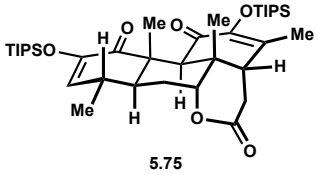

Enone (+)-**5.75**

^{1}H NMR (500 MHz, $CDCl_3$)

δ 5.60 (d, 1H, J = 2.4 Hz)	2.46–2.40 (m, 1H)	1.78–1.73 (m, 1H)
4.25 (t, 1H, J = 2.6 Hz)	2.35 (dd, 1H, J = 12.0, 6.8 Hz)	1.54 (s, 3H)
2.99 (s, 1H)	2.05 (dt, 1H, J = 14.4, 3.2 Hz)	1.28–1.22 (m, 3H)
2.96 (dd, 1H, J = 18.8, 6.8 Hz)	1.87 (s, 3H)	1.20–1.14 (m, 6H)
2.58 (dd, 1H, J = 18.7, 12.0 Hz)	1.85–1.82 (m, 1H)	1.07–1.04 (m, 39H)

^{13}C NMR (126 MHz, $CDCl_3$)

δ 198.9	125.8	43.9	22.8	14.1 (3C)
191.1	82.5	37.2	19.2	13.2 (3C)
169.8	47.1	32.0	18.4 (6C)	13.1
144.6 (2C)	45.9	31.7	18.2 (6C)	
129.1	45.7	26.1	16.0	

HRMS (ES+) calculated for $C_{38}H_{64}O_6Si_2Na$ $[M+Na]^+$: 695.4139, found 695.4130

TLC: R_f = 0.33 (30% v/v ethyl acetate in hexanes)

$[\alpha]_D^{22}$ + 26.3 (c = 1.0, $CHCl_3$)

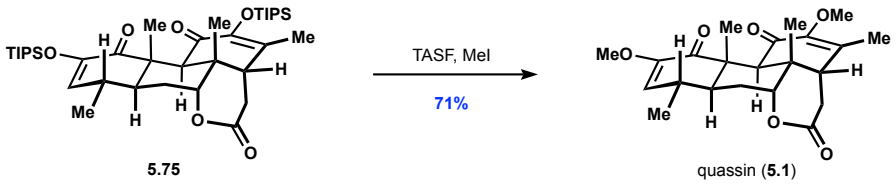

Quassin (+)-**5.1**. A dram vial was charged with enone (+)-**5.75** (12.0 mg, 0.0178 mmol) and dissolved in THF (0.2 mL). Then MeI (22 μL, 0.35 mmol) was added followed by slow addition of TASF (14.7 mg, 0.0534 mmol) as a suspension in THF (0.8 mL). After stirring vigorously for 1 h the mixture was diluted with saturated aqueous NaHCO3 (10 mL) and EtOAc (10 mL). The phases were separated, and the aqueous layer was extracted twice with EtOAc (20 mL combined). The organic layers were combined and washed with brine (5 mL). The organic layer was dried over anhydrous sodium sulfate, filtered, and concentrated under reduced pressure. Purification by preparative thin layer chromatography (eluent: 70% v/v ethyl acetate in hexanes) afforded quassin (+)-**5.1** (4.9 mg, 71%) as a white solid.

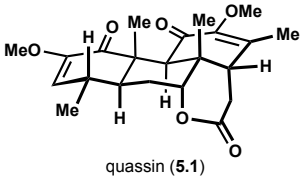

Quassin (+)-**5.1**

^{1}H NMR (500 MHz, $CDCl_3$)

δ 5.30 (d, 1H, J = 2.3 Hz)	2.99 (s, 1H)	1.90–1.78 (m, 2H)
4.28 (m, 1H)	2.61 (dd, 1H, J = 18.6, 11.9 Hz)	1.88 (s, 3H)
3.67 (s, 3H)	2.51–2.45 (m, 1H)	1.56 (s, 3H)
3.58 (s, 3H)	2.39 (dd, 1H, J = 11.8, 7.0 Hz)	1.20 (s, 3H)
2.99 (dd, 1H, J = 18.6, 7.1 Hz)	2.09 (dt, 1H, J = 14.3, 2.8 Hz)	1.12 (d, 3H, J = 6.9 Hz)

^{13}C NMR (126 MHz, $CDCl_3$)*

δ 197.8	137.4	46.6	31.7	15.4
190.9	116.3	46.3	31.2	12.7
169.1	82.1	45.8	25.8	
148.3	59.3	43.2	22.4	
148.0	55.0	37.1	19.5	

*$CDCl_3$ calibrated to 77.0 ppm for comparison purposes

HRMS (ES+) calculated for $C_{22}H_{29}O_6$ $[M+H]^+$: 389.1964, found 389.1960

TLC: R_f = 0.25 (70% v/v ethyl acetate in hexanes)

$[\alpha]_D^{22}$ + 34.9 (c = 1.0, $CHCl_3$)

Comparison of ^{13}C NMR data for synthetic quassin (+)-**5.1** to literature values ($CDCl_3$; Δ, ppm)

This Work	Shing et al. (commercial) [31a]	Δ
197.8	197.8	0.0
190.9	190.9	0.0
169.1	169.1	0.0
148.3	148.2	+0.1
148.0	147.9	+0.1
137.4	137.6	–0.2
116.3	116.3	0.0
82.1	81.9	+0.2
59.3	59.3	0.0
55.0	54.9	+0.1
46.6	46.5	+0.1
46.3	46.2	+0.1
45.8	45.8	0.0
43.2	43.2	0.0
37.1	37.0	+0.1
31.7	31.6	+0.1
31.2	31.1	+0.1
25.8	25.8	0.0
22.4	22.2	+0.2
19.5	19.4	+0.1
15.4	15.3	+0.1
12.7	12.7	0.0

This Work	Shing et al. (synthetic) [31b]	Δ
197.8	197.8	0.0
190.9	191.0	–0.1
169.1	169.1	0.0
148.3	148.3	0.0
148.0	148.0	0.0
137.4	137.5	–0.1
116.3	116.3	0.0
82.1	82.0	+0.1
59.3	59.3	0.0
55.0	55.0	0.0
46.6	46.6	0.0
46.3	46.2	+0.1
45.8	45.8	0.0
43.2	43.2	0.0
37.1	37.1	0.0
31.7	31.6	+0.1
31.2	31.2	0.0
25.8	25.8	0.0
22.4	22.3	+0.1
19.5	19.4	+0.1
15.4	15.4	0.0
12.7	12.7	0.0

5.5 References and Notes

1. For reviews on the synthesis and biological activity of quassinoids see: (a) Polonsky, J. Quassinoid Bitter Principles. *Fortschritte Der Chemie Organischer Naturstoffe* **1973**, 101. (b) Guo, Z.; Vangapandu, S.; Sindelar, R. W.; Walker, L. A.; Sindelar, R. D. Biologically active quassinoids and their chemistry: potential leads for drug design. *Curr. Med. Chem.* **2005**, *12*, 173. (c) Curcino Vieira, I. J.; Braz-Filho, A. R. Quassinoids: structual diversity, biological activity and studies synthetic. *Studies in Nat. Prod. Chem.* **2005**, *33*, 433. (d) Spino, C. The ever-challenging quassinoids. *Synlett*, **2006**, *1*, 0023. (e) Fiaschetti, G.; Grotzer, M.A.; Shalaby, T.; Castelletti, A.; Arcaro, A. Quassinoids: from traditional drugs to new cancer therapeutics. *Curr. Med. Chem*. **2011**, *18*, 316. (f) Houël, E.; Stien, D.; Bourdy, G.; Deharo, E. Quassinoids: anticancer and antimalarial activities. *Natural Products* **2013**, 3775. (g) Li, Z.; Ruan. J.-y.; Sun, F.; Yan, J.-j.; Wang, J.-l.; Zhang, Z.-x.; Wang, T. Relationship between structural characteristics and plant sources along with pharmacology research of quassinoids. *Chem. Pharm. Bull.* **2019**, *67*, 654. (h) Duan, Z.-K.; Zhang, Z.-J.; Dong, S.-H.; Wang, Y.-X.; Song, S.-J.; Huang, X.-X. Quassinoids: phytochemistry and antitumor prospect. *Phytochemistry* **2021**, *187*, 112769.
2. Thomas, W. P.; Pronin S. V. A concise enantioselective approach to quassinoids. *J. Am. Chem. Soc.* **2022**, *144*, 118.
3. (a) Grieco, P. A.; Ferrino, S.; Vidari, G. Total synthesis of dl-quassin. *J. Am. Chem. Soc.* **1980**, *102*, 7586. (b) Vidari, G.; Ferriño, S.; Grieco, P. A. Quassinoids: total synthesis of dl-quassin. *J. Am. Chem. Soc*. **1984**, *106*, 3539.
4. Kim, M.; Kawada, K.; Gross, R. S.; Watt, D. S. An enantioselective synthesis of (+)-picrasin B, (+)-Δ^2-picrasin B, and (+)-quassin from the R-(−) enantiomer of the Wieland-Miescher ketone. *J. Org. Chem.* **1990**, *55*, 504.
5. (a) Stojanac, N.; Sood, A.; Stojanac, Ž.; Valenta, Z. A synthetic approach to quassin. Introduction of functionality and stereochemistry by a Diels-Alder reaction. *Can. J. Chem.* **1975**, 53, 619. (b) Stojanac, N.; Stojanac, Ž.; White, P. S.; Valenta, Z. A synthetic approach to quassin. Synthesis of a ring A seco derivative. *Can. J. Chem.* **1979**, *57*, 3346. (c) Stojanac, N.; Valenta, Z. Total synthesis of d,l-quassin. *Can. J. Chem.* **1991**, *69*, 853.
6. (a) Shing, T. K. M.; Jiang, Q.; Mak, T. C. W. Total synthesis of (+)-quassin from (+)-carvone. *J. Org. Chem.* **1998**, *63*, 2056. (b) Shing, T. K. M.; Jiang, Q. Total synthesis of (+)-quassin. *J. Org. Chem.* **2000**, *65*, 7059.
7. For innovative approaches to the quassinoids in the 21st century, see: (a) Barrero, A. F.; Alvarez-Manzaneda, E. J.; Alvarez-Manzaneda, R.; Chahboun, R.; Meneses, R.; Cuerva, J. M.; Aparicio, M.; Romera, J. L. Approach to the synthesis of antitumor quassinoids from labdane diterpenes: an efficient synthesis of a picrasane-related intermediate. *Org. Lett.* **2001**, *3*, 647. (b) Spino, C.; Hill, B.; Dubé, P.; Gingras, S. A diene-transmissive approach to the quassinoid skeleton. *Can. J. Chem.* **2003**, *81*, 81. (c) Perreault, S.; Spino, C. Meldrum's acid-derived thione dienophile in a convergent and stereoselective synthesis of a tetracyclic quassinoid intermediate. *Org. Lett.* **2006**, *8*, 4385. (d) Marcos, I. S.; García, N.; Sexmero, M. J.; Hernandez, F. A.; Escola, M. A.; Basabe, P.; Díez, D.; Urones, J. G. Synthetic studies towards picrasane quassinoids. *Tetrahedron* **2007**, *63*, 2335. (e) Caron, P.-Y.; Deslongchamps, P. Versatile strategy to access tricycles related to quassinoids and triterpenes. *Org. Lett.* **2010**, *12*, 508. (f) Burns, D. J.; Mommer, S.; O'Brien, P.; Taylor, R. J. K.; Whitwood, A. C.; Hachisu, S. Stereocontrolled synthesis of the AB rings of

samaderine C. *Org. Lett.* **2013**, *15*, 394. (g) Ravindar, K.; Caron, P.-Y.; Deslongchamps, P. Anionic polycyclization entry to tricycles related to quassinoids and terpenoids: a stereocontrolled total synthesis of (+)-cassaine. *J. Org. Chem.* **2014**, *79*, 7979. (h) Usui, K.; Suzuki, T.; Nakada, M. A highly stereoselective intramolecular Diels−Alder reaction for construction of the AB ring moiety of bruceantin. *Tetrahedron Lett.* **2015**, *56*, 1247. (i) Oki, Y.; Nakada, M. Research on Au(I)-catalyzed ene-yne cycloisomerization for construction of quassinoid scaffold. *Tetrahedron Lett.* **2018**, *59*, 926. (j) Condakes, M. L.; Rosen, R. Z.; Harwood, S. J.; Maimone, T. J. A copper-catalyzed double coupling enables a 3-step synthesis of the quassinoid core architecture. *Chem. Sci.* **2019**, *10*, 768.

8. For relevant studies, see: (a) Valenta, Z.; Papadopoulos, S.; Podesva, C. Quassin and neoquassin. *Tetrahedron* **1961**, *15*, 100. (b) ref. 5a

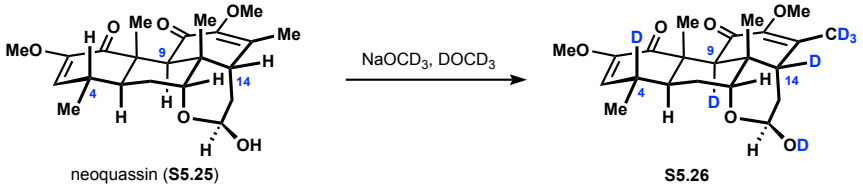

neoquassin (**S5.25**) **S5.26**

9. Mandell, L.; Lee, D. E.; Courtney, L. F. Toward the total synthesis of quassin. *J. Org. Chem.* **1982**, *47*, 610
10. Liu, D.; Canales, E.; Corey, E. J. Chiral oxazaborolidine−aluminum bromide complexes are unusually powerful and effective catalysts for enantioselective Diels–Alder reactions. *J. Am. Chem. Soc.* **2007**, *129*, 1498.
11. (a) Chen, M. S.; White, C. M. Combined effects on selectivity in Fe-catalyzed methylene oxidation. *Science* **2010**, *327*, 566. (b) Gormisky, P. E.; White, C. M. Catalyst-controlled aliphatic C–H oxidations with a predictive model for site-selectivity. *J. Am. Chem. Soc.* **2013**, 135, 38, 14052. (c) White, C. M.; Zhao, J. Aliphatic C–H oxidations for late-stage functionalization. *J. Am. Chem. Soc.* **2018**, *140*, 13988
12. (a) Schmidt, V. A.; Quinn, R. K.; Brusoe, A. T.; Alexanian, E. J. Site-selective aliphatic C–H bromination using *N*-bromoamides and visible light. *J. Am. Chem. Soc.* **2014**, *136*, 14389. (b) For a relevant C–H chlorination, see: Quinn, R. K.; Könst, Z. A.; Michalak, S. E.; Schmidt, Y.; Szklarski, A. R.; Flores, A. R.; Nam, S.; Horne, D. A.; Vanderwal, C. D.; Alexanian, E. J. Site-Selective Aliphatic C-H Chlorination Using N-Chloroamides Enables a Synthesis of Chlorolissoclimide. *J. Am. Chem. Soc.* **2016**, *138*, 696. (c) Carestia, A. M.; Ravelli, D.; Alexanian, E. J. Reagent-dictated site selectivity in intermolecular aliphatic C–H functionalizations using nitrogen-centered radicals: *Chem. Sci.* **2018**, *9,* 5360. (d) Tierney, M. M.; Crespi, S.; Ravelli, D.; Alexanian, E. J. Identifying amidyl radicals for intermolecular C–H functionalizations. *J. Org. Chem.* **2019**, *84,* 12983.
13. For relevant examples, see ref. 11, ref. 12 and: Hong, B.; Luo, T.; Lei, X. Late-Stage Diversification of Natural Products. *ACS Cent. Sci.* **2020**, *6*, 622.
14. It is not clear how aromatization occurs to form **5.43** and it is possible that it is a result of radical capture by adventitious molecular oxygen following Giese addition. Although all annulation reactions were degassed by freeze-pump-thaw technique, preliminary reactions were run on small scale (0.05 mmol), so it is plausible that some oxygen was still present in these reactions. Therefore, it cannot be ruled out that the difference in yield of **5.43** is

simply a reflection of the quantity of adventitious molecular oxygen present in the reaction vessel.

15. We were unable to find other examples in the literature of *trans-syn-cis* perhydro-phenanthrenes adopting twist-boat conformations. The related structures found showed chair configurations, see: Caron, P.Y-.; Deslongchamps, P. Versatile strategy to access tricycles related to quassinoids and triterpenes. *Org. Lett.* **2010**, *12*, 508.
16. Nicolaou, K. C.; Zhong, Y.-L.; Baran, P. S. A new method for the one-step synthesis of α,β,-unsaturated carbonyl systems from saturated alcohols and carbonyl compounds. *J. Am. Chem. Soc.* **2000**, *122*, 7596.
17. Huang, D.; Schuppe, A. W.; Liang, M. Z.; Newhouse, T. R. Scalable procedure for the fragmentation of hydroperoxides mediated by copper and iron tetrafluoroborate salts. *Org. Biomol. Chem.* **2016**, *14*, 6197.
18. At the time of writing prices from Sigma–Aldrich are: (+)-3-methylcyclohexanone (**5.45**) $120/5g; (–)-isopulegol (**5.46**) $153/1kg.
19. The C7 stereocenter could be epimerized with basic aluminum oxide (Brockmann grade IV) in refluxing toluene d. r. 6:1, K_2CO_3 in *sec*-butanol at 100 ºC d. r. 2:1 or NaH in toluene at 50 ºC d. r. 6:1. Epimerization of TMS ether **S5.22** with NaH in THF epimerized C9, the TMS ether was also cleaved under the reaction conditions/work up delivering TMS ether **S5.27**, confirmed by X-ray crystallography, see Appendix C. Notably, this *trans-anti-trans* perhydro-phenanthrene adopted an all-chair configuration in the solid state, presumably precluding facile epimerization of the equatorial C7 alcohol to the desired axial orientation. TMS ether **S5.27** was also observed during prolonged epimerizations with basic aluminum oxide.

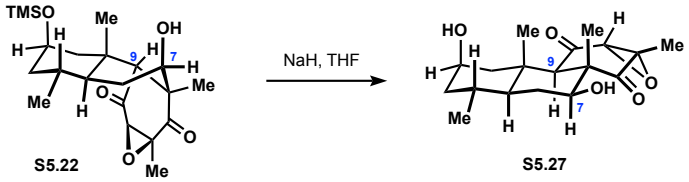

20. Egi, M.; Ota, Y.; Nishimura, Y.; Shimizu, K.; Azechi, K.; Akai, S. Efficient intramolecular cyclizations of phenoxyethynyl diols into multisubstituted α,β-unsaturated lactones. *Org. Lett.* **2013**, *15*, 4150.
21. Shing performed an S_N2' reduction of a related unsaturated epoxylactone that inspired these inquiries, see ref. 6b.
22. We initially postulated that this solvent effect may be due to discrepancies in the ratio of enol- vs keto-tautomer, but ^1H NMR experiments in $CDCl_3$, C_6D_6, and CD_3OD indicated only presence of the enol-tautomer.
23. The efficiency of this SeO_2 mediate oxidation was highly sensitive to solvent effects, where dimethyl acetamide provided the optimal results. This type of SeO_2 mediated oxidation was originally reported by Magnus, see: Magnus, P.; Mugrage, B. New trialkylsilyl enol ether chemistry. Regiospecific and stereospecific sequential electrophilic addition. *J. Am. Chem. Soc*. **1990**, *112*, 462.
24. Omura, K.; Sharma, A. K.; Swern, D. Dimethyl sulfoxide-trifluoroacetic anhydride. New reagent for oxidation of alcohols to carbonyls. *J. Org. Chem.* **1976**, *41*, 957.
25. The following procedures have not been optimized.

26. Lifchits, O.; Demoulin, N.; List, B. Direct asymmetric α-benzoyloxylation of cyclic ketones. *Angew. Chem. Int. Ed.* **2011**, *50*, 9680.
27. Lombardo, L. Methylenation of carbonyl compounds with Zn-CH_2Br_2-$TiCl_4$. Application to gibberellins. *Tetrahedron Lett.* **1982**, *23*, 4293.
28. Yamamoto, K.; Hentemann, M. F.; Allen J. F.; Danishefsky, S. J. *Chem. Eur. J.* **2003**, *9*, 3242.
29. Obradors, C.; Martinez, R. M.; Shenvi, R. A. Ph(*i*-PrO)SiH_2: an exceptional reductant for metal-catalyzed hydrogen atom transfers. *J. Am. Chem. Soc.* **2016**, *138*, 4962.
30. Enantiopurity was assessed by HPLC (Chiralcel OD-H (w/o guard); 1.0 mL/min; 0.3% v/v *i*-PrOH in hexanes; 254nm): tR = 18.384, 26.676 min.
31. (a) For ^{13}C NMR resonance values of commercial (+)-quassin see reported spectrum on S56 of the supporting information: Shing, T. K. M.; Jiang, Q. Total synthesis of (+)-quassin. *J. Org. Chem*. **2000**, 65, 7059. (b) Shing, T. K. M.; Jian, Q.; Mak, T. C. W. Total synthesis of (+)-quassin from (+)-carvone. *J. Org. Chem.* **1998**, *63*, 2056.

Appendix A: NMR Spectra for Chapter 3

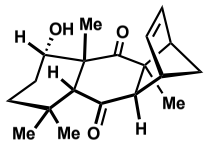

3.18 (1H NMR, 500 MHz, $CDCl_3$)

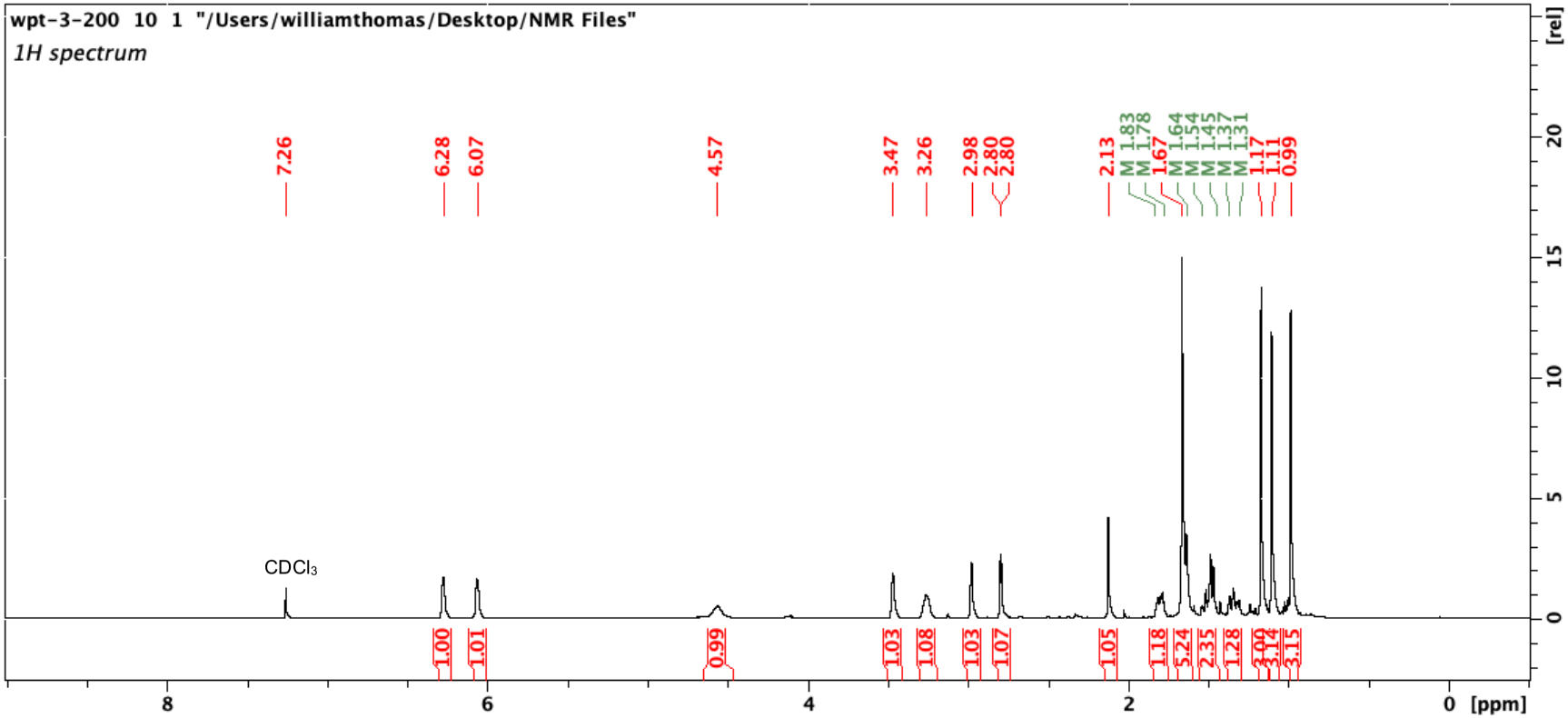

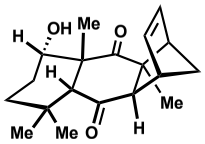

3.18 (^{13}C NMR, 126 MHz, $CDCl_3$)

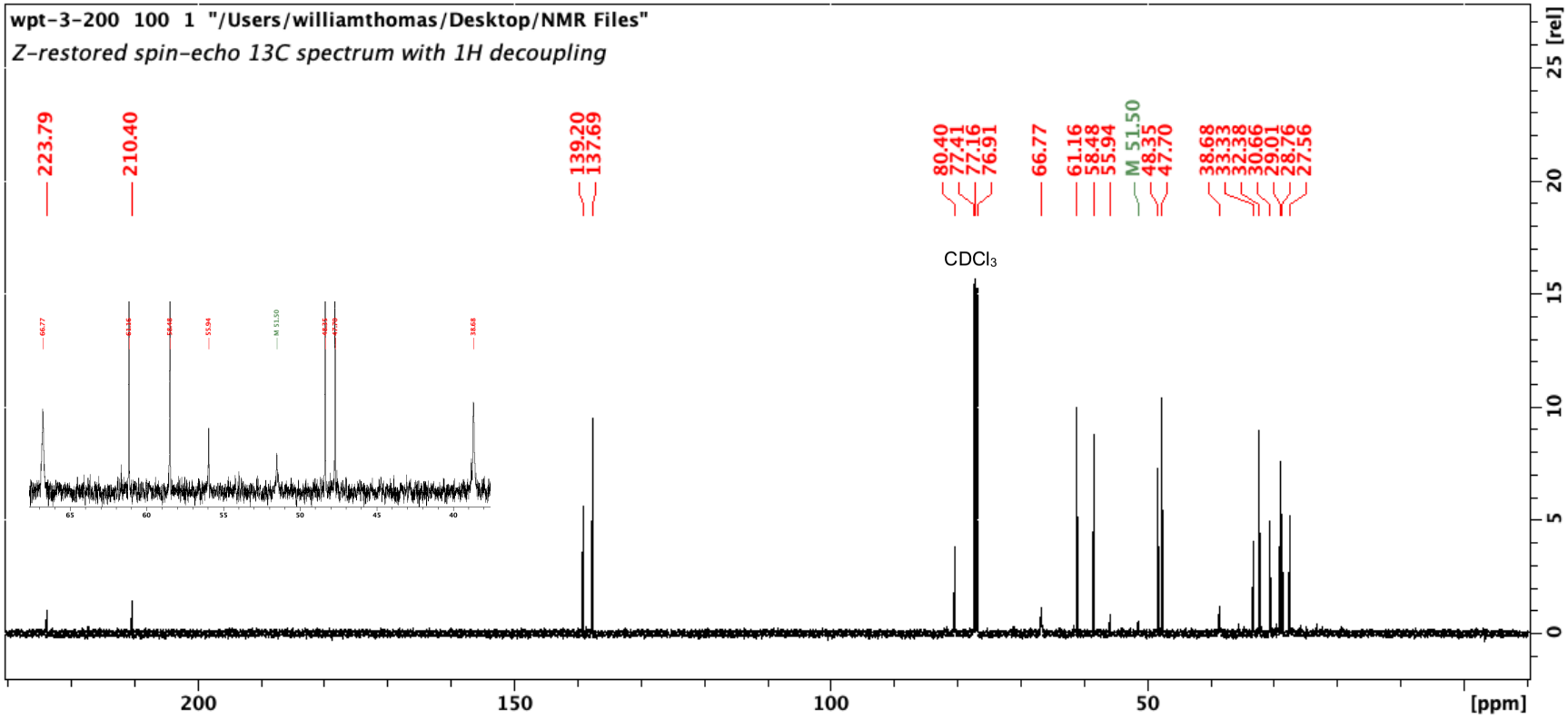

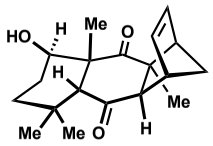

3.19 (^{1}H NMR, 500 MHz, $CDCl_3$)

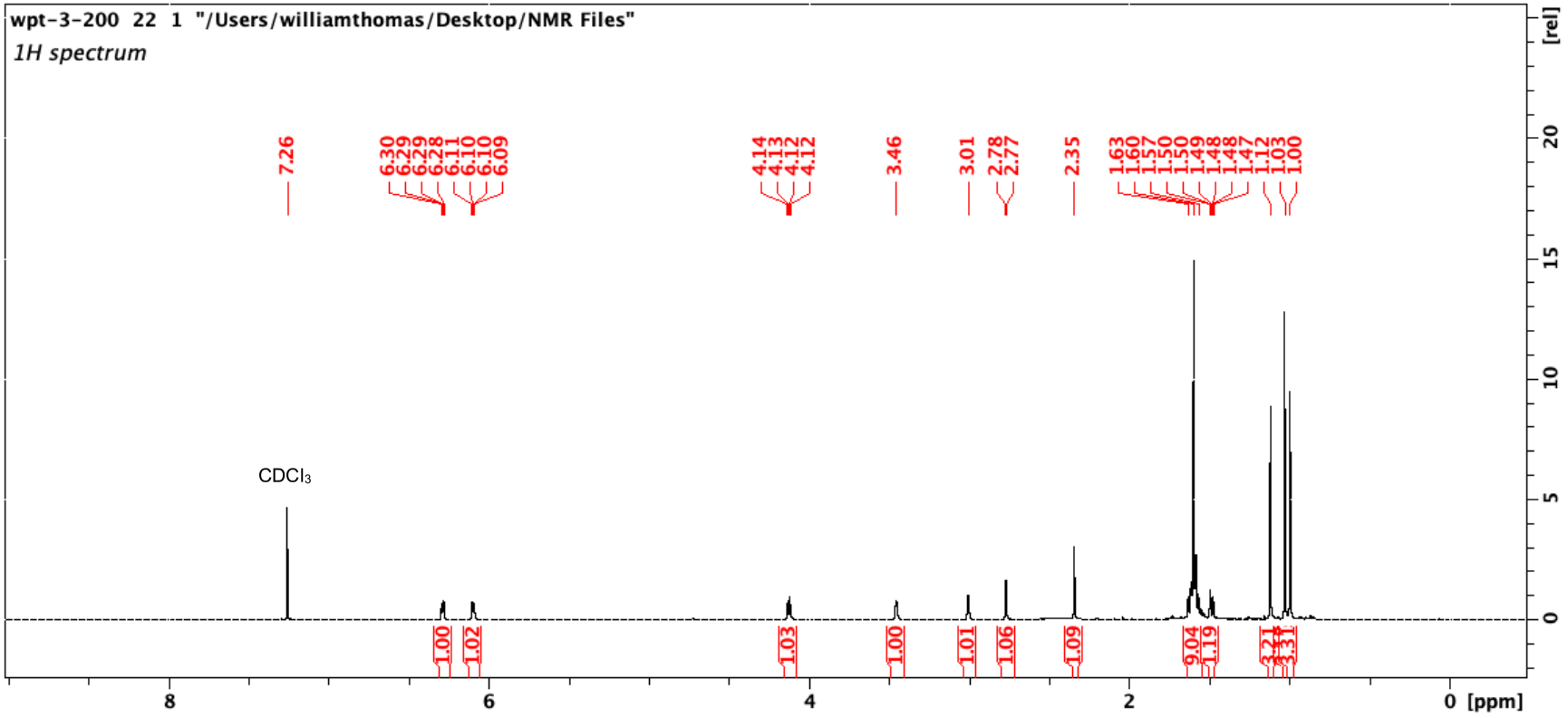

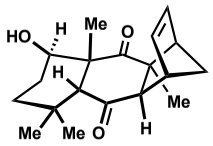

3.19 (^{13}C NMR, 126 MHz, $CDCl_3$)

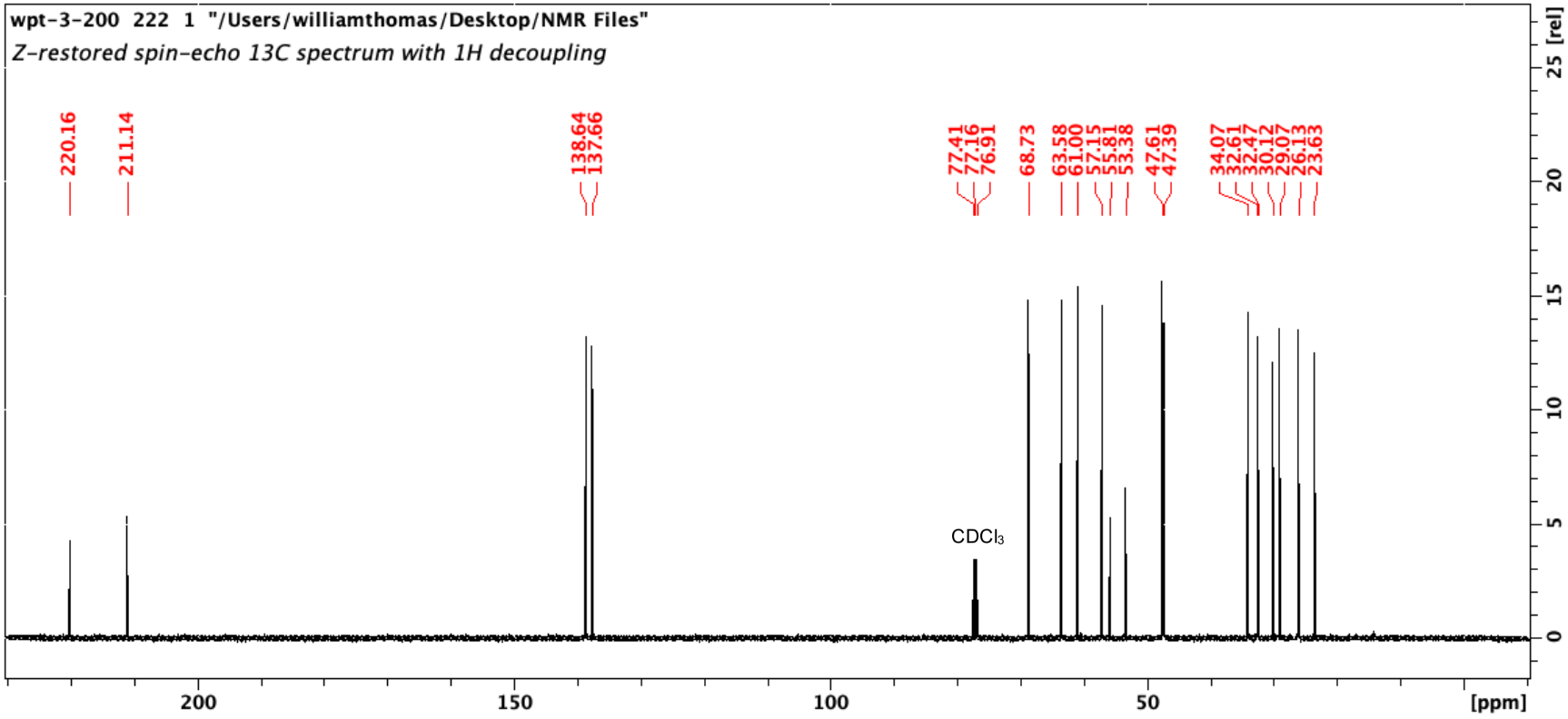

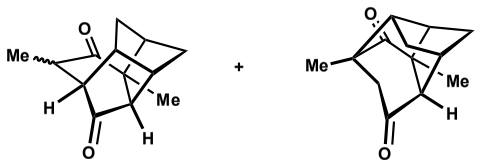

wpt-8-47 2 1 "/opt/NMR Files"

1H spectrum

1:1 mixture of **3.20** and **3.21**
(^{1}H NMR, 500 MHz, $CDCl_3$)

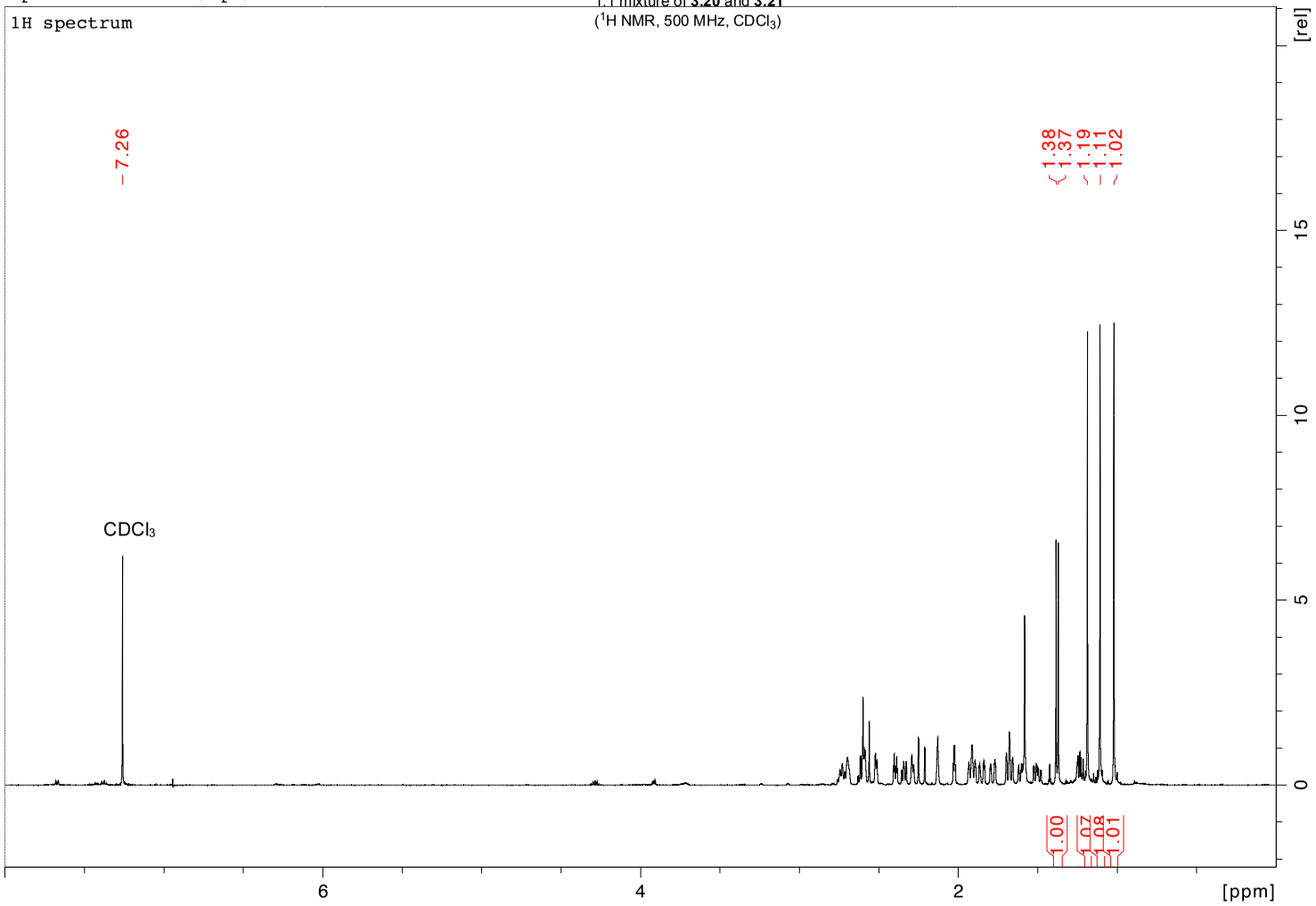

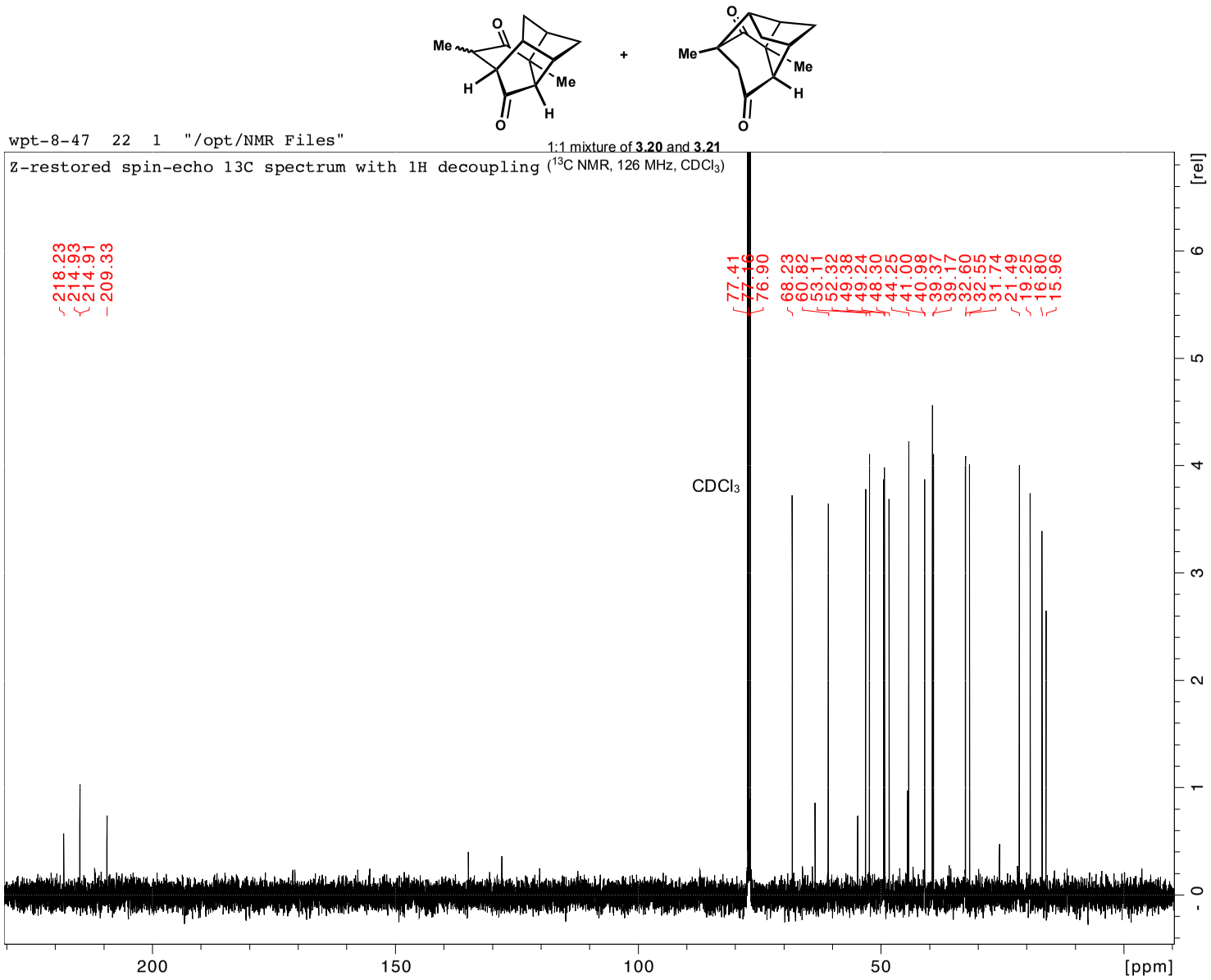
Me
O
H
Me
H
O
+
Me
O
Me
H
O
wpt-8-47 22 1 "/opt/NMR Files"
1:1 mixture of 3.20 and 3.21
Z-restored spin-echo 13C spectrum with 1H decoupling (13C NMR, 126 MHz, CDCl3)
218.23
214.93
214.91
209.33
77.41
77.16
76.90
68.23
60.82
53.11
52.32
49.38
49.24
48.30
44.25
41.00
40.98
39.37
39.17
32.60
32.55
31.74
21.49
19.25
16.80
15.96
CDCl3
[rel]
6
5
4
3
2
1
0
200
150
100
50
[ppm]

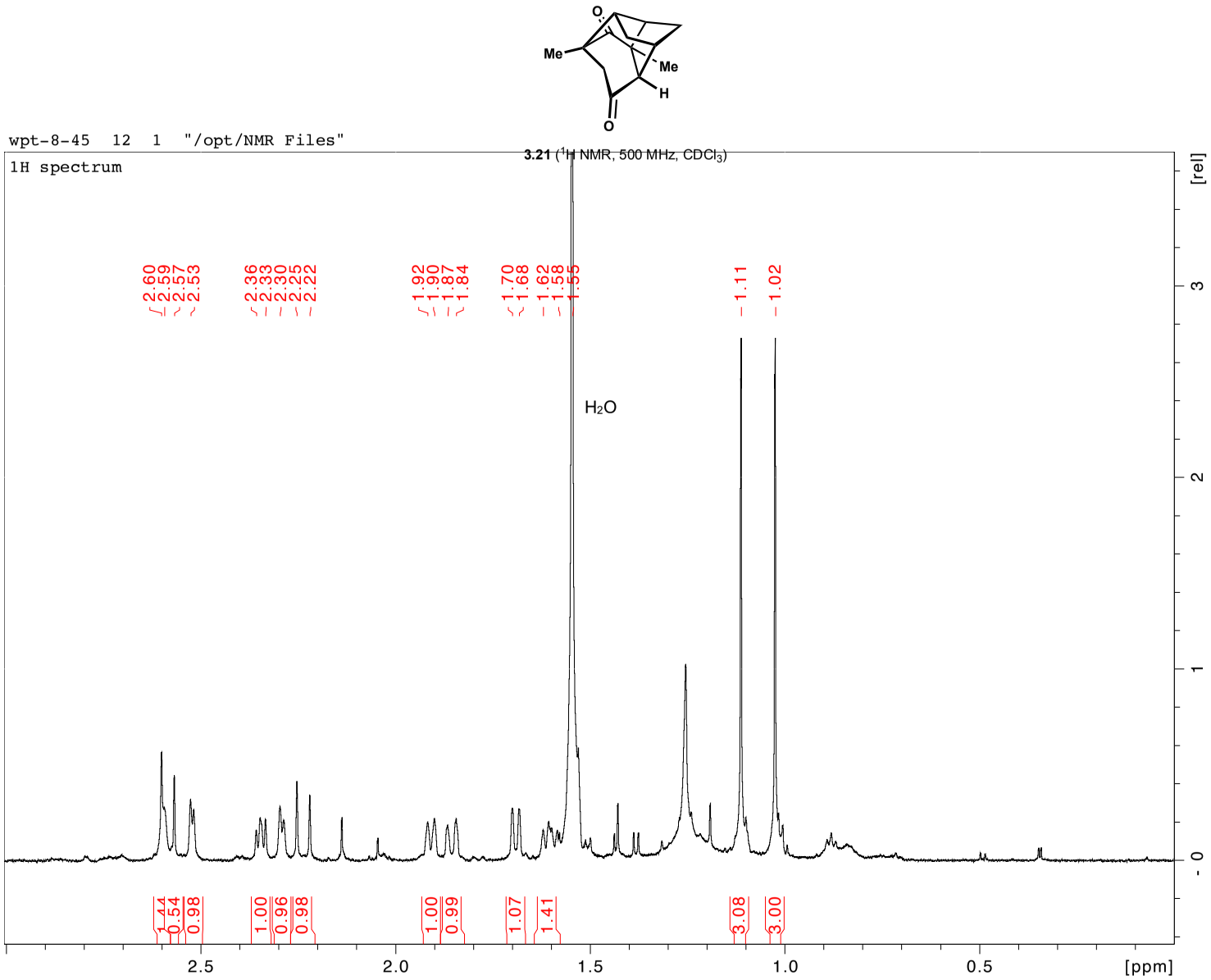
Me
Me
H
O
O
wpt-8-45 12 1 "/opt/NMR Files"
1H spectrum
3.21 (1H NMR, 500 MHz, CDCl3)
2.60
2.59
2.57
2.53
2.36
2.33
2.30
2.25
2.22
1.92
1.90
1.87
1.84
1.70
1.68
1.62
1.58
1.55
1.11
1.02
H2O
1.44
0.54
0.98
1.00
0.96
0.98
1.00
0.99
1.07
1.41
3.08
3.00
2.5
2.0
1.5
1.0
0.5
[ppm]
[rel]
3
2
1
0

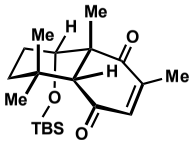

3.23 (^{1}H NMR, 500 MHz, $CDCl_3$)

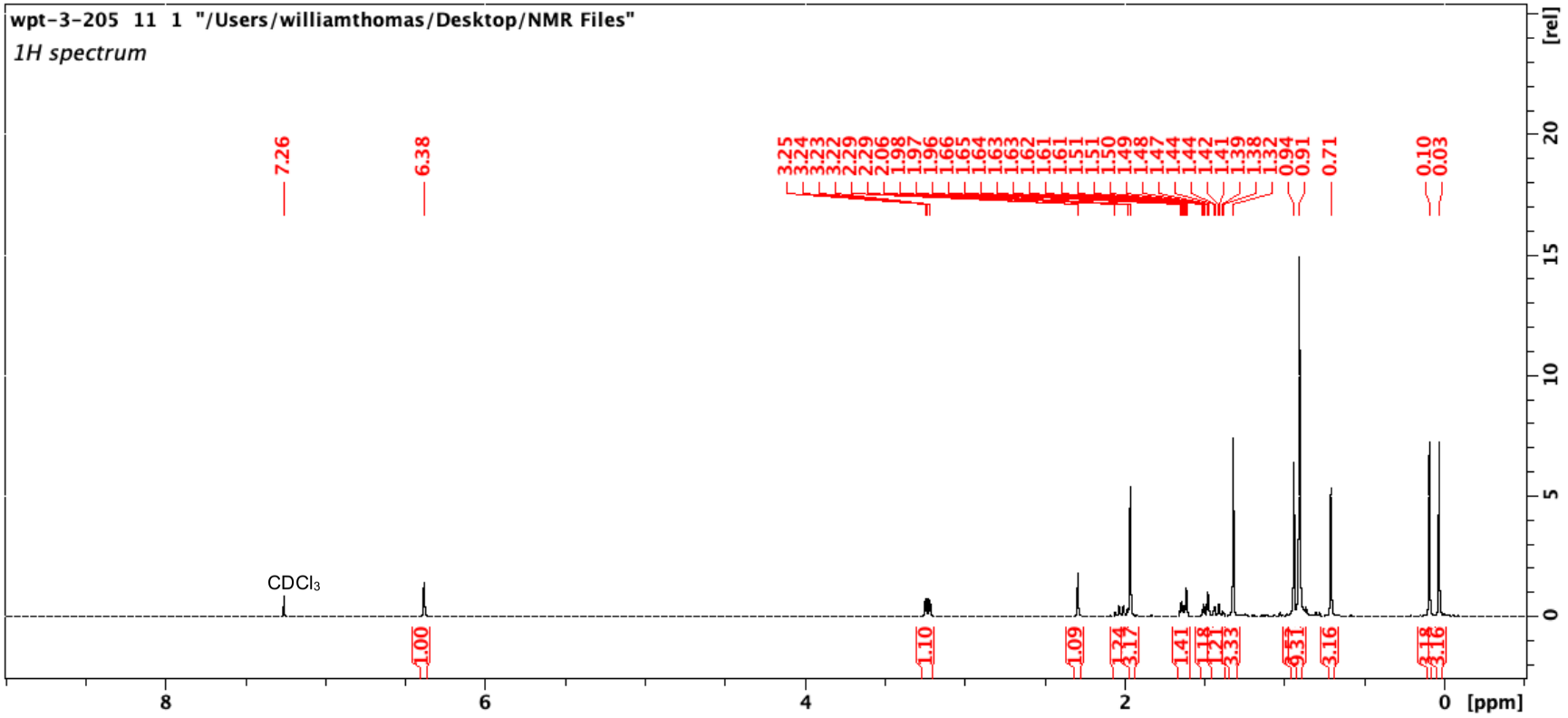

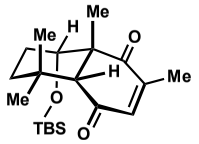

3.23 (^{13}C NMR, 126 MHz, $CDCl_3$)

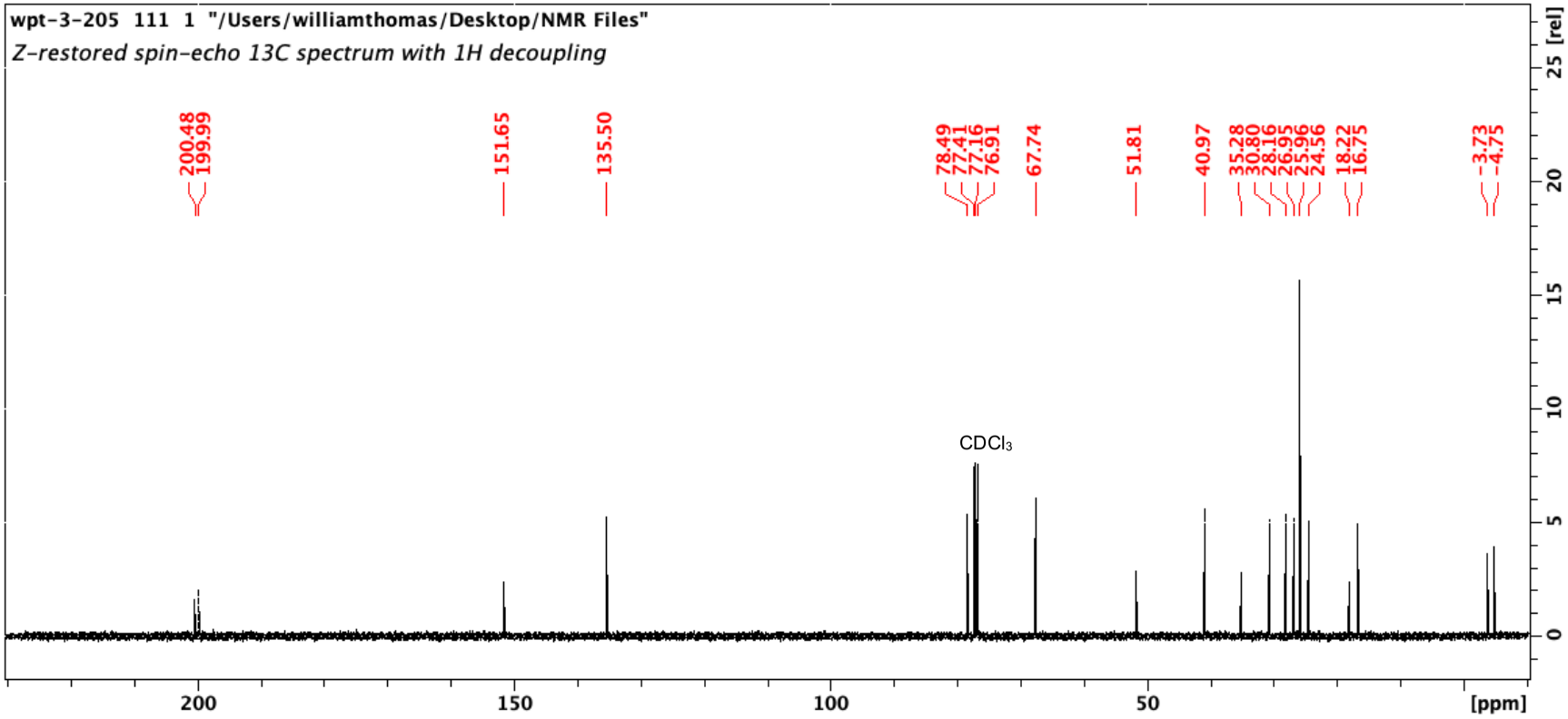

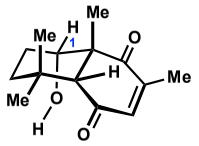

wpt-1-236 2 1 "/opt/NMR Files"

3.30 (^{1}H NMR, 500 MHz, $CDCl_3$)

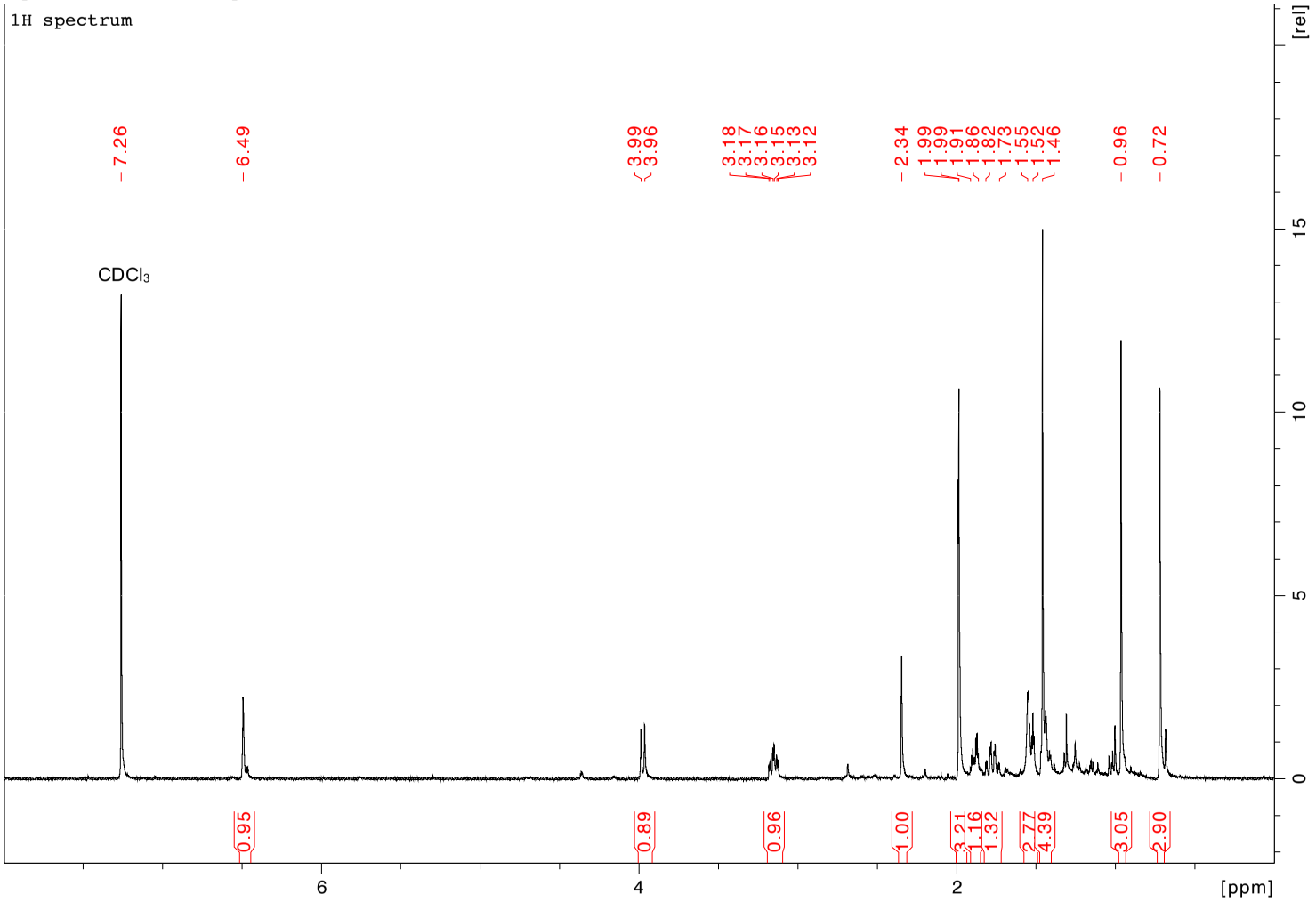

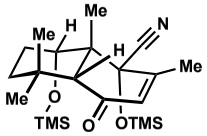

wpt-1-283 22 1 "/opt/NMR Files"

3.31 (^{1}H NMR, 500 MHz, $CDCl_3$)

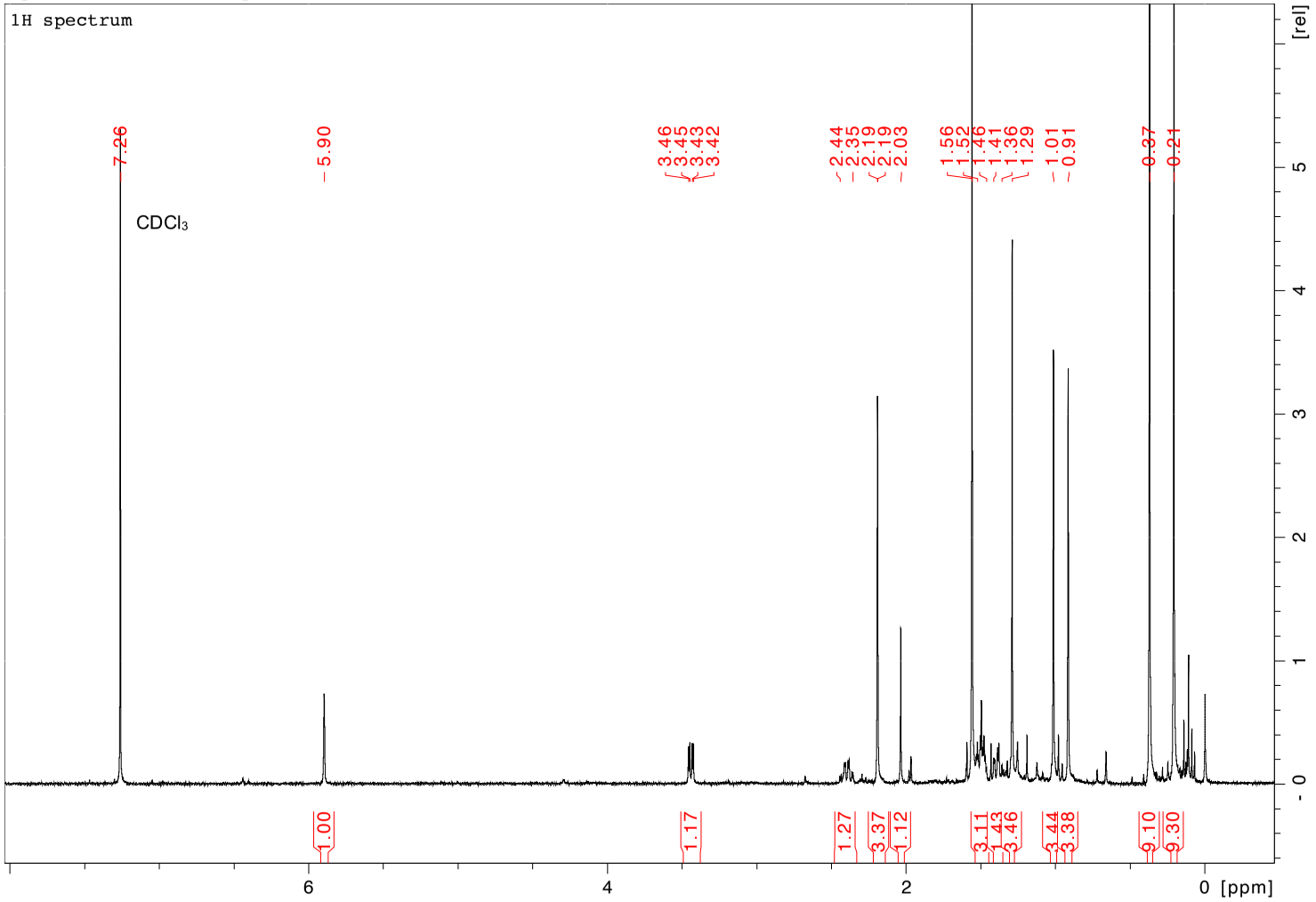

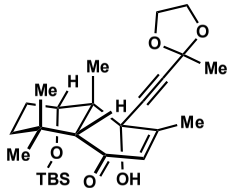

3.34 (^{1}H NMR, 500 MHz, $CDCl_3$)

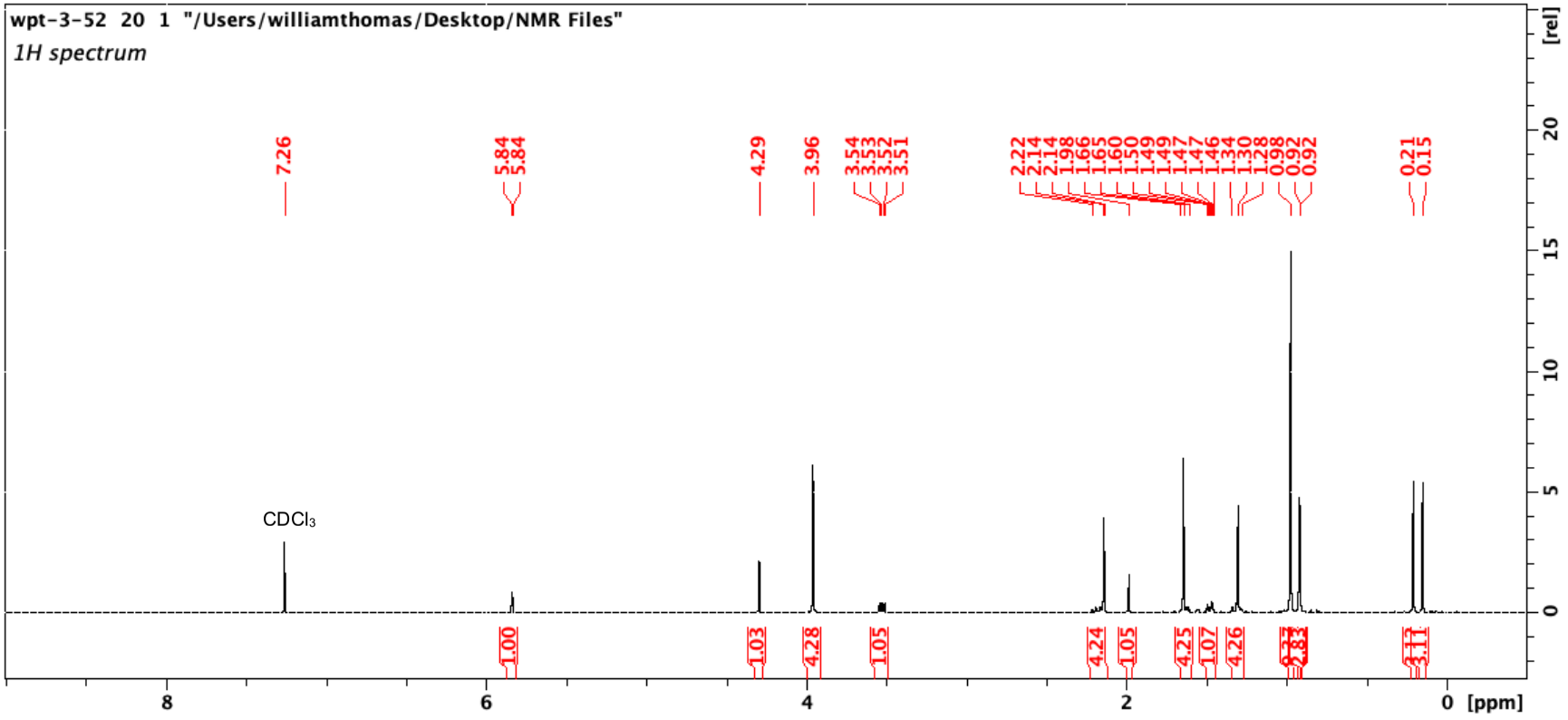

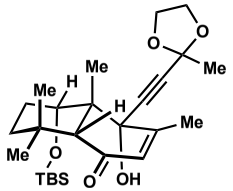

3.34 (^{13}C NMR, 126 MHz, $CDCl_3$)

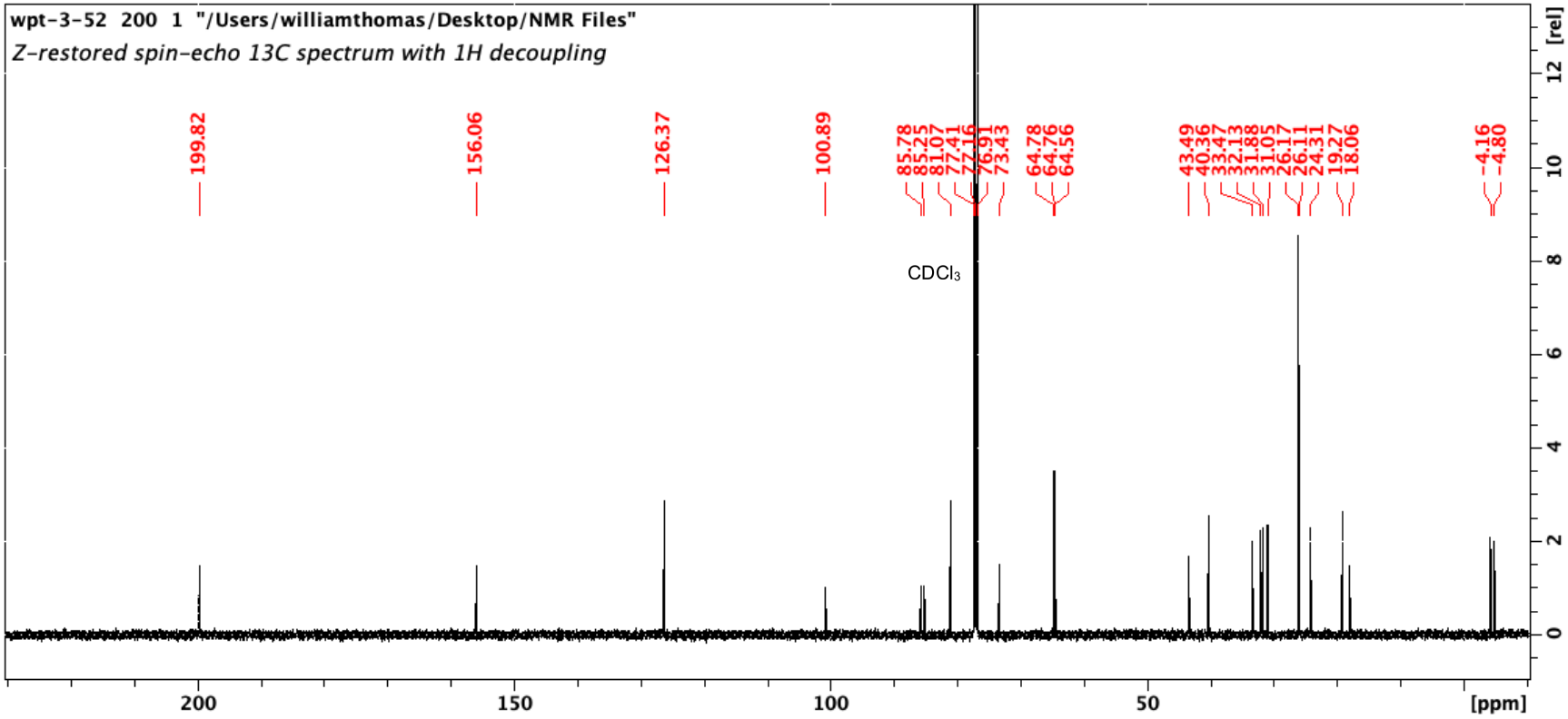

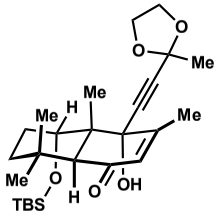

3.35 (^{1}H NMR, 500 MHz, $CDCl_3$)

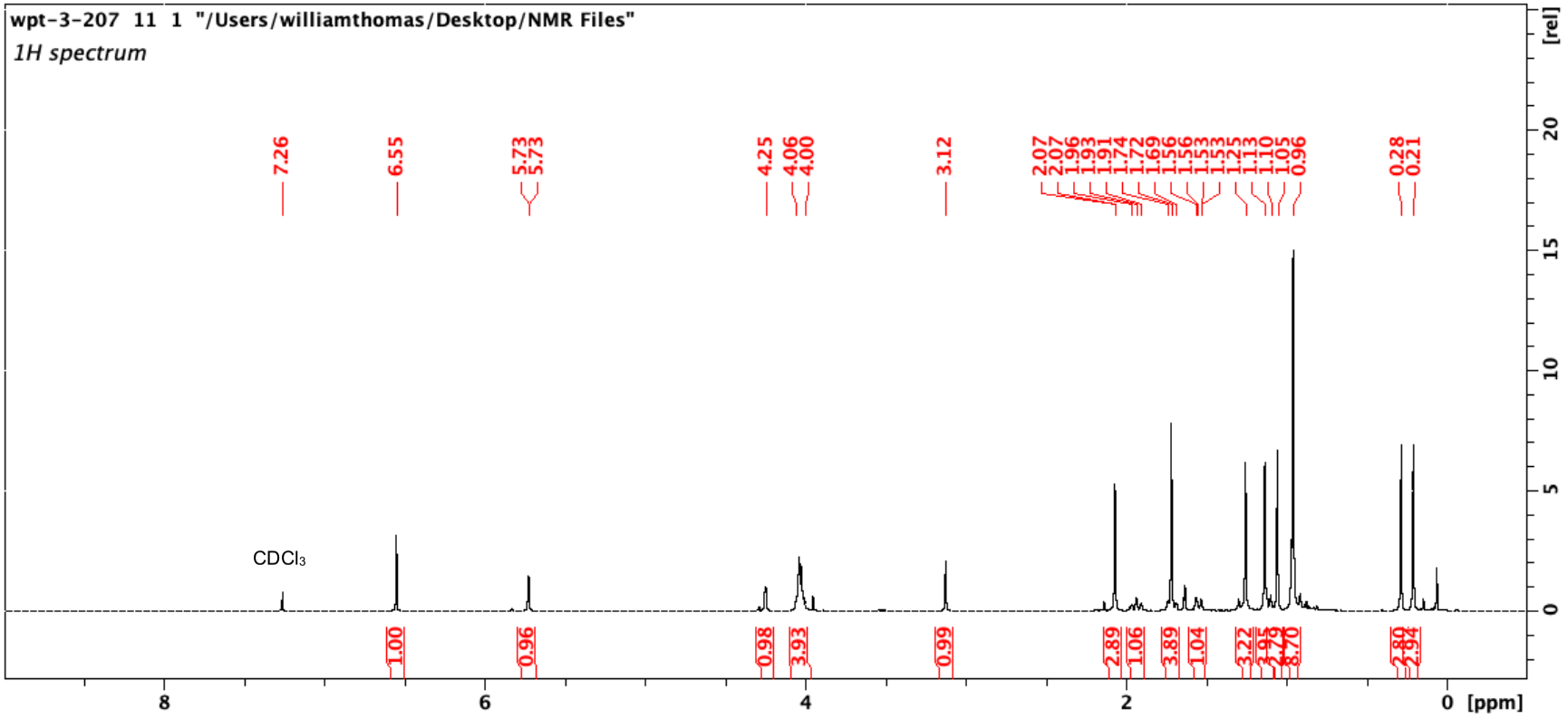

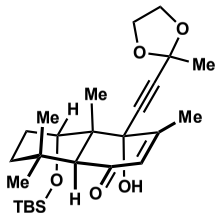

3.35 (^{13}C NMR, 126 MHz, $CDCl_3$)

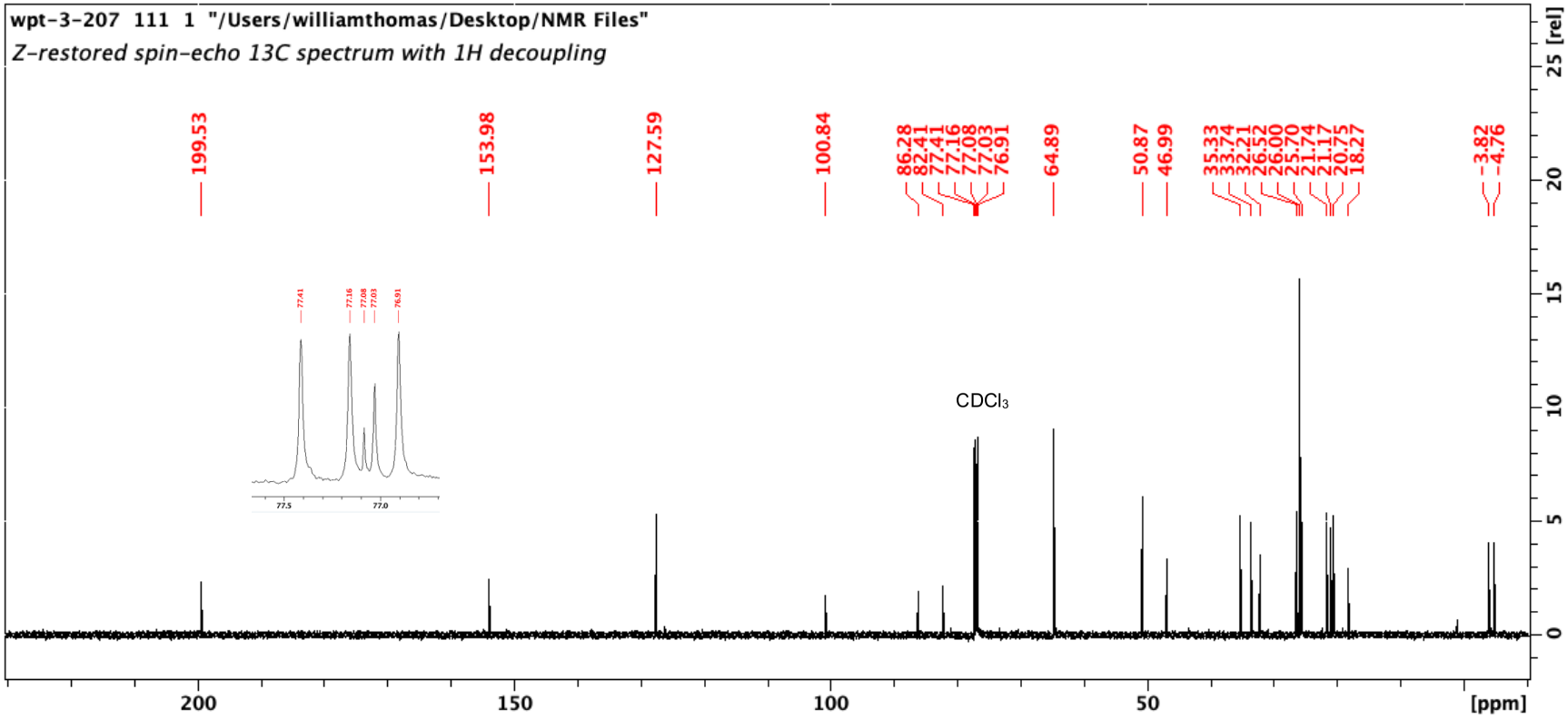

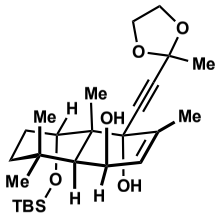

3.36 (^{1}H NMR, 500 MHz, $CDCl_3$)

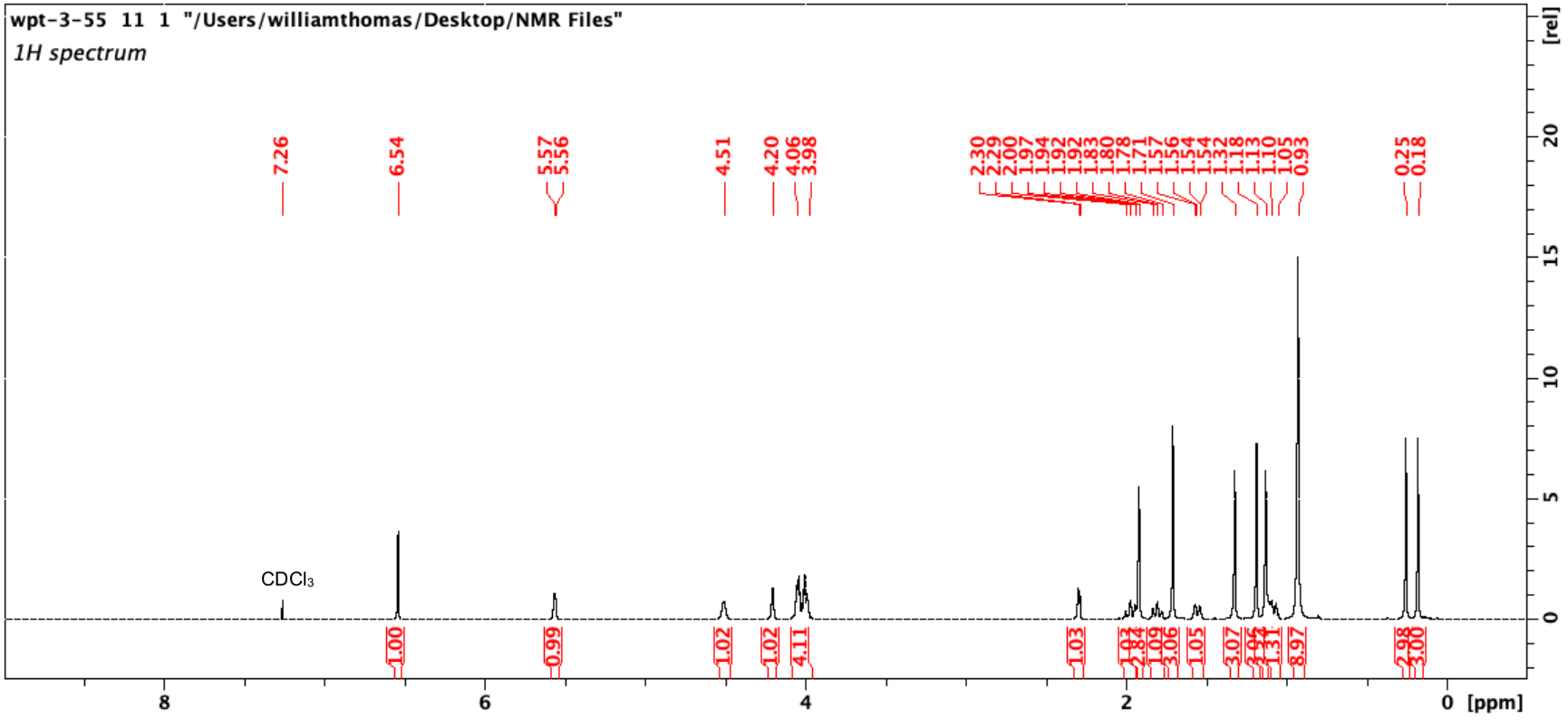

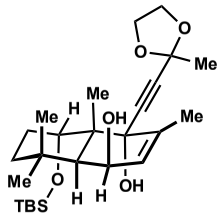

3.36 (^{13}C NMR, 126 MHz, $CDCl_3$)

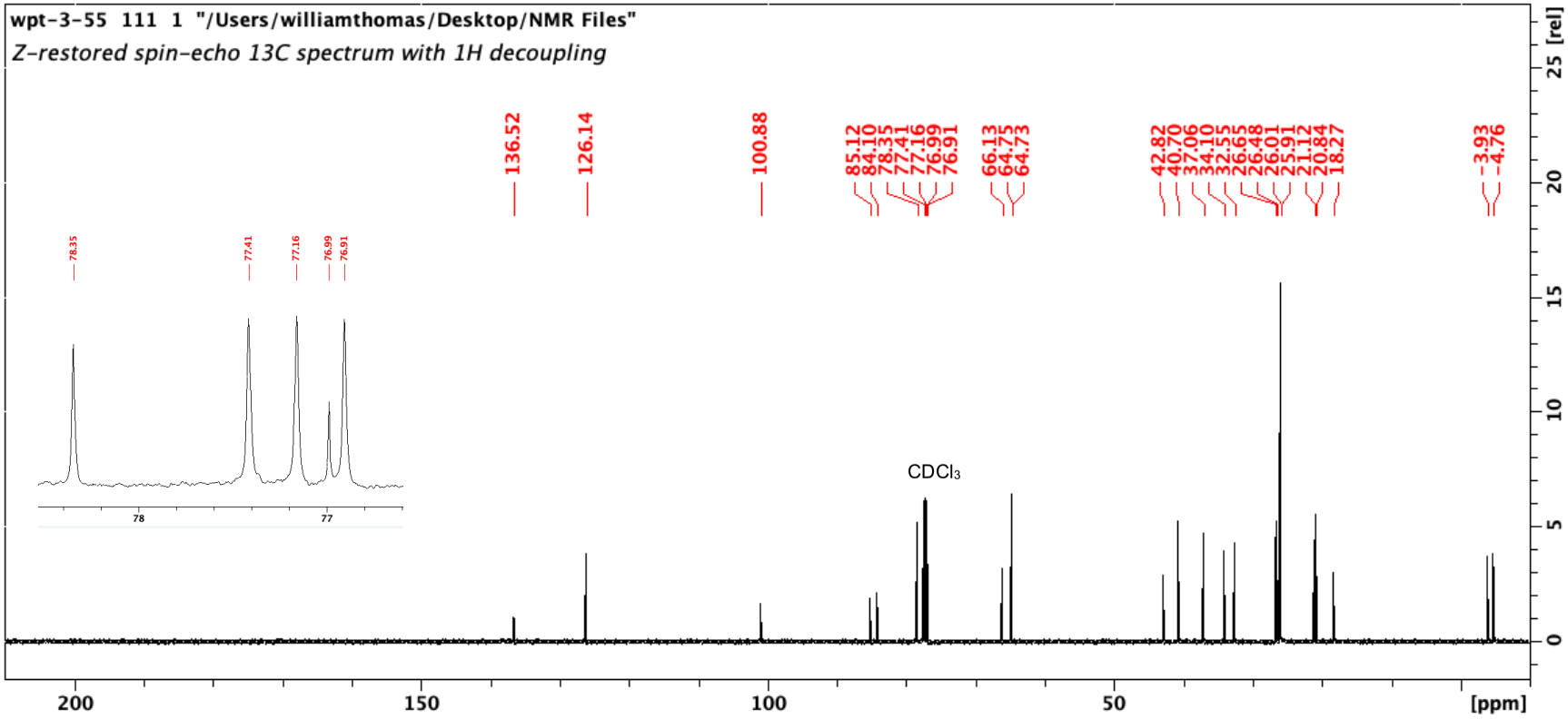

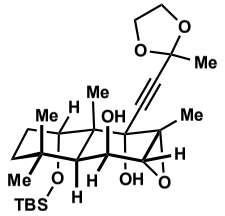

3.37 (^{1}H NMR, 500 MHz, $CDCl_3$)

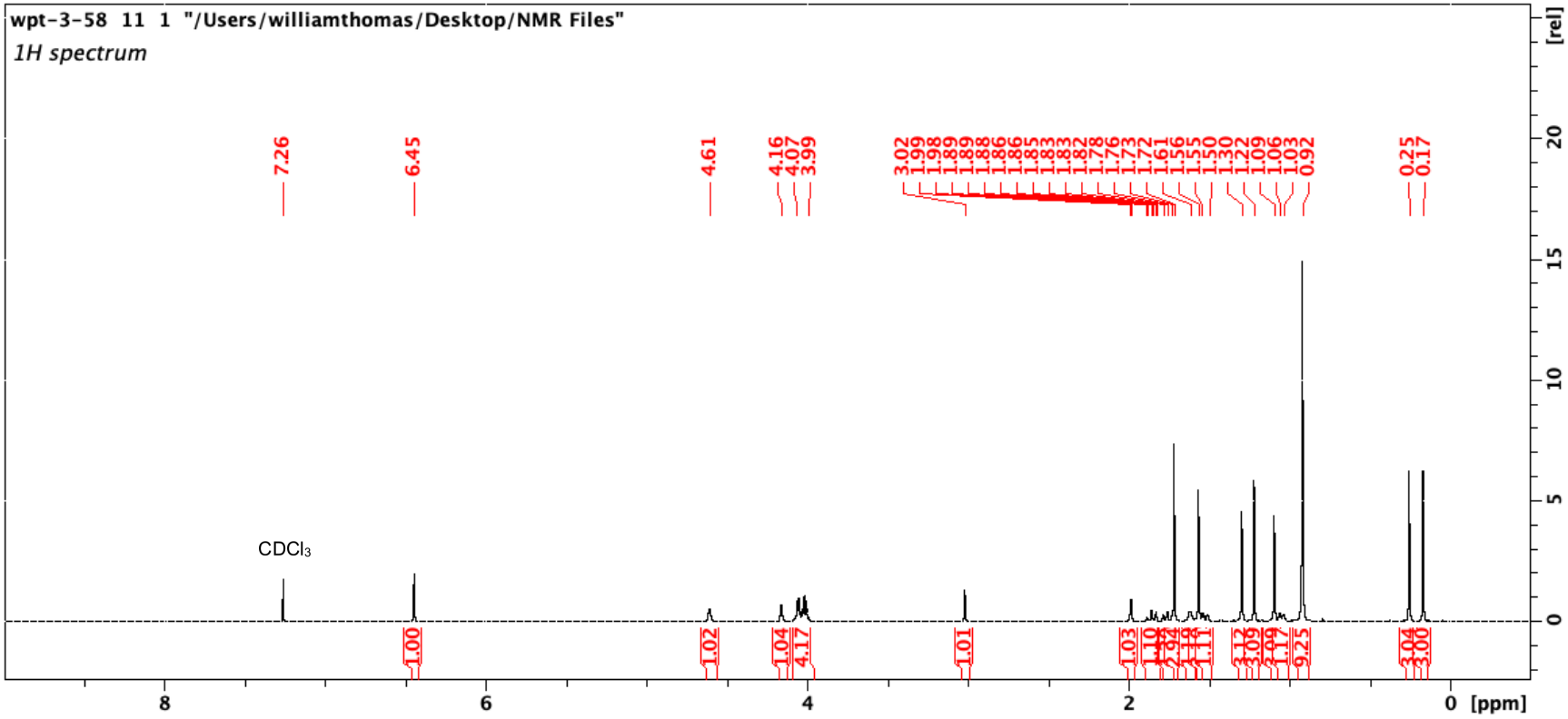

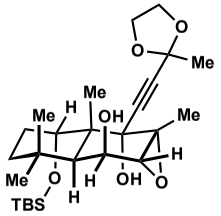

3.37 (^{13}C NMR, 126 MHz, $CDCl_3$)

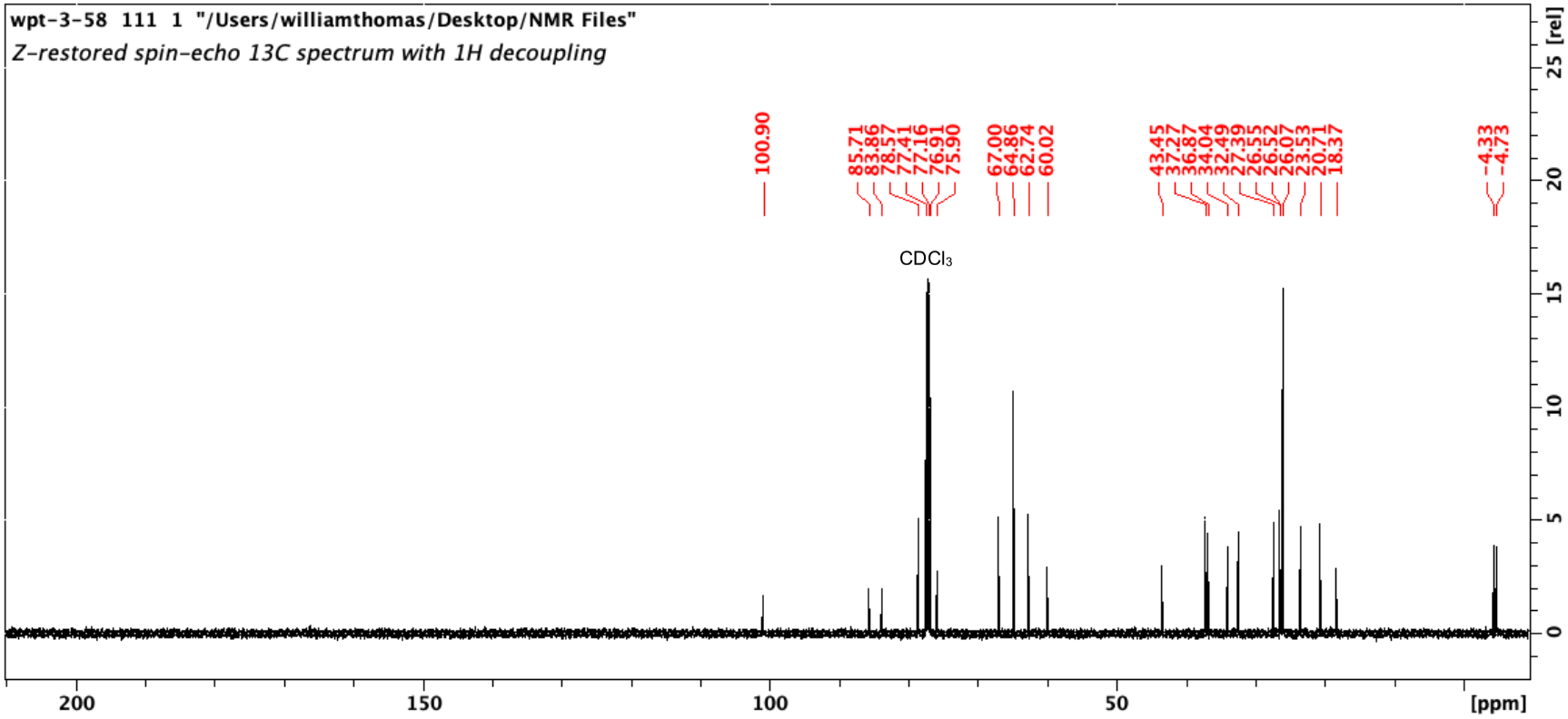

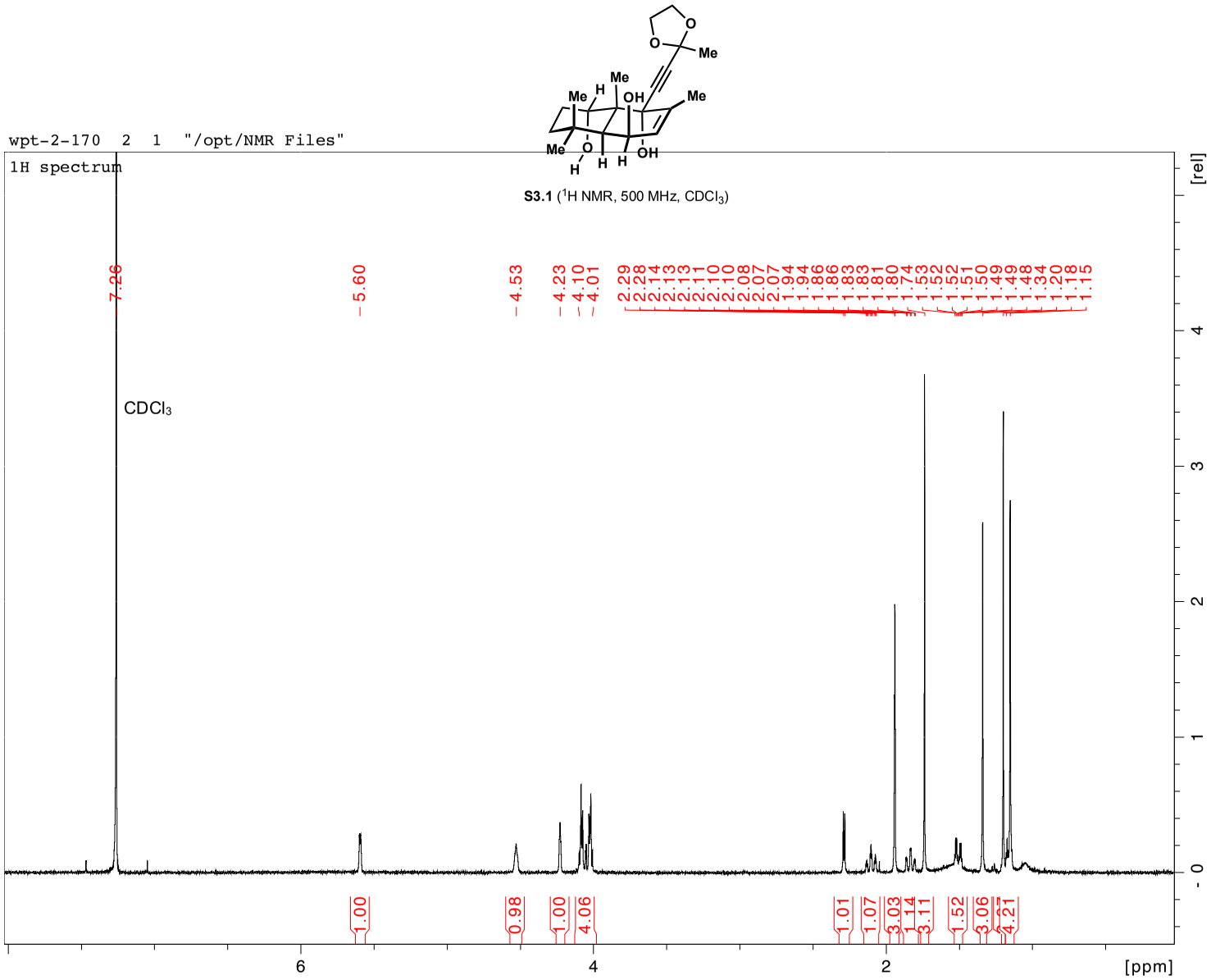

S3.1 (^{1}H NMR, 500 MHz, $CDCl_3$)

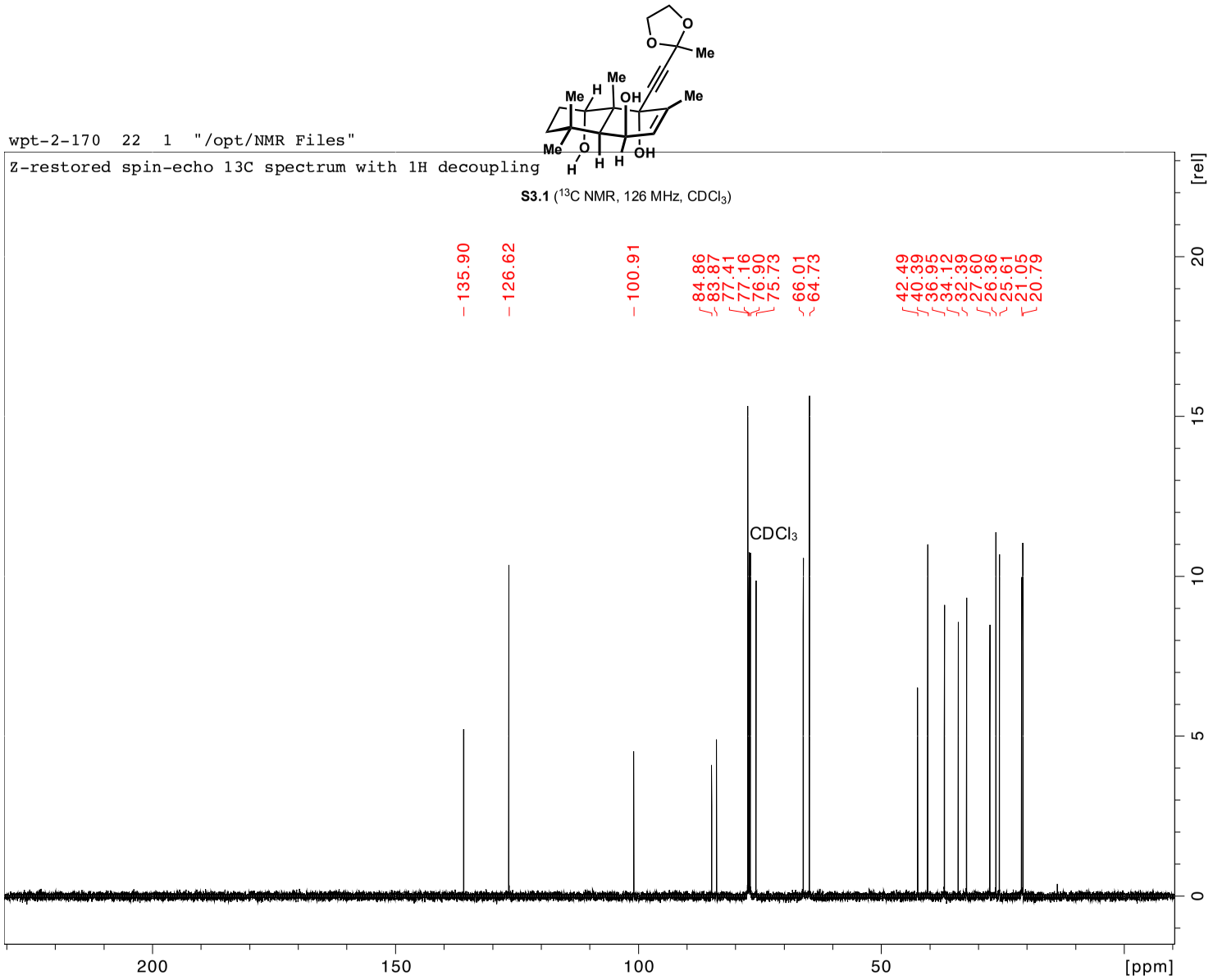
wpt-2-170 22 1 "/opt/NMR Files"
Z-restored spin-echo 13C spectrum with 1H decoupling
S3.1 (13C NMR, 126 MHz, CDCl3)
135.90
126.62
100.91
84.86
83.87
77.41
77.16
76.90
75.73
66.01
64.73
42.49
40.39
36.95
34.12
32.39
27.60
26.36
25.61
21.05
20.79
CDCl3
[rel]
[ppm]

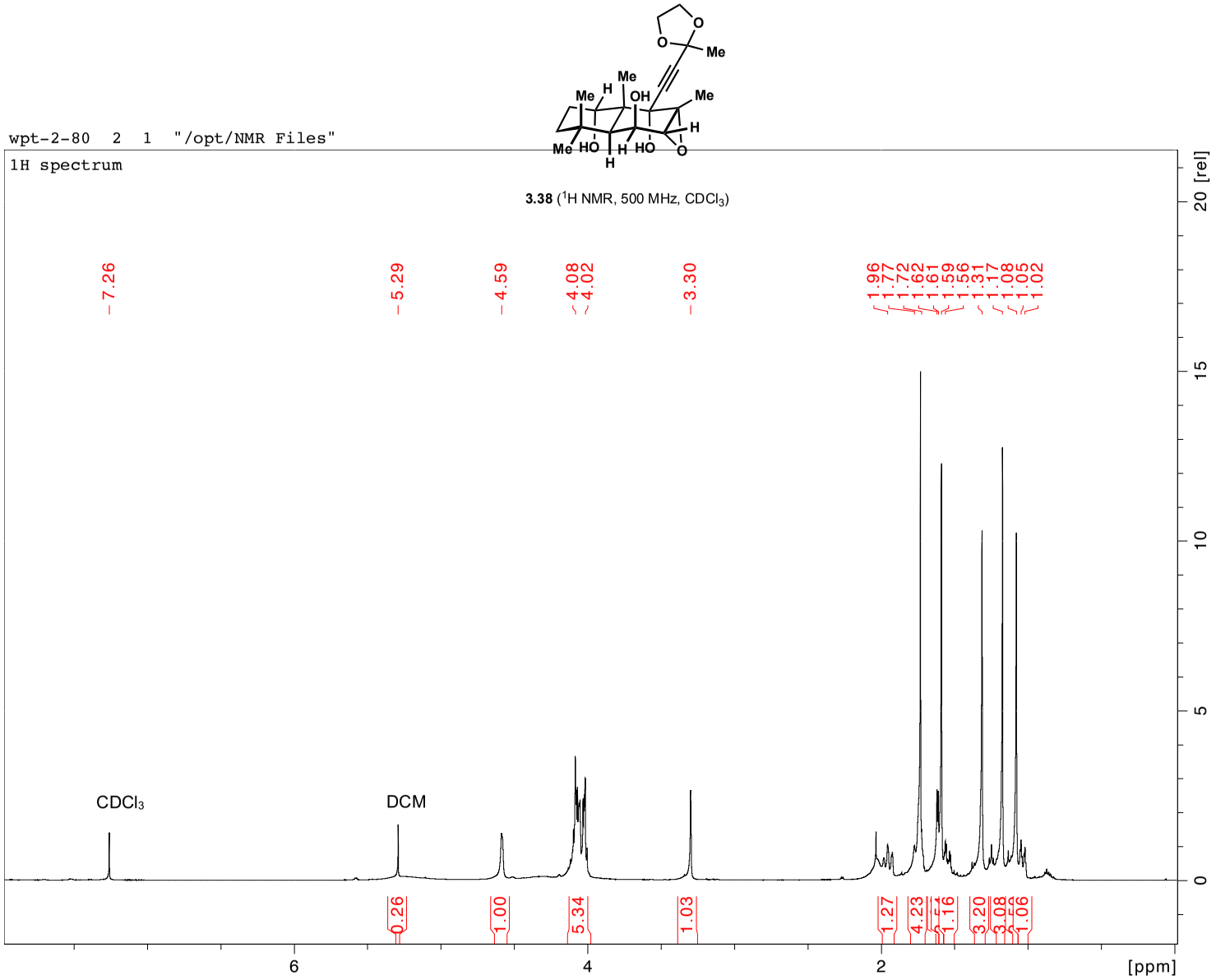
wpt-2-80 2 1 "/opt/NMR Files"
1H spectrum
3.38 (1H NMR, 500 MHz, CDCl3)
7.26
5.29
4.59
4.08
4.02
3.30
1.96
1.77
1.72
1.62
1.61
1.59
1.56
1.31
1.17
1.08
1.05
1.02
CDCl3
DCM
0.26
1.00
5.34
1.03
1.27
4.23
1.16
3.20
3.08
1.06
6
4
2
[ppm]
20 [rel]
15
10
5
0

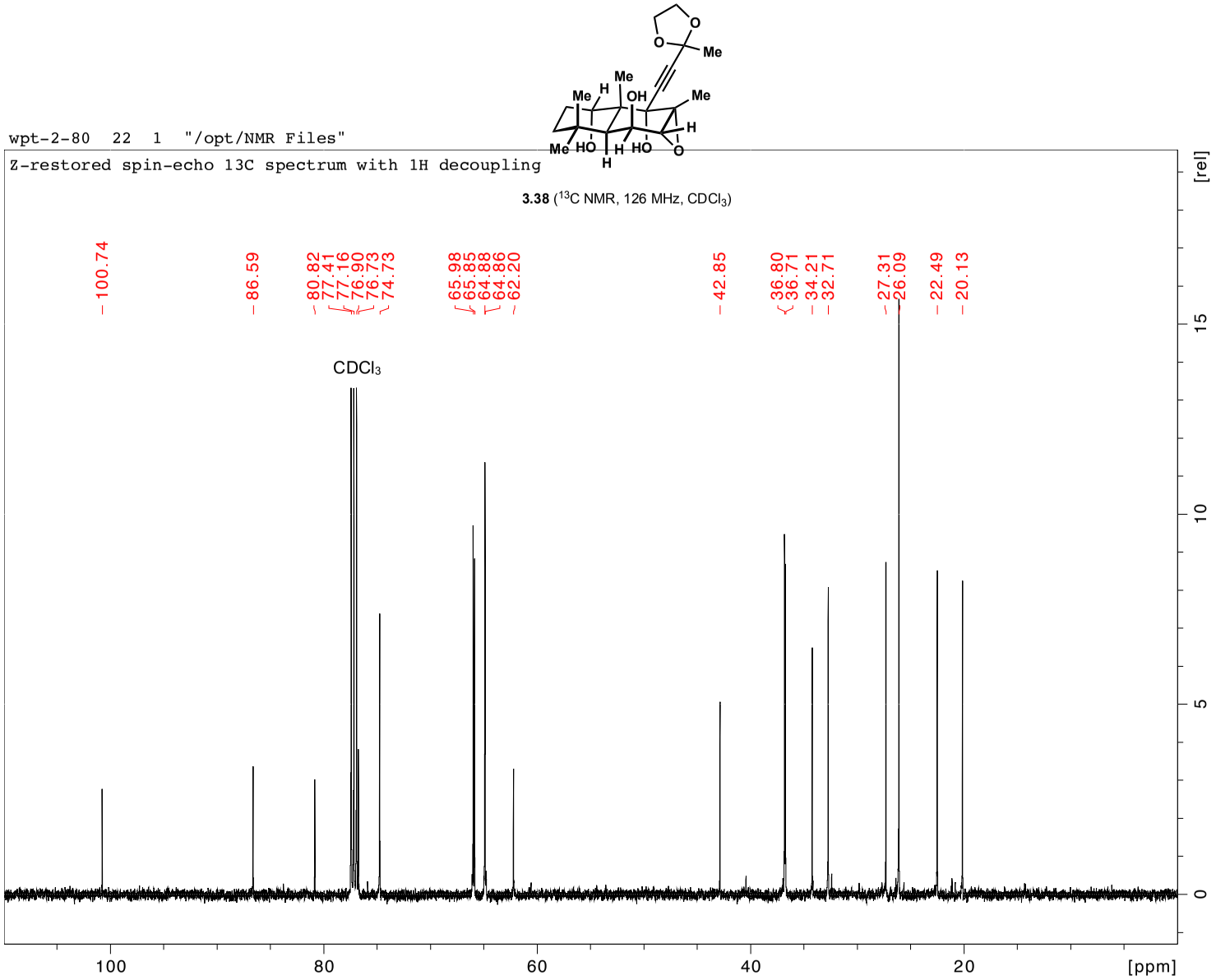
wpt-2-80 22 1 "/opt/NMR Files"
Z-restored spin-echo 13C spectrum with 1H decoupling
3.38 (13C NMR, 126 MHz, CDCl3)
100.74
86.59
80.82
77.41
77.16
76.90
76.73
74.73
65.98
65.85
64.88
64.86
62.20
42.85
36.80
36.71
34.21
32.71
27.31
26.09
22.49
20.13
CDCl3
[rel]
0
5
10
15
100
80
60
40
20
[ppm]

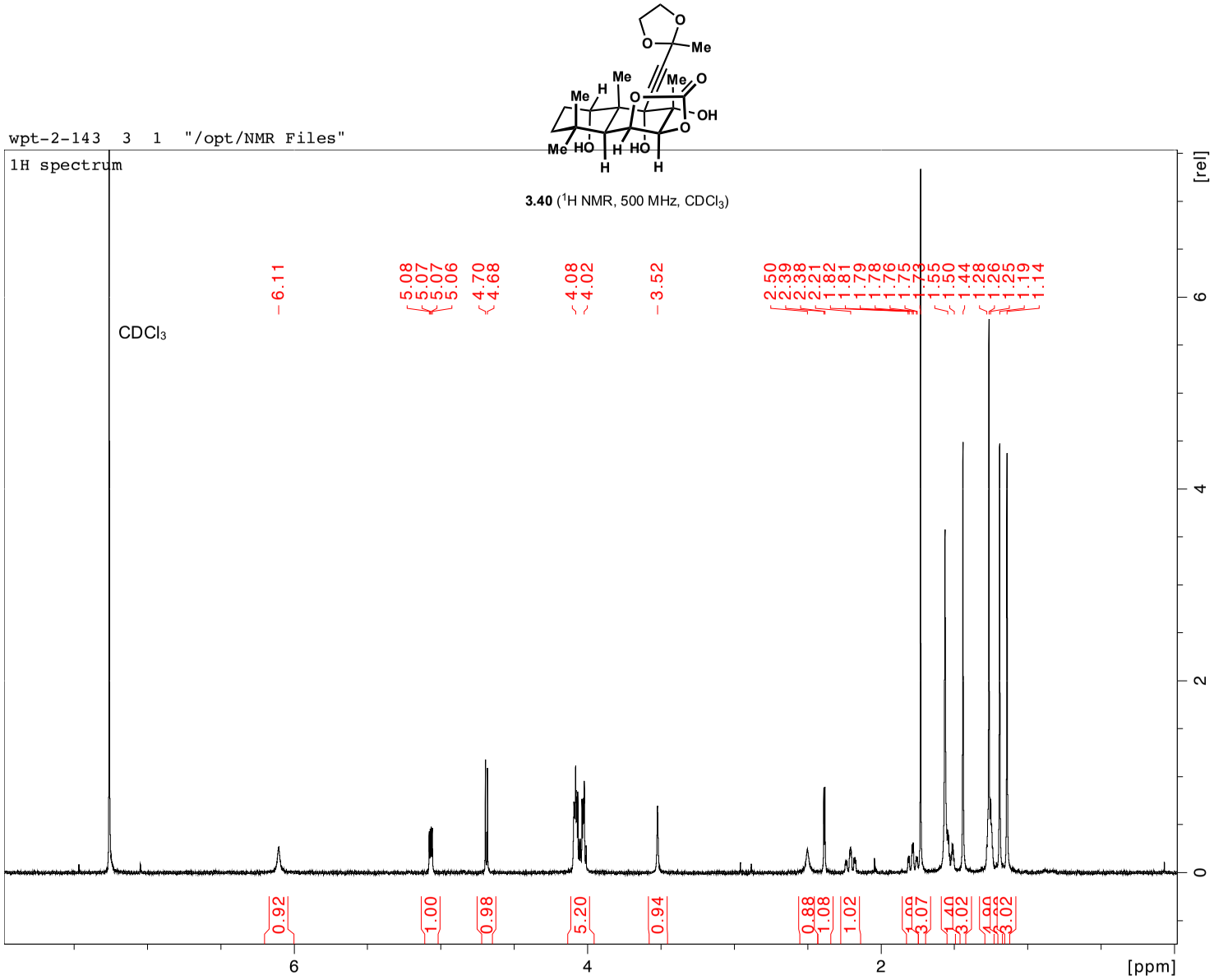
wpt-2-143 3 1 "/opt/NMR Files"
1H spectrum
CDCl3
3.40 (1H NMR, 500 MHz, CDCl3)
6.11
5.08
5.07
5.07
5.06
4.70
4.68
4.08
4.02
3.52
2.50
2.39
2.38
2.21
1.82
1.81
1.79
1.78
1.76
1.75
1.73
1.55
1.50
1.44
1.28
1.26
1.25
1.19
1.14
0.92
1.00
0.98
5.20
0.94
0.88
1.08
1.02
3.07
1.40
3.02
3.02
[rel]
[ppm]

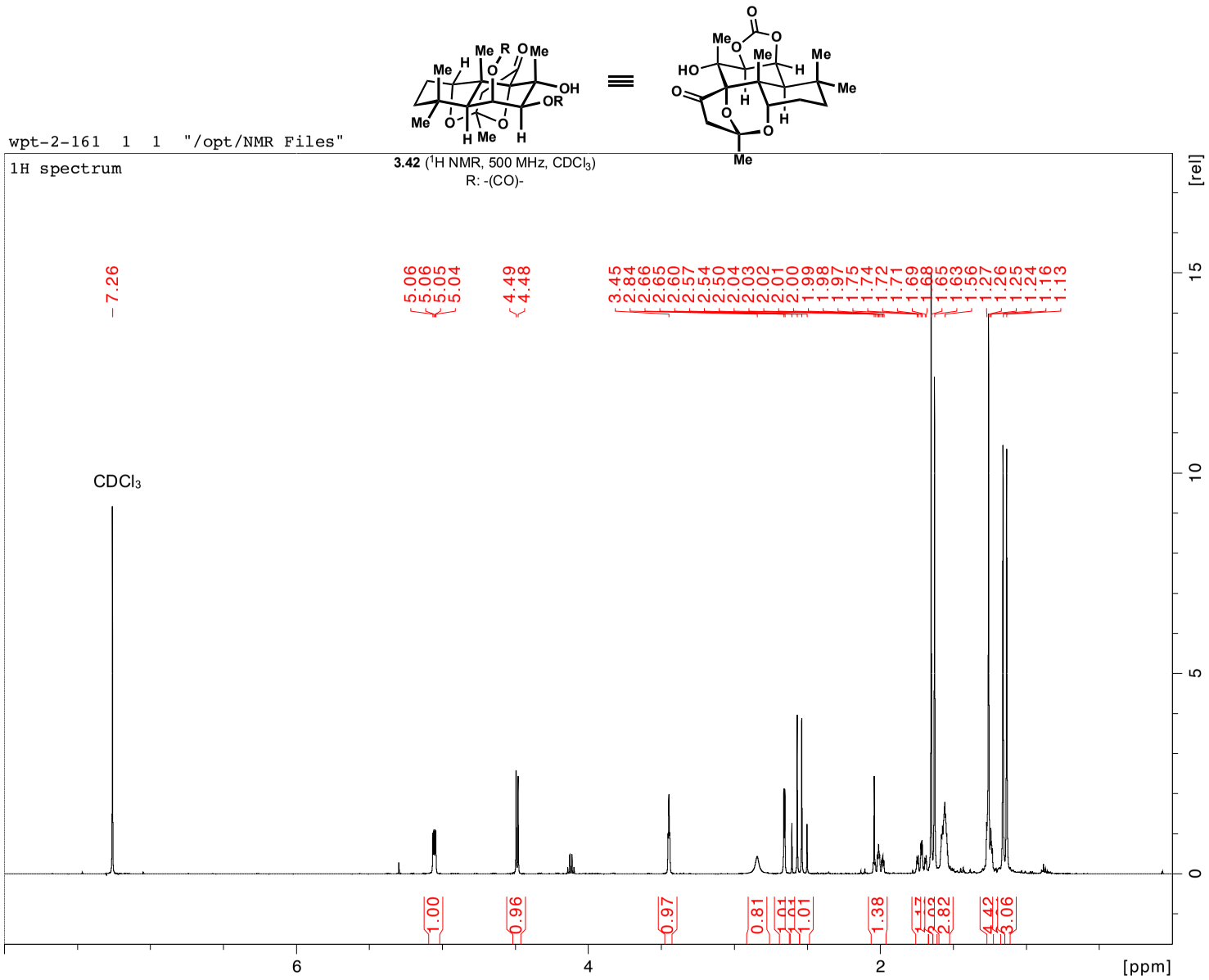
wpt-2-161 1 1 "/opt/NMR Files"
1H spectrum
3.42 (1H NMR, 500 MHz, CDCl3)
R: -(CO)-
CDCl3
7.26
5.06
5.05
5.04
4.49
4.48
3.45
2.84
2.66
2.65
2.60
2.57
2.54
2.50
2.04
2.03
2.02
2.01
2.00
1.99
1.98
1.97
1.75
1.74
1.72
1.71
1.69
1.68
1.65
1.63
1.56
1.27
1.26
1.25
1.24
1.16
1.13
1.00
0.96
0.97
0.81
1.01
1.01
1.38
2.82
4.42
3.06
[rel]
[ppm]

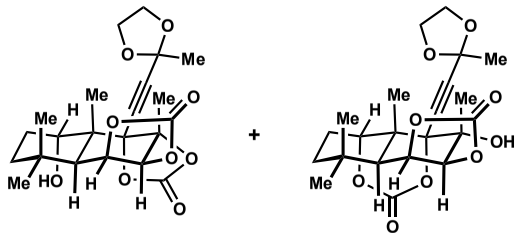

1:3 mixture of **3.43 and 3.44** (^{1}H NMR, 500 MHz, $CDCl_3$)

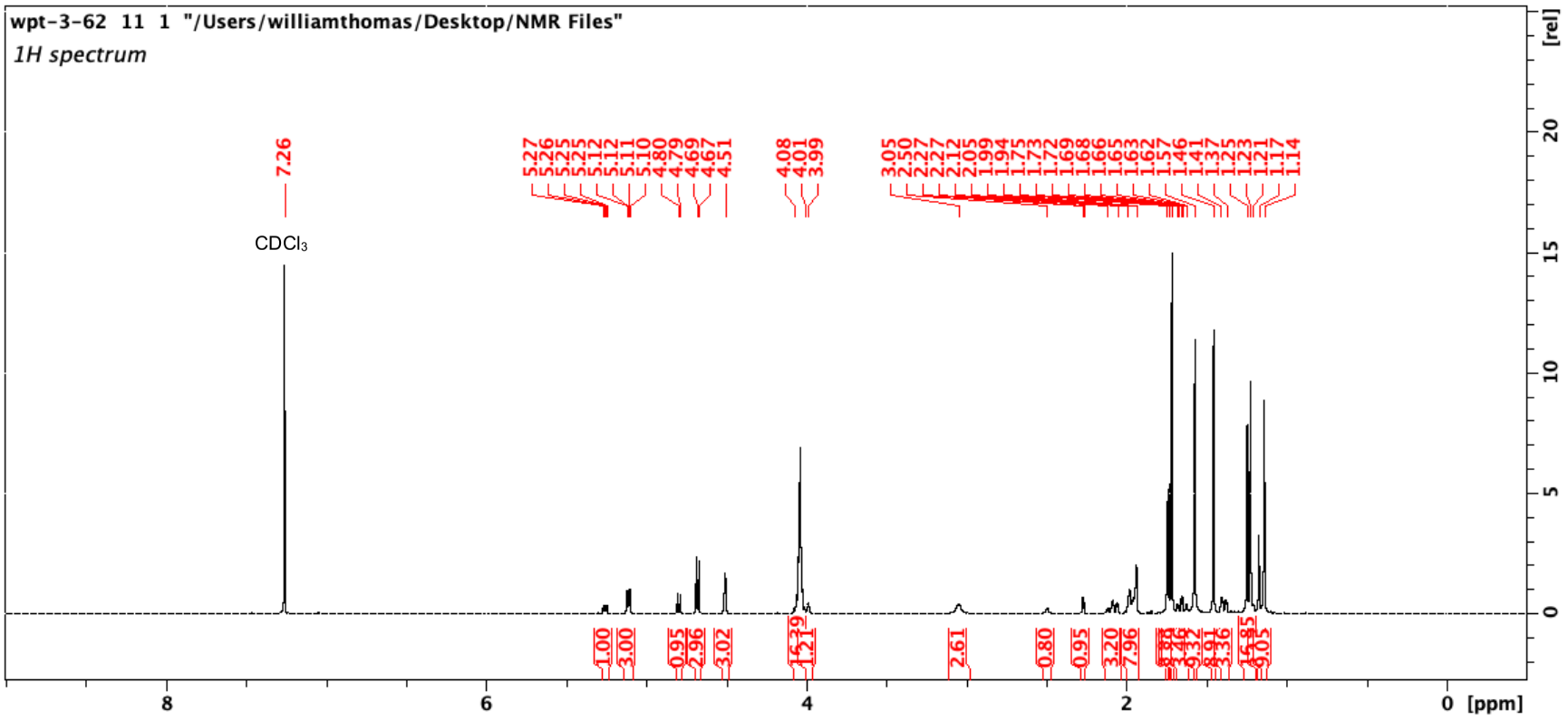

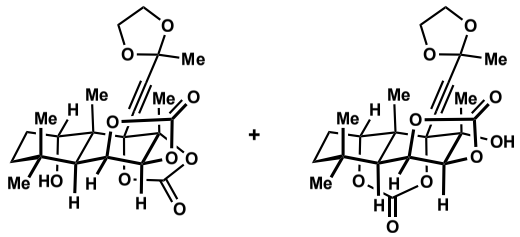

1:3 mixture of **3.43 and 3.44** (^{13}C NMR, 126 MHz, $CDCl_3$)

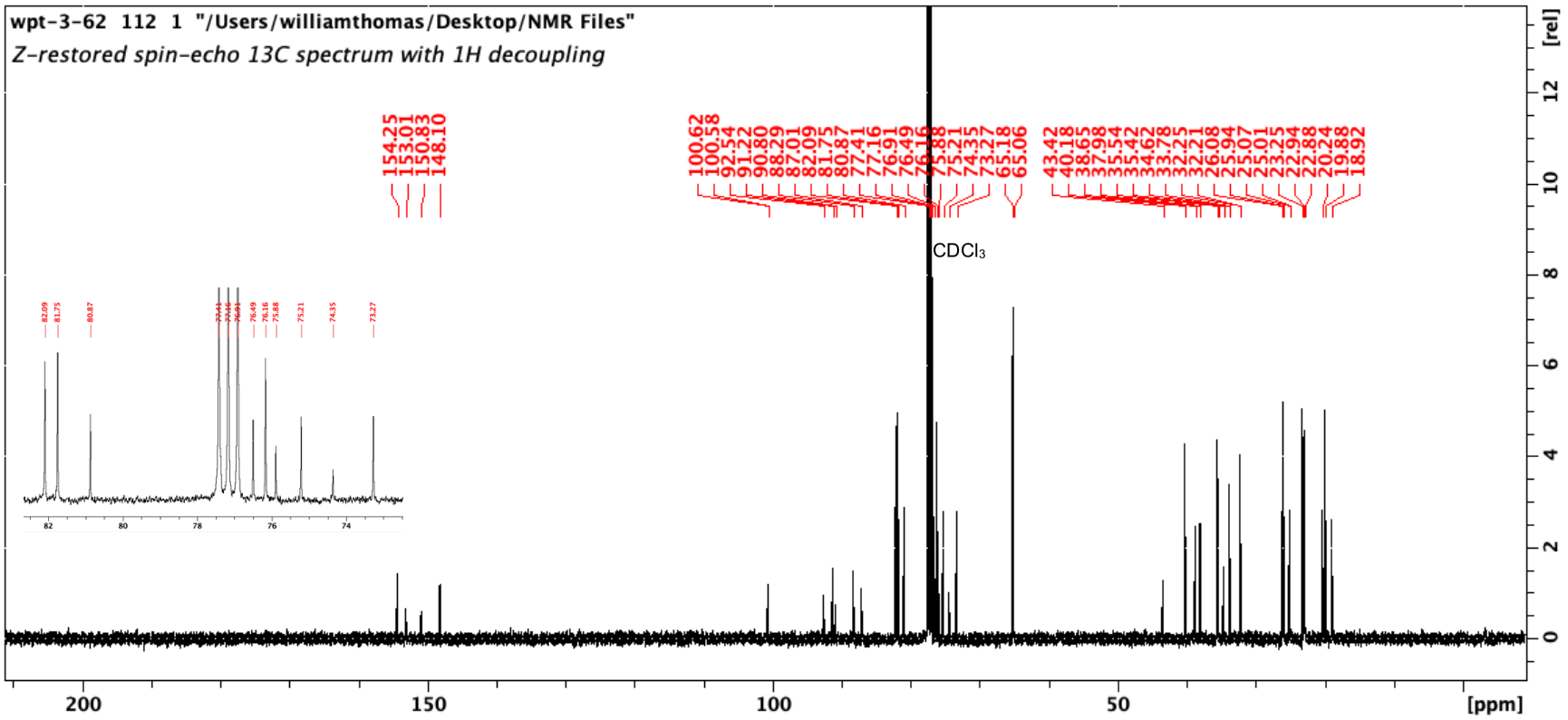

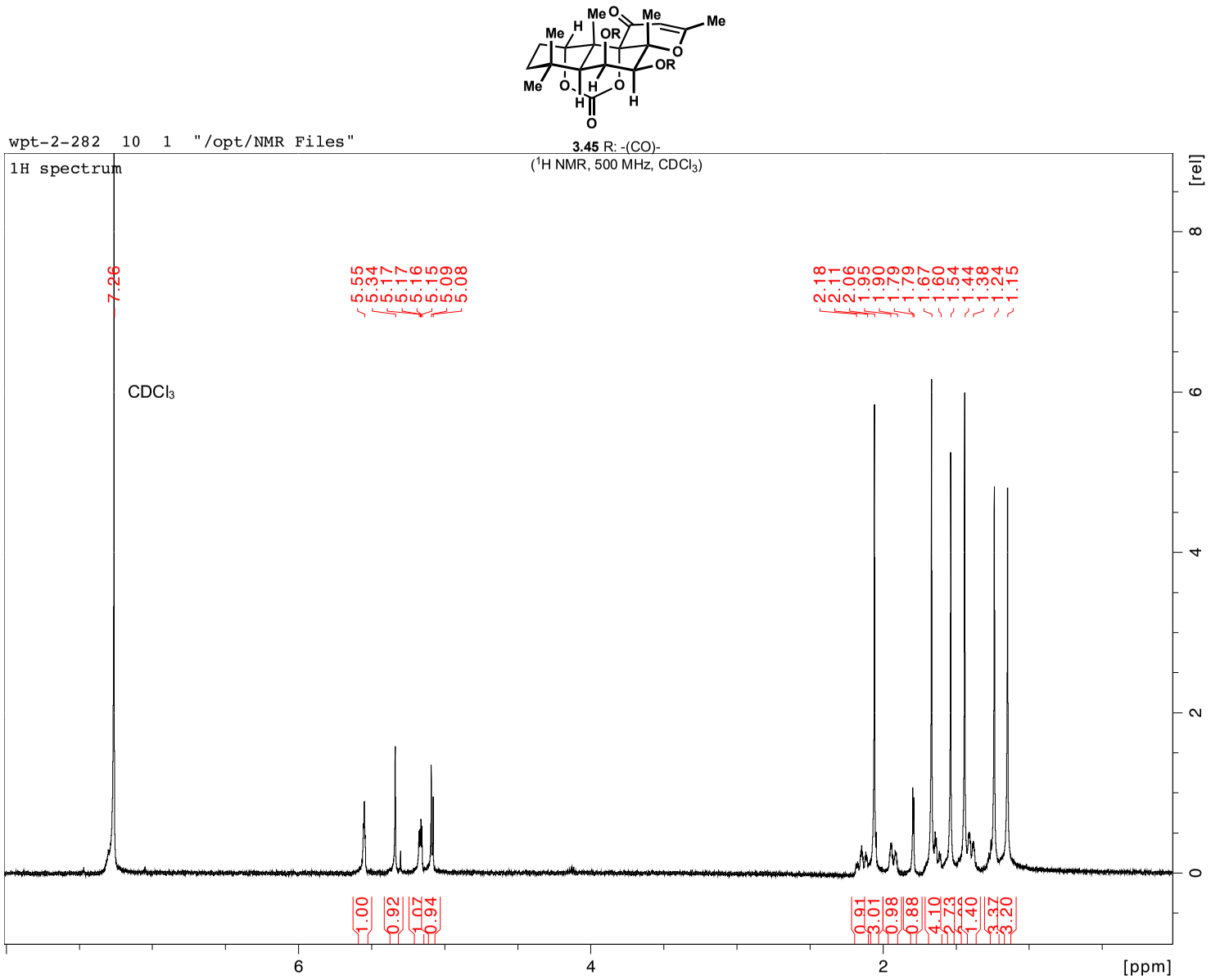
wpt-2-282 10 1 "/opt/NMR Files"
1H spectrum
3.45 R: -(CO)-
(1H NMR, 500 MHz, CDCl3)
CDCl3
7.26
5.55
5.34
5.17
5.17
5.16
5.15
5.09
5.08
2.18
2.11
2.06
1.95
1.90
1.79
1.79
1.67
1.60
1.54
1.44
1.38
1.24
1.15
1.00
0.92
1.07
0.94
0.91
3.01
0.98
0.88
4.10
2.73
2.23
1.40
3.37
3.20
[rel]
[ppm]

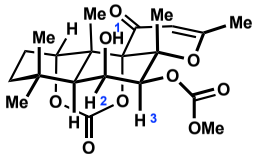

3.51 (^{1}H NMR, 500 MHz, $CDCl_3$)

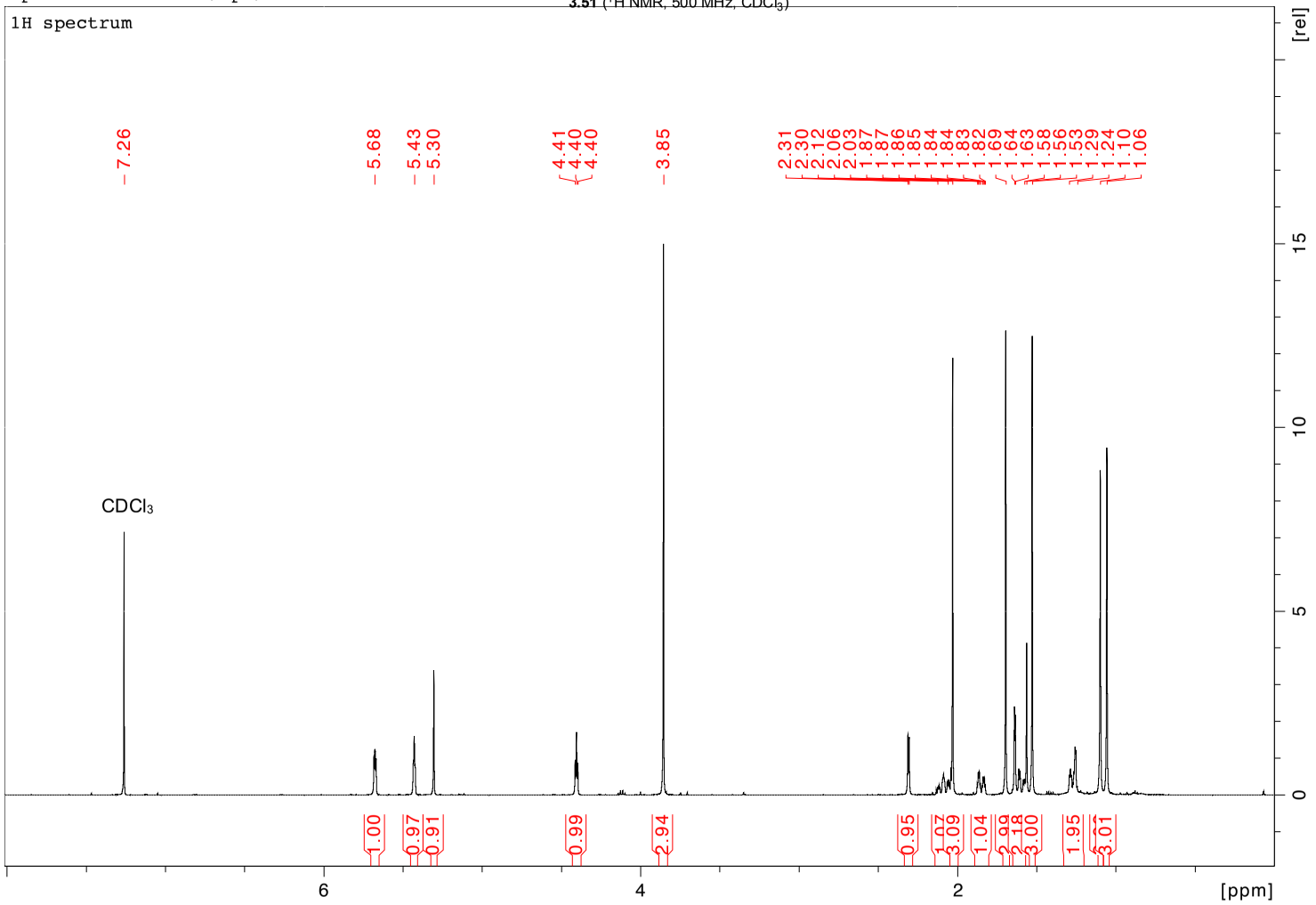

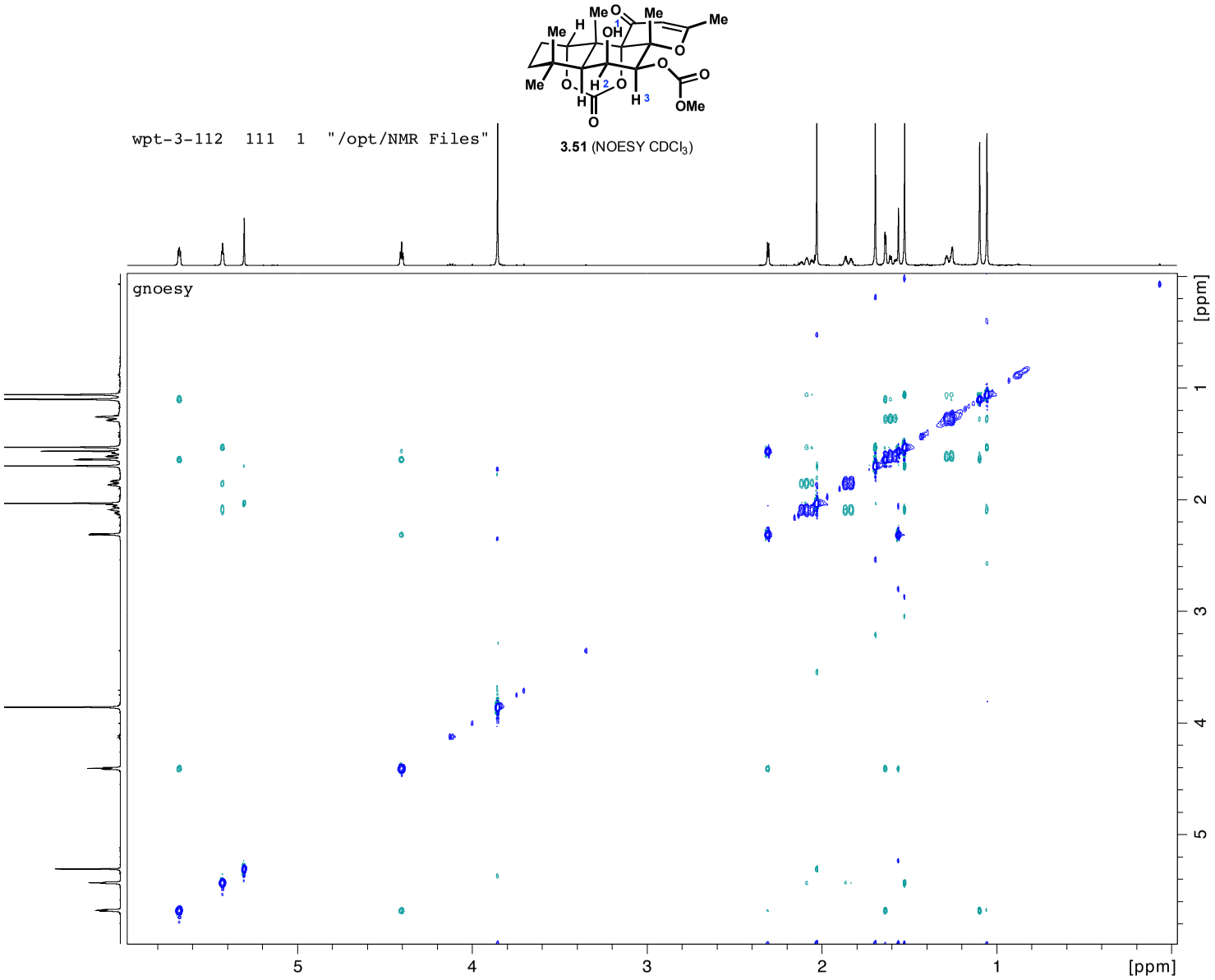

3.51 (NOESY $CDCl_3$)

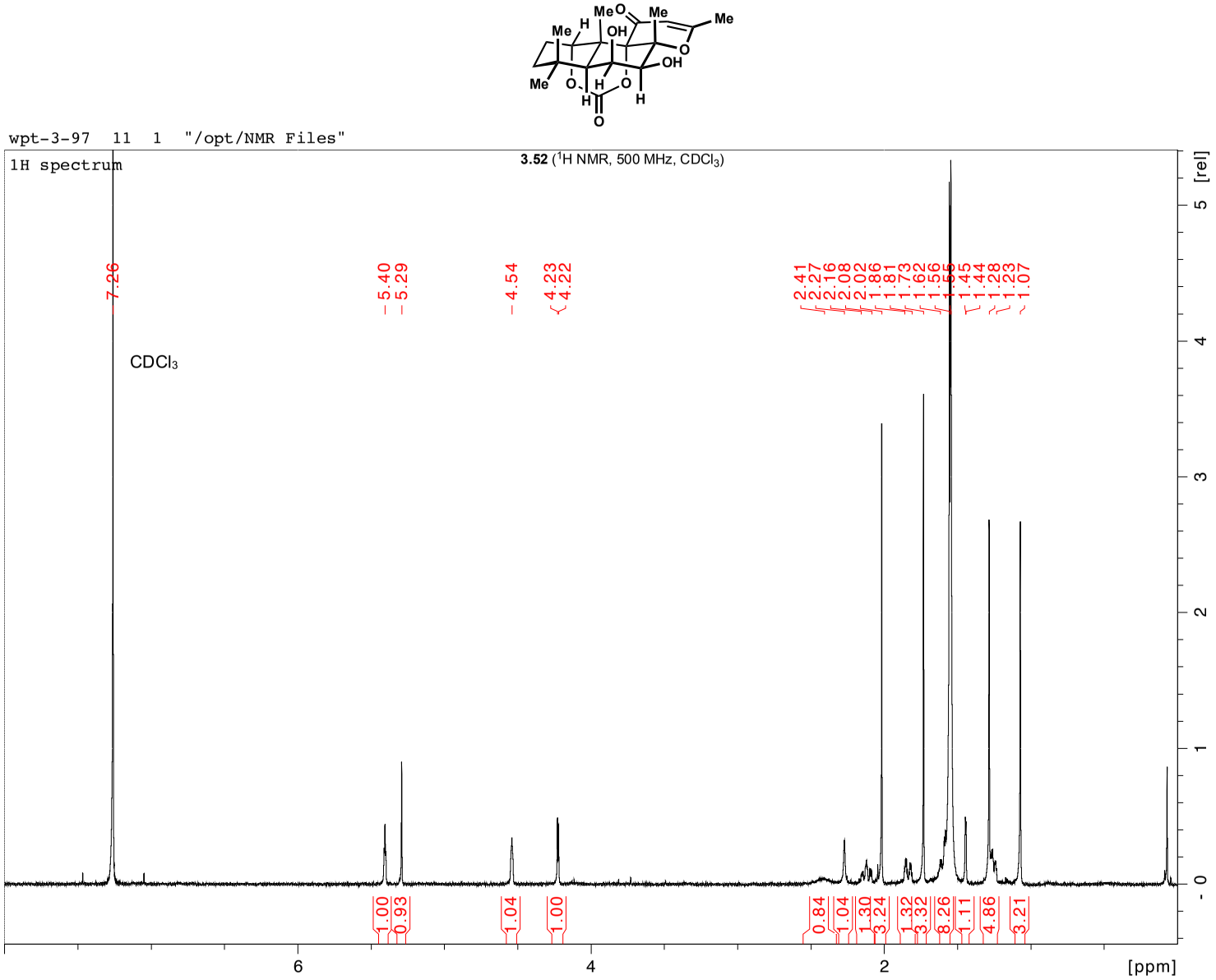
wpt-3-97 11 1 "/opt/NMR Files"
1H spectrum
3.52 (1H NMR, 500 MHz, CDCl3)
7.26
5.40
5.29
4.54
4.23
4.22
2.41
2.27
2.16
2.08
2.02
1.86
1.81
1.73
1.62
1.56
1.55
1.45
1.44
1.28
1.23
1.07
CDCl3
1.00
0.93
1.04
1.00
0.84
1.04
1.30
3.24
1.32
3.32
8.26
1.11
4.86
3.21
6
4
2
[ppm]
5 [rel]
4
3
2
1
0

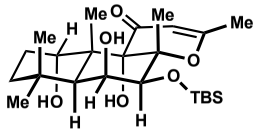

S3.2 (^{1}H NMR, 500 MHz, $CDCl_3$)

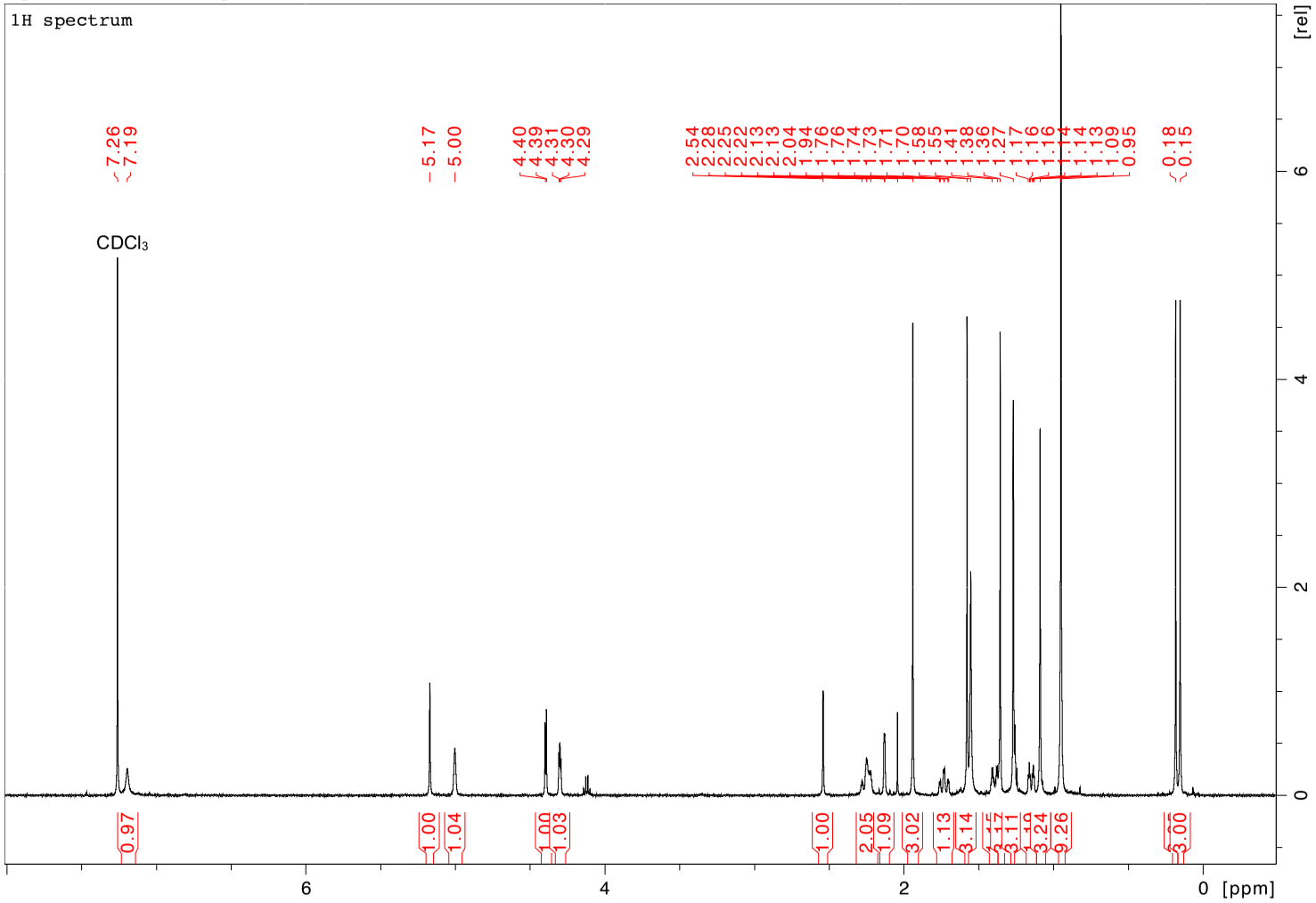

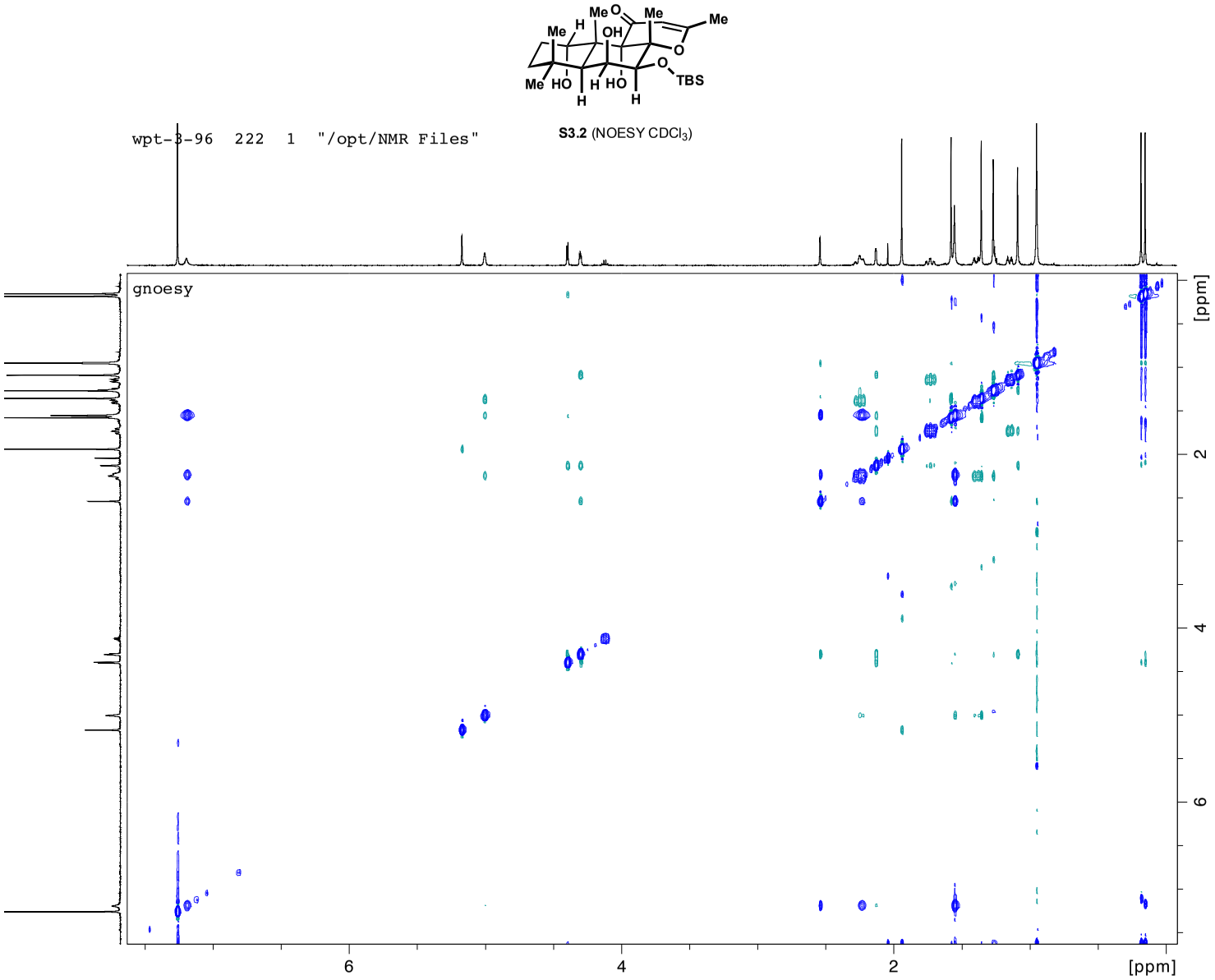

S3.2 (NOESY $CDCl_3$)

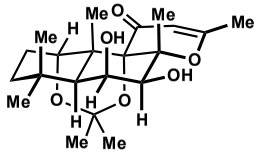

3.54 (^{1}H NMR, 500 MHz, $CDCl_3$)

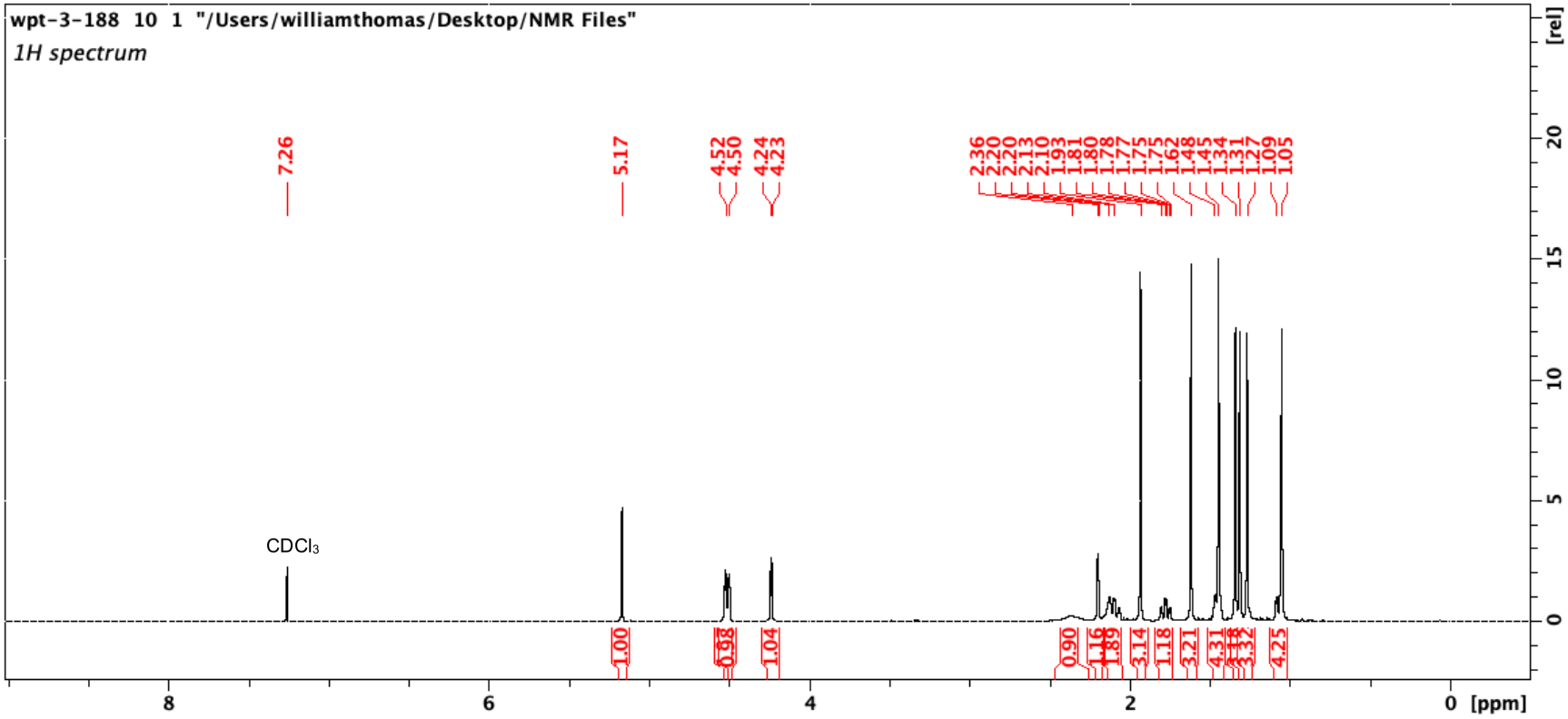

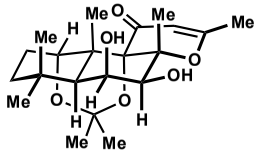

3.54 (^{13}C NMR, 126 MHz, $CDCl_3$)

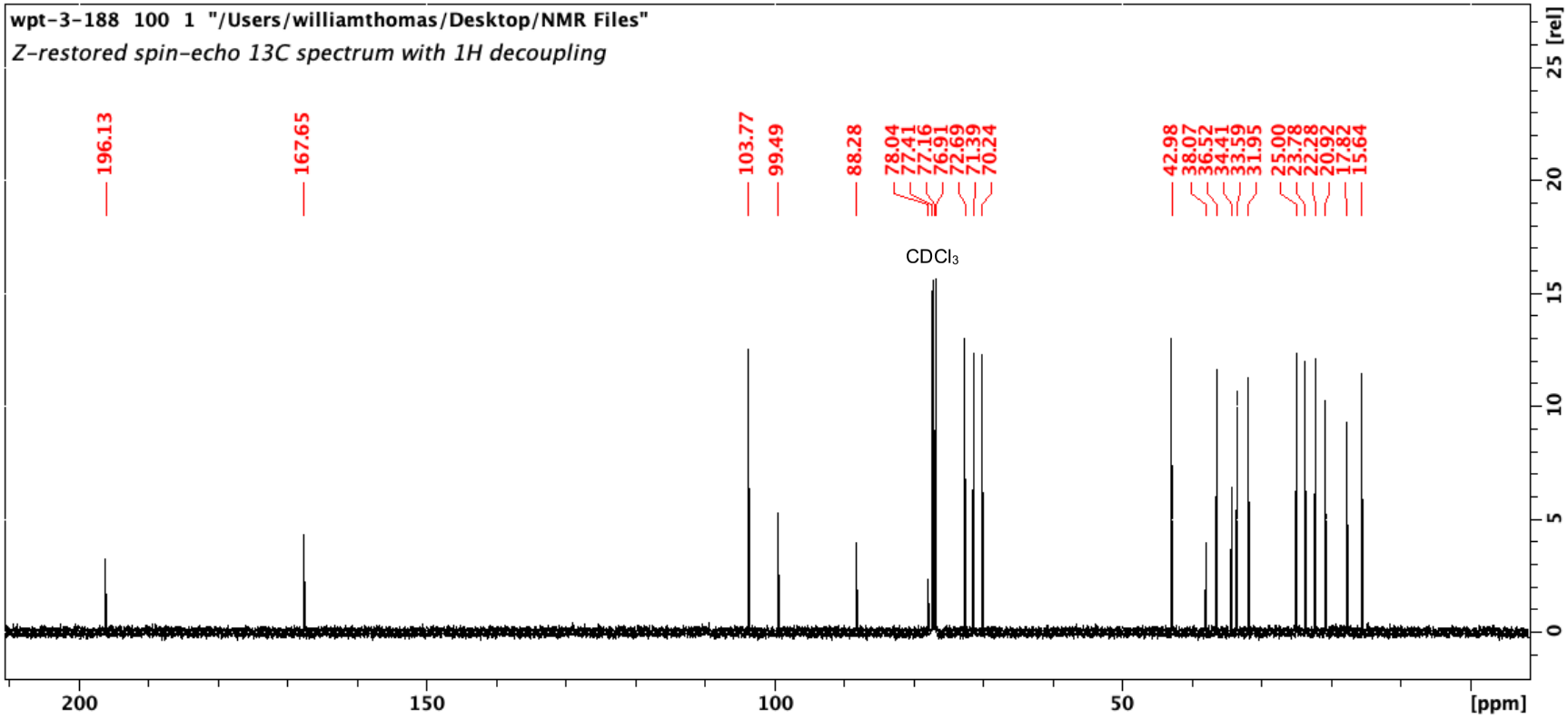

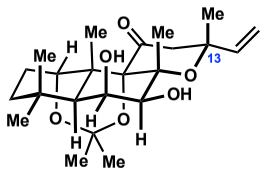

3.55 d. r. 5:1 at C13 (^{1}H NMR, 500 MHz, $CDCl_3$)

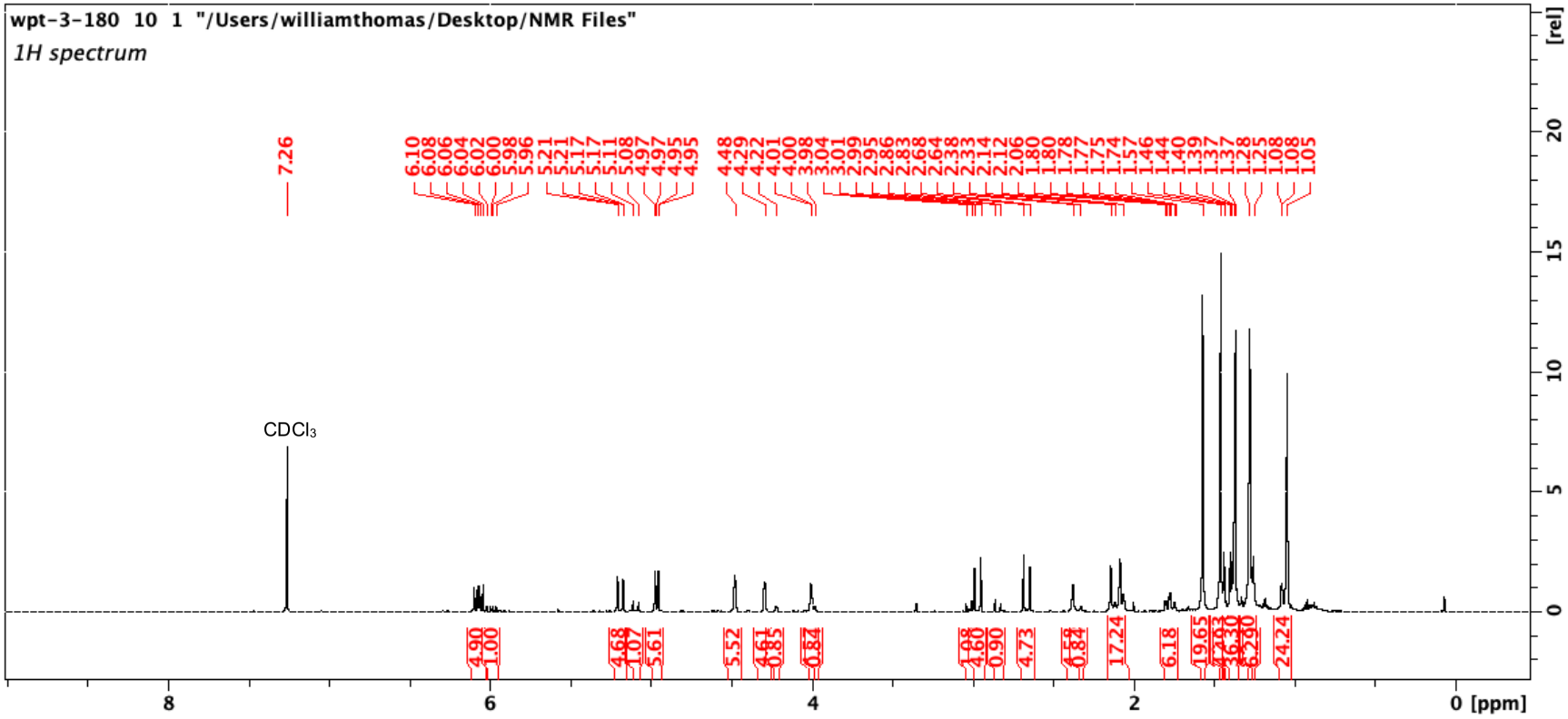

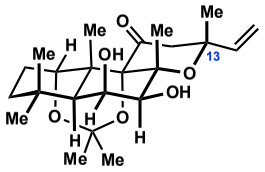

3.55 d. r. 5:1 at C13 (^{13}C NMR, 126 MHz, $CDCl_3$)

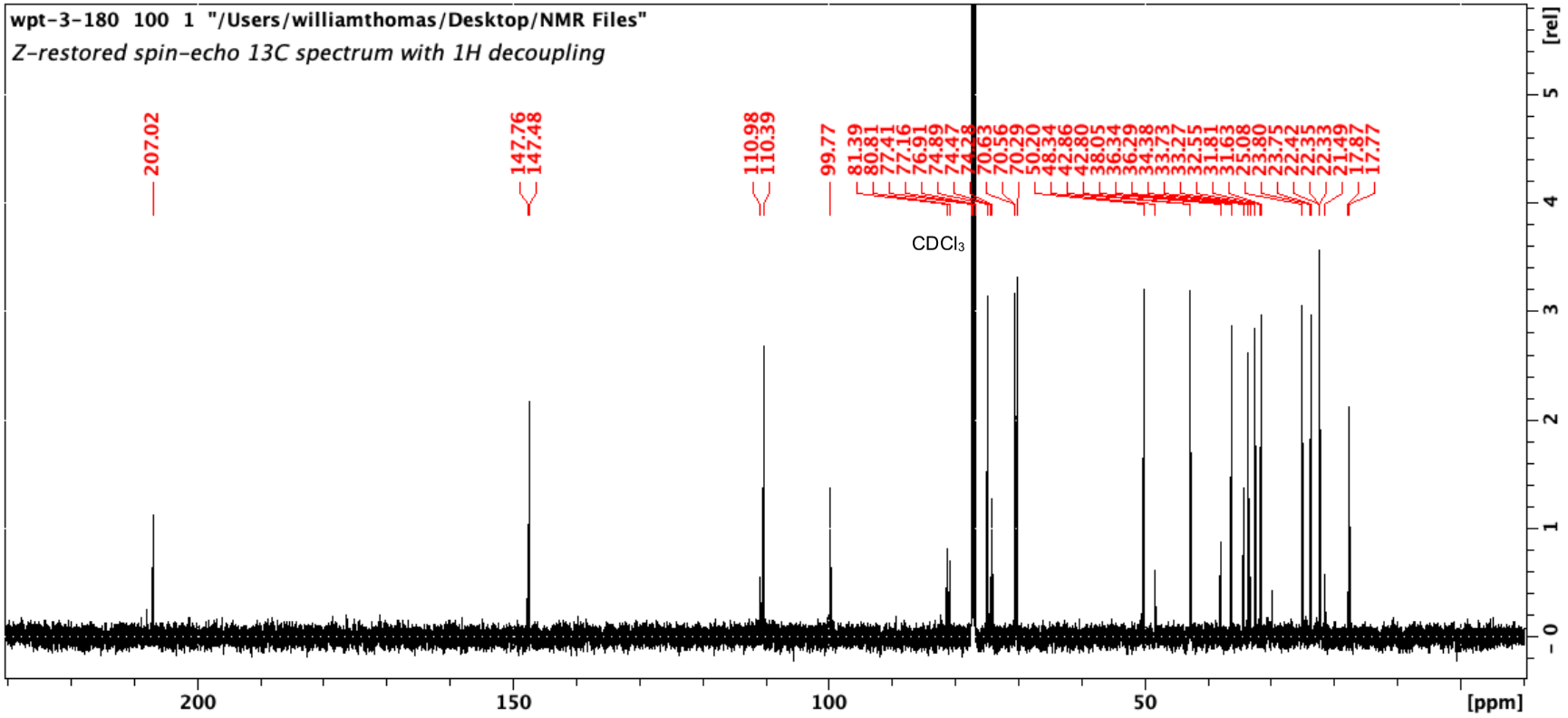

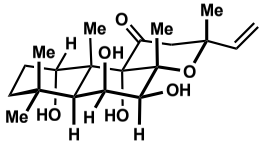

3.59 (^{1}H NMR, 500 MHz, $CDCl_3$)

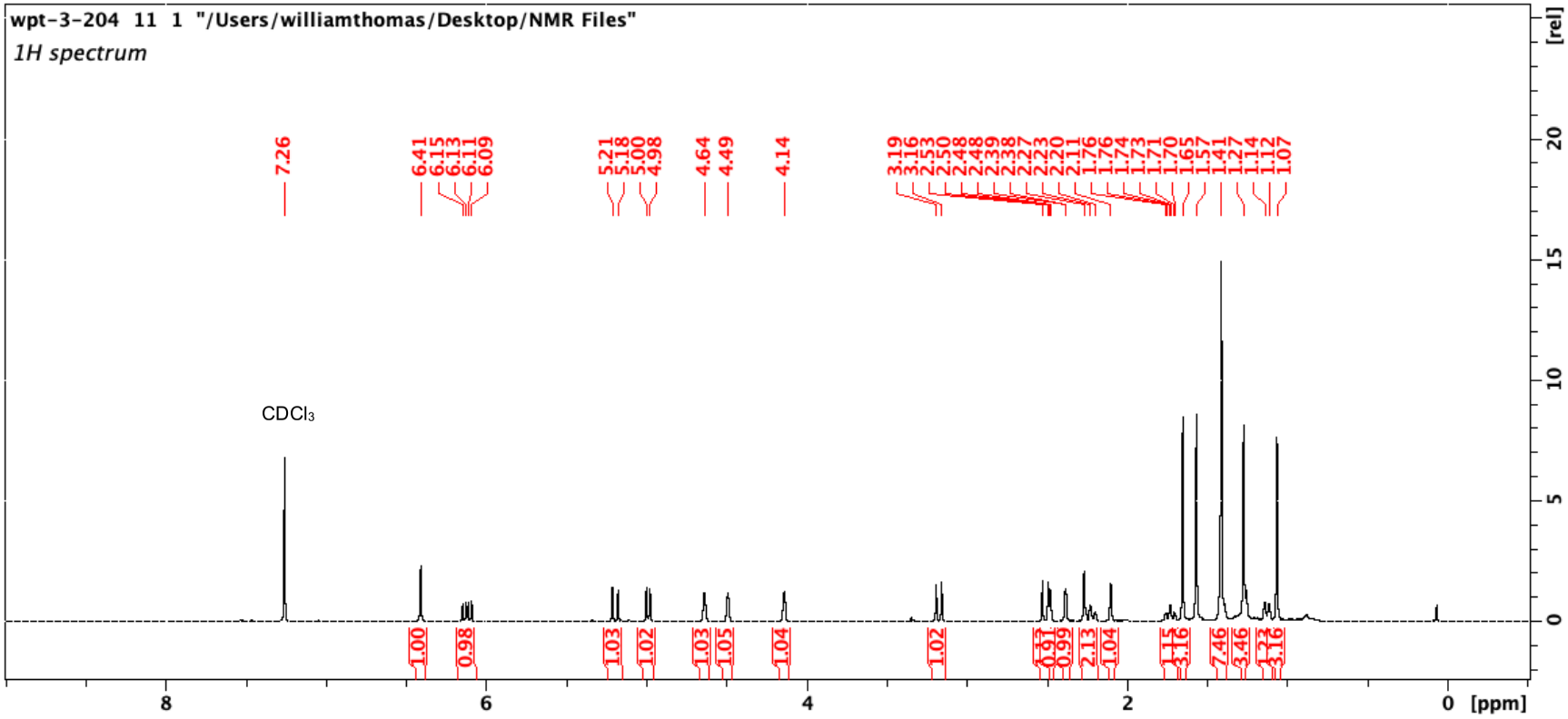

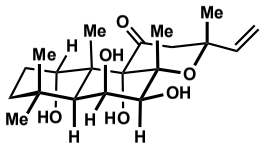

3.59 (^{13}C NMR, 126 MHz, $CDCl_3$)

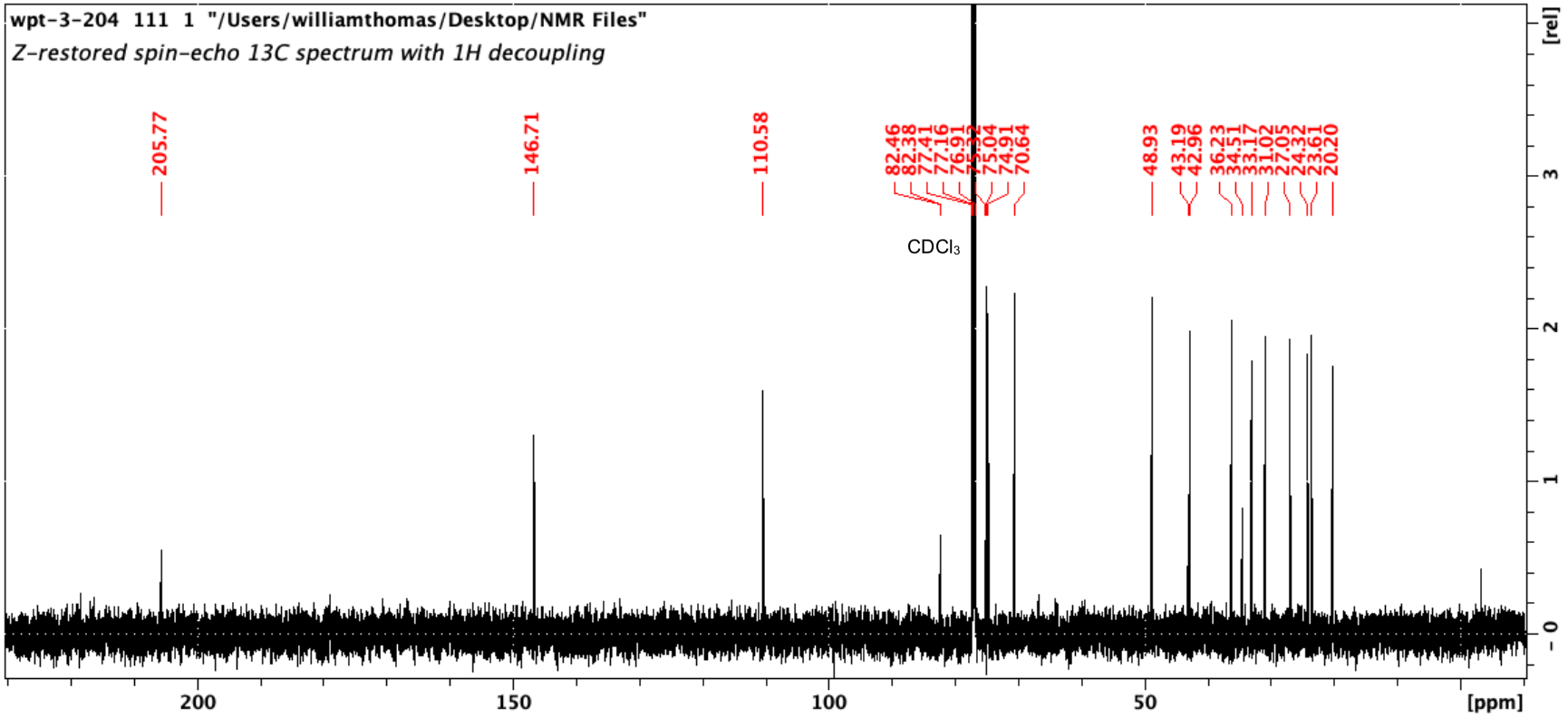

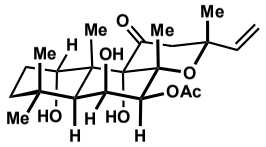

forskolin (**3.1**) (^{1}H NMR, 500 MHz, $CDCl_3$)

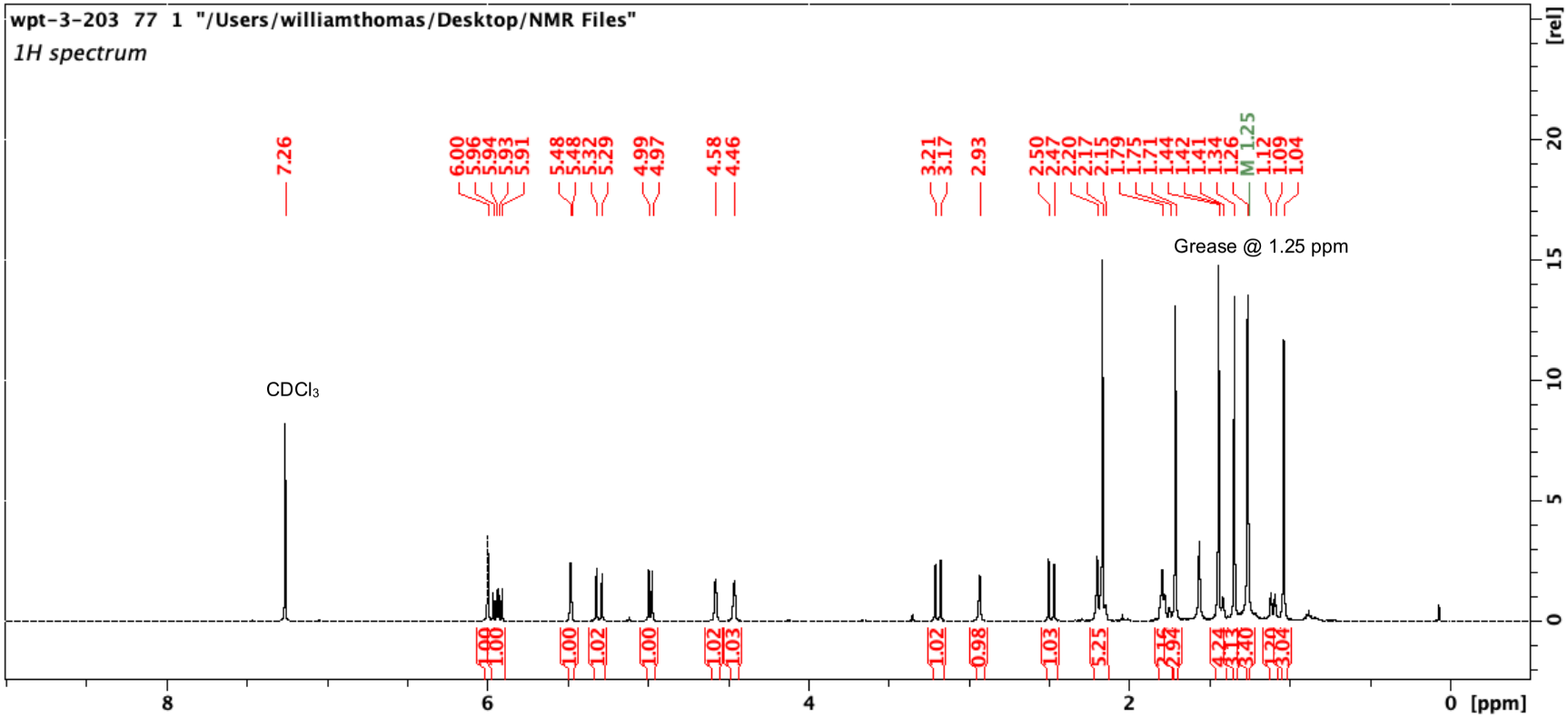

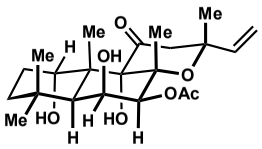

forskolin (**3.1**) (^{13}C NMR, 126 MHz, $CDCl_3$)

*$CDCl_3$ calibrated to 77.2 ppm for comparison purposes.[9]

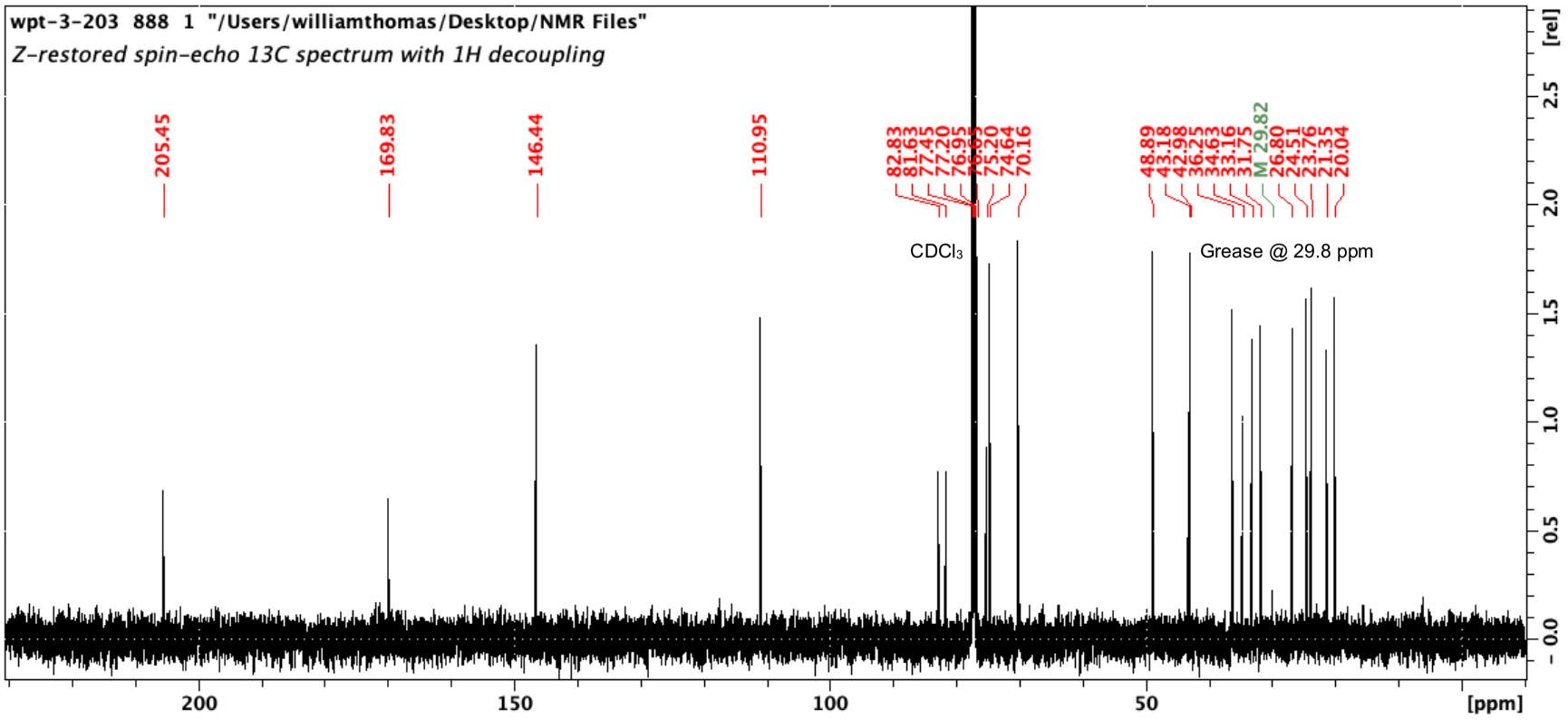

Appendix B: NMR Spectra for Chapter 5

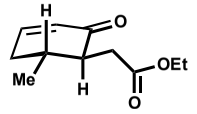

S5.2 (^{1}H NMR, 500 MHz, $CDCl_3$)

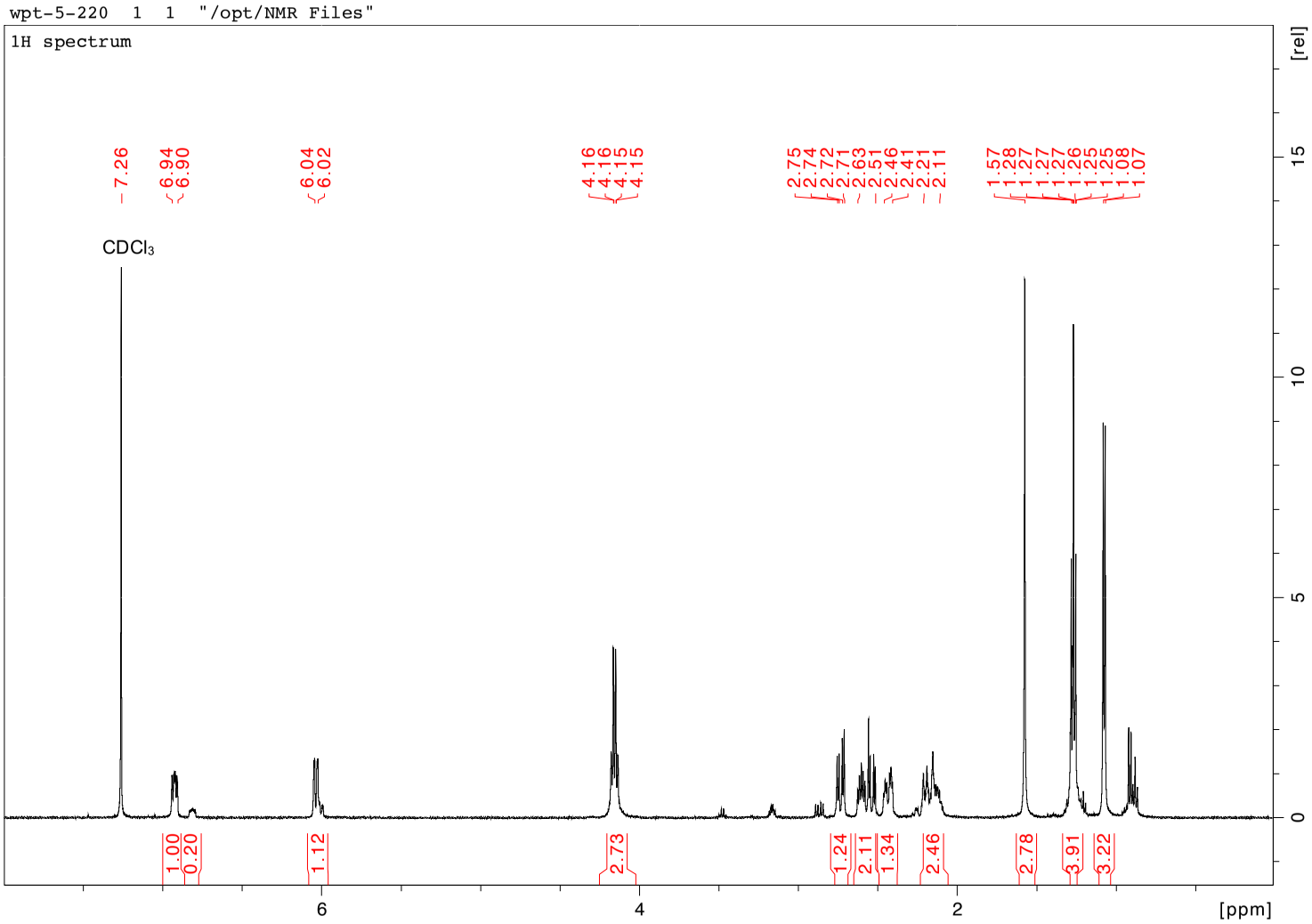

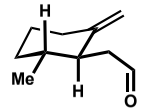

5.16 (^{1}H NMR, 500 MHz, $CDCl_3$)

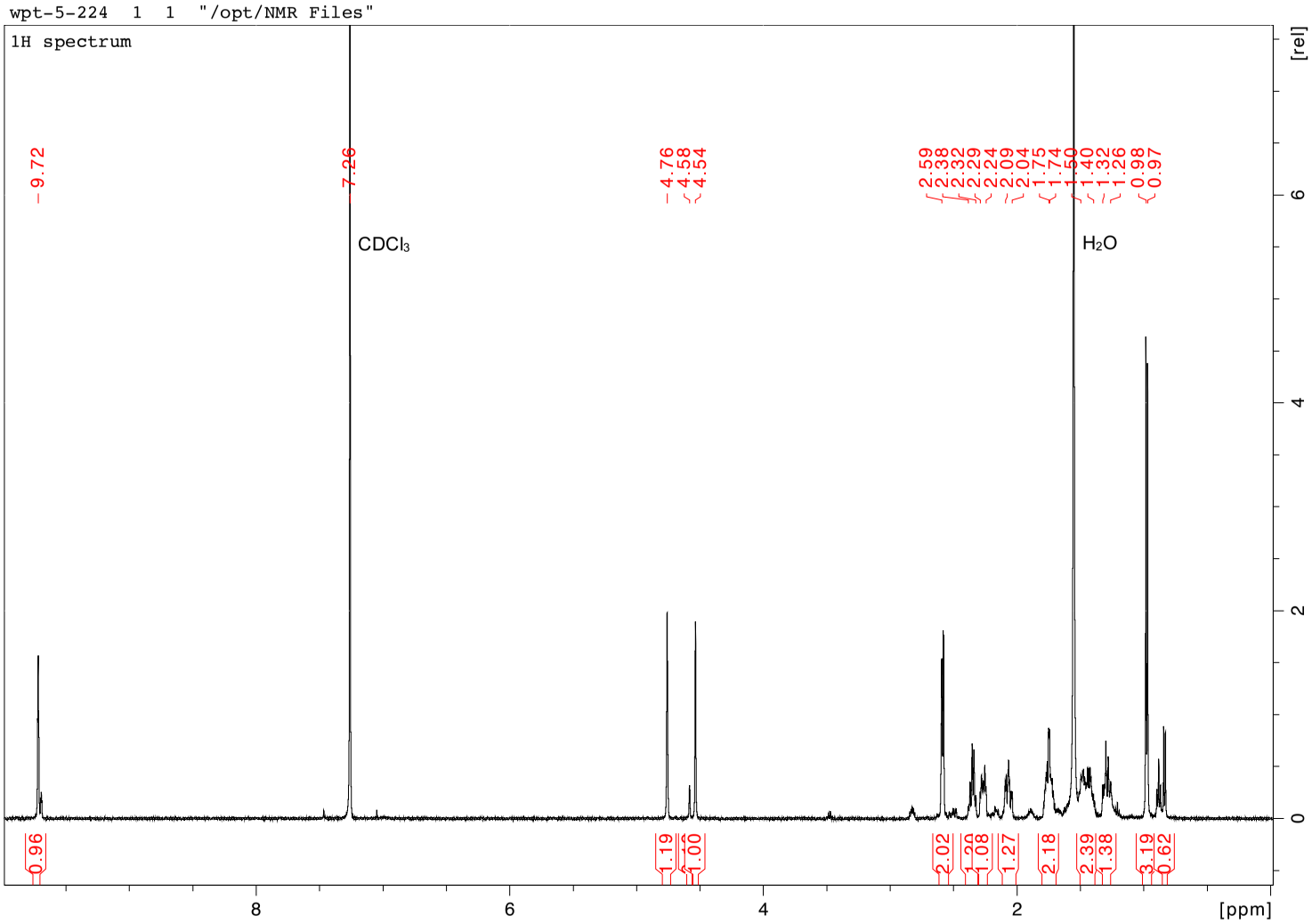

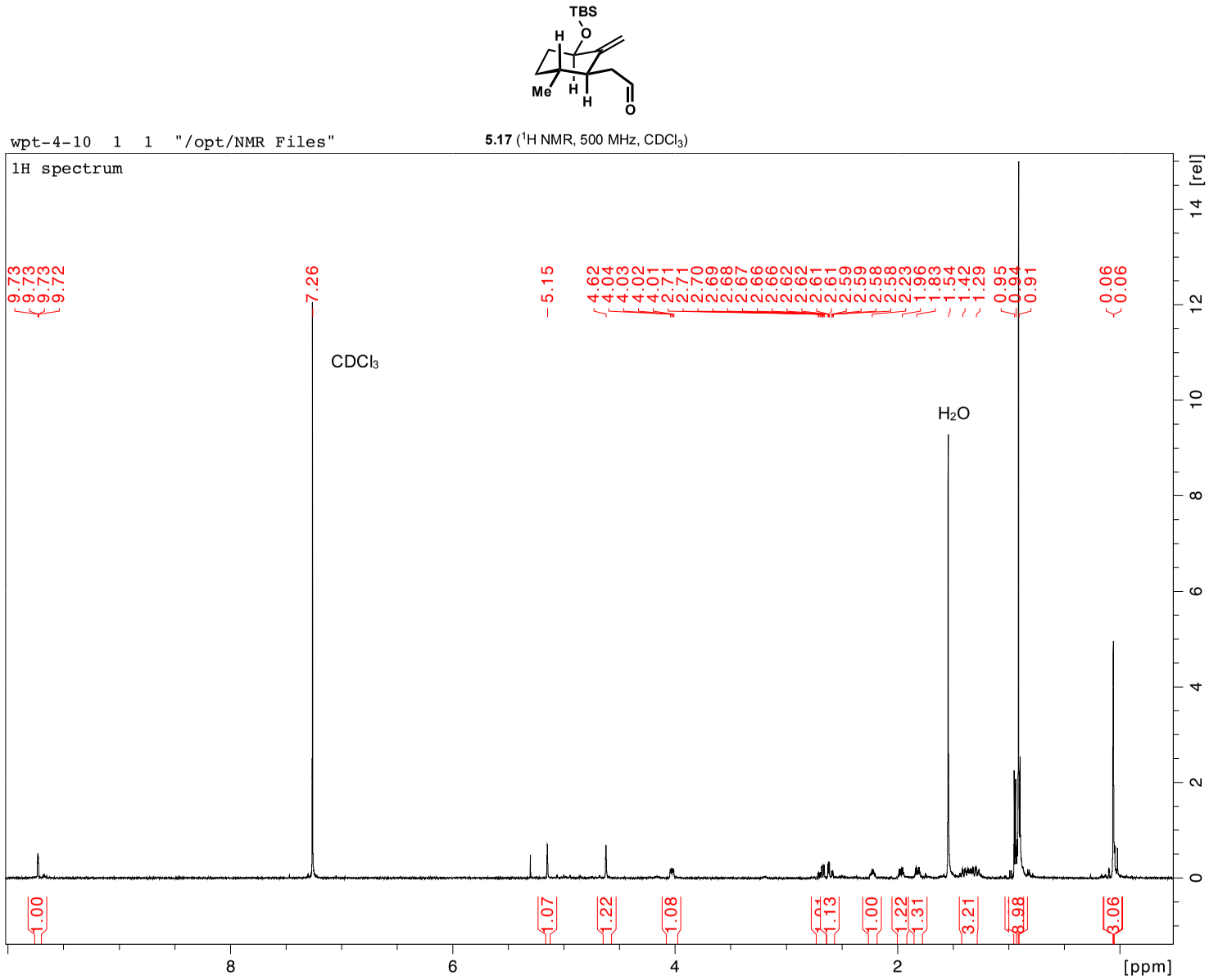
TBS
H
O
Me
H
H
O
wpt-4-10 1 1 "/opt/NMR Files"
5.17 (1H NMR, 500 MHz, CDCl3)
1H spectrum
9.73
9.73
9.72
7.26
5.15
4.62
4.04
4.03
4.02
4.01
2.71
2.70
2.69
2.68
2.67
2.66
2.66
2.62
2.61
2.59
2.59
2.58
2.58
2.23
1.96
1.83
1.54
1.42
1.29
0.95
0.94
0.91
0.06
0.06
CDCl3
H2O
1.00
1.07
1.22
1.08
1.13
1.00
1.22
1.31
3.21
8.98
3.06
8
6
4
2
[ppm]
14 [rel]
12
10
8
6
4
2
0

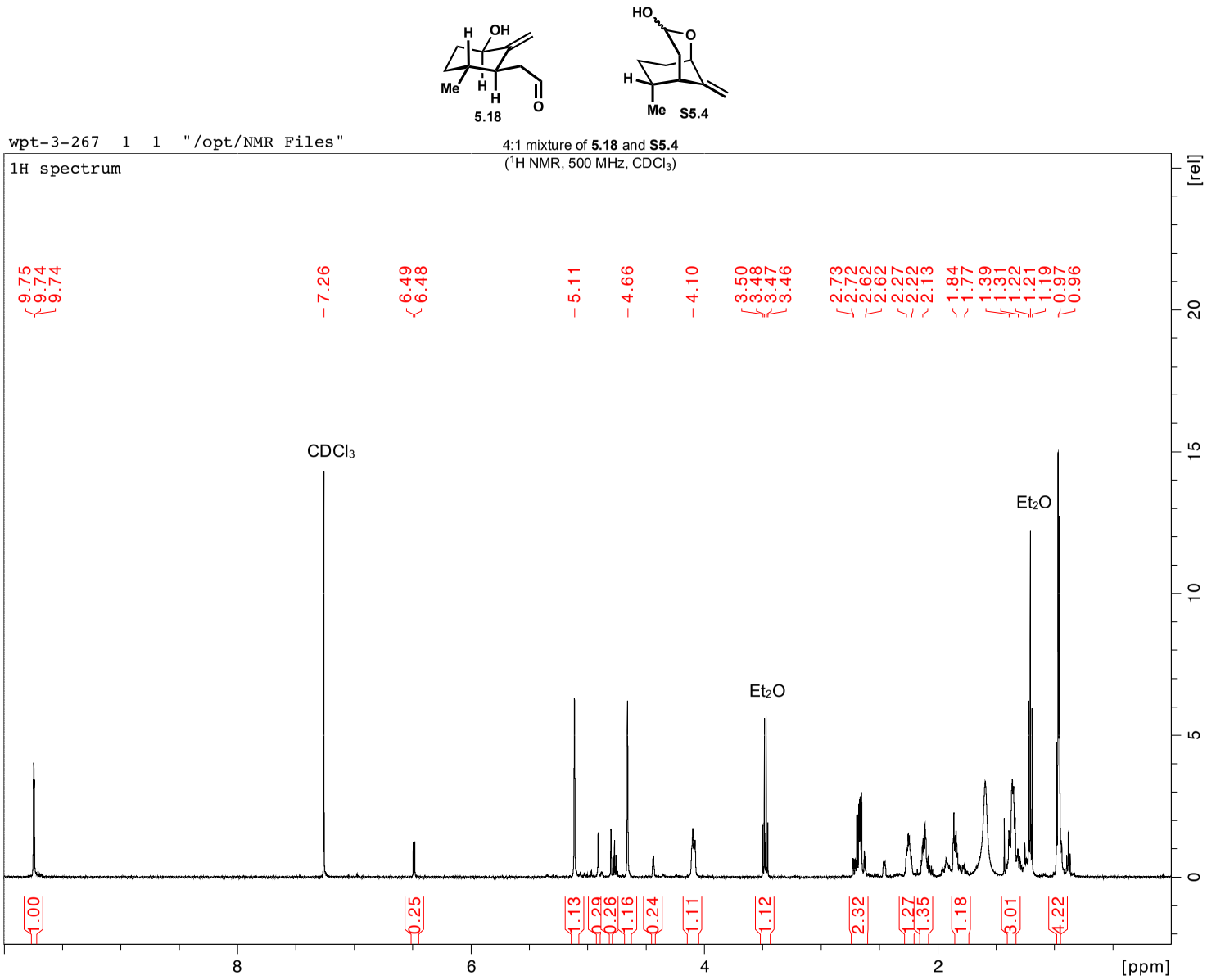
5.18
S5.4
wpt-3-267 1 1 "/opt/NMR Files"
1H spectrum
4:1 mixture of 5.18 and S5.4
(1H NMR, 500 MHz, CDCl3)
9.75
9.74
9.74
7.26
6.49
6.48
5.11
4.66
4.10
3.50
3.48
3.47
3.46
2.73
2.72
2.62
2.62
2.27
2.22
2.13
1.84
1.77
1.39
1.31
1.22
1.21
1.19
0.97
0.96
CDCl3
Et2O
Et2O
1.00
0.25
1.13
0.29
0.26
1.16
0.24
1.11
1.12
2.32
1.27
1.35
1.18
3.01
4.22
8
6
4
2
[ppm]
[rel]
0
5
10
15
20

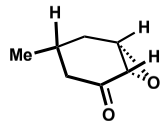

S5.6 (^{1}H NMR, 500 MHz, $CDCl_3$)

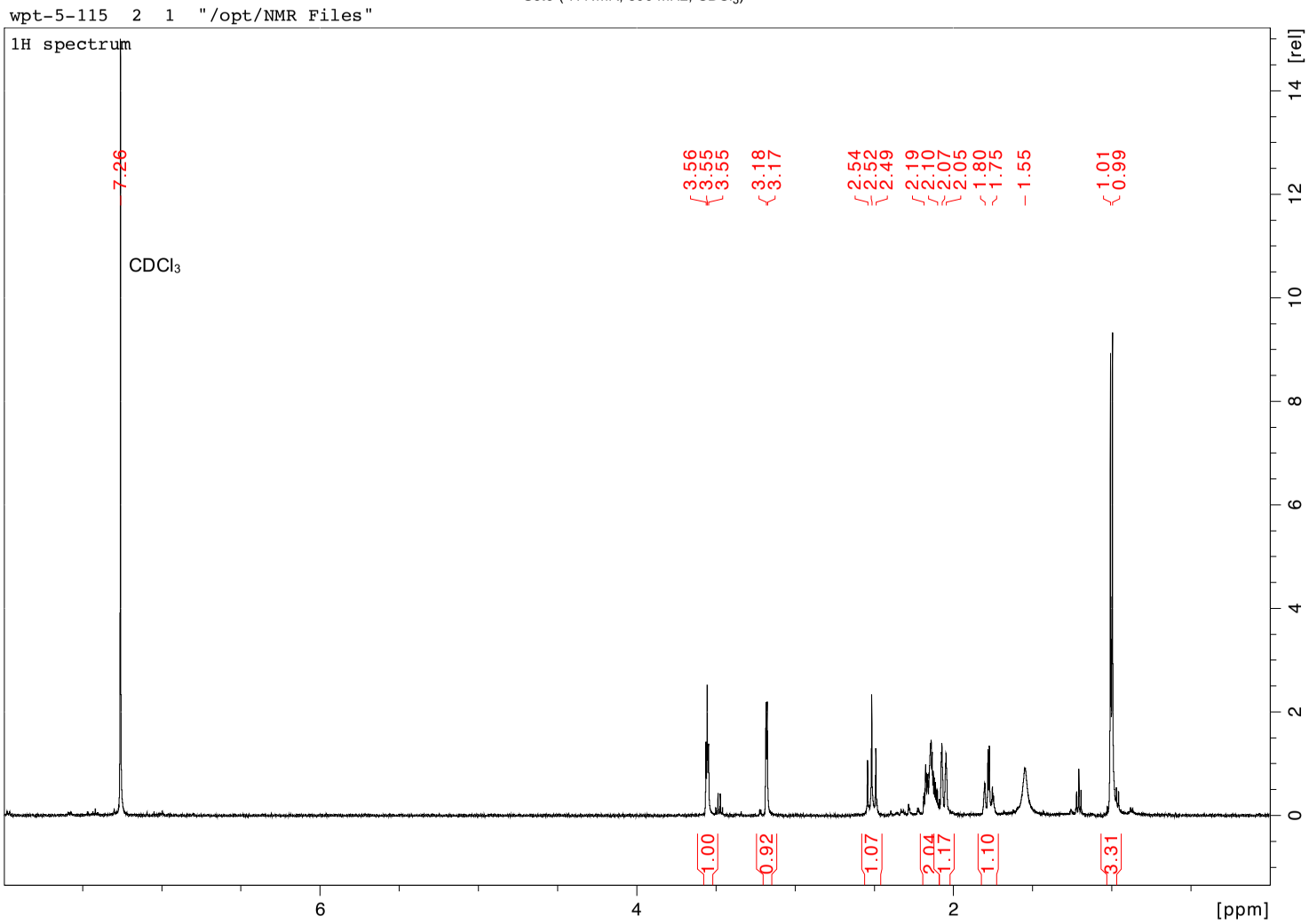

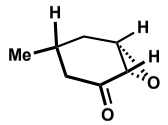

S5.6 (^{13}C NMR, 126 MHz, $CDCl_3$)

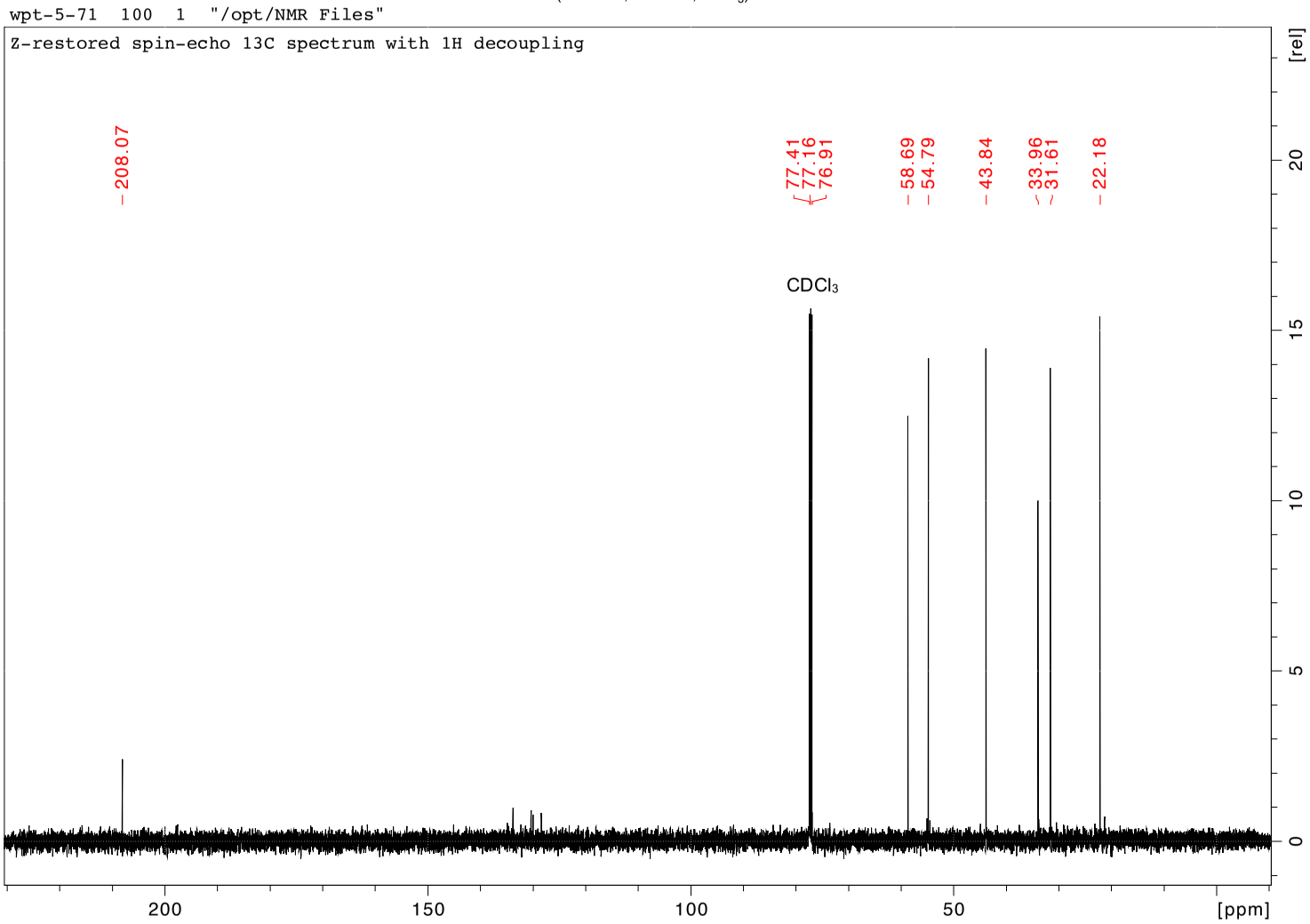

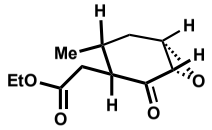

S5.7 (^{1}H NMR, 500 MHz, $CDCl_3$)

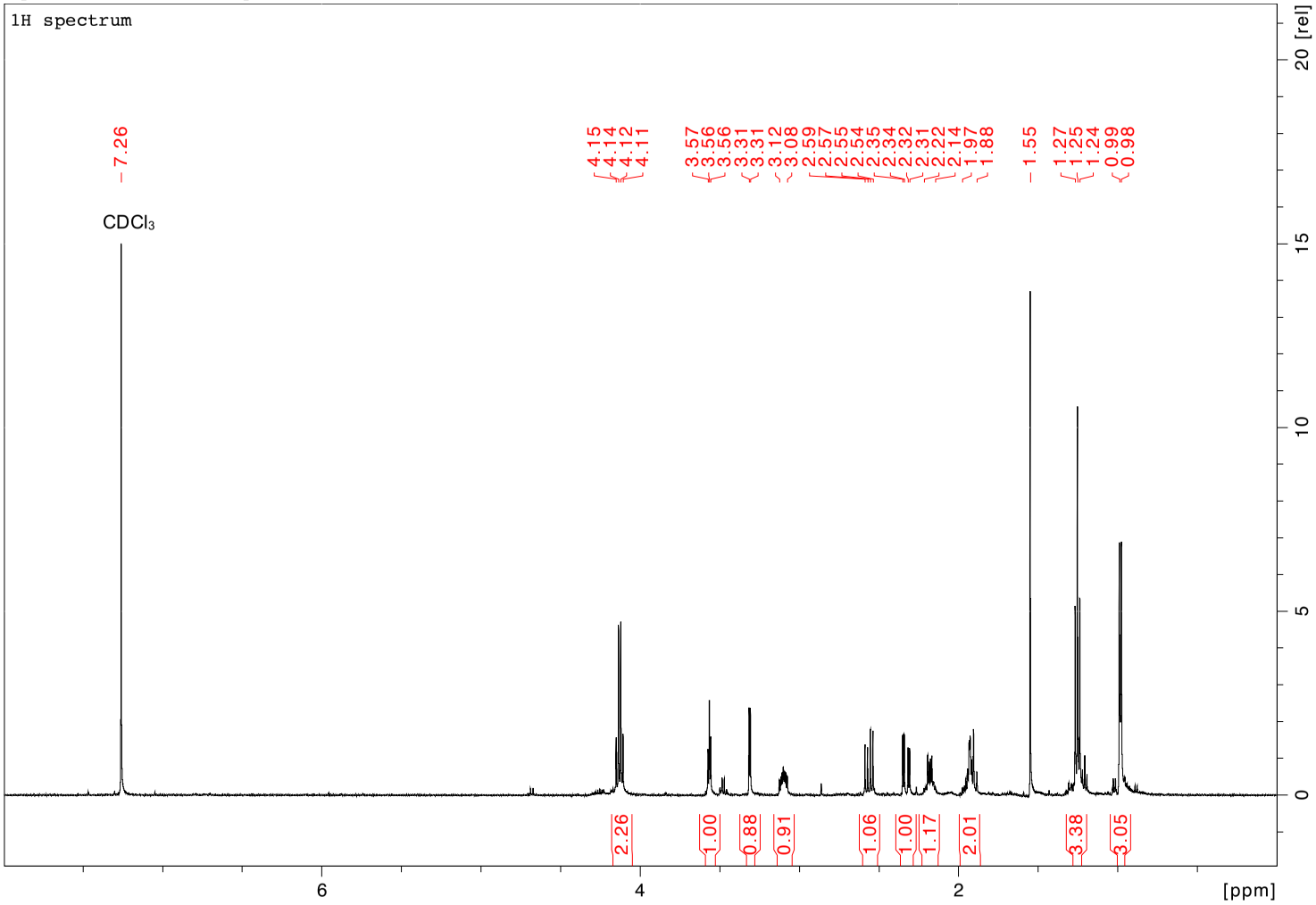

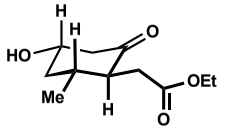

S5.8 (^{1}H NMR, 500 MHz, $CDCl_3$)

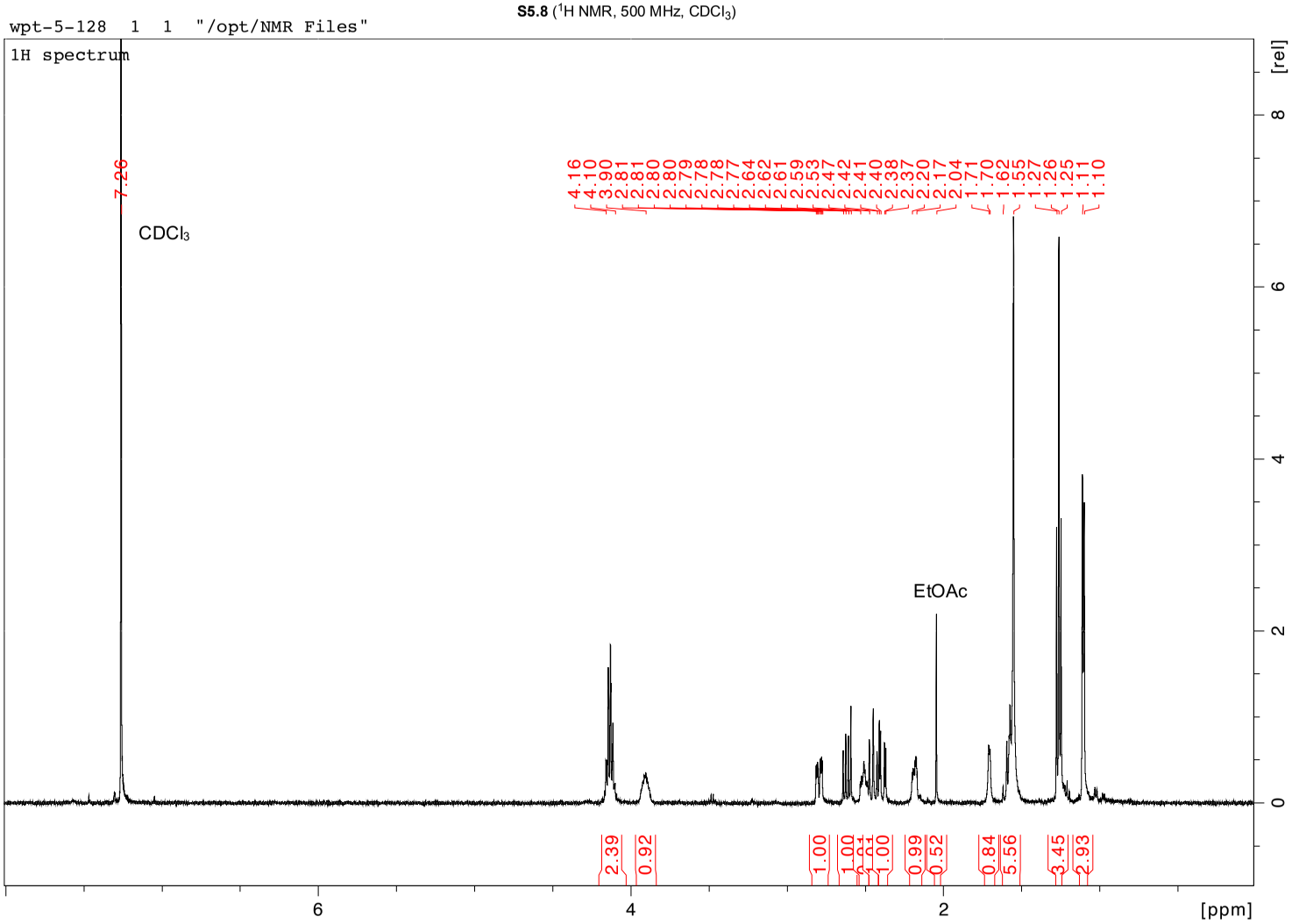

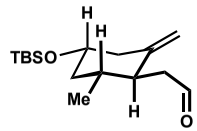

5.19 (^{1}H NMR, 500 MHz, $CDCl_3$)

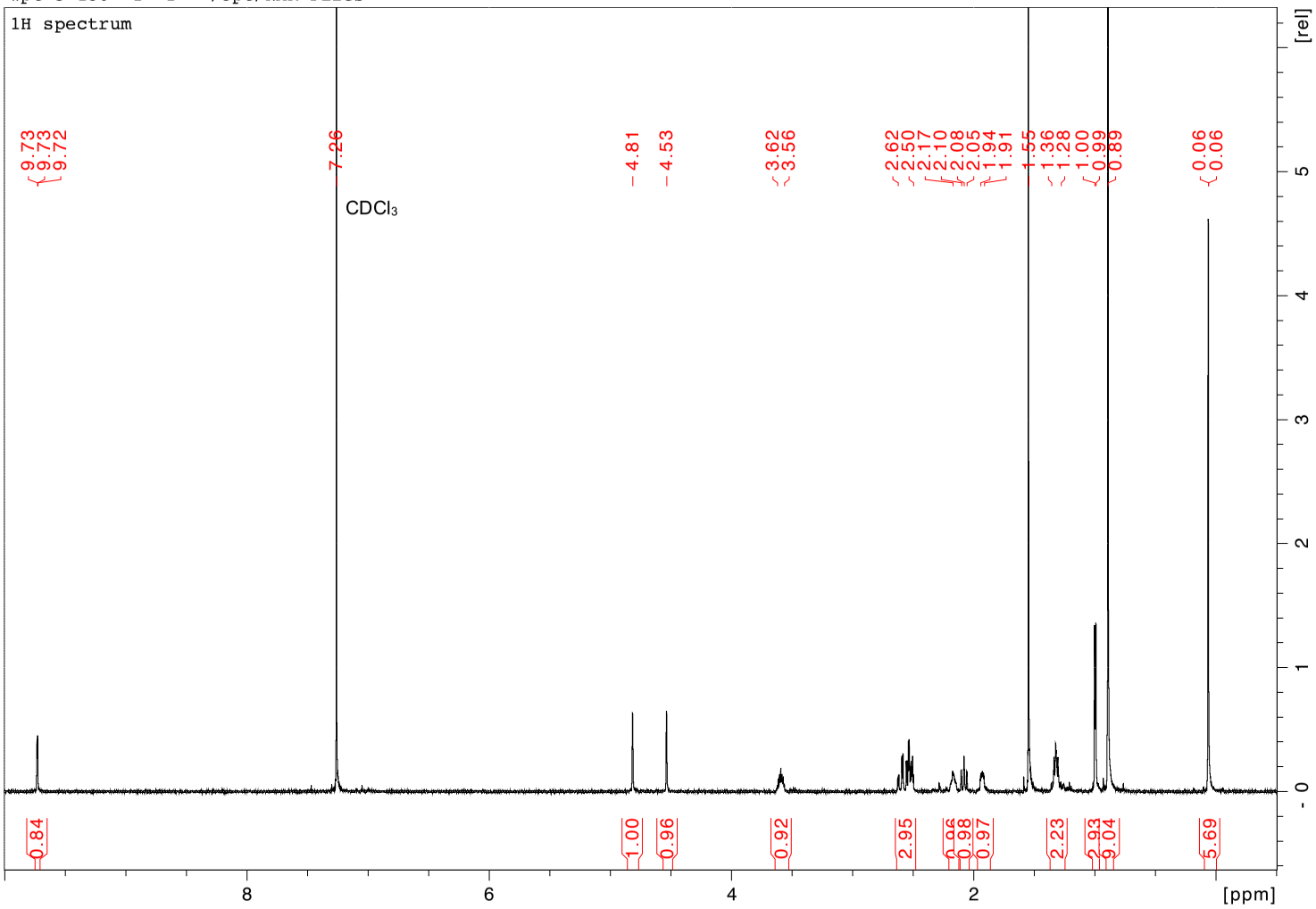

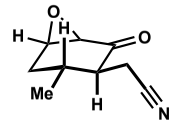

5.48 (^{1}H NMR, 500 MHz, $CDCl_3$)

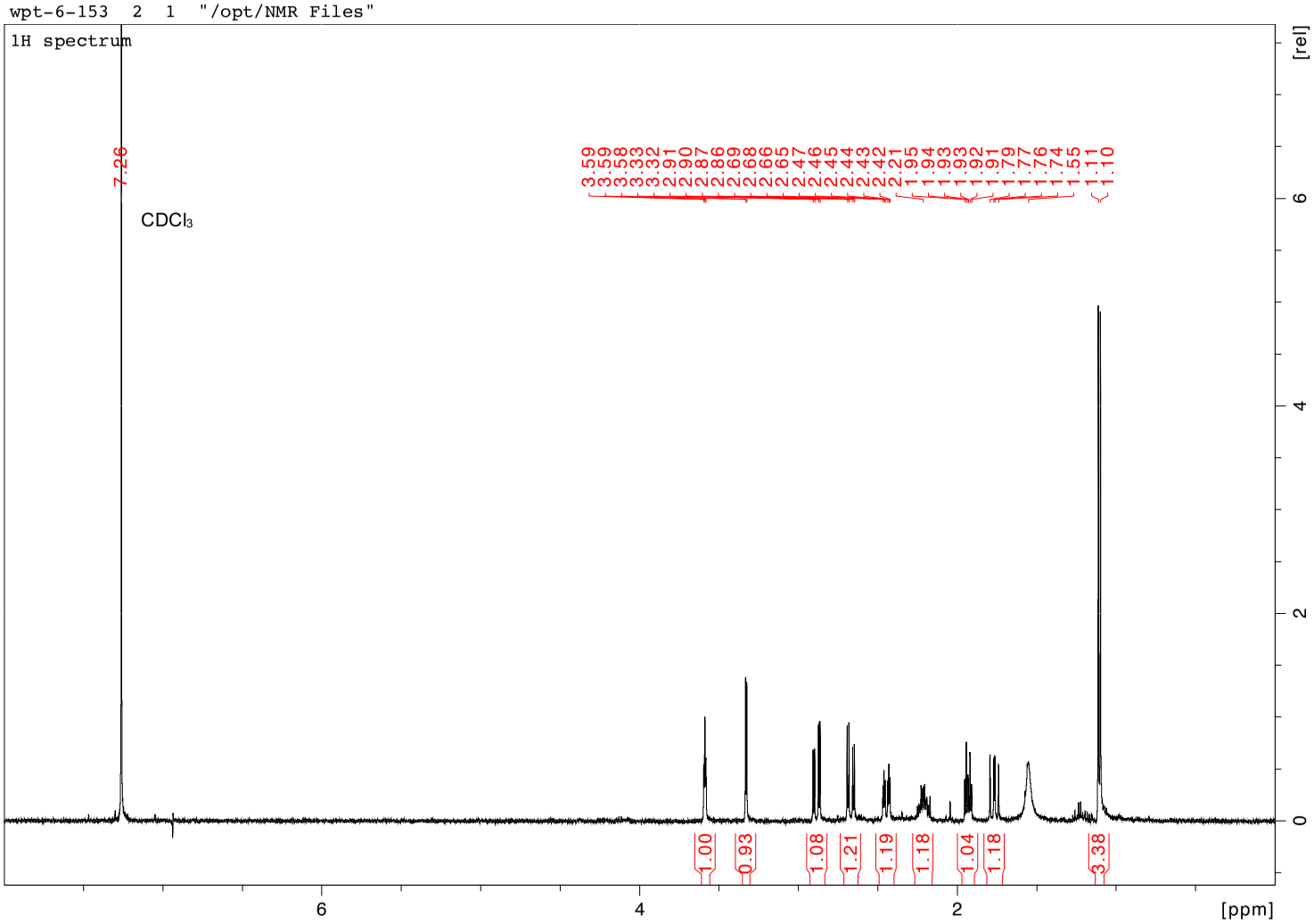

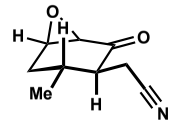

5.48 (^{13}C NMR, 126 MHz, $CDCl_3$)

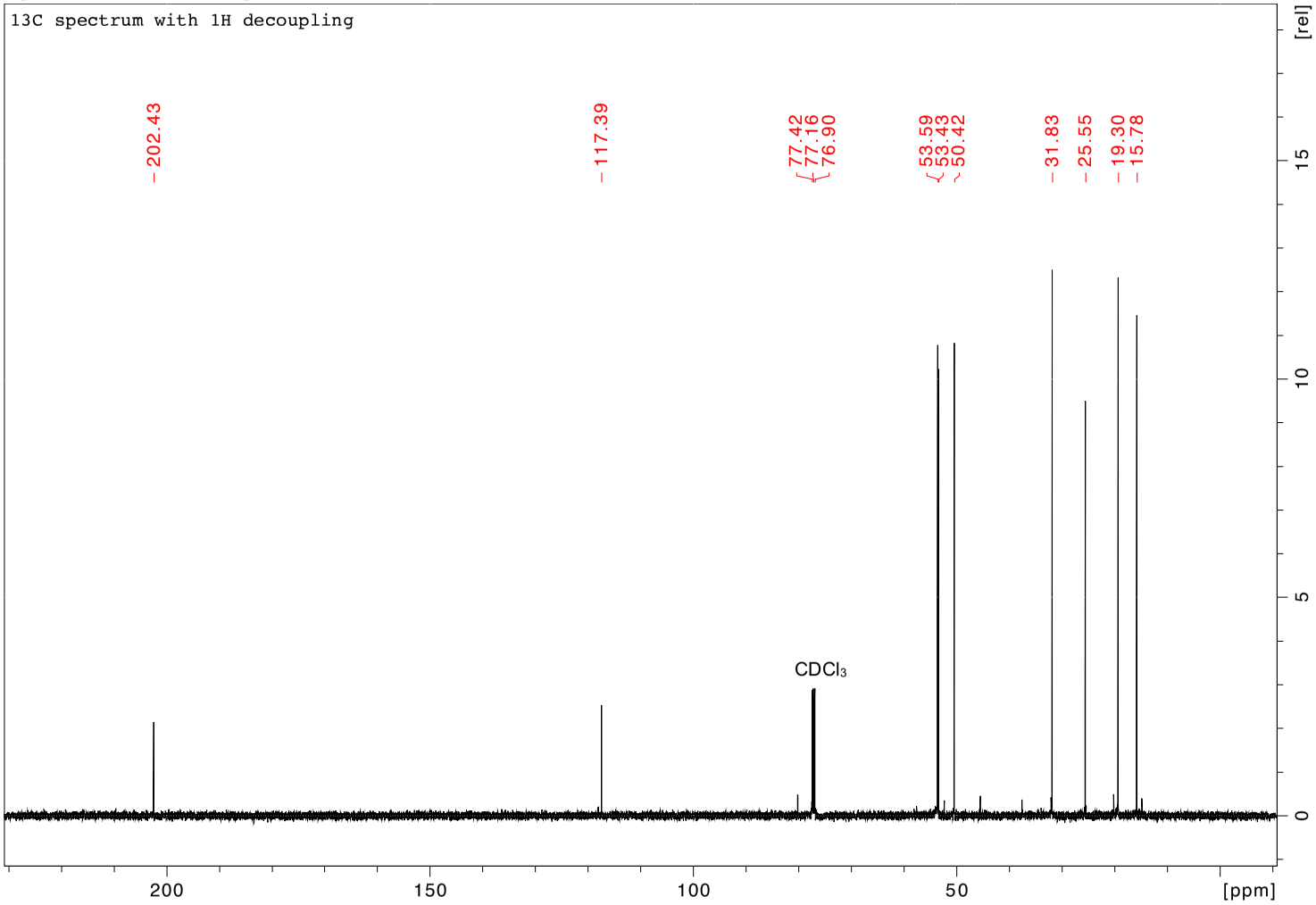

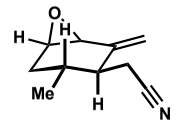

S5.9 (^{1}H NMR, 500 MHz, $CDCl_3$)

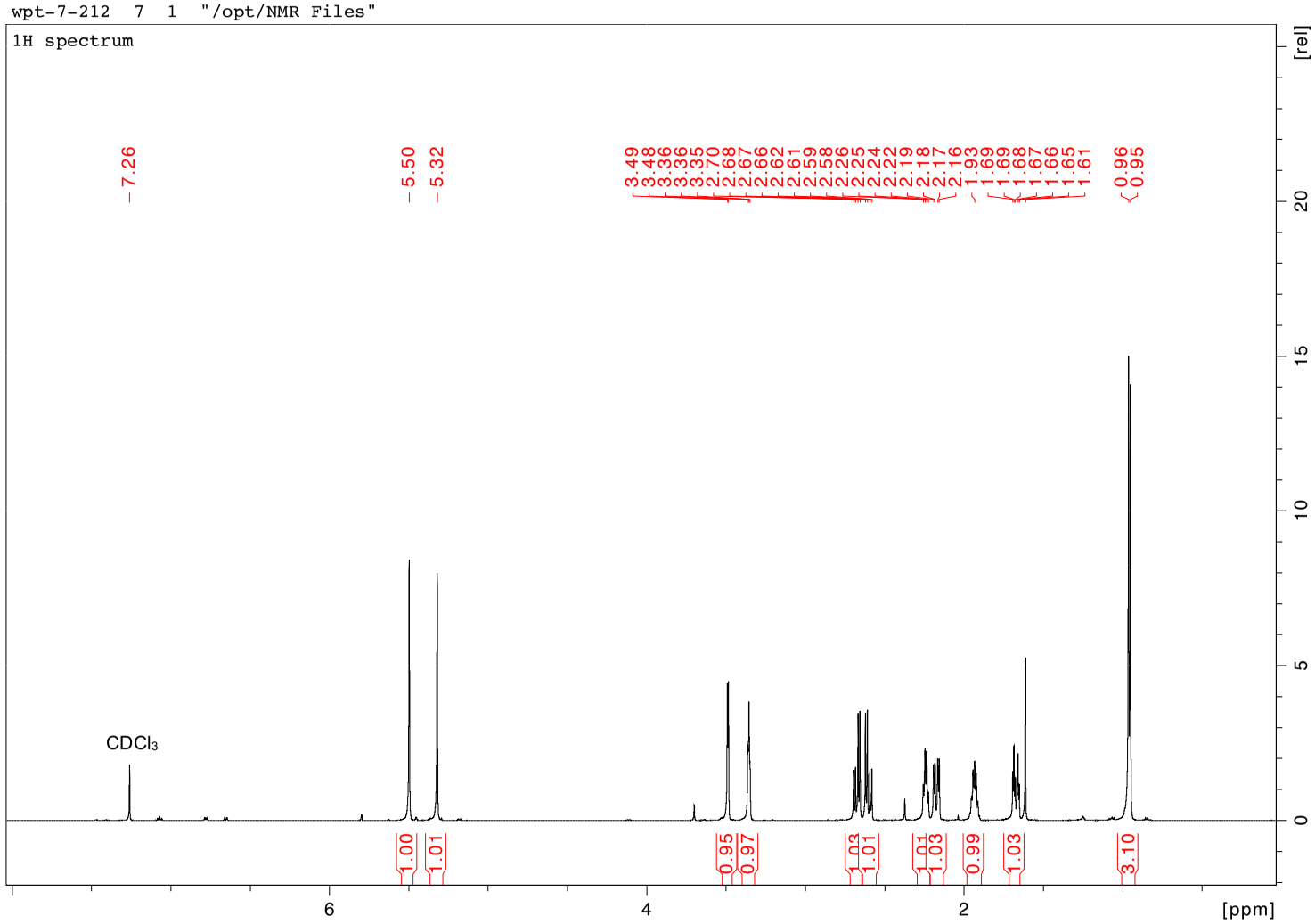

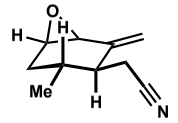

S5.9 (^{13}C NMR, 126 MHz, $CDCl_3$)

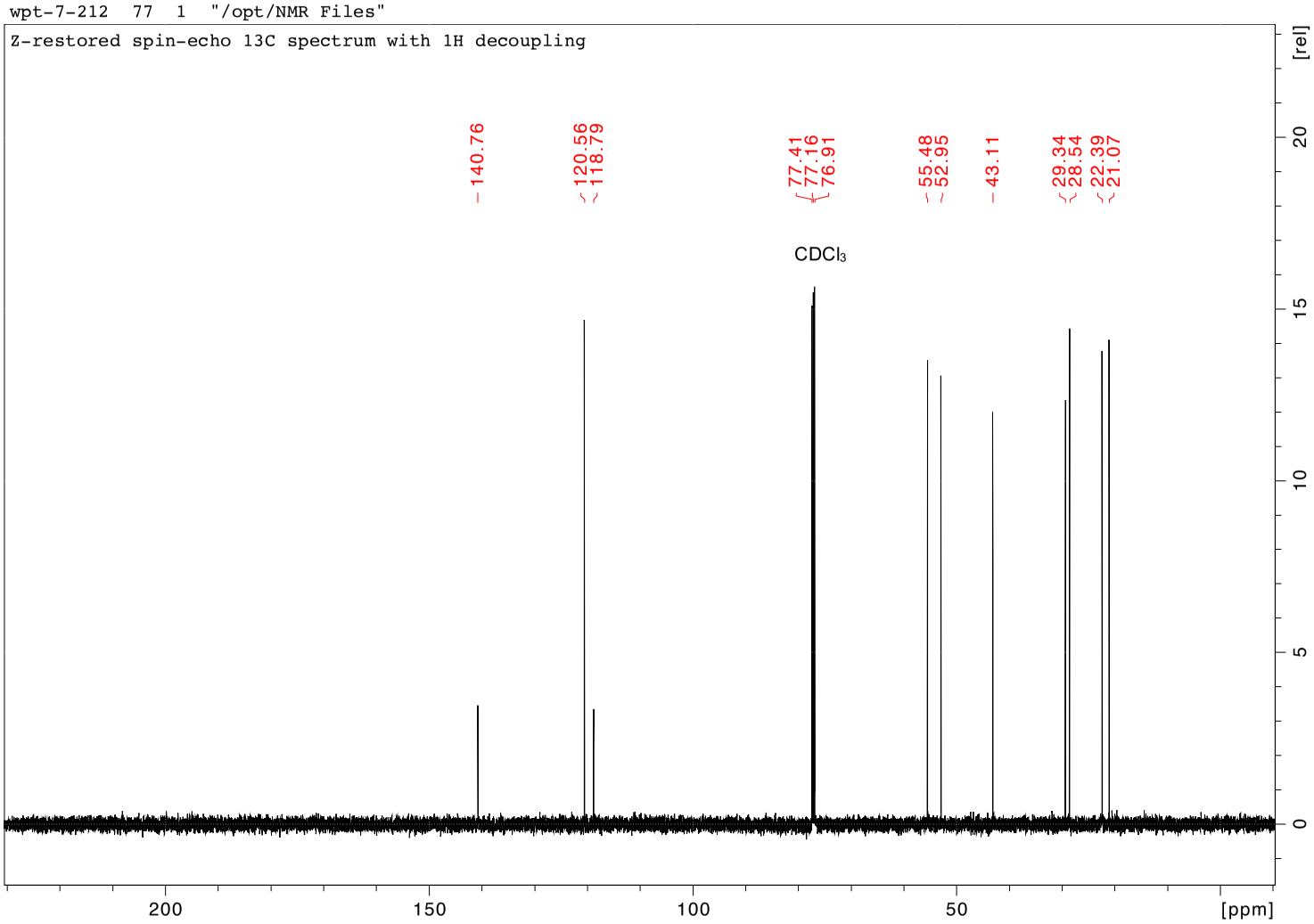

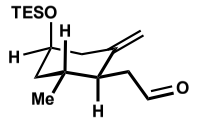

5.49 (^{1}H NMR, 500 MHz, $CDCl_3$)

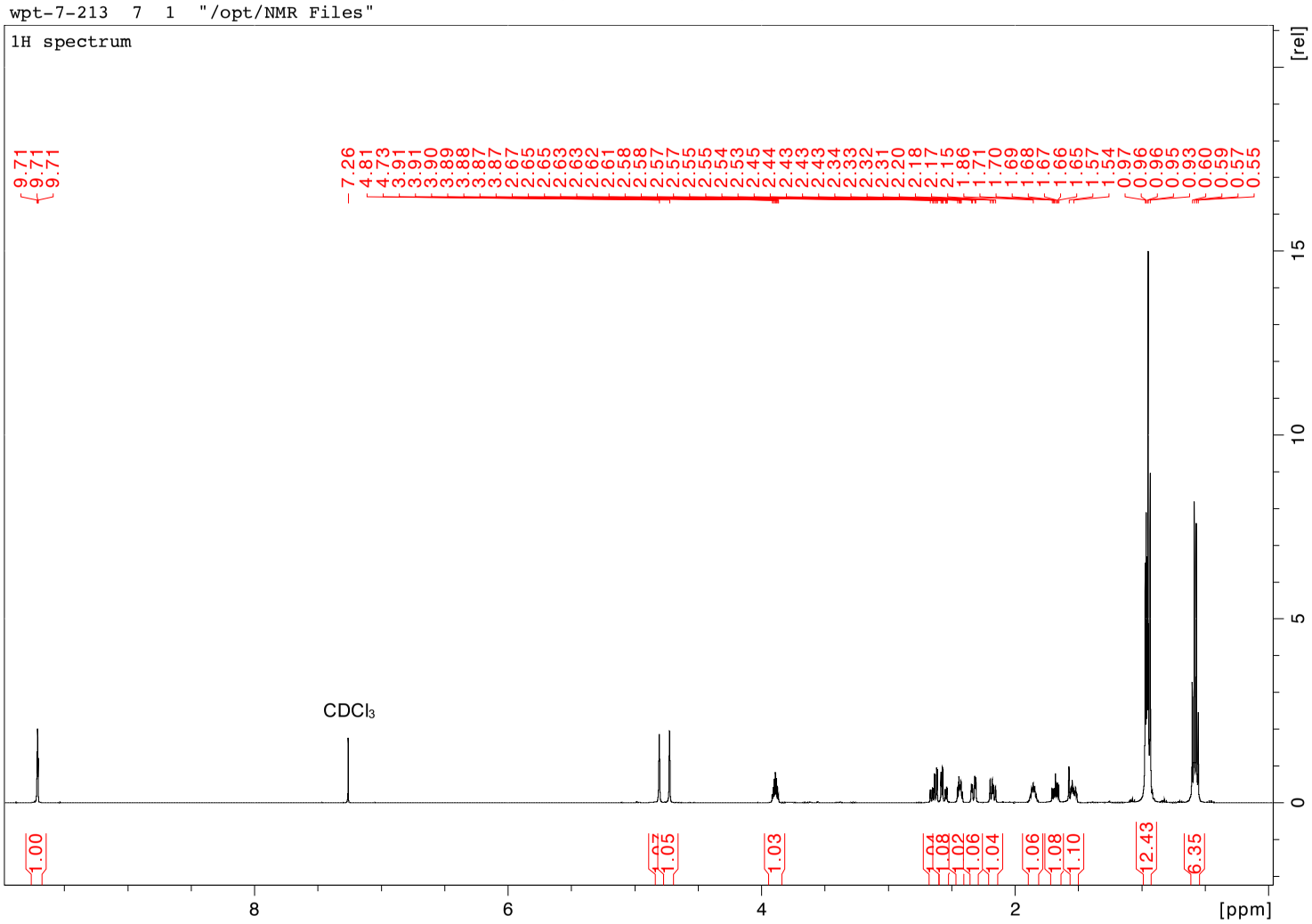

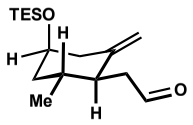

5.49 (^{13}C NMR, 126 MHz, $CDCl_3$)

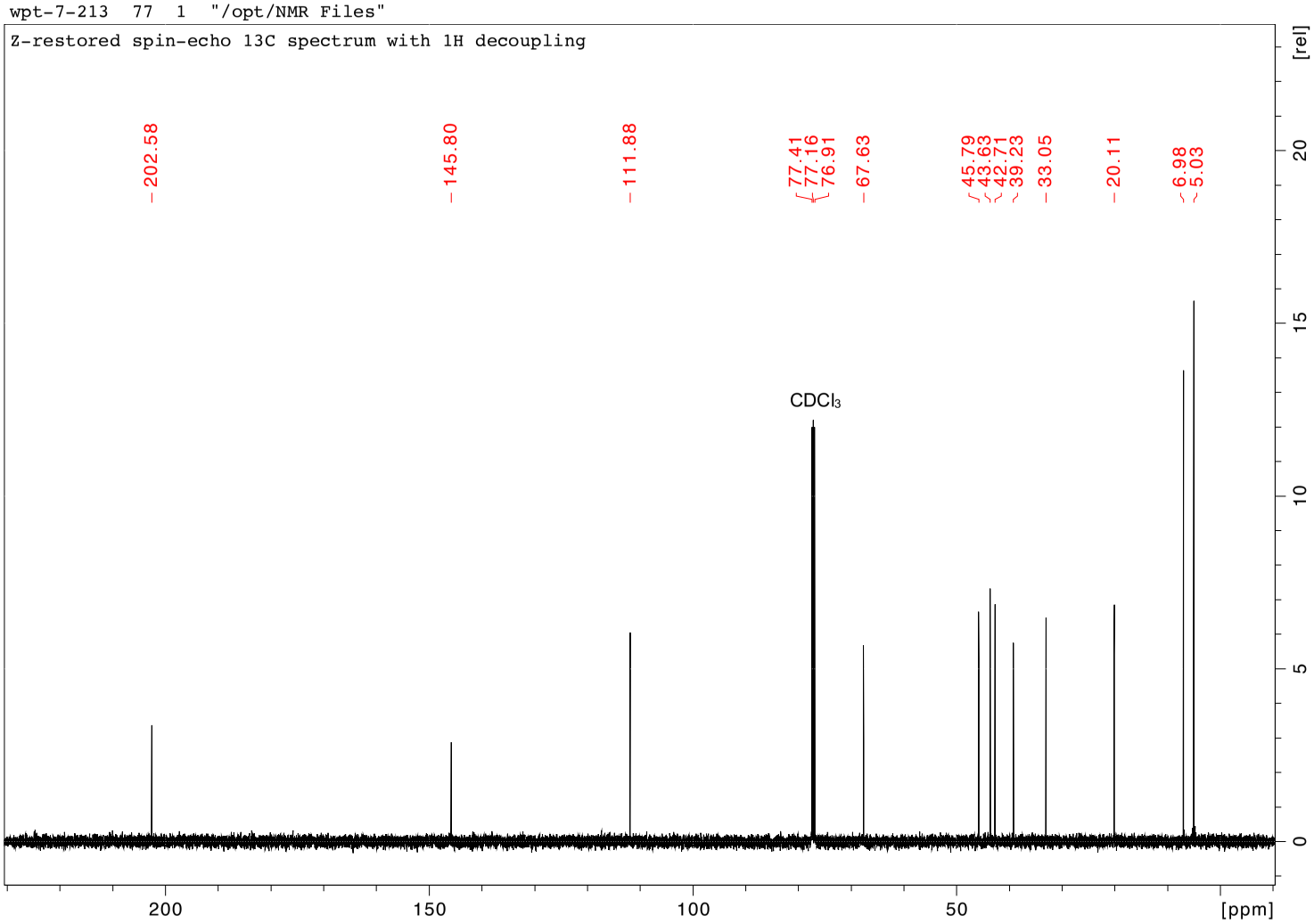

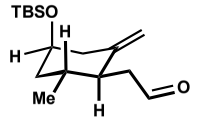

5.20 (^{1}H NMR, 500 MHz, $CDCl_3$)

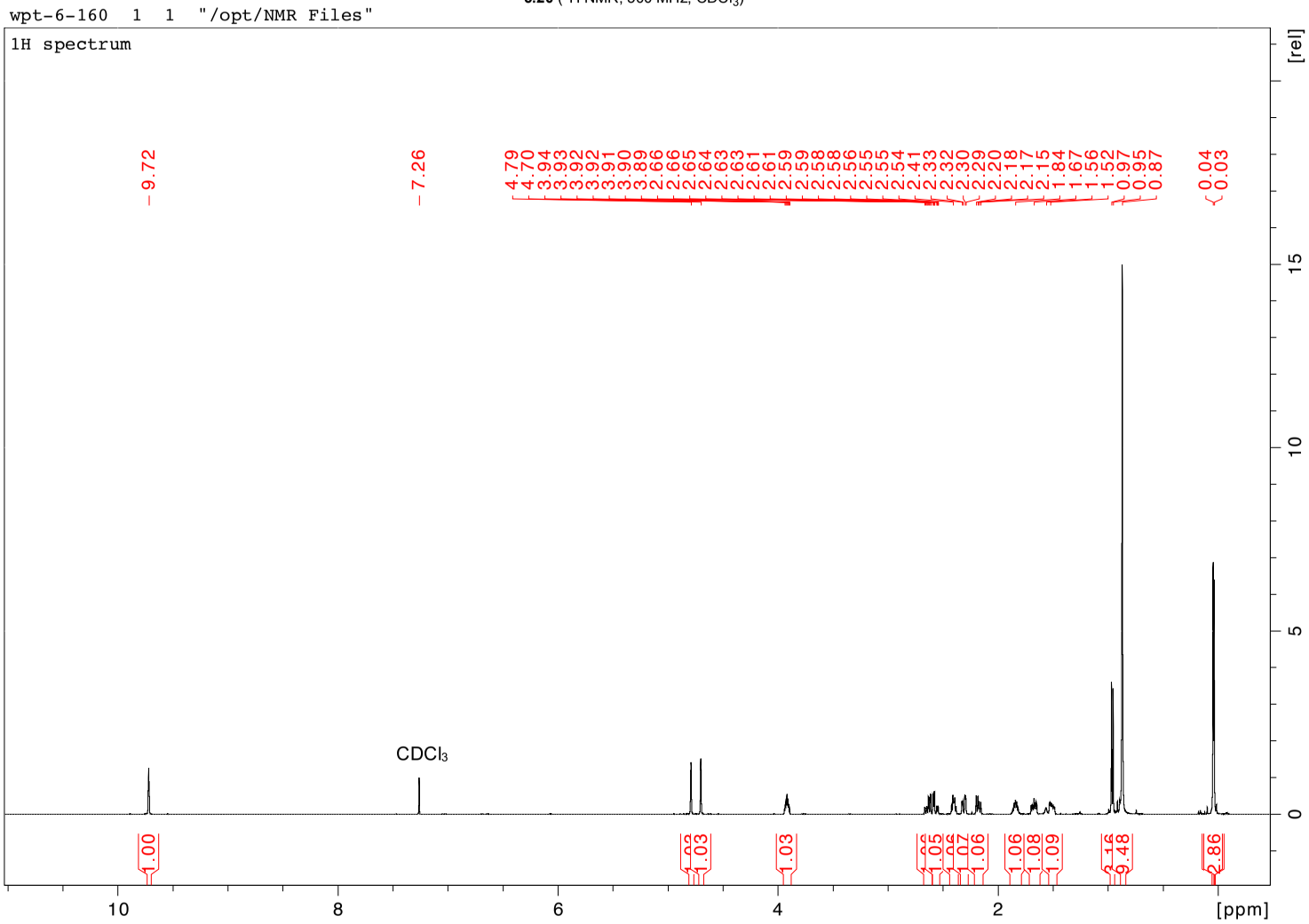

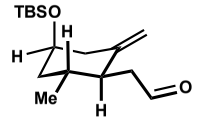

5.20 (^{13}C NMR, 126 MHz, $CDCl_3$)

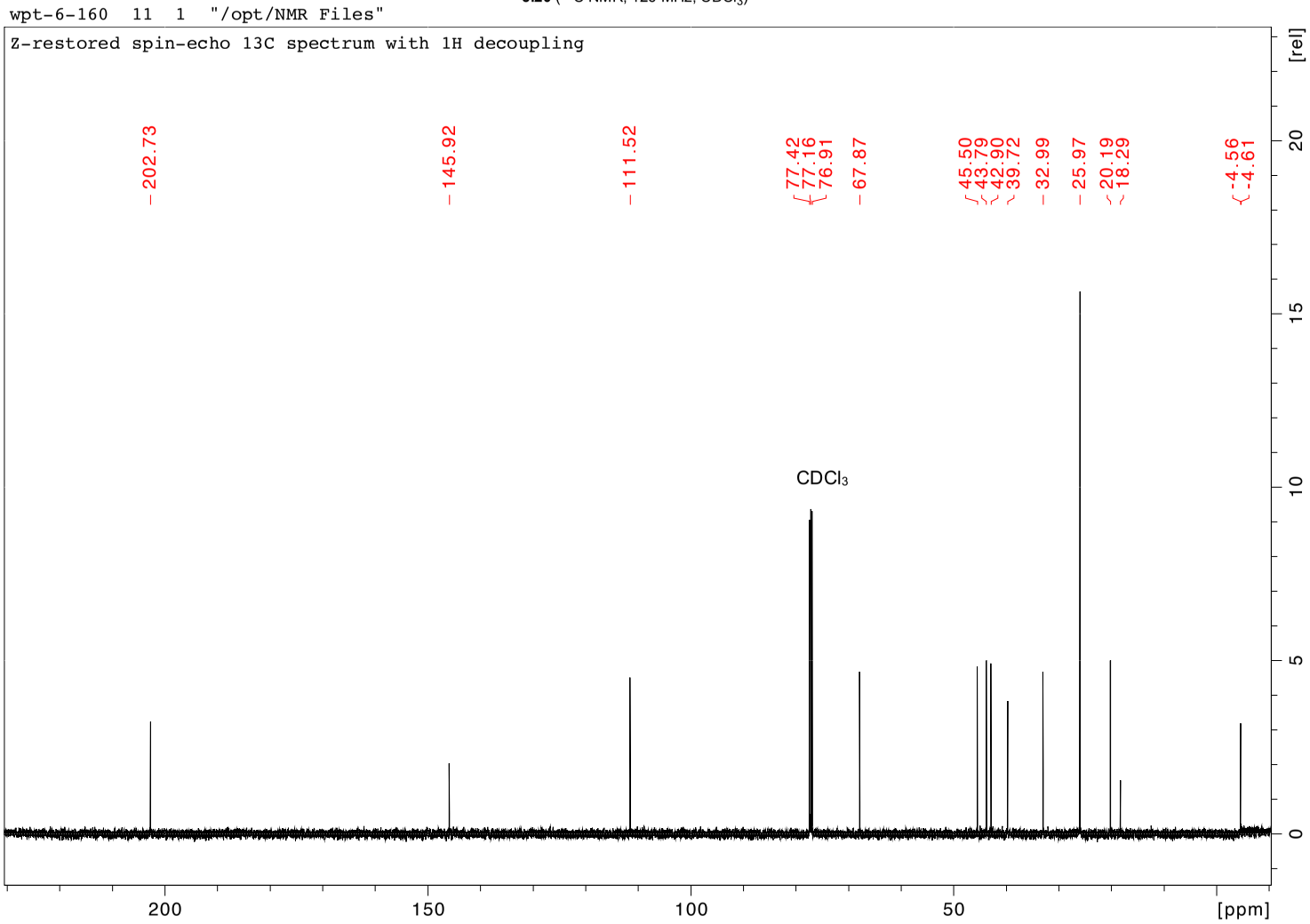

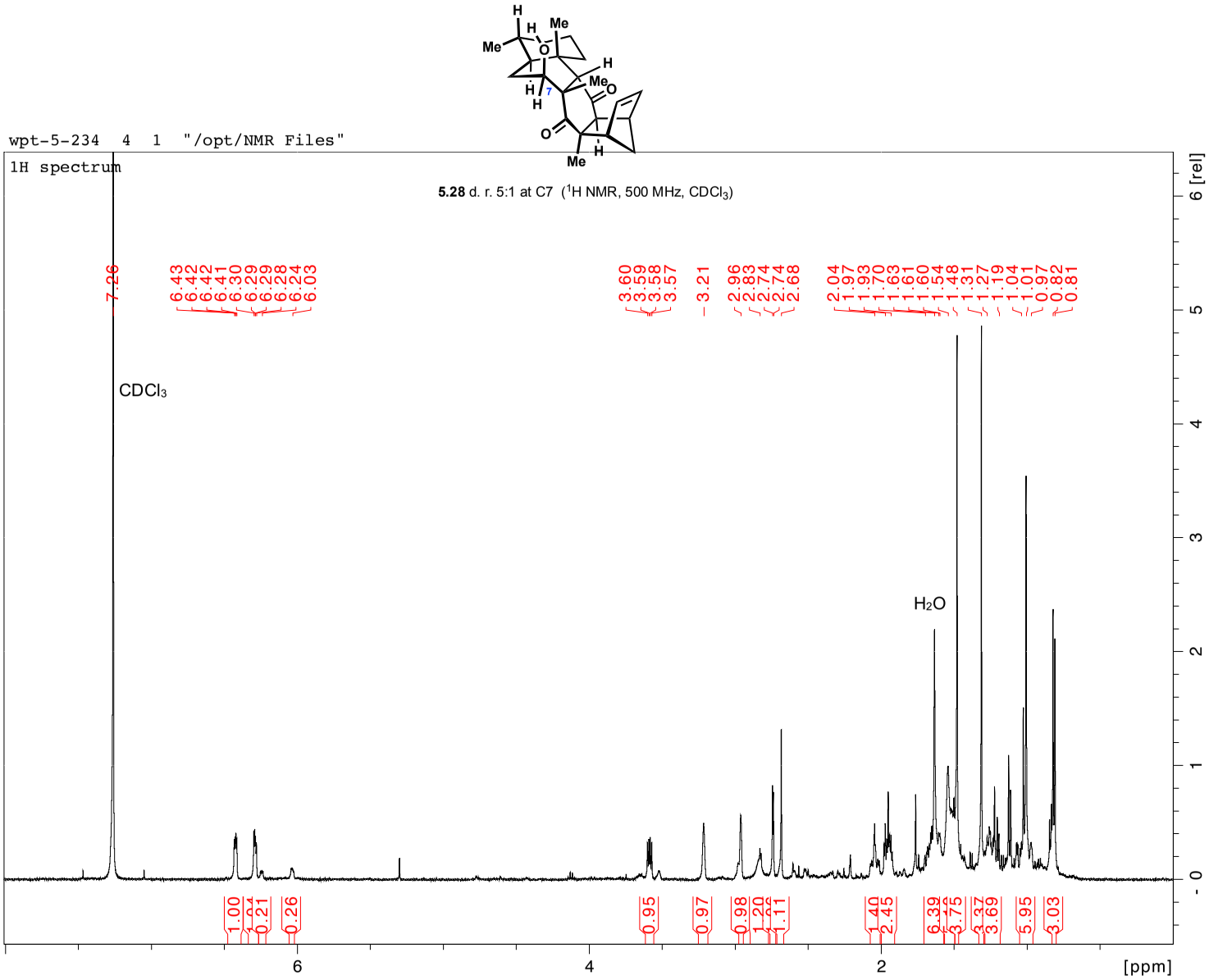
wpt-5-234 4 1 "/opt/NMR Files"
1H spectrum
5.28 d. r. 5:1 at C7 (1H NMR, 500 MHz, CDCl3)
7.26
6.43
6.42
6.42
6.41
6.30
6.29
6.29
6.28
6.24
6.03
3.60
3.59
3.58
3.57
3.21
2.96
2.83
2.74
2.74
2.68
2.04
1.97
1.93
1.70
1.63
1.61
1.60
1.54
1.48
1.31
1.27
1.19
1.04
1.01
0.97
0.82
0.81
CDCl3
H2O
1.00
0.95
0.97
0.98
1.40
2.45
6.39
3.75
3.69
5.95
3.03
6
4
2
[ppm]
6 [rel]

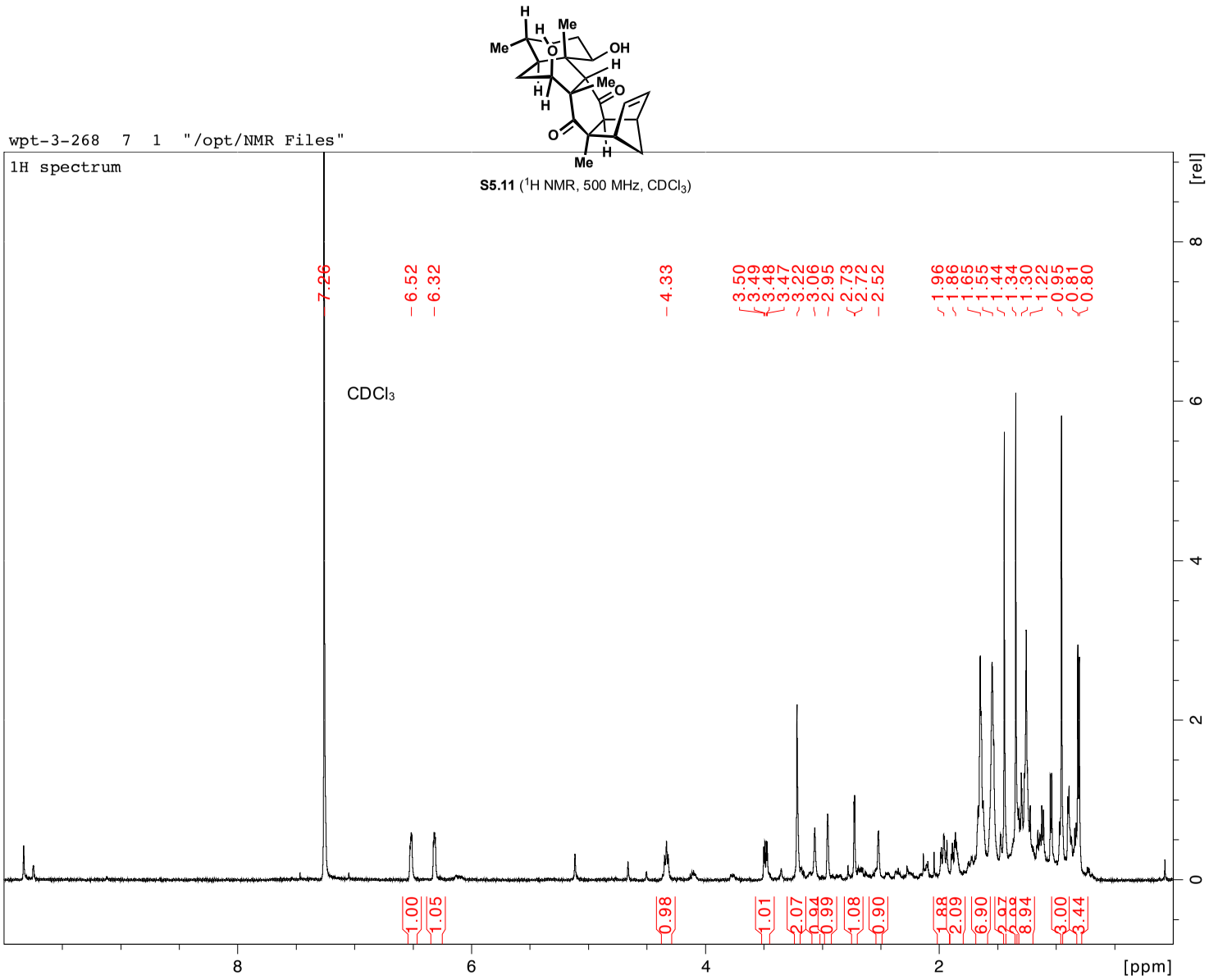

S5.11 (^{1}H NMR, 500 MHz, $CDCl_3$)

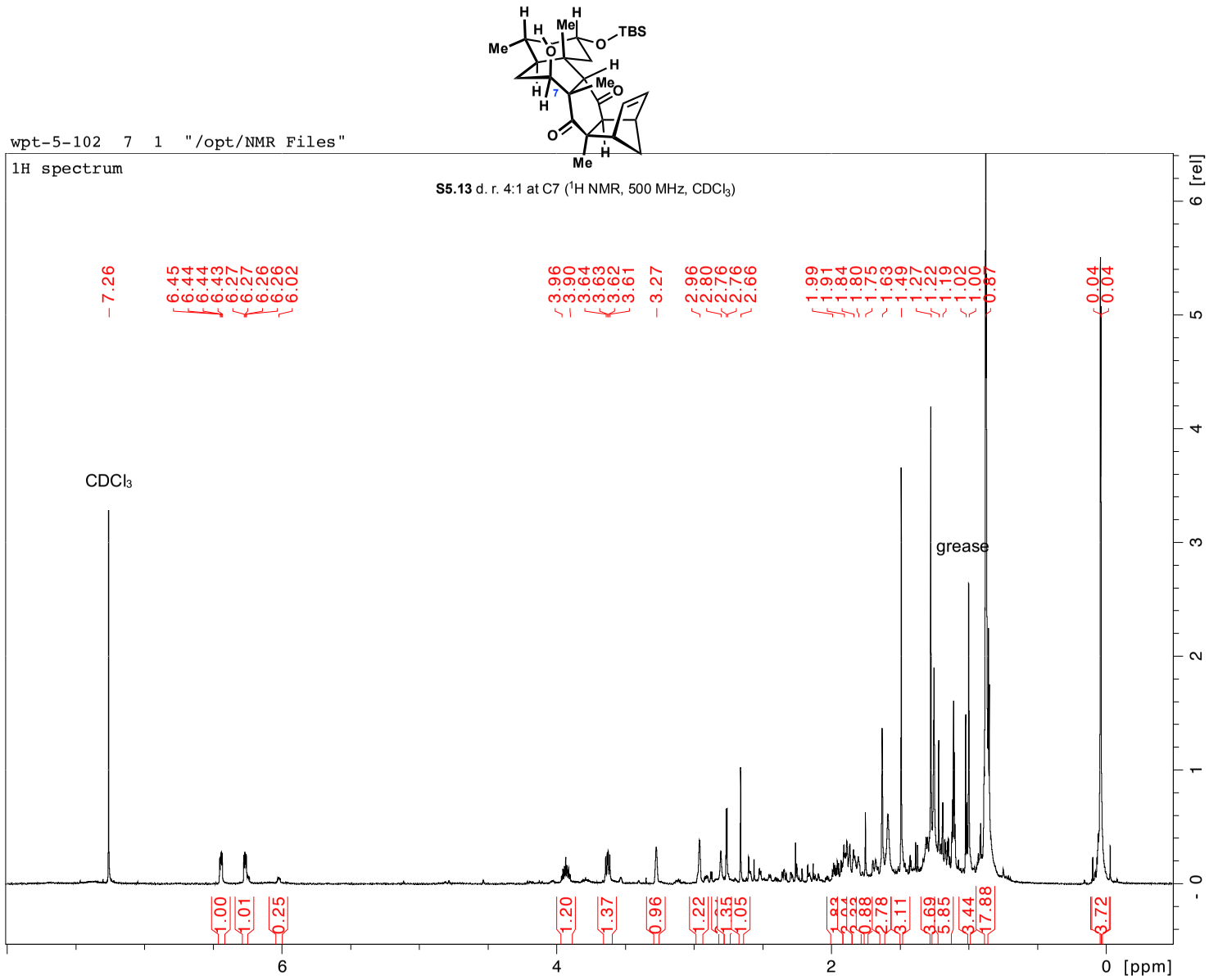
wpt-5-102 7 1 "/opt/NMR Files"
1H spectrum
S5.13 d. r. 4:1 at C7 (1H NMR, 500 MHz, CDCl3)
TBS
Me
CDCl3
grease
7.26
6.45
6.44
6.44
6.43
6.27
6.27
6.26
6.26
6.02
3.96
3.90
3.64
3.63
3.62
3.61
3.27
2.96
2.80
2.76
2.76
2.66
1.99
1.91
1.84
1.80
1.75
1.63
1.49
1.27
1.22
1.19
1.02
1.00
0.87
0.04
0.04
1.00
1.01
0.25
1.20
1.37
0.96
1.22
1.35
1.05
2.82
2.22
0.88
2.78
3.11
3.69
5.85
3.44
17.88
3.72
6
4
2
0 [ppm]
6 [rel]
5
4
3
2
1
0

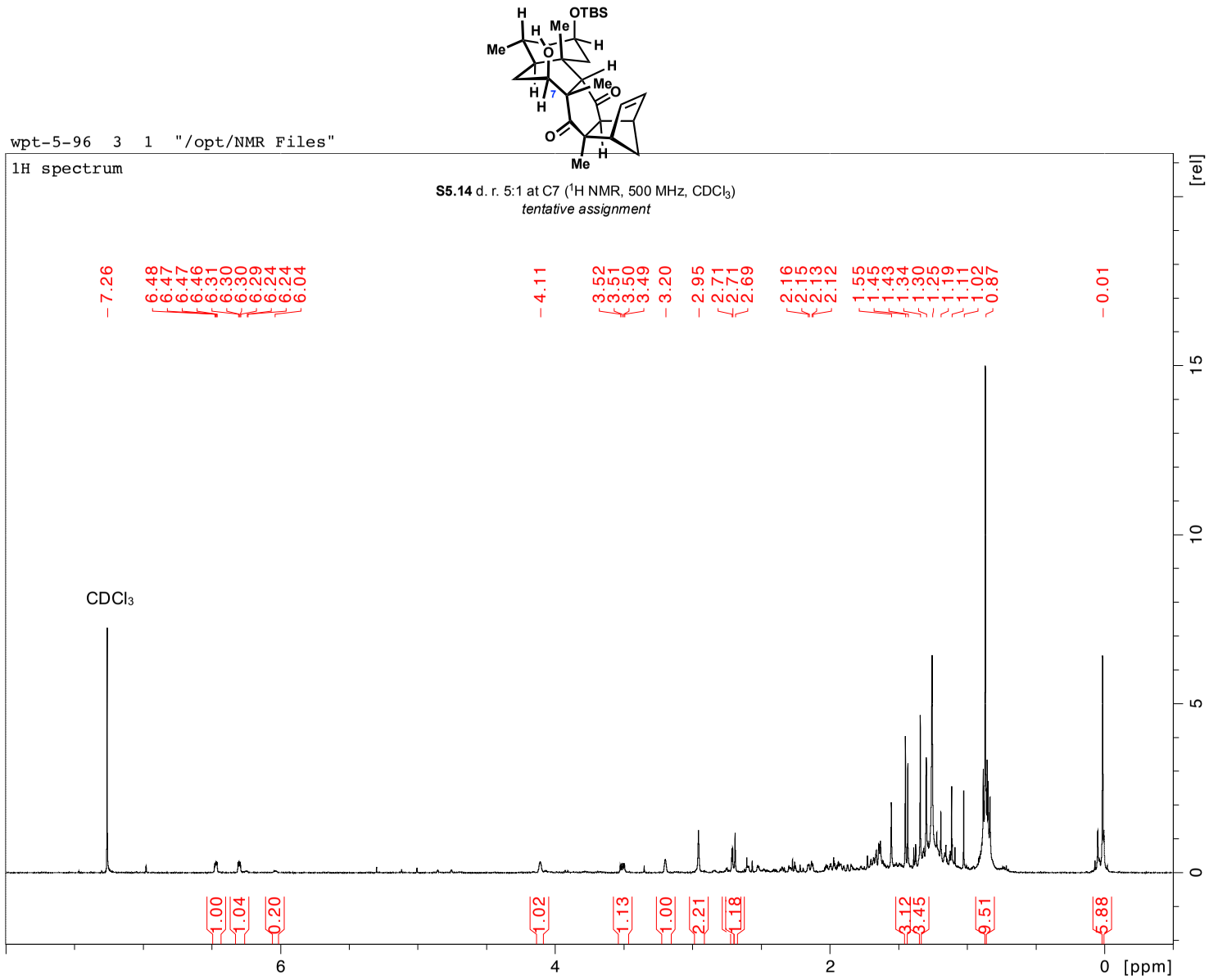
wpt-5-96 3 1 "/opt/NMR Files"
1H spectrum
S5.14 d. r. 5:1 at C7 (1H NMR, 500 MHz, CDCl3)
tentative assignment
OTBS
Me
O
H
7
CDCl3
7.26
6.48
6.47
6.47
6.46
6.31
6.30
6.30
6.29
6.24
6.24
6.04
4.11
3.52
3.51
3.50
3.49
3.20
2.95
2.71
2.71
2.69
2.16
2.15
2.13
2.12
1.55
1.45
1.43
1.34
1.30
1.25
1.19
1.11
1.02
0.87
0.01
1.00
1.04
0.20
1.02
1.13
1.00
2.21
1.18
3.12
3.45
9.51
5.88
6
4
2
0
[ppm]
[rel]
15
10
5
0

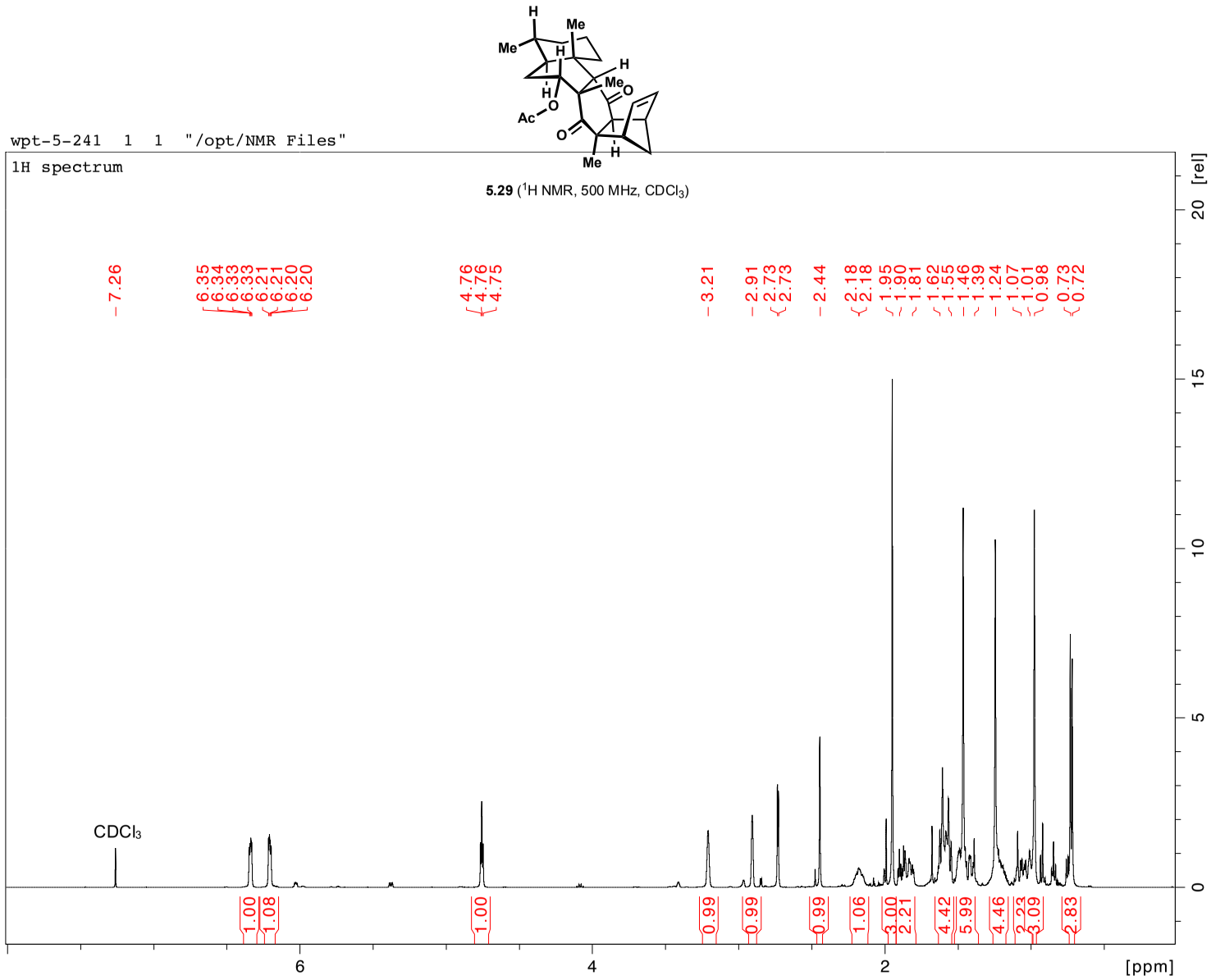
wpt-5-241 1 1 "/opt/NMR Files"
1H spectrum
5.29 (1H NMR, 500 MHz, CDCl3)
7.26
6.35
6.34
6.33
6.33
6.21
6.21
6.20
6.20
4.76
4.76
4.75
3.21
2.91
2.73
2.73
2.44
2.18
2.18
1.95
1.90
1.81
1.62
1.55
1.46
1.39
1.24
1.07
1.01
0.98
0.73
0.72
CDCl3
1.00
1.08
1.00
0.99
0.99
0.99
1.06
3.00
2.21
4.42
5.99
4.46
2.23
3.09
2.83
6
4
2
[ppm]
20
15
10
5
0
[rel]

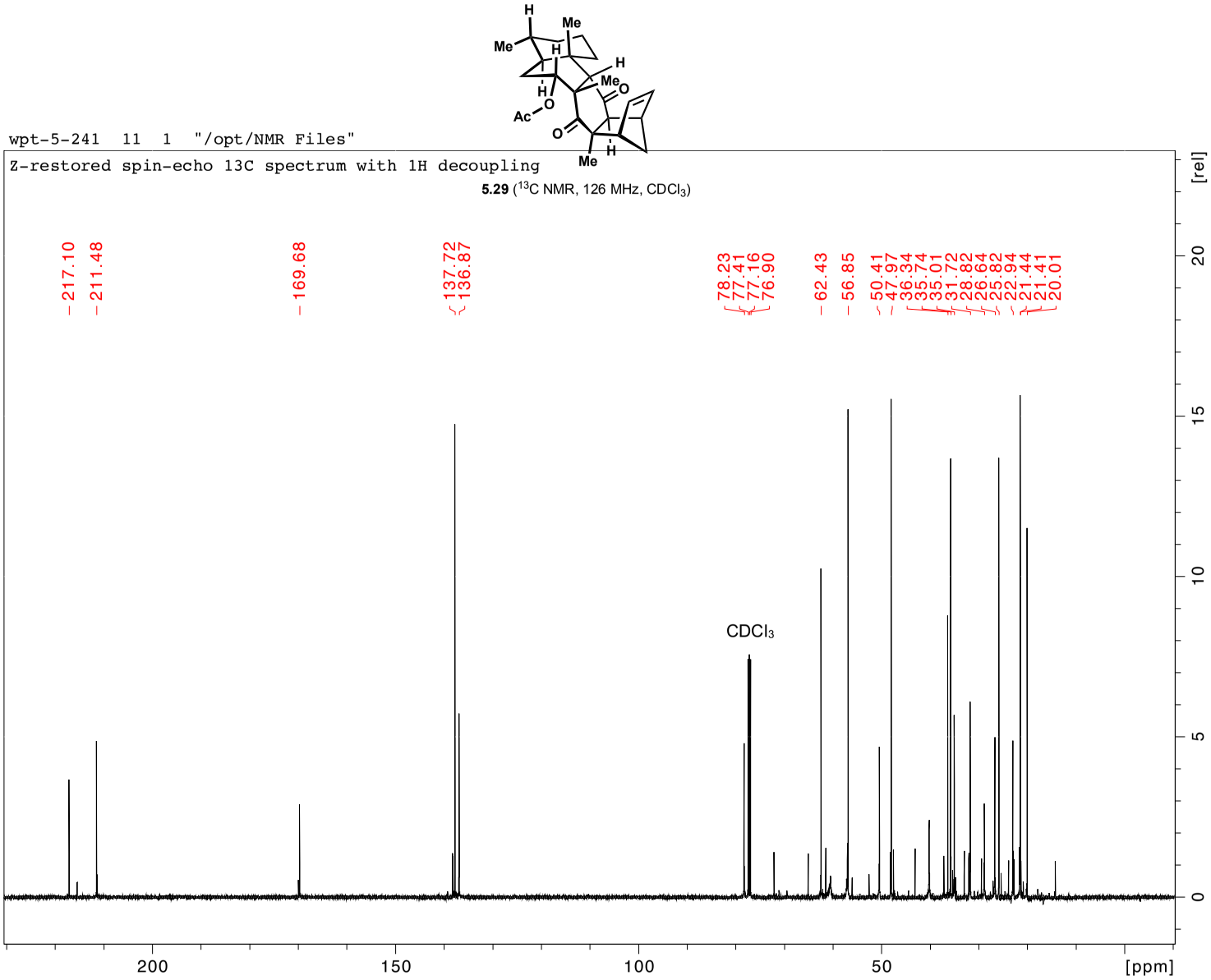
wpt-5-241 11 1 "/opt/NMR Files"
Z-restored spin-echo 13C spectrum with 1H decoupling
5.29 (13C NMR, 126 MHz, CDCl3)
217.10
211.48
169.68
137.72
136.87
78.23
77.41
77.16
76.90
62.43
56.85
50.41
47.97
36.34
35.74
35.01
31.72
28.82
26.64
25.82
22.94
21.44
21.41
20.01
CDCl3
[rel]
[ppm]

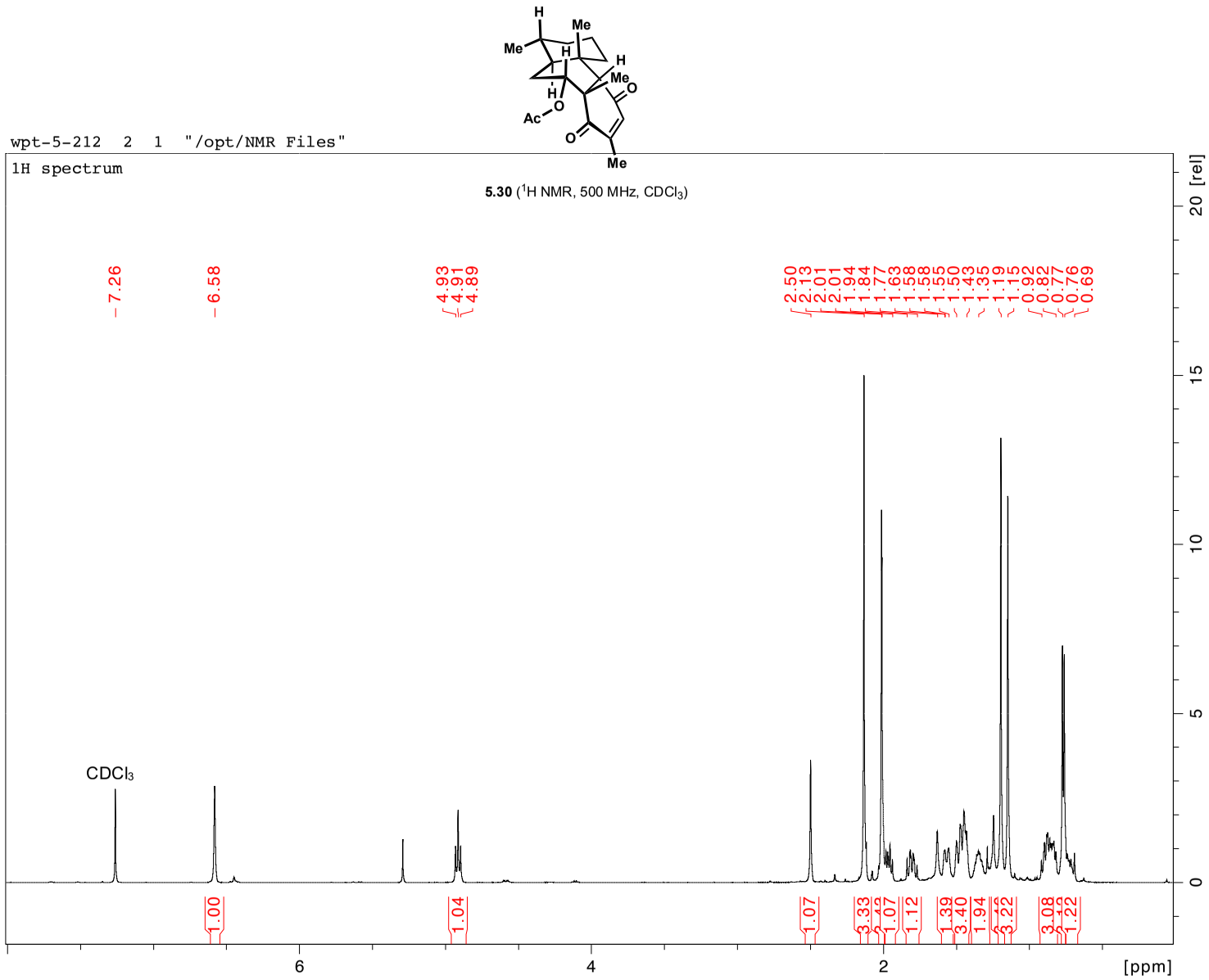
wpt-5-212 2 1 "/opt/NMR Files"
1H spectrum
5.30 (1H NMR, 500 MHz, CDCl3)
7.26
6.58
4.93
4.91
4.89
2.50
2.13
2.01
2.01
1.94
1.84
1.77
1.63
1.58
1.58
1.55
1.50
1.43
1.35
1.19
1.15
0.92
0.82
0.77
0.76
0.69
CDCl3
1.00
1.04
1.07
3.33
2.15
1.07
1.12
1.39
3.40
1.94
2.26
3.22
3.08
2.19
1.22
20 [rel]
15
10
5
0
6
4
2
[ppm]

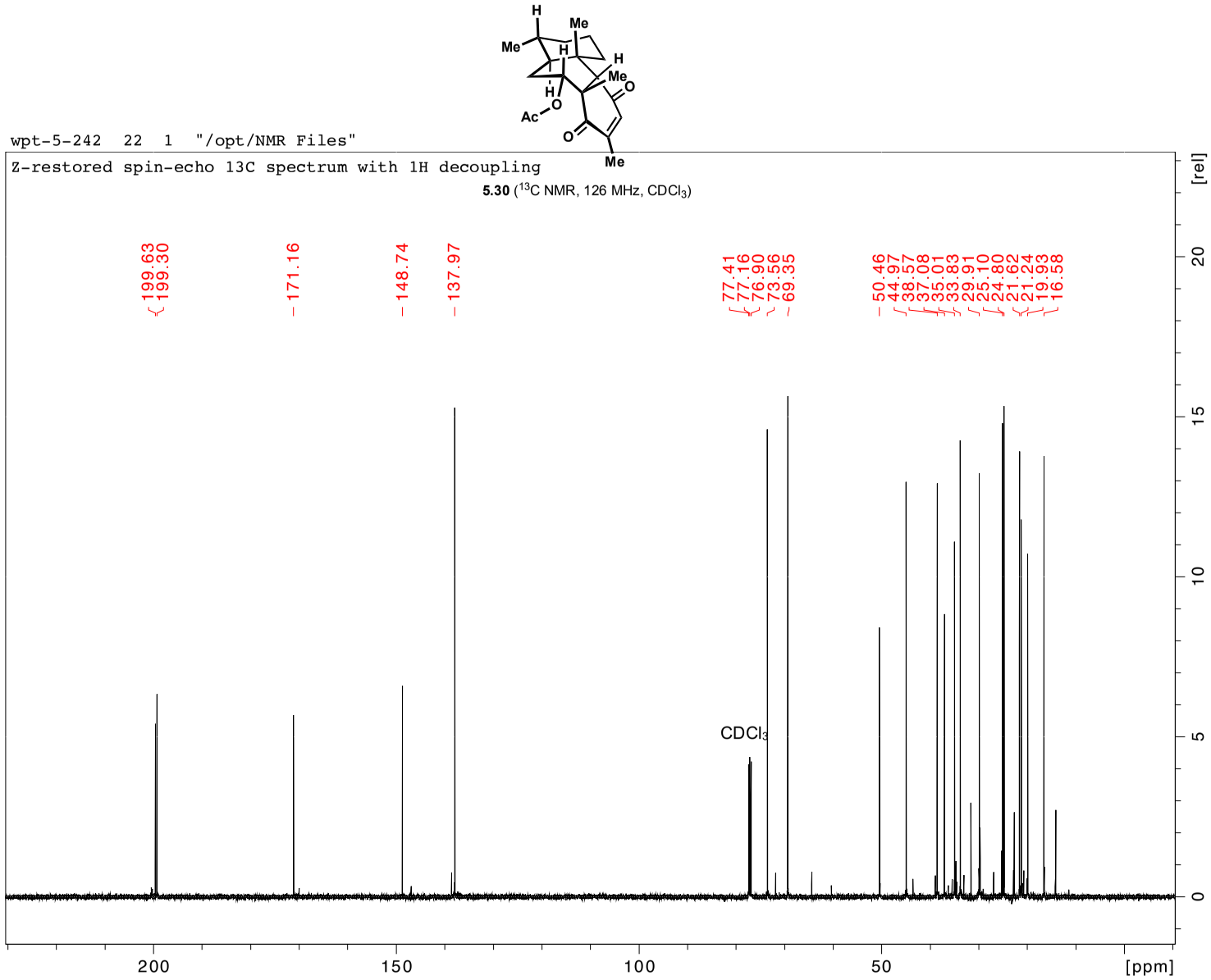
wpt-5-242 22 1 "/opt/NMR Files"
Z-restored spin-echo 13C spectrum with 1H decoupling
5.30 (13C NMR, 126 MHz, CDCl3)
199.63
199.30
171.16
148.74
137.97
77.41
77.16
76.90
73.56
69.35
50.46
44.97
38.57
37.08
35.01
33.83
29.91
25.10
24.80
21.62
21.24
19.93
16.58
CDCl3
[rel]
[ppm]

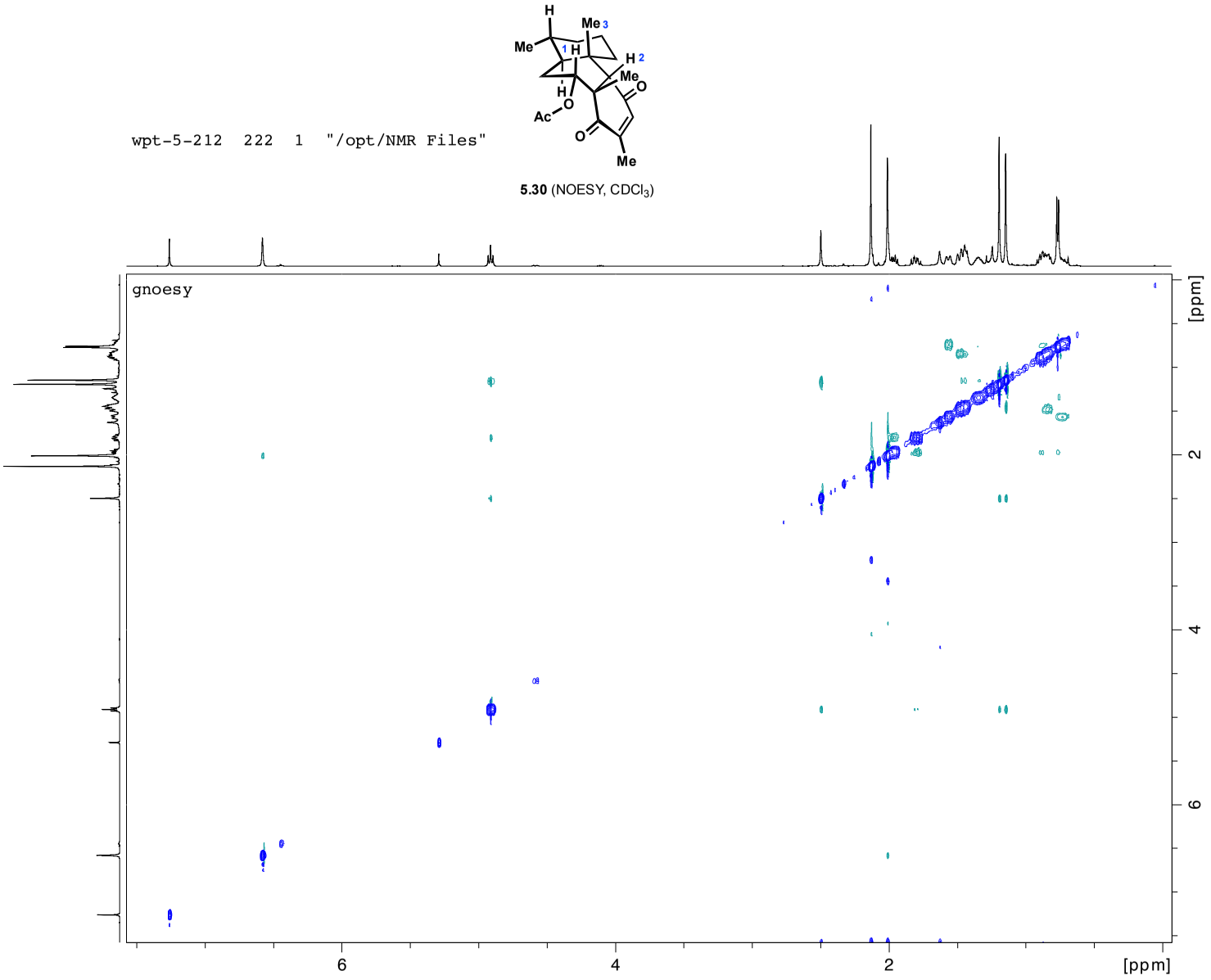

5.30 (NOESY, $CDCl_3$)

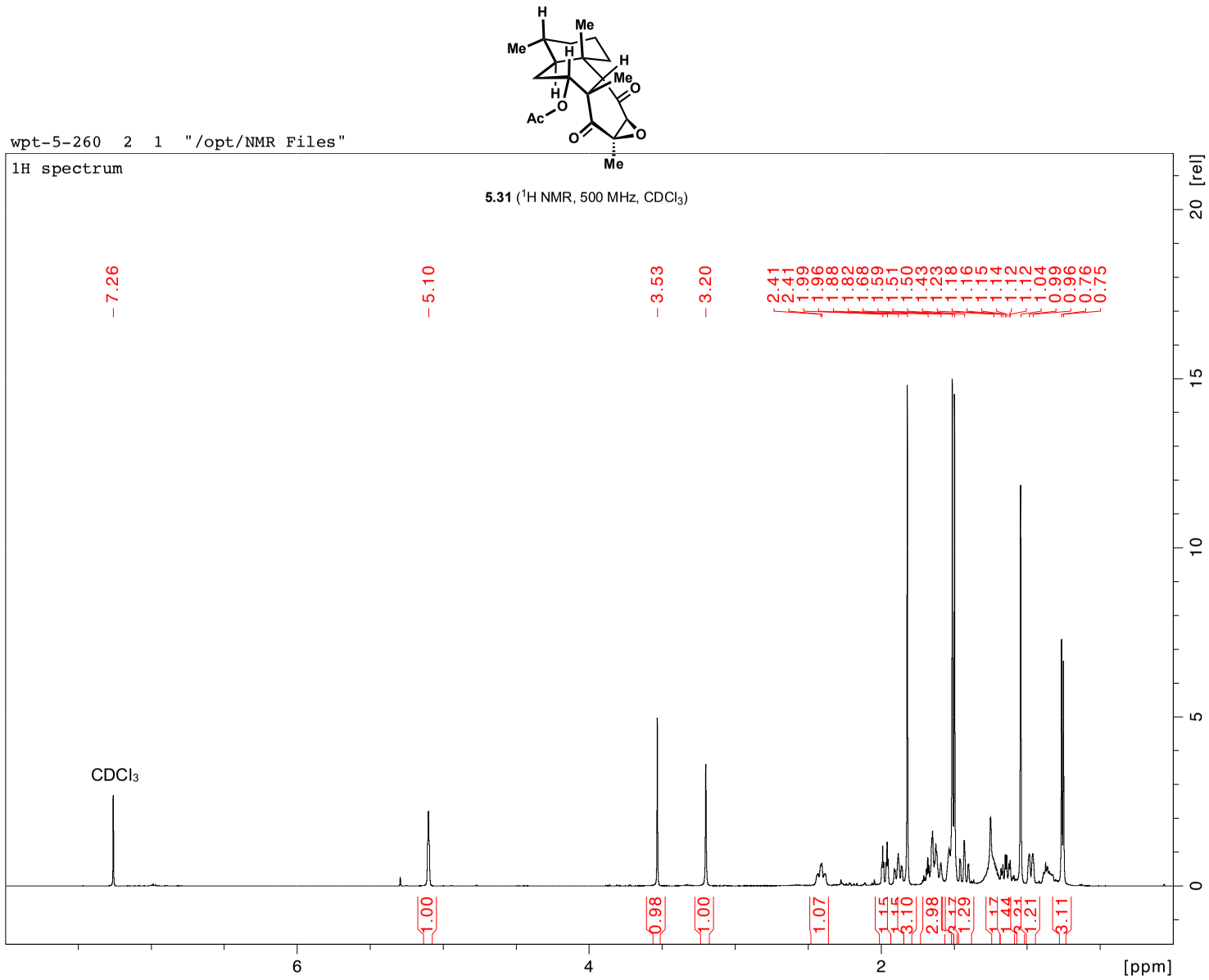
wpt-5-260 2 1 "/opt/NMR Files"
1H spectrum
5.31 (1H NMR, 500 MHz, CDCl3)
7.26
5.10
3.53
3.20
2.41
2.41
1.99
1.96
1.88
1.82
1.68
1.59
1.51
1.50
1.43
1.23
1.18
1.16
1.15
1.14
1.12
1.12
1.04
0.99
0.96
0.76
0.75
CDCl3
1.00
0.98
1.00
1.07
1.15
1.15
3.10
2.98
2.17
1.29
1.17
1.44
2.21
3.11
6
4
2
[ppm]
20
15
10
5
0
[rel]

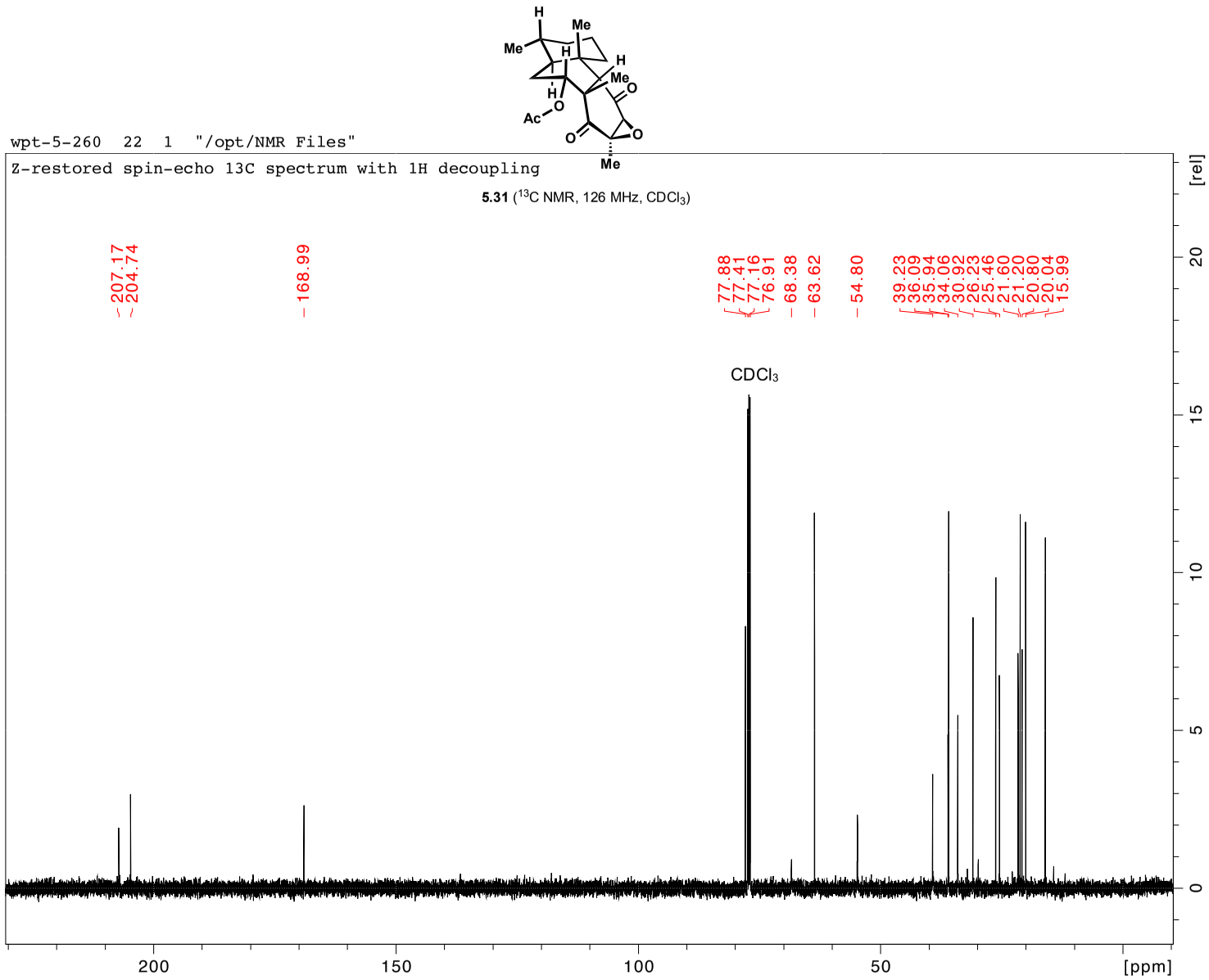
wpt-5-260 22 1 "/opt/NMR Files"
Z-restored spin-echo 13C spectrum with 1H decoupling
5.31 (13C NMR, 126 MHz, CDCl3)
207.17
204.74
168.99
77.88
77.41
77.16
76.91
68.38
63.62
54.80
39.23
36.09
35.94
34.06
30.92
26.23
25.46
21.60
21.20
20.80
20.04
15.99
CDCl3
[rel]
[ppm]

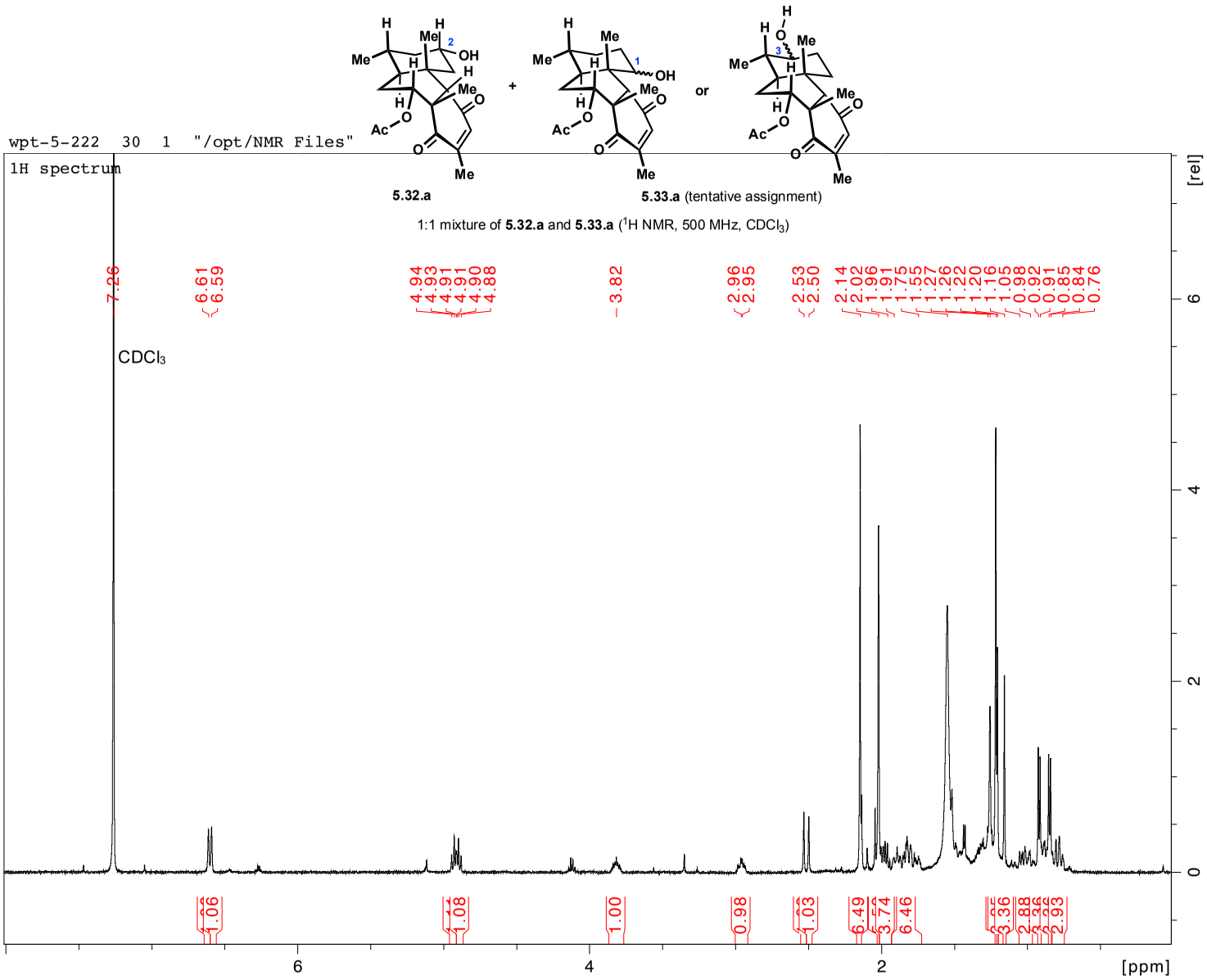
wpt-5-222 30 1 "/opt/NMR Files"
1H spectrum
5.32.a
5.33.a (tentative assignment)
1:1 mixture of 5.32.a and 5.33.a (1H NMR, 500 MHz, CDCl3)
7.26
CDCl3
6.61
6.59
4.94
4.93
4.91
4.91
4.90
4.88
3.82
2.96
2.95
2.53
2.50
2.14
2.02
1.96
1.91
1.75
1.55
1.27
1.26
1.22
1.20
1.16
1.05
0.98
0.92
0.91
0.85
0.84
0.76
1.06
1.08
1.00
0.98
1.03
6.49
3.74
6.46
2.36
2.88
2.93
[rel]
[ppm]

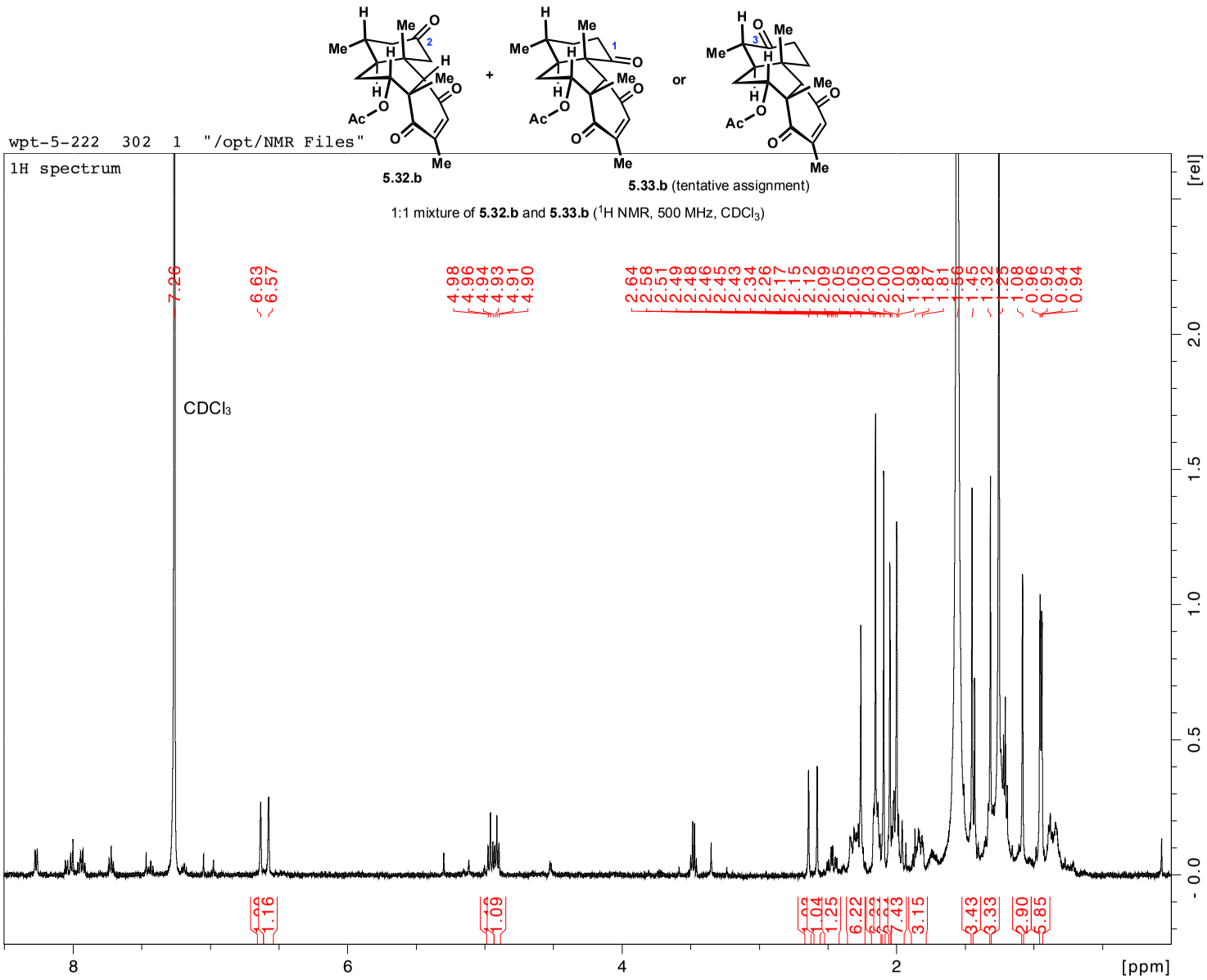
wpt-5-222 302 1 "/opt/NMR Files"
1H spectrum
5.32.b
5.33.b (tentative assignment)
1:1 mixture of 5.32.b and 5.33.b (1H NMR, 500 MHz, CDCl3)
CDCl3
[rel]
[ppm]

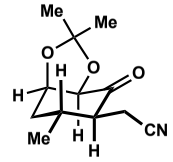

wpt-7-82 8 1 "/opt/NMR Files"

S5.16 (^{1}H NMR, 500 MHz, $CDCl_3$)

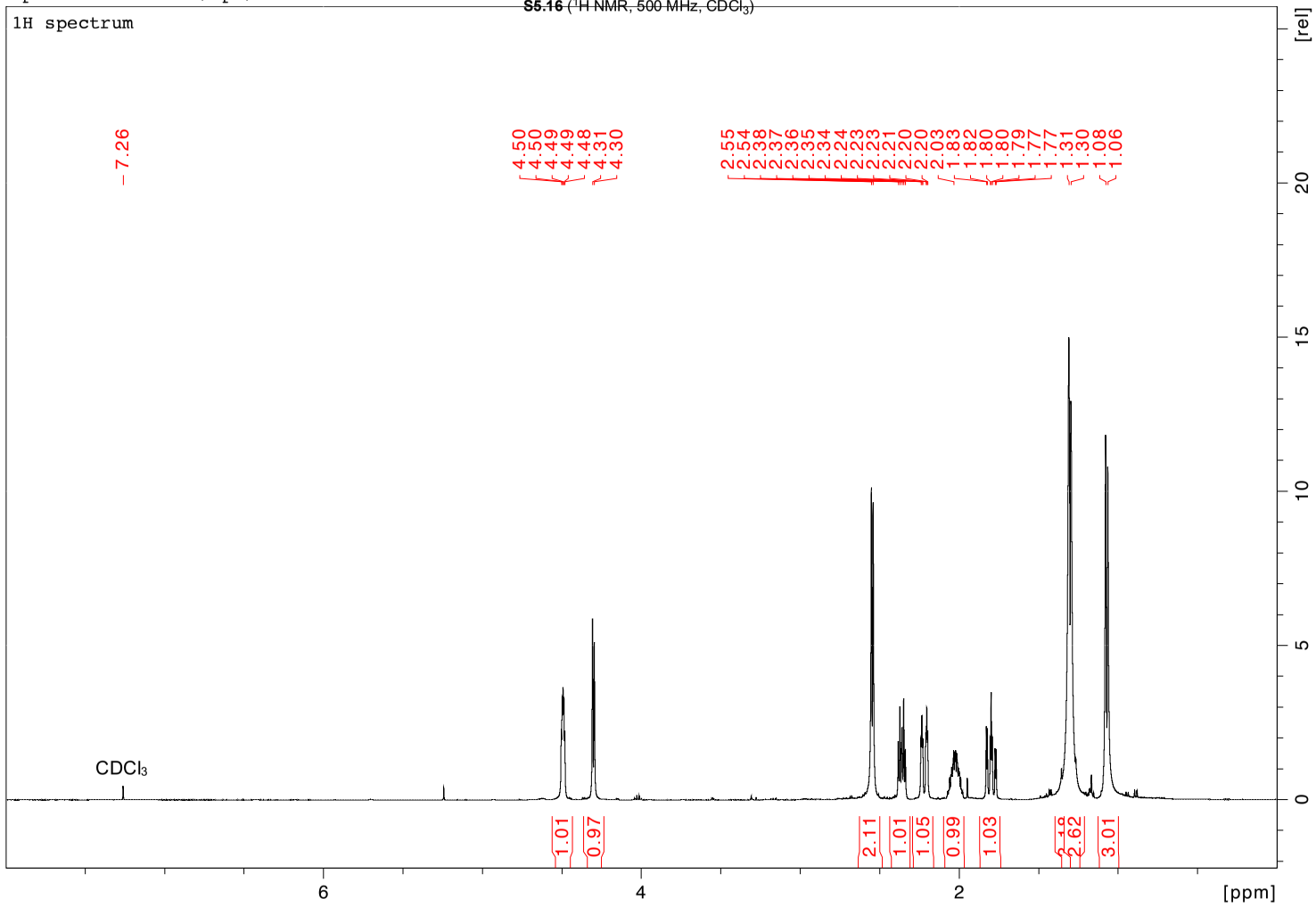

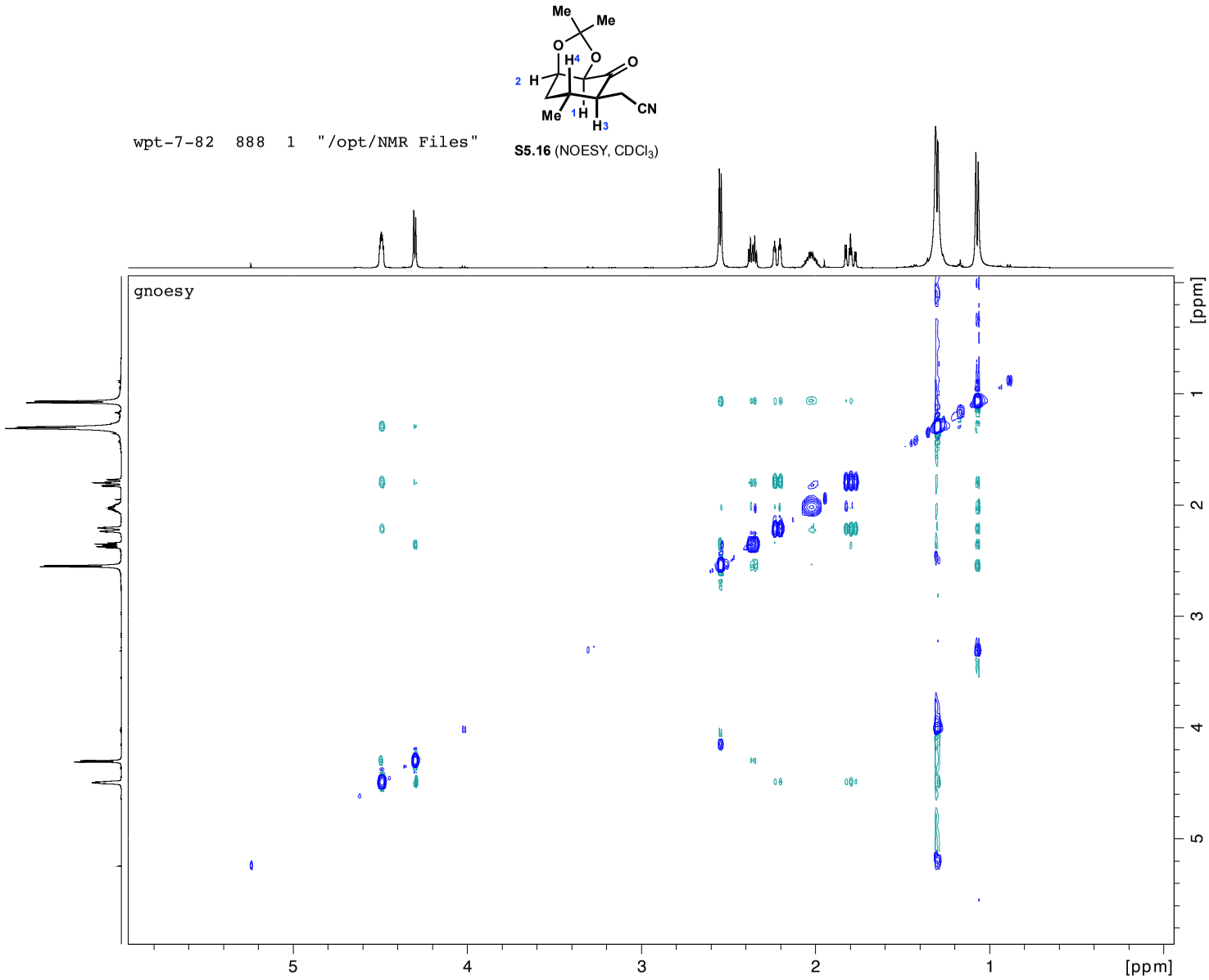
Me
Me
O
O
H4
O
2 H
O
CN
Me
1H
H3
wpt-7-82 888 1 "/opt/NMR Files"
S5.16 (NOESY, CDCl3)
gnoesy
5
4
3
2
1
[ppm]
[ppm]

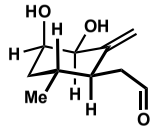

5.44 (^{1}H NMR, 500 MHz, $CDCl_3$)

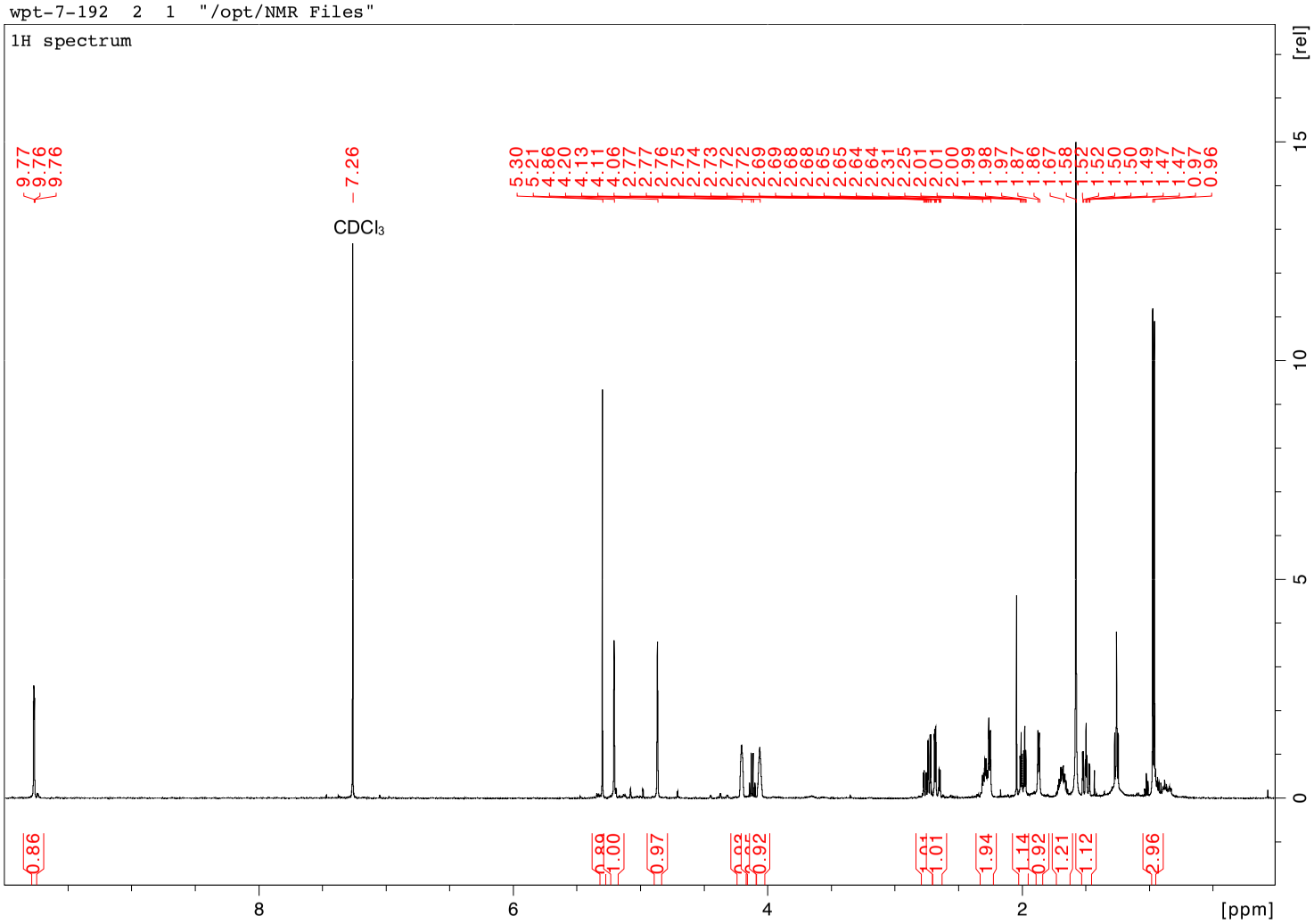

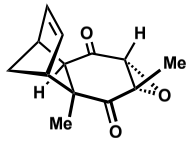

5.52 (^{1}H NMR, 500 MHz, $CDCl_3$)

wpt-6-152 1 1 "/opt/NMR Files"

1H spectrum

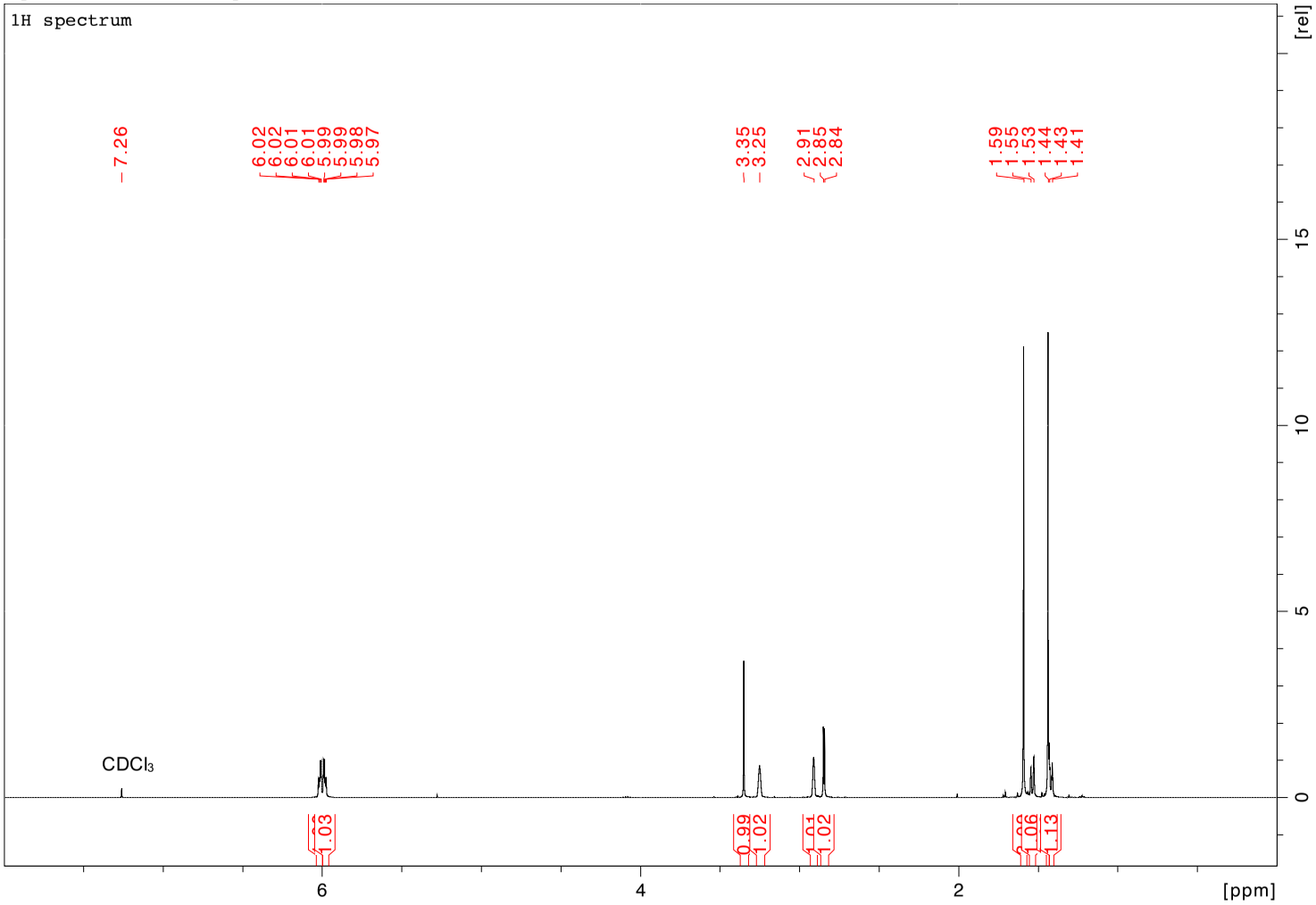

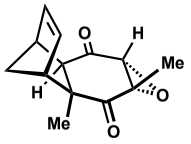

5.52 (^{13}C NMR, 126 MHz, $CDCl_3$)

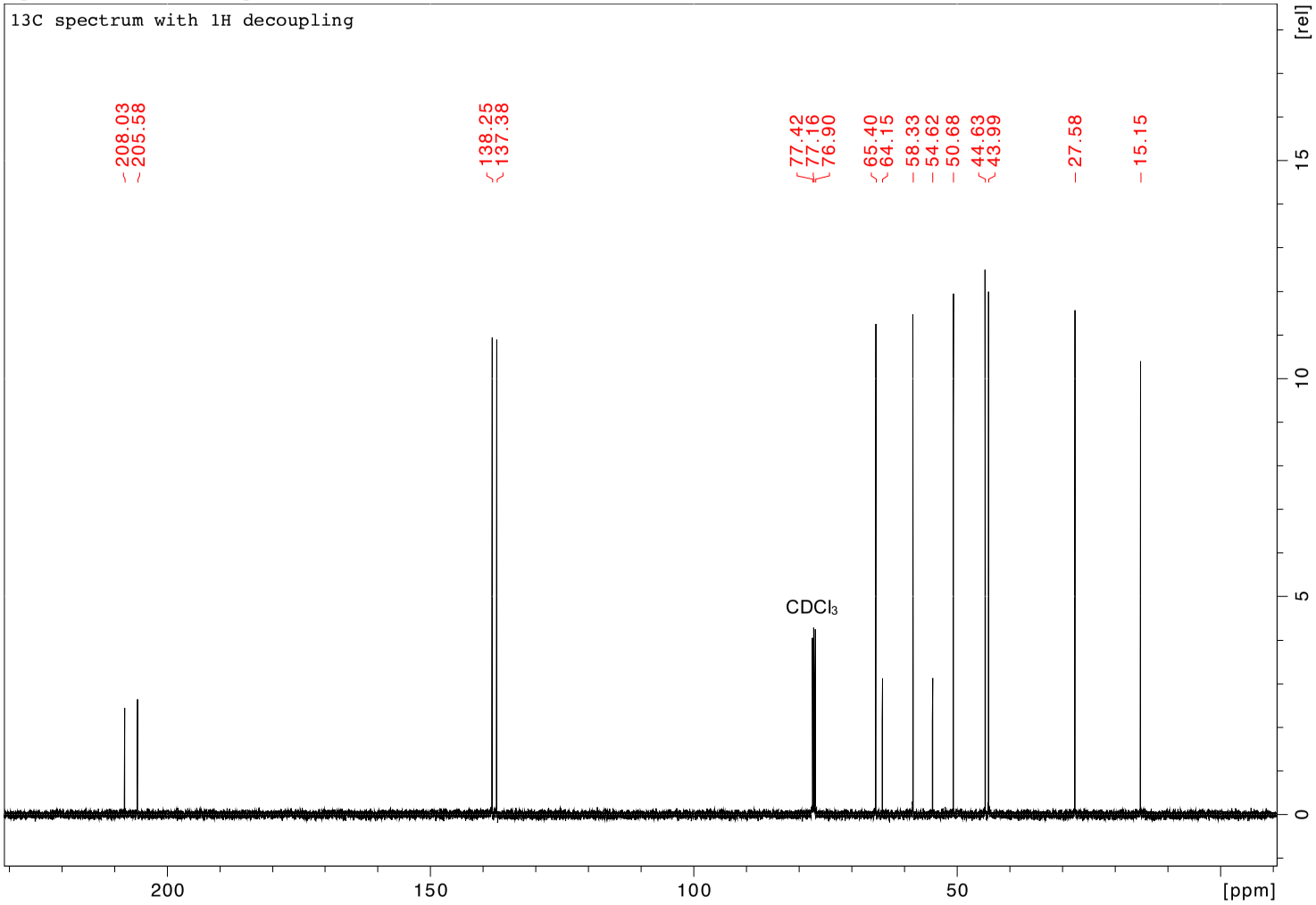

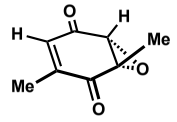

5.36 (^{1}H NMR, 500 MHz, $CDCl_3$)

wpt-6-29 2 1 "/opt/NMR Files"

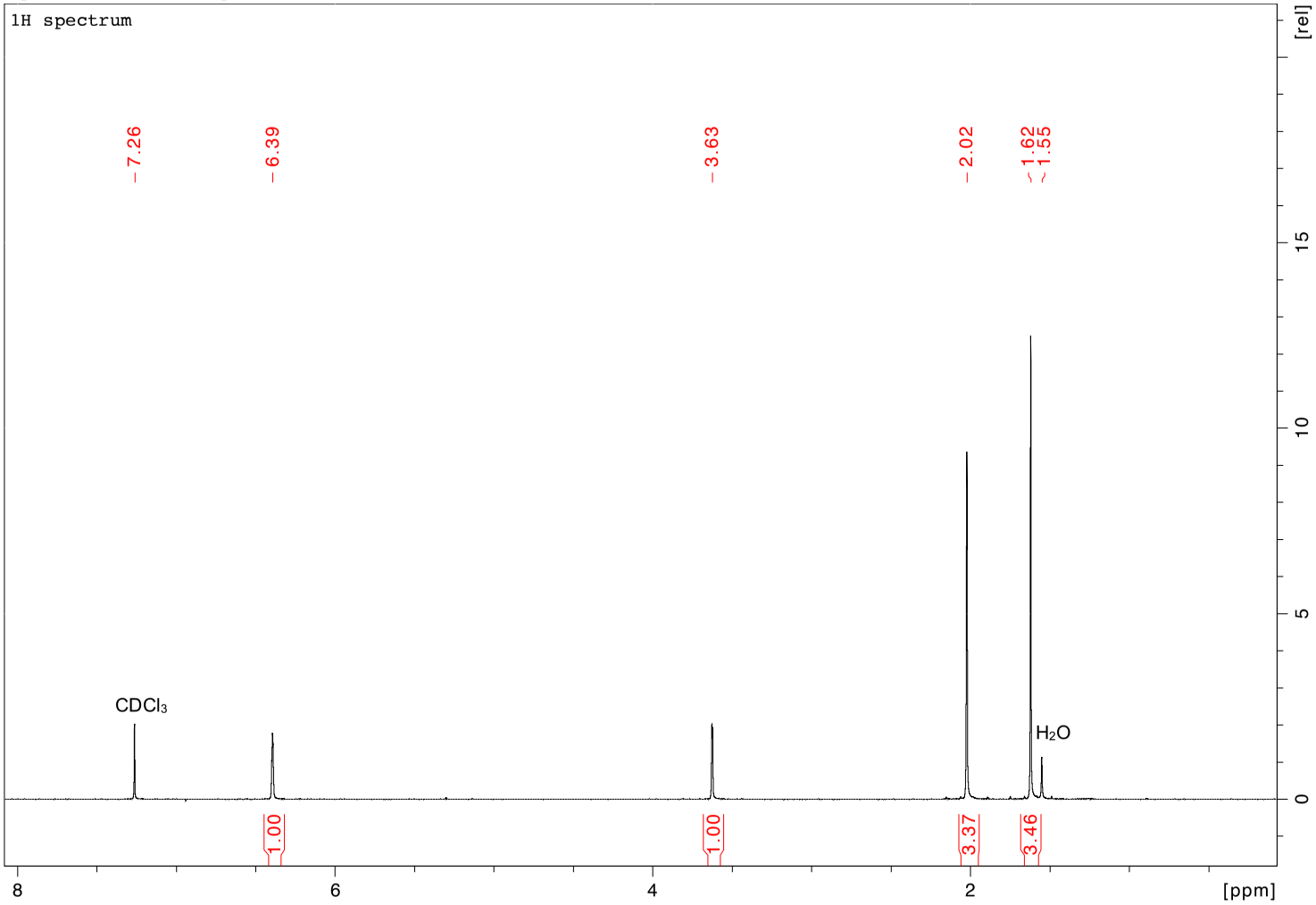

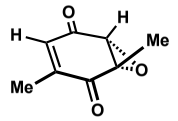

5.36 (^{13}C NMR, 126 MHz, $CDCl_3$)

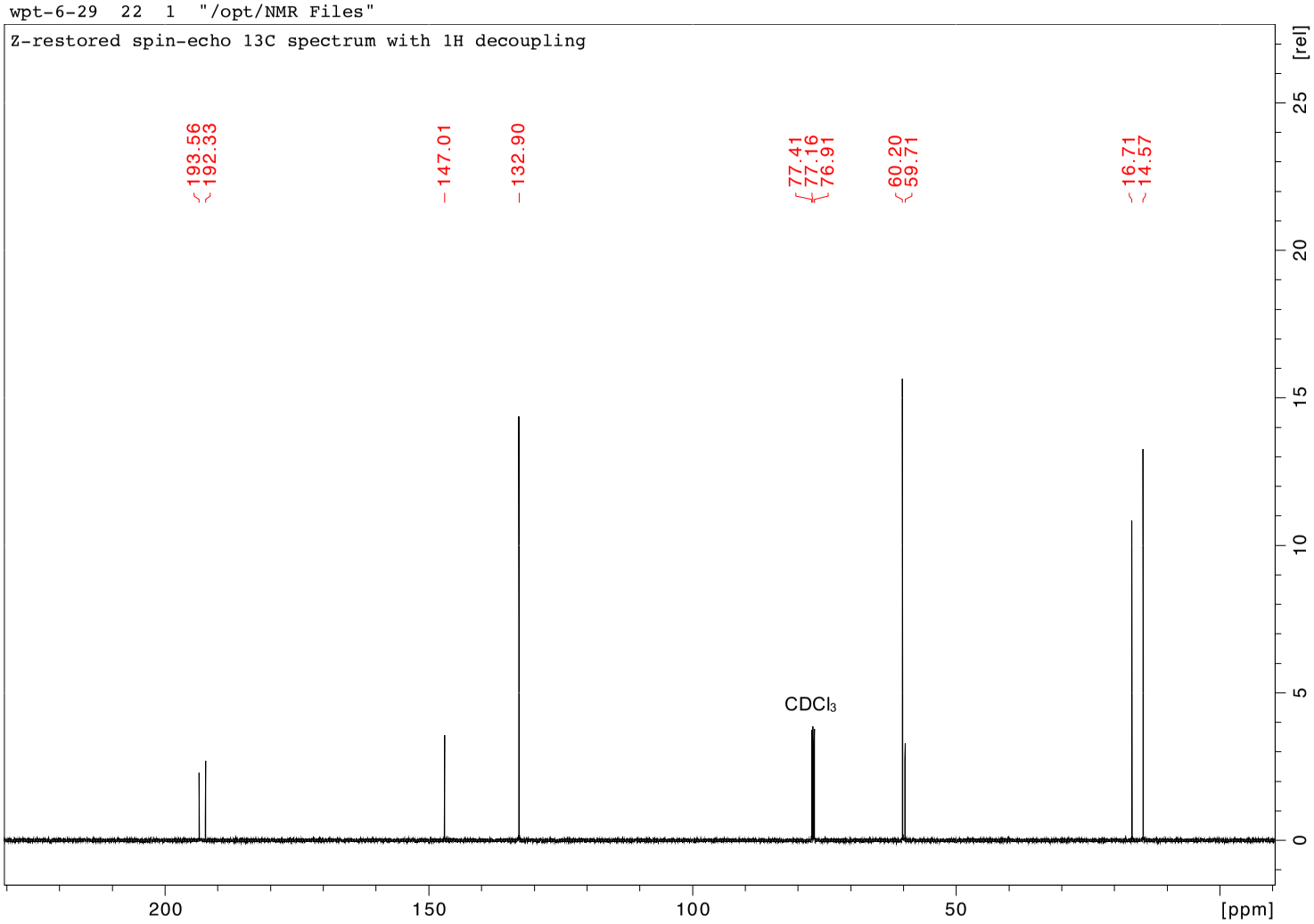

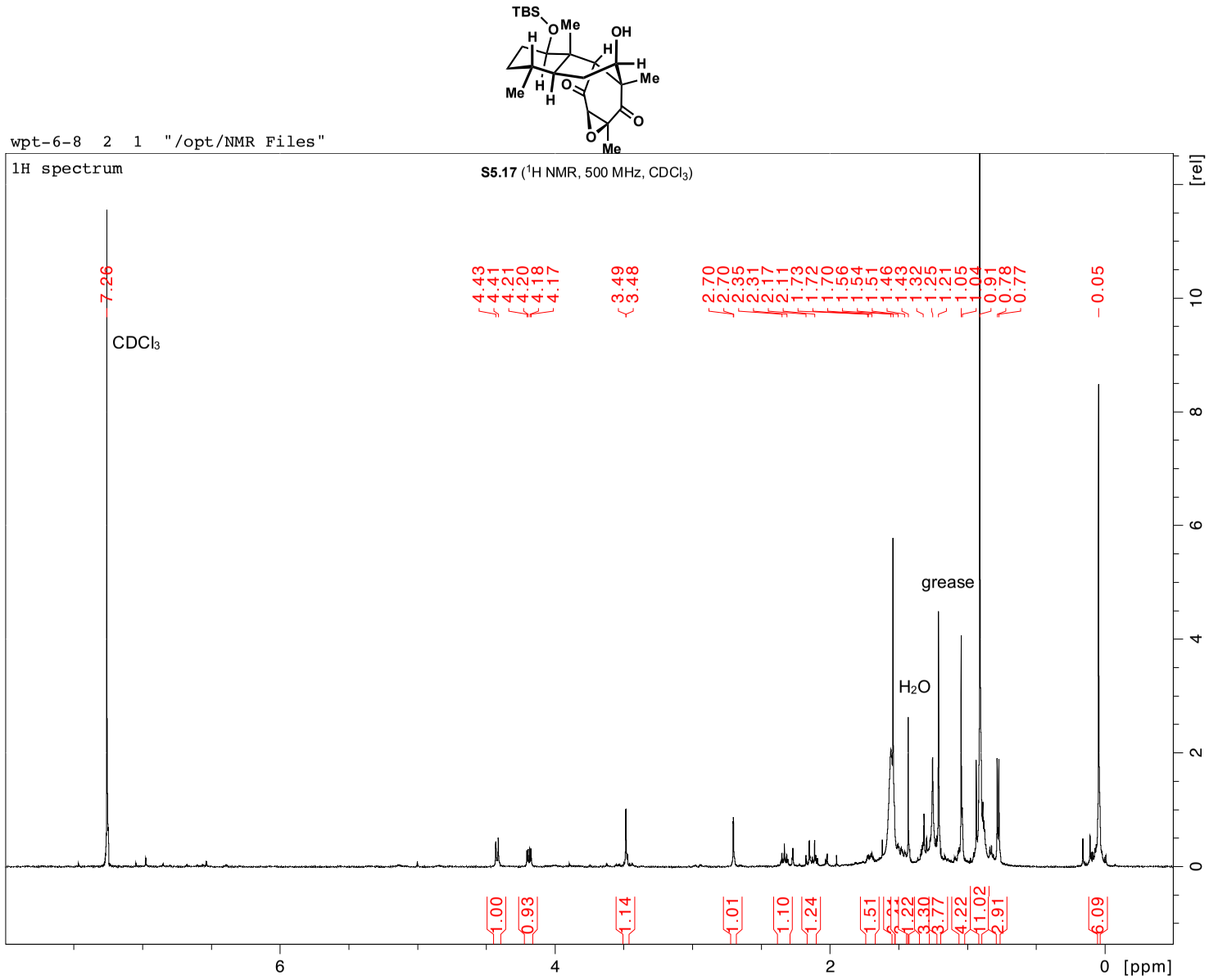
TBS
O
Me
H
OH
H
H
Me
Me
H
H
O
O
O
Me
wpt-6-8 2 1 "/opt/NMR Files"
1H spectrum
S5.17 (1H NMR, 500 MHz, CDCl3)
7.26
CDCl3
4.43
4.41
4.21
4.20
4.18
4.17
3.49
3.48
2.70
2.70
2.35
2.31
2.17
2.11
1.73
1.72
1.70
1.56
1.54
1.51
1.46
1.43
1.32
1.25
1.21
1.05
1.04
0.91
0.78
0.77
0.05
grease
H2O
1.00
0.93
1.14
1.01
1.10
1.24
1.51
1.22
3.30
3.77
4.22
11.02
2.91
6.09
[rel]
0
2
4
6
8
10
6
4
2
0
[ppm]

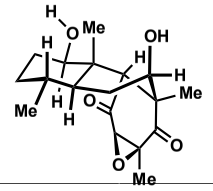

wpt-7-57 8 1 "/opt/NMR Files"

1H spectrum

S5.18 (^{1}H NMR, 500 MHz, $CDCl_3$)

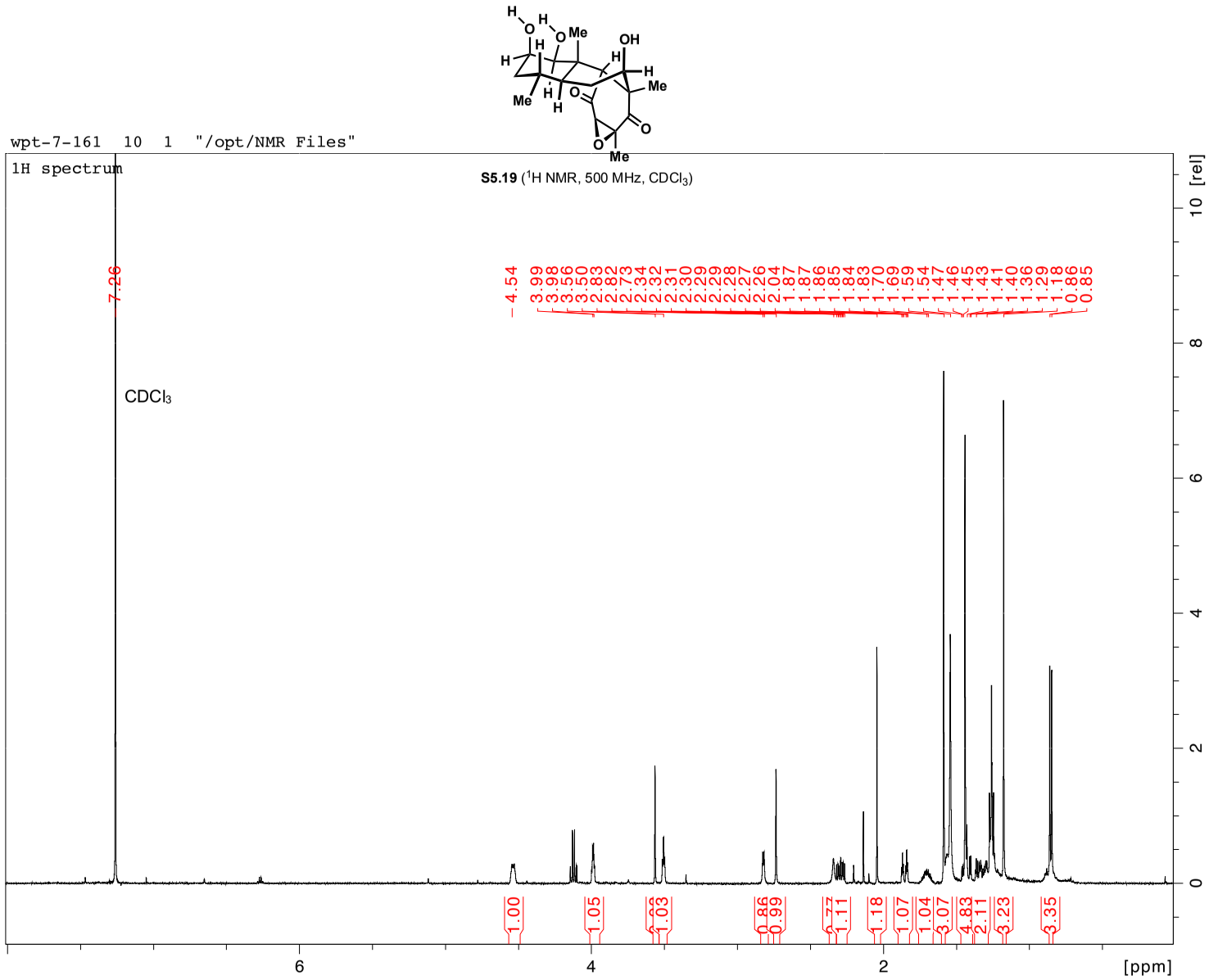

S5.19 (^{1}H NMR, 500 MHz, $CDCl_3$)

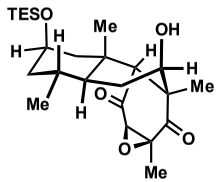

wpt-7-214 7 1 "/opt/NMR Files"

1H spectrum

5.53 (^{1}H NMR, 500 MHz, $CDCl_3$)

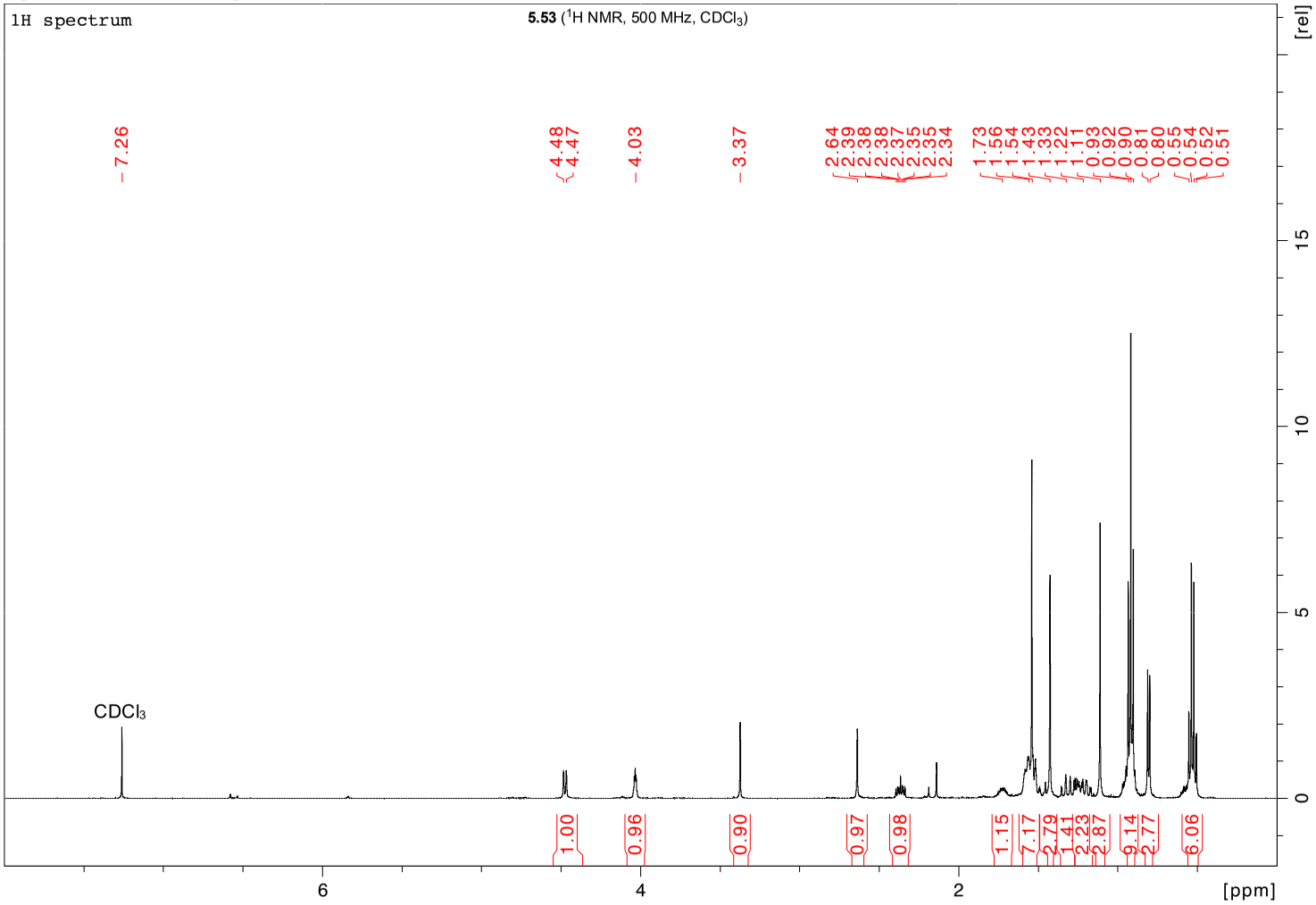

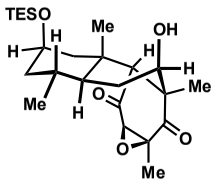

wpt-7-214 77 1 "/opt/NMR Files"

13C spectrum with 1H decoupling

5.53 (^{13}C NMR, 126 MHz, $CDCl_3$)

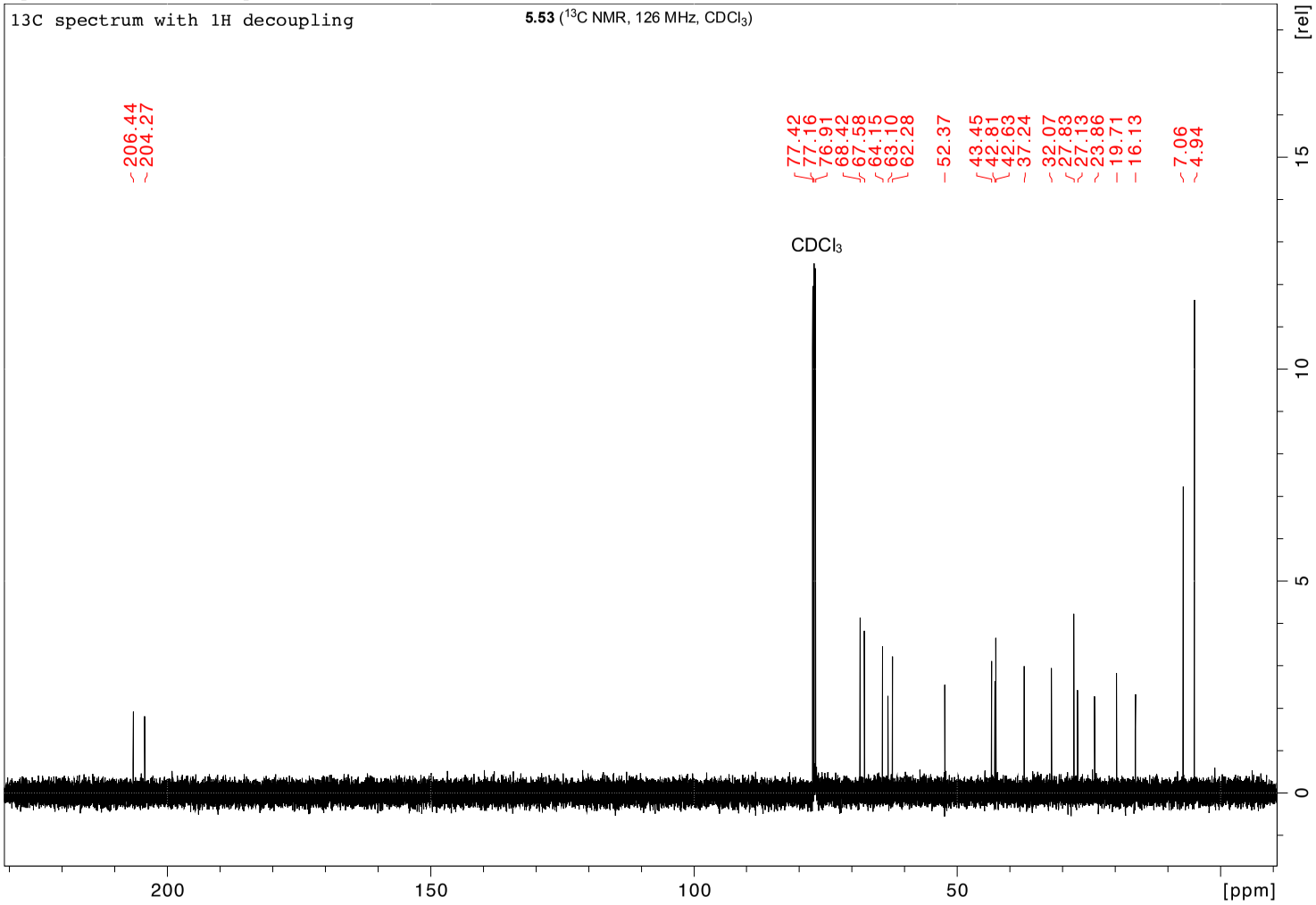

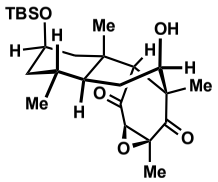

wpt-6-294 7 1 "/opt/NMR Files"

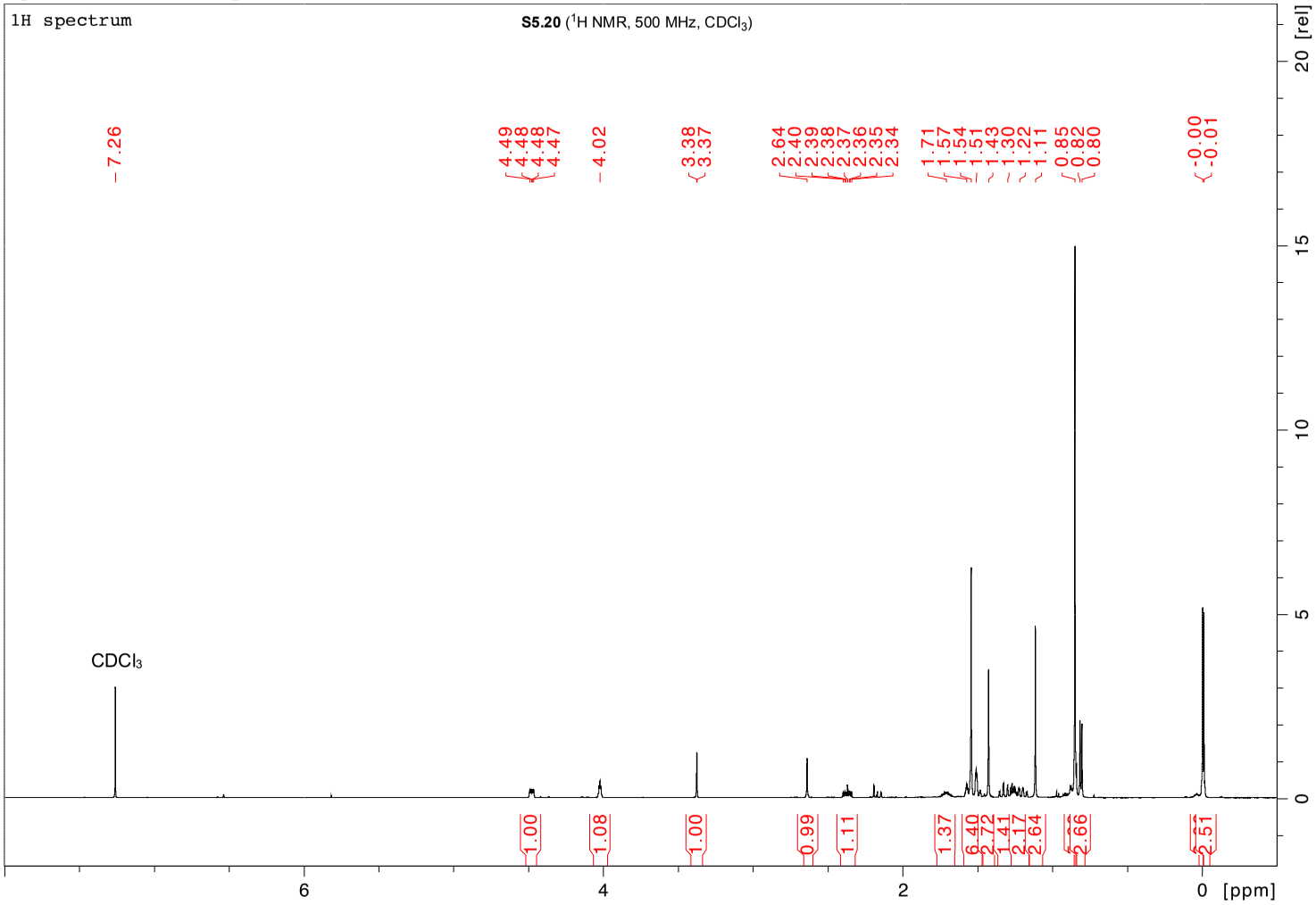

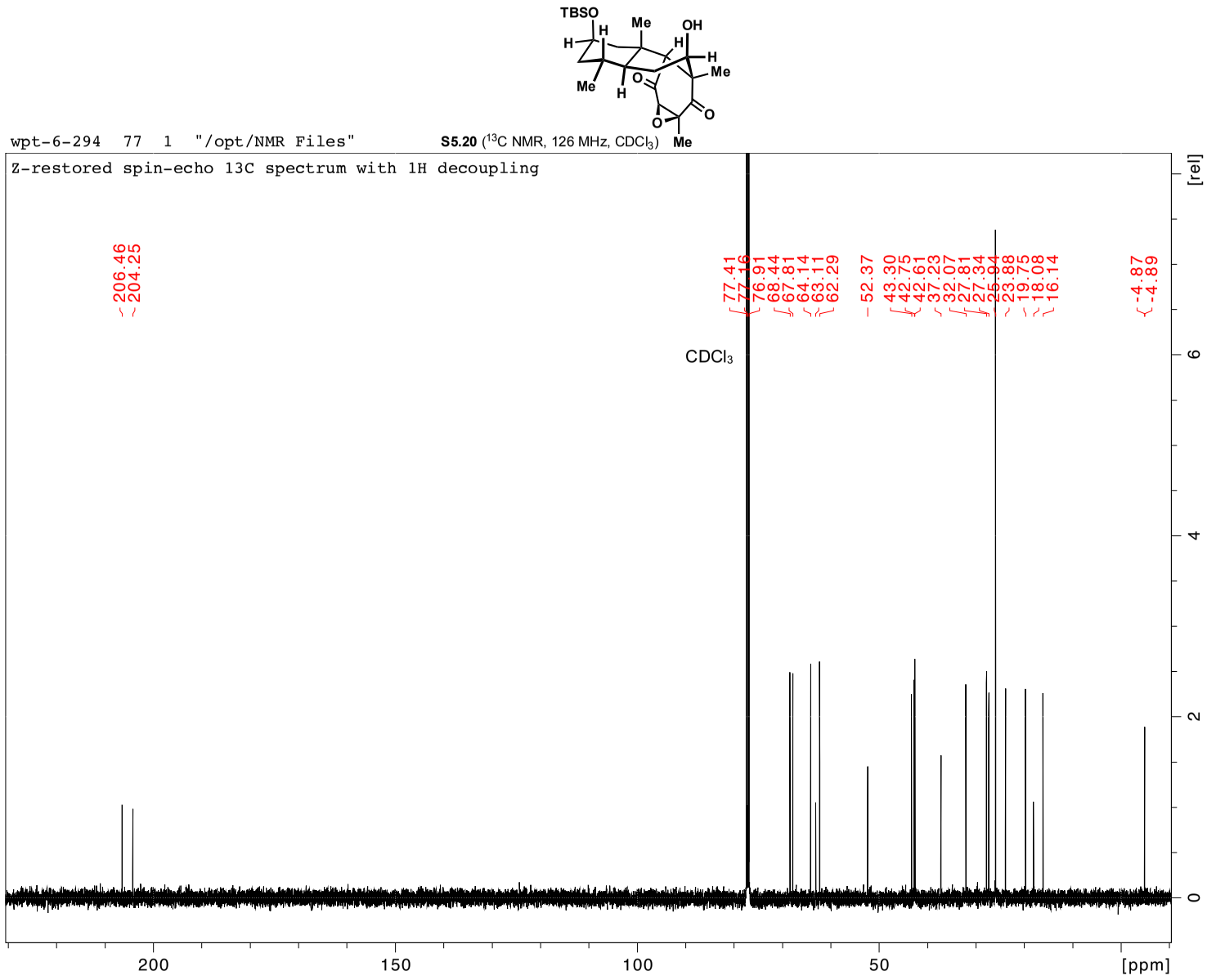
TBSO
Me
OH
H
H
H
H
Me
Me
H
O
O
O
Me
wpt-6-294 77 1 "/opt/NMR Files"
S5.20 (13C NMR, 126 MHz, CDCl3)
Z-restored spin-echo 13C spectrum with 1H decoupling
206.46
204.25
77.41
77.16
76.91
68.44
67.81
64.14
63.11
62.29
52.37
43.30
42.75
42.61
37.23
32.07
27.81
27.34
25.94
23.88
19.75
18.08
16.14
-4.87
-4.89
CDCl3
[rel]
0
2
4
6
200
150
100
50
[ppm]

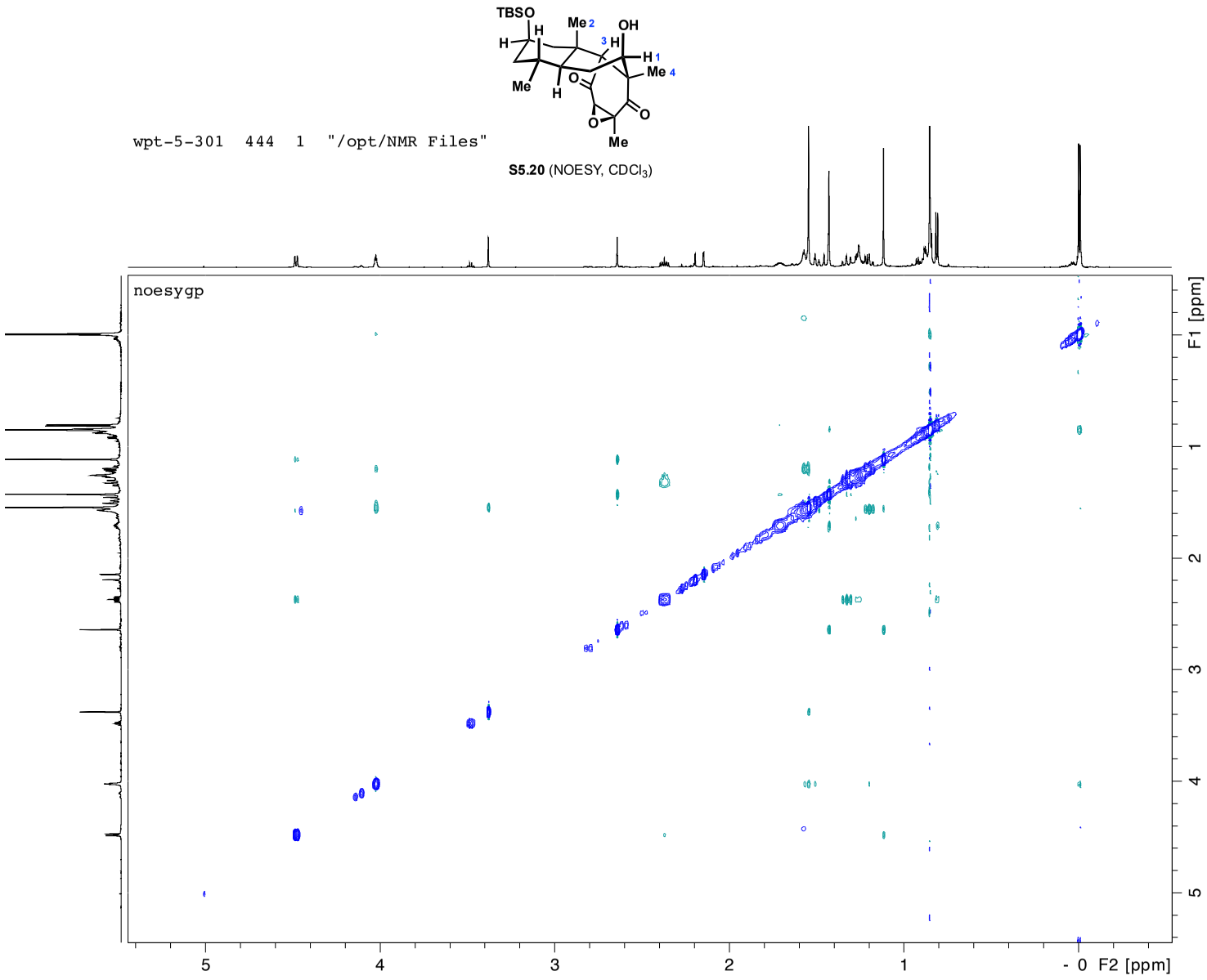
TBSO
H
H
Me 2
OH
3 H
H 1
Me 4
Me
H
O
O
O
Me
wpt-5-301 444 1 "/opt/NMR Files"
S5.20 (NOESY, CDCl3)
noesygp
F1 [ppm]
F2 [ppm]
5
4
3
2
1
0

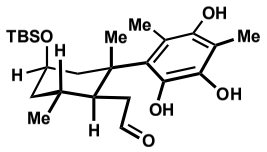

wpt-8-44 294 1 "/opt/NMR Files"

S5.21 (^{1}H NMR, 500 MHz, $CDCl_3$)

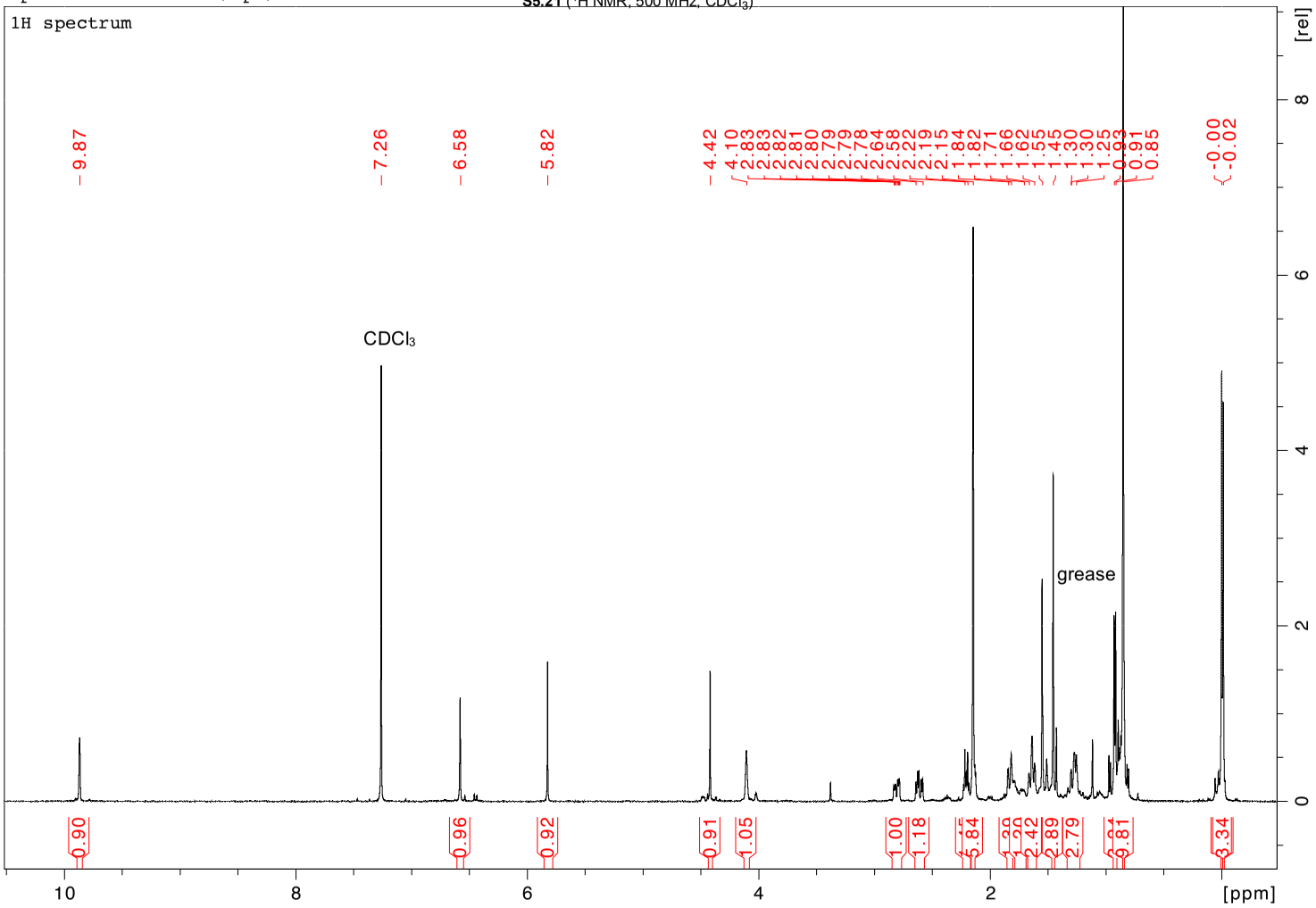

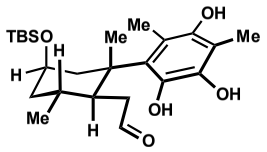

S5.21 (^{13}C NMR, 126 MHz, $CDCl_3$)

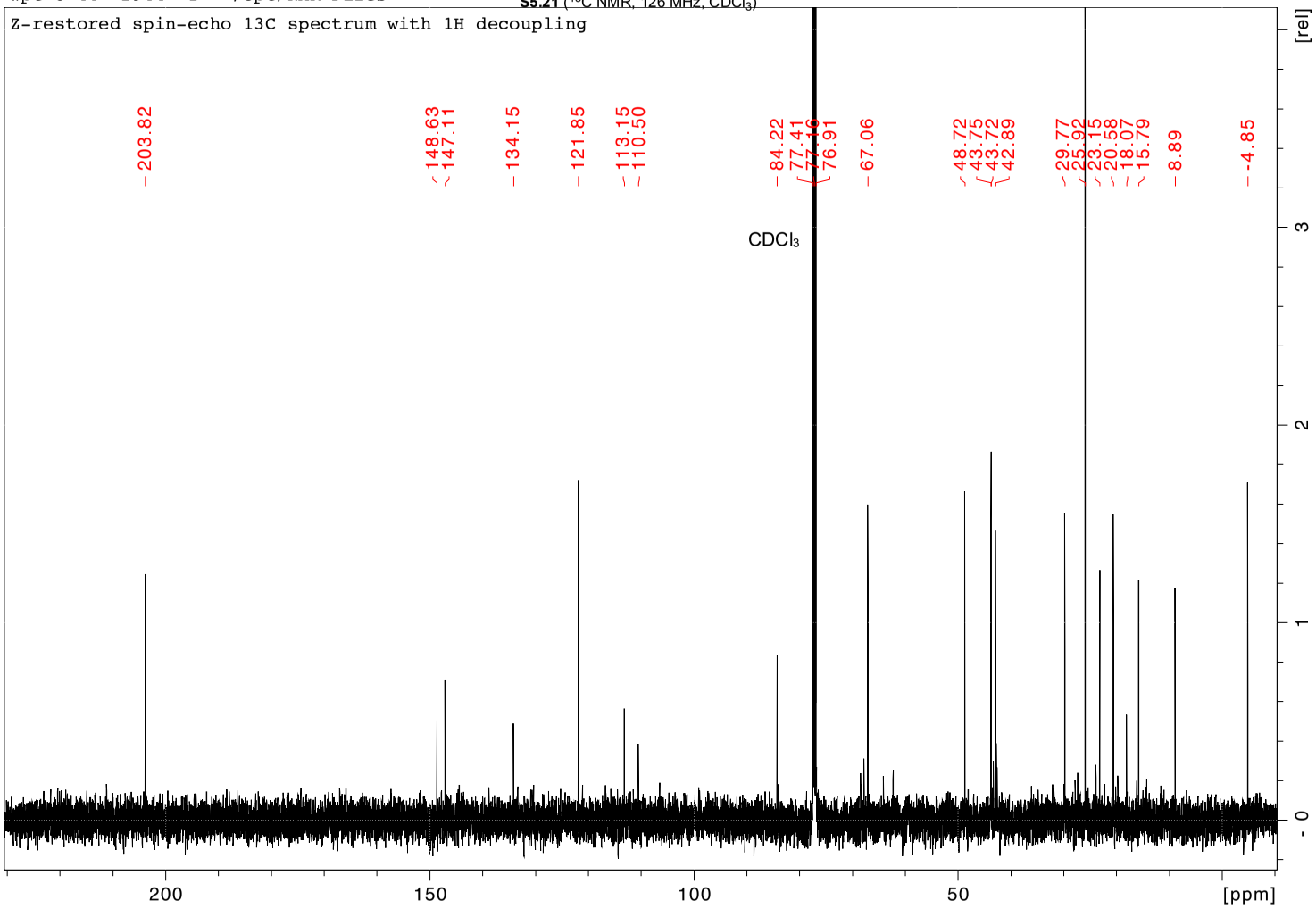

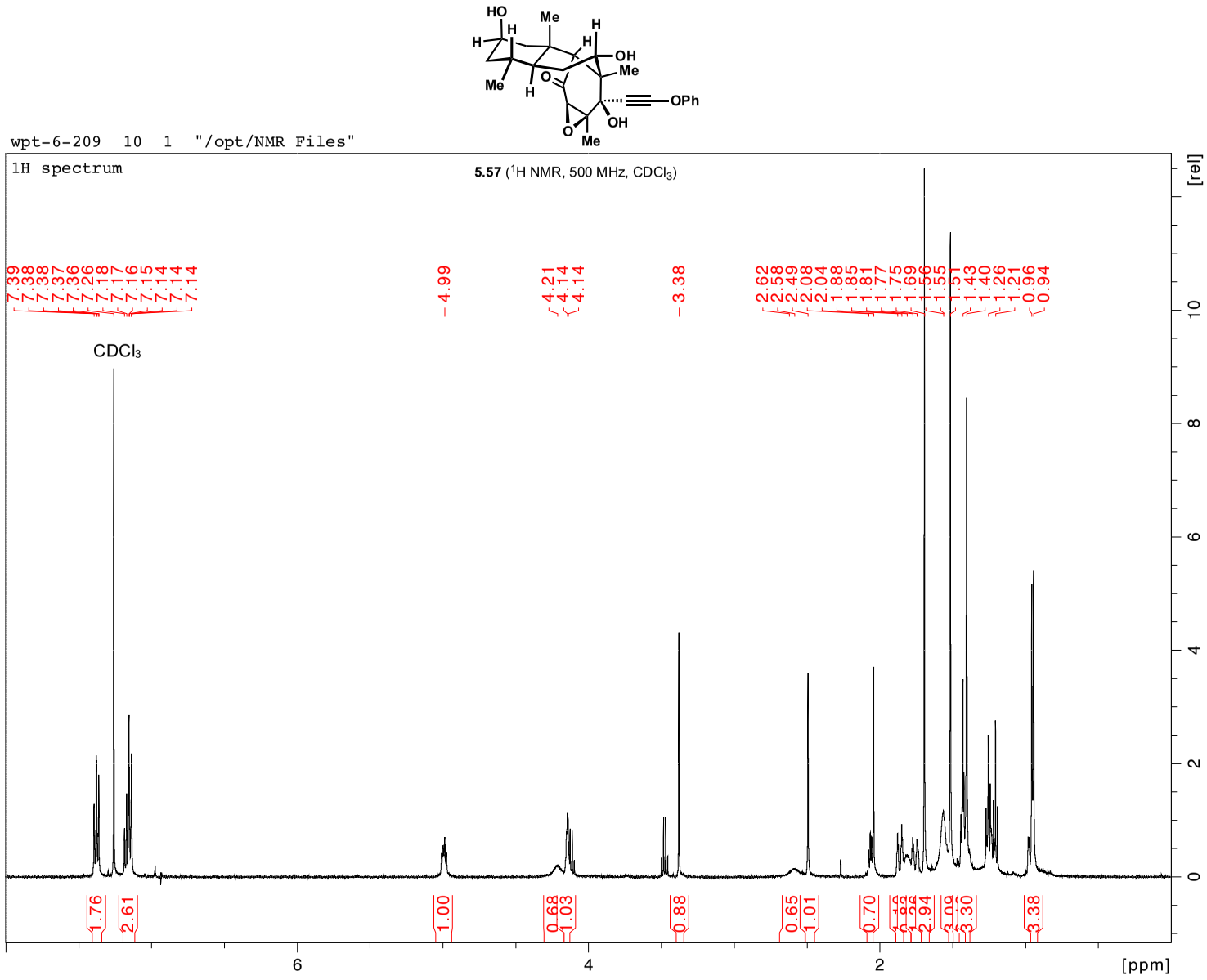
wpt-6-209 10 1 "/opt/NMR Files"
1H spectrum
5.57 (1H NMR, 500 MHz, CDCl3)
CDCl3
[rel]
[ppm]

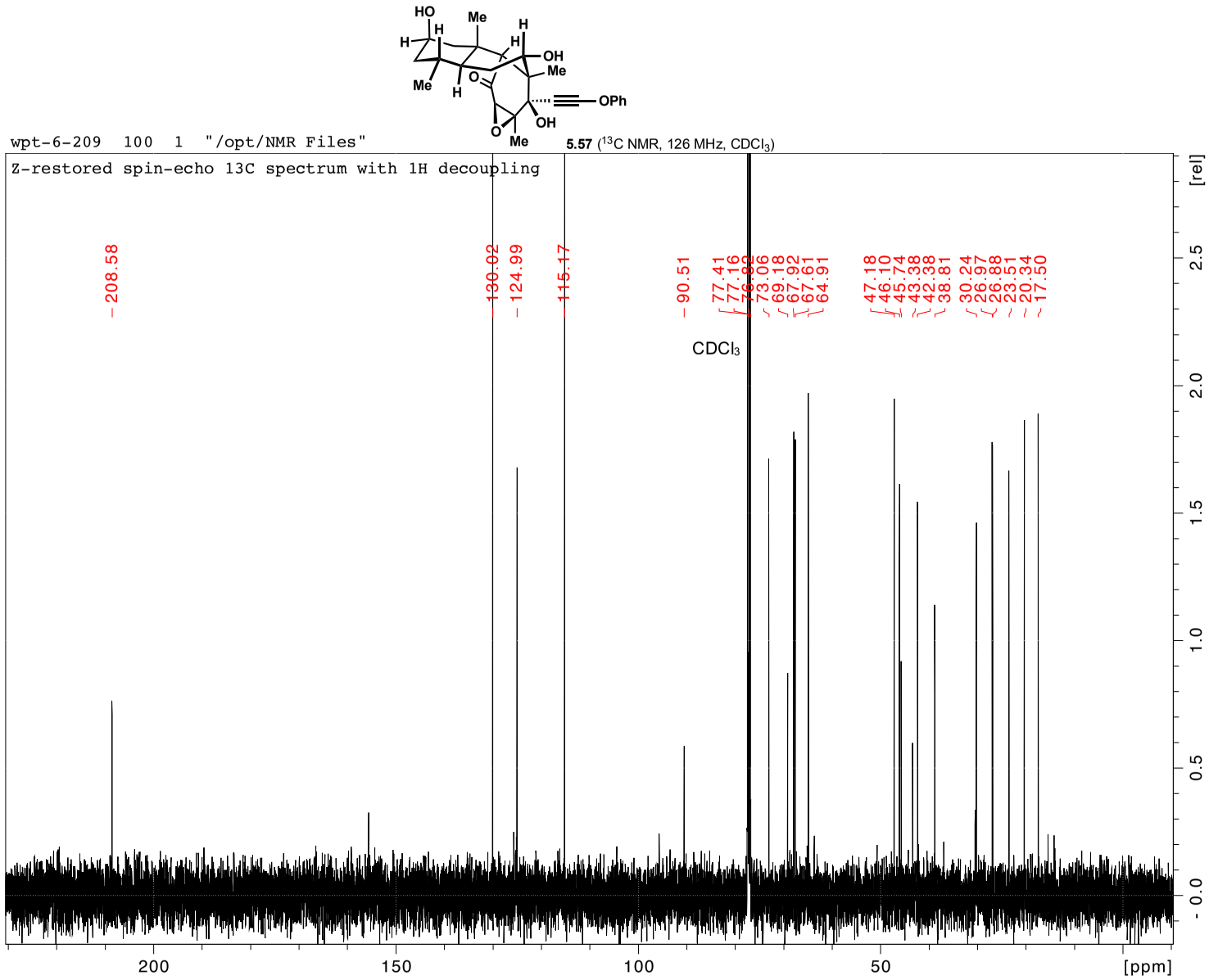
wpt-6-209 100 1 "/opt/NMR Files"
5.57 (13C NMR, 126 MHz, CDCl3)
Z-restored spin-echo 13C spectrum with 1H decoupling
208.58
130.02
124.99
115.17
90.51
77.41
77.16
76.92
73.06
69.18
67.92
67.61
64.91
47.18
46.10
45.74
43.38
42.38
38.81
30.24
26.97
26.88
23.51
20.34
17.50
CDCl3
[rel]
2.5
2.0
1.5
1.0
0.5
0.0
200
150
100
50
[ppm]

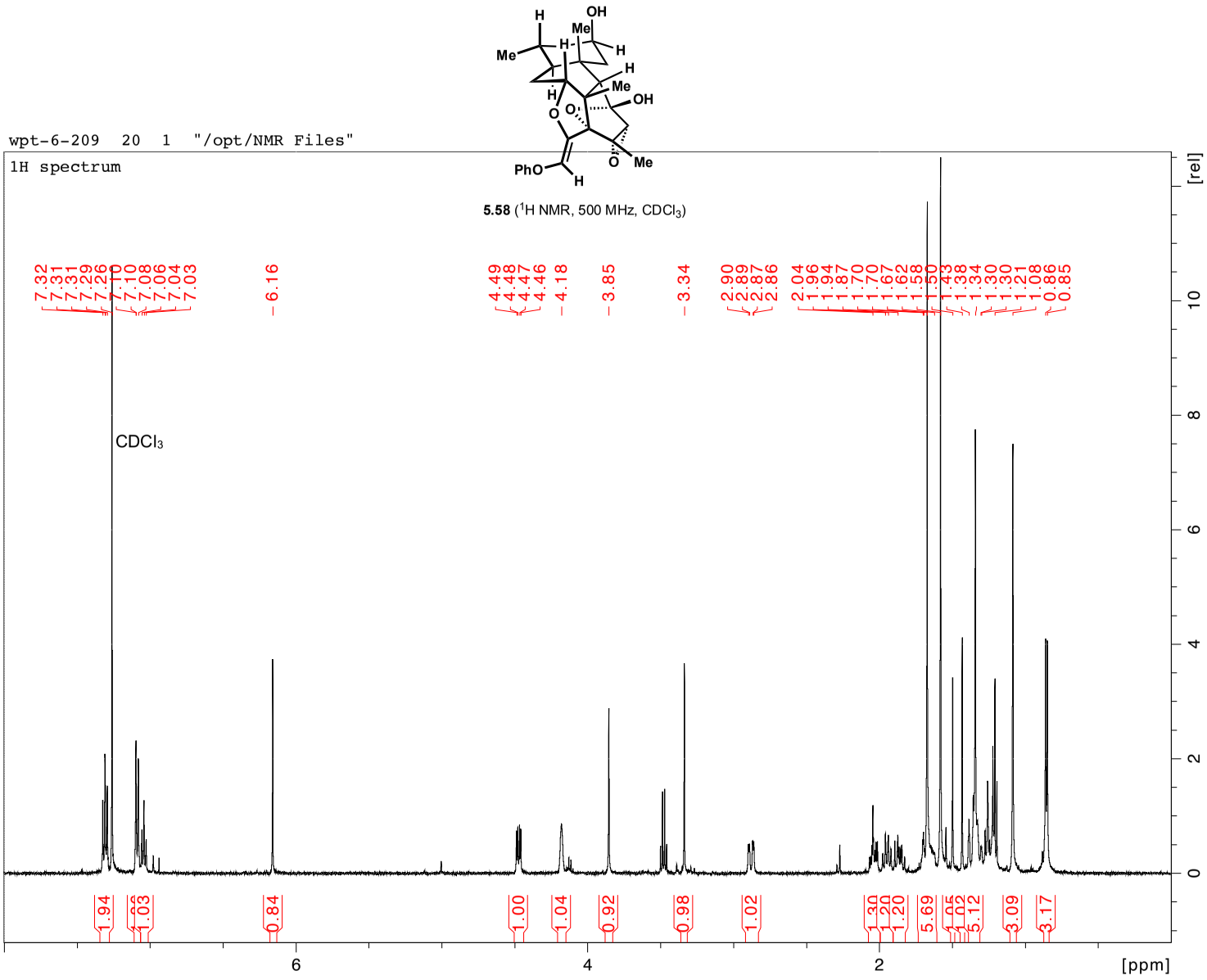
wpt-6-209 20 1 "/opt/NMR Files"
1H spectrum
5.58 (1H NMR, 500 MHz, CDCl3)
CDCl3
[rel]
[ppm]

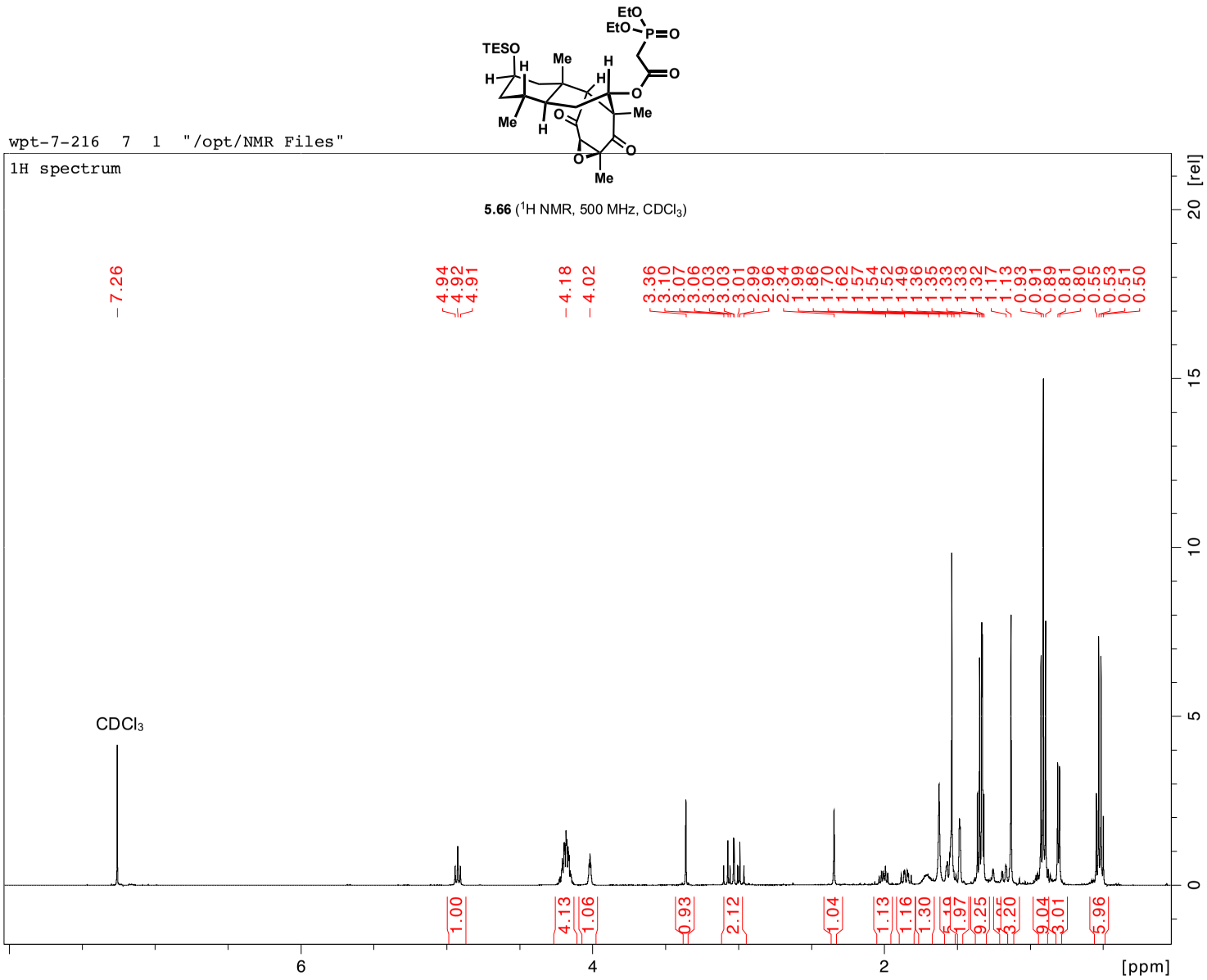
wpt-7-216 7 1 "/opt/NMR Files"
1H spectrum
5.66 (1H NMR, 500 MHz, CDCl3)
7.26
4.94
4.92
4.91
4.18
4.02
3.36
3.10
3.07
3.06
3.03
3.03
3.01
2.99
2.96
2.34
1.99
1.86
1.70
1.62
1.57
1.54
1.52
1.49
1.36
1.35
1.33
1.33
1.32
1.17
1.13
0.93
0.91
0.89
0.81
0.80
0.55
0.53
0.51
0.50
CDCl3
1.00
4.13
1.06
0.93
2.12
1.04
1.13
1.16
1.30
1.97
9.25
3.20
9.04
3.01
5.96
[rel]
[ppm]

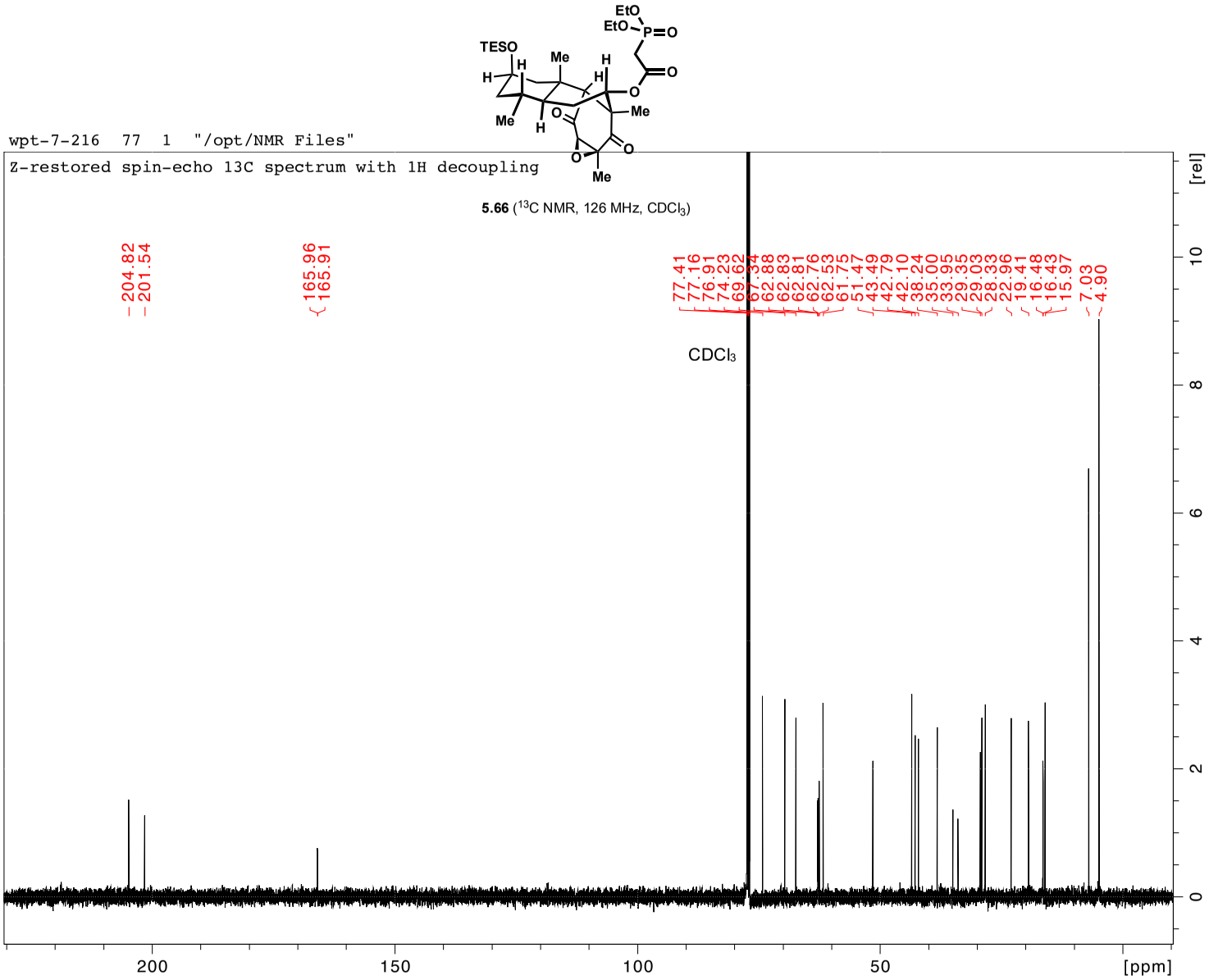
wpt-7-216 77 1 "/opt/NMR Files"
Z-restored spin-echo 13C spectrum with 1H decoupling
5.66 (13C NMR, 126 MHz, CDCl3)
204.82
201.54
165.96
165.91
77.41
77.16
76.91
74.23
69.62
67.34
62.88
62.83
62.81
62.76
62.53
61.75
51.47
43.49
42.79
42.10
38.24
35.00
33.95
29.35
29.03
28.33
22.96
19.41
16.48
16.43
15.97
7.03
4.90
CDCl3
[rel]
[ppm]

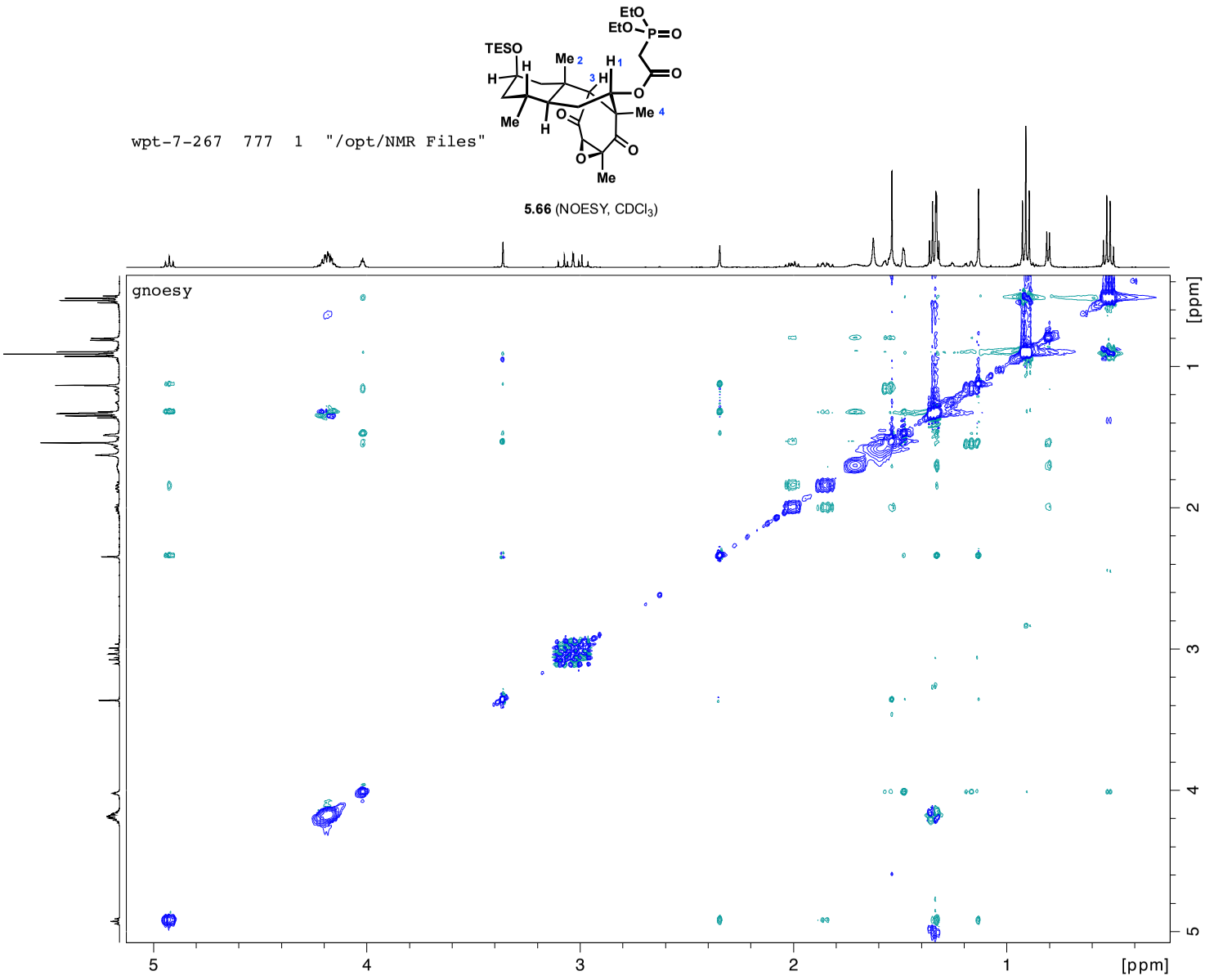
wpt-7-267 777 1 "/opt/NMR Files"
EtO
EtO
P=O
TESO
H
H
Me 2
H 1
3 H
O
O
Me 4
Me
H
O
O
O
Me
5.66 (NOESY, CDCl3)
gnoesy
[ppm]
1
2
3
4
5
5
4
3
2
1
[ppm]

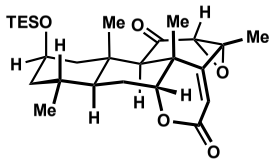

wpt-7-217 10 1 "/opt/NMR Files"

S5.23 (^{1}H NMR, 500 MHz, $CDCl_3$)

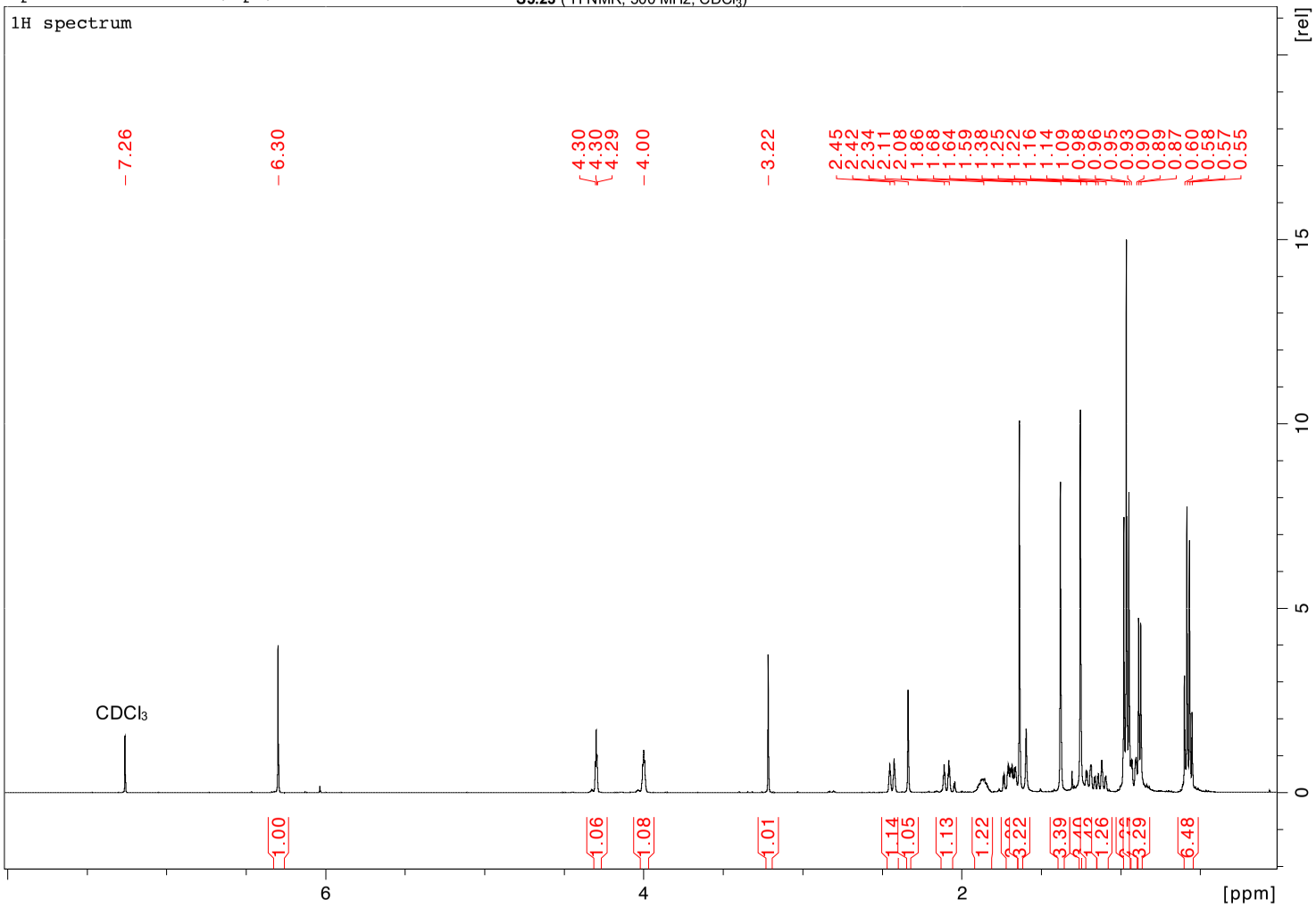

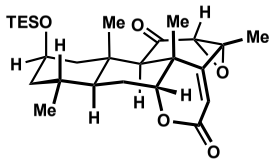

S5.23 (^{13}C NMR, 126 MHz, $CDCl_3$)

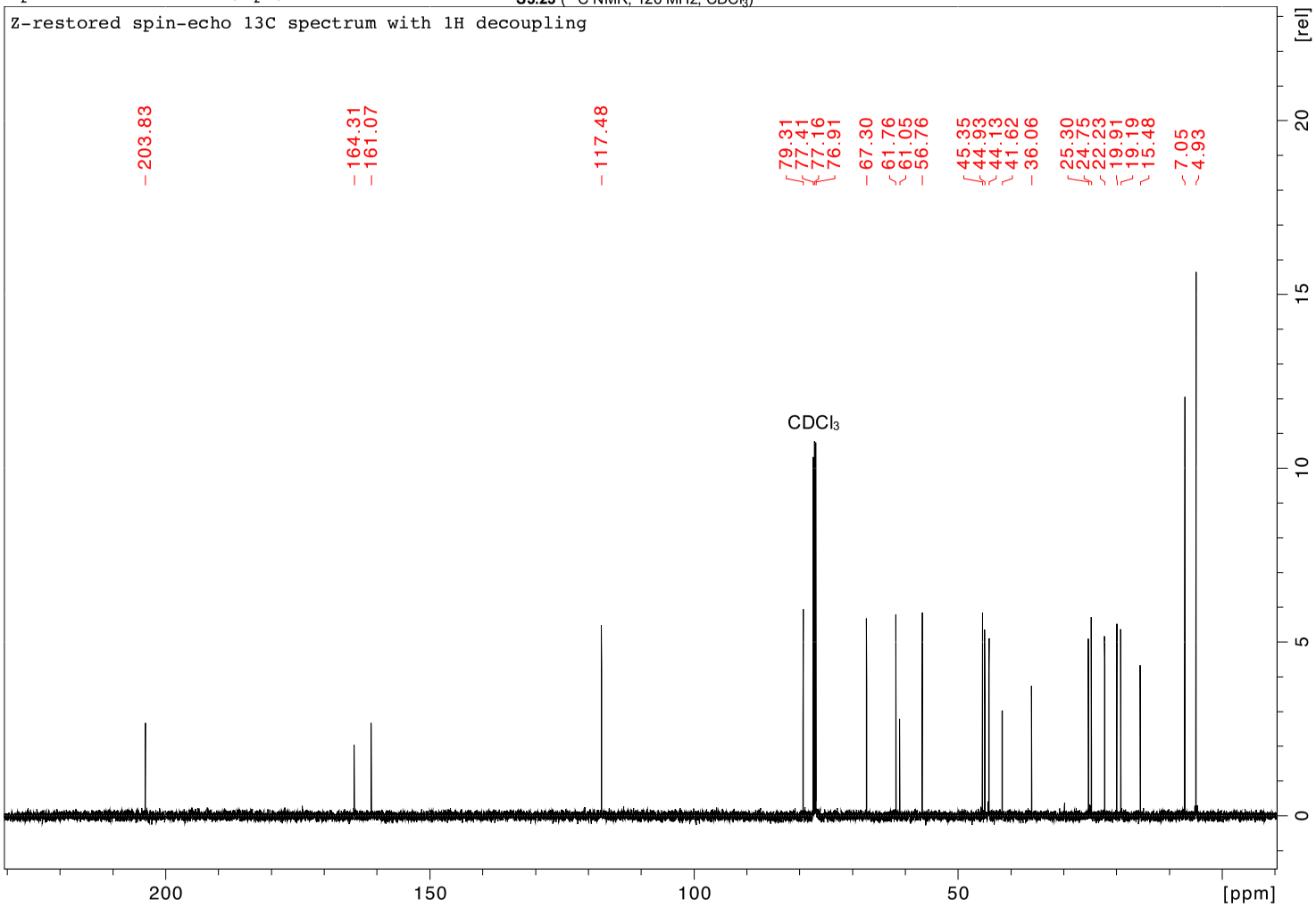

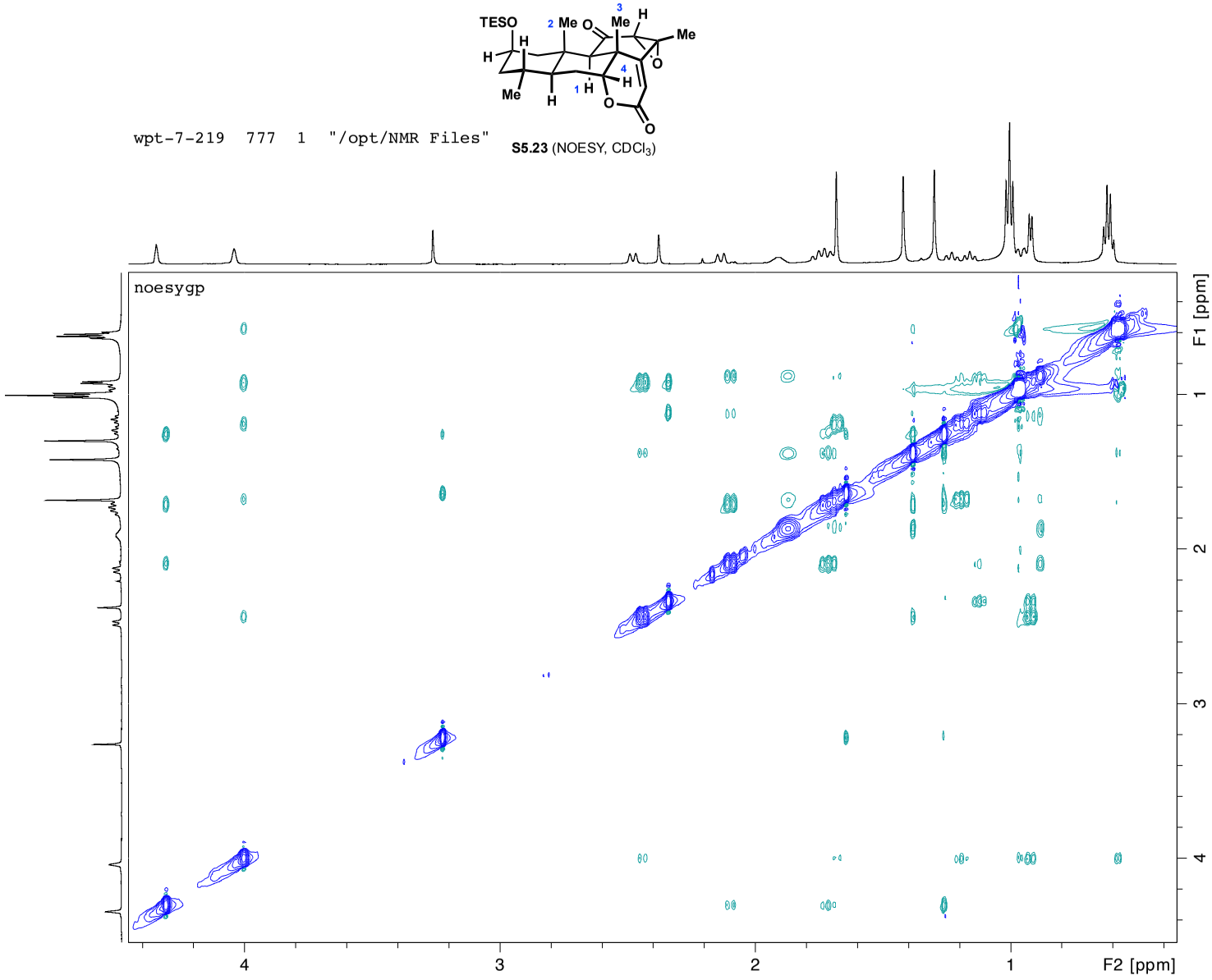
TESO
2 Me
O
3
Me
H
Me
H
H
Me
H
1 H
4
H
O
O
O
wpt-7-219 777 1 "/opt/NMR Files"
S5.23 (NOESY, CDCl3)
noesygp
F1 [ppm]
F2 [ppm]
1
2
3
4

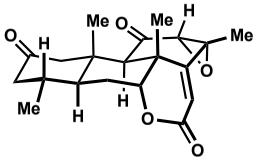

wpt-7-218 7 1 "/opt/NMR Files"

1H spectrum

5.67 (^{1}H NMR, 500 MHz, $CDCl_3$)

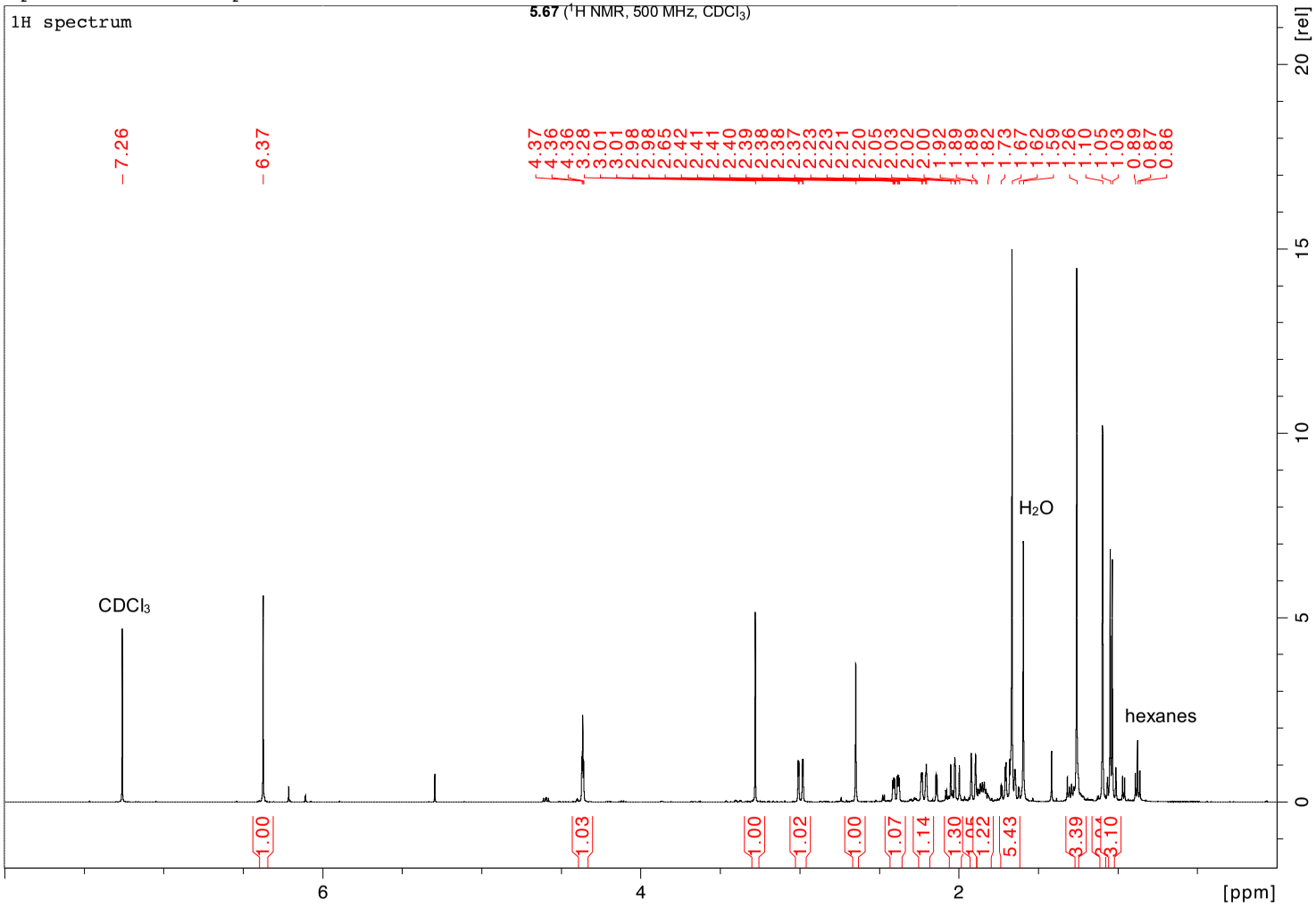

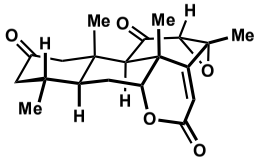

5.67 (^{13}C NMR, 126 MHz, $CDCl_3$)

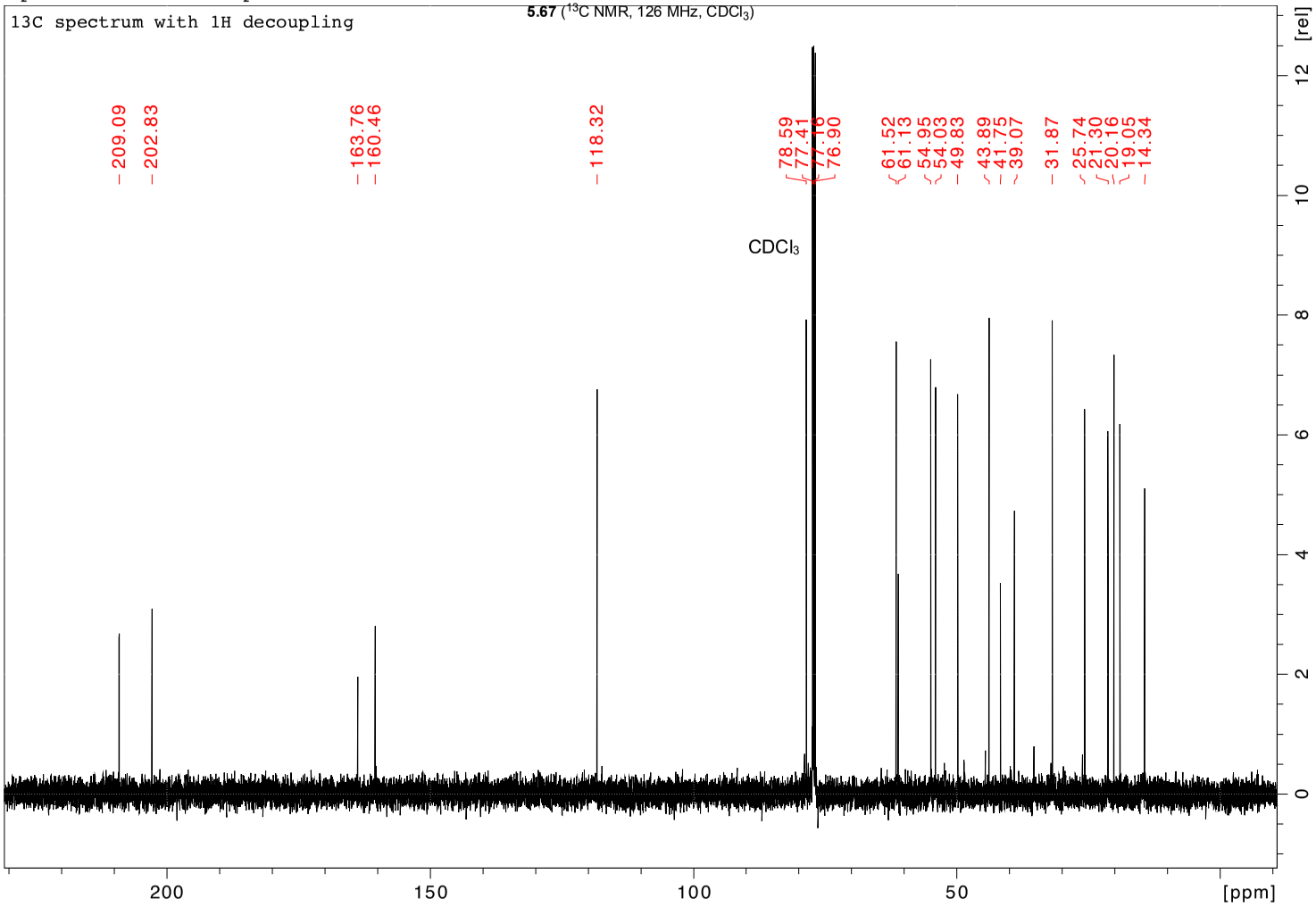

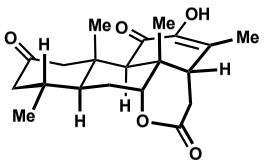

wpt-7-264 9 1 "/opt/NMR Files"

5.72 (^{1}H NMR, 500 MHz, C_6D_6)

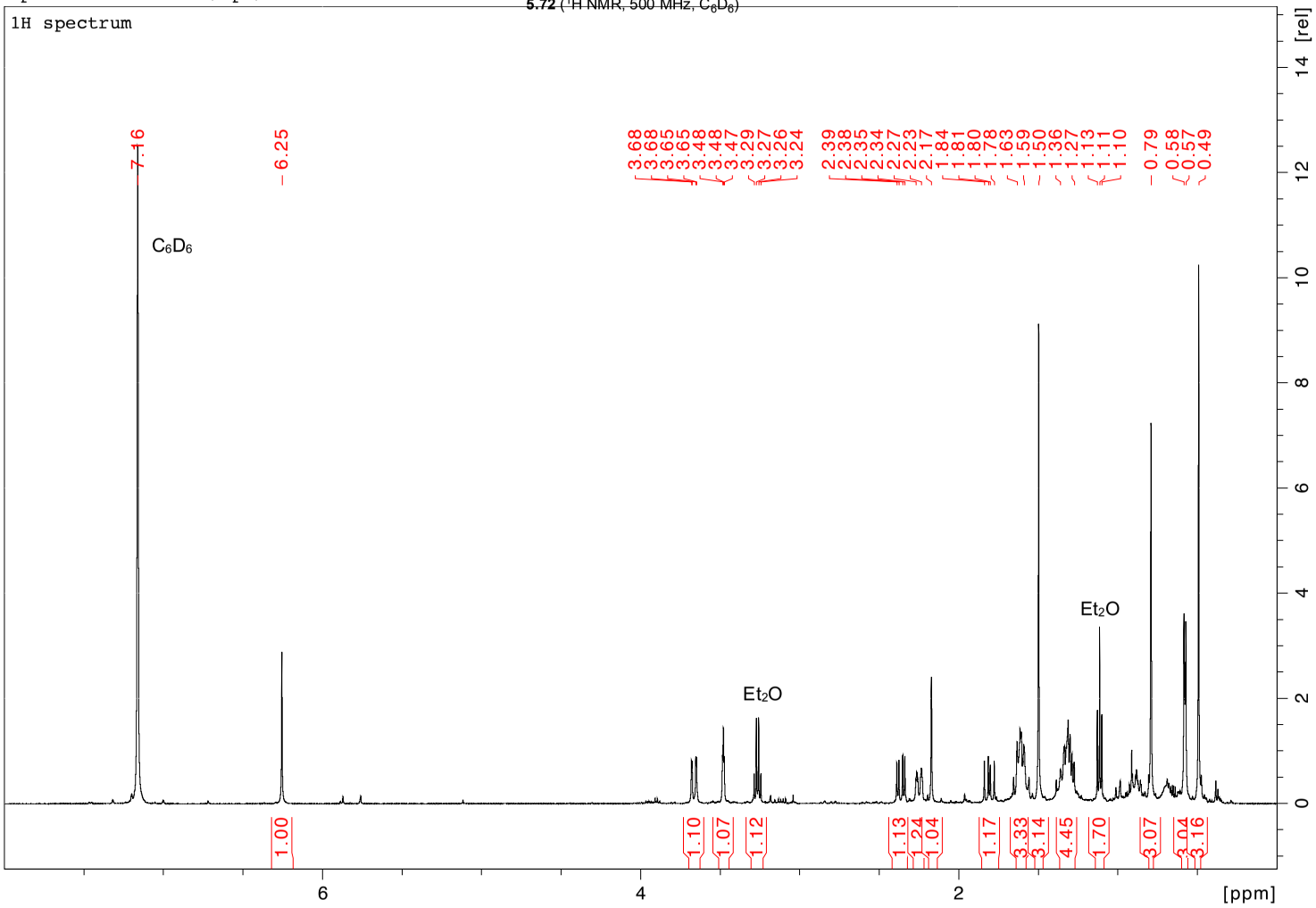

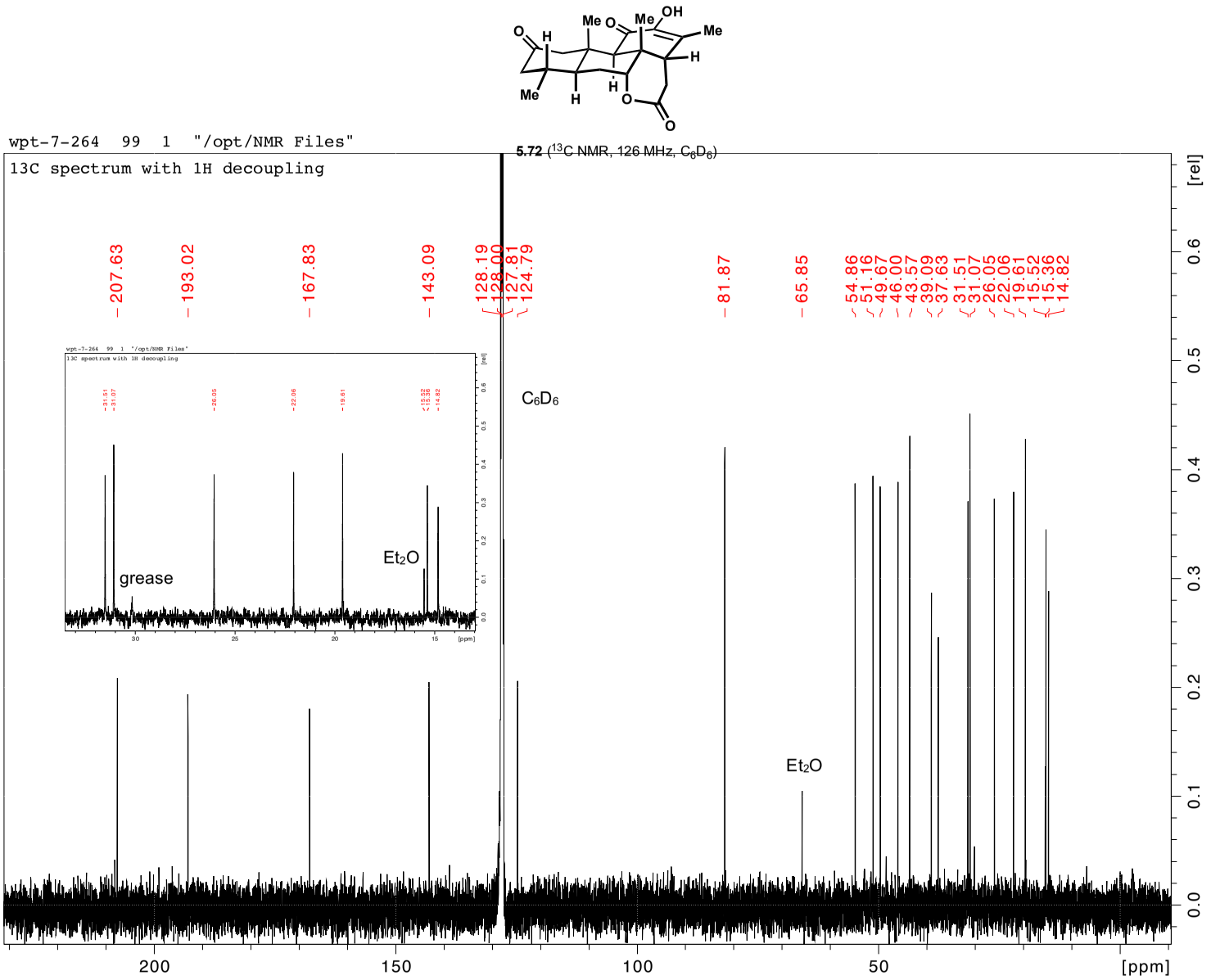

5.72 (^{13}C NMR, 126 MHz, C_6D_6)

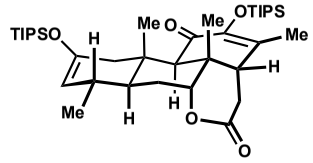

5.73 (^{1}H NMR, 500 MHz, $CDCl_3$)

wpt-7-265 77 1 "/opt/NMR Files"

1H spectrum

7.26
4.69
4.28
3.03
3.00
2.97
2.96
2.94
2.92
2.50
2.39
2.32
2.06
2.03
1.93
1.87
1.76
1.73
1.62
1.58
1.27
1.21
1.20
1.15
1.13
1.11
1.08
1.06
1.05
1.04
1.03
1.01
0.96
0.95

$CDCl_3$

0.91
1.00
0.96
0.93
2.93
1.14
1.01
2.81
0.96
0.92
7.39
5.92
36.05
3.10

20 [rel]
15
10
5
0
6
4
2
[ppm]

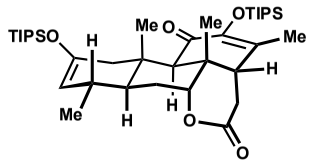

5.73 (^{13}C NMR, 126 MHz, $CDCl_3$)

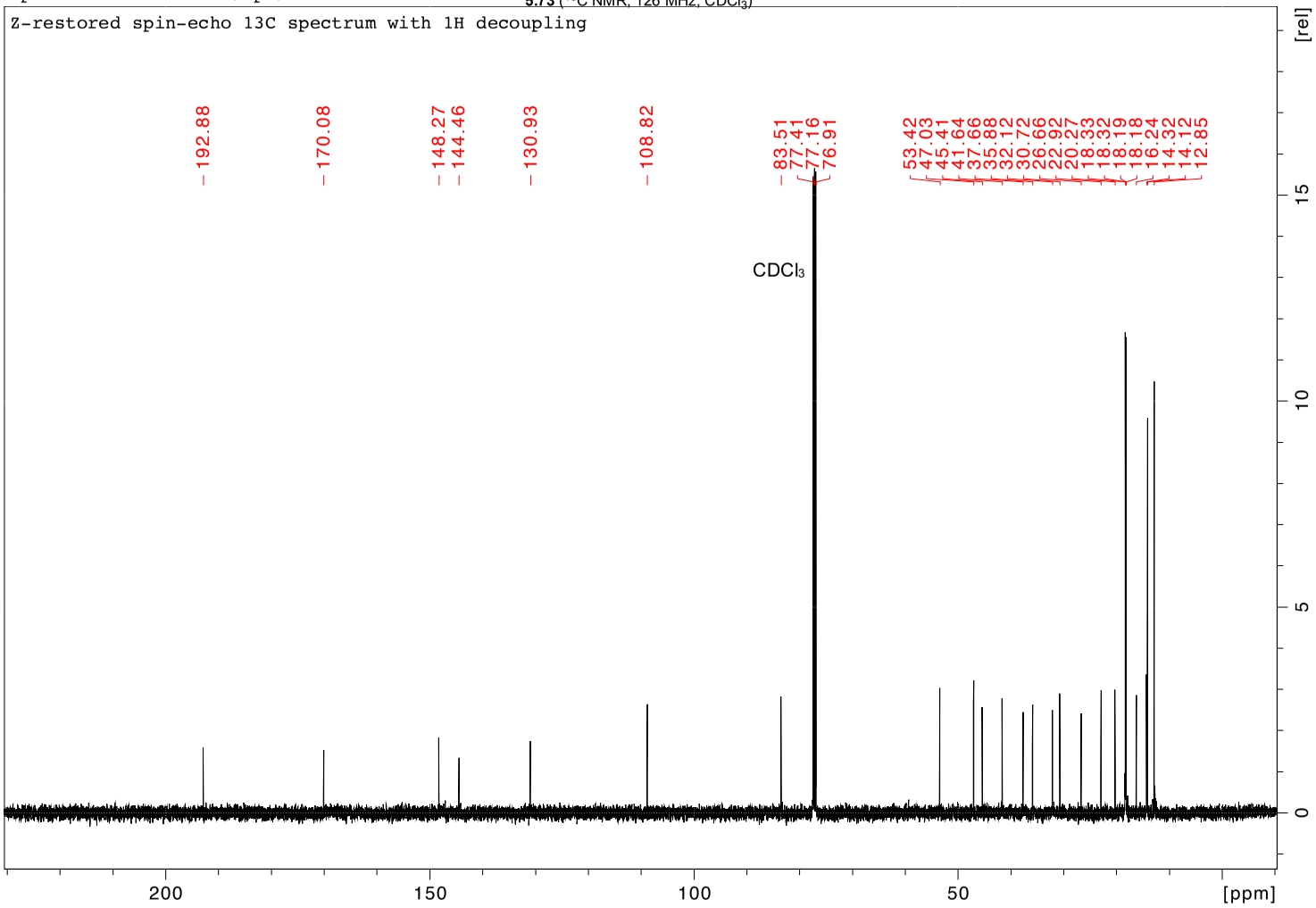

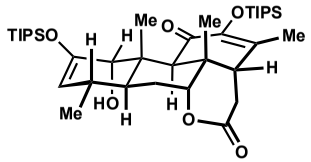

wpt-7-269 7 1 "/opt/NMR Files"

5.74 (^{1}H NMR, 500 MHz, $CDCl_3$)

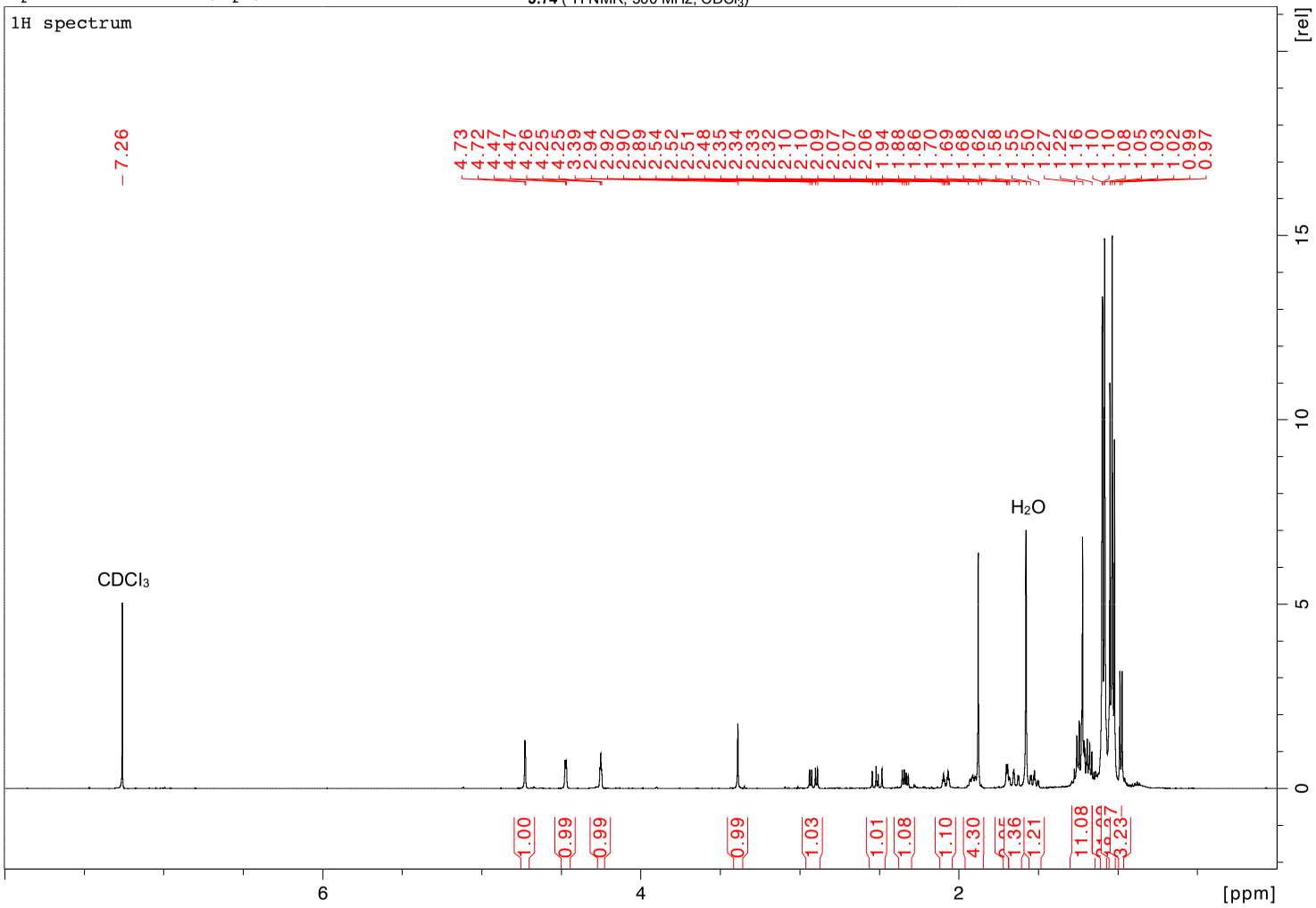

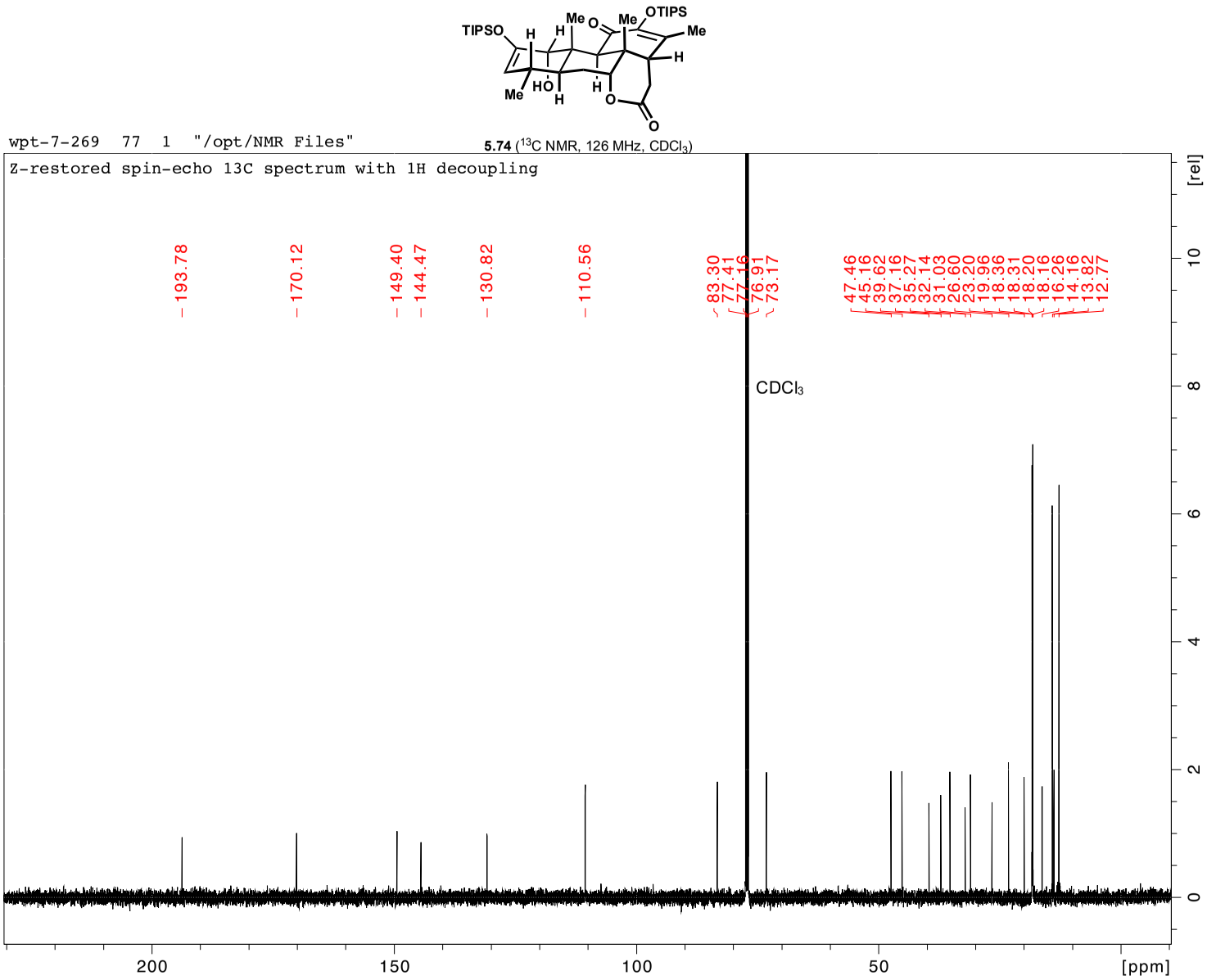
TIPSO
H
H
Me
O
Me
OTIPS
Me
H
Me
HO
H
H
O
O
wpt-7-269 77 1 "/opt/NMR Files"
5.74 (13C NMR, 126 MHz, CDCl3)
Z-restored spin-echo 13C spectrum with 1H decoupling
193.78
170.12
149.40
144.47
130.82
110.56
83.30
77.41
77.16
76.91
73.17
47.46
45.16
39.62
37.16
35.27
32.14
31.03
26.60
23.20
19.96
18.36
18.31
18.20
18.16
16.26
14.16
13.82
12.77
CDCl3
[rel]
0
2
4
6
8
10
200
150
100
50
[ppm]

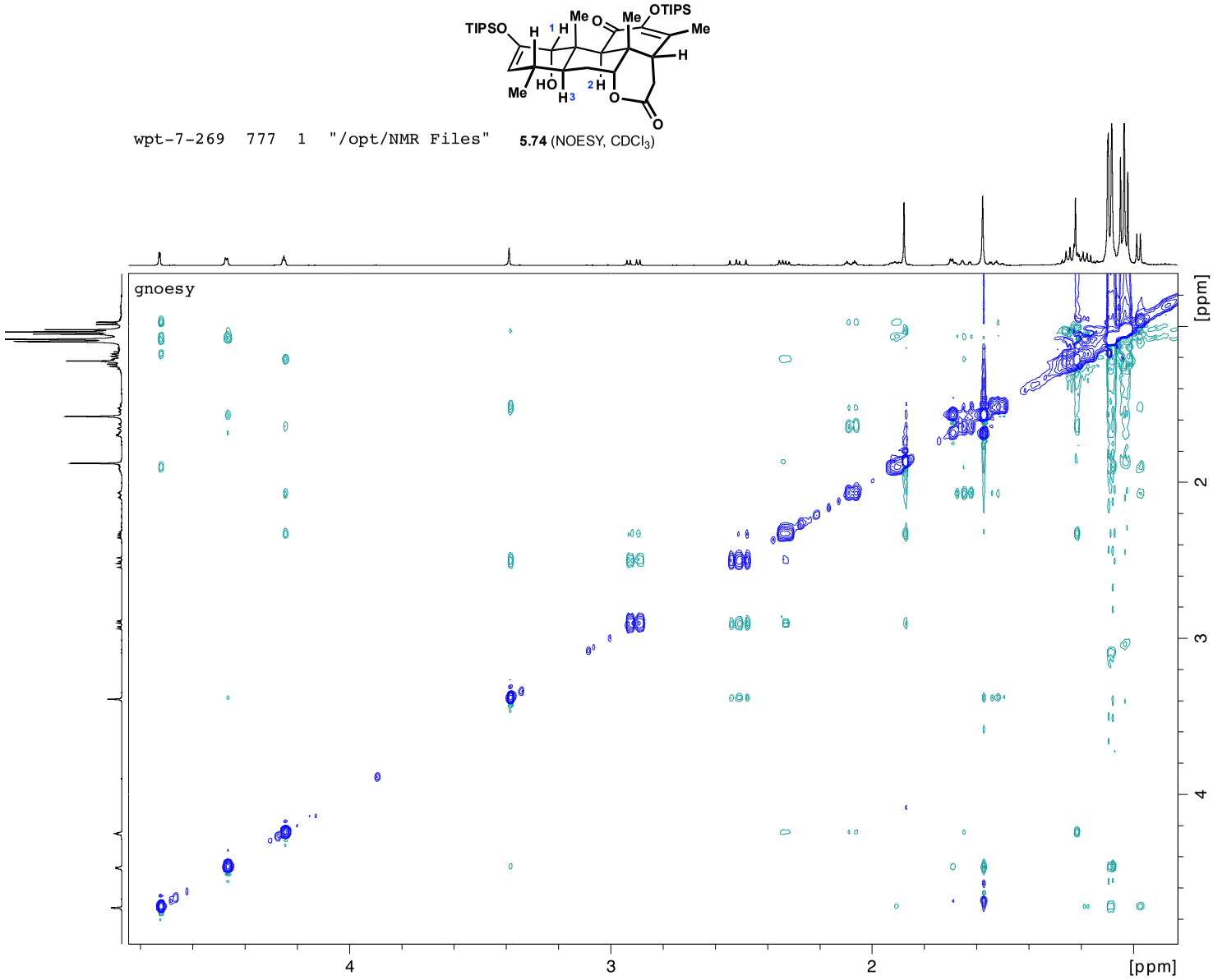
TIPSO
H
1H
Me
O
Me
OTIPS
Me
H
HO
Me
H3
2H
O
O
wpt-7-269 777 1 "/opt/NMR Files"
5.74 (NOESY, CDCl3)
gnoesy
[ppm]
4
3
2
[ppm]

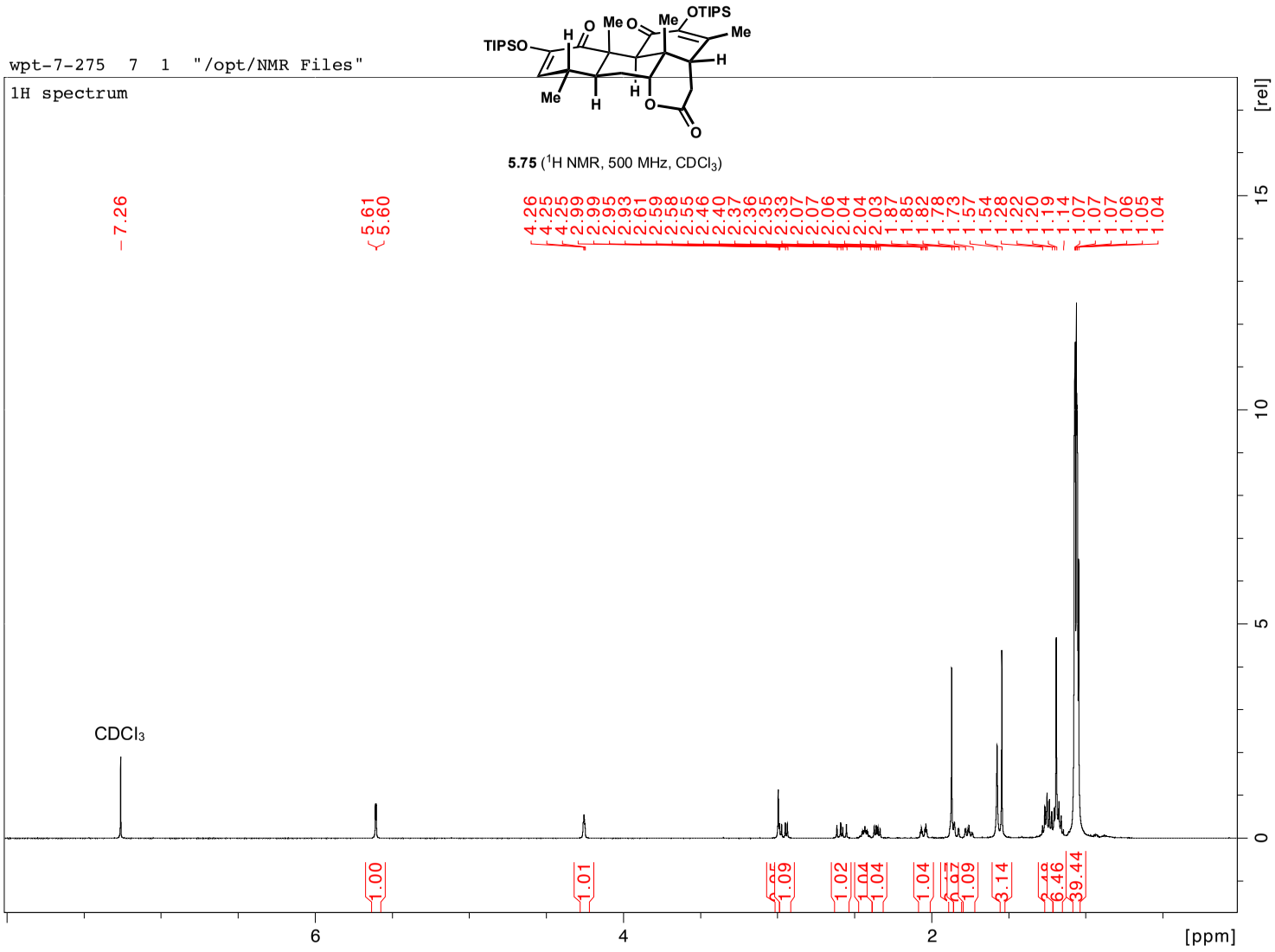
wpt-7-275 7 1 "/opt/NMR Files"
1H spectrum
TIPSO
OTIPS
Me
H
O
Me
O
Me
Me
H
H
Me
H
O
O
5.75 (1H NMR, 500 MHz, CDCl3)
7.26
5.61
5.60
4.26
4.25
4.25
2.99
2.95
2.93
2.61
2.59
2.58
2.55
2.46
2.40
2.37
2.36
2.35
2.33
2.07
2.07
2.06
2.04
2.04
2.03
1.87
1.85
1.82
1.78
1.73
1.57
1.54
1.28
1.22
1.20
1.19
1.14
1.07
1.07
1.07
1.06
1.05
1.04
CDCl3
1.00
1.01
1.09
1.02
1.04
1.04
1.04
1.09
3.14
6.46
39.44
6
4
2
[ppm]
[rel]
15
10
5
0

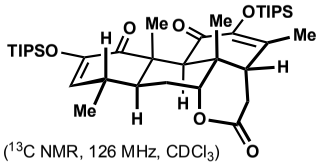

5.75 (^{13}C NMR, 126 MHz, $CDCl_3$)

wpt-7-275 77 1 "/opt/NMR Files"

Z-restored spin-echo 13C spectrum with 1H decoupling

198.87
191.06
169.82
144.60
144.58
129.10
125.76
82.45
77.42
77.16
76.91
47.05
45.91
45.69
43.85
37.18
31.98
31.69
26.07
22.82
19.16
18.43
18.37
18.22
18.18
15.96
14.05
13.18
13.10
$CDCl_3$

[rel]
0
2
4
6
8
10
12
14
200
150
100
50
[ppm]

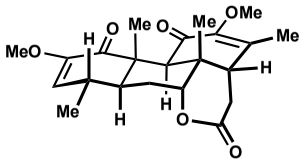

wpt-7-276 70 1 "/opt/NMR Files"

quassin, **5.1** (^{1}H NMR, 500 MHz, $CDCl_3$)

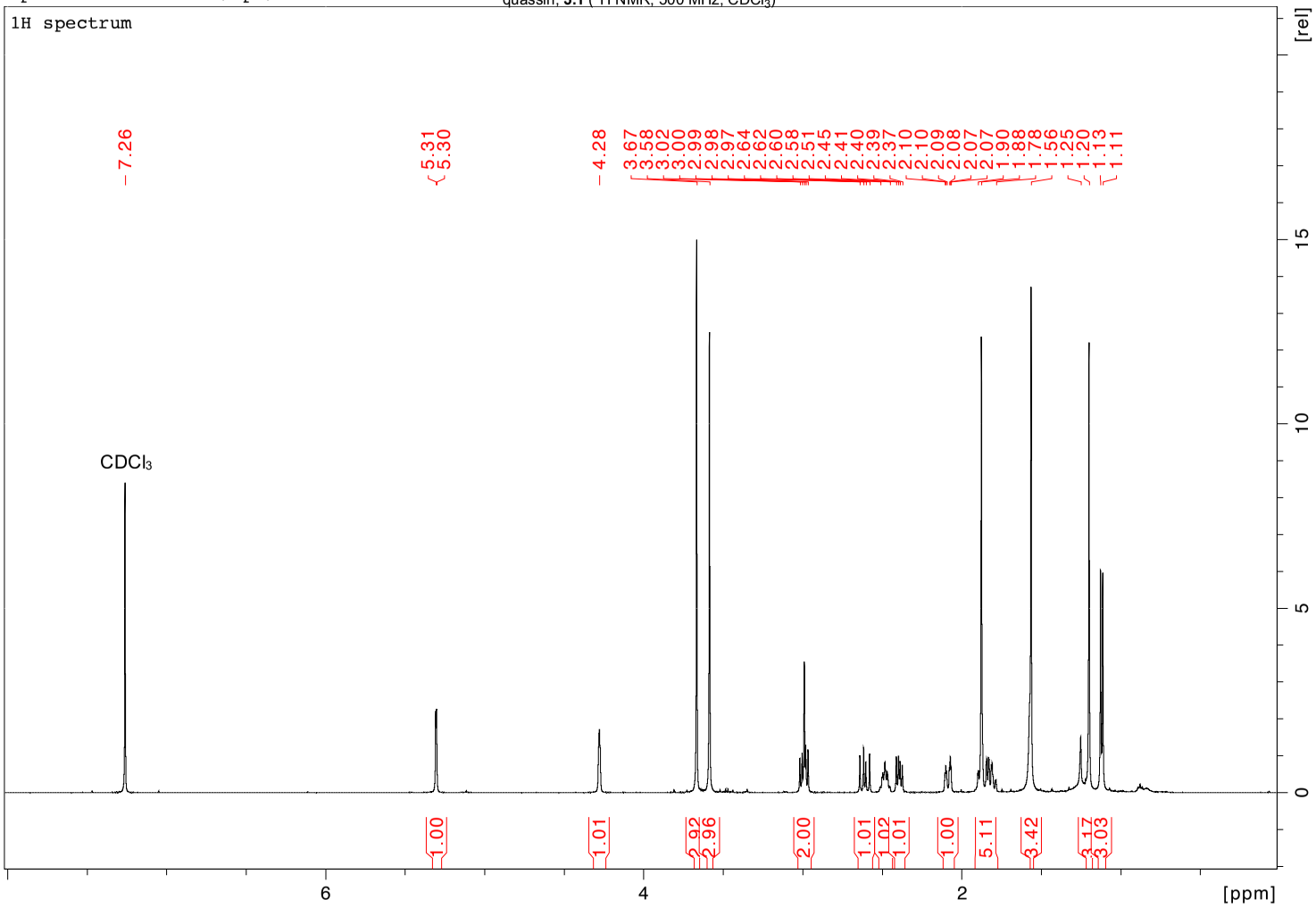

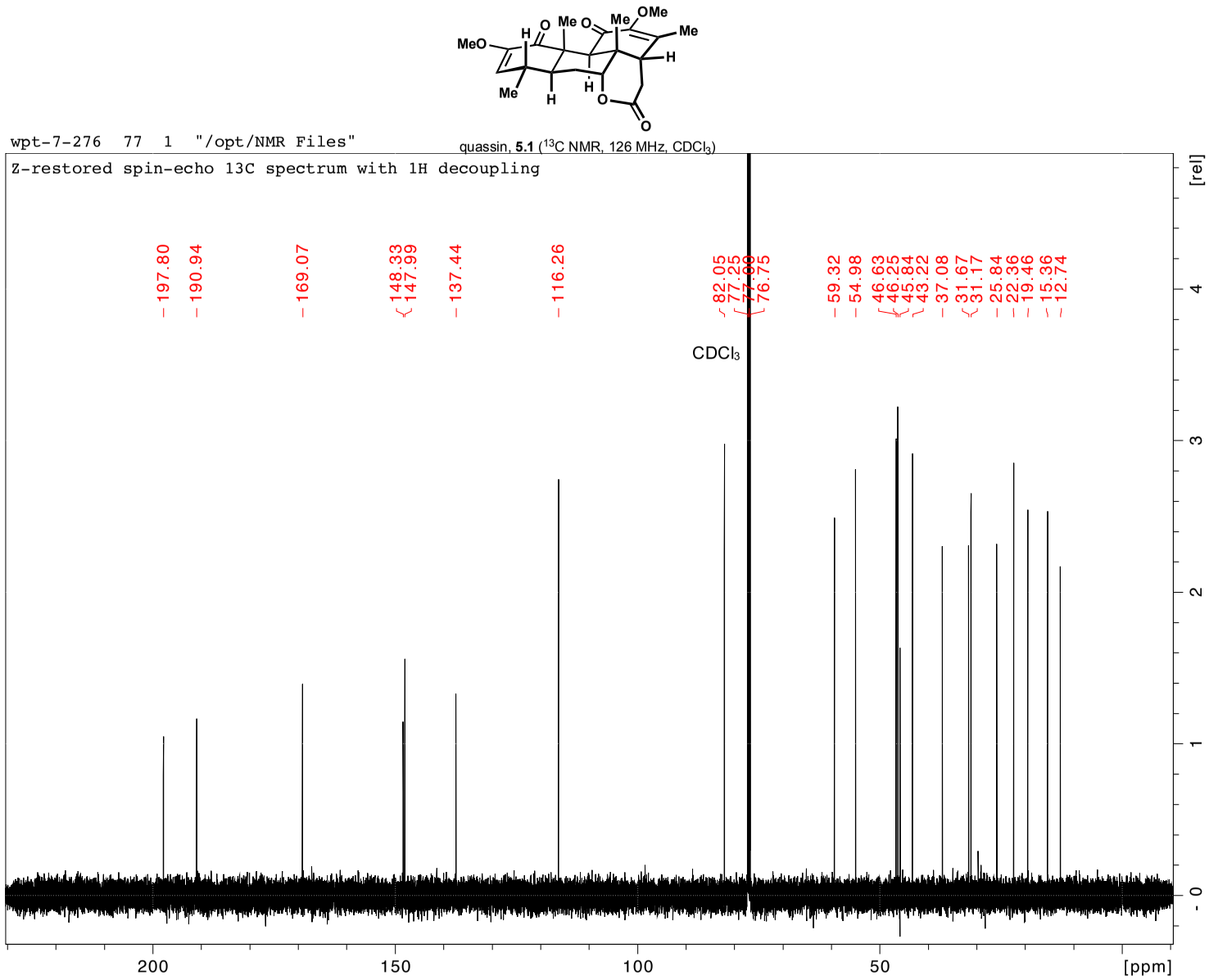
wpt-7-276 77 1 "/opt/NMR Files"
quassin, 5.1 (13C NMR, 126 MHz, CDCl3)
Z-restored spin-echo 13C spectrum with 1H decoupling
197.80
190.94
169.07
148.33
147.99
137.44
116.26
82.05
77.25
77.00
76.75
59.32
54.98
46.63
46.25
45.84
43.22
37.08
31.67
31.17
25.84
22.36
19.46
15.36
12.74
CDCl3
[rel]
0
1
2
3
4
200
150
100
50
[ppm]

Appendix C: X-Ray Crystallographic Data

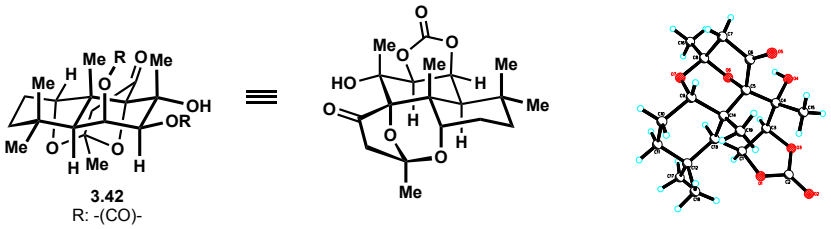

Table 1. Crystal data and structure refinement for **3.42**.

Identification code	3.42 (William Thomas)	
Empirical formula	$C_{19}H_{26}O_7$	
Formula weight	366.40	
Temperature	133(2) K	
Wavelength	0.71073 Å	
Crystal system	Tetragonal	
Space group	$I\bar{4}$	
Unit cell dimensions	a = 21.500(5) Å	□ = 90°.
	b = 21.500(5) Å	□ = 90°.
	c = 7.8999(19) Å	□ = 90°.
Volume	3651.7(19) Å^3	
Z	8	
Density (calculated)	1.333 Mg/m^3	
Absorption coefficient	0.101 mm^{-1}	
F(000)	1568	
Crystal color	colorless	
Crystal size	0.267 x 0.214 x 0.155 mm^3	
Theta range for data collection	1.339 to 25.495°	
Index ranges	$-25 \le h \le 25$, $-25 \le k \le 25$, $-9 \le l \le 9$	
Reflections collected	19116	
Independent reflections	3393 [R(int) = 0.0544]	
Completeness to theta = 25.242°	99.9 %	
Absorption correction	Semi-empirical from equivalents	
Max. and min. transmission	0.8620 and 0.7703	
Refinement method	Full-matrix least-squares on F^2	
Data / restraints / parameters	3393 / 0 / 244	
Goodness-of-fit on F^2	1.176	

Final R indices [I>2sigma(I) = 3073 data]	R1 = 0.0671, wR2 = 0.1417
R indices (all data, 0.83 Å)	R1 = 0.0741, wR2 = 0.1453
Largest diff. peak and hole	0.333 and -0.286 e.Å^{-3}

Table 2. Atomic coordinates (x 10^4) and equivalent isotropic displacement parameters (Å^2 x 10^3)
for 3.42. U(eq) is defined as one third of the trace of the orthogonalized U^{ij} tensor.

	x	y	z	U(eq)
O(1)	3386(2)	-1556(2)	4883(5)	17(1)
O(2)	2763(2)	-1296(2)	7094(6)	22(1)
O(3)	2616(2)	-2200(2)	5681(5)	16(1)
O(4)	3025(2)	-3597(2)	5573(6)	21(1)
O(5)	4575(2)	-3784(2)	6355(6)	24(1)
O(6)	3702(2)	-3486(2)	2773(5)	15(1)
O(7)	4606(2)	-3305(2)	1231(5)	19(1)
C(1)	3323(3)	-2025(3)	3529(7)	17(1)
C(2)	2917(3)	-1643(3)	5977(8)	16(1)
C(3)	2991(3)	-2552(3)	4468(8)	14(1)
C(4)	3390(3)	-3035(3)	5393(8)	15(1)
C(5)	3954(3)	-3191(3)	4270(8)	14(1)
C(6)	4385(3)	-3708(3)	4919(8)	19(1)
C(7)	4545(3)	-4122(3)	3416(8)	19(1)
C(8)	4223(3)	-3775(3)	1942(7)	15(1)
C(9)	4864(3)	-2884(3)	2444(8)	23(2)
C(10)	5190(3)	-2370(4)	1423(9)	28(2)
C(11)	4730(3)	-1967(4)	465(9)	30(2)
C(12)	4230(3)	-1664(3)	1573(9)	26(2)
C(13)	3913(3)	-2201(3)	2613(8)	19(1)
C(14)	4348(3)	-2621(3)	3668(8)	15(1)
C(15)	3551(3)	-2850(3)	7198(8)	21(1)
C(16)	3978(3)	-4180(3)	546(8)	24(2)
C(17)	3742(3)	-1378(4)	387(9)	33(2)
C(18)	4509(3)	-1141(4)	2663(9)	33(2)
C(19)	4693(3)	-2315(3)	5175(8)	22(1)

Table 3. Bond lengths [Å] and angles [°] for 3.42.

O(1)-C(2)	1.341(7)
O(1)-C(1)	1.476(7)
O(2)-C(2)	1.202(7)
O(3)-C(2)	1.379(7)
O(3)-C(3)	1.463(7)
O(4)-C(4)	1.448(7)
O(4)-H(4)	0.83(10)
O(5)-C(6)	1.216(7)
O(6)-C(8)	1.440(7)
O(6)-C(5)	1.447(7)
O(7)-C(8)	1.419(7)
O(7)-C(9)	1.430(8)
C(1)-C(13)	1.508(8)
C(1)-C(3)	1.531(8)
C(1)-H(1A)	1.0000
C(3)-C(4)	1.534(8)
C(3)-H(3A)	1.0000
C(4)-C(15)	1.520(8)
C(4)-C(5)	1.540(8)
C(5)-C(6)	1.534(8)
C(5)-C(14)	1.565(9)
C(6)-C(7)	1.524(9)
C(7)-C(8)	1.547(9)
C(7)-H(7A)	0.9900
C(7)-H(7B)	0.9900
C(8)-C(16)	1.502(8)
C(9)-C(10)	1.537(10)
C(9)-C(14)	1.575(8)
C(9)-H(9A)	1.0000
C(10)-C(11)	1.516(10)
C(10)-H(10A)	0.9900
C(10)-H(10B)	0.9900
C(11)-C(12)	1.532(10)
C(11)-H(11A)	0.9900

C(11)-H(11B)	0.9900
C(12)-C(17)	1.536(9)
C(12)-C(18)	1.538(11)
C(12)-C(13)	1.571(9)
C(13)-C(14)	1.545(8)
C(13)-H(13A)	1.0000
C(14)-C(19)	1.550(8)
C(15)-H(15A)	0.9800
C(15)-H(15B)	0.9800
C(15)-H(15C)	0.9800
C(16)-H(16A)	0.9800
C(16)-H(16B)	0.9800
C(16)-H(16C)	0.9800
C(17)-H(17A)	0.9800
C(17)-H(17B)	0.9800
C(17)-H(17C)	0.9800
C(18)-H(18A)	0.9800
C(18)-H(18B)	0.9800
C(18)-H(18C)	0.9800
C(19)-H(19A)	0.9800
C(19)-H(19B)	0.9800
C(19)-H(19C)	0.9800

C(2)-O(1)-C(1)	107.7(4)
C(2)-O(3)-C(3)	107.6(4)
C(4)-O(4)-H(4)	109(6)
C(8)-O(6)-C(5)	105.6(4)
C(8)-O(7)-C(9)	114.2(5)
O(1)-C(1)-C(13)	116.2(5)
O(1)-C(1)-C(3)	101.3(4)
C(13)-C(1)-C(3)	116.1(5)
O(1)-C(1)-H(1A)	107.5
C(13)-C(1)-H(1A)	107.5
C(3)-C(1)-H(1A)	107.5
O(2)-C(2)-O(1)	126.4(6)
O(2)-C(2)-O(3)	122.2(5)

O(1)-C(2)-O(3)	111.3(5)
O(3)-C(3)-C(1)	101.1(4)
O(3)-C(3)-C(4)	110.3(5)
C(1)-C(3)-C(4)	118.1(5)
O(3)-C(3)-H(3A)	109.0
C(1)-C(3)-H(3A)	109.0
C(4)-C(3)-H(3A)	109.0
O(4)-C(4)-C(15)	104.5(5)
O(4)-C(4)-C(3)	107.9(5)
C(15)-C(4)-C(3)	113.3(5)
O(4)-C(4)-C(5)	107.6(5)
C(15)-C(4)-C(5)	114.8(5)
C(3)-C(4)-C(5)	108.3(5)
O(6)-C(5)-C(6)	100.5(4)
O(6)-C(5)-C(4)	105.7(4)
C(6)-C(5)-C(4)	116.2(5)
O(6)-C(5)-C(14)	107.3(5)
C(6)-C(5)-C(14)	110.0(5)
C(4)-C(5)-C(14)	115.5(5)
O(5)-C(6)-C(7)	124.9(6)
O(5)-C(6)-C(5)	127.7(6)
C(7)-C(6)-C(5)	107.4(5)
C(6)-C(7)-C(8)	101.7(5)
C(6)-C(7)-H(7A)	111.4
C(8)-C(7)-H(7A)	111.4
C(6)-C(7)-H(7B)	111.4
C(8)-C(7)-H(7B)	111.4
H(7A)-C(7)-H(7B)	109.3
O(7)-C(8)-O(6)	109.0(5)
O(7)-C(8)-C(16)	109.1(5)
O(6)-C(8)-C(16)	108.1(5)
O(7)-C(8)-C(7)	112.5(5)
O(6)-C(8)-C(7)	102.3(5)
C(16)-C(8)-C(7)	115.4(5)
O(7)-C(9)-C(10)	106.3(5)
O(7)-C(9)-C(14)	111.5(5)

C(10)-C(9)-C(14)	112.7(6)
O(7)-C(9)-H(9A)	108.8
C(10)-C(9)-H(9A)	108.8
C(14)-C(9)-H(9A)	108.8
C(11)-C(10)-C(9)	112.0(5)
C(11)-C(10)-H(10A)	109.2
C(9)-C(10)-H(10A)	109.2
C(11)-C(10)-H(10B)	109.2
C(9)-C(10)-H(10B)	109.2
H(10A)-C(10)-H(10B)	107.9
C(10)-C(11)-C(12)	114.5(6)
C(10)-C(11)-H(11A)	108.6
C(12)-C(11)-H(11A)	108.6
C(10)-C(11)-H(11B)	108.6
C(12)-C(11)-H(11B)	108.6
H(11A)-C(11)-H(11B)	107.6
C(11)-C(12)-C(17)	107.6(6)
C(11)-C(12)-C(18)	110.9(6)
C(17)-C(12)-C(18)	108.3(6)
C(11)-C(12)-C(13)	106.9(6)
C(17)-C(12)-C(13)	108.5(5)
C(18)-C(12)-C(13)	114.4(6)
C(1)-C(13)-C(14)	113.4(5)
C(1)-C(13)-C(12)	115.6(5)
C(14)-C(13)-C(12)	116.6(5)
C(1)-C(13)-H(13A)	102.8
C(14)-C(13)-H(13A)	102.8
C(12)-C(13)-H(13A)	102.8
C(13)-C(14)-C(19)	117.1(5)
C(13)-C(14)-C(5)	107.1(5)
C(19)-C(14)-C(5)	111.0(5)
C(13)-C(14)-C(9)	107.8(5)
C(19)-C(14)-C(9)	106.7(5)
C(5)-C(14)-C(9)	106.7(5)
C(4)-C(15)-H(15A)	109.5
C(4)-C(15)-H(15B)	109.5

H(15A)-C(15)-H(15B)	109.5
C(4)-C(15)-H(15C)	109.5
H(15A)-C(15)-H(15C)	109.5
H(15B)-C(15)-H(15C)	109.5
C(8)-C(16)-H(16A)	109.5
C(8)-C(16)-H(16B)	109.5
H(16A)-C(16)-H(16B)	109.5
C(8)-C(16)-H(16C)	109.5
H(16A)-C(16)-H(16C)	109.5
H(16B)-C(16)-H(16C)	109.5
C(12)-C(17)-H(17A)	109.5
C(12)-C(17)-H(17B)	109.5
H(17A)-C(17)-H(17B)	109.5
C(12)-C(17)-H(17C)	109.5
H(17A)-C(17)-H(17C)	109.5
H(17B)-C(17)-H(17C)	109.5
C(12)-C(18)-H(18A)	109.5
C(12)-C(18)-H(18B)	109.5
H(18A)-C(18)-H(18B)	109.5
C(12)-C(18)-H(18C)	109.5
H(18A)-C(18)-H(18C)	109.5
H(18B)-C(18)-H(18C)	109.5
C(14)-C(19)-H(19A)	109.5
C(14)-C(19)-H(19B)	109.5
H(19A)-C(19)-H(19B)	109.5
C(14)-C(19)-H(19C)	109.5
H(19A)-C(19)-H(19C)	109.5
H(19B)-C(19)-H(19C)	109.5

Table 4. Anisotropic displacement parameters ($Å^2$ x 10^3) for 3.42. The anisotropic displacement factor exponent takes the form: $-2\pi^2[h^2 a^{*2} U^{11} + ... + 2 h k a^* b^* U^{12}]$

	U^{11}	U^{22}	U^{33}	U^{23}	U^{13}	U^{12}
O(1)	13(2)	20(2)	17(2)	-1(2)	2(2)	2(2)
O(2)	27(3)	26(2)	15(2)	-3(2)	0(2)	6(2)
O(3)	15(2)	18(2)	15(2)	-2(2)	1(2)	4(2)
O(4)	22(2)	19(2)	21(2)	4(2)	4(2)	-5(2)
O(5)	20(2)	36(3)	17(2)	1(2)	-3(2)	8(2)
O(6)	9(2)	22(2)	14(2)	-4(2)	2(2)	1(2)
O(7)	15(2)	31(3)	12(2)	-1(2)	2(2)	-2(2)
C(1)	18(3)	23(3)	11(3)	2(3)	-1(2)	5(3)
C(2)	5(3)	22(3)	20(3)	7(3)	-6(2)	2(2)
C(3)	16(3)	14(3)	12(3)	0(2)	3(2)	5(2)
C(4)	11(3)	14(3)	20(3)	4(3)	3(3)	2(2)
C(5)	11(3)	13(3)	18(3)	-5(2)	-4(2)	8(2)
C(6)	7(3)	27(3)	22(3)	7(3)	2(2)	-3(2)
C(7)	17(3)	19(3)	21(3)	0(3)	-4(3)	1(3)
C(8)	10(3)	25(3)	11(3)	1(3)	6(2)	0(3)
C(9)	13(3)	42(4)	13(3)	-4(3)	-3(2)	1(3)
C(10)	4(3)	56(5)	24(3)	0(4)	5(3)	-4(3)
C(11)	17(3)	52(5)	20(3)	9(3)	5(3)	-6(3)
C(12)	23(4)	37(4)	18(3)	8(3)	4(3)	3(3)
C(13)	12(3)	32(4)	12(3)	1(3)	1(2)	2(3)
C(14)	5(3)	26(3)	15(3)	-1(3)	-1(2)	0(2)
C(15)	22(3)	28(4)	13(3)	-1(3)	-3(3)	0(3)
C(16)	27(4)	27(4)	19(3)	-2(3)	-1(3)	-5(3)
C(17)	24(4)	54(5)	20(4)	12(4)	3(3)	-1(3)
C(18)	24(4)	46(5)	28(4)	13(3)	6(3)	-1(3)
C(19)	14(3)	36(4)	18(3)	1(3)	-3(3)	5(3)

Table 5. Hydrogen coordinates (x 10^4) and isotropic displacement parameters (Å^2 x 10^3) for 3.42.

	x	y	z	U(eq)
H(4)	2960(40)	-3740(40)	4620(120)	50(30)
H(1A)	3027	-1856	2669	21
H(3A)	2707	-2771	3663	17
H(7A)	4375	-4547	3560	23
H(7B)	5001	-4149	3242	23
H(9A)	5182	-3109	3132	27
H(10A)	5434	-2105	2203	34
H(10B)	5482	-2562	610	34
H(11A)	4523	-2226	-404	36
H(11B)	4963	-1636	-131	36
H(13A)	3760	-2488	1708	22
H(15A)	3699	-2419	7213	31
H(15B)	3877	-3125	7633	31
H(15C)	3180	-2886	7911	31
H(16A)	3727	-4516	1033	37
H(16B)	4326	-4359	-88	37
H(16C)	3719	-3931	-218	37
H(17A)	3442	-1138	1054	49
H(17B)	3524	-1710	-222	49
H(17C)	3948	-1103	-428	49
H(18A)	4201	-1005	3499	49
H(18B)	4623	-790	1936	49
H(18C)	4880	-1296	3247	49
H(19A)	4808	-2635	6000	34
H(19B)	4420	-2008	5715	34
H(19C)	5070	-2107	4763	34

Table 6. Torsion angles [°] for 3.42.

C(2)-O(1)-C(1)-C(13)	-154.7(5)
C(2)-O(1)-C(1)-C(3)	-27.8(5)
C(1)-O(1)-C(2)-O(2)	-168.3(6)
C(1)-O(1)-C(2)-O(3)	12.1(6)
C(3)-O(3)-C(2)-O(2)	-169.4(5)
C(3)-O(3)-C(2)-O(1)	10.2(6)
C(2)-O(3)-C(3)-C(1)	-26.7(5)
C(2)-O(3)-C(3)-C(4)	99.0(5)
O(1)-C(1)-C(3)-O(3)	32.0(5)
C(13)-C(1)-C(3)-O(3)	158.9(5)
O(1)-C(1)-C(3)-C(4)	-88.3(6)
C(13)-C(1)-C(3)-C(4)	38.6(8)
O(3)-C(3)-C(4)-O(4)	87.6(6)
C(1)-C(3)-C(4)-O(4)	-157.0(5)
O(3)-C(3)-C(4)-C(15)	-27.6(7)
C(1)-C(3)-C(4)-C(15)	87.7(6)
O(3)-C(3)-C(4)-C(5)	-156.2(5)
C(1)-C(3)-C(4)-C(5)	-40.8(7)
C(8)-O(6)-C(5)-C(6)	-44.2(5)
C(8)-O(6)-C(5)-C(4)	-165.4(5)
C(8)-O(6)-C(5)-C(14)	70.7(5)
O(4)-C(4)-C(5)-O(6)	51.5(6)
C(15)-C(4)-C(5)-O(6)	167.3(5)
C(3)-C(4)-C(5)-O(6)	-64.9(6)
O(4)-C(4)-C(5)-C(6)	-58.9(6)
C(15)-C(4)-C(5)-C(6)	56.9(7)
C(3)-C(4)-C(5)-C(6)	-175.3(5)
O(4)-C(4)-C(5)-C(14)	170.0(5)
C(15)-C(4)-C(5)-C(14)	-74.2(7)
C(3)-C(4)-C(5)-C(14)	53.6(6)
O(6)-C(5)-C(6)-O(5)	-157.2(6)
C(4)-C(5)-C(6)-O(5)	-43.7(9)
C(14)-C(5)-C(6)-O(5)	89.9(7)
O(6)-C(5)-C(6)-C(7)	23.2(6)

C(4)-C(5)-C(6)-C(7)	136.7(5)
C(14)-C(5)-C(6)-C(7)	-89.8(6)
O(5)-C(6)-C(7)-C(8)	-175.6(6)
C(5)-C(6)-C(7)-C(8)	4.1(6)
C(9)-O(7)-C(8)-O(6)	61.6(6)
C(9)-O(7)-C(8)-C(16)	179.4(5)
C(9)-O(7)-C(8)-C(7)	-51.2(7)
C(5)-O(6)-C(8)-O(7)	-71.2(5)
C(5)-O(6)-C(8)-C(16)	170.4(5)
C(5)-O(6)-C(8)-C(7)	48.1(6)
C(6)-C(7)-C(8)-O(7)	86.6(6)
C(6)-C(7)-C(8)-O(6)	-30.2(6)
C(6)-C(7)-C(8)-C(16)	-147.4(5)
C(8)-O(7)-C(9)-C(10)	-173.1(5)
C(8)-O(7)-C(9)-C(14)	-50.0(7)
O(7)-C(9)-C(10)-C(11)	68.2(7)
C(14)-C(9)-C(10)-C(11)	-54.2(7)
C(9)-C(10)-C(11)-C(12)	56.2(8)
C(10)-C(11)-C(12)-C(17)	-169.8(6)
C(10)-C(11)-C(12)-C(18)	71.8(8)
C(10)-C(11)-C(12)-C(13)	-53.5(8)
O(1)-C(1)-C(13)-C(14)	74.4(7)
C(3)-C(1)-C(13)-C(14)	-44.7(7)
O(1)-C(1)-C(13)-C(12)	-64.1(7)
C(3)-C(1)-C(13)-C(12)	176.8(5)
C(11)-C(12)-C(13)-C(1)	-168.4(5)
C(17)-C(12)-C(13)-C(1)	-52.6(7)
C(18)-C(12)-C(13)-C(1)	68.4(7)
C(11)-C(12)-C(13)-C(14)	54.5(7)
C(17)-C(12)-C(13)-C(14)	170.2(6)
C(18)-C(12)-C(13)-C(14)	-68.7(8)
C(1)-C(13)-C(14)-C(19)	-71.9(7)
C(12)-C(13)-C(14)-C(19)	66.2(7)
C(1)-C(13)-C(14)-C(5)	53.5(7)
C(12)-C(13)-C(14)-C(5)	-168.5(5)
C(1)-C(13)-C(14)-C(9)	167.9(5)

C(12)-C(13)-C(14)-C(9)	-54.0(7)
O(6)-C(5)-C(14)-C(13)	56.8(6)
C(6)-C(5)-C(14)-C(13)	165.3(5)
C(4)-C(5)-C(14)-C(13)	-60.8(6)
O(6)-C(5)-C(14)-C(19)	-174.2(5)
C(6)-C(5)-C(14)-C(19)	-65.7(6)
C(4)-C(5)-C(14)-C(19)	68.2(6)
O(6)-C(5)-C(14)-C(9)	-58.3(5)
C(6)-C(5)-C(14)-C(9)	50.1(6)
C(4)-C(5)-C(14)-C(9)	-176.0(5)
O(7)-C(9)-C(14)-C(13)	-67.6(7)
C(10)-C(9)-C(14)-C(13)	51.7(7)
O(7)-C(9)-C(14)-C(19)	165.8(5)
C(10)-C(9)-C(14)-C(19)	-74.8(6)
O(7)-C(9)-C(14)-C(5)	47.1(6)
C(10)-C(9)-C(14)-C(5)	166.5(5)

Table 7. Hydrogen bonds for 3.42 [Å and °].

D-H...A	d(D-H)	d(H...A)	d(D...A)	<(DHA)
O(4)-H(4)...O(2)#1	0.83(10)	2.53(9)	3.236(7)	144(8)
O(4)-H(4)...O(6)	0.83(10)	2.23(9)	2.659(6)	112(7)

Symmetry transformations used to generate equivalent atoms:
#1 -x+1/2,-y-1/2,z-1/2

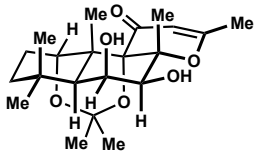

3.54

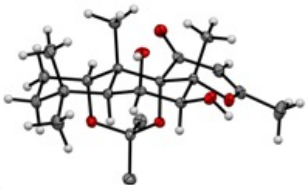

Table 1. Crystal data and structure refinement for **3.54**

Identification code	3.54 (William Thomas)	
Empirical formula	C_{21} H_{32} O_6	
Formula weight	380.46	
Temperature	133(2) K	
Wavelength	0.71073 Å	
Crystal system	Monoclinic	
Space group	$P2_1/c$	
Unit cell dimensions	a = 11.3869(6) Å	□ = 90°.
	b = 11.0755(6) Å	□ = 106.0167(7)°.
	c = 16.4649(9) Å	□ = 90°.
Volume	1995.87(19) $Å^3$	
Z	4	
Density (calculated)	1.266 Mg/m^3	
Absorption coefficient	0.091 mm^{-1}	
F(000)	824	
Crystal color	colorless	
Crystal size	0.417 x 0.356 x 0.193 mm^3	
Theta range for data collection	1.861 to 28.854°	
Index ranges	$-15 \le h \le 15$, $-14 \le k \le 14$, $-21 \le l \le 21$	
Reflections collected	23515	
Independent reflections	4932 [R(int) = 0.0231]	
Completeness to theta = 25.500°	100.0 %	
Absorption correction	Semi-empirical from equivalents	
Max. and min. transmission	0.8621 and 0.8233	
Refinement method	Full-matrix least-squares on F^2	
Data / restraints / parameters	4932 / 0 / 372	
Goodness-of-fit on F^2	1.032	
Final R indices [I>2sigma(I) = 4236 data]	R1 = 0.0362, wR2 = 0.0946	

R indices (all data, 0.74 Å)	R1 = 0.0433, wR2 = 0.1004
Largest diff. peak and hole	0.411 and -0.220 e.Å^{-3}

Table 2. Atomic coordinates (x 10^4) and equivalent isotropic displacement parameters (Å^2 x 10^3)
for 3.54. U(eq) is defined as one third of the trace of the orthogonalized U^{ij} tensor.

	x	y	z	U(eq)
O(1)	9068(1)	125(1)	8530(1)	17(1)
O(2)	6951(1)	42(1)	8314(1)	14(1)
O(3)	7195(1)	3076(1)	8613(1)	19(1)
O(4)	4621(1)	536(1)	7730(1)	16(1)
O(5)	4250(1)	-131(1)	6015(1)	17(1)
O(6)	6047(1)	1080(1)	5529(1)	18(1)
C(1)	7740(1)	1345(1)	7378(1)	13(1)
C(2)	7656(1)	272(1)	6746(1)	14(1)
C(3)	8744(1)	167(1)	6339(1)	19(1)
C(4)	9930(1)	121(1)	7068(1)	22(1)
C(5)	10062(1)	1171(1)	7686(1)	21(1)
C(6)	8982(1)	1239(1)	8064(1)	16(1)
C(7)	8124(1)	-106(1)	8916(1)	16(1)
C(8)	6728(1)	1155(1)	7842(1)	13(1)
C(9)	6552(1)	2169(1)	8449(1)	16(1)
C(10)	5555(1)	1922(1)	8814(1)	18(1)
C(11)	4696(1)	1095(1)	8467(1)	18(1)
C(12)	5429(1)	984(1)	7234(1)	14(1)
C(13)	5424(1)	-40(1)	6612(1)	13(1)
C(14)	6383(1)	121(1)	6127(1)	15(1)
C(15)	7656(1)	2607(1)	6961(1)	17(1)
C(16)	8853(1)	1166(1)	5714(1)	25(1)
C(17)	8627(1)	-1038(1)	5858(1)	26(1)
C(18)	8199(1)	-1441(1)	9122(1)	22(1)
C(19)	8280(1)	650(1)	9716(1)	21(1)
C(20)	3713(1)	690(1)	8845(1)	30(1)
C(21)	4838(1)	2132(1)	6786(1)	18(1)

Table 3. Bond lengths [Å] and angles [°] for 3.54.

O(1)-C(7)	1.4144(12)
O(1)-C(6)	1.4414(12)
O(2)-C(7)	1.4368(11)
O(2)-C(8)	1.4412(11)
O(3)-C(9)	1.2291(13)
O(4)-C(11)	1.3440(12)
O(4)-C(12)	1.4747(11)
O(5)-C(13)	1.4271(11)
O(6)-C(14)	1.4258(12)
C(1)-C(15)	1.5493(14)
C(1)-C(6)	1.5514(13)
C(1)-C(8)	1.5627(13)
C(1)-C(2)	1.5646(13)
C(2)-C(14)	1.5342(14)
C(2)-C(3)	1.5669(14)
C(3)-C(17)	1.5393(16)
C(3)-C(16)	1.5401(15)
C(3)-C(4)	1.5403(15)
C(4)-C(5)	1.5247(17)
C(5)-C(6)	1.5258(14)
C(7)-C(18)	1.5142(15)
C(7)-C(19)	1.5289(15)
C(8)-C(9)	1.5522(13)
C(8)-C(12)	1.5522(13)
C(9)-C(10)	1.4495(14)
C(10)-C(11)	1.3466(15)
C(11)-C(20)	1.4911(15)
C(12)-C(13)	1.5270(13)
C(12)-C(21)	1.5299(14)
C(13)-C(14)	1.5303(14)

C(7)-O(1)-C(6)	116.49(8)
C(7)-O(2)-C(8)	117.50(7)
C(11)-O(4)-C(12)	116.90(8)
C(15)-C(1)-C(6)	108.89(8)

C(15)-C(1)-C(8)	111.99(8)
C(6)-C(1)-C(8)	106.32(8)
C(15)-C(1)-C(2)	113.89(8)
C(6)-C(1)-C(2)	107.66(8)
C(8)-C(1)-C(2)	107.74(8)
C(14)-C(2)-C(1)	113.46(8)
C(14)-C(2)-C(3)	114.89(8)
C(1)-C(2)-C(3)	115.47(8)
C(17)-C(3)-C(16)	106.90(9)
C(17)-C(3)-C(4)	107.75(9)
C(16)-C(3)-C(4)	109.24(9)
C(17)-C(3)-C(2)	108.56(9)
C(16)-C(3)-C(2)	116.89(9)
C(4)-C(3)-C(2)	107.19(8)
C(5)-C(4)-C(3)	113.49(9)
C(4)-C(5)-C(6)	111.57(9)
O(1)-C(6)-C(5)	103.37(8)
O(1)-C(6)-C(1)	111.47(8)
C(5)-C(6)-C(1)	112.44(8)
O(1)-C(7)-O(2)	110.22(8)
O(1)-C(7)-C(18)	105.96(8)
O(2)-C(7)-C(18)	104.47(8)
O(1)-C(7)-C(19)	111.47(8)
O(2)-C(7)-C(19)	113.36(8)
C(18)-C(7)-C(19)	110.88(9)
O(2)-C(8)-C(9)	107.87(7)
O(2)-C(8)-C(12)	103.78(7)
C(9)-C(8)-C(12)	103.57(7)
O(2)-C(8)-C(1)	109.51(7)
C(9)-C(8)-C(1)	117.45(8)
C(12)-C(8)-C(1)	113.62(8)
O(3)-C(9)-C(10)	123.42(9)
O(3)-C(9)-C(8)	123.91(9)
C(10)-C(9)-C(8)	112.66(8)
C(11)-C(10)-C(9)	120.87(10)
O(4)-C(11)-C(10)	123.59(9)

O(4)-C(11)-C(20)	111.76(9)
C(10)-C(11)-C(20)	124.65(10)
O(4)-C(12)-C(13)	103.58(7)
O(4)-C(12)-C(21)	106.68(8)
C(13)-C(12)-C(21)	112.02(8)
O(4)-C(12)-C(8)	108.20(7)
C(13)-C(12)-C(8)	110.52(8)
C(21)-C(12)-C(8)	115.05(8)
O(5)-C(13)-C(12)	110.10(8)
O(5)-C(13)-C(14)	108.46(8)
C(12)-C(13)-C(14)	113.05(8)
O(6)-C(14)-C(13)	110.67(8)
O(6)-C(14)-C(2)	113.70(8)
C(13)-C(14)-C(2)	110.19(8)

Table 4. Anisotropic displacement parameters ($Å^2$ x 10^3) for 3.54. The anisotropic displacement factor exponent takes the form: $-2\pi^2[h^2 a^{*2} U^{11} + ... + 2 h k a^* b^* U^{12}]$

	U^{11}	U^{22}	U^{33}	U^{23}	U^{13}	U^{12}
O(1)	12(1)	21(1)	18(1)	5(1)	3(1)	2(1)
O(2)	12(1)	15(1)	12(1)	2(1)	1(1)	0(1)
O(3)	18(1)	18(1)	20(1)	-5(1)	4(1)	-2(1)
O(4)	12(1)	22(1)	16(1)	-2(1)	5(1)	-2(1)
O(5)	16(1)	20(1)	13(1)	1(1)	0(1)	-5(1)
O(6)	25(1)	18(1)	12(1)	3(1)	3(1)	0(1)
C(1)	12(1)	14(1)	14(1)	1(1)	3(1)	0(1)
C(2)	15(1)	14(1)	14(1)	1(1)	5(1)	2(1)
C(3)	19(1)	21(1)	19(1)	2(1)	9(1)	3(1)
C(4)	15(1)	28(1)	25(1)	4(1)	10(1)	5(1)
C(5)	12(1)	28(1)	24(1)	4(1)	5(1)	-1(1)
C(6)	13(1)	18(1)	16(1)	2(1)	2(1)	-1(1)
C(7)	12(1)	21(1)	14(1)	3(1)	1(1)	0(1)
C(8)	12(1)	13(1)	12(1)	0(1)	2(1)	1(1)
C(9)	15(1)	17(1)	13(1)	-1(1)	1(1)	2(1)
C(10)	19(1)	21(1)	17(1)	-4(1)	7(1)	2(1)
C(11)	16(1)	22(1)	18(1)	-1(1)	6(1)	3(1)

C(12)	12(1)	16(1)	13(1)	0(1)	3(1)	0(1)
C(13)	14(1)	14(1)	11(1)	1(1)	1(1)	-1(1)
C(14)	18(1)	14(1)	12(1)	0(1)	4(1)	0(1)
C(15)	18(1)	14(1)	18(1)	1(1)	4(1)	-1(1)
C(16)	25(1)	30(1)	22(1)	6(1)	13(1)	1(1)
C(17)	30(1)	26(1)	27(1)	-3(1)	16(1)	6(1)
C(18)	18(1)	21(1)	22(1)	7(1)	0(1)	1(1)
C(19)	18(1)	28(1)	13(1)	0(1)	1(1)	-1(1)
C(20)	24(1)	41(1)	31(1)	-10(1)	16(1)	-8(1)
C(21)	17(1)	16(1)	18(1)	1(1)	1(1)	4(1)

Table 5. Hydrogen coordinates (x 10^4) and isotropic displacement parameters (Å^2 x 10^3) for 3.54.

	x	y	z	U(eq)
H(5)	3794(15)	-614(15)	6203(10)	37(4)
H(6)	5914(14)	747(14)	5036(10)	34(4)
H(2A)	7746(11)	-459(11)	7099(8)	13(3)
H(4A)	9948(13)	-651(13)	7379(9)	25(3)
H(4B)	10626(13)	103(13)	6837(9)	27(4)
H(5A)	10154(13)	1957(13)	7405(9)	25(3)
H(5B)	10797(14)	1059(13)	8165(9)	29(4)
H(6A)	9068(11)	1923(11)	8451(8)	15(3)
H(10A)	5533(12)	2351(12)	9319(9)	22(3)
H(13A)	5612(11)	-786(11)	6937(8)	12(3)
H(14A)	6375(11)	-657(12)	5809(8)	16(3)
H(15A)	7275(14)	3187(14)	7249(9)	31(4)
H(15B)	7194(13)	2601(13)	6360(9)	27(4)
H(15C)	8465(15)	2911(14)	6988(10)	36(4)
H(16A)	9500(15)	911(15)	5450(11)	44(5)
H(16B)	9103(13)	1955(14)	5989(9)	29(4)
H(16C)	8103(15)	1277(14)	5256(10)	36(4)
H(17A)	9411(14)	-1211(14)	5733(10)	34(4)
H(17B)	7970(14)	-1011(13)	5301(10)	32(4)

H(17C)	8466(14)	-1715(14)	6211(9)	31(4)
H(18A)	8097(13)	-1907(12)	8605(9)	24(3)
H(18B)	7560(14)	-1665(13)	9409(9)	32(4)
H(18C)	8987(14)	-1629(13)	9501(9)	31(4)
H(19A)	8417(13)	1515(13)	9618(9)	27(4)
H(19B)	8975(13)	350(13)	10148(9)	26(3)
H(19C)	7561(13)	568(13)	9919(9)	27(3)
H(20A)	3749(15)	1157(15)	9366(11)	42(4)
H(20B)	3817(18)	-187(19)	8990(12)	63(6)
H(20C)	2928(18)	765(17)	8448(12)	55(5)
H(21A)	3978(15)	1961(14)	6527(10)	36(4)
H(21B)	5180(14)	2357(14)	6327(10)	35(4)
H(21C)	4883(12)	2789(13)	7174(9)	24(3)

Table 6. Torsion angles [°] for 3.54.

C(15)-C(1)-C(2)-C(14)	-69.78(10)
C(6)-C(1)-C(2)-C(14)	169.39(8)
C(8)-C(1)-C(2)-C(14)	55.08(10)
C(15)-C(1)-C(2)-C(3)	65.86(11)
C(6)-C(1)-C(2)-C(3)	-54.98(10)
C(8)-C(1)-C(2)-C(3)	-169.28(8)
C(14)-C(2)-C(3)-C(17)	-54.30(11)
C(1)-C(2)-C(3)-C(17)	170.69(9)
C(14)-C(2)-C(3)-C(16)	66.64(12)
C(1)-C(2)-C(3)-C(16)	-68.37(12)
C(14)-C(2)-C(3)-C(4)	-170.43(8)
C(1)-C(2)-C(3)-C(4)	54.56(11)
C(17)-C(3)-C(4)-C(5)	-170.62(9)
C(16)-C(3)-C(4)-C(5)	73.59(11)
C(2)-C(3)-C(4)-C(5)	-53.95(12)
C(3)-C(4)-C(5)-C(6)	57.20(12)
C(7)-O(1)-C(6)-C(5)	-176.24(8)
C(7)-O(1)-C(6)-C(1)	-55.24(11)
C(4)-C(5)-C(6)-O(1)	63.56(10)
C(4)-C(5)-C(6)-C(1)	-56.79(11)

C(15)-C(1)-C(6)-O(1)	174.66(8)
C(8)-C(1)-C(6)-O(1)	53.82(10)
C(2)-C(1)-C(6)-O(1)	-61.42(10)
C(15)-C(1)-C(6)-C(5)	-69.80(11)
C(8)-C(1)-C(6)-C(5)	169.36(8)
C(2)-C(1)-C(6)-C(5)	54.12(10)
C(6)-O(1)-C(7)-O(2)	50.63(11)
C(6)-O(1)-C(7)-C(18)	163.11(8)
C(6)-O(1)-C(7)-C(19)	-76.16(10)
C(8)-O(2)-C(7)-O(1)	-51.88(11)
C(8)-O(2)-C(7)-C(18)	-165.32(8)
C(8)-O(2)-C(7)-C(19)	73.86(11)
C(7)-O(2)-C(8)-C(9)	-73.29(10)
C(7)-O(2)-C(8)-C(12)	177.26(8)
C(7)-O(2)-C(8)-C(1)	55.62(10)
C(15)-C(1)-C(8)-O(2)	-172.15(8)
C(6)-C(1)-C(8)-O(2)	-53.33(9)
C(2)-C(1)-C(8)-O(2)	61.86(9)
C(15)-C(1)-C(8)-C(9)	-48.72(11)
C(6)-C(1)-C(8)-C(9)	70.10(10)
C(2)-C(1)-C(8)-C(9)	-174.71(8)
C(15)-C(1)-C(8)-C(12)	72.33(10)
C(6)-C(1)-C(8)-C(12)	-168.85(8)
C(2)-C(1)-C(8)-C(12)	-53.66(10)
O(2)-C(8)-C(9)-O(3)	120.76(10)
C(12)-C(8)-C(9)-O(3)	-129.65(10)
C(1)-C(8)-C(9)-O(3)	-3.50(14)
O(2)-C(8)-C(9)-C(10)	-58.33(10)
C(12)-C(8)-C(9)-C(10)	51.26(10)
C(1)-C(8)-C(9)-C(10)	177.41(8)
O(3)-C(9)-C(10)-C(11)	163.19(10)
C(8)-C(9)-C(10)-C(11)	-17.72(14)
C(12)-O(4)-C(11)-C(10)	-8.32(14)
C(12)-O(4)-C(11)-C(20)	171.46(9)
C(9)-C(10)-C(11)-O(4)	-6.79(17)
C(9)-C(10)-C(11)-C(20)	173.46(11)

C(11)-O(4)-C(12)-C(13)	163.00(8)
C(11)-O(4)-C(12)-C(21)	-78.65(10)
C(11)-O(4)-C(12)-C(8)	45.67(11)
O(2)-C(8)-C(12)-O(4)	48.14(9)
C(9)-C(8)-C(12)-O(4)	-64.46(9)
C(1)-C(8)-C(12)-O(4)	166.99(7)
O(2)-C(8)-C(12)-C(13)	-64.63(9)
C(9)-C(8)-C(12)-C(13)	-177.22(8)
C(1)-C(8)-C(12)-C(13)	54.23(10)
O(2)-C(8)-C(12)-C(21)	167.29(8)
C(9)-C(8)-C(12)-C(21)	54.70(10)
C(1)-C(8)-C(12)-C(21)	-73.85(10)
O(4)-C(12)-C(13)-O(5)	68.68(9)
C(21)-C(12)-C(13)-O(5)	-45.91(11)
C(8)-C(12)-C(13)-O(5)	-175.63(8)
O(4)-C(12)-C(13)-C(14)	-169.85(7)
C(21)-C(12)-C(13)-C(14)	75.56(10)

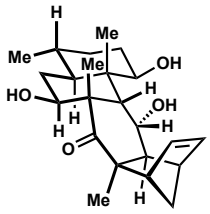

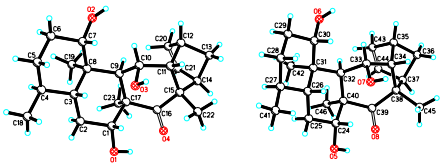

S5.12

Table 1. Crystal data and structure refinement for **S5.12.**

Identification code	S5.12 (William Thomas)	
Empirical formula	$C_{23}\ H_{34}\ O_4$	
Formula weight	374.50	
Temperature	133(2) K	
Wavelength	0.71073 Å	
Crystal system	Monoclinic	
Space group	$P2_1$	
Unit cell dimensions	a = 8.0189(5) Å	□ = 90°.
	b = 11.4531(7) Å	□ = 95.3189(8)°.
	c = 22.2367(14) Å	□ = 90°.
Volume	2033.5(2) Å^3	
Z	4	
Density (calculated)	1.223 Mg/m^3	
Absorption coefficient	0.082 mm^{-1}	
F(000)	816	
Crystal color	colorless	
Crystal size	0.514 x 0.364 x 0.092 mm^3	
Theta range for data collection	1.840 to 28.262°	
Index ranges	$-10 \le h \le 10$, $-15 \le k \le 14$, $-29 \le l \le 29$	
Reflections collected	20244	
Independent reflections	9277 [R(int) = 0.0234]	
Completeness to theta = 25.242°	99.9 %	
Absorption correction	Semi-empirical from equivalents	
Max. and min. transmission	0.8621 and 0.7986	
Refinement method	Full-matrix least-squares on F^2	
Data / restraints / parameters	9277 / 1 / 691	
Goodness-of-fit on F^2	1.024	
Final R indices [I>2sigma(I) = 8080 data]	R1 = 0.0398, wR2 = 0.0920	

R indices (all data, 0.75 Å)	R1 = 0.0500, wR2 = 0.0975
Largest diff. peak and hole	0.317 and -0.190 e.Å^{-3}

Table 2. Atomic coordinates (x 10^4) and equivalent isotropic displacement parameters (Å^2 x 10^3)
for S5.12. U(eq) is defined as one third of the trace of the orthogonalized U^{ij} tensor.

	x	y	z	U(eq)
O(1)	7094(2)	-1439(2)	268(1)	23(1)
O(2)	-868(2)	-134(1)	-357(1)	21(1)
O(3)	2176(2)	-2948(2)	227(1)	20(1)
O(4)	6064(2)	-1444(2)	1377(1)	34(1)
C(1)	5330(3)	-1573(2)	103(1)	16(1)
C(2)	5030(3)	-1243(2)	-558(1)	18(1)
C(3)	3199(3)	-1392(2)	-796(1)	16(1)
C(4)	2867(3)	-1211(2)	-1484(1)	21(1)
C(5)	1034(3)	-1493(2)	-1673(1)	24(1)
C(6)	-162(3)	-770(2)	-1337(1)	22(1)
C(7)	220(3)	-889(2)	-653(1)	16(1)
C(8)	2061(3)	-610(2)	-432(1)	14(1)
C(9)	2376(3)	-860(2)	270(1)	13(1)
C(10)	1464(3)	-1937(2)	480(1)	14(1)
C(11)	1540(3)	-2083(2)	1164(1)	17(1)
C(12)	528(3)	-1237(3)	1545(1)	27(1)
C(13)	1254(3)	-1639(3)	2179(1)	31(1)
C(14)	3048(3)	-1285(3)	2070(1)	30(1)
C(15)	3324(3)	-2048(2)	1494(1)	19(1)
C(16)	4621(3)	-1441(2)	1147(1)	20(1)
C(17)	4268(3)	-845(2)	522(1)	16(1)
C(18)	4004(4)	-1961(3)	-1842(1)	31(1)
C(19)	2346(3)	699(2)	-549(1)	19(1)
C(20)	1259(4)	-17(3)	1539(1)	34(1)
C(21)	2753(4)	-48(3)	1854(1)	37(1)
C(22)	3972(4)	-3271(3)	1676(1)	29(1)
C(23)	4980(3)	407(2)	594(1)	23(1)

O(5)	6655(2)	-4522(2)	4935(1)	24(1)
O(6)	-1247(2)	-3010(1)	4410(1)	17(1)
O(7)	1669(2)	-5827(1)	5060(1)	18(1)
O(8)	5790(2)	-4292(2)	6057(1)	32(1)
C(24)	4868(3)	-4607(2)	4807(1)	17(1)
C(25)	4490(3)	-4403(2)	4137(1)	19(1)
C(26)	2625(3)	-4505(2)	3941(1)	16(1)
C(27)	2218(3)	-4448(2)	3250(1)	21(1)
C(28)	341(3)	-4597(2)	3088(1)	24(1)
C(29)	-727(3)	-3765(2)	3426(1)	21(1)
C(30)	-257(3)	-3828(2)	4106(1)	15(1)
C(31)	1619(3)	-3601(2)	4284(1)	14(1)
C(32)	2010(3)	-3743(2)	4990(1)	13(1)
C(33)	1052(3)	-4738(2)	5270(1)	14(1)
C(34)	1211(3)	-4722(2)	5959(1)	17(1)
C(35)	284(3)	-3748(2)	6294(1)	25(1)
C(36)	1086(4)	-3985(3)	6941(1)	31(1)
C(37)	2867(3)	-3738(2)	6778(1)	26(1)
C(38)	3023(3)	-4681(2)	6262(1)	19(1)
C(39)	4323(3)	-4246(2)	5858(1)	19(1)
C(40)	3920(3)	-3761(2)	5208(1)	15(1)
C(41)	3167(4)	-5389(3)	2929(1)	31(1)
C(42)	2013(3)	-2336(2)	4101(1)	18(1)
C(43)	1060(4)	-2568(3)	6184(1)	28(1)
C(44)	2598(4)	-2565(2)	6475(1)	28(1)
C(45)	3617(4)	-5860(3)	6526(1)	28(1)
C(46)	4715(3)	-2535(2)	5207(1)	21(1)

Table 3. Bond lengths [Å] and angles [°] for S5.12.

O(1)-C(1)	1.436(3)
O(1)-H(1)	0.84(3)
O(2)-C(7)	1.431(3)
O(2)-H(2)	0.81(3)
O(3)-C(10)	1.431(3)
O(3)-H(3)	0.83(3)

O(4)-C(16)	1.221(3)
C(1)-C(2)	1.515(3)
C(1)-C(17)	1.561(3)
C(1)-H(1A)	0.93(3)
C(2)-C(3)	1.523(3)
C(2)-H(2A)	0.95(3)
C(2)-H(2B)	1.00(3)
C(3)-C(4)	1.543(3)
C(3)-C(8)	1.558(3)
C(3)-H(3A)	0.94(3)
C(4)-C(5)	1.526(3)
C(4)-C(18)	1.528(3)
C(4)-H(4A)	0.99(3)
C(5)-C(6)	1.515(4)
C(5)-H(5A)	0.98(3)
C(5)-H(5B)	0.96(3)
C(6)-C(7)	1.531(3)
C(6)-H(6A)	0.95(3)
C(6)-H(6B)	0.99(3)
C(7)-C(8)	1.545(3)
C(7)-H(7A)	0.98(3)
C(8)-C(19)	1.542(3)
C(8)-C(9)	1.583(3)
C(9)-C(10)	1.529(3)
C(9)-C(17)	1.568(3)
C(9)-H(9A)	0.96(3)
C(10)-C(11)	1.526(3)
C(10)-H(10A)	0.97(3)
C(11)-C(15)	1.546(3)
C(11)-C(12)	1.563(3)
C(11)-H(11A)	0.96(3)
C(12)-C(20)	1.515(4)
C(12)-C(13)	1.544(4)
C(12)-H(12A)	0.88(3)
C(13)-C(14)	1.535(4)
C(13)-H(13A)	0.98(3)

C(13)-H(13B)	0.97(4)
C(14)-C(21)	1.508(4)
C(14)-C(15)	1.583(3)
C(14)-H(14A)	1.01(3)
C(15)-C(16)	1.520(3)
C(15)-C(22)	1.535(4)
C(16)-C(17)	1.550(3)
C(17)-C(23)	1.547(3)
C(18)-H(18A)	0.97(4)
C(18)-H(18B)	0.98(3)
C(18)-H(18C)	0.96(4)
C(19)-H(19A)	0.96(3)
C(19)-H(19B)	0.93(3)
C(19)-H(19C)	0.96(3)
C(20)-C(21)	1.331(4)
C(20)-H(20A)	0.97(3)
C(21)-H(21A)	0.99(4)
C(22)-H(22A)	0.94(3)
C(22)-H(22B)	0.98(4)
C(22)-H(22C)	0.98(3)
C(23)-H(23A)	0.98(3)
C(23)-H(23B)	0.98(3)
C(23)-H(23C)	0.96(3)
O(5)-C(24)	1.439(3)
O(5)-H(5)	0.84(3)
O(6)-C(30)	1.437(3)
O(6)-H(6)	0.84(3)
O(7)-C(33)	1.436(3)
O(7)-H(7)	0.80(3)
O(8)-C(39)	1.219(3)
C(24)-C(25)	1.511(3)
C(24)-C(40)	1.562(3)
C(24)-H(24A)	0.95(3)
C(25)-C(26)	1.522(3)
C(25)-H(25A)	0.95(3)
C(25)-H(25B)	0.97(3)

C(26)-C(27)	1.543(3)
C(26)-C(31)	1.556(3)
C(26)-H(26A)	0.96(3)
C(27)-C(28)	1.524(4)
C(27)-C(41)	1.534(3)
C(27)-H(27A)	0.98(3)
C(28)-C(29)	1.525(3)
C(28)-H(28A)	0.96(3)
C(28)-H(28B)	1.02(3)
C(29)-C(30)	1.526(3)
C(29)-H(29A)	1.04(3)
C(29)-H(29B)	0.93(3)
C(30)-C(31)	1.542(3)
C(30)-H(30A)	0.98(3)
C(31)-C(42)	1.546(3)
C(31)-C(32)	1.579(3)
C(32)-C(33)	1.538(3)
C(32)-C(40)	1.563(3)
C(32)-H(32A)	0.98(3)
C(33)-C(34)	1.525(3)
C(33)-H(33A)	0.96(3)
C(34)-C(38)	1.546(3)
C(34)-C(35)	1.567(3)
C(34)-H(34A)	0.96(3)
C(35)-C(43)	1.517(4)
C(35)-C(36)	1.545(4)
C(35)-H(35A)	0.96(3)
C(36)-C(37)	1.533(4)
C(36)-H(36A)	0.96(3)
C(36)-H(36B)	0.97(4)
C(37)-C(44)	1.509(4)
C(37)-C(38)	1.588(3)
C(37)-H(37A)	0.95(3)
C(38)-C(39)	1.522(3)
C(38)-C(45)	1.531(4)
C(39)-C(40)	1.553(3)

C(40)-C(46)	1.542(3)
C(41)-H(41A)	0.99(4)
C(41)-H(41B)	0.96(3)
C(41)-H(41C)	0.93(4)
C(42)-H(42A)	0.96(3)
C(42)-H(42B)	0.94(3)
C(42)-H(42C)	0.98(3)
C(43)-C(44)	1.338(4)
C(43)-H(43A)	0.96(3)
C(44)-H(44A)	0.98(3)
C(45)-H(45A)	0.96(3)
C(45)-H(45B)	0.96(3)
C(45)-H(45C)	0.97(4)
C(46)-H(46A)	0.94(3)
C(46)-H(46B)	1.00(3)
C(46)-H(46C)	1.01(3)

C(1)-O(1)-H(1)	103(2)
C(7)-O(2)-H(2)	111(2)
C(10)-O(3)-H(3)	109(2)
O(1)-C(1)-C(2)	106.57(17)
O(1)-C(1)-C(17)	111.64(18)
C(2)-C(1)-C(17)	113.60(18)
O(1)-C(1)-H(1A)	111.0(16)
C(2)-C(1)-H(1A)	106.0(16)
C(17)-C(1)-H(1A)	107.9(16)
C(1)-C(2)-C(3)	111.64(18)
C(1)-C(2)-H(2A)	105.8(16)
C(3)-C(2)-H(2A)	112.1(16)
C(1)-C(2)-H(2B)	108.8(15)
C(3)-C(2)-H(2B)	112.0(16)
H(2A)-C(2)-H(2B)	106(2)
C(2)-C(3)-C(4)	113.59(18)
C(2)-C(3)-C(8)	110.37(18)
C(4)-C(3)-C(8)	112.47(18)
C(2)-C(3)-H(3A)	107.0(16)

C(4)-C(3)-H(3A)	106.4(16)
C(8)-C(3)-H(3A)	106.5(16)
C(5)-C(4)-C(18)	110.1(2)
C(5)-C(4)-C(3)	108.60(18)
C(18)-C(4)-C(3)	112.6(2)
C(5)-C(4)-H(4A)	109.0(16)
C(18)-C(4)-H(4A)	108.0(16)
C(3)-C(4)-H(4A)	108.4(16)
C(6)-C(5)-C(4)	112.7(2)
C(6)-C(5)-H(5A)	111.9(17)
C(4)-C(5)-H(5A)	108.9(16)
C(6)-C(5)-H(5B)	111.4(17)
C(4)-C(5)-H(5B)	107.7(17)
H(5A)-C(5)-H(5B)	104(2)
C(5)-C(6)-C(7)	111.39(19)
C(5)-C(6)-H(6A)	111.2(18)
C(7)-C(6)-H(6A)	105.4(17)
C(5)-C(6)-H(6B)	111.2(17)
C(7)-C(6)-H(6B)	109.1(16)
H(6A)-C(6)-H(6B)	108(2)
O(2)-C(7)-C(6)	109.25(18)
O(2)-C(7)-C(8)	109.51(18)
C(6)-C(7)-C(8)	113.25(18)
O(2)-C(7)-H(7A)	109.8(16)
C(6)-C(7)-H(7A)	106.2(15)
C(8)-C(7)-H(7A)	108.7(15)
C(19)-C(8)-C(7)	107.42(18)
C(19)-C(8)-C(3)	111.58(18)
C(7)-C(8)-C(3)	107.73(17)
C(19)-C(8)-C(9)	109.30(18)
C(7)-C(8)-C(9)	109.67(16)
C(3)-C(8)-C(9)	111.06(16)
C(10)-C(9)-C(17)	111.95(17)
C(10)-C(9)-C(8)	114.25(17)
C(17)-C(9)-C(8)	114.34(16)
C(10)-C(9)-H(9A)	103.5(15)

C(17)-C(9)-H(9A)	107.8(15)
C(8)-C(9)-H(9A)	103.9(15)
O(3)-C(10)-C(11)	108.86(18)
O(3)-C(10)-C(9)	108.18(16)
C(11)-C(10)-C(9)	114.70(18)
O(3)-C(10)-H(10A)	109.5(16)
C(11)-C(10)-H(10A)	106.8(15)
C(9)-C(10)-H(10A)	108.7(16)
C(10)-C(11)-C(15)	114.83(17)
C(10)-C(11)-C(12)	119.8(2)
C(15)-C(11)-C(12)	103.34(18)
C(10)-C(11)-H(11A)	106.6(16)
C(15)-C(11)-H(11A)	105.8(16)
C(12)-C(11)-H(11A)	105.3(16)
C(20)-C(12)-C(13)	99.8(2)
C(20)-C(12)-C(11)	110.3(2)
C(13)-C(12)-C(11)	98.0(2)
C(20)-C(12)-H(12A)	117(2)
C(13)-C(12)-H(12A)	115.5(19)
C(11)-C(12)-H(12A)	113(2)
C(14)-C(13)-C(12)	93.3(2)
C(14)-C(13)-H(13A)	112.0(18)
C(12)-C(13)-H(13A)	114.4(18)
C(14)-C(13)-H(13B)	111.4(18)
C(12)-C(13)-H(13B)	113.5(18)
H(13A)-C(13)-H(13B)	111(3)
C(21)-C(14)-C(13)	100.2(2)
C(21)-C(14)-C(15)	106.9(2)
C(13)-C(14)-C(15)	100.7(2)
C(21)-C(14)-H(14A)	115.6(19)
C(13)-C(14)-H(14A)	119.5(17)
C(15)-C(14)-H(14A)	112.1(18)
C(16)-C(15)-C(22)	108.7(2)
C(16)-C(15)-C(11)	114.66(18)
C(22)-C(15)-C(11)	112.2(2)
C(16)-C(15)-C(14)	108.2(2)

C(22)-C(15)-C(14)	111.1(2)
C(11)-C(15)-C(14)	101.86(18)
O(4)-C(16)-C(15)	116.9(2)
O(4)-C(16)-C(17)	117.6(2)
C(15)-C(16)-C(17)	125.45(19)
C(23)-C(17)-C(16)	106.27(19)
C(23)-C(17)-C(1)	109.92(18)
C(16)-C(17)-C(1)	103.67(18)
C(23)-C(17)-C(9)	112.51(19)
C(16)-C(17)-C(9)	113.98(17)
C(1)-C(17)-C(9)	110.06(17)
C(4)-C(18)-H(18A)	113(2)
C(4)-C(18)-H(18B)	113(2)
H(18A)-C(18)-H(18B)	108(3)
C(4)-C(18)-H(18C)	110(2)
H(18A)-C(18)-H(18C)	109(3)
H(18B)-C(18)-H(18C)	103(3)
C(8)-C(19)-H(19A)	112.0(18)
C(8)-C(19)-H(19B)	111.1(18)
H(19A)-C(19)-H(19B)	103(2)
C(8)-C(19)-H(19C)	112.1(18)
H(19A)-C(19)-H(19C)	107(2)
H(19B)-C(19)-H(19C)	111(2)
C(21)-C(20)-C(12)	107.5(3)
C(21)-C(20)-H(20A)	133(2)
C(12)-C(20)-H(20A)	118.8(19)
C(20)-C(21)-C(14)	107.4(3)
C(20)-C(21)-H(21A)	125.9(19)
C(14)-C(21)-H(21A)	126.2(19)
C(15)-C(22)-H(22A)	109(2)
C(15)-C(22)-H(22B)	109(2)
H(22A)-C(22)-H(22B)	108(3)
C(15)-C(22)-H(22C)	109(2)
H(22A)-C(22)-H(22C)	113(3)
H(22B)-C(22)-H(22C)	109(3)
C(17)-C(23)-H(23A)	110.7(18)

C(17)-C(23)-H(23B)	110.0(19)
H(23A)-C(23)-H(23B)	108(3)
C(17)-C(23)-H(23C)	110(2)
H(23A)-C(23)-H(23C)	112(3)
H(23B)-C(23)-H(23C)	106(2)
C(24)-O(5)-H(5)	107(2)
C(30)-O(6)-H(6)	105(2)
C(33)-O(7)-H(7)	109(2)
O(5)-C(24)-C(25)	106.83(18)
O(5)-C(24)-C(40)	111.97(18)
C(25)-C(24)-C(40)	113.84(18)
O(5)-C(24)-H(24A)	108.1(16)
C(25)-C(24)-H(24A)	109.1(16)
C(40)-C(24)-H(24A)	106.8(16)
C(24)-C(25)-C(26)	111.81(18)
C(24)-C(25)-H(25A)	106.9(16)
C(26)-C(25)-H(25A)	110.9(16)
C(24)-C(25)-H(25B)	110.1(16)
C(26)-C(25)-H(25B)	112.9(16)
H(25A)-C(25)-H(25B)	104(2)
C(25)-C(26)-C(27)	113.15(18)
C(25)-C(26)-C(31)	110.42(18)
C(27)-C(26)-C(31)	112.87(18)
C(25)-C(26)-H(26A)	106.4(15)
C(27)-C(26)-H(26A)	105.9(15)
C(31)-C(26)-H(26A)	107.6(16)
C(28)-C(27)-C(41)	109.4(2)
C(28)-C(27)-C(26)	110.14(18)
C(41)-C(27)-C(26)	111.4(2)
C(28)-C(27)-H(27A)	106.5(16)
C(41)-C(27)-H(27A)	111.8(16)
C(26)-C(27)-H(27A)	107.4(16)
C(27)-C(28)-C(29)	113.6(2)
C(27)-C(28)-H(28A)	108.6(17)
C(29)-C(28)-H(28A)	108.9(17)
C(27)-C(28)-H(28B)	113.0(16)

C(29)-C(28)-H(28B)	107.8(16)
H(28A)-C(28)-H(28B)	104(2)
C(28)-C(29)-C(30)	111.15(19)
C(28)-C(29)-H(29A)	112.3(15)
C(30)-C(29)-H(29A)	110.6(15)
C(28)-C(29)-H(29B)	110.0(18)
C(30)-C(29)-H(29B)	107.7(17)
H(29A)-C(29)-H(29B)	105(2)
O(6)-C(30)-C(29)	109.81(18)
O(6)-C(30)-C(31)	109.72(17)
C(29)-C(30)-C(31)	113.10(18)
O(6)-C(30)-H(30A)	111.1(15)
C(29)-C(30)-H(30A)	106.7(15)
C(31)-C(30)-H(30A)	106.4(15)
C(30)-C(31)-C(42)	107.99(18)
C(30)-C(31)-C(26)	107.44(17)
C(42)-C(31)-C(26)	111.50(17)
C(30)-C(31)-C(32)	109.71(16)
C(42)-C(31)-C(32)	109.37(18)
C(26)-C(31)-C(32)	110.77(17)
C(33)-C(32)-C(40)	112.06(17)
C(33)-C(32)-C(31)	114.70(17)
C(40)-C(32)-C(31)	114.16(16)
C(33)-C(32)-H(32A)	104.2(15)
C(40)-C(32)-H(32A)	106.6(14)
C(31)-C(32)-H(32A)	103.9(14)
O(7)-C(33)-C(34)	109.73(18)
O(7)-C(33)-C(32)	108.18(16)
C(34)-C(33)-C(32)	113.57(18)
O(7)-C(33)-H(33A)	106.6(17)
C(34)-C(33)-H(33A)	107.2(14)
C(32)-C(33)-H(33A)	111.3(16)
C(33)-C(34)-C(38)	115.25(18)
C(33)-C(34)-C(35)	119.1(2)
C(38)-C(34)-C(35)	103.82(18)
C(33)-C(34)-H(34A)	106.2(15)

C(38)-C(34)-H(34A)	107.0(16)
C(35)-C(34)-H(34A)	104.5(16)
C(43)-C(35)-C(36)	99.5(2)
C(43)-C(35)-C(34)	109.73(19)
C(36)-C(35)-C(34)	98.2(2)
C(43)-C(35)-H(35A)	118.2(19)
C(36)-C(35)-H(35A)	117.2(17)
C(34)-C(35)-H(35A)	111.7(18)
C(37)-C(36)-C(35)	93.60(19)
C(37)-C(36)-H(36A)	113.2(19)
C(35)-C(36)-H(36A)	113.0(19)
C(37)-C(36)-H(36B)	110.4(19)
C(35)-C(36)-H(36B)	114.2(18)
H(36A)-C(36)-H(36B)	111(3)
C(44)-C(37)-C(36)	99.9(2)
C(44)-C(37)-C(38)	107.50(19)
C(36)-C(37)-C(38)	100.61(19)
C(44)-C(37)-H(37A)	115.1(19)
C(36)-C(37)-H(37A)	120.4(17)
C(38)-C(37)-H(37A)	111.6(18)
C(39)-C(38)-C(45)	108.0(2)
C(39)-C(38)-C(34)	114.79(18)
C(45)-C(38)-C(34)	112.8(2)
C(39)-C(38)-C(37)	107.94(19)
C(45)-C(38)-C(37)	111.5(2)
C(34)-C(38)-C(37)	101.65(19)
O(8)-C(39)-C(38)	117.5(2)
O(8)-C(39)-C(40)	117.6(2)
C(38)-C(39)-C(40)	124.86(19)
C(46)-C(40)-C(39)	106.08(18)
C(46)-C(40)-C(24)	109.89(17)
C(39)-C(40)-C(24)	103.88(18)
C(46)-C(40)-C(32)	112.34(18)
C(39)-C(40)-C(32)	114.06(17)
C(24)-C(40)-C(32)	110.18(17)
C(27)-C(41)-H(41A)	114(2)

C(27)-C(41)-H(41B)	109(2)
H(41A)-C(41)-H(41B)	111(3)
C(27)-C(41)-H(41C)	109(2)
H(41A)-C(41)-H(41C)	105(3)
H(41B)-C(41)-H(41C)	109(3)
C(31)-C(42)-H(42A)	114.3(18)
C(31)-C(42)-H(42B)	110.6(18)
H(42A)-C(42)-H(42B)	105(2)
C(31)-C(42)-H(42C)	109.6(17)
H(42A)-C(42)-H(42C)	110(2)
H(42B)-C(42)-H(42C)	107(2)
C(44)-C(43)-C(35)	107.3(3)
C(44)-C(43)-H(43A)	126.5(19)
C(35)-C(43)-H(43A)	126.2(19)
C(43)-C(44)-C(37)	107.5(2)
C(43)-C(44)-H(44A)	123.7(18)
C(37)-C(44)-H(44A)	128.8(18)
C(38)-C(45)-H(45A)	108(2)
C(38)-C(45)-H(45B)	106(2)
H(45A)-C(45)-H(45B)	111(3)
C(38)-C(45)-H(45C)	114(2)
H(45A)-C(45)-H(45C)	106(3)
H(45B)-C(45)-H(45C)	111(3)
C(40)-C(46)-H(46A)	112(2)
C(40)-C(46)-H(46B)	110.1(17)
H(46A)-C(46)-H(46B)	111(3)
C(40)-C(46)-H(46C)	108.2(18)
H(46A)-C(46)-H(46C)	109(2)
H(46B)-C(46)-H(46C)	107(2)

Table 4. Anisotropic displacement parameters ($Å^2$ x 10^3) for S5.12. The anisotropic displacement factor exponent takes the form: $-2\pi^2[h^2 a^{*2} U^{11} + ... + 2 h k a^* b^* U^{12}]$

	U^{11}	U^{22}	U^{33}	U^{23}	U^{13}	U^{12}
O(1)	12(1)	31(1)	27(1)	8(1)	3(1)	1(1)
O(2)	17(1)	17(1)	29(1)	5(1)	8(1)	3(1)
O(3)	24(1)	14(1)	22(1)	0(1)	9(1)	-3(1)
O(4)	19(1)	56(1)	26(1)	12(1)	-5(1)	-4(1)
C(1)	11(1)	18(1)	20(1)	3(1)	3(1)	0(1)
C(2)	18(1)	18(1)	21(1)	2(1)	7(1)	2(1)
C(3)	18(1)	14(1)	15(1)	1(1)	5(1)	1(1)
C(4)	29(1)	20(1)	14(1)	4(1)	5(1)	1(1)
C(5)	34(1)	24(1)	14(1)	2(1)	-2(1)	0(1)
C(6)	21(1)	24(1)	20(1)	2(1)	-5(1)	0(1)
C(7)	16(1)	16(1)	18(1)	2(1)	1(1)	2(1)
C(8)	15(1)	12(1)	13(1)	1(1)	2(1)	1(1)
C(9)	14(1)	13(1)	12(1)	-1(1)	2(1)	0(1)
C(10)	14(1)	15(1)	15(1)	1(1)	1(1)	0(1)
C(11)	17(1)	19(1)	15(1)	4(1)	3(1)	-1(1)
C(12)	20(1)	42(2)	18(1)	-1(1)	6(1)	8(1)
C(13)	30(1)	46(2)	16(1)	0(1)	7(1)	7(1)
C(14)	30(1)	43(2)	15(1)	-6(1)	0(1)	1(1)
C(15)	17(1)	26(1)	14(1)	2(1)	1(1)	1(1)
C(16)	19(1)	24(1)	17(1)	0(1)	1(1)	-1(1)
C(17)	14(1)	17(1)	17(1)	1(1)	1(1)	-2(1)
C(18)	42(2)	33(2)	19(1)	-1(1)	11(1)	5(1)
C(19)	22(1)	14(1)	21(1)	2(1)	3(1)	0(1)
C(20)	49(2)	30(2)	26(1)	-5(1)	12(1)	14(1)
C(21)	51(2)	35(2)	25(1)	-16(1)	9(1)	-5(1)
C(22)	26(1)	35(2)	26(1)	11(1)	3(1)	8(1)
C(23)	23(1)	17(1)	29(1)	-3(1)	1(1)	-7(1)
O(5)	13(1)	27(1)	32(1)	7(1)	5(1)	2(1)
O(6)	16(1)	14(1)	22(1)	0(1)	5(1)	1(1)
O(7)	24(1)	12(1)	19(1)	2(1)	9(1)	-2(1)
O(8)	18(1)	48(1)	28(1)	8(1)	-5(1)	-3(1)

C(24)	13(1)	14(1)	26(1)	3(1)	5(1)	1(1)
C(25)	17(1)	17(1)	23(1)	2(1)	10(1)	3(1)
C(26)	21(1)	13(1)	15(1)	0(1)	8(1)	1(1)
C(27)	31(1)	18(1)	15(1)	1(1)	8(1)	2(1)
C(28)	33(1)	24(1)	14(1)	0(1)	2(1)	-3(1)
C(29)	22(1)	25(1)	15(1)	2(1)	-2(1)	-1(1)
C(30)	19(1)	12(1)	15(1)	0(1)	2(1)	1(1)
C(31)	16(1)	12(1)	13(1)	1(1)	3(1)	1(1)
C(32)	15(1)	12(1)	12(1)	-1(1)	2(1)	-1(1)
C(33)	13(1)	14(1)	14(1)	0(1)	2(1)	-1(1)
C(34)	18(1)	17(1)	15(1)	1(1)	3(1)	-4(1)
C(35)	24(1)	33(2)	20(1)	-7(1)	8(1)	-4(1)
C(36)	39(2)	36(2)	18(1)	-6(1)	8(1)	-10(1)
C(37)	33(1)	30(1)	15(1)	-4(1)	0(1)	-10(1)
C(38)	21(1)	23(1)	14(1)	2(1)	-1(1)	-4(1)
C(39)	18(1)	19(1)	18(1)	-1(1)	-1(1)	-2(1)
C(40)	13(1)	16(1)	17(1)	2(1)	2(1)	-1(1)
C(41)	46(2)	31(2)	18(1)	-4(1)	12(1)	7(1)
C(42)	20(1)	14(1)	19(1)	3(1)	4(1)	1(1)
C(43)	39(2)	26(1)	22(1)	-10(1)	9(1)	3(1)
C(44)	42(2)	23(1)	22(1)	-11(1)	8(1)	-8(1)
C(45)	32(2)	29(1)	23(1)	10(1)	-6(1)	-3(1)
C(46)	18(1)	17(1)	27(1)	-2(1)	3(1)	-5(1)

Table 5. Hydrogen coordinates (x 10^4) and isotropic displacement parameters ($Å^2$ x 10^3) for S5.12.

	x	y	z	U(eq)
H(1)	7160(40)	-1450(30)	646(15)	35
H(2)	-1470(40)	-510(30)	-151(14)	31
H(3)	1640(40)	-3530(30)	320(13)	30
H(1A)	5010(30)	-2350(30)	127(12)	20
H(2A)	5750(30)	-1730(30)	-765(12)	22
H(2B)	5430(30)	-430(30)	-610(12)	22
H(3A)	2910(30)	-2170(30)	-720(12)	19
H(4A)	3080(30)	-390(30)	-1575(12)	25
H(5A)	820(30)	-1400(30)	-2110(13)	29
H(5B)	870(30)	-2320(30)	-1610(12)	29
H(6A)	-1280(40)	-1030(30)	-1421(12)	26
H(6B)	-110(30)	60(30)	-1449(12)	26
H(7A)	-10(30)	-1710(30)	-555(12)	20
H(9A)	1830(30)	-220(20)	451(11)	16
H(10A)	290(30)	-1880(20)	334(11)	17
H(11A)	1110(30)	-2850(30)	1237(12)	20
H(12A)	-570(40)	-1310(30)	1469(13)	32
H(13A)	840(40)	-1200(30)	2514(14)	37
H(13B)	1160(40)	-2480(30)	2242(13)	37
H(14A)	3980(40)	-1390(30)	2403(14)	36
H(18A)	5190(40)	-1760(30)	-1768(15)	46
H(18B)	3690(40)	-1940(30)	-2277(16)	46
H(18C)	3870(40)	-2770(30)	-1744(15)	46
H(19A)	3520(40)	900(30)	-505(13)	29
H(19B)	1890(30)	1160(30)	-259(13)	29
H(19C)	1910(30)	930(30)	-949(13)	29
H(20A)	660(40)	580(30)	1296(14)	41
H(21A)	3580(40)	600(30)	1893(14)	44
H(22A)	5060(40)	-3210(30)	1874(15)	44
H(22B)	4050(40)	-3740(30)	1313(16)	44

H(22C)	3170(40)	-3640(30)	1925(15)	44
H(23A)	4120(40)	950(30)	710(13)	35
H(23B)	5350(40)	680(30)	212(14)	35
H(23C)	5960(40)	410(30)	878(14)	35
H(5)	6860(40)	-4480(30)	5313(14)	36
H(6)	-1980(40)	-3420(30)	4551(13)	26
H(7)	1350(40)	-6340(30)	5263(13)	27
H(24A)	4540(30)	-5380(30)	4901(12)	21
H(25A)	5110(30)	-4970(30)	3936(12)	22
H(25B)	4960(30)	-3660(30)	4023(12)	22
H(26A)	2290(30)	-5270(20)	4060(11)	19
H(27A)	2500(30)	-3660(30)	3120(12)	25
H(28A)	40(40)	-5380(30)	3175(13)	28
H(28B)	0(30)	-4500(30)	2639(13)	28
H(29A)	-660(30)	-2910(30)	3274(12)	25
H(29B)	-1850(40)	-3970(30)	3354(12)	25
H(30A)	-480(30)	-4630(30)	4229(11)	18
H(32A)	1550(30)	-3030(20)	5155(11)	15
H(33A)	-120(30)	-4710(20)	5138(11)	17
H(34A)	720(30)	-5440(20)	6082(11)	20
H(35A)	-910(40)	-3820(30)	6225(13)	30
H(36A)	720(40)	-3450(30)	7233(14)	37
H(36B)	990(40)	-4780(30)	7073(14)	37
H(37A)	3790(40)	-3780(30)	7079(13)	31
H(41A)	4400(50)	-5280(30)	2961(15)	47
H(41B)	2720(40)	-5430(30)	2511(16)	47
H(41C)	3000(40)	-6110(30)	3113(15)	47
H(42A)	3180(40)	-2170(30)	4098(12)	26
H(42B)	1620(30)	-1800(30)	4376(13)	26
H(42C)	1420(30)	-2160(30)	3704(13)	26
H(43A)	550(40)	-1950(30)	5941(13)	34
H(44A)	3380(40)	-1910(30)	6463(13)	34
H(45A)	2930(40)	-6060(30)	6842(15)	43
H(45B)	4770(40)	-5750(30)	6682(14)	43
H(45C)	3510(40)	-6500(30)	6239(15)	43
H(46A)	5700(40)	-2490(30)	5467(13)	31

H(46B)	3880(40)	-1930(30)	5311(13)	31
H(46C)	4990(30)	-2360(30)	4785(13)	31

Table 6. Torsion angles [°] for S5.12.

O(1)-C(1)-C(2)-C(3)	177.94(19)
C(17)-C(1)-C(2)-C(3)	-58.7(3)
C(1)-C(2)-C(3)-C(4)	-173.0(2)
C(1)-C(2)-C(3)-C(8)	59.6(2)
C(2)-C(3)-C(4)-C(5)	174.8(2)
C(8)-C(3)-C(4)-C(5)	-58.9(3)
C(2)-C(3)-C(4)-C(18)	52.7(3)
C(8)-C(3)-C(4)-C(18)	178.9(2)
C(18)-C(4)-C(5)-C(6)	-179.6(2)
C(3)-C(4)-C(5)-C(6)	56.7(3)
C(4)-C(5)-C(6)-C(7)	-54.8(3)
C(5)-C(6)-C(7)-O(2)	176.3(2)
C(5)-C(6)-C(7)-C(8)	53.9(3)
O(2)-C(7)-C(8)-C(19)	-56.0(2)
C(6)-C(7)-C(8)-C(19)	66.2(2)
O(2)-C(7)-C(8)-C(3)	-176.33(16)
C(6)-C(7)-C(8)-C(3)	-54.1(2)
O(2)-C(7)-C(8)-C(9)	62.7(2)
C(6)-C(7)-C(8)-C(9)	-175.12(19)
C(2)-C(3)-C(8)-C(19)	67.6(2)
C(4)-C(3)-C(8)-C(19)	-60.4(2)
C(2)-C(3)-C(8)-C(7)	-174.72(18)
C(4)-C(3)-C(8)-C(7)	57.3(2)
C(2)-C(3)-C(8)-C(9)	-54.6(2)
C(4)-C(3)-C(8)-C(9)	177.40(18)
C(19)-C(8)-C(9)-C(10)	155.39(19)
C(7)-C(8)-C(9)-C(10)	37.9(2)
C(3)-C(8)-C(9)-C(10)	-81.1(2)
C(19)-C(8)-C(9)-C(17)	-73.8(2)
C(7)-C(8)-C(9)-C(17)	168.69(18)
C(3)-C(8)-C(9)-C(17)	49.7(2)

C(17)-C(9)-C(10)-O(3)	-64.8(2)
C(8)-C(9)-C(10)-O(3)	67.2(2)
C(17)-C(9)-C(10)-C(11)	56.9(2)
C(8)-C(9)-C(10)-C(11)	-171.13(18)
O(3)-C(10)-C(11)-C(15)	68.6(2)
C(9)-C(10)-C(11)-C(15)	-52.8(3)
O(3)-C(10)-C(11)-C(12)	-167.5(2)
C(9)-C(10)-C(11)-C(12)	71.2(3)
C(10)-C(11)-C(12)-C(20)	-68.2(3)
C(15)-C(11)-C(12)-C(20)	61.1(2)
C(10)-C(11)-C(12)-C(13)	-171.7(2)
C(15)-C(11)-C(12)-C(13)	-42.4(2)
C(20)-C(12)-C(13)-C(14)	-50.7(2)
C(11)-C(12)-C(13)-C(14)	61.6(2)
C(12)-C(13)-C(14)-C(21)	51.2(2)
C(12)-C(13)-C(14)-C(15)	-58.3(2)
C(10)-C(11)-C(15)-C(16)	21.8(3)
C(12)-C(11)-C(15)-C(16)	-110.5(2)
C(10)-C(11)-C(15)-C(22)	-102.7(2)
C(12)-C(11)-C(15)-C(22)	125.0(2)
C(10)-C(11)-C(15)-C(14)	138.4(2)
C(12)-C(11)-C(15)-C(14)	6.1(2)
C(21)-C(14)-C(15)-C(16)	49.7(3)
C(13)-C(14)-C(15)-C(16)	153.9(2)
C(21)-C(14)-C(15)-C(22)	168.9(2)
C(13)-C(14)-C(15)-C(22)	-86.9(2)
C(21)-C(14)-C(15)-C(11)	-71.5(2)
C(13)-C(14)-C(15)-C(11)	32.7(2)
C(22)-C(15)-C(16)-O(4)	-50.0(3)
C(11)-C(15)-C(16)-O(4)	-176.4(2)
C(14)-C(15)-C(16)-O(4)	70.7(3)
C(22)-C(15)-C(16)-C(17)	128.5(2)
C(11)-C(15)-C(16)-C(17)	2.1(3)
C(14)-C(15)-C(16)-C(17)	-110.7(3)
O(4)-C(16)-C(17)-C(23)	-54.3(3)
C(15)-C(16)-C(17)-C(23)	127.2(2)

O(4)-C(16)-C(17)-C(1)	61.6(3)
C(15)-C(16)-C(17)-C(1)	-117.0(2)
O(4)-C(16)-C(17)-C(9)	-178.8(2)
C(15)-C(16)-C(17)-C(9)	2.7(3)
O(1)-C(1)-C(17)-C(23)	47.0(2)
C(2)-C(1)-C(17)-C(23)	-73.6(2)
O(1)-C(1)-C(17)-C(16)	-66.3(2)
C(2)-C(1)-C(17)-C(16)	173.15(19)
O(1)-C(1)-C(17)-C(9)	171.41(17)
C(2)-C(1)-C(17)-C(9)	50.9(2)
C(10)-C(9)-C(17)-C(23)	-151.80(19)
C(8)-C(9)-C(17)-C(23)	76.3(2)
C(10)-C(9)-C(17)-C(16)	-30.7(3)
C(8)-C(9)-C(17)-C(16)	-162.65(19)
C(10)-C(9)-C(17)-C(1)	85.2(2)
C(8)-C(9)-C(17)-C(1)	-46.7(2)
C(13)-C(12)-C(20)-C(21)	33.6(3)
C(11)-C(12)-C(20)-C(21)	-68.8(3)
C(12)-C(20)-C(21)-C(14)	0.4(3)
C(13)-C(14)-C(21)-C(20)	-34.4(3)
C(15)-C(14)-C(21)-C(20)	70.1(3)
O(5)-C(24)-C(25)-C(26)	178.37(19)
C(40)-C(24)-C(25)-C(26)	-57.5(3)
C(24)-C(25)-C(26)-C(27)	-173.1(2)
C(24)-C(25)-C(26)-C(31)	59.3(2)
C(25)-C(26)-C(27)-C(28)	178.1(2)
C(31)-C(26)-C(27)-C(28)	-55.6(3)
C(25)-C(26)-C(27)-C(41)	56.5(3)
C(31)-C(26)-C(27)-C(41)	-177.2(2)
C(41)-C(27)-C(28)-C(29)	175.1(2)
C(26)-C(27)-C(28)-C(29)	52.3(3)
C(27)-C(28)-C(29)-C(30)	-52.4(3)
C(28)-C(29)-C(30)-O(6)	178.21(19)
C(28)-C(29)-C(30)-C(31)	55.3(3)
O(6)-C(30)-C(31)-C(42)	-59.4(2)
C(29)-C(30)-C(31)-C(42)	63.6(2)

O(6)-C(30)-C(31)-C(26)	-179.78(16)
C(29)-C(30)-C(31)-C(26)	-56.8(2)
O(6)-C(30)-C(31)-C(32)	59.7(2)
C(29)-C(30)-C(31)-C(32)	-177.28(19)
C(25)-C(26)-C(31)-C(30)	-175.10(18)
C(27)-C(26)-C(31)-C(30)	57.1(2)
C(25)-C(26)-C(31)-C(42)	66.8(2)
C(27)-C(26)-C(31)-C(42)	-61.0(2)
C(25)-C(26)-C(31)-C(32)	-55.3(2)
C(27)-C(26)-C(31)-C(32)	176.96(18)
C(30)-C(31)-C(32)-C(33)	38.0(2)
C(42)-C(31)-C(32)-C(33)	156.28(18)
C(26)-C(31)-C(32)-C(33)	-80.4(2)
C(30)-C(31)-C(32)-C(40)	169.25(18)
C(42)-C(31)-C(32)-C(40)	-72.5(2)
C(26)-C(31)-C(32)-C(40)	50.8(2)
C(40)-C(32)-C(33)-O(7)	-64.1(2)
C(31)-C(32)-C(33)-O(7)	68.1(2)
C(40)-C(32)-C(33)-C(34)	58.0(2)
C(31)-C(32)-C(33)-C(34)	-169.79(18)
O(7)-C(33)-C(34)-C(38)	68.4(2)
C(32)-C(33)-C(34)-C(38)	-52.8(3)
O(7)-C(33)-C(34)-C(35)	-167.19(19)
C(32)-C(33)-C(34)-C(35)	71.6(3)
C(33)-C(34)-C(35)-C(43)	-67.2(3)
C(38)-C(34)-C(35)-C(43)	62.6(2)
C(33)-C(34)-C(35)-C(36)	-170.4(2)
C(38)-C(34)-C(35)-C(36)	-40.6(2)
C(43)-C(35)-C(36)-C(37)	-51.1(2)
C(34)-C(35)-C(36)-C(37)	60.6(2)
C(35)-C(36)-C(37)-C(44)	51.4(2)
C(35)-C(36)-C(37)-C(38)	-58.6(2)
C(33)-C(34)-C(38)-C(39)	20.2(3)
C(35)-C(34)-C(38)-C(39)	-111.9(2)
C(33)-C(34)-C(38)-C(45)	-104.1(2)
C(35)-C(34)-C(38)-C(45)	123.8(2)

C(33)-C(34)-C(38)-C(37)	136.4(2)
C(35)-C(34)-C(38)-C(37)	4.3(2)
C(44)-C(37)-C(38)-C(39)	51.1(3)
C(36)-C(37)-C(38)-C(39)	155.1(2)
C(44)-C(37)-C(38)-C(45)	169.5(2)
C(36)-C(37)-C(38)-C(45)	-86.4(2)
C(44)-C(37)-C(38)-C(34)	-70.1(2)
C(36)-C(37)-C(38)-C(34)	34.0(2)
C(45)-C(38)-C(39)-O(8)	-47.0(3)
C(34)-C(38)-C(39)-O(8)	-173.8(2)
C(37)-C(38)-C(39)-O(8)	73.7(3)
C(45)-C(38)-C(39)-C(40)	132.3(2)
C(34)-C(38)-C(39)-C(40)	5.5(3)
C(37)-C(38)-C(39)-C(40)	-107.0(2)
O(8)-C(39)-C(40)-C(46)	-56.2(3)
C(38)-C(39)-C(40)-C(46)	124.5(2)
O(8)-C(39)-C(40)-C(24)	59.6(3)
C(38)-C(39)-C(40)-C(24)	-119.6(2)
O(8)-C(39)-C(40)-C(32)	179.6(2)
C(38)-C(39)-C(40)-C(32)	0.3(3)
O(5)-C(24)-C(40)-C(46)	47.2(2)
C(25)-C(24)-C(40)-C(46)	-74.1(2)
O(5)-C(24)-C(40)-C(39)	-65.9(2)
C(25)-C(24)-C(40)-C(39)	172.77(19)
O(5)-C(24)-C(40)-C(32)	171.50(17)
C(25)-C(24)-C(40)-C(32)	50.2(2)
C(33)-C(32)-C(40)-C(46)	-151.69(18)
C(31)-C(32)-C(40)-C(46)	75.8(2)
C(33)-C(32)-C(40)-C(39)	-30.9(2)
C(31)-C(32)-C(40)-C(39)	-163.45(18)
C(33)-C(32)-C(40)-C(24)	85.4(2)
C(31)-C(32)-C(40)-C(24)	-47.1(2)
C(36)-C(35)-C(43)-C(44)	33.6(2)
C(34)-C(35)-C(43)-C(44)	-68.7(2)
C(35)-C(43)-C(44)-C(37)	0.3(3)
C(36)-C(37)-C(44)-C(43)	-34.4(2)

C(38)-C(37)-C(44)-C(43)	70.1(3)

Table 7. Hydrogen bonds for S5.12 [Å and °].

D-H...A	d(D-H)	d(H...A)	d(D...A)	<(DHA)
O(1)-H(1)...O(4)	0.84(3)	1.92(3)	2.672(3)	149(3)
O(2)-H(2)...O(1)#1	0.81(3)	1.88(3)	2.693(2)	175(3)
O(3)-H(3)...O(2)#2	0.83(3)	1.94(4)	2.739(2)	161(3)
O(5)-H(5)...O(8)	0.84(3)	1.94(3)	2.665(3)	143(3)
O(6)-H(6)...O(5)#1	0.84(3)	1.92(3)	2.748(2)	170(3)
O(7)-H(7)...O(6)#3	0.80(3)	2.05(3)	2.798(2)	156(3)

Symmetry transformations used to generate equivalent atoms:
#1 x-1,y,z #2 -x,y-1/2,-z #3 -x,y-1/2,-z+1

C(8)-C(12)-C(13)-C(14)	-54.16(10)
O(5)-C(13)-C(14)-O(6)	51.20(10)
C(12)-C(13)-C(14)-O(6)	-71.19(10)
O(5)-C(13)-C(14)-C(2)	177.82(8)
C(12)-C(13)-C(14)-C(2)	55.43(10)
C(1)-C(2)-C(14)-O(6)	68.28(10)
C(3)-C(2)-C(14)-O(6)	-67.63(11)
C(1)-C(2)-C(14)-C(13)	-56.62(10)
C(3)-C(2)-C(14)-C(13)	167.47(8)

Table 7. Hydrogen bonds for 3.54 [Å and °].

D-H...A	d(D-H)	d(H...A)	d(D...A)	<(DHA)
O(5)-H(5)...O(3)#1	0.861(17)	1.911(17)	2.7539(11)	165.8(15)
O(6)-H(6)...O(5)#2	0.866(16)	1.822(17)	2.6849(11)	174.7(15)
C(6)-H(6A)...O(3)	0.978(13)	2.561(12)	3.1796(13)	121.2(9)

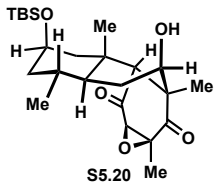

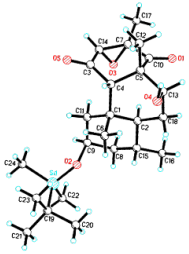

Symmetry transformations used to generate equivalent atoms:
#1 -x+1,y-1/2,-z+3/2 #2 -x+1,-y,-z+1

Table 1. Crystal data and structure refinement for **S5.20**

Identification code	S5.20 (Will Thomas)	
Empirical formula	C_{24} H_{40} O_5 Si	
Formula weight	436.65	
Temperature	133(2) K	
Wavelength	0.71073 Å	
Crystal system	Orthorhombic	
Space group	$P2_12_12_1$	
Unit cell dimensions	a = 7.3693(15) Å	□ = 90°.
	b = 11.979(3) Å	□ = 90°.
	c = 28.099(6) Å	□ = 90°.
Volume	2480.4(9) Å^3	
Z	4	
Density (calculated)	1.169 Mg/m^3	
Absorption coefficient	0.125 mm^{-1}	
F(000)	952	
Crystal color	colorless	
Crystal size	0.340 x 0.207 x 0.104 mm^3	
Theta range for data collection	1.449 to 28.316°	
Index ranges	$-9 \le h \le 9$, $-15 \le k \le 15$, $-37 \le l \le 37$	
Reflections collected	53752	
Independent reflections	6165 [R(int) = 0.0521]	
Completeness to theta = 25.242°	100.0 %	
Absorption correction	Semi-empirical from equivalents	

Max. and min. transmission	0.8621 and 0.8148
Refinement method	Full-matrix least-squares on F^2
Data / restraints / parameters	6165 / 0 / 284
Goodness-of-fit on F^2	1.049
Final R indices [I>2sigma(I) = 5736 data]	R1 = 0.0315, wR2 = 0.0772
R indices (all data, 0.75 Å)	R1 = 0.0355, wR2 = 0.0797
Absolute structure parameter	0.00(4)
Largest diff. peak and hole	0.317 and -0.171 e.Å^{-3}

Table 2. Atomic coordinates (x 10^4) and equivalent isotropic displacement parameters (Å^2 x 10^3)
for **S5.20**. U(eq) is defined as one third of the trace of the orthogonalized U^{ij} tensor.

	x	y	z	U(eq)
Si(1)	8625(1)	2947(1)	7065(1)	16(1)
O(1)	5915(2)	2404(1)	4879(1)	20(1)
O(2)	8578(2)	4839(1)	4764(1)	17(1)
O(3)	5753(2)	6789(1)	4556(1)	20(1)
O(4)	1619(2)	5451(1)	5395(1)	19(1)
O(5)	7596(2)	3700(1)	6657(1)	20(1)
C(1)	5694(2)	4461(1)	5703(1)	11(1)
C(2)	4910(2)	4164(1)	5191(1)	11(1)
C(3)	6114(2)	3411(1)	4892(1)	13(1)
C(4)	7506(2)	3933(2)	4571(1)	15(1)
C(5)	7253(2)	5092(2)	4399(1)	14(1)
C(6)	5750(2)	5789(1)	4621(1)	13(1)
C(7)	4257(2)	5174(1)	4886(1)	11(1)
C(8)	3186(2)	5996(1)	5201(1)	14(1)
C(9)	4348(2)	6431(2)	5617(1)	16(1)
C(10)	6058(2)	5737(1)	5732(1)	12(1)
C(11)	6906(2)	6064(2)	6216(1)	14(1)
C(12)	8683(2)	5422(2)	6294(1)	17(1)
C(13)	8504(2)	4160(2)	6247(1)	16(1)
C(14)	7496(2)	3829(1)	5792(1)	14(1)
C(15)	4255(2)	4088(2)	6071(1)	15(1)

C(16)	7964(3)	5462(2)	3923(1)	22(1)
C(17)	3042(2)	4723(2)	4478(1)	14(1)
C(18)	7300(3)	7319(2)	6247(1)	21(1)
C(19)	9640(4)	1667(2)	6794(1)	37(1)
C(20)	10514(3)	3751(2)	7346(1)	31(1)
C(21)	6775(3)	2613(2)	7503(1)	22(1)
C(22)	5879(3)	3710(2)	7668(1)	30(1)
C(23)	5326(3)	1872(2)	7272(1)	37(1)
C(24)	7573(3)	2006(2)	7940(1)	35(1)

Table 3. Bond lengths [Å] and angles [°] for S5.20.

Si(1)-O(5)	1.6448(13)
Si(1)-C(20)	1.867(2)
Si(1)-C(19)	1.869(2)
Si(1)-C(21)	1.880(2)
O(1)-C(3)	1.216(2)
O(2)-C(4)	1.447(2)
O(2)-C(5)	1.448(2)
O(3)-C(6)	1.212(2)
O(4)-C(8)	1.434(2)
O(5)-C(13)	1.442(2)
C(1)-C(15)	1.547(2)
C(1)-C(14)	1.548(2)
C(1)-C(10)	1.554(2)
C(1)-C(2)	1.592(2)
C(2)-C(3)	1.518(2)
C(2)-C(7)	1.558(2)
C(3)-C(4)	1.504(2)
C(4)-C(5)	1.481(2)
C(5)-C(16)	1.503(2)
C(5)-C(6)	1.522(2)
C(6)-C(7)	1.519(2)
C(7)-C(8)	1.540(2)
C(7)-C(17)	1.554(2)
C(8)-C(9)	1.541(2)

C(9)-C(10)	1.544(2)
C(10)-C(11)	1.547(2)
C(11)-C(12)	1.534(3)
C(11)-C(18)	1.535(2)
C(12)-C(13)	1.523(3)
C(13)-C(14)	1.531(2)
C(21)-C(23)	1.533(3)
C(21)-C(24)	1.542(3)
C(21)-C(22)	1.542(3)

O(5)-Si(1)-C(20)	110.84(9)
O(5)-Si(1)-C(19)	110.47(9)
C(20)-Si(1)-C(19)	107.29(12)
O(5)-Si(1)-C(21)	103.83(8)
C(20)-Si(1)-C(21)	111.98(10)
C(19)-Si(1)-C(21)	112.48(11)
C(4)-O(2)-C(5)	61.52(11)
C(13)-O(5)-Si(1)	123.57(11)
C(15)-C(1)-C(14)	109.81(13)
C(15)-C(1)-C(10)	111.60(14)
C(14)-C(1)-C(10)	108.95(13)
C(15)-C(1)-C(2)	106.93(13)
C(14)-C(1)-C(2)	110.34(13)
C(10)-C(1)-C(2)	109.20(13)
C(3)-C(2)-C(7)	109.79(13)
C(3)-C(2)-C(1)	114.86(13)
C(7)-C(2)-C(1)	115.77(13)
O(1)-C(3)-C(4)	118.44(15)
O(1)-C(3)-C(2)	122.42(16)
C(4)-C(3)-C(2)	118.95(14)
O(2)-C(4)-C(5)	59.26(11)
O(2)-C(4)-C(3)	117.33(14)
C(5)-C(4)-C(3)	119.99(15)
O(2)-C(5)-C(4)	59.22(11)
O(2)-C(5)-C(16)	117.18(15)
C(4)-C(5)-C(16)	121.52(16)

O(2)-C(5)-C(6)	108.33(13)
C(4)-C(5)-C(6)	118.15(14)
C(16)-C(5)-C(6)	117.22(15)
O(3)-C(6)-C(7)	123.67(16)
O(3)-C(6)-C(5)	118.64(16)
C(7)-C(6)-C(5)	117.56(14)
C(6)-C(7)-C(8)	110.06(13)
C(6)-C(7)-C(17)	102.90(13)
C(8)-C(7)-C(17)	110.53(13)
C(6)-C(7)-C(2)	114.99(13)
C(8)-C(7)-C(2)	109.87(13)
C(17)-C(7)-C(2)	108.25(13)
O(4)-C(8)-C(7)	109.92(13)
O(4)-C(8)-C(9)	108.18(14)
C(7)-C(8)-C(9)	111.54(14)
C(8)-C(9)-C(10)	115.39(14)
C(9)-C(10)-C(11)	112.12(13)
C(9)-C(10)-C(1)	112.26(13)
C(11)-C(10)-C(1)	111.32(13)
C(12)-C(11)-C(18)	108.72(15)
C(12)-C(11)-C(10)	110.19(14)
C(18)-C(11)-C(10)	112.00(14)
C(13)-C(12)-C(11)	114.22(15)
O(5)-C(13)-C(12)	110.50(15)
O(5)-C(13)-C(14)	110.02(14)
C(12)-C(13)-C(14)	111.87(14)
C(13)-C(14)-C(1)	115.07(14)
C(23)-C(21)-C(24)	109.25(18)
C(23)-C(21)-C(22)	108.77(18)
C(24)-C(21)-C(22)	109.10(17)
C(23)-C(21)-Si(1)	110.57(14)
C(24)-C(21)-Si(1)	110.16(14)
C(22)-C(21)-Si(1)	108.96(13)

Table 4. Anisotropic displacement parameters ($Å^2$ x 10^3) for S5.20. The anisotropic displacement factor exponent takes the form: $-2\pi^2[h^2 a^{*2} U^{11} + ... + 2 h k a^* b^* U^{12}]$

	U^{11}	U^{22}	U^{33}	U^{23}	U^{13}	U^{12}
Si(1)	18(1)	17(1)	12(1)	1(1)	-2(1)	3(1)
O(1)	21(1)	11(1)	27(1)	-2(1)	-3(1)	1(1)
O(2)	11(1)	21(1)	19(1)	0(1)	-2(1)	-1(1)
O(3)	22(1)	13(1)	25(1)	4(1)	-1(1)	-2(1)
O(4)	11(1)	29(1)	17(1)	-2(1)	1(1)	0(1)
O(5)	16(1)	29(1)	14(1)	8(1)	-1(1)	0(1)
C(1)	11(1)	13(1)	10(1)	0(1)	0(1)	-1(1)
C(2)	10(1)	10(1)	12(1)	1(1)	0(1)	0(1)
C(3)	12(1)	14(1)	12(1)	-1(1)	-4(1)	2(1)
C(4)	14(1)	18(1)	14(1)	-3(1)	2(1)	2(1)
C(5)	12(1)	18(1)	13(1)	0(1)	-1(1)	-3(1)
C(6)	12(1)	16(1)	10(1)	1(1)	-4(1)	-2(1)
C(7)	10(1)	12(1)	12(1)	1(1)	-1(1)	1(1)
C(8)	12(1)	14(1)	17(1)	-1(1)	0(1)	3(1)
C(9)	16(1)	14(1)	16(1)	-3(1)	-1(1)	3(1)
C(10)	11(1)	12(1)	12(1)	-1(1)	-1(1)	0(1)
C(11)	14(1)	17(1)	12(1)	-1(1)	1(1)	-2(1)
C(12)	14(1)	24(1)	12(1)	1(1)	-2(1)	-3(1)
C(13)	12(1)	23(1)	12(1)	4(1)	0(1)	2(1)
C(14)	13(1)	15(1)	14(1)	1(1)	-1(1)	2(1)
C(15)	14(1)	18(1)	13(1)	3(1)	1(1)	-2(1)
C(16)	23(1)	28(1)	16(1)	1(1)	5(1)	-6(1)
C(17)	12(1)	17(1)	14(1)	0(1)	-2(1)	-2(1)
C(18)	24(1)	19(1)	18(1)	-5(1)	-2(1)	-5(1)
C(19)	53(2)	27(1)	30(1)	-1(1)	11(1)	13(1)
C(20)	25(1)	40(1)	28(1)	3(1)	-10(1)	-5(1)
C(21)	24(1)	24(1)	17(1)	6(1)	1(1)	1(1)
C(22)	28(1)	37(1)	23(1)	3(1)	6(1)	9(1)
C(23)	36(1)	35(1)	39(1)	7(1)	-1(1)	-14(1)
C(24)	37(1)	44(1)	24(1)	18(1)	5(1)	9(1)

Table 5. Hydrogen coordinates (x 10^4) and isotropic displacement parameters (Å^2 x 10^3) for S5.20.

	x	y	z	U(eq)
H(4)	860(40)	5390(20)	5167(9)	35(7)
H(2A)	3791	3715	5254	13
H(4A)	8152	3414	4349	18
H(8A)	2784	6642	5002	17
H(9A)	3579	6461	5906	19
H(9B)	4729	7205	5544	19
H(10A)	6977	5915	5481	14
H(11A)	6037	5859	6475	17
H(12A)	9592	5689	6061	20
H(12B)	9148	5598	6616	20
H(13A)	9752	3835	6232	19
H(14A)	7233	3019	5805	17
H(14B)	8309	3958	5517	17
H(15A)	4655	4299	6392	23
H(15B)	4104	3276	6055	23
H(15C)	3096	4452	6001	23
H(16A)	9072	5046	3847	33
H(16B)	8237	6262	3933	33
H(16C)	7047	5319	3678	33
H(17A)	2556	5351	4294	22
H(17B)	2036	4291	4613	22
H(17C)	3766	4243	4269	22
H(18A)	7906	7484	6549	31
H(18B)	6158	7736	6229	31
H(18C)	8089	7540	5982	31
H(19A)	10465	1882	6536	55
H(19B)	8672	1193	6666	55
H(19C)	10316	1254	7037	55
H(20A)	11364	3997	7099	47
H(20B)	11150	3274	7575	47

H(20C)	10018	4404	7510	47
H(22A)	4944	3545	7906	44
H(22B)	5322	4084	7394	44
H(22D)	6801	4199	7808	44
H(23A)	4352	1728	7502	55
H(23D)	5874	1163	7175	55
H(23B)	4825	2252	6993	55
H(24D)	6598	1836	8165	53
H(24A)	8475	2486	8094	53
H(24B)	8153	1310	7837	53

Table 6. Torsion angles [°] for S5.20.

C(20)-Si(1)-O(5)-C(13)	58.82(17)
C(19)-Si(1)-O(5)-C(13)	-59.96(17)
C(21)-Si(1)-O(5)-C(13)	179.23(14)
C(15)-C(1)-C(2)-C(3)	-123.27(15)
C(14)-C(1)-C(2)-C(3)	-3.88(19)
C(10)-C(1)-C(2)-C(3)	115.84(15)
C(15)-C(1)-C(2)-C(7)	107.10(15)
C(14)-C(1)-C(2)-C(7)	-133.52(14)
C(10)-C(1)-C(2)-C(7)	-13.80(18)
C(7)-C(2)-C(3)-O(1)	-132.34(17)
C(1)-C(2)-C(3)-O(1)	95.14(19)
C(7)-C(2)-C(3)-C(4)	42.6(2)
C(1)-C(2)-C(3)-C(4)	-89.95(18)
C(5)-O(2)-C(4)-C(3)	-110.33(17)
O(1)-C(3)-C(4)-O(2)	-140.48(16)
C(2)-C(3)-C(4)-O(2)	44.4(2)
O(1)-C(3)-C(4)-C(5)	150.99(16)
C(2)-C(3)-C(4)-C(5)	-24.1(2)
C(4)-O(2)-C(5)-C(16)	-112.22(18)
C(4)-O(2)-C(5)-C(6)	112.41(15)
C(3)-C(4)-C(5)-O(2)	105.87(17)
O(2)-C(4)-C(5)-C(16)	104.97(18)

C(3)-C(4)-C(5)-C(16)	-149.16(16)
O(2)-C(4)-C(5)-C(6)	-95.53(15)
C(3)-C(4)-C(5)-C(6)	10.3(2)
O(2)-C(5)-C(6)-O(3)	101.20(18)
C(4)-C(5)-C(6)-O(3)	165.46(16)
C(16)-C(5)-C(6)-O(3)	-34.2(2)
O(2)-C(5)-C(6)-C(7)	-82.76(17)
C(4)-C(5)-C(6)-C(7)	-18.5(2)
C(16)-C(5)-C(6)-C(7)	141.89(16)
O(3)-C(6)-C(7)-C(8)	-20.1(2)
C(5)-C(6)-C(7)-C(8)	164.10(14)
O(3)-C(6)-C(7)-C(17)	97.74(19)
C(5)-C(6)-C(7)-C(17)	-78.08(17)
O(3)-C(6)-C(7)-C(2)	-144.79(16)
C(5)-C(6)-C(7)-C(2)	39.4(2)
C(3)-C(2)-C(7)-C(6)	-49.87(18)
C(1)-C(2)-C(7)-C(6)	82.18(17)
C(3)-C(2)-C(7)-C(8)	-174.68(13)
C(1)-C(2)-C(7)-C(8)	-42.63(18)
C(3)-C(2)-C(7)-C(17)	64.54(17)
C(1)-C(2)-C(7)-C(17)	-163.41(13)
C(6)-C(7)-C(8)-O(4)	171.47(13)
C(17)-C(7)-C(8)-O(4)	58.48(17)
C(2)-C(7)-C(8)-O(4)	-60.92(17)
C(6)-C(7)-C(8)-C(9)	-68.54(18)
C(17)-C(7)-C(8)-C(9)	178.47(14)
C(2)-C(7)-C(8)-C(9)	59.07(18)
O(4)-C(8)-C(9)-C(10)	103.40(16)
C(7)-C(8)-C(9)-C(10)	-17.6(2)
C(8)-C(9)-C(10)-C(11)	-167.26(14)
C(8)-C(9)-C(10)-C(1)	-41.1(2)
C(15)-C(1)-C(10)-C(9)	-61.99(17)
C(14)-C(1)-C(10)-C(9)	176.58(13)
C(2)-C(1)-C(10)-C(9)	56.00(17)
C(15)-C(1)-C(10)-C(11)	64.63(17)
C(14)-C(1)-C(10)-C(11)	-56.80(17)

C(2)-C(1)-C(10)-C(11)	-177.38(13)
C(9)-C(10)-C(11)-C(12)	-175.30(14)
C(1)-C(10)-C(11)-C(12)	57.99(18)
C(9)-C(10)-C(11)-C(18)	-54.14(19)
C(1)-C(10)-C(11)-C(18)	179.16(14)
C(18)-C(11)-C(12)-C(13)	-176.97(14)
C(10)-C(11)-C(12)-C(13)	-53.87(19)
Si(1)-O(5)-C(13)-C(12)	-108.62(15)
Si(1)-O(5)-C(13)-C(14)	127.37(14)
C(11)-C(12)-C(13)-O(5)	-74.17(18)
C(11)-C(12)-C(13)-C(14)	48.8(2)
O(5)-C(13)-C(14)-C(1)	74.50(18)
C(12)-C(13)-C(14)-C(1)	-48.7(2)
C(15)-C(1)-C(14)-C(13)	-69.81(18)
C(10)-C(1)-C(14)-C(13)	52.70(18)
C(2)-C(1)-C(14)-C(13)	172.57(14)
O(5)-Si(1)-C(21)-C(23)	65.01(16)
C(20)-Si(1)-C(21)-C(23)	-175.35(15)
C(19)-Si(1)-C(21)-C(23)	-54.43(18)
O(5)-Si(1)-C(21)-C(24)	-174.12(15)
C(20)-Si(1)-C(21)-C(24)	-54.49(18)
C(19)-Si(1)-C(21)-C(24)	66.43(18)
O(5)-Si(1)-C(21)-C(22)	-54.48(15)
C(20)-Si(1)-C(21)-C(22)	65.15(16)
C(19)-Si(1)-C(21)-C(22)	-173.93(15)

Table 7. Hydrogen bonds for S5.20 [Å and °].

D-H...A	d(D-H)	d(H...A)	d(D...A)	<(DHA)
O(4)-H(4)...O(2)#1	0.86(3)	2.13(3)	2.9508(18)	161(2)

Symmetry transformations used to generate equivalent atoms:
#1 x-1,y,z

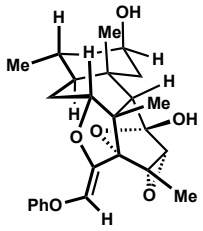

5.58

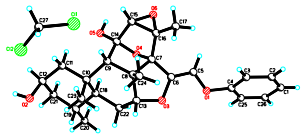

Table 1. Crystal data and structure refinement for **5.58.**

Identification code	5.58 (William Thomas)	
Empirical formula	$C_{26}H_{32}O_6 \bullet CH_2Cl_2$	
Formula weight	525.44	
Temperature	133(2) K	
Wavelength	0.71073 Å	
Crystal system	Monoclinic	
Space group	*C*2	
Unit cell dimensions	a = 18.1918(8) Å	□ = 90°.
	b = 10.7661(5) Å	□ = 96.3646(7)°.
	c = 12.8675(6) Å	□ = 90°.
Volume	2504.6(2) $Å^3$	
Z	4	
Density (calculated)	1.393 Mg/m^3	
Absorption coefficient	0.301 mm^{-1}	
F(000)	1112	
Crystal color	colorless	
Crystal size	0.345 x 0.261 x 0.256 mm^3	
Theta range for data collection	1.592 to 30.375°	
Index ranges	$-25 \le h \le 25$, $-14 \le k \le 15$, $-18 \le l \le 18$	
Reflections collected	31215	
Independent reflections	7342 [R(int) = 0.0304]	
Completeness to theta = 25.242°	100.0 %	
Absorption correction	Semi-empirical from equivalents	
Max. and min. transmission	0.8622 and 0.8210	
Refinement method	Full-matrix least-squares on F^2	
Data / restraints / parameters	7342 / 1 / 418	
Goodness-of-fit on F^2	1.042	
Final R indices [I>2sigma(I) = 6940 data]	R1 = 0.0347, wR2 = 0.0838	

R indices (all data, 0.70 Å)	R1 = 0.0378, wR2 = 0.0856
Absolute structure parameter	-0.001(17)
Largest diff. peak and hole	0.566 and -0.443 e.Å^{-3}

Table 2. Atomic coordinates (x 10^4) and equivalent isotropic displacement parameters (Å^2 x 10^3)
for 5.58. U(eq) is defined as one third of the trace of the orthogonalized U^{ij} tensor.

	x	y	z	U(eq)
O(1)	5262(1)	7567(1)	1031(1)	13(1)
O(2)	4972(1)	5443(1)	1549(1)	10(1)
O(3)	5394(1)	4688(1)	3790(1)	17(1)
O(4)	1761(1)	3178(2)	1568(1)	24(1)
O(5)	4047(1)	5561(1)	150(1)	14(1)
O(6)	6873(1)	5186(1)	3979(1)	17(1)
C(1)	4355(1)	5860(2)	2991(1)	10(1)
C(2)	4582(1)	4613(2)	3539(1)	12(1)
C(3)	4387(1)	3392(2)	2958(2)	15(1)
C(4)	3808(1)	3434(2)	1984(1)	12(1)
C(5)	3368(1)	2209(2)	1870(2)	16(1)
C(6)	2818(1)	2239(2)	882(2)	20(1)
C(7)	2295(1)	3343(2)	830(2)	17(1)
C(8)	2717(1)	4565(2)	1018(1)	14(1)
C(9)	3296(1)	4572(2)	1992(1)	11(1)
C(10)	3766(1)	5774(2)	2007(1)	11(1)
C(11)	4276(1)	6014(2)	1128(1)	11(1)
C(12)	4492(1)	7404(2)	1188(1)	13(1)
C(13)	5058(1)	7508(2)	2093(1)	11(1)
C(14)	5081(1)	6172(2)	2502(1)	10(1)
C(15)	4138(1)	6795(2)	3796(2)	16(1)
C(16)	3874(1)	1079(2)	1835(2)	26(1)
C(17)	2881(1)	4603(2)	2976(1)	15(1)
C(18)	5277(1)	8624(2)	2750(2)	17(1)
C(19)	5676(1)	5635(2)	3241(1)	12(1)
C(20)	6390(1)	5927(2)	3346(1)	13(1)

C(21)	7552(1)	5670(2)	4371(1)	14(1)
C(22)	7641(1)	6881(2)	4715(2)	17(1)
C(23)	8334(1)	7266(2)	5181(2)	21(1)
C(24)	8923(1)	6447(2)	5283(2)	23(1)
C(25)	8143(1)	4843(2)	4451(2)	17(1)
C(26)	8831(1)	5240(2)	4910(2)	21(1)
C(27)	1292(1)	8238(2)	1795(3)	34(1)
Cl(1)	2257(1)	8420(1)	1922(1)	34(1)
Cl(2)	1024(1)	6682(1)	1596(1)	45(1)

Table 3. Bond lengths [Å] and angles [°] for 5.58.

O(1)-C(12)	1.448(2)
O(1)-C(13)	1.457(2)
O(2)-C(14)	1.452(2)
O(2)-C(11)	1.457(2)
O(3)-C(19)	1.372(2)
O(3)-C(2)	1.478(2)
O(4)-C(7)	1.443(2)
O(4)-H(4)	0.79(3)
O(5)-C(11)	1.372(2)
O(5)-H(5)	0.79(3)
O(6)-C(20)	1.383(2)
O(6)-C(21)	1.384(2)
C(1)-C(15)	1.527(3)
C(1)-C(2)	1.551(3)
C(1)-C(14)	1.561(2)
C(1)-C(10)	1.568(2)
C(2)-C(3)	1.534(3)
C(2)-H(2A)	0.97(3)
C(3)-C(4)	1.547(2)
C(3)-H(3A)	0.92(3)
C(3)-H(3B)	0.99(3)
C(4)-C(9)	1.540(3)
C(4)-C(5)	1.541(3)
C(4)-H(4A)	0.94(3)

C(5)-C(16)	1.528(3)
C(5)-C(6)	1.529(3)
C(5)-H(5A)	0.99(3)
C(6)-C(7)	1.519(3)
C(6)-H(6A)	0.95(3)
C(6)-H(6B)	0.91(3)
C(7)-C(8)	1.529(3)
C(7)-H(7A)	0.99(3)
C(8)-C(9)	1.545(2)
C(8)-H(8A)	1.00(3)
C(8)-H(8B)	1.02(3)
C(9)-C(17)	1.544(2)
C(9)-C(10)	1.550(3)
C(10)-C(11)	1.560(3)
C(10)-H(10A)	0.97(3)
C(11)-C(12)	1.546(3)
C(12)-C(13)	1.471(2)
C(12)-H(12A)	0.95(3)
C(13)-C(18)	1.497(3)
C(13)-C(14)	1.530(3)
C(14)-C(19)	1.477(2)
C(15)-H(15A)	0.95(3)
C(15)-H(15B)	0.97(3)
C(15)-H(15C)	0.93(3)
C(16)-H(16A)	0.99(4)
C(16)-H(16B)	0.99(4)
C(16)-H(16C)	0.98(4)
C(17)-H(17A)	0.99(3)
C(17)-H(17B)	0.97(3)
C(17)-H(17C)	0.98(3)
C(18)-H(18A)	0.94(3)
C(18)-H(18B)	0.93(3)
C(18)-H(18C)	0.93(3)
C(19)-C(20)	1.329(3)
C(20)-H(20A)	0.91(3)
C(21)-C(22)	1.380(3)

C(21)-C(25)	1.391(3)
C(22)-C(23)	1.397(3)
C(22)-H(22A)	0.97(3)
C(23)-C(24)	1.384(3)
C(23)-H(23A)	0.89(3)
C(24)-C(26)	1.389(3)
C(24)-H(24A)	0.93(3)
C(25)-C(26)	1.390(3)
C(25)-H(25A)	0.89(3)
C(26)-H(26A)	0.91(3)
C(27)-Cl(1)	1.756(3)
C(27)-Cl(2)	1.756(3)
C(27)-H(27A)	0.91(4)
C(27)-H(27B)	0.98(4)

C(12)-O(1)-C(13)	60.83(11)
C(14)-O(2)-C(11)	96.71(12)
C(19)-O(3)-C(2)	110.52(14)
C(7)-O(4)-H(4)	104(2)
C(11)-O(5)-H(5)	111(2)
C(20)-O(6)-C(21)	118.63(15)
C(15)-C(1)-C(2)	109.76(15)
C(15)-C(1)-C(14)	115.13(15)
C(2)-C(1)-C(14)	100.04(14)
C(15)-C(1)-C(10)	112.51(14)
C(2)-C(1)-C(10)	116.07(15)
C(14)-C(1)-C(10)	102.70(13)
O(3)-C(2)-C(3)	108.92(15)
O(3)-C(2)-C(1)	105.15(14)
C(3)-C(2)-C(1)	119.01(14)
O(3)-C(2)-H(2A)	106.1(15)
C(3)-C(2)-H(2A)	107.8(16)
C(1)-C(2)-H(2A)	109.2(16)
C(2)-C(3)-C(4)	118.00(16)
C(2)-C(3)-H(3A)	107.7(18)
C(4)-C(3)-H(3A)	107.5(17)

C(2)-C(3)-H(3B)	104.6(16)
C(4)-C(3)-H(3B)	110.4(16)
H(3A)-C(3)-H(3B)	108(2)
C(9)-C(4)-C(5)	111.97(14)
C(9)-C(4)-C(3)	112.11(15)
C(5)-C(4)-C(3)	110.57(16)
C(9)-C(4)-H(4A)	107.4(17)
C(5)-C(4)-H(4A)	106.0(17)
C(3)-C(4)-H(4A)	108.5(15)
C(16)-C(5)-C(6)	109.48(18)
C(16)-C(5)-C(4)	112.13(17)
C(6)-C(5)-C(4)	110.19(16)
C(16)-C(5)-H(5A)	107.9(17)
C(6)-C(5)-H(5A)	107.5(16)
C(4)-C(5)-H(5A)	109.6(17)
C(7)-C(6)-C(5)	113.78(17)
C(7)-C(6)-H(6A)	107.4(19)
C(5)-C(6)-H(6A)	106.7(18)
C(7)-C(6)-H(6B)	105.8(19)
C(5)-C(6)-H(6B)	112.8(19)
H(6A)-C(6)-H(6B)	110(3)
O(4)-C(7)-C(6)	109.73(17)
O(4)-C(7)-C(8)	111.43(17)
C(6)-C(7)-C(8)	111.41(15)
O(4)-C(7)-H(7A)	108.2(16)
C(6)-C(7)-H(7A)	107.2(17)
C(8)-C(7)-H(7A)	108.7(18)
C(7)-C(8)-C(9)	114.69(16)
C(7)-C(8)-H(8A)	108.2(16)
C(9)-C(8)-H(8A)	109.3(16)
C(7)-C(8)-H(8B)	103.1(16)
C(9)-C(8)-H(8B)	111.8(15)
H(8A)-C(8)-H(8B)	109(2)
C(4)-C(9)-C(17)	111.95(15)
C(4)-C(9)-C(8)	110.40(15)
C(17)-C(9)-C(8)	108.34(14)

C(4)-C(9)-C(10)	109.27(14)
C(17)-C(9)-C(10)	106.94(15)
C(8)-C(9)-C(10)	109.87(14)
C(9)-C(10)-C(11)	120.09(15)
C(9)-C(10)-C(1)	112.73(14)
C(11)-C(10)-C(1)	99.67(13)
C(9)-C(10)-H(10A)	107.3(16)
C(11)-C(10)-H(10A)	108.6(15)
C(1)-C(10)-H(10A)	107.8(16)
O(5)-C(11)-O(2)	110.65(14)
O(5)-C(11)-C(12)	116.05(15)
O(2)-C(11)-C(12)	100.61(13)
O(5)-C(11)-C(10)	117.51(15)
O(2)-C(11)-C(10)	102.87(13)
C(12)-C(11)-C(10)	107.06(14)
O(1)-C(12)-C(13)	59.89(11)
O(1)-C(12)-C(11)	110.84(15)
C(13)-C(12)-C(11)	105.33(15)
O(1)-C(12)-H(12A)	116.7(16)
C(13)-C(12)-H(12A)	124.2(16)
C(11)-C(12)-H(12A)	123.3(16)
O(1)-C(13)-C(12)	59.29(11)
O(1)-C(13)-C(18)	114.47(15)
C(12)-C(13)-C(18)	128.83(16)
O(1)-C(13)-C(14)	111.35(14)
C(12)-C(13)-C(14)	101.03(14)
C(18)-C(13)-C(14)	124.36(16)
O(2)-C(14)-C(19)	110.70(14)
O(2)-C(14)-C(13)	102.79(13)
C(19)-C(14)-C(13)	125.45(15)
O(2)-C(14)-C(1)	100.47(13)
C(19)-C(14)-C(1)	104.43(14)
C(13)-C(14)-C(1)	110.38(14)
C(1)-C(15)-H(15A)	111.3(19)
C(1)-C(15)-H(15B)	110.8(18)
H(15A)-C(15)-H(15B)	108(3)

C(1)-C(15)-H(15C)	109.7(19)
H(15A)-C(15)-H(15C)	104(3)
H(15B)-C(15)-H(15C)	113(3)
C(5)-C(16)-H(16A)	108(2)
C(5)-C(16)-H(16B)	108(2)
H(16A)-C(16)-H(16B)	109(3)
C(5)-C(16)-H(16C)	113(2)
H(16A)-C(16)-H(16C)	108(3)
H(16B)-C(16)-H(16C)	110(3)
C(9)-C(17)-H(17A)	111.7(17)
C(9)-C(17)-H(17B)	110.3(18)
H(17A)-C(17)-H(17B)	105(2)
C(9)-C(17)-H(17C)	110.7(17)
H(17A)-C(17)-H(17C)	107(2)
H(17B)-C(17)-H(17C)	111(2)
C(13)-C(18)-H(18A)	108.4(19)
C(13)-C(18)-H(18B)	112.1(19)
H(18A)-C(18)-H(18B)	109(3)
C(13)-C(18)-H(18C)	111(2)
H(18A)-C(18)-H(18C)	109(3)
H(18B)-C(18)-H(18C)	107(2)
C(20)-C(19)-O(3)	122.77(16)
C(20)-C(19)-C(14)	127.68(17)
O(3)-C(19)-C(14)	109.42(15)
C(19)-C(20)-O(6)	118.19(17)
C(19)-C(20)-H(20A)	124.4(17)
O(6)-C(20)-H(20A)	117.0(17)
C(22)-C(21)-O(6)	122.80(17)
C(22)-C(21)-C(25)	121.18(18)
O(6)-C(21)-C(25)	115.94(17)
C(21)-C(22)-C(23)	119.14(19)
C(21)-C(22)-H(22A)	121.6(17)
C(23)-C(22)-H(22A)	119.2(17)
C(24)-C(23)-C(22)	120.3(2)
C(24)-C(23)-H(23A)	122.2(19)
C(22)-C(23)-H(23A)	117.4(19)

C(23)-C(24)-C(26)	120.03(19)
C(23)-C(24)-H(24A)	123(2)
C(26)-C(24)-H(24A)	117(2)
C(26)-C(25)-C(21)	119.1(2)
C(26)-C(25)-H(25A)	121.7(19)
C(21)-C(25)-H(25A)	119.1(19)
C(24)-C(26)-C(25)	120.2(2)
C(24)-C(26)-H(26A)	120(2)
C(25)-C(26)-H(26A)	120(2)
Cl(1)-C(27)-Cl(2)	112.28(14)
Cl(1)-C(27)-H(27A)	115(2)
Cl(2)-C(27)-H(27A)	102(2)
Cl(1)-C(27)-H(27B)	107(2)
Cl(2)-C(27)-H(27B)	107(2)
H(27A)-C(27)-H(27B)	113(3)

Table 4. Anisotropic displacement parameters ($Å^2$ x 10^3) for 5.58. The anisotropic displacement factor exponent takes the form: $-2\pi^2[h^2 a^{*2} U^{11} + ... + 2 h k a^* b^* U^{12}]$

	U^{11}	U^{22}	U^{33}	U^{23}	U^{13}	U^{12}
O(1)	10(1)	18(1)	11(1)	2(1)	0(1)	-4(1)
O(2)	8(1)	13(1)	9(1)	-2(1)	-1(1)	1(1)
O(3)	10(1)	22(1)	17(1)	7(1)	-3(1)	-2(1)
O(4)	12(1)	40(1)	21(1)	2(1)	3(1)	-10(1)
O(5)	12(1)	23(1)	8(1)	0(1)	0(1)	-7(1)
O(6)	9(1)	16(1)	24(1)	4(1)	-5(1)	0(1)
C(1)	8(1)	15(1)	8(1)	0(1)	1(1)	0(1)
C(2)	9(1)	18(1)	10(1)	3(1)	0(1)	0(1)
C(3)	14(1)	15(1)	16(1)	3(1)	-1(1)	1(1)
C(4)	10(1)	14(1)	12(1)	0(1)	2(1)	0(1)
C(5)	16(1)	15(1)	18(1)	-1(1)	3(1)	-4(1)
C(6)	20(1)	20(1)	19(1)	-4(1)	1(1)	-8(1)
C(7)	11(1)	26(1)	14(1)	0(1)	0(1)	-7(1)
C(8)	8(1)	22(1)	13(1)	3(1)	-1(1)	-3(1)
C(9)	7(1)	15(1)	11(1)	2(1)	1(1)	-1(1)

C(10)	8(1)	14(1)	10(1)	0(1)	0(1)	1(1)
C(11)	8(1)	14(1)	10(1)	0(1)	0(1)	-1(1)
C(12)	9(1)	15(1)	12(1)	2(1)	-1(1)	-1(1)
C(13)	9(1)	12(1)	12(1)	0(1)	1(1)	0(1)
C(14)	8(1)	12(1)	9(1)	-1(1)	1(1)	0(1)
C(15)	14(1)	23(1)	13(1)	-5(1)	3(1)	1(1)
C(16)	26(1)	17(1)	37(1)	-3(1)	5(1)	-2(1)
C(17)	10(1)	22(1)	13(1)	1(1)	3(1)	-1(1)
C(18)	17(1)	15(1)	20(1)	-5(1)	1(1)	-1(1)
C(19)	12(1)	15(1)	9(1)	0(1)	0(1)	1(1)
C(20)	11(1)	15(1)	13(1)	1(1)	-1(1)	2(1)
C(21)	10(1)	18(1)	13(1)	3(1)	-1(1)	-1(1)
C(22)	15(1)	19(1)	16(1)	0(1)	1(1)	-1(1)
C(23)	23(1)	21(1)	19(1)	-3(1)	0(1)	-8(1)
C(24)	16(1)	34(1)	19(1)	2(1)	-4(1)	-8(1)
C(25)	14(1)	17(1)	19(1)	1(1)	-2(1)	2(1)
C(26)	12(1)	29(1)	22(1)	4(1)	-3(1)	3(1)
C(27)	23(1)	22(1)	60(2)	-4(1)	11(1)	4(1)
Cl(1)	26(1)	48(1)	30(1)	-9(1)	6(1)	0(1)
Cl(2)	45(1)	29(1)	65(1)	-12(1)	30(1)	-7(1)

Table 5. Hydrogen coordinates (x 10^4) and isotropic displacement parameters (Å^2 x 10^3) for 5.58.

	x	y	z	U(eq)
H(4)	1380(19)	3080(30)	1210(30)	36
H(5)	4286(16)	5840(30)	-270(20)	21
H(2A)	4379(14)	4580(30)	4210(20)	15
H(3A)	4216(15)	2850(30)	3430(20)	18
H(3B)	4865(15)	3080(30)	2770(20)	18
H(4A)	4058(14)	3500(30)	1380(20)	14
H(5A)	3079(15)	2110(30)	2480(20)	20
H(6A)	3102(17)	2300(30)	310(20)	24
H(6B)	2524(17)	1550(30)	810(20)	24

H(7A)	2026(15)	3360(30)	120(20)	21
H(8A)	2349(15)	5240(30)	1080(20)	17
H(8B)	2956(15)	4680(30)	350(20)	17
H(10A)	3430(15)	6470(20)	2030(20)	13
H(12A)	4164(14)	8050(30)	950(20)	15
H(15A)	4538(17)	6960(30)	4320(20)	25
H(15B)	3729(17)	6490(30)	4140(20)	25
H(15C)	4042(17)	7560(30)	3480(20)	25
H(16A)	3562(19)	330(30)	1740(30)	39
H(16B)	4184(19)	1020(30)	2520(30)	39
H(16C)	4190(20)	1110(30)	1260(30)	39
H(17A)	2533(17)	3900(30)	2990(20)	22
H(17B)	2577(16)	5340(30)	2970(20)	22
H(17C)	3231(16)	4550(30)	3620(20)	22
H(18A)	5126(17)	9340(30)	2360(20)	26
H(18B)	5785(17)	8660(30)	2940(20)	26
H(18C)	5048(16)	8610(30)	3360(20)	26
H(20A)	6594(15)	6530(30)	2970(20)	16
H(22A)	7230(16)	7460(30)	4670(20)	20
H(23A)	8371(16)	8040(30)	5430(20)	25
H(24A)	9393(17)	6670(30)	5580(20)	28
H(25A)	8075(16)	4080(30)	4180(20)	21
H(26A)	9216(17)	4700(30)	4980(20)	26
H(27A)	1050(20)	8620(40)	1230(30)	41
H(27B)	1122(19)	8510(40)	2460(30)	41

Table 6. Torsion angles [°] for 5.58.

C(19)-O(3)-C(2)-C(3)	113.38(17)
C(19)-O(3)-C(2)-C(1)	-15.22(19)
C(15)-C(1)-C(2)-O(3)	-93.40(16)
C(14)-C(1)-C(2)-O(3)	28.06(16)
C(10)-C(1)-C(2)-O(3)	137.64(15)
C(15)-C(1)-C(2)-C(3)	144.30(16)
C(14)-C(1)-C(2)-C(3)	-94.23(17)

C(10)-C(1)-C(2)-C(3)	15.4(2)
O(3)-C(2)-C(3)-C(4)	-135.69(16)
C(1)-C(2)-C(3)-C(4)	-15.3(2)
C(2)-C(3)-C(4)-C(9)	-22.7(2)
C(2)-C(3)-C(4)-C(5)	-148.41(17)
C(9)-C(4)-C(5)-C(16)	178.62(18)
C(3)-C(4)-C(5)-C(16)	-55.6(2)
C(9)-C(4)-C(5)-C(6)	56.4(2)
C(3)-C(4)-C(5)-C(6)	-177.81(16)
C(16)-C(5)-C(6)-C(7)	-179.03(18)
C(4)-C(5)-C(6)-C(7)	-55.3(2)
C(5)-C(6)-C(7)-O(4)	-72.5(2)
C(5)-C(6)-C(7)-C(8)	51.4(2)
O(4)-C(7)-C(8)-C(9)	73.6(2)
C(6)-C(7)-C(8)-C(9)	-49.3(2)
C(5)-C(4)-C(9)-C(17)	66.79(19)
C(3)-C(4)-C(9)-C(17)	-58.1(2)
C(5)-C(4)-C(9)-C(8)	-54.00(19)
C(3)-C(4)-C(9)-C(8)	-178.94(15)
C(5)-C(4)-C(9)-C(10)	-174.94(15)
C(3)-C(4)-C(9)-C(10)	60.12(18)
C(7)-C(8)-C(9)-C(4)	50.9(2)
C(7)-C(8)-C(9)-C(17)	-72.1(2)
C(7)-C(8)-C(9)-C(10)	171.45(16)
C(4)-C(9)-C(10)-C(11)	56.85(19)
C(17)-C(9)-C(10)-C(11)	178.21(15)
C(8)-C(9)-C(10)-C(11)	-64.4(2)
C(4)-C(9)-C(10)-C(1)	-60.10(18)
C(17)-C(9)-C(10)-C(1)	61.26(18)
C(8)-C(9)-C(10)-C(1)	178.63(15)
C(15)-C(1)-C(10)-C(9)	-105.44(17)
C(2)-C(1)-C(10)-C(9)	22.2(2)
C(14)-C(1)-C(10)-C(9)	130.19(15)
C(15)-C(1)-C(10)-C(11)	126.04(16)
C(2)-C(1)-C(10)-C(11)	-106.35(16)
C(14)-C(1)-C(10)-C(11)	1.66(16)

C(14)-O(2)-C(11)-O(5)	175.58(14)
C(14)-O(2)-C(11)-C(12)	52.34(15)
C(14)-O(2)-C(11)-C(10)	-58.09(15)
C(9)-C(10)-C(11)-O(5)	32.0(2)
C(1)-C(10)-C(11)-O(5)	155.50(15)
C(9)-C(10)-C(11)-O(2)	-89.79(17)
C(1)-C(10)-C(11)-O(2)	33.69(16)
C(9)-C(10)-C(11)-C(12)	164.68(15)
C(1)-C(10)-C(11)-C(12)	-71.83(16)
C(13)-O(1)-C(12)-C(11)	-96.10(16)
O(5)-C(11)-C(12)-O(1)	-87.18(18)
O(2)-C(11)-C(12)-O(1)	32.22(17)
C(10)-C(11)-C(12)-O(1)	139.36(14)
O(5)-C(11)-C(12)-C(13)	-150.29(16)
O(2)-C(11)-C(12)-C(13)	-30.89(17)
C(10)-C(11)-C(12)-C(13)	76.25(17)
C(12)-O(1)-C(13)-C(18)	-122.07(18)
C(12)-O(1)-C(13)-C(14)	90.39(16)
C(11)-C(12)-C(13)-O(1)	105.52(15)
O(1)-C(12)-C(13)-C(18)	98.1(2)
C(11)-C(12)-C(13)-C(18)	-156.42(19)
O(1)-C(12)-C(13)-C(14)	-108.40(15)
C(11)-C(12)-C(13)-C(14)	-2.88(17)
C(11)-O(2)-C(14)-C(19)	167.71(15)
C(11)-O(2)-C(14)-C(13)	-56.11(15)
C(11)-O(2)-C(14)-C(1)	57.79(14)
O(1)-C(13)-C(14)-O(2)	-24.83(17)
C(12)-C(13)-C(14)-O(2)	36.32(16)
C(18)-C(13)-C(14)-O(2)	-168.55(16)
O(1)-C(13)-C(14)-C(19)	102.51(19)
C(12)-C(13)-C(14)-C(19)	163.66(17)
C(18)-C(13)-C(14)-C(19)	-41.2(3)
O(1)-C(13)-C(14)-C(1)	-131.27(14)
C(12)-C(13)-C(14)-C(1)	-70.12(16)
C(18)-C(13)-C(14)-C(1)	85.0(2)
C(15)-C(1)-C(14)-O(2)	-159.05(14)

C(2)-C(1)-C(14)-O(2)	83.41(14)
C(10)-C(1)-C(14)-O(2)	-36.41(16)
C(15)-C(1)-C(14)-C(19)	86.20(18)
C(2)-C(1)-C(14)-C(19)	-31.34(17)
C(10)-C(1)-C(14)-C(19)	-151.17(14)
C(15)-C(1)-C(14)-C(13)	-51.06(19)
C(2)-C(1)-C(14)-C(13)	-168.60(14)
C(10)-C(1)-C(14)-C(13)	71.57(17)
C(2)-O(3)-C(19)-C(20)	177.91(17)
C(2)-O(3)-C(19)-C(14)	-5.9(2)
O(2)-C(14)-C(19)-C(20)	93.0(2)
C(13)-C(14)-C(19)-C(20)	-31.0(3)
C(1)-C(14)-C(19)-C(20)	-159.68(19)
O(2)-C(14)-C(19)-O(3)	-82.97(18)
C(13)-C(14)-C(19)-O(3)	153.00(17)
C(1)-C(14)-C(19)-O(3)	24.35(19)
O(3)-C(19)-C(20)-O(6)	4.8(3)
C(14)-C(19)-C(20)-O(6)	-170.64(17)
C(21)-O(6)-C(20)-C(19)	-159.26(17)
C(20)-O(6)-C(21)-C(22)	39.3(3)
C(20)-O(6)-C(21)-C(25)	-144.01(18)
O(6)-C(21)-C(22)-C(23)	174.58(18)
C(25)-C(21)-C(22)-C(23)	-2.0(3)
C(21)-C(22)-C(23)-C(24)	0.8(3)
C(22)-C(23)-C(24)-C(26)	0.8(3)
C(22)-C(21)-C(25)-C(26)	1.5(3)
O(6)-C(21)-C(25)-C(26)	-175.27(18)
C(23)-C(24)-C(26)-C(25)	-1.3(3)
C(21)-C(25)-C(26)-C(24)	0.2(3)

Table 7. Hydrogen bonds for 5.58 [Å and °].

D-H...A	d(D-H)	d(H...A)	d(D...A)	<(DHA)
O(4)-H(4)...O(1)#1	0.79(3)	2.09(4)	2.815(2)	151(3)
O(5)-H(5)...O(1)#2	0.79(3)	2.30(3)	2.996(2)	148(3)

O(5)-H(5)...O(2)#2	0.79(3)	2.28(3)	2.9729(19)	147(3)

Symmetry transformations used to generate equivalent atoms:
#1 x-1/2,y-1/2,z #2 -x+1,y,-z

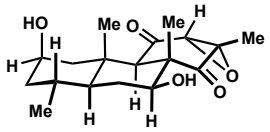

S5.27

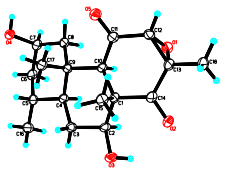

Table 1. Crystal data and structure refinement for **S5.27**.

Identification code	S5.27 (William Thomas)	
Empirical formula	C_{18} H_{26} O_5	
Formula weight	322.39	
Temperature	93(2) K	
Wavelength	0.71073 Å	
Crystal system	Monoclinic	
Space group	$P2_1$	
Unit cell dimensions	a = 8.496(2) Å	□ = 90°.
	b = 9.772(3) Å	□ = 108.094(3)°.
	c = 10.408(3) Å	□ = 90°.
Volume	821.4(4) $Å^3$	
Z	2	
Density (calculated)	1.303 Mg/m^3	
Absorption coefficient	0.094 mm^{-1}	
F(000)	348	
Crystal color	colorless	
Crystal size	0.346 x 0.341 x 0.080 mm^3	
Theta range for data collection	2.059 to 27.100°	
Index ranges	$-10 \le h \le 10$, $-12 \le k \le 12$, $-13 \le l \le 13$	
Reflections collected	8994	
Independent reflections	3626 [R(int) = 0.0490]	
Completeness to theta = 25.242°	99.8 %	
Absorption correction	Semi-empirical from equivalents	
Max. and min. transmission	0.8621 and 0.6251	
Refinement method	Full-matrix least-squares on F^2	
Data / restraints / parameters	3626 / 1 / 286	
Goodness-of-fit on F^2	1.034	
Final R indices [I>2sigma(I) = 3204 data]	R1 = 0.0468, wR2 = 0.1120	
R indices (all data, 0.78 Å)	R1 = 0.0559, wR2 = 0.1193	

Largest diff. peak and hole 0.293 and -0.196 e.Å^{-3}

Table 2. Atomic coordinates (x 10^4) and equivalent isotropic displacement parameters (Å^2 x 10^3)
for S5.27. U(eq) is defined as one third of the trace of the orthogonalized U^{ij} tensor.

	x	y	z	U(eq)
O(1)	2648(3)	2124(2)	1233(2)	23(1)
O(2)	5519(3)	4116(2)	861(3)	24(1)
O(3)	8844(3)	3292(3)	1655(3)	26(1)
O(4)	7893(3)	-3440(2)	4446(3)	22(1)
O(5)	4547(3)	494(2)	4374(2)	25(1)
C(1)	6636(4)	2264(3)	2445(3)	18(1)
C(2)	7882(4)	2075(3)	1635(3)	20(1)
C(3)	9108(4)	911(3)	2179(4)	20(1)
C(4)	8222(4)	-466(3)	2196(4)	18(1)
C(5)	9410(4)	-1711(4)	2569(3)	21(1)
C(6)	8346(5)	-3030(3)	2312(4)	22(1)
C(7)	7055(4)	-3086(3)	3048(3)	21(1)
C(8)	6044(4)	-1735(3)	2910(3)	19(1)
C(9)	7089(4)	-386(3)	3127(3)	17(1)
C(10)	5837(4)	824(3)	2581(3)	16(1)
C(11)	4562(4)	1055(3)	3321(3)	20(1)
C(12)	3247(4)	2117(3)	2698(3)	20(1)
C(13)	3625(4)	3286(4)	1935(3)	20(1)
C(14)	5288(4)	3280(3)	1670(3)	19(1)
C(15)	7459(4)	2981(3)	3839(4)	21(1)
C(16)	10662(4)	-1774(4)	1769(4)	26(1)
C(17)	8140(4)	-231(3)	4644(4)	20(1)
C(18)	2725(5)	4637(4)	1865(4)	24(1)

Table 3. Bond lengths [Å] and angles [°] for S5.27.

O(1)-C(12)	1.449(4)
O(1)-C(13)	1.461(4)
O(2)-C(14)	1.231(4)

O(3)-C(2)	1.440(4)
O(3)-H(3)	0.81(5)
O(4)-C(7)	1.449(4)
O(4)-H(4)	0.80(5)
O(5)-C(11)	1.229(4)
C(1)-C(14)	1.541(4)
C(1)-C(2)	1.556(4)
C(1)-C(15)	1.567(5)
C(1)-C(10)	1.588(4)
C(2)-C(3)	1.528(4)
C(2)-H(2A)	1.04(4)
C(3)-C(4)	1.545(4)
C(3)-H(3A)	0.99(4)
C(3)-H(3B)	0.97(4)
C(4)-C(5)	1.551(4)
C(4)-C(9)	1.566(4)
C(4)-H(4A)	1.06(4)
C(5)-C(16)	1.541(5)
C(5)-C(6)	1.549(5)
C(5)-H(5A)	1.02(4)
C(6)-C(7)	1.522(5)
C(6)-H(6A)	1.00(4)
C(6)-H(6B)	0.92(5)
C(7)-C(8)	1.557(4)
C(7)-H(7A)	0.97(4)
C(8)-C(9)	1.566(4)
C(8)-H(8A)	1.01(4)
C(8)-H(8B)	0.98(4)
C(9)-C(17)	1.561(5)
C(9)-C(10)	1.573(4)
C(10)-C(11)	1.528(4)
C(10)-H(10A)	1.01(4)
C(11)-C(12)	1.515(5)
C(12)-C(13)	1.482(5)
C(12)-H(12A)	0.95(4)
C(13)-C(18)	1.516(5)

C(13)-C(14)	1.522(4)
C(15)-H(15A)	0.98(4)
C(15)-H(15B)	0.99(4)
C(15)-H(15C)	0.98(5)
C(16)-H(16A)	0.95(5)
C(16)-H(16B)	1.00(5)
C(16)-H(16C)	0.99(5)
C(17)-H(17A)	0.98(5)
C(17)-H(17B)	0.99(4)
C(17)-H(17C)	0.96(4)
C(18)-H(18A)	0.97(5)
C(18)-H(18B)	0.98(5)
C(18)-H(18C)	0.96(5)

C(12)-O(1)-C(13)	61.2(2)
C(2)-O(3)-H(3)	107(4)
C(7)-O(4)-H(4)	102(3)
C(14)-C(1)-C(2)	108.2(3)
C(14)-C(1)-C(15)	104.0(2)
C(2)-C(1)-C(15)	111.8(3)
C(14)-C(1)-C(10)	110.4(2)
C(2)-C(1)-C(10)	109.0(2)
C(15)-C(1)-C(10)	113.2(3)
O(3)-C(2)-C(3)	106.9(3)
O(3)-C(2)-C(1)	111.9(3)
C(3)-C(2)-C(1)	112.8(3)
O(3)-C(2)-H(2A)	108(2)
C(3)-C(2)-H(2A)	109(2)
C(1)-C(2)-H(2A)	108(2)
C(2)-C(3)-C(4)	112.0(3)
C(2)-C(3)-H(3A)	106(2)
C(4)-C(3)-H(3A)	112(2)
C(2)-C(3)-H(3B)	108(2)
C(4)-C(3)-H(3B)	112(2)
H(3A)-C(3)-H(3B)	106(3)
C(3)-C(4)-C(5)	113.8(3)

C(3)-C(4)-C(9)	111.0(3)
C(5)-C(4)-C(9)	111.2(3)
C(3)-C(4)-H(4A)	104(2)
C(5)-C(4)-H(4A)	107(2)
C(9)-C(4)-H(4A)	110(2)
C(16)-C(5)-C(6)	109.7(3)
C(16)-C(5)-C(4)	113.6(3)
C(6)-C(5)-C(4)	108.0(3)
C(16)-C(5)-H(5A)	108(2)
C(6)-C(5)-H(5A)	108(2)
C(4)-C(5)-H(5A)	109(2)
C(7)-C(6)-C(5)	114.6(3)
C(7)-C(6)-H(6A)	111(2)
C(5)-C(6)-H(6A)	106(2)
C(7)-C(6)-H(6B)	108(3)
C(5)-C(6)-H(6B)	110(3)
H(6A)-C(6)-H(6B)	106(3)
O(4)-C(7)-C(6)	107.9(3)
O(4)-C(7)-C(8)	112.4(3)
C(6)-C(7)-C(8)	112.7(3)
O(4)-C(7)-H(7A)	106(2)
C(6)-C(7)-H(7A)	110(2)
C(8)-C(7)-H(7A)	108(2)
C(7)-C(8)-C(9)	115.4(2)
C(7)-C(8)-H(8A)	109(2)
C(9)-C(8)-H(8A)	112(2)
C(7)-C(8)-H(8B)	105(3)
C(9)-C(8)-H(8B)	106(3)
H(8A)-C(8)-H(8B)	109(3)
C(17)-C(9)-C(4)	111.2(3)
C(17)-C(9)-C(8)	110.4(3)
C(4)-C(9)-C(8)	107.3(3)
C(17)-C(9)-C(10)	113.7(3)
C(4)-C(9)-C(10)	106.9(3)
C(8)-C(9)-C(10)	106.9(2)
C(11)-C(10)-C(9)	115.8(2)

C(11)-C(10)-C(1)	107.7(2)
C(9)-C(10)-C(1)	116.0(2)
C(11)-C(10)-H(10A)	107(2)
C(9)-C(10)-H(10A)	105(2)
C(1)-C(10)-H(10A)	104(2)
O(5)-C(11)-C(12)	118.5(3)
O(5)-C(11)-C(10)	126.0(3)
C(12)-C(11)-C(10)	115.5(3)
O(1)-C(12)-C(13)	59.8(2)
O(1)-C(12)-C(11)	115.2(3)
C(13)-C(12)-C(11)	120.2(3)
O(1)-C(12)-H(12A)	114(2)
C(13)-C(12)-H(12A)	119(3)
C(11)-C(12)-H(12A)	116(3)
O(1)-C(13)-C(12)	59.0(2)
O(1)-C(13)-C(18)	116.9(3)
C(12)-C(13)-C(18)	120.5(3)
O(1)-C(13)-C(14)	108.8(3)
C(12)-C(13)-C(14)	117.5(3)
C(18)-C(13)-C(14)	118.5(3)
O(2)-C(14)-C(13)	118.4(3)
O(2)-C(14)-C(1)	122.4(3)
C(13)-C(14)-C(1)	119.2(3)
C(1)-C(15)-H(15A)	108(3)
C(1)-C(15)-H(15B)	108(2)
H(15A)-C(15)-H(15B)	115(3)
C(1)-C(15)-H(15C)	109(3)
H(15A)-C(15)-H(15C)	109(4)
H(15B)-C(15)-H(15C)	107(4)
C(5)-C(16)-H(16A)	114(3)
C(5)-C(16)-H(16B)	112(3)
H(16A)-C(16)-H(16B)	107(4)
C(5)-C(16)-H(16C)	109(3)
H(16A)-C(16)-H(16C)	107(4)
H(16B)-C(16)-H(16C)	107(4)
C(9)-C(17)-H(17A)	111(3)

C(9)-C(17)-H(17B)	114(2)
H(17A)-C(17)-H(17B)	108(4)
C(9)-C(17)-H(17C)	108(3)
H(17A)-C(17)-H(17C)	107(4)
H(17B)-C(17)-H(17C)	108(4)
C(13)-C(18)-H(18A)	109(3)
C(13)-C(18)-H(18B)	111(3)
H(18A)-C(18)-H(18B)	107(4)
C(13)-C(18)-H(18C)	107(3)
H(18A)-C(18)-H(18C)	113(4)
H(18B)-C(18)-H(18C)	111(4)

Table 4. Anisotropic displacement parameters ($Å^2$ x 10^3) for S5.27. The anisotropic displacement factor exponent takes the form: $-2\pi^2[h^2 a^{*2} U^{11} + ... + 2 h k a^* b^* U^{12}]$

	U^{11}	U^{22}	U^{33}	U^{23}	U^{13}	U^{12}
O(1)	23(1)	17(1)	28(1)	-2(1)	6(1)	-2(1)
O(2)	27(1)	16(1)	32(1)	5(1)	11(1)	2(1)
O(3)	25(1)	14(1)	42(1)	2(1)	15(1)	-2(1)
O(4)	23(1)	16(1)	29(1)	5(1)	9(1)	0(1)
O(5)	27(1)	20(1)	30(1)	4(1)	13(1)	3(1)
C(1)	20(2)	11(1)	23(2)	1(1)	6(1)	1(1)
C(2)	23(2)	12(1)	28(2)	1(1)	12(1)	-1(1)
C(3)	21(2)	16(2)	26(2)	0(1)	10(1)	0(1)
C(4)	19(2)	12(1)	24(2)	1(1)	9(1)	0(1)
C(5)	22(2)	16(2)	26(2)	2(1)	9(1)	4(1)
C(6)	28(2)	12(2)	28(2)	1(1)	11(1)	3(1)
C(7)	26(2)	12(2)	24(2)	0(1)	7(1)	0(1)
C(8)	20(2)	11(1)	26(2)	1(1)	7(1)	0(1)
C(9)	16(2)	11(1)	24(2)	1(1)	8(1)	0(1)
C(10)	19(2)	10(1)	22(2)	0(1)	7(1)	-2(1)
C(11)	21(2)	13(1)	25(2)	-2(1)	8(1)	-2(1)
C(12)	18(2)	16(2)	28(2)	-1(1)	8(1)	-2(1)
C(13)	23(2)	14(1)	24(2)	0(1)	7(1)	0(1)
C(14)	24(2)	10(1)	23(2)	-3(1)	7(1)	-2(1)

C(15)	23(2)	13(2)	25(2)	-3(1)	6(1)	-2(1)
C(16)	26(2)	19(2)	36(2)	2(2)	14(1)	4(2)
C(17)	22(2)	15(2)	24(2)	1(1)	8(1)	1(1)
C(18)	27(2)	17(2)	31(2)	2(1)	12(2)	4(1)

Table 5. Hydrogen coordinates (x 10^4) and isotropic displacement parameters (Å^2 x 10^3) for S5.27.

	x	y	z	U(eq)
H(3)	8200(60)	3890(50)	1280(50)	38
H(4)	7150(60)	-3700(50)	4700(50)	33
H(2A)	7210(50)	1870(40)	640(40)	24
H(3A)	9790(50)	1200(40)	3090(40)	24
H(3B)	9840(50)	870(40)	1640(40)	24
H(4A)	7480(50)	-610(40)	1170(40)	22
H(5A)	10050(50)	-1660(50)	3570(40)	25
H(6A)	7820(50)	-3090(40)	1320(40)	27
H(6B)	9020(50)	-3790(50)	2560(40)	27
H(7A)	6290(50)	-3820(40)	2690(40)	25
H(8A)	5340(50)	-1780(50)	3530(40)	23
H(8B)	5330(50)	-1710(50)	1970(40)	23
H(10A)	5210(50)	570(40)	1610(40)	20
H(12A)	2410(50)	2220(40)	3120(40)	25
H(15A)	8490(50)	2490(50)	4300(40)	31
H(15B)	6630(50)	3010(50)	4330(40)	31
H(15C)	7720(50)	3930(50)	3680(40)	31
H(16A)	11450(60)	-1060(50)	1970(50)	39
H(16B)	10110(50)	-1760(60)	770(50)	39
H(16C)	11300(60)	-2640(50)	1990(50)	39
H(17A)	7470(60)	100(40)	5190(40)	30
H(17B)	9110(50)	380(50)	4800(40)	30
H(17C)	8540(50)	-1120(50)	4980(40)	30
H(18A)	3330(60)	5200(50)	2630(50)	37
H(18B)	1620(60)	4490(50)	1940(50)	37

H(18C)	2670(60)	5050(50)	1010(50)	37

Table 6. Torsion angles [°] for S5.27.

C(14)-C(1)-C(2)-O(3)	69.1(3)
C(15)-C(1)-C(2)-O(3)	-45.0(4)
C(10)-C(1)-C(2)-O(3)	-170.8(3)
C(14)-C(1)-C(2)-C(3)	-170.3(3)
C(15)-C(1)-C(2)-C(3)	75.7(3)
C(10)-C(1)-C(2)-C(3)	-50.2(3)
O(3)-C(2)-C(3)-C(4)	-179.4(3)
C(1)-C(2)-C(3)-C(4)	57.1(4)
C(2)-C(3)-C(4)-C(5)	172.7(3)
C(2)-C(3)-C(4)-C(9)	-60.8(4)
C(3)-C(4)-C(5)-C(16)	-48.7(4)
C(9)-C(4)-C(5)-C(16)	-175.0(3)
C(3)-C(4)-C(5)-C(6)	-170.6(3)
C(9)-C(4)-C(5)-C(6)	63.1(3)
C(16)-C(5)-C(6)-C(7)	-179.9(3)
C(4)-C(5)-C(6)-C(7)	-55.5(4)
C(5)-C(6)-C(7)-O(4)	-77.9(3)
C(5)-C(6)-C(7)-C(8)	46.8(4)
O(4)-C(7)-C(8)-C(9)	77.1(3)
C(6)-C(7)-C(8)-C(9)	-45.1(4)
C(3)-C(4)-C(9)-C(17)	-67.7(3)
C(5)-C(4)-C(9)-C(17)	60.2(3)
C(3)-C(4)-C(9)-C(8)	171.5(3)
C(5)-C(4)-C(9)-C(8)	-60.6(3)
C(3)-C(4)-C(9)-C(10)	57.1(3)
C(5)-C(4)-C(9)-C(10)	-175.1(2)
C(7)-C(8)-C(9)-C(17)	-70.2(3)
C(7)-C(8)-C(9)-C(4)	51.2(4)
C(7)-C(8)-C(9)-C(10)	165.6(3)
C(17)-C(9)-C(10)-C(11)	-58.8(4)
C(4)-C(9)-C(10)-C(11)	178.0(3)
C(8)-C(9)-C(10)-C(11)	63.2(3)

C(17)-C(9)-C(10)-C(1)	68.8(4)
C(4)-C(9)-C(10)-C(1)	-54.4(3)
C(8)-C(9)-C(10)-C(1)	-169.1(3)
C(14)-C(1)-C(10)-C(11)	-58.6(3)
C(2)-C(1)-C(10)-C(11)	-177.3(2)
C(15)-C(1)-C(10)-C(11)	57.6(3)
C(14)-C(1)-C(10)-C(9)	169.9(3)
C(2)-C(1)-C(10)-C(9)	51.1(3)
C(15)-C(1)-C(10)-C(9)	-74.0(3)
C(9)-C(10)-C(11)-O(5)	8.6(4)
C(1)-C(10)-C(11)-O(5)	-123.1(3)
C(9)-C(10)-C(11)-C(12)	-173.6(3)
C(1)-C(10)-C(11)-C(12)	54.7(3)
C(13)-O(1)-C(12)-C(11)	-111.7(3)
O(5)-C(11)-C(12)-O(1)	-143.5(3)
C(10)-C(11)-C(12)-O(1)	38.5(4)
O(5)-C(11)-C(12)-C(13)	148.2(3)
C(10)-C(11)-C(12)-C(13)	-29.8(4)
C(12)-O(1)-C(13)-C(18)	-111.0(3)
C(12)-O(1)-C(13)-C(14)	111.4(3)
C(11)-C(12)-C(13)-O(1)	103.3(3)
O(1)-C(12)-C(13)-C(18)	105.0(3)
C(11)-C(12)-C(13)-C(18)	-151.7(3)
O(1)-C(12)-C(13)-C(14)	-96.3(3)
C(11)-C(12)-C(13)-C(14)	7.0(5)
O(1)-C(13)-C(14)-O(2)	104.4(3)
C(12)-C(13)-C(14)-O(2)	168.5(3)
C(18)-C(13)-C(14)-O(2)	-32.4(4)
O(1)-C(13)-C(14)-C(1)	-77.3(3)
C(12)-C(13)-C(14)-C(1)	-13.2(4)
C(18)-C(13)-C(14)-C(1)	145.9(3)
C(2)-C(1)-C(14)-O(2)	-23.0(4)
C(15)-C(1)-C(14)-O(2)	96.1(4)
C(10)-C(1)-C(14)-O(2)	-142.2(3)
C(2)-C(1)-C(14)-C(13)	158.8(3)
C(15)-C(1)-C(14)-C(13)	-82.1(3)

C(10)-C(1)-C(14)-C(13)	39.6(4)

Table 7. Hydrogen bonds for S5.27 [Å and °].

D-H...A	d(D-H)	d(H...A)	d(D...A)	<(DHA)
O(3)-H(3)...O(2)	0.81(5)	2.19(5)	2.805(4)	132(5)
O(4)-H(4)...O(5)#1	0.80(5)	2.12(5)	2.911(4)	172(5)

Symmetry transformations used to generate equivalent atoms:
#1 -x+1,y-1/2,-z+1